Heterogeneous catalytic conversion of non-edible lipid biomass to biochemicals

Konvertering av ikke-spiselig lipidrik biomasse til biokjemikalier ved heterogen katalyse

Philosophiae Doctor (PhD) Thesis

Mangesh Ramesh Avhad

Department of Mathematical Sciences and Technology
Faculty of Environmental Science and Technology
Norwegian University of Life Sciences

Ås (2016)

Thesis number 2016:84
ISSN 1894-6402
ISBN 978-82-575-1400-6

Supervisor:

Dr. Jorge Mario Marchetti
Associate Professor, Department of Mathematical Sciences and Technology
Norwegian University of Life Sciences (NMBU)
P. O. Box 5003 IMT, N-1432, Ås, Norway

Evaluation Committee:

Dr. Rasmus Fehrmann
Professor, Department of Chemistry
Denmark University of Technology (DTU)
Department of Chemistry Building 207, DK-2800 Lyngby, Denmark

Dr. Tanja Barth
Professor, Department of Chemistry
University of Bergen (UiB)
Realfagbygget, Allégt. 41 / P. O. Box 7803, 5020 Bergen, Norway

Dr. Knut Kvaal
Professor, Department of Mathematical Science and Technology
Norwegian University of Life Sciences (NMBU)
P. O. Box 5003 IMT, N-1432, Ås, Norway

The research described in this thesis was conducted in the Reaction Engineering and Catalysis group at the Norwegian University of Life Sciences, Norway. This work was financially supported by IMT-NMBU under the project number 1301051406.

- *Dedicated to my beloved parents*

“All Birds find shelter during a rain. But eagle avoids rain by flying above the clouds. Problems are common, but attitude makes the difference!”

- *Dr. A.P.J. Abdul Kalam*

Acknowledgements

The completion of this thesis is credited to the support and encouragement of people encompassing my supervisor, family members, colleagues, and well-wishers. I am privileged to acknowledge all those people who contributed in many ways to make this journey memorable and an unforgettable experience for me.

First, I would like to express my heartfelt and sincere gratitude to my research supervisor Associate Professor Jorge M. Marchetti. I believe you were an exceptional leader, who offered the work responsibilities with freedom. I sincerely thank you for keeping your door always open for scientific as well as informal discussions. Our frequent meetings have been vital in guiding me in the right direction throughout the research tenure. Your immense support, constructive working culture, and discipline have always inspired me to work harder and achieve more. I have learnt a lot from you, both as a scientist and as a person. I would like to show my gratefulness also to Anna Saltberg, Björn Saltberg, and Lukas Saltberg Marchetti for all the delightful gatherings at your place. This makes my time in a country half a world away from home more enjoyable..

I am deeply indebted also to Professor José Aracil and Professor Mercedes Martínez for providing an opportunity to perform the research activities at the Complutense University of Madrid, Spain through the NILS mobility grant. The collaboration was fruitful, and your knowledge and vast experience in the field allowed me to conduct research in the right direction all through my stay. A special thanks to Marcos Sánchez for his unconditional assistance. Marcos, you helped me in a way only a brother could do. I would like to thank also Marta Serrano, Abderrahim Bouaid, and Elisa Peña for involving me in both professional and social activities. The time spent in Spain has been one of the best of my life that I treasure so much and keep with me for the rest of my life.

I wish to extend my gratitude to Professor Andrzej Stankiewicz, Lalit Gangurde, and George Tsalidis for the cooperation in performing the characterization of the catalytic materials at the Delft University of Technology, The Netherlands.

I would like to thank Sandeep Sharma from the Department of Chemistry, Biotechnology and Food Science (IKBM) for the moisture analysis, as well as Ranjana Pathak and Niveditha U.

Katyayini from the Centre for Climate Regulated Plant Research (SKP) for the microscopic imaging. Sigurd Flaatten, Hans O. D. Kristiansen, Glenn A. Knutheim, Christine Spiten, Tor K. Vara, Ulrik v. Rør, Eivind Bachmann, Espen Vinsand, Johanne Solheim, Steffen Aasen, Fahad Jamil, and Ibrahim Temel from the Department of Mathematical Sciences and Technology (IMT) are acknowledged for the heat of combustion analysis.

I am grateful to Petter Heyerdahl, Cecilia Futsæther, Knut Kvaal, and Arne Svendsen for their contribution in collecting the avocado seeds, and involving me in the coffee-break discussions. I would like to acknowledge the support and advice from the administration staff of IMT: Anita H. Habbestad, Mona V. Kristiansen, Anne-Karin S. Pettersen, Berit H. Lindstad, Rune Grønnevik, and Tone Rasmussen. Frode Hilmarsen, Hassan A. Nur, and Jon Asper are acknowledged for their technical assistance. Thank you Andreas Flø and Signe Kroken for all the assistance in developing the laboratory, and helping me in getting to the University on the day-1 of my Ph.D.

I would like to thank Aleksander Hykkerud, Miriam Osborg, Yadessa Keneni, Shemelis Gebremariam, and Valeria Verdinelli for maintaining an enjoyable working atmosphere.

It is also a pleasure to thank Professor Shantaram Bonde and Professor Ranjana Bhadane for their unconditional support and advices. Had I not been fortunate enough to get an opportunity to do research with you, I might have never realized how much you care for the progression of your students. I believe the better way of thanking you would be through my future contribution to the scientific community.

I sincerely thank the well-wishers during my journey at the National Chemical Laboratory, and Nowrosjee Wadia College. I thank the people of Abasaheb Garware College for introducing me to the world of hiking and camping; I never stopped thereafter. Joining the National Cadet Corps was one of the wisest decisions I made in my life that taught me the importance of discipline and equality at a right age.

Hrishikesh Deshpande, Nitin Rukhe, and Tushar Sakpal, thank you for being beside me through the thick and thin in my life. Thank you my brothers for helping my parents at times in my absence. Recollecting the moments spent with you all have always brought smile to my face. I am enormously happy that the distance did not tarnish our relation. Thank you, Durgesh Lad.

Finally, I would like to thank my beloved family. I would have not come to this point without their moral values, sacrifice, love, and blessings. I would like to pay high regards to my parents, Smt. Hemlata R. Avhad and Shri. Ramesh J. Avhad for educating me with the human ethical values, and then allowing me to be as ambitious as I wanted. Do remember, always, *'मागे उभा मंगेश, पुढे उभा मंगेश'*.

To my sister Smt. Meghana A. Avhad-Khade, thank you for your constant love, and ensuring that I become a conscientious person. A special thanks to my brother-in-law Professor Amitkumar S. Khade for buzzing a reviving alarm for my advancements. My deepest gratitude to my nephew Avaneesh for bringing joy and happiness into our lives.

I am grateful to the Norwegian University of Life Sciences and the Department of Mathematical Sciences and Technology for providing the financial support for my Ph.D.

My Ph.D. journey has come to an end with plenty of beautiful and unforgettable moments that I highly treasure and keep with me for rest of my life.

Summary

The use of fuel increases consistently given the high demand for energy. This demand is mostly met by fossil fuels. Considering the uncertainties connected to fossil fuel reserves and the related natural effects of their use, the interest in renewable energy is continuously growing. Plant biomass, being renewable, has been pointed out as the potential equivalent to petroleum for the sustainable production of fuels, chemicals, and carbon-based materials. Biofuels, such as biodiesel from plant oils are becoming attractive as an alternative to petrodiesel and believed to be the future fuels for the transportation sector. Biodiesel is considered as the fastest growing industry worldwide because of its natural advantages and production from renewable assets. Still, high costs and the constrained accessibility of plant oil resources limit the wider use of this alternative biofuel. Feedstocks that compete with food crops have been put in question for their sustainability as the food process show an upsurge. Use of the type of catalysts is an additional factor that contributes to the total production expenses. The usage of homogenous catalysts multiplies the processing stages. From the perspective of ensuring widespread consumption of biodiesel, the utilization of cost-effective lipid biomass and catalysts is a key. The prime objective of the present PhD thesis is to use an active and inexpensive heterogeneous catalyst for the conversion of non-edible lipid biomass to biochemicals, with an emphasis on biodiesel. Additionally, the thesis attempted to integrate the processing stages for biodiesel production through the reactive extraction methodology. The latter part of the present thesis includes the mathematical modelling of the experimental findings, which would allow the design engineers to select the suitable operating parameters for the respective process.

The present PhD thesis is based on seven scientific papers that systematically examined different aspects of lipid biomass, catalytic materials, the process integration, and the mathematical modelling for biochemicals production. It is evident from the deluge of available publications that biodiesel production is receiving renewed interest and intensive research. Therefore, the work started with an extensive literature study of the state of the art of diverse lipid biomass and catalytic materials for biodiesel production (**Paper I** and **II**). An in-depth study of literature hinted the need of utilizing non-food grade lipid biomass and cost-effective, but heterogeneous catalysts for biodiesel production. As a continuation of previous research work, the initial activity in the present PhD project involved the application of non-edible lipid

feedstock for the synthesis of biodiesel and a value-added by-product over a heterogeneous catalyst. A set of experiments was designed to conduct the statistical analysis for the determination of factors influencing the process and to develop a model equation predicting the optimal conditions affecting the process. The study additionally established a mathematical model to simulate the reaction kinetics, and investigate a step controlling the process (**Paper III**). Based on the reaction chemistry, the catalyst was later structurally modified and the performance of the same was tested for a single-step biodiesel production from non-edible crude plant oil. This work presented a novel method for the preparation of a solid catalyst. The experimental part of this study involved a comparison between different catalysts, and examining the impact of different variables on the performance of the best heterogeneous catalyst selected for the transformation of crude oil to biodiesel. The statistical analysis was conducted to understand the parameters influencing the process, and derive a model equation predicting the optimal conditions affecting the process (**Paper IV**). In **Paper V**, the same heterogeneous catalyst was applied for the conversion of refined oil to biodiesel. Firstly, the impact of three reaction parameters on the oil conversion as well as biodiesel yield was carefully examined in the experimental section. Secondly, the physical and fuel properties of biodiesel were determined. Thirdly, a model equation was established to predict the optimal conditions affecting the process through the statistical analysis. Finally, a previously developed mathematical model was applied for the present heterogeneously catalyzed chemical process to describe the kinetics of triglycerides consumption as well as biodiesel formation.

In the process integration context, the drying process of waste seeds comprising lipid bodies was carried out as a preliminary step for the reactive extraction in **Paper VI**. The effects of different temperatures on the degree of moisture evaporation and the physical appearance of seeds was systematically monitored. In addition, this study carefully examined the impact of the pretreatment of seeds on the drying mechanism. In **Paper VII**, a novel semi-theoretical mathematical model was presented, which provided an excellent simulation of the drying kinetics of seeds. The accuracy of the presented model was verified by comparing with those frequently applied for predicting the drying kinetics of biomass. The dried seeds were subsequently utilized for the reactive extraction process for biochemicals production, wherein the effects of the processing methodology, temperatures, and pressures were investigated.

Sammendrag

Bruken av drivstoff øker konsekvent grunnet den høye etterspørselen etter energi. Dette kravet dekkes stort sett av fossilt brensel. Grunnet usikkerheten knyttet til fossile reserver og konsekvenser ved bruk, er interessen for fornybar energi stadig voksende. Biomasse fra planter, som er fornybar, har blitt pekt ut som det potensielle alternativet til petroleum for bærekraftig produksjon av drivstoff, kjemikalier, og karbonbaserte materialer. Biodrivstoff, for eksempel biodiesel fra planteoljer, er et godt alternativ til petrodiesel og antas å være det fremtidige drivstoffet for transportsektoren. Biodiesel er regnet som den raskest voksende industrien over hele verden på grunn av sine naturlige fortrinn og produksjon fra fornybare ressurser. Høye kostnader og begrenset tilgjengelighet av planteoljeressurser begrenser større bruk av dette alternative biobrenselet. Råstoffer som konkurrerer med matproduksjon har blitt utfordret på bærekraft ettersom matproduksjonen øker. Bruk av katalysatorer er en ytterligere faktor som bidrar til de totale produksjonskostnadene. Bruken av homogene katalysatorer øker antall behandlingstrinn. Fra perspektivet om å sikre utbredt forbruk av biodiesel, er utnyttelse av kostnadseffektiv lipid biomasse og katalysatorer en nøkkel. Hovedmålsettingen for denne avhandlingen er å bruke en aktiv og rimelig heterogen katalysator for konvertering av ikke-spiselig lipid biomasse til biokjemikalier, med vekt på biodiesel. I tillegg har arbeidet forsøkt å integrere behandlingstrinn for biodieselproduksjon gjennom reaktiv utvinningsmetodikk. Den siste delen av avhandlingen er en matematisk modellering av de eksperimentelle funn, som tillater designingeniører til å velge passende rammebetingelsene for de respektive prosessene.

Denne doktorgradsavhandlingen er basert på syv vitenskapelige artikler som systematisk undersøker ulike aspekter av lipid biomasse, katalytiske materialer, prosessintegrasjon, og matematisk modellering av biokjemikalieproduksjon. Det store antallet av tilgjengelige publikasjoner som biodieselprodusentene mottar har fornyet interessen og intensivert forskningen. Derfor startet arbeidet med avhandlingen med en omfattende litteraturstudie av statusen til ulike lipide biomasser og katalytiske materialer for biodieselproduksjon (**artikkel I** og **II**). En grundig studie av litteraturen antydet behovet for å utnytte ikke-spiselig lipid biomasse og kostnadseffektivitet med heterogene katalysatorer for biodieselproduksjon. Som en videreføring av forskningsarbeidet, involverte det første arbeidet i dette prosjektet bruk av ikke-spiselig lipid råstoff for syntese av biodiesel og et verdiøkende biprodukt over en

heterogen katalysator. Et sett av eksperimenter ble utviklet for å utføre den statistiske analysen for bestemmelse av faktorer som påvirker prosessen, samt for å utvikle en modell for en ligning som forutsier de optimale forhold som påvirker prosessen. Studien har i tillegg etablert en matematisk modell for å simulere reaksjonskinetikk og undersøke et trinn som styrer prosessen (**artikkel III**). Basert på reaksjonskjemi, ble katalysatoren senere strukturelt modifisert og utførelsen av det samme ble testet for en enkelttrinnsproduksjon av biodiesel fra ikke-spiselig rå planteolje. Dette arbeidet representerer en ny fremgangsmåte for fremstilling av en fast katalysator. Den eksperimentelle delen av denne studien involverte en sammenligning mellom forskjellige katalysatorer, og å undersøke virkningen av forskjellige variable på resultatene av den beste heterogene katalysatoren valgt for transformasjonen av råolje til biodiesel. Den statistiske analysen ble utført for å forstå de parameterne som påvirker prosessen, og utledet en modelligning som kan forutsi optimale betingelser som påvirker prosessen (**artikkel IV**). I **artikkel V** ble den tilsvarende heterogene katalysatoren anvendt for omdannelse av raffinert olje til biodiesel. Først ble virkningen av tre reaksjonsparametere på oljekonvertering samt biodieselutbyttet nøye undersøkt i den eksperimentelle delen. Deretter ble de fysikalske egenskapene og brenselsegenskapene til biodiesel bestemt, før en modelligning ble etablert for å forutsi optimale forhold som påvirker prosessen gjennom statistisk analyse. Til slutt ble en tidligere utviklet matematisk modell anvendt for den heterogent katalyserte kjemiske prosessen for å beskrive kinetikken av triglyseridforbruk samt biodieselformasjonen.

I prosessintegrasjonen ble tørkingen av avfallskimer som omfatter lipid-legemer utført som et innledende trinn for den reaktive ekstraksjonen i **artikkel VI**. Effekten av forskjellige temperaturer på graden av tørking og det fysiske utseendet til frøene ble systematisk overvåket. I tillegg har denne studien nøye undersøkt effekten av forbehandling av frø til tørkemekanisme. I **artikkel VII**, ble en ny halvteoretisk matematisk modell presentert, noe som ga en utmerket simulering av tørkekinetikken for frø. Nøyaktigheten av den presenterte modellen ble verifisert ved å sammenligne med de som ofte anvendes for å forutsi tørkekinetikken av biomasse. De tørkede frøene ble deretter anvendt for den reaktive utvinningsprosessen for produksjon av biokjemikalier, karakterisert ved at effekten av forskjellige og behandlingsmetodikk, temperaturer og trykk ble undersøkt.

List of articles

Paper I

Avhad MR, Marchetti JM. A review on recent advancement in catalytic materials for biodiesel production. *Renewable and Sustainable Energy Reviews*. 2015: 50; 696-718.

Paper II

Avhad MR, Marchetti JM. Innovation in solid heterogeneous catalysis for the generation of economically viable and ecofriendly biodiesel: A review. *Catalysis reviews: Science and Engineering*. 2016: 58(2); 157-208.

Paper III

Avhad MR, Sánchez M, Peña E, Bouaid A, Martínez M, Aracil J, Marchetti JM. Renewable production of value-added jojobyl alcohols and biodiesel using a naturally-derived heterogeneous green catalyst. *Fuel*. 2016: 179; 332-338.

Paper IV

Avhad MR, Sánchez M, Bouaid A, Martínez M, Aracil J, Marchetti JM. Glycerol-activated calcium oxide catalyst for the methanolysis of crude *jatropha curcas* oil. Submitted to *Fuel*.

Paper V

Avhad MR, Sánchez M, Bouaid A, Martínez M, Aracil J, Marchetti JM. Modeling chemical kinetics of avocado oil ethanolysis catalyzed by solid glycerol-enriched calcium oxide. Accepted by *Energy Conversion and Management*. 2016. http://dx.doi.org/10.1016/j.enconman.2016.07.060

Paper VI

Avhad MR, Marchetti JM. Temperature and pretreatment effects on the drying of Hass avocado seeds. *Biomass and Bioenergy*. 2015: 83; 467-473.

Paper VII

Avhad MR, Marchetti JM. Mathematical modelling of the drying kinetics of Hass avocado seeds. *Industrial Crops and Products*. 2016: 91; 76-87.

Additional scientific contribution

Oral presentations

Avhad MR, Sánchez M, Bouaid A, Martínez M, Aracil J, Marchetti JM. Glycerol-activated calcium oxide catalyst for biodiesel production from crude *jatropha curcas* oil. FineCat 2016-Symposium on heterogeneous catalysis for fine chemicals. April 6-7, 2016. Palermo, Italy.

Avhad MR, Sánchez M, Peña E, Bouaid A, Martínez M, Aracil J, Marchetti JM. Investigation of catalytic activity of thermally treated waste mussel shells for biodiesel production from jojoba oil. International Congress and Expo on Biofuels and Bioenergy. August 25-27, 2015. Valencia, Spain.

Avhad MR, Marchetti JM. Effect of pretreatment and temperature on the drying kinetics of Hass avocado seeds. The Energy and Material Research Conference. February 25-27, 2015. Madrid, Spain.

Poster presentations

Avhad MR, Sánchez M, Bouaid A, Martínez M, Aracil J, Marchetti JM. Modelling chemical kinetics jojoba oil butanolysis catalyzed by CaO. 24th European Biomass Conference and Exhibition. June 6-9, 2016. Amsterdam, The Netherlands.

Avhad MR, Sánchez M, Peña E, Bouaid A, Martínez M, Aracil J, Marchetti JM. Investigation of efficiency of waste mussel shells derived calcium oxide catalyst for biodiesel production from several oils. International Symposium on Green Chemistry Conference. May 3-7, 2015. La Rochelle, France.

Avhad MR, Marchetti JM. Time dependent mathematical modeling for the temperature dependent drying of Hass avocado seed. Time dependent mathematical modelling for the temperature dependent drying of Hass avocado seeds. 21st International Congress of Chemical and Process Engineering. August 23-27, 2014. Prague, Czech Republic.

Avhad MR, Marchetti JM. Time dependent mathematical modeling for the temperature dependent drying of Hass avocado seed. Determination of physical properties of Hass and Fuerte avocado seed at various drying temperature: A comparative study. 21st International Congress of Chemical and Process Engineering. August 23-27, 2014. Prague, Czech Republic.

Avhad MR, Marchetti JM. Effect of temperature on different pretreated Sharwil avocado seeds for biofuel generation. Renewable Energy Research Conference. June 16-18, 2014. Oslo, Norway.

Avhad MR, Marchetti JM. Effect of different temperatures on the germination of Hass avocado seeds. Renewable Energy Research Conference. June 16-18, 2014. Oslo, Norway.

Book chapters

Marchetti JM, Avhad MR. Economic assessment for biodiesel production. *Biofuel production and processing technology*. *Taylor and Francis*. 2016. Edited by Riazi MR and Chiaramonti D. Accepted and under editorial processing.

Marchetti JM, Avhad MR. Uses of enzymes for biodiesel production. *Handbook of Biotechnology for Renewable Fuels: Technology Assessments, Emerging Industrial Applications, and Future Outlooks*. *Elsevier*. Edited by Hosseini M. Under preparation.

Articles

Sánchez M, Avhad MR, Marchetti JM, Martínez M, Aracil J. Enhancement of the jojobyl alcohols and biodiesel production using a renewable catalyst in a pressurized reactor. *Energy Conversion and Management*. 2016: 126; 1047-1053.

Sánchez M, Avhad MR, Marchetti JM, Martínez M, Aracil J. Jojoba Oil: A state of the art review and future prospects. Submitted to *Energy Conversion and Management*.

Avhad MR, Osborg MV, Marchetti JM. Modeling chemical kinetics of acetic acid esterification catalyzed by the cation-exchange resins. Under preparation.

Avhad MR, Sánchez M, Marchetti JM. Techno-economic assessment of glycerol-enriched calcium oxide catalyzed single-step methanolysis of crude *jatropha curcas* oil. Under preparation.

Serrano M. Avhad MR, Marchetti JM. Techno-economic assessment of avocado oil ethanolysis catalyzed by solid glycerol-enriched calcium oxide. Under preparation.

List of abbreviations

AOCS	American Oil Chemists' Society
ASTM	American Society for Testing and Materials
CaDg	Calcium diglyceroxide
CaO	Calcium oxide
CJCO	Crude *jatropha curcas* oil
DAGs	Diacylglycerols
EU	European Union
FAAEs	Fatty acid alkyl esters
FABEs	Fatty acid butyl esters
FAEEs	Fatty acid ethyl esters
FAMEs	Fatty acid methyl esters
FFAs	Free fatty acids
GC	Gas chromatography
MAGs	Monoacylglycerols
MSC	Model selection criteria
REM	Reactive extraction methodology
RSM	Response surface methodology
SWE	Sum of weighted errors
TAGs	Triacylglycerols
TGA	Thermogravimetric analysis
XRD	X-ray diffraction

Table of Contents

1. Introduction

1.1. General introduction

Energy is a basic requirement for human existence; and the demand for the same has been significantly increasing because of the augmenting human population. According to the International Energy Outlook 2016 set by the U.S. Energy Information Administration, the total world energy consumption will grow by 48 % between 2012 and 2040 [1]. The majority of the energy is utilized for the industrial applications, transportation, and the power generation sector. In the present situation, the conventional fossil fuel resources, such as gasoline, liquefied petroleum gas, diesel fuel, and natural gas supply the foremost amount of energy. The energy consumption for the transportation sector is increasing at an annual rate of 1.4 %, accounting for 49 % growth from 2012 to 2040 [1]. The utilization of fossil fuel resources for the energy production, however, has several hazardous impacts on the ecosystem, such as large greenhouse gas emissions, the climate change, and acid rain. Furthermore, a consistent fear of dwindling reserves of crude oil and oscillating fuel prices have made todays necessity to find an alternative resources of energy which are sustainable, renewable, environmentally friendly, economically competitive, and easily available [2].

The European Union (EU) Renewable Energy Directive 2009/28/EC set a target of increasing the share of renewable energy use in the EU from 8.5 % in 2005 to 20 % by 2020 with the motive to promote cleaner transport, limit the greenhouse gas emissions, and stimulate innovation and the technological development. In addition to the overall target for renewables, all member states have to reach a target of 10 % share of renewable energy for transportation [3, 4]. Plant biomass, the only current sustainable source of organic carbon, has been considered as the promising equivalent to petroleum for the production of fuel and value-added chemicals. The establishment of plant biomass based energy is anticipated to minimize the entire dependency on the utilization of fossil fuels. Additionally, biomass feedstocks feature a closed carbon cycle in which the carbon dioxide released during the energy conversion is recaptured by the existing plants *via* photosynthesis during biomass regrowth [5, 6]. The ‘Roadmap for Biomass Technologies’ set by the U.S. Department of Energy has predicted that by 2030, 20 % of transportation fuel and 25 % of chemicals would be produced from biomass [7].

Biofuels have aroused much attention in the green-tech revolution in parallel to energy demand and the climate change around the world. Among different biofuels, biodiesel has been gaining substantial relevance as a potential alternative or additive to current petroleum-derived diesel not only because this oxygenated fuel can be synthesized from oil-rich biomass but also for the reason that it offers minor environmental toxicity and is biodegradable in nature [8, 9]. The combustion of biodiesel offers net carbon dioxide emissions reduction of 78 % (based on the lifecycle analysis), 48 % less carbon monoxide, 47 % less particulate matters, and 67 % less hydrocarbons, when compared with petroleum based diesel fuel [10, 11]. The biofuels barometer presented by the EurObserv'ER indicated that the biodiesel amounted for 79.7 %, in energy content, of the total biofuel consumption [12]. The breakdown of total EU biofuel consumption, in energy content, in year 2014 for transport by biofuel type is shown in Figure 1.1. Whereas, the share of biofuel types consumed in several EU countries in 2014 for transport can be seen in Figure 1.2.

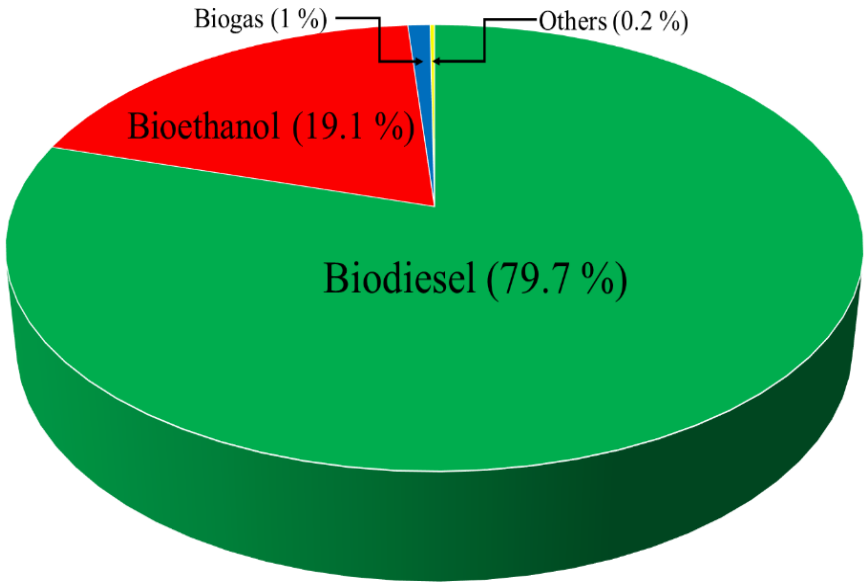

Figure 1.1: Breakdown of total EU biofuel consumption in 2014 for transport by biofuel type [12].

The biodiesel consumption for the EU transport increased by 7.8 % in the year 2014, when compared to that of in 2013. A graphical representation showing a comparison of biodiesel consumption in the EU countries for transport between the year 2013 and 2014 is presented in Figure 1.3.

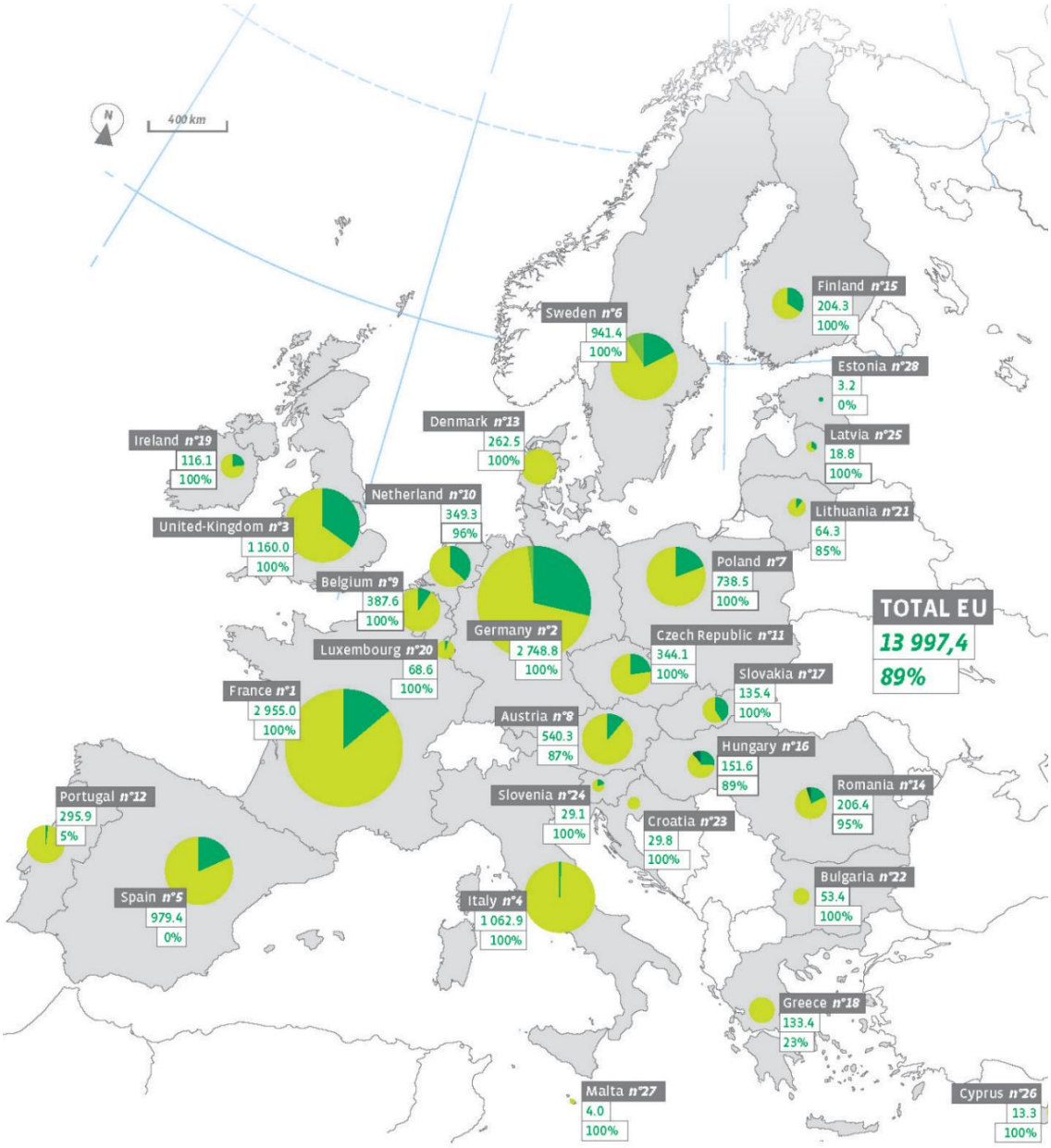

Figure 1.2: Share of biofuel types consumed in the EU countries in 2014 for transport. ■-Biodiesel, ■-Bioethanol, ■-Biogas, ■-Others (Pure used vegetable oil and unspecified biofuel) [12]. *Figure reprinted with permission from EurObserv'ER.*

In Norway, Perstorp chemical company located in Fredrikstad produces a large-scale biodiesel from rapeseed oil. This company aims further developments in improving biodiesel winter performance and the application of non-crop based feedstocks [13]. The available literature suggests that the residual fish oil, animal fats, and grease traps are potential raw materials for producing large amounts of biodiesel in Norway [14, 15]. The three largest cities of Norway: Oslo, Trondheim, and Bergen are believed to supply foremost quantity of these feedstocks [14].

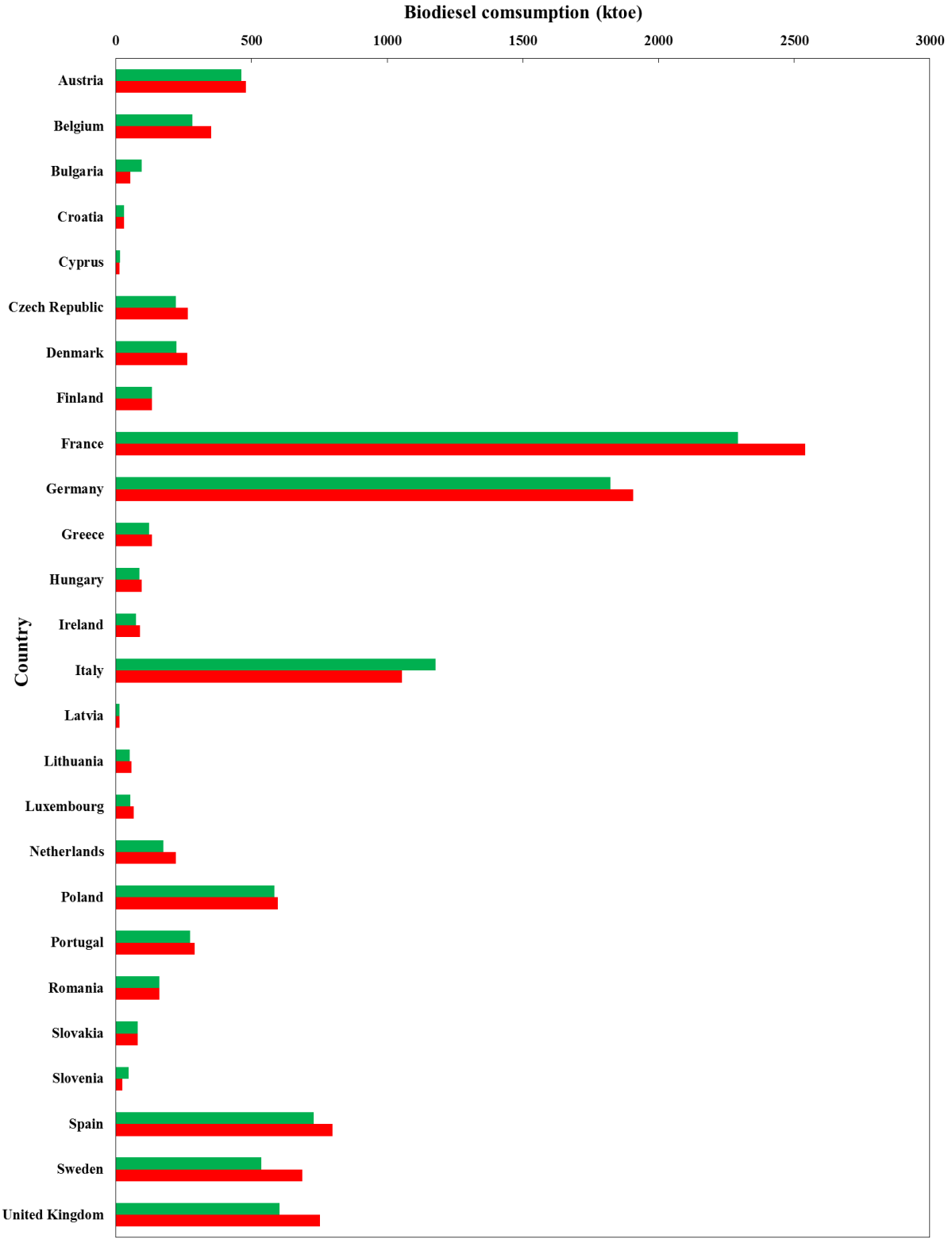

Figure 1.3: Biodiesel consumption for transport in the European Union. ■-2013, ■-2014 [12].

For Denmark, biodiesel and bioethanol data is mixed due to confidentiality, so the figure contains both bioethanol and biodiesel. EU countries having no or insignificant consumption of biodiesel are not included in the figure.

According to the Clean Cities Alternative Fuel Price Report published by the U.S. Department of Energy in April 2016 [16], the retail price of biodiesel (B99/B100) in April 2016 was $ 2.81 per gallon, which is higher when compared with that of conventional petroleum diesel ($ 2.13 per gallon). The usage of refined vegetable oils, expensive catalytic materials, and multiple processing stages for biodiesel production have been contributing in making biodiesel expensive. In such context, consistent efforts are engaged in reducing the production cost of biodiesel to make it profitable and expand its consumption. The present thesis is centered on the consensus that sustainable biodiesel generation is a requirement for the future of cleaner transportation. Concretely, we focused our efforts on the utilization of cost-competitive materials and the process integration with the perspective of reducing the production cost of biodiesel. The thesis attempts to furnish insights into the below listed important segments:

- Second generation lipid biomass: Non-edible plant oils
- Cost-effective heterogeneous catalysis
- Process integration: Reactive extraction methodology
- Mathematical modelling

1.2. Research objectives

The challenges in biodiesel production involves the utilization of proficient as well as cost-effective materials. The type of feedstocks, catalytic materials, and the processing technology applied for biodiesel production have a significant impact on the final cost of this biofuel. In pursuit of this, the prime objectives of the present research includes: (i) use of non-edible lipid biomass for the production of biochemicals, with an emphasis on biodiesel (**Paper III-IV**), (ii) the application of active and inexpensive "green" heterogeneous catalytic system for the alcoholysis reactions (**Paper III-V**), (iii) the reactive extraction of Hass avocado seeds for the generation of biochemicals (**Paper VI**), and (iv) the mathematical modelling of the experimental findings that would allow the design engineers to choose the most suitable operating conditions for the respective process (**Paper III-V, VII**). A part of the present thesis also dedicates to follow the principles of green chemistry, wherein all materials utilized for the production of biochemicals are available from renewable natural resources.

1.3. Organization of the thesis

The different stages of the present thesis are addressed in each of the seven publications. A description of the contents of each publication is given below.

Paper I presents a general introduction to the existing variety of lipid biomass, catalysts, and methodologies applied for biodiesel production. The lipid feedstocks were initially categorized, then the oil content in the plant seeds and the fatty acid profile of edible as well as non-edible plant oils was tabulated. Subsequently, the necessity for the transformation of oil to biodiesel was elucidated, followed with an overview of different processes applied for the oil conversion. Recently tested several homogeneous as well as heterogeneous acid and base catalysts along with the most suitable operating reaction parameters applied for biodiesel production were systematically reviewed. Moreover, the article drives the attention towards the non-traditional developments in catalysis and the processing technology for biodiesel production.

Paper II thoroughly discussed the reaction mechanism for the homogeneous base-, homogeneous acid-, heterogeneous base-, and heterogeneous acid-catalyzed alcoholysis process. The advantages and disadvantages of homogeneous as well as heterogeneous catalysts for biodiesel production were presented. This article provided an extensive information about different kinds of single alkaline earth metal oxides, supported alkali metals, supported alkaline earth metals, ion-exchange resins, zirconia-based, silica-based, heteropoly acids, and carbon-based heterogeneous catalysts for biodiesel production. Furthermore, this article discussed the factors influencing the performance of heterogeneous catalysts and biodiesel production.

In **Paper III**, we presented the transformation of jojoba oil to biodiesel and value-added jojobyl alcohols using the renewable natural resources. The *Mytilus Galloprovincialis* shells derived calcium oxide (CaO) was utilized to accelerate the alcoholysis process between jojoba oil and butanol, wherein the impact of temperature, time, butanol-to-oil molar ratio, and the catalyst amount was systematically investigated. The article also presented a mathematical model describing the kinetics of the process.

Paper IV showed how the structurally modified CaO displays superior catalytic activity than CaO. The novel catalyst was applied for a single-step methanolysis process of crude *jatropha curcas* oil (CJCO) having high content of free fatty acids (FFAs). The activity of different

laboratory-synthesized and commercial catalysts was compared to find the best catalyst for the present study. The statistical analysis determining the interaction between the reaction variables, and their influence on the methanolysis process was also presented.

The aim of **Paper V** was focused on the application of glycerol-enriched CaO catalyst for the transesterification between avocado oil and ethanol, in which the effect of temperature, ethanol-to-oil molar ratio, and the catalyst amount on the process was carefully examined. The simulation studies were conducted and a mathematical model was employed for predicting the kinetics of the process. The research article also provides the detail information about the physical and fuel properties of avocado oil and the synthesized biodiesel.

The effects of different temperatures on the degree of moisture evaporation from Hass avocado seeds were presented in **Paper VI**. In this article, we explained the necessity of the physical treatment of seed before placing it for the drying process. The impact two different surrounding conditions on the physical appearance as well as on the quality of Hass avocado seeds was also demonstrated. In **Paper VII**, we establish a new semi-theoretical mathematical model that provides a superior simulation of the drying kinetics of Hass avocado seeds, when compared with those frequently applied for describing the drying process of biomass seeds.

2. Research background

2.1. Sustainability and Green chemistry

It is difficult to imagine how life in the 21st century would be, were it not for the advances made by the chemical industry throughout the 19th and 20th centuries. Virtually, every aspect of modern day life is affected by the chemical industry in some way. During the industrial revolution the prime focus was on the discovery of new processes, but not on sustainability and waste minimization. As a result, lot of waste was generated from various chemical and pharmaceutical processes. It is also true that at present the chemical industry is inexorably linked with the petroleum industry as its primary source of raw materials. These circumstances hinting the necessity for transforming the orthodox reaction concepts to the environmental benign processes have paved the way for sustainable chemistry. Citizens in the EU are being made increasingly aware of the need for sustainable development. Since recent years, many industrial sectors have understood the importance of sustainable development and become responsive for running their business using a new perspective [17].

The United Nations Commission on Environment and Development in 1987 came with the ideology of sustainable development as "*Meeting the needs of the present generation without endangering the possibilities of future generations to meet their own needs*" [18].

If sustainability is the ultimate objective, then the vital tool to accomplish it is green chemistry. The term "green chemistry" was coined in the early 1990's by Paul Anastas and John Warner [19] of the U.S. Environmental Protection Agency as "*To promote innovative chemical technologies that reduces or eliminates the use or generation of hazardous substances in the design, manufacture, and application of chemical products*".

This concept is embodied in the twelve principles, which could be paraphrased as:

- Waste prevention instead of remediation
- Atom efficiency
- Less hazardous/toxic chemicals
- Safer products by design
- Innocuous solvents and auxiliaries

- Energy efficient by design
- Preferably renewable raw materials
- Shorter syntheses route (avoid derivatization)
- Catalytic rather than stoichiometric reagents
- Design products for degradation
- Analytical methodologies for pollution prevention
- Inherently safer processes

The industry and academia have widely accepted the above doctrine of green chemistry. The replacements of outdated processes using stoichiometric reagents with greener catalytic alternatives have led to significant minimization in waste generation. The step further in achieving sustainable chemical industry will be the one in which the renewable raw materials would be deployed for the synthesis of chemicals. The final point is particularly pertinent when we discuss sustainable development. If a product is substituted for a more 'sustainable' and 'environmental friendly' alternative, the introduced product must not have an inferior technical performance. This is an equally key point that the utilization of renewable materials cannot be considered an appropriate substitute if the technical performance of the products generated from renewable raw materials is poor than for materials derived from fossil fuels. Regardless of the pressing need, merely utilizing a renewable feedstock does not automatically constitute a greener process. If the synthesis of the desired end product still remains energy intensive, wasteful and/or dangerous, then the process cannot be considered green and sustainable even if it has a feedstock based on a renewable resource [20].

2.2. Biodiesel

Sir Rudolf Diesel invented the diesel engine from a thermodynamic viewpoint. The first documented use of a vegetable oil as fuel for a diesel engine occurred at the Paris World Exposition in 1900, when peanut oil was used to power one of the diesel engines exhibited by the French Otto Company [21]. On April 1, 1935, a commission on fuels was established in the Belgian Department of Colonies in order to study systematically the production and use of fuels obtained from local products. This resulted in the first documentation on biodiesel as the Belgian patent 422877 was awarded to C. G. Chavanne on August 31, 1937 at the University of Brussels.

Right through 1940s, several reports on the use of vegetable oils to provide European tropical colonies with a certain degree of self-sufficiency have been reported [21, 22]. However, the full exploration of biodiesel only came into light in the 1980s as a result of renewed interest in renewable energy sources for reducing greenhouse gas emissions and alleviating the depletion of fossil fuel reserves [23]. Biodiesel is the colloquial name for "fatty acid alkyl esters" (FAAEs). According to the American Society for Testing and Materials (ASTM), "*Biodiesel is defined as the monoalkyl esters derivative from lipid feedstocks, such as vegetable oils or animal fats"* [24]. Biodiesel has been recognized as a potential alternative or additive to the conventional petroleum diesel because of the following characteristics:

- It has both physical and fuel properties adjacent to those of petroleum diesel, and therefore, can be directly used in a diesel engine with no or little engine modifications [25-27].
- It is renewable, biodegradable, environmentally less toxic, and has good combustion efficiency [25-27].
- Its combustion has negligible impact on the greenhouse effect because the generated carbon dioxide would be recycled through the photosynthesis process [28].
- It presents higher flashpoint, better lubricating efficiency, low sulfur concentration, and superior cetane number, when compared to that of petroleum diesel [28, 29].
- Its higher flashpoint of 423 K, in contrast to 337 K of petroleum diesel, make it easy to handle and safe to store [9, 29].
- The presence of more than 10 % oxygen in biodiesel would accelerate the rate of fuel combustion and minimize the generation of pollutants, such as particulate matter, carbon monoxide, and polycyclic aromatic hydrocarbons [30].

However, the prime drawback of the use of biodiesel is that the temperature within the engine cylinders is raised due to the enhanced fuel combustion. This amplified temperature stimulates the production of nitrogen oxide gas, which in comparison is higher than that produced from the conventional diesel fuel [31]. The heating value of biodiesel and its parent oils is approximately 10% less than those of petroleum based diesel fuel on a similar mass basis. The overall physical and fuel properties of this oxygenated biofuel, however, are dependent on the nature of lipid biomass [25].

2.3. Lipid biomass

In current scenarios, the price of plant oils accounts for about 60–80% of the total production cost of biodiesel [32, 33]. The requirement of edible plant oils has been increasing abruptly in the last few decades for two prime industrial reasons: first for the food industries, and second being its use as a biodiesel feedstock. Generally, edible oils are used for biodiesel production; like rapeseed (canola) in northern Europe, soybean in the United States of America and Argentina, coconut and sunflower oil in tropical regions [34, 35]. Around 95 % of the world total biodiesel is produced from approximately 84, 13, and 3 % amount of rapeseed, sunflower, and palm oil, respectively [36]. Since recent few years, consistent scientific efforts are underway in finding a non-edible source of oil-rich biomass for the synthesis of fuel and chemicals. This is because the use of edible oil for biodiesel production result in the rise of food prices, deforestation, and biodiversity threatening concerns in some developing nations around the world [35, 37]. Non-edible lipid feedstocks, such as *jatropha curcas, pongamia pinnata, and madhuca indica* oil are utilized for biodiesel production in India [29]. Different types of lipid feedstocks, along with their botanical name and seed oil content, tested for biodiesel production are categorically tabulated in **Paper I**. Furthermore, the fatty acid composition of edible and non-edible plant oils are also listed in **Paper I**. There are two kinds of fatty acids: the saturated fatty acids containing a single carbon bond and the unsaturated fatty acids, which includes one or more carbon-carbon double bonds. The most common fatty acids found in plant oils are palmitic acid (16:0), stearic acid (18:0), oleic acid (18:1), linoleic acid (18:2), and linolenic acid (18:3). The other fatty acids present in some oils are myristic acid (14:0), palmitoleic acid (16:1), arachidic acid (20:0), and erucic acid (22:1). Other than fatty acids, phospholipids, carotenes, tocopherols, sulphur compounds, and water constitute the chemical composition of the plant oils [25, 38, 39]. The following write-up provides a description of feedstocks utilized for biochemical production in the present thesis.

2.3.1. Jojoba oil

Jojoba plants, botanically known as *Simmonsdia Chinensis*, is native to the Sonoran and Mohave deserts of Arizona, Mexico, and southern California; these days also cultivated in several Middle East and Latin American nations [40, 41]. The agriculture of jojoba plants is both profitable and trouble-free because it grows strong in soil even of marginal fertility, resists

soil alkalinity, requires less water, needs less maintenance, survive in temperature of up to 45 ^{o}C, and has a long life span [42]. Jojoba seeds constituents for approximately 40-50 wt. % oil on dry basis [40, 43]. The world total production of jojoba seeds from the year 2006 to 2014 is shown in Figure 2.1.

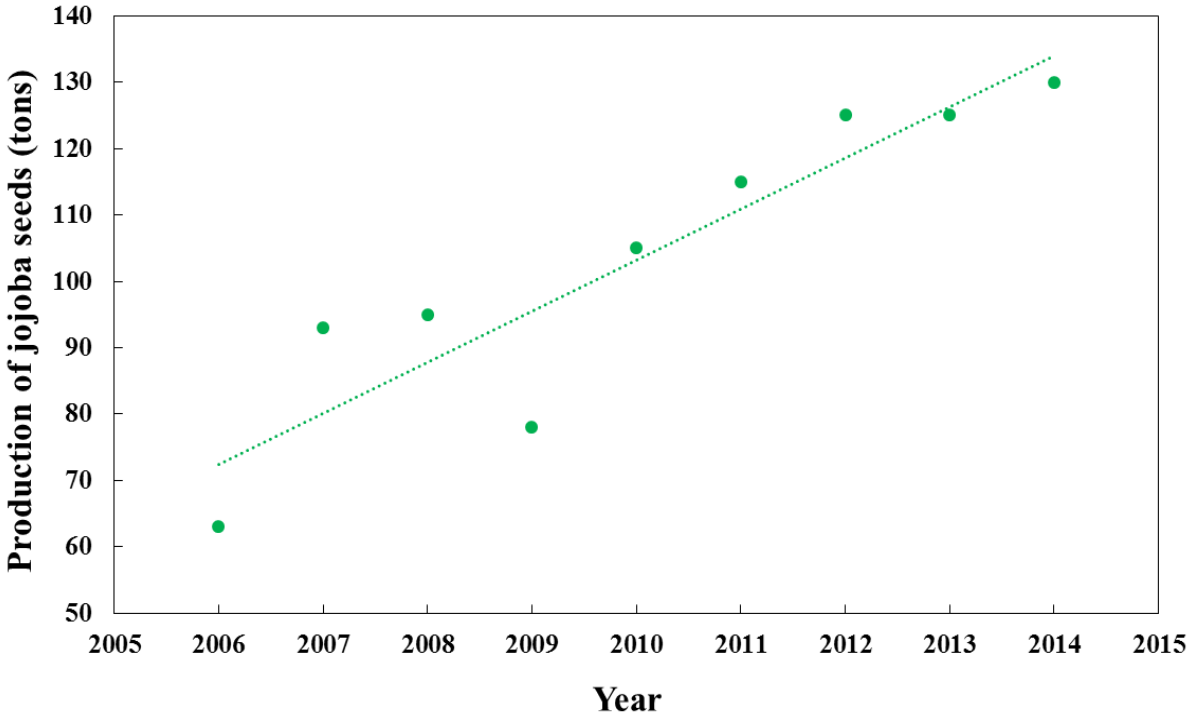

Figure 2.1: World total production of jojoba seeds [44].

Jojoba oil is a light golden color fluid that differs profoundly from other seed oils because of the absence of the glycerol molecules. The chemical structure of the same could be explained as a mixture of esters of straight long-chain fatty acids and fatty alcohols [40]. The chemical structure of jojoba oil is presented in Figure 2.2.

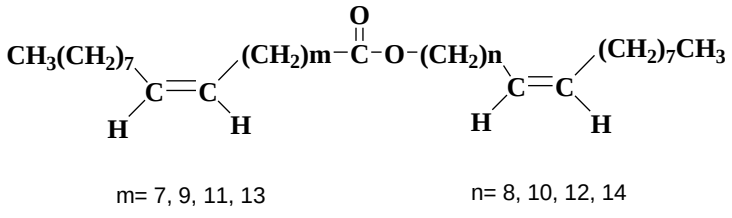

Figure 2.2: Chemical structure of jojoba oil.

The available reports indicate that jojoba oil is not poisonous to human, but is poorly digestible and is not considered a part of the human food chain; hence, is categorized as the non-edible oil [45]. Nevertheless, jojoba oil and its derivatives find their valuable importance in different

sectors of industries. The alcoholysis process would enable the transformation of jojoba oil to FAAEs and jojobyl alcohols (11-eicosenol, 13-docosenol, and 15-tetracosenol). Jojobyl alcohols find their relevance in the pharmaceuticals, cosmetic, and coating industry [40, 43, 46], while, FAAEs could be utilized as biofuel in the high-speed machinery. Additionally, the leftover solid residue obtained after the extraction of jojoba oil have a heating value higher than 13 MJ kg^{-1} and could be used for direct combustion or as a substrate for the biogasification process [42, 47]. The environmental as well as economic benefits gained through the appropriate utilization of jojobyl alcohols, FAAEs and jojoba leftover could lead to a successful jojoba based biorefinery [41, 48] and encourage the expansion of agriculture of jojoba plant. From the above-discussed points, it is considered that jojoba based biomass is a potential renewable energy resource.

2.3.2. *Jatropha curcas* oil

Jatropha curcas oil is one of the most promising feedstocks for biodiesel production. *Jatropha curcas* is a small tree or large shrub belonging to the Euphoribiaceae family. The name '*jatropha*' derives from Greek words '*jatros'* (meaning physician) and '*trophe'* (meaning nutrition) as it has several medicinal values [32]. However, oil derived from *jatropha* is non-edible due to the presence of two toxic components, named curcin and phorbol esters, in the seeds [49, 50]. The *jatropha* plants grows naturally in tropical and sub-tropical regions in Asia and Africa. This plant is well adapted to arid and semi-arid conditions, and can grow on the non-cultivated and degraded wasteland [34, 37]. Because of the leaf shedding activity, *jatropha* plant becomes highly adaptable in harsh environment because the decomposition of the shed leaves would provide nutrients for the shrub [32]. The cultivation of this plant in wastelands would help the soil to regain its nutrients and will be able to assist in carbon restoration and sequestration. This plant bears fruit starting on the second year of its plantation, the economic yield stabilizes from fifth year, and live up to 50 years [37]. Depending on the variety, oil content ranges from 35 to 40 % in seed and 50 to 60 % in kernel, with oleic acid (C18:1) and linoleic acid (C18:2) as its major fatty acids. Since, *jatropha* oil consists mainly of oleic and linoleic acid, the biodiesel produced has good low temperature properties [50]. Apart from being one of the potential feedstocks for biodiesel production, *jatropha* oil has other applications, such as producing soap and biocides [49].

2.3.3. Hass avocado seeds

According to the statistics division of the Food and Agriculture organization of the United Nations [44], the world total production of avocado fruit from the year 1993 until 2013 was augmented by 58.30 %; the aggregate production of fruit being 4.71 million tons in the year 2013. The world total production of Hass avocado fruit from the year 2006 to 2013 is shown in Figure 2.3.

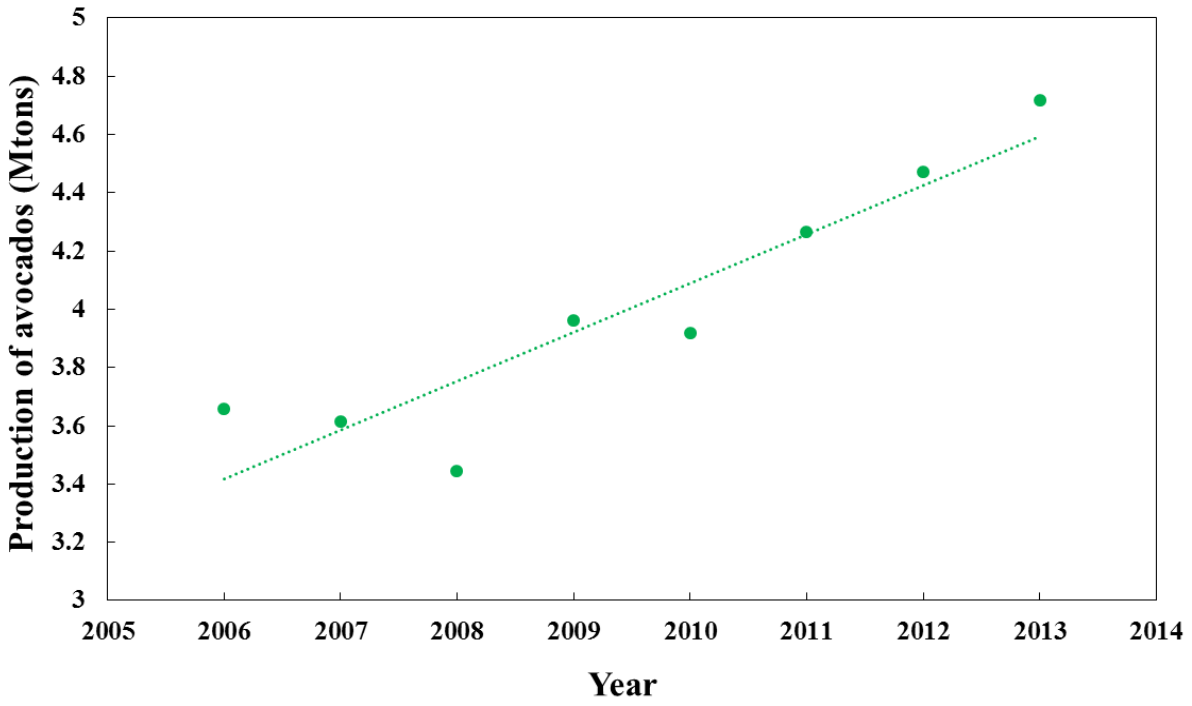

Figure 2.3: World total production of avocado fruit [44].

The consistent rise in agriculture of avocado fruit is attributed to its increasing requirement as a consequence of numerous benefits of the same on human health [51]. The presence of micro- and macro-nutrients, such as minerals, dietary fibers, proteins, lipids, vitamins, and phytochemicals in the fruit pulp is the prime reason for the consistent rise in its requirement. Among the different varieties of avocado fruit, Hass variety is commonly grown because of its longer shelf life and demand in foreign markets. The augmenting demand for such a nutrient dense fruit has resulted in the growth of export business. Mexico is the top producer of Hass avocado fruits. According to the report published by the USDA Foreign Agricultural Service in November 2014, Mexico has been exporting avocados to 21 countries; the nations which are the top importers of avocado fruit include, the United States, Japan, Canada, and Costa Rica [52]. It is however important to note that only the pulp of the fruit is consumed; the seed of

Hass avocado, which constituents on an average 13 % of the total weight of the fresh fruit, is considered as an agricultural waste and is discarded with no further application. Therefore, it could be estimated that in the year 2013 alone, approximately 613 thousand tonnes of avocado seeds were treated as a waste material. The average share of the pulp, skin, and seed in Hass avocado fruit is presented in Figure 2.4.

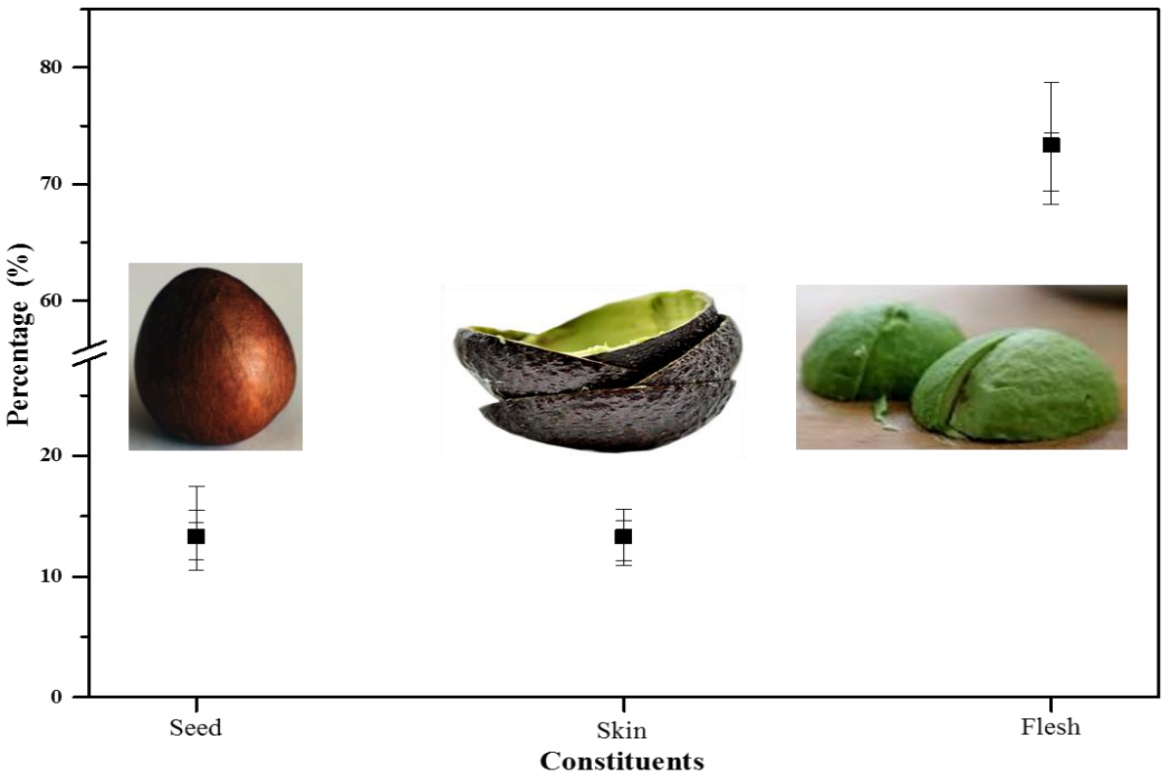

Figure 2.4: Constituents of Hass avocado fruit [53].

In addition, there are reports suggesting that avocado plant leaves and, fruit seed and skin are all potentially poisonous to animals and cannot be served as food because of the presence of substance named persin. The consumption of avocado waste by animals could trigger several hazardous effects, such as fluid accumulation around the heart, difficulty in breathing, and even death due to oxygen deprivation. The natural orange pigments reside in Hass avocado seeds, which can be extracted in the presence of water and utilize in the food and the cosmetics industries [54]. Furthermore, the polyphenolic components are also present in Hass avocado seeds and can possibly be extracted [55]. The research articles focused on the availability of the starch compounds in avocado seeds are also available [56, 57]. The carbon material synthesized from avocado seeds holds the capability to be served as an adsorbent for the treatment of the aquatic systems [58, 59]. In addition, few reports also indicated the existence of lipid

components in avocado seeds, which depending on the physico-chemical properties could be utilized as combustible oil, or be transformed to biofuel [60, 61]. In the present thesis, Hass avocado seeds were applied for the reactive extraction methodology for the generation of combustible biofuel.

2.4. Biodiesel production

The direct use of peanut oil in a diesel engine was recognized to be the first step towards the invention of plant oils based renewable biofuel. Plant oils can be used as direct fuel for the combustion engine, but their viscosity is much higher than that of common petroleum diesel fuel. The kinematic viscosity of plant oils fluctuates around 10–17 times higher than that of petroleum diesel. A long-term use of plant oils as a fuel in the diesel engine could cause severe problems, such as thickening and gelling of the lubricating oil, and ring sticking; thus, resulting in incomplete combustion of fuel, and increasing the exhaust smoke level [62, 63]. Therefore, plant oils are converted to biodiesel (FAAEs). During the transformation, the glycerol backbone of triacylglycerols (TAGs) is required to be stripped off. The resulting FAAEs has been responsible for a significant reduction in the kinematic viscosity compared to its parent oils. The conversion of TAGs into fatty acid methyl esters (FAMEs) or fatty acid ethyl esters (FAEEs) reduces the molecular weight to one third of that of the TAGs, and reduces the kinematic viscosity by a factor of about eight [64].

The methodologies employed for transforming plant oils to biodiesel include: thermal cracking (pyrolysis), micro-emulsion, and the alcoholysis process [36, 65]. A brief overview of the above-mentioned methodologies applied for biodiesel production are presented in **Paper I**. Among different possible routes, the alcoholysis process is well known and most frequently performed for the conversion of plant oils to biodiesel [66, 67]. The alcoholysis process is also known as transesterification of TAGs and/or esterification of fatty acids. The transesterification reaction has been gaining ever-increasing attention not only in the biodiesel industry but also in the polymer, paint, detergent, and pharmaceutical industries for the generation of intermediates [68-70]. In a TAGs based plant oils, three long chain fatty acids are attached to a glycerol structure. During the transesterification reaction, the fatty acid chains are released from the glycerol skeleton to interact with an alcohol to produce biodiesel and the byproduct, glycerol. In a stoichiometric transesterification reaction, one TAGs molecule reacts with three

alcohol molecules to produce three molecules of FAAEs and a single molecule of glycerol. This process consists of three sequential reversible reactions wherein TAGs is converted stepwise to diacylglycerols (DAGs), monoacylglycerols (MAGs), and finally to glycerol, accompanied with the generation of esters during each step. A general reaction and a sequence for the transesterification process is shown in Figure 2.5 and Figure 2.6, respectively.

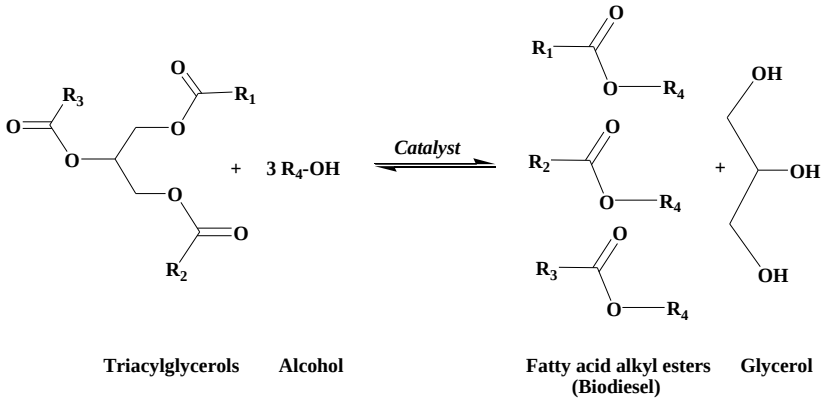

Figure 2.5: General transesterification reaction of TAGs based plant oils.

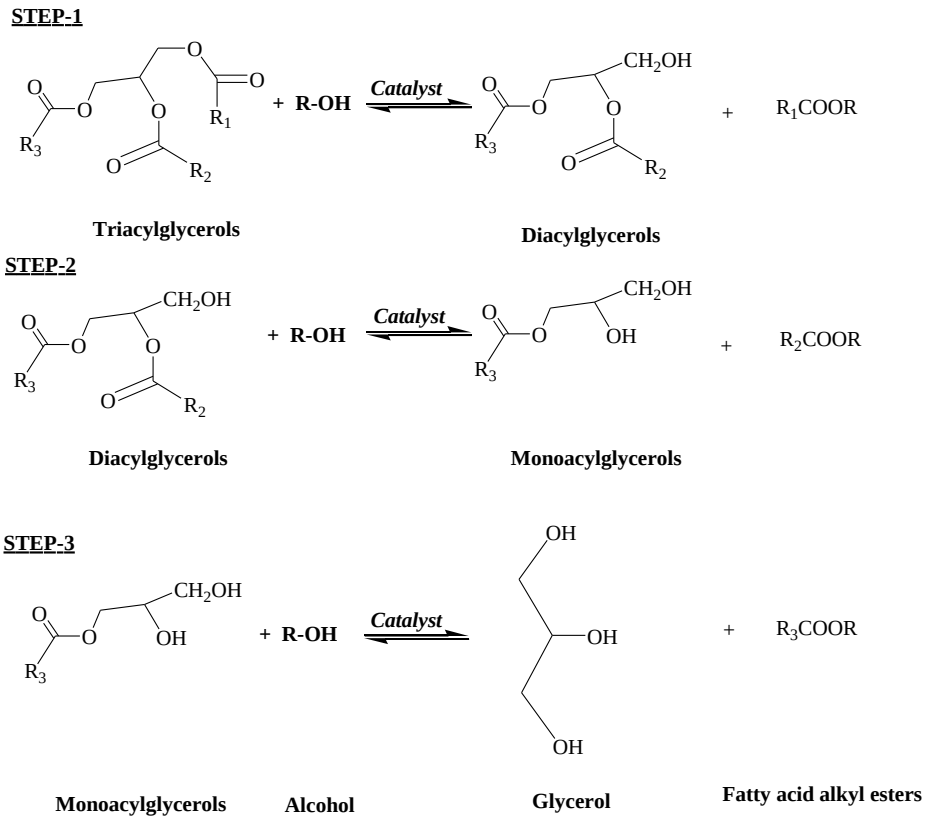

Figure 2.6: Stepwise transesterification reaction of TAGs based plant oils.

The transesterification reaction of non-TAGs based plant oil, such as jojoba oil, is a single step process, in which a molecule of jojoba oil reacts with an alcohol to produce a molecule of fatty acid alcohols and a molecule of FAAEs. A general schematic representation for the transesterification reaction of jojoba oil is presented in Figure 2.7.

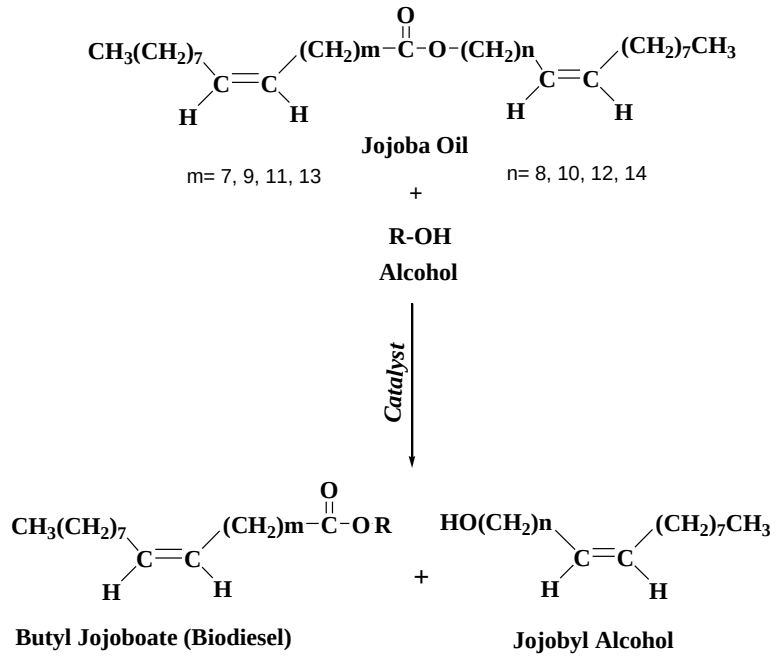

Figure 2.7: General transesterification reaction of non-TAGs based plant oils.

The esterification is a single step process, in which a molecule of FFAs reacts with a molecule of alcohol to yield a single molecule of biodiesel and water. A general reaction for the esterification process is shown in Figure 2.8.

Figure 2.8: Esterification reaction of fatty acids.

Both transesterification and esterification reactions are reversible processes, and therefore, an excess of alcohol is usually required to shift the reaction equilibrium towards the formation of products. The types of alcohol that could be used for the alcoholysis reactions include short chain, long chain, and cyclic alcohols; however, methanol and ethanol are widely utilized because of their superior reactivity, polarity, availability, and low cost [71].

In general, a catalytic material is employed to accelerate the alcoholysis process. The catalysts applied for the alcoholysis reaction can be classified as homogeneous or heterogeneous catalysts; which further could be subdivided into three categories: acid, base, and acid-base bi-functional catalysts.

2.5. Catalysis

The term 'Catalysis', a Greek word implying 'loosen' and 'down', was coined by Berzelius in 1836 when he observed that chemical reactions occurred by the catalytic contact [72, 73]. Lemoine in 1877 explained for the first time that a catalyst cannot influence the position of the equilibrium; it can only alter the rate at which it can be reached. Later in 1895, Ostwald proposed a definition, which stated, "*a catalyst accelerates a chemical reaction without affecting the position of the equilibrium*" [74, 75]. Catalysis is important to the development of environmentally benign and sustainable processes, and a corner stone to the concept of green chemistry. It plays an important role in the development of green, efficient, and economical industrial processes for the production of chemicals, drug intermediates, and fuels. The accomplishments of any chemical plant would depend on the catalyst technology it uses. Therefore, catalysis became the backbone to the chemical industry contributing substantially to our societal needs and wealth. The continuous discovery of novel catalytic processes is leading to major innovations in chemical processing. Areas of the industry where homogeneous catalysts are used include: Hydroformylation (Rhodium and Cobalt based catalysts), Hydrocyanation in DuPont (Nickel based catalyst), Metochlor in Novartis (sulfuric acid, Iridium based catalyst), Glycidol (diethyl tartrate), amongst others [76]. While, the sectors of the industry where heterogeneous catalysts are used include: Hydrogenation (Zinc and Copper based catalysts, Raney Nickel), Oxidation reaction (Vanadium and Silver based catalysts), Alkylation (Silica supported phosphoric acid catalyst), Olefin reactions (supported Chromium oxide catalysts), amongst others [77].

2.5.1. Homogeneous catalysis for biodiesel production

The ability of homogeneous catalysts to promote the production of biodiesel in a short reaction time using mild reaction conditions have resulted in its widespread utilization. The base-catalyzed transesterification reactions are faster than the one catalyzed by acidic materials. The most commonly applied homogeneous base catalysts for biodiesel production are hydroxides

and alkoxides of alkali metals, such as sodium hydroxide (NaOH), potassium hydroxide (KOH), sodium methoxide (CH_3ONa), potassium methoxide (KCH_3O), and sodium ethoxide (C_2H_5ONa), as these catalysts are soluble in polar reactants. However, KOH and NaOH catalyst are frequently utilized for the industrial production of biodiesel due to several reasons, such as (i) low cost and easy availability, (ii) ability to catalyze the transesterification reaction at relative low operative temperature, and (iii) high biodiesel yield could be obtained in short reaction time [78, 79]. However, it is worth noting that these basic homogeneous catalysts face a variety of technical hurdles that limit their use for biodiesel production. For instance, the usage of such catalysts is restricted only for refined oils (containing less than 0.5 wt. % FFAs or acid value less than 1 mg KOH g^{-1}) and under anhydrous conditions [80]. The inexpensive feedstocks containing high concentration of FFAs and moisture are known to cause a detrimental effect on the catalytic performance of homogeneous base catalysts. The base catalysts are not suitable for such raw materials because of the occurrence of inevitable saponification reaction between the catalyst and FFAs. The generation of soap could promote the formation of stable emulsions that prevent the separation of FAAEs from glycerol; consequently, less biodiesel yield is achieved. Hence, the additional separation and purification equipment are required, which makes biodiesel production more expensive [81]. The reaction of FFAs with base catalyst leading towards the formation of soap is shown in Figure 2.9. Furthermore, the presence of moisture in the reaction medium would hydrolyze formed alkyl esters; thus, minimizing the biodiesel yield.

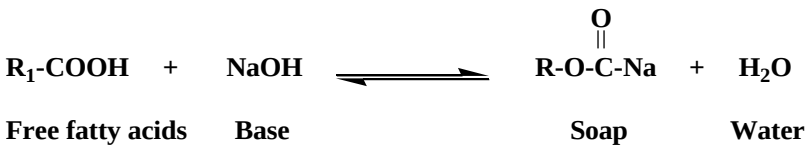

Figure 2.9: Saponification reaction of free fatty acid.

The use of acid catalysts could be a possible option to solve the above-mentioned drawbacks associated with the usage of low-grade raw materials for biodiesel production. Though acid-catalyzed transesterification reaction is slower than the homogeneous base-catalyzed one, it is worth understanding that the performance of these catalysts is not strongly affected by the presence of FFAs in the feedstocks. Furthermore, acid catalysts can simultaneously assist both transesterification and esterification reaction of TAGs and FFAs, respectively. Hence, acid

catalysts are expected to be successfully utilized for the synthesis of biodiesel from low-grade feedstocks, such as waste cooking oil, industrial waste oils, animal fats, wax, and grease. However, the requirement of severe reaction operative conditions (high reaction temperature, prolonged reaction time, and high alcohol amount) to promote the reaction rate and biodiesel yield in the case of acid-catalyzed alcoholysis reactions have been a major reason of concern for its upscaling on an industrial platform [82-84]. Furthermore, the use of these acid catalysts might also lead towards complicated and costly neutralization steps, and give rise to human safety and corrosion of equipment related concerns. The leading homogeneous acid catalysts used for the alcoholysis process are sulfuric acid (H_2SO_4), and hydrochloric acid (HCl); while other homogeneous acid catalysts tested for the alcoholysis reaction include nitric acid (HNO_3), aluminium chloride ($AlCl_3$), phosphoric acid (H_3PO_4), and organic sulfonic acid [85, 86]. The performance of recently tested homogeneous base as well as acid catalysts along with the applied operating conditions are discussed in **Paper I**. Whereas, the possible reaction pathway for the homogeneous base-catalyzed as well as acid-catalyzed alcoholysis reaction is shown in **Paper II**. Homogeneous catalysts generally are miscible in the reaction mixture, and therefore are difficult to be removed and recycled. Hence, serious scientific efforts are engaged in finding stable and active heterogeneous catalysts that would not lixiviate into the alcoholysis reaction mixture.

2.5.2. Heterogeneous catalysis for biodiesel production

Heterogeneous catalysis is the pillar of modern chemical technology. The technical problems related to the utilization of homogeneous catalysts for biodiesel production is anticipated to be minimized by its replacement with a heterogeneous catalytic system. The concentration of metals or other elements arising from the catalyst in the obtained biodiesel, or glycerol, could be notably reduced when solid catalysts are utilized. A successful application of heterogeneous catalyst is expected to quench multiple separation and purification steps, and decrease the amount of post-treatment wastewater and other contaminants; thus, downsizing the processing equipment, and empowering a continuous biodiesel production. The process intensification of biodiesel production by heterogenizing the reaction is expected to improve the economics of the process only if the catalyst is neither consumed nor dissolved in the reaction medium, which in return would facilitate its separation from the post-reaction mixture [11, 87]. A broad range

of heterogeneous catalytic materials have been lately researched for biodiesel production; the performance of those to assist the alcoholysis reaction under different operating conditions, along with their synthesis route and the physico-chemical properties are systematically reviewed in **Paper I** and **II**.

The heterogeneously-catalyzed alcoholysis reaction is carried out on the surface of the catalyst, depending heavily on the interconnected system of large pores, strength, and porosity; while, the reaction controlling step could be the adsorption, surface reaction or the desorption step. The prime drawbacks of the solid catalysts is their limited catalytic active centers in comparison to their homogeneous counterparts and, in general, severe operating conditions are required to achieve oil conversion similar to that obtained by the homogenous-catalyzed processes [88]. Also, the mass transfer concern associated with the use heterogeneous catalyst due to the presence of three phases (oil/alcohol/catalyst) in most of the reaction systems could be allied to the slower reaction rate for the transformation of lipid feedstock to biodiesel [89]. It is also worth noting that the complicated and time consuming synthesis procedure, and high price of materials required for the synthesis of heterogeneous catalysts might also contribute to the total cost of the process; hence, making biodiesel more expensive. Furthermore, the poisoning of the active centers of catalysts when exposed to the surrounding atmospheric medium could also affect the stability and activity of catalysts; in this case, having the detail information about to the physical and chemical properties of solid materials become mandatory.

2.5.3. Calcium oxide

A wide range of heterogeneous base materials have been tested to catalyze the alcoholysis reactions, such as CaO [90-92], magnesium oxide [93-95], strontium oxide [91, 92, 96], barium oxide [92, 97], supported alkali metals [98-102], supported alkaline earth metals [103-105], mixed metal oxides [106-108], hydrotalcites [33, 109, 110], and anion-exchange resins [111, 112]. Among the numerous heterogeneous catalysts utilized to assist the alcoholysis reaction, CaO catalyst has been extensively researched not only because it possesses high basicity, low solubility, and superior activity but also due to its simple synthesis procedure and low cost. Another reason for its increasing popularity is the abundance of natural resources of calcium. The natural materials are inactive in their available form, but after thermal treatment, they were found to display good activity to accelerate the alcoholysis reactions. Waste natural resources,

such as crab shells [113], egg shells [113, 114], capiz shells [115], snail shells [116], oyster shells [117], amongst others, have been tested as precursors for the CaO synthesis. The appropriate utilization of these naturally available waste materials for the synthesis of CaO catalyst is expected to decrease the entire dependency on limestone rocks that are non-renewable sources of calcium carbonate ($CaCO_3$). However, the major drawback associated to the use of CaO catalyst is its deactivation when exposed to the surrounding carbon dioxide and moisture. This poisoning effect alters and blocks the active catalytic sites. The CaO based catalyst have been utilized in several forms like, neat [94, 118], mixed oxides [107, 119, 120], supported [104, 121], doped [122, 123], amongst others [124, 125]. Apart from the above-mentioned CaO based catalysts, the catalytic activity of glycerol-CaO complex, characterized as calcium diglyceroxide (CaDg), for the alcoholysis reaction have been also investigated [126-130]. León-Reina et al. [131] described CaDg as a set of molecular calcium tetramers interlinked by H-bonds, and reported its superior catalytic activity for the alcoholysis reaction when compared with CaO catalyst. The superior activity of CaDg catalyst was because of availability of basic oxygen anion after the interruption of the crystal structure at the surface, which can abstract proton from OH group of methanol leading towards the formation of surface methoxide ion. The recent studies have reported that CaO experiences material transformation during the progression of the alcoholysis of TAGs based plant oils, due to its reaction with the generated glycerol. The initial stage of the alcoholysis reaction is catalyzed by the CaO phase of the catalyst, after which the material reacts with the co-generated glycerol and is transformed to CaDg. CaDg material was characterized as weakly basic in nature and chemically stable. Because CaDg displayed superior catalytic activity than CaO for the alcoholysis reaction, and is not prone for deactivation due to the surrounding air and moisture, it was recommended to transform CaO to CaDg compounds before applying for the alcoholysis process [132, 133].

2.6. Catalyst characterization

The characterization of the catalysts helps to understand their properties, so that materials can be designed or improved to meet the desired requirements. The following write-up provides a brief account of the theory and principles of the characterization techniques used for the current study. In the present thesis, the catalyst characterization was limited to X-ray diffraction and thermal analysis to investigate only the chemical and thermal properties of the materials, respectively.

2.6.1. X-ray diffraction

X-Ray diffraction (XRD) is one of the fundamental techniques employed for catalyst characterization. It has been an important technique for determining the structure of materials characterized by long-range order. It is used to identify crystalline phase(s) of catalysts by means of lattice structural parameters and crystallinity [134]. X-rays are highly intrusive electromagnetic radiations, which are electrically neutral. Their frequency lies between the ultra-violet (UV) and gamma radiations, and their wavelength (λ) range from approximately 0.04 to 1000 Å. For diffraction applications, X-rays with only shorter wavelengths ranging from few Å to 0.1 Å (1- 12keV) are used because these are comparable to the size of the atoms. Therefore, the X-rays are ideally suited for deducing the structural arrangement of atoms and molecules for various materials. The diffraction method involves the interaction between the incident monochromatized X-rays (like Cu Kα or Mo Kα source) with the atoms of a periodic lattice.

X-rays scattered by atoms in an ordered lattice interfere constructively as per Bragg's law [135]:

$$n\lambda = 2d \sin\theta;\ n = 1, 2, 3,\ldots \tag{2.1}$$

where, λ is the wavelength of the X-rays, d is the distance between two lattice planes, θ is the angle between the incoming X-rays and the normal to the reflecting lattice plane, and n is the integer called order of the reflection.

By measuring the angle 2θ, under which constructively interfering X-rays leave the crystal, the Bragg's equation gives the corresponding lattice spacing, which is characteristic for a particular compound. Width of the diffraction peaks signifies the dimension of the reflecting planes. It is known that the width of a diffraction peak increases when the crystallite size is reduced below a certain limit (< 100 nm). Therefore, XRD patterns can be used to estimate the average crystallite size of very small crystallites using XRD line broadening by applying the Scherrer formula [136]:

$$t = 0.9\lambda / \beta\text{Cos}\,\theta \tag{2.2}$$

where, t is the thickness of the crystallites (in Å), λ is the wavelength of X-rays, θ is the diffraction angle and β is the full width at half maxima of the diffraction peak.

2.6.2. Thermal analysis

Thermo analytical techniques involve the measurements of the response of a solid under study (energy or mass released or consumed) as a function of temperature (or time), when it is heated in a programmed method. Thermogravimetry (TG) is a technique that measures the change in mass of a material as a function of temperature and time, in a controlled manner. This variation in mass can be either a loss of mass (vapor emission) or a gain of mass (gas fixation). It is ideally used to assess volatile content, thermal stability, degradation characteristics, aging/lifetime breakdown, sintering behavior, and the reaction kinetics [137].

2.7. Process integration: reactive extraction methodology

The processing of oil-rich biomass involves various stages, such as the oil extraction, purification, degumming, deacidification, and dewaxing, before it can be transesterified/esterified into FAAEs [138]. The oil extraction process typically includes a physical method, such as screw press extraction, or a chemical method, such as solvent extraction using hexane. However, the solvent extraction procedure is expensive, complex, and poses health as well as safety hazard due to handling of flammable and explosive solvent. On the other hand, mechanical pressing often yields less oil than the solvent extraction because of high residual oil remaining in the leftover biomass [139]. In an attempt to cut down the processing steps and use of multiple solvents, the integration of extraction and alcoholysis has been recently developed, which is known as the reactive extraction methodology (REM). It is a process in which the extraction and the transesterification/esterification proceed simultaneously in a single step. The uniqueness of the current methodology is that alcohol acts as both an extraction solvent and alcoholysis reagent. The REM differs from the conventional biodiesel production process in which the oil-bearing material contacts with alcohol directly instead of reacting with pre-extracted oil. The addition of catalyst to the process is anticipated to accelerate the transformation of oil to biodiesel and also minimize the need of high energy for the biodiesel production process [140]. Moreover, the use of solid lipid biomass rather than refined oil could certainly reduce the feedstock cost. Few available reports have pointed out that this process provides higher extraction efficiency and subsequently lead to higher biodiesel yield than those obtained from the conventional reaction [141-143]. This could be possible because the lipid biomass consisting of polar components (phospholipids) can be extracted by

the alcohol during the REM, which is not possible by the conventional methods [139]. Therefore, the integration of extraction and alcoholysis of lipid to produce biodiesel attracts attention from an engineering perspective. However, it is worth noting that the reactive extraction product yield could be different for different biological materials, because the extraction efficiency is heavily influenced by the seed sample matrix, the molecular structure and size of the solute, and the presence of other components [144]. A higher amount of alcohol is required for the REM process, when compared to that used for the conventional alcoholysis reactions. Furthermore, though the REM eliminates the requirement of two independent processes, the separation of residue, catalyst, and products remains one area of concern. Lian et al. [145] reported a study concluding that the separation of the biomass leftover, catalyst, and products is possible with the use of integrated apparatus consisting of separate chambers for the catalyst, which is placed underneath the lipid biomass holder, while the alcohol flows through different chambers.

2.8. Product analysis

Biodiesel is produced from plant oils of varying origin and value. Therefore, determining the fuel quality is of high relevance to guarantee the engine performance without any difficulties and ensure its successful commercialization. The utilization of low-quality biodiesel or the presence of contaminants in this biofuel could cause several engine problems. In order to protect consumers from unknowingly purchasing substandard fuel, several strict guidelines for the quality of biodiesel are set in various countries that needs to be fulfilled before its introduction into the market. The mostly referred specifications include the ASTM D6751 or EN 14214 standards for biodiesel. There are also some other standards available globally, such as American Oil Chemists' Society (AOCS), Germany (DIN 51606), Austria (ON), and Czech Republic (CSN) [36, 67].

2.8.1. Kinematic viscosity

The kinematic viscosity refers to the degree of fluidity, and is determined by measuring the amount of time taken for a given measure of liquid to pass through an orifice of a specified size [37]. The kinematic viscosity of biodiesel must not be greater than 6 and 5 mm^2s^{-1} according to the ASTM D445 and EN 3104 specifications respectively, because higher values of viscosity

gives rise to poor fuel atomization, incomplete combustion, and carbon deposition on the injector [146].

2.8.2. Cloud point and Pour point

Since the kinematic viscosity of diesel fuel is a strong function of temperature and usually increases at lower temperatures, operating engines at cold climate regions is often challenging, and therefore, the low temperature flow properties of fuel must be monitored closely. This is because even a partial solidification of biodiesel may cause blockage of the fuel lines and filters, problems in starting, and engine damage due to inadequate lubrication. These properties can be examined by cloud point (CP), and pour point (PP). The CP is defined as the temperature at which a cloud of wax crystals first appear when the fuel is cooled under controlled conditions during a standard test [29]. At temperatures below CP, crystals grow larger and agglomerate together to the point that they prevent the fluid to flow. The PP is the temperature at which the amount of wax form of a solution is sufficient to gel the fuel; thus, it is the lowest temperature at which the fuel can flow [29].

2.8.3. Cold filter plugging point

The cold filter plugging point (CFPP) is used as indicator of low temperature operability of fuels and defines the fuels limit of filterability. CFPP refers to the temperature at which the test filter starts to plug due to fuel components that have started to gel or crystallize [37].

2.8.4. Oxidation stability

Biodiesel is susceptible to oxidation, which leads to fuel degradation; therefore, the oxidation stability of biodiesel is crucially important as it determines resistance to chemical changes brought about by oxidation reaction. Oxidation stability of biodiesel depends greatly on the fatty acid composition and the degree of unsaturation. The saturated FAAEs is more stable than the unsaturated ones, while polyunsaturated FAAEs is at least twice as reactive to auto-oxidation than the monounsaturated FAAEs. For the same number of double bond per molecule, FAAEs with a longer chain or higher molecular weight would be less prone to auto-oxidation due to the lower molar concentration of double bond. In addition to the degree of unsaturation, the position at which double bonds are located in an unsaturated molecule is also an important parameter to determine the oxidation stability of biodiesel. In presence of oxygen at high

temperature, the oxidation reaction takes place and the oxidation derivatives are transferred to the measuring chamber containing Millipore water. The increase in conductivity of water is detected as the oxidation derivatives are transferred into water. The induction time is defined as the time required for the conductivity of water to be increased rapidly and is used as an indication of biodiesel oxidation stability [50]. The oxidation stability of biodiesel must be minimum 3 and 8 hour according to the ASTM D675 and EN 14112 specifications, respectively [36].

2.8.5. Iodine number and Peroxide value

The oxidation stability of biodiesel can also be evaluated by Iodine number (IN) and Peroxide value (PV). IN allows determination of the degree of unsaturation of biodiesel. The IN is determined by measuring the amount of I_2 that reacts by addition to carbon–carbon double bonds. This property greatly influences the oxidation stability and polymerization of glycerides. The major flaw of this technique as an oxidation stability indicator is that it does not take into account the positions at which double bonds are located in a molecule, which has been proven a contributing factor for autoxidation of fatty acids. According to the EN 14111 official specification, the IN must not be greater than 120 mg I_2 g^{-1}. PV of biodiesel increases when FAAEs oxidation initiates and propagates to form peroxides and hydroperoxides. PV is not a very suitable parameter for determining oxidation stability because its value drops during further degradation of hydroperoxides to form secondary oxidation derivatives [37].

2.8.6. Moisture content

Water in biodiesel reduces the heat of combustion. This means more smoke, harder starting, and less power. Water will cause corrosion of vital fuel system components, such as fuel pumps, injector pumps, and fuel tubes. Water, as it approaches 0 ºC begins to form ice crystals. These crystals provide sites of nucleation and accelerate the gelling of the residual fuel. While biodiesel is generally considered to be insoluble in water, it actually takes up considerably more amount of water than diesel fuel. Water is part of the respiration system of most microbes. Biodiesel is a great food for microbes and water is necessary for microbe respiration. The presence of water accelerates the growth of microbe colonies, which can seriously plug up a

fuel system. The standard of water content and sediment for biodiesel in ASTM D2709 and EN ISO 12937 specifications is maximum 0.05 % (vol. %) [37].

2.8.7. Acid value

The acid value (AV) measures the content of FFAs in the fuel sample. AV is a measure of the amount of carboxylic acid groups in a chemical compound, such as a fatty acid, or in a mixture of compounds. This property is specified to ensure proper ageing of the fuel. Various standards have fixed the value of this parameter in the range of 0.5–0.8 mg KOH g^{-1}. Higher acid content can cause severe corrosion in the fuel supply system and the internal combustion engine [8, 36].

3. Experimental section

This section will provide a brief overview of the materials and methodologies applied for experimental as well as theoretical investigations. **Paper I** and **II** have helped in selecting an appropriate lipid feedstocks and solid catalytic material for the alcoholysis processes in the present thesis. Both **Paper I** and **II** do not include the description of the laboratory based work because the articles were based on the literature study.

3.1. Catalyst preparation

3.1.1. Preparation of calcium oxide

The *Mytilus Galloprovincialis* (mussel) shells required for the synthesis of CaO in **Paper III-V** were obtained from one of the local fish markets in Madrid, Spain. The *M. Galloprovincialis* shells were cleaned under the flow of tap water to remove the adsorbed superfluous materials, and dried in an oven, set at 100 ºC, for 60 min. This shells were subsequently pulverized, placed in a silica crucible and calcined in a ceramic muffle heating furnace, set at 800 ºC, for 360 min. The heating furnace was shut down after 360 min of the calcination process and allowed to cool. The obtained white colored solid was removed from the furnace, preserved in an airtight container to avoid poisoning due to ambient air while handling or weighing, and utilized instantaneously for the butanolysis process (**Paper III**) and for the synthesis of CaDg (**Paper IV-V**).

3.1.2. Preparation of Calcium diglyceroxide

For the synthesis of CaDg catalyst, a measured amount of CaO and glycerol were initially added into an airtight three-neck curved bottom glass reactor. Then, an appropriate volume of crude *jatropha curcas* oil (CJCO) (**Paper IV**) or avocado oil (**Paper V**) was poured into the reactor and the mixture was vigorously stirred at 60 ºC for 60 min using 350 rpm stirring intensity under atmospheric pressure. Instead of following the reported procedures for the preparation of calcium diglyceroxide in the presence [127, 131] or absence [126, 147] of alcohol, this work presented a novel method for the preparation of CaDg in which the catalyst was synthesized in the presence of lipid feedstock.

3.1.3. Other catalysts

Commercial catalysts, such as Melamine, Amberlyst 16, Amberlyst A21, Amberlyst BD20, Dowex 50W, Dowex Marathon MR-3, and calcium oxide were applied for the initial screening of the alcoholysis of plant oils.

3.2. Experimental reactions

Jojoba oil in **Paper III** was supplied by Jojoba Israel (Kibbutz Hatzerim, Israel). Iberinco (Spain) provided the CJCO in **Paper IV**. In **Paper V**, avocado oil was purchased from Jedwards International, Inc. (Braintree, USA). The fatty acid composition and the physico-chemical properties of jojoba oil and CJCO were determined earlier, in accordance to the AOCS official methods and the ASTM methods, and the results were published elsewhere [43, 148]. The suppliers provided the fatty acid profile and some properties of avocado oil. Few properties of avocado oil we determined in the laboratory at the Department of Chemical Engineering of the Universidad Complutense Madrid, Spain. The physico-chemical properties as well as the fatty acid composition of avocado oil, CJCO, and jojoba oil used in the present thesis are tabulated in Table 3.1. The CaO-catalyzed butanolysis of jojoba oil (**Paper III**), CaDg-catalyzed methanolysis of CJCO (**Paper IV**), and CaDg catalyst assisted avocado oil ethanolysis (**Paper V**) reactions were conducted in a three-neck curved bottom glass reactor of 250 cm^3 volume capacity. Both the diameter and length of the glass reactor is equivalent to 12.0 cm. The middle neck of the reactor was used to insert the mechanical stirrer equipped with an impeller of 6.0 cm diameter placed centrically close to the bottom. One of the side necks was fitted with the water cooling condenser; while the other neck, was fitted with a rubber cork through which the aliquots of the reaction mixture were periodically withdrawn using a glass syringe. The glass reactor was immersed into a thermostatically controlled water bath (Heto-Holten A/S, Denmark), the temperature of which was controlled by a PID controller with 1 ºC precision. The speed of the mechanical stirrer was monitored by a motor (Eurostar Basic IKA). In **Paper III-V**, the catalyst was separated from the post-reaction mixture through the centrifugation process carried out at 1500 rpm for 15 min.

Table 3.1: Physico-chemical properties and fatty acid composition of plant oils [43, 148].

Parameters	Avocado oil	CJCO [148]	Jojoba oil [43]
Kinematic viscosity (cSt)	41.66	34.7	26.6
Iodine value (g I_2 100 g^{-1})	83.75	103.91	83
Moisture content (%)	0.03	0.05	0.03
Oxidation stability (h)	18.38	8.36	41.3
Acid value (%)	0.1*	24.8 (mg KOH g^{-1})	0.36
Fatty acid composition (%)			
Palmitic acid (C 16:0)	13.0*	13.0	C 34-36: 0.2
Palmitoleic acid (C 16:1)	2.1*	0.9	C 38: 6.6
Margaric acid (C 17:0)	-	0.1	C40: 30.2
Margaric oleic acid (C 17:1)	-	0.1	C 42: 50.9
Stearic acid (C 18:0)	2.5*	5.8	C 44: 9.0
Oleic acid (C 18:1)	68.9*	40.4	C 46-50: 0.9
Linoleic acid (C 18:2)	11.2*	39.0	-
Linolenic acid (C 18:3)	0.6*	0.2	-
Araquic acid (C 20:0)	-	0.2	-
Eicosenoic acid (C 20:1)	-	0.1	-
Erucic acid (C 22:1)	-	0.1	-
Lignoceric acid (C 22:2)	-	0.1	-

*- *Information provided by the suppliers.*

For the characterization purpose, high quantity of biodiesel was produced from avocado oil using a homogeneous catalyst in **Paper V**. A large-scale biodiesel production was carried out in a semi-batch 3 dm^3 capacity glass reactor, equipped with the mechanical stirrer, water condenser, distillation unit, and decantation valve. The potassium methoxide-catalyzed avocado oil ethanolysis reaction was performed at 75 ºC for 60 min, using 2 dm^3 of oil, 1 wt. % catalyst amount, ethanol-to-oil molar ratio of 6:1, and 600 rpm stirring intensity. Avocado oil was first added to the reactor, and the system temperature was raised to the desired set point. Once the system temperature was stable at the set point, potassium methoxide catalyst dissolved in ethanol was poured to the reactor. After the ethanolysis reaction, excess amount of ethanol was removed using the distillation unit attached to a vacuum pump (70 mg Hg). The glycerol phase was separated from the biodiesel one through the decantation process. The trace amount

of catalyst present in the FAEEs phase was removed using the water-washing step. The water-washing step was repeated until the pH value of the wastewater reached approximately neutral. The distillation process was repeated to eliminate the trace amount of water present in FAEEs.

3.3. Reactive extraction of Hass avocado seeds

Riped Hass avocado fruits for **Paper VI** were purchased from a local market of Norway. Before applying Hass avocado seeds for the in-situ extraction and reaction process, the seed samples were dried to eliminate water residing inside the seed. After the reactive extraction process, the heat of combustion of seed leftover was determined.

3.3.1. Moisture evaporation step

Hass avocado seeds were pulverized using a bowl-shaped mortar-pestle, while, the slicing pretreatment process was done using a stainless steel slicer. The detailed dimensions of the seed samples is presented in **Paper VI**. All the seed samples were kept in separate pyrex glass petri plates and then placed in the heating furnace (Narbetherm P300, Germany) for the drying process. To understand the rate of moisture evaporation, the seed samples were weighed on a digital balance machine having 0.01 g accuracy (Mettler-Toledo, PG 5002 Delta Range, Switzerland) at a predetermined time interval taking less than 15 seconds to weigh the samples. The drying experiments were performed for 5760 min.

3.3.2. Reactive extraction process

The in-situ extraction and alcoholysis experiments were performed in the presence or absence of CaO catalyst using two different set-ups: the experiments with the operating temperature below the boiling point of ethanol were conducted in a glass reactor (Quark; 500 cm^3 volume capacity), while those with higher than the boiling point of ethanol were performed in a Parr autoclave (Parr instrument company, USA; 500 cm^3 volume capacity) batch reactor. The autoclave temperature is regulated using PID controller with 1 ºC precision. Two different chillers were used to control the temperature of the autoclave and for the protection of rotator placed above the autoclave. The dried powder of Hass avocado seeds and a measured volume of ethanol were initially added to the reactor. The experiments in the glass reactor were performed at 75 ºC for 330 min using 500 rpm stirring intensity at an atmospheric pressure condition. The internal diameter of the glass reactor and the length of the magnetic stirrer was

10 and 5 cm, respectively. A water condenser was attached to one of the side necks of the glass reactor, while a rubber cork was fitted to the other side neck through which the aliquots of the reaction mixture were periodically removed using a plastic syringe. The effects of different temperatures and pressures on the reactive extraction process of Hass avocado seeds was studied in a Parr autoclave reactor. The experiments were performed at different temperatures (75, 150, 225 ºC), at the respective system pressures, for 330 min using 500 rpm stirring intensity. The internal diameter of the autoclave was 8.2 cm; while, the mechanical stirrer was equipped with dual impellers of 4.5 cm individually. The aliquots of the reaction mixture were periodically withdrawn through the valve attached to the autoclave.

3.4. Characterization

3.4.1. Catalyst characterization

The X-ray diffraction and thermal analysis of catalysts were performed at the Process and Energy Department of the Delft University of Technology, The Netherlands.

3.4.1.1. X-ray diffraction

The XRD patterns of the catalysts reported in this thesis were collected using Bruker D5005 diffractometer equipped with Huber incident-beam monochromator and Braun PSD detector. The data collection was done at room temperature using monochromatic Cu Kα1 radiation (λ= 0.154056 nm) in the 2θ region between 10 and 80°, step size 0.038° 2θ. Samples of about 20 mg were deposited on a Si ⟨510⟩ wafer and were rotated during measurement. The data evaluation was done using the Bruker program EVA.

3.4.1.2. Thermal analysis

In the present work, the TG measurements of the samples were performed with a Thermal Advantage (SDT Q600) thermogravimetric analyzer. The samples were placed in alumina crucible in amounts varying between 3 and 25 mg, and the purge flow rate was 100 ml min^{-1}. Experimental runs were performed in a nitrogen atmosphere. The TG analyses started with a temperature equilibration at 25 ºC, after which the samples were heated at a ramp rate of 5 ºC min^{-1} to 800 ºC. The residence time at 800 ºC was 20 min.

3.4.2. Biomass characterization

3.4.2.1. Microscopic imaging

The microscopic imaging of Hass avocado seeds was performed using Leica DM5000 B microscope (Leica Microsystems, Germany). Scalpel was used to cut the seed embryo to achieve a sample film of approximately 1 µm. The sliced seed samples were then immediately placed on a glass slide for staining purpose. Toluidine Blue was used as a staining agent.

3.4.2.2. Moisture analysis

The initial and equilibrium (after the drying process) moisture content in Hass avocado seeds were determined using the automated Karl Fischer (KF) volumetric system (Metrohm, Tampa, FL, USA) consisting of an oven sample unit (Model 774) for water extraction, a dosing device (Model 901) connected to two mechanical burettes (Model 80; one for titrant and other for methanol) for control of titrant, and a titration cell with electrode and stirrer (Model 801). The complete system was operated by a computer using the software Tiamo 2.3, for the data analysis. The initial and the equilibrium moisture content, in the case of the pretreated seed samples, was measured thrice and the average of the analyzed value was considered.

The moisture content in the seed samples was determined according to the following equation:

$$\text{Moisture content (\%)} = \frac{V\ (mL) \cdot 5\left(g\ L^{-1}\right) \cdot 0.1}{m\ (g)} \tag{3.1}$$

where, 5 g L^{-1} is the concentration of water equivalents in the titrant, V is the total volume of titrant consumed during the titration, and m is the initial weight of the sample.

3.4.2.3. Heat of combustion

The gross calorific value of Hass avocado seeds, before and after the reactive extraction process, was determined using a Parr 1341 plain jacket oxygen bomb calorimeter (Parr Instrument Company, USA) equipped with a stirrer and Parr model 6775 digital thermometer. The test samples were placed in a crucible of the combustion chamber. The isolated chamber of the bomb calorimeter was filled with 20 bar oxygen for the completion of seed combustion. The combustion chamber is immersed in a vessel having 2000 ml water. A mechanical stirrer was introduced to ensure uniform system temperature throughout the water container. By means

of an ignition wire, the seed samples were ignited; successively, the rise in temperature due to the combustion was measured as the water around the chamber is heated. The ignition wire is weighed before and after the ignition. The calorific value was measured thrice and the average of the analyzed value was considered.

The calorific value of the seed samples (E_s) was determined using the following equation:

$$E_s = \frac{C \cdot \Delta T - \epsilon_w \cdot m_w}{m_s} \quad (3.2)$$

where, C is the heat capacity for the bomb calorimeter, ΔT is the temperature rise of the water, ϵ_w the calorific value for the ignition wire, m_w the mass of burned wire, and m_s is the mass of the seed sample. For the current experiments, a Parr fuse wire having ϵ_w of 1400 cal g^{-1} was used. The heat capacity (C) for the reported bomb calorimeter was calculated to be 10.21 kJ K^{-1} using benzoic acid as a standard sample (calorific value: 26.42 kJ g^{-1}).

The standard deviation for the experimental findings were calculated according to the following equation:

$$\sigma = \sqrt{\frac{1}{N}\sum_{i=1}^{N}(E_{s,i} - \overline{E_s})^2} \quad (3.3)$$

where, N is the number of measurements, $E_{s,i}$ is the individual measurements and $\overline{E_s}$ is the mean value of the measurements.

3.4.3. Product analysis

3.4.3.1. Gas chromatography

The reaction samples in **Paper III-V** were analyzed to determine the oil conversion and biodiesel yield using the gas chromatography (GC) analyzer (Hewlett-Packard HP-5890 Series II) equipped with a flame ionization detector and a fused silica capillary column (12 m length, 0.31 mm internal diameter, and 0.71 µm thickness). A Hewlett-Packard 3396SA integrator was connected to the chromatograph. The injection system was split-splitless, and helium was the carrier gas at a 1 mL min^{-1} flowrate. The injector and the detector temperature were set at 275 and 325 ºC, respectively. The GC column temperature was initially held at 130 ºC for 1 min, then raised at 2 ºC min^{-1} to 160 ºC, and finally heating at a ramp rate of 30 ºC min^{-1} to 320 ºC. n-octyl octonoate was used as an internal standard and the extracted reaction samples were

dissolved in carbon disulfide. The GC analysis was conducted by injecting 1.0 µL volume of the prepared samples into the instrument.

The plant oil conversion ($X_{plant\ oil}$) is expressed as

$$X_{plant\ oil} = \frac{Initial\ moles\ of\ TAGs - Final\ moles\ of\ TAGS}{Initial\ moles\ of\ TAGs}\ \text{x}\ 100\ \% \qquad (3.4)$$

The FAAEs yield is expressed as

$$FAAEs\ yield = \frac{Total\ moles\ of\ FAAEs}{3\ \text{x}\ Moles\ of\ plant\ oil}\ \text{x}\ 100\ \% \qquad (3.5)$$

The physical and fuel properties of biodiesel produced from avocado oil in **Paper V** were analyzed using different instruments, the details of which and the official methods followed are listed in Table 3.2.

Table 3.2: Analytical tools and official methods used for the characterization purpose.

Properties	Standards	Equipment
Kinetic viscosity	ASTM D445	Cannon-Fenske viscometer
Iodine number	AOCS Cd 1-25	Metrohm Switzerland, Model 702 SM Titrino
Peroxide	AOCS cd 8-53	Metrohm Switzerland, Model 702 SM Titrino
Moisture	EN ISO 12937	Metrohm Switzerland, Model 702 SM Titrino
Acid value	ASTM D664	Metrohm Switzerland, Model 702 SM Titrino
Oxidation stability	AOCS Cd 12b-92	Metrohm Switzerland, Model 743 Rancimat instrument
Cloud point	ASTM D 2500	ISL CPP 97-2
Pour point	ASTM D 97	ISL CPP 97-2
Cold filter plugging point	ASTM D6371	ISL CPP 97-2

3.5. Mathematical modelling

This section illustrates the procedure applied for performing the statistical analysis of the alcoholysis processes (**Paper III**-**V**), simulating the chemical kinetics of the alcoholysis reactions (**Paper III** and **V**), and modelling the drying kinetics of Hass avocado seeds (**Paper VII**).

3.5.1. Statistical analysis

In **Paper III-V**, the interactions within the reaction variables, their influence on the alcoholysis reaction, and the optimum parameters affecting the alcoholysis process were determined by means of the response surface methodology (RSM). The regression analyses was conducted by designing a set of experiments, the results of which were fitted to a two-level factorial design for the application of the RSM using the Statgraphics centurion XV software (Statpoint technologies, Inc., USA). The linear and non-linear stage of the two-level factorial design consisted of four experiments each, along with four replicates of the center points. The non-linear stage of the two-factorial design is also known as the star-points and coded as ± α. The distance between the origin and the star-points is expressed as $\alpha = 2^{n/4}$. n is the number of experimental parameters utilized for the statistical analysis (in the present studies: n = 2 and α = 1.41). The linear, center-points, and non-linear stage of the experimental design were combined to form a central composite design, and utilized to investigate the influence of alcohol-to-oil molar ratio and the catalyst loading on all three alcoholysis processes. However, a successful implementation of such method requires an appropriate selection of the independent variables, levels, and the response. For **Paper III-V**, alcohol-to-oil molar ratio and the catalyst amount were considered as the investigating factors; while, the jojoba oil conversion, CJCO conversion, and FAEEs yield was selected as the response in **Paper III**, **IV**, and **V**, respectively. The model equations were used to elucidate the interaction between the variables, and predict the optimum conditions affecting the alcoholysis processes.

3.5.2. Chemical kinetics

The curve fitting procedure for the reaction kinetics of the CaO-catalyzed jojoba oil butanolysis process (**Paper III**) and the CaDg-catalyzed avocado oil ethanolysis process (**Paper V**) was performed using Aspen custom modeler software (Version 8.4, Aspen Technology, Inc., USA).

In **Paper III**, the overall alcoholysis reaction between jojoba oil and n-butanol, in the presence of solid CaO catalyst with stoichiometry was represented as:

$$\mathrm{J} + \mathrm{B} \overset{catalyst}{\longleftrightarrow} \mathrm{JA} + \mathrm{FABEs} \tag{3.6}$$

where, J is jojoba oil, B is n-butanol, JA is jojobyl alcohols, and FABEs is Fatty Acid Butyl Esters.

In **Paper V**, the stoichiometry of transesterification reaction between avocado oil and ethanol requires a mole TAGs and three moles of ethanol to produce three moles of FAEEs and a mole of glycerol. The overall avocado oil ethanolysis is shown as:

$$\text{TAGs} + 3\,\text{E} \xleftrightarrow{Catalyst} 3\,\text{FAEEs} + \text{G} \tag{3.7}$$

where, E is ethanol, and G is glycerol.

The stepwise ethanolysis process is represented as:

$$\text{TAGs} + \text{E} \xleftrightarrow{Catalyst} \text{FAEEs} + \text{DAGs} \tag{3.8}$$

$$\text{DAGs} + \text{E} \xleftrightarrow{Catalyst} \text{FAEEs} + \text{MAGs} \tag{3.9}$$

$$\text{MAGs} + \text{E} \xleftrightarrow{Catalyst} \text{FAEEs} + \text{G} \tag{3.10}$$

For the purpose of modelling the reaction kinetics the above-mentioned alcoholysis processes, following commonly applied assumptions were taken into considerations:

- The reaction mixture was perfectly mixed, and its composition, catalyst distribution and temperature were uniform throughout the process because the reaction was performed in a batch reactor under continuous, vigorous stirring (**Paper III** and **V**).
- The contribution of homogeneous and thermal catalysis is insignificant (**Paper III** and **V**).
- The internal diffusion rate inside the catalyst particles does not influence the rate of the butanolysis reaction because of low porosity and small surface area of CaO catalyst (**Paper III**).
- The possibility of the formation of the calcium glyceroxide catalytic active centers was not existent because of the characteristics of jojoba oil (**Paper III**).
- The proportion of FFAs in avocado oil was negligible, hence the FFAs neutralization is insignificant (**Paper V**).
- The saponification reaction is negligible and the catalyst concentration remains constant during the ethanolysis process (**Paper V**).
- Because of the nature of the catalyst, the initial mass transfer step resistance is not existent (**Paper V**).

In **Paper III**, a mathematical model predicting the variation in the concentration of jojoba oil over the applied range of experimental conditions was developed. While in **Paper V**, a mathematical model describing the change in the TAGs and FAEEs concentration is studied. The selection of an appropriate mathematical model for the described alcoholysis process was based on the statistical parameters, such as the sum of weighted errors (SWE) and the model selection criteria (MSC). The mathematical expression for the MSC is presented as:

$$MSC = ln\left[\frac{\sum(\beta_{exp,i}-\beta_{exp,a})^2}{\sum(\beta_{exp,i}-\beta_{pre,i})^2}\right] - \frac{2p}{n} \quad (3.11)$$

where, $\beta_{exp,i}$ is the experimental data at i^{th} reaction time; $\beta_{exp,a}$ is an average of the experimental data; $\beta_{pre,i}$ is the predicted values at i^{th} reaction time; p is the number of the parameter involved in the model; n is the number of the experimental data.

3.5.3. Drying kinetics of Hass avocado seeds

In **Paper VII**, the capability of a newly established mathematical model to simulate the drying kinetics of pretreated and non-pretreated Hass avocado seeds was compared with three well-known and widely used semi-theoretical mathematical models.

Depending upon the characteristics of Hass avocado seeds, following assumptions were taken into consideration:

- The initial moisture content in Hass avocado seeds is high and uniformly distributed throughout the mass of the seed.
- The initial stage of the drying process was air temperature dependent.
- The change in the water content in Hass avocado seed during the initial period of drying was non-linear and the constant drying rate period is not existent.
- Resistance to mass transfer at the surface is negligible compared to the internal resistance of the sample.
- The drying process resulted in slight shrinkage of Hass avocado seeds.

The evaluation of the goodness of fit of the models to describe the drying curves was determined based on their coefficient of determination (R^2), square error (χ^2), root mean square error (E_{RMS}), and mean bias error (MBE).

The expression for the above mentioned parameters were written as:

$$R^2 = \frac{\sum_{i=1}^{N}\left(MR_{exp,i} - \overline{MR}_{pre,i}\right) * \left(MR_{exp,i} - \overline{MR}_{pre,i}\right)}{\sqrt{\sum_{i=1}^{N}\left(MR_{exp,i} - \overline{MR}_{pre,i}\right)^2 * \sum_{i=1}^{N}\left(MR_{exp,i} - \overline{MR}_{pre,i}\right)^2}} \quad (3.12)$$

$$\chi^2 = \frac{\sum_{i=1}^{N}\left(MR_{exp,i} - MR_{pre,i}\right)^2}{N - z} \quad (3.13)$$

$$E_{RMS} = \left[\frac{1}{N}\sum_{i=1}^{N}\left(MR_{exp,i} - MR_{pre,i}\right)^2\right]^{1/2} \quad (3.14)$$

$$MBE = \frac{1}{N}\sum_{i=1}^{N}\left(MR_{exp,i} - MR_{pre,i}\right) \quad (3.15)$$

where, $MR_{exp,i}$ is the *i*th experimental dimensionless moisture ratio; $MR_{pre,i}$ is the *i*th predicted dimensionless moisture ratio; N is the number of observation; z is the number of constants in the model.

4. Experimental results and discussion

The research activities involved in the present thesis initiated as a continuation of previous research work. Formerly, the methanolysis of jojoba oil over CaO catalyst derived from *M. Galloprovincialis* shells was carried out by Sánchez et al. [149]. The reported study registered jojoba oil conversion of 93.3 % after 600 min of methanolysis reaction performed at 65 ºC, using methanol-to-oil molar ratio of 9:1, catalyst amount of 8 wt. %, and 350 rpm stirring intensity. However, the published report concluded the existence of mass transfer limitations when methanol was used as a reactant for the CaO-catalyzed alcoholysis process of jojoba oil. With a challenge to eliminate the mass transfer concerns, we started the experimental study focused on examining the impact of different alcohols on the progression of the CaO-catalyzed alcoholysis reaction of jojoba oil. Using the above-mentioned operating parameters, we performed the CaO-catalyzed alcoholysis of jojoba oil using alcohols with an increasing order of their chain length, such as ethanol, propanol, and n-butanol. After the initial screening, we observed that the ethanolysis and propanolysis resulted in an insignificant oil conversion; whereas, the jojoba oil conversion improved when butanol was utilized, but still lower than that obtained from the methanolysis process. This was supposed to be because of unfavorable operating parameters. In order to have a better understanding of the reaction route and improve the oil conversion, we systematically investigated the influence of butanol-to-oil molar ratio, temperature, time, and catalyst loading on the CaO-catalyzed butanolysis of jojoba oil as presented below.

4.1. Calcium oxide-catalyzed alcoholysis process

In **Paper III**, the CaO-catalyzed butanolysis of jojoba oil was performed in a glass reactor and the progress of the reaction was systematically monitored by taking aliquots (approx. 1 mL) of the reaction mixture at a specified time intervals (100, 200, 300, 400, 500, 600 min). First, the impact of three different temperatures (65, 75, and 85 ºC) on the mentioned butanolysis process was studied keeping constant butanol-to-oil molar ratio of 10:1 and 12 wt. % catalyst amount. The experimental results for the effect of different temperatures on the jojoba oil conversion are presented in Figure 4.1. The obtained results indicated that the reaction temperature had a positive impact on the described butanolysis process. The rise in temperature resulted in the

reduction of reaction time. To achieve approximately 20 % conversion of jojoba oil, the reaction time decreased from 600 min to 200 min when temperature was raised from 65 ºC to 85 ºC. Using 85 ºC reaction temperature, jojoba oil conversion higher than 52 % was obtained after 600 min of the CaO-catalyzed jojoba oil butanolysis process. Further extending the reaction time to 1800 min, maximum jojoba oil conversion of 96.11 % was achieved.

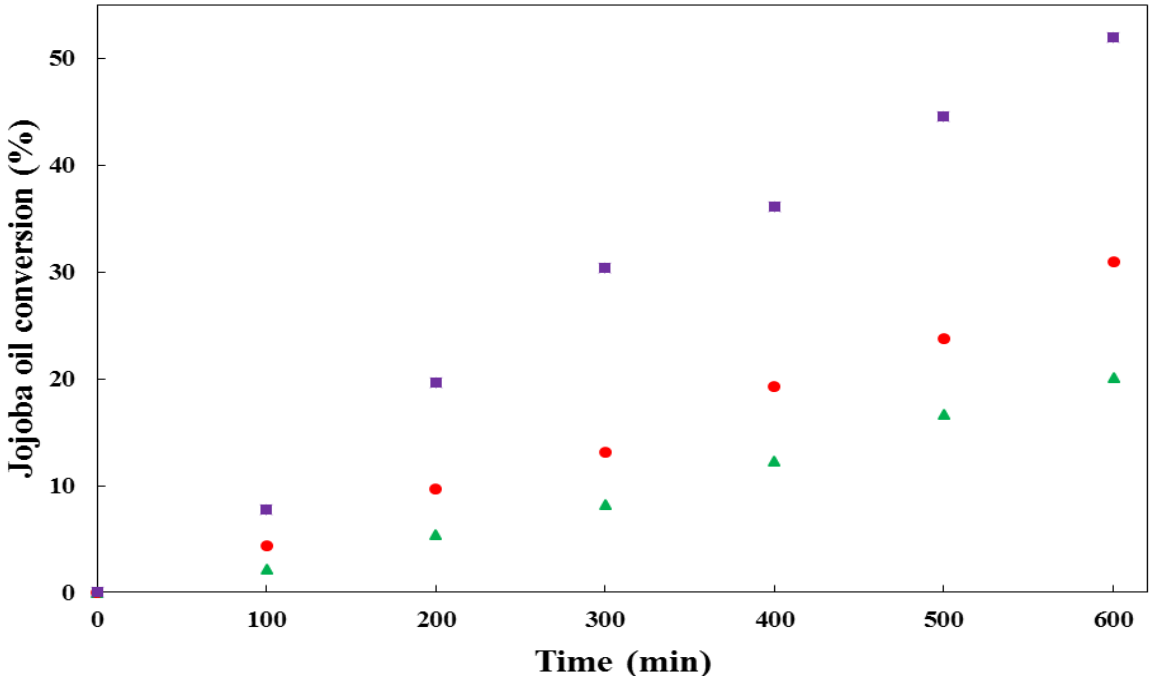

Figure 4.1: Impact of reaction temperature on the jojoba oil conversion. Temperature- (▲): 65 ºC, (●): 75 ºC, (■): 85 ºC. Catalyst loading 12 wt. %, butanol-to-oil molar ratio: 10:1, time: 600 min, stirring intensity: 350 rpm.

Secondly, we studied the effect of five different butanol-to-molar ratio on the CaO-catalyzed jojoba oil butanolysis process, keeping fixed reaction temperature of 85 ºC and 12 wt. % catalyst amount. Increasing butanol-to-oil molar ratio from 6 to 12.8:1 resulted in the augmentation of jojoba oil conversion from 39.00 to 58.93 % after 600 min of reaction time. The experimental results for the effect of butanol-to-oil molar ratio (6 to 12.8:1) on the jojoba oil conversion are presented in Figure 4.2. However, further amplifying the butanol-to-oil molar ratio to 14:1 directed the drop in the jojoba oil conversion to 46.02 %. This could be because the presence of higher amount of n-butanol than the optimal value resulted in the dilution of the reaction mixture that prevented the interaction between jojoba oil and butoxide ions chemisorbed on the CaO catalytic sites. The presented explanation was in agreement with the

literature [150]. The observed drop in the jojoba oil conversion when butanol-to-oil molar ratio was increased from 12.8 to 14:1 are shown in Figure 4.3.

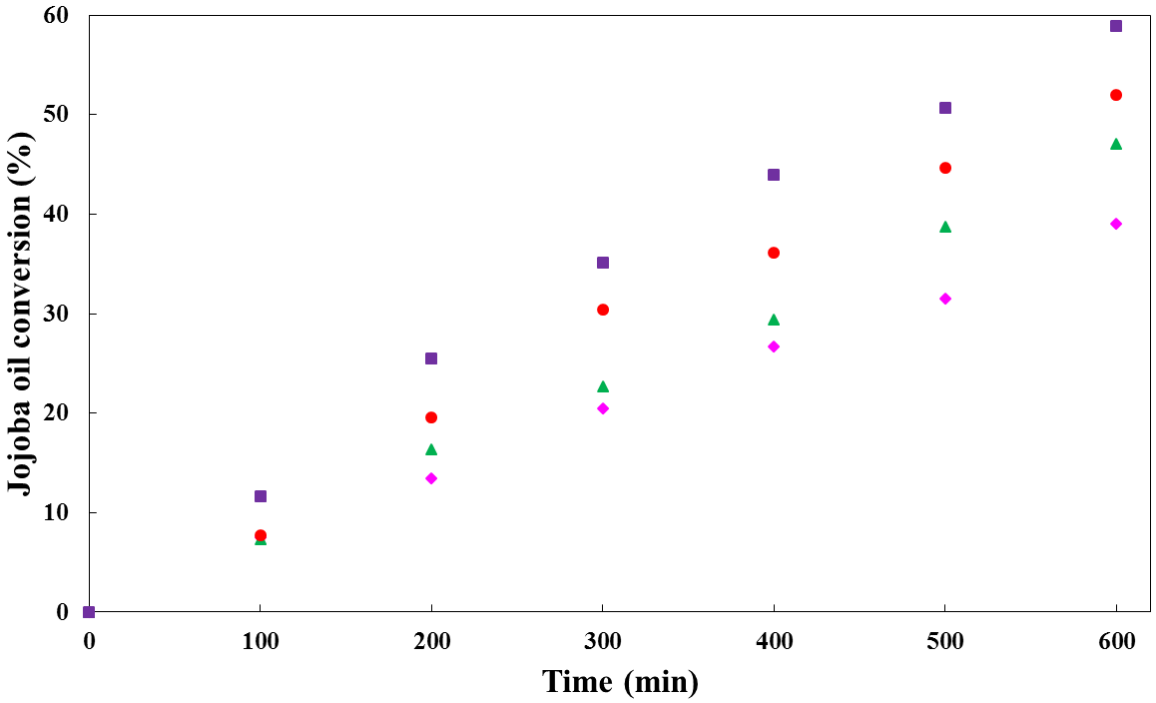

Figure 4.2: Impact of n-butanol concentration on the jojoba oil conversion. Butanol-to-oil molar ratio- (♦): 6:1, (▲): 7.2:1, (●): 10:1, (■): 12.8:1. Temperature: 85 ºC, Catalyst loading: 12 wt. %, Time: 600 min, Stirring intensity: 350 rpm.

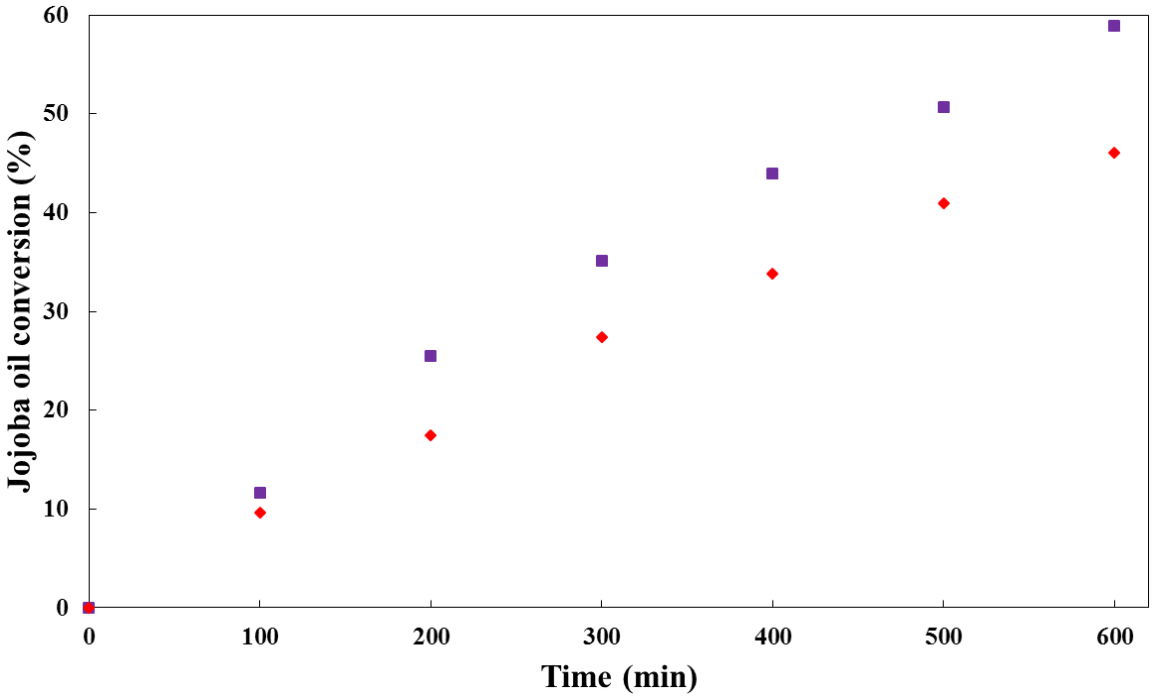

Figure 4.3: Impact of n-butanol concentration on the jojoba oil conversion. Butanol-to-oil molar ratio- (■): 12.8:1, (♦) 14:1. Temperature: 85 ºC, Catalyst loading 12 wt. %, Time: 600 min, Stirring intensity: 350 rpm.

In the experimental findings, we finally examined the effect of five different catalyst loading ranging between 6.3 and 17.7 wt. % (w.r.t. reaction mixture) on the rate of the described butanolysis process, setting the reaction temperature and butanol-to-oil molar ratio to 85 ºC and 10:1, respectively. Increase in the catalyst loading from 6.3 to 16 wt. % resulted in the acceleration of the rate of butanolysis reaction. The maximum jojoba oil conversion of 59.30 % was recorded after 600 min of the CaO-catalyzed butanolysis reaction. This is attributed to the increase in the availability of the catalytic active centers; thus, producing additional number of butoxide ions. The experimental results for the effect of the catalyst amount (6.3 to 16 wt. %) on the jojoba oil conversion are presented in Figure 4.4. However, further rise in the catalyst loading to 17.7 wt. % resulted in lowering of jojoba oil conversion to 53.71 %. This was because of increase in the kinematic viscosity of the reaction mixture. It is supposed that the rise in the kinematic viscosity of the reaction mixture obstructed the interaction between the reactant molecules due to the external mass transfer resistance [116, 151]. The obtained fall in the jojoba oil conversion when the catalyst amount was raised from 16 to 17.7 wt. % is shown in Figure 4.5.

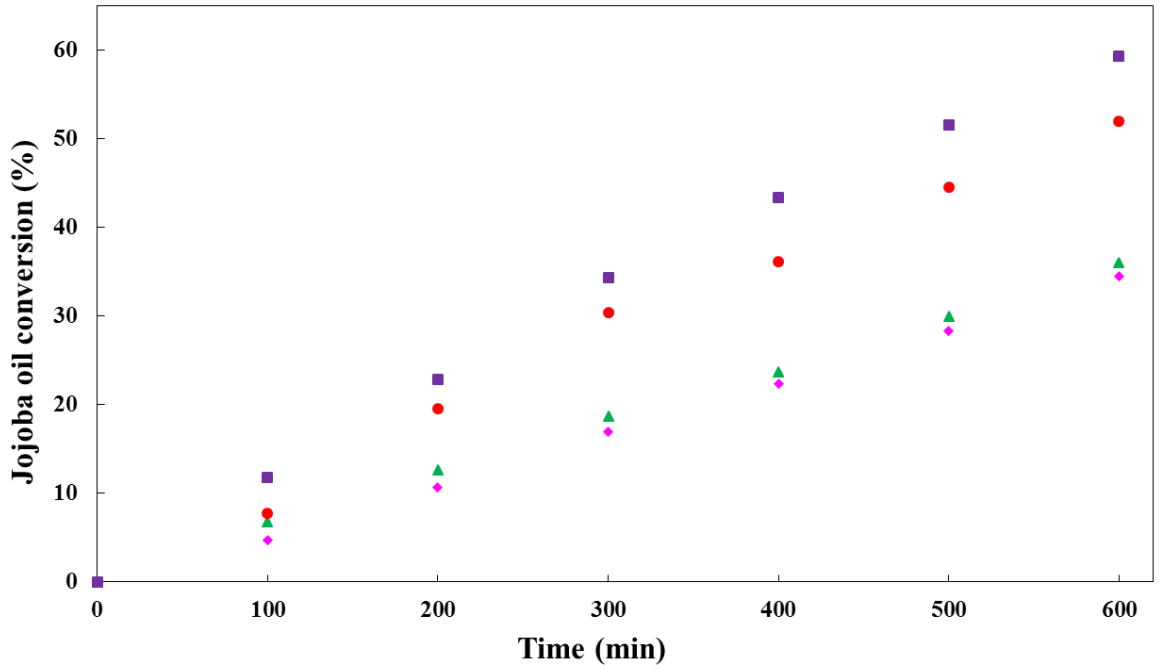

Figure 4.4: Impact of catalyst loading on the jojoba oil conversion. Catalyst loading- (♦): 6.3 wt. %, (▲): 8 wt. %, (●): 12 wt. %, (■): 16 wt. %. Temperature: 85 ºC, butanol-to-oil molar ratio: 10:1, Time: 600 min, Stirring intensity: 350 rpm.

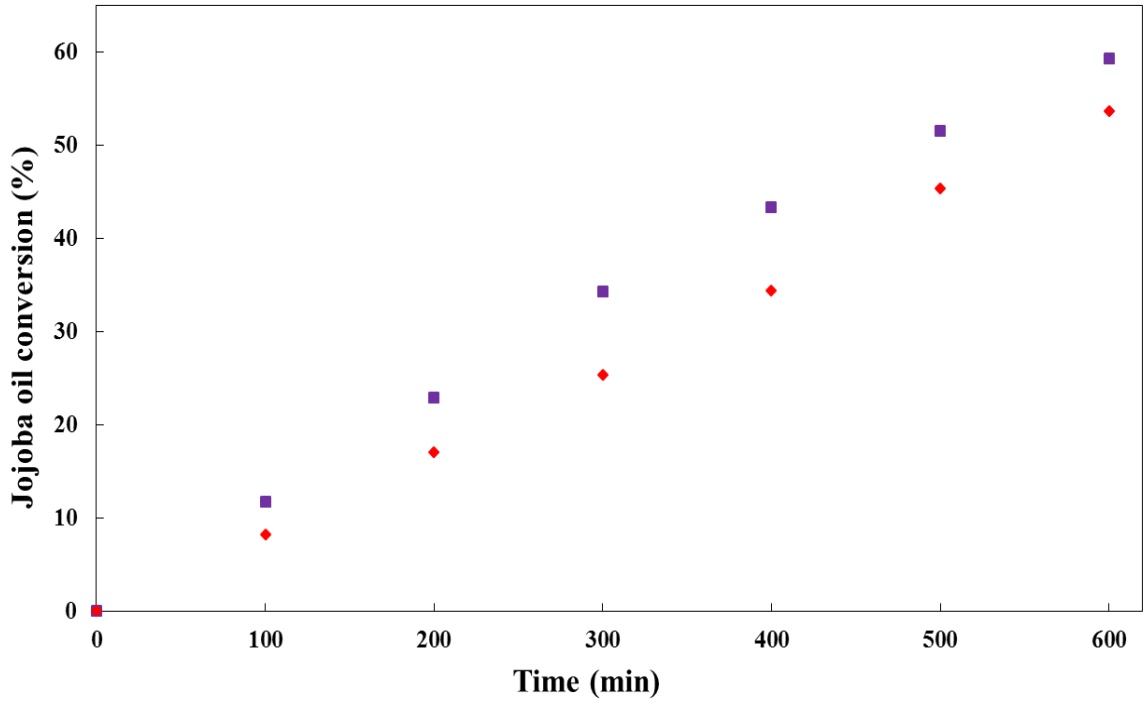

Figure 4.5: Impact of catalyst loading on the jojoba oil conversion. Catalyst loading- (■): 16 wt. %, (♦) 17.7 wt. %. Temperature: 85 ºC, butanol-to-oil molar ratio: 10:1, Time: 600 min, Stirring intensity: 350 rpm.

The CaO-catalyzed methanolysis of jojoba oil was a tri-phasic reaction system (liquid-liquid-solid), while, the butanolysis was a biphasic one (liquid-solid) because of the miscibility between jojoba oil and butanol. From the graphical curves, it was clear that the present study did not experience sigmoidal reaction pathway as observed in the case of the methanolysis process [149]. After the successful application of heterogeneous CaO catalyst for the butanolysis of jojoba oil, we focused our research towards investigating the capability of this catalyst for the alcoholysis of other non-edible lipid biomass. For this purpose, we used crude *jatropha curcas* oil having high content of FFAs. However, it is worth noting that jojoba oil is a non-TAGs based plant oil, while, CJCO consists of fatty acids attached to the glycerol skeleton. That means, glycerol is produced as a by-product during the alcoholysis reaction of TAGs based plant oil. Considering this aspect is of high relevance because a careful literature study suggested that CaO reacts with glycerol during the alcoholysis reaction [131, 132, 147]. Therefore, only the initial stage of the alcoholysis process of TAGs based plant oil is catalyzed by CaO material. Once the glycerol is generated in the reaction mixture, it reacts with CaO. The glycerol-enriched CaO was considered to further accelerate the alcoholysis process. Because the glycerol-CaO complex was characterized as chemically stable heterogeneous

catalyst and not prone for deactivation due to the surrounding air and moisture, Kouzu et al. [132] and López et al. [133] recommended to transform CaO to CaDg compounds before applying for the alcoholysis process. The present study presented a novel method for the preparation of CaDg, and the resultant catalyst was applied for the CJCO alcoholysis process. Since the newly synthesized heterogeneous catalyst was tested for a single-step alcoholysis of crude oil having high FFAs content for the first time, we performed the CJCO alcoholysis process using commonly used alcohol, i.e. methanol.

4.2. Calcium diglyceroxide-catalyzed alcoholysis process

4.2.1. *Jatropha curcas* methanolysis process

After the glycerol activation process of CaO in the presence of crude *jatropha curcas* oil (CJCO), temperature of the reaction system was shifted to the desired set point. Subsequently, a measured volume of methanol was charged into the reactor; and this was considered as the starting time of the methanolysis reaction. This study first screened the ability of different calcium-based catalysts for a single-step methanolysis of CJCO, and selected an appropriate catalyst for further study. Among the different laboratory-synthesized and commercial catalysts, CaDg assisted highest CJCO conversion. The oil conversion was improved by 3.88 times when the *M. Galloprovincialis* shells derived CaO was applied for the glycerol activation process prior to its utilization for the described methanolysis reaction. The presence of hydrophobic as well as hydrophilic sites on the surface of CaDg, in comparison to the polar surface of CaO, favor the approach of TAGs and alcohol to the catalytic sites [127, 131]. The utilization of CaDg catalyst assisted in 93.56 % oil conversion, when the methanolysis reaction was performed at 65 ºC for 420 min, using methanol-to-oil molar ratio of 9:1, catalyst amount of 15 wt. %, glycerol dose (in the case of glycerol activated catalyst) of 10 % w.r.t. catalyst weight, and 350 rpm stirring intensity. A graphical representation of the study evaluating the efficiency of different catalysts to assist the CJCO methanolysis reaction is shown in Figure 4.6. Using the CaDg catalyst, the present work systematically investigated the influence of different variables, such as the glycerol dose, temperature, time, methanol-to-oil molar ratio, and catalyst amount on the CJCO conversion. The study of variables effects on the methanolysis process initiated with examining the impact of glycerol dose on the CJCO conversion. The obtained results suggested that increasing the glycerol dose from 5 to 10 % (w.r.t. cat. wt.)

resulted in the rise of oil conversion from 85.60 to 93.56 %; however, further increase in the glycerol dose had an insignificant impact on the CJCO conversion. Therefore, the present study concluded that the glycerol dose of 10 % (w.r.t. cat. wt.) was appropriate. Next, we observed temperature be a critical factor affecting not only in increasing the oil conversion but also the activation of the glycerol-enriched CaO catalyst. Approximately identical and low oil conversion obtained at reaction temperature of 45 and 55 ºC hinted that the catalytic phase of glycerol-enriched CaO were not activated at these temperatures. The obtained experimental findings can be correlated with that reported by Kouzu et al. [152], where it was stated that CaDg was interacted with methanol at 60 ºC temperature. Therefore, the reaction temperature of 65 ºC was concluded as optimum for the described methanolysis process.

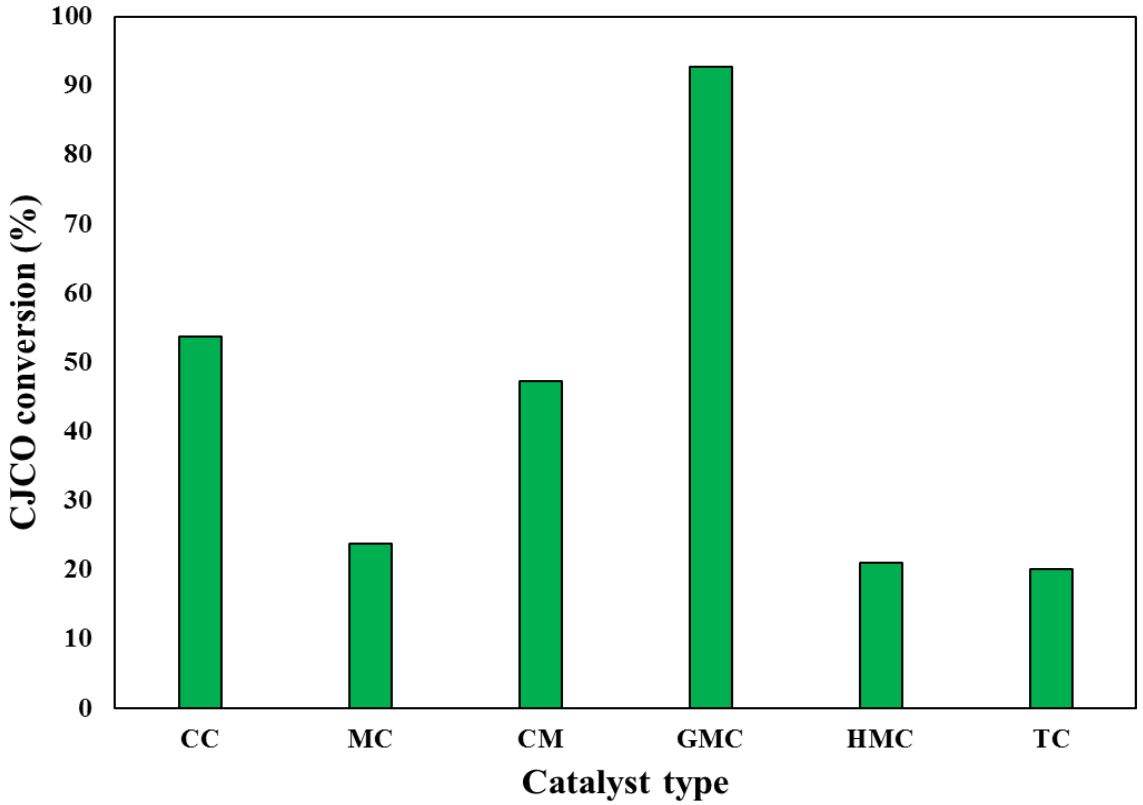

Figure 4.6: CJCO conversion using different types of catalyst. CC: commercial CaO, MC: mussel shells derived CaO, CM: calcium methoxide, GMC: glycerol-activated mussel shells derived CaO (CaDg), HMC: Homogeneous contribution of mussel shells derived CaO, TC: thermal catalysis. Reaction temperature: 65 ºC, time: 420 min, CaO catalyst loading: 15 wt. %, glycerol dosage: 10 % (only in the case of GMC), methanol-to-CJCO molar ratio: 9:1, stirring intensity: 350 rpm.

The impact of time was further investigated, using reaction temperature of 65 ºC, catalyst loading of 15 wt. %, glycerol dose of 10 % (w.r.t. cat. wt.), methanol-to-CJCO molar ratio of 9:1, and 350 rpm stirring intensity. The obtained results suggested that the methanolysis

reaction progressed until 420 min, enabling 93.56 % oil conversion; however, further extending the process time resulted in an insignificant improvement in the oil conversion. The graphical representations depicting the impact of glycerol dose, temperature, and time on the CJCO conversion is shown in **Paper IV**.

Subsequently, a set of experiment was designed to investigate the influence of five different methanol-to-CJCO molar ratio and catalyst amount on the described methanolysis process. The experimental results showed that the CJCO conversion augmented gradually with increasing amount of methanol. The increase in methanol-to-CJCO molar ratio from 4.8 to 9:1 resulted in the elevation of CJCO conversion from 80.93 to 93.56 %; however, further increase in the mole ratio of methanol-to-CJCO to 12:1 resulted only in slight improvement in the oil conversion. The effect of the mole ratio of methanol-to-CJCO, varied from 4.8 to 13.2:1, on the CJCO conversion is shown in Figure 4.7.

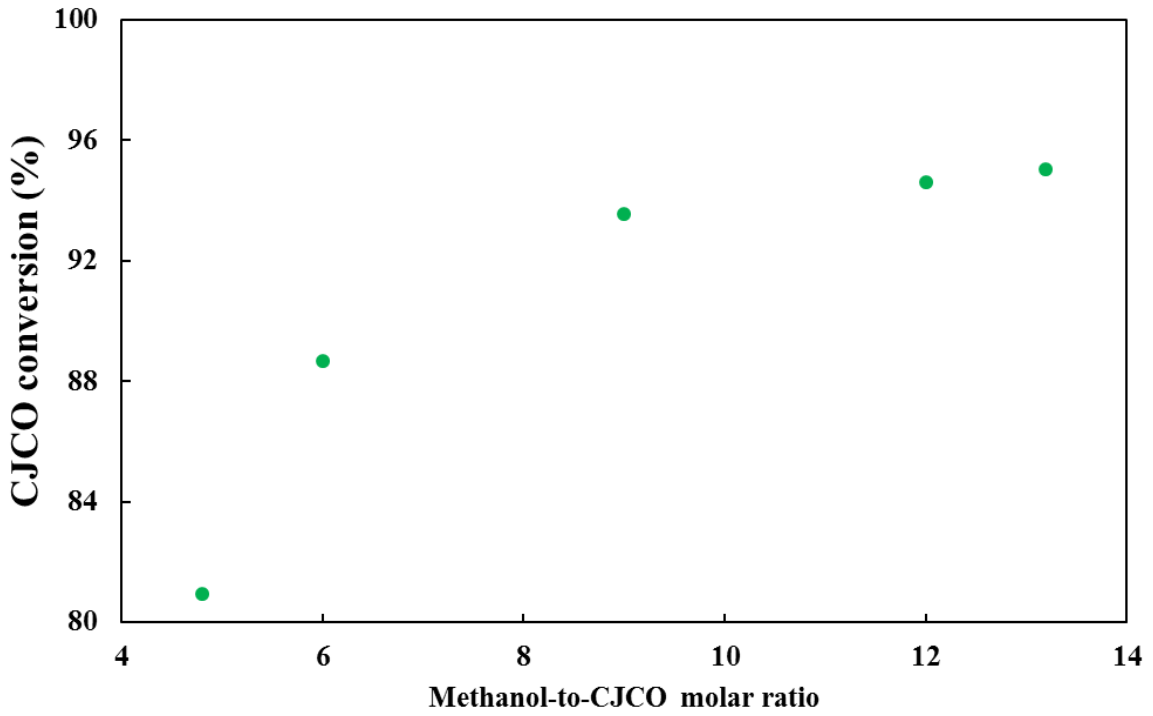

Figure 4.7: Effect of methanol-to-oil molar ratio on CJCO conversion. Reaction temperature: 65 ºC, time: 420 min, CaO catalyst amount: 15 wt. %, glycerol dose: 10 %, stirring intensity: 350 rpm.

The impact of five different catalyst amount on the described methanolysis reaction was also examined, using constant glycerol dose of 10 % (w.r.t. cat. wt.), temperature of 65 ºC, time of 420 min, methanol-to-CJCO molar ratio of 9:1, and 350 rpm stirring intensity. The experimental results indicated that increase in the catalyst loading from 10.8 to 15 wt. %

resulted in the augmentation of CJCO conversion from 84.30 to 93.56 %. However, insignificant improvement in oil conversion observed when the catalyst amount was further increased was indicative of the catalyst amount of 15 wt. % being optimum for the described methanolysis reaction. The increase in the viscosity of the reaction mixture caused due to higher catalyst loading could be the reason for stagnation in the advancement of the CJCO methanolysis process. The effect of catalyst amount, ranging between 10.8 and 19.2 wt. %, on the CJCO conversion is presented in Figure 4.8.

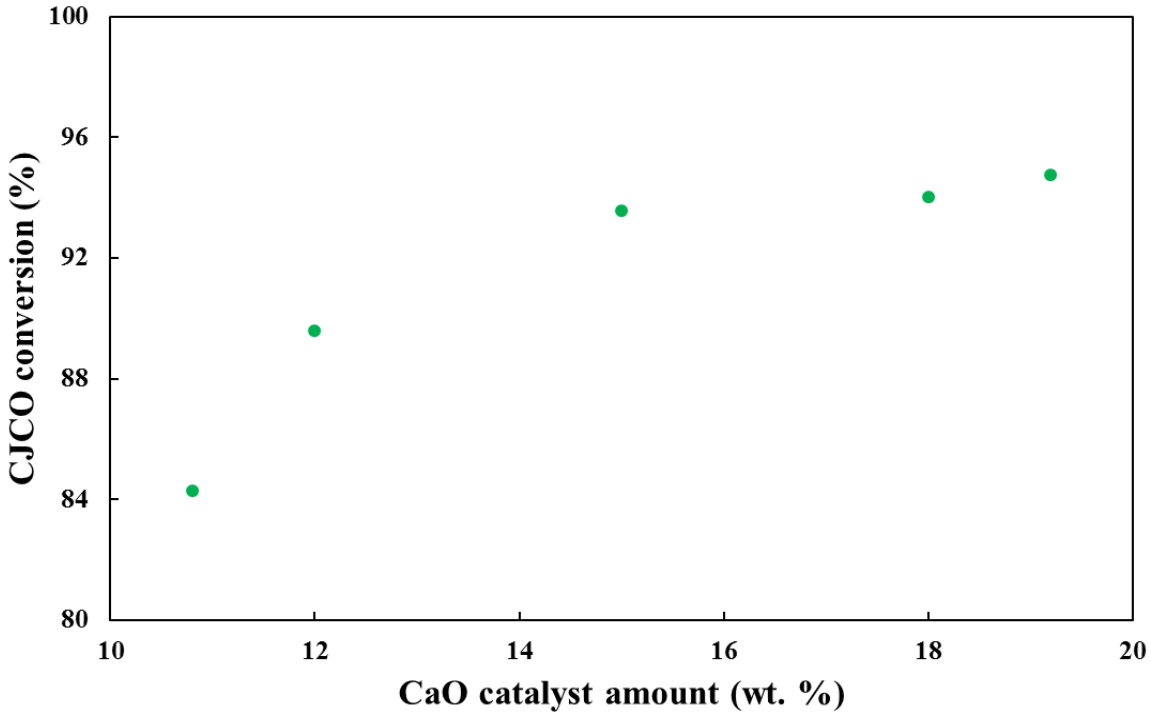

Figure 4.8: Effect of catalyst amount on CJCO conversion. Reaction temperature: 65 °C, time: 420 min, glycerol dose: 10 %, methanol-to-CJCO molar ratio: 9:1, stirring intensity: 350 rpm.

The post-reaction mixture was centrifuged for the separation of different phases (methanol-biodiesel-glycerol-catalyst) of the components. The biodiesel phase was washed with water to remove calcium soap, if any, lixiviated into the reaction products during the methanolysis process. The trace amount of methanol as well as water present in the biodiesel phase were subsequently removed using a rotary evaporator attached to a vacuum pump (10 mg Hg), set at 60 °C, for 30 min. The acid value of the produced biodiesel was subsequently determined. The acid value of CJCO was determined to be 24.75 mg KOH g^{-1}, which subsequently dropped to 0.18 mg KOH g^{-1} after its transformation to biodiesel. The acid value of biodiesel was found to follow the official EN 14104 and ASTM D664 specifications [153].

After the completion of the above-mentioned two studies, we planned a research strategy to utilize another non-edible lipid biomass, Hass avocado seeds. In this case, we attempted a step further to integrate the processing stages for biodiesel production through the reactive extraction methodology (REM) using CaDg catalyst. To ensure if CaDg is a right catalyst for the alcoholysis of extracted lipid bodies from Hass avocado seeds, we carried out a separate study focused on the utilization of CaDg catalyst to assist the alcoholysis of refined avocado pulp oil. Because the use of ethanol was planned for the in-situ extraction of lipid bodies from Hass avocado seeds and the transformation of extractable lipid to biodiesel, the ethanolysis of avocado oil catalyzed by CaDg was performed.

4.2.2. Avocado oil ethanolysis process

In **Paper V**, the ethanolysis of avocado oil was performed after the glycerol activation process of CaO, in the presence of oil. The aliquots (approx. 1 mL) of the reaction mixture were withdrawn at a specific time intervals (1, 2.5, 5, 10, 20, 40, 60, and 120 min) to understand the progression of the reaction. The extracted samples were immediately applied to a rota-evaporator, attached to a vacuum pump (10 mg Hg), set at 70 ºC, for 30 min to eliminate the residual ethanol. During the experimental findings, this study systematically examined the impact of temperature, ethanol-to-oil molar ratio, and catalyst amount on the variation in the concentration of TAGs and FAEEs with reaction time. Initially, the effect of three different temperatures (55, 65, and 75 ºC) on the described ethanolysis process was studied keeping constant ethanol-to-oil molar ratio of 9:1, catalyst amount of 7 wt. %, time of 120 min, and 350 rpm stirring intensity. The experimental results for the effect of temperature on the change in the concentration of TAGs and FAEEs are presented in Figure 4.9 and 4.10, respectively. The increase in the reaction temperature accelerated the drop in TAGs concentration and increase the FAEEs concentrations. The rise in temperature from 55 to 75 ºC resulted in the reduction of reaction time from 120 to 40 min to produce nearly equal amount of biodiesel. Therefore, reaction temperature of 75 ºC was found to be optimal for the described ethanolysis process. Secondly, the effect of ethanol-to-oil molar ratio on the described ethanolysis process was investigated using fixed reaction temperature of 75 ºC, time of 120 min, catalyst amount of 7 wt. %, and 350 rpm stirring intensity. The variation in the TAGs and FAEEs concentration with the change in ethanol-to-oil molar ratio is shown in Figure 4.11 and 4.12, respectively. The

experimental findings indicated that the increase in ethanol-to-oil molar ratio significantly affected the rate of the CaDg-catalyzed avocado oil ethanolysis process. To achieve approximately similar FAEEs concentration, the reaction time decreased from 40 to 10 min when ethanol-to-oil molar ratio was raised from 6 to 12:1. Though the rise in ethanol-to-oil molar ratio from 9 to 12:1 improved the rate of the ethanolysis reaction, an insignificant difference in the final TAGs and biodiesel concentration was observed. Therefore, ethanol-to-oil molar ratio of 9:1 was considered appropriate for the described ethanolysis process under the investigated range of experimental conditions.

Finally, the effect of three different catalyst amount (4, 7, and 10 wt. %) on the mentioned ethanolysis process was also examined setting the constant reaction temperature of 75 ºC, ethanol-to-oil molar ratio of 9:1, time of 120 min, and 350 rpm stirring intensity. The experimental results of the study evaluating the effect of the catalyst amount on the variation in the TAGs and FAEEs concentration are shown in Figure 4.13 and 4.14, respectively. A faster drop in the TAGs concentration and the rise in the FAEEs concentration was observed with an increase in the catalyst amount. This is attributed to an increase in the availability of the catalytic active centers; thus, providing an additional number of ethoxide ions for the reaction. The increase in the catalyst amount from 4 to 10 wt. % reduced the ethanolysis reaction time from 60 to 20 min to achieve around similar biodiesel concentration. However, when the catalyst amount was raised from 7 to 10 wt. %, a minor difference in the final TAGs as well as the biodiesel concentration was obtained; therefore, the catalyst amount of 7 wt. % was considered optimal for the described ethanolysis process.

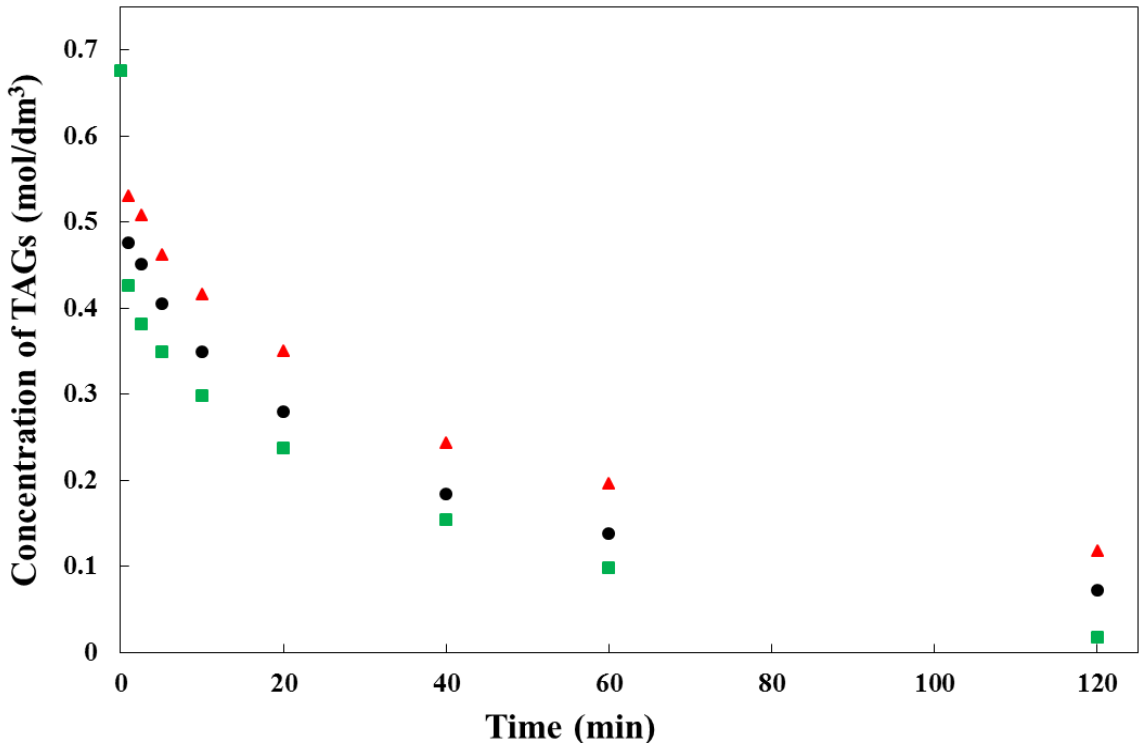

Figure 4.9: Effect of temperature on the change in TAGs concentration. (▲- 55 ºC, ●- 65 ºC, ■- 75 ºC).

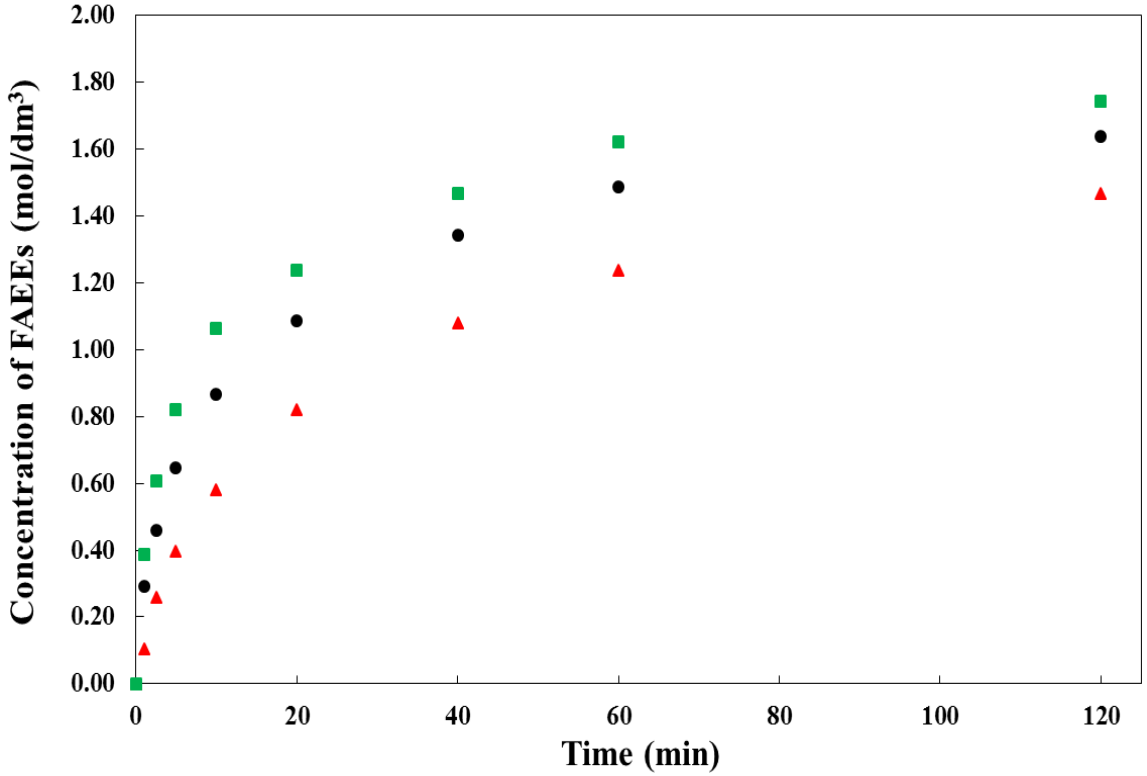

Figure 4.10: Effect of temperature on the change in FAEEs concentration. (▲- 55 ºC, ●- 65 ºC, ■- 75 ºC).

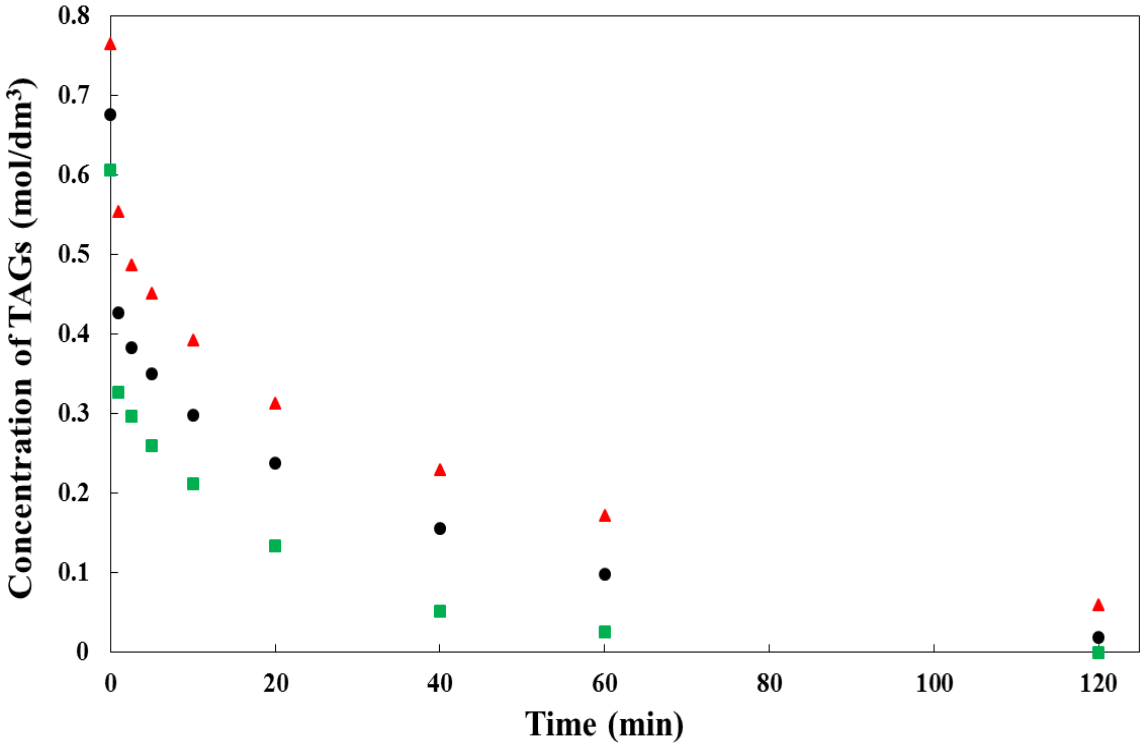

Figure 4.11: Effect of ethanol-to-oil molar ratio on the change in TAGs concentration. (▲-6:1, ●-9:1, ■-12:1).

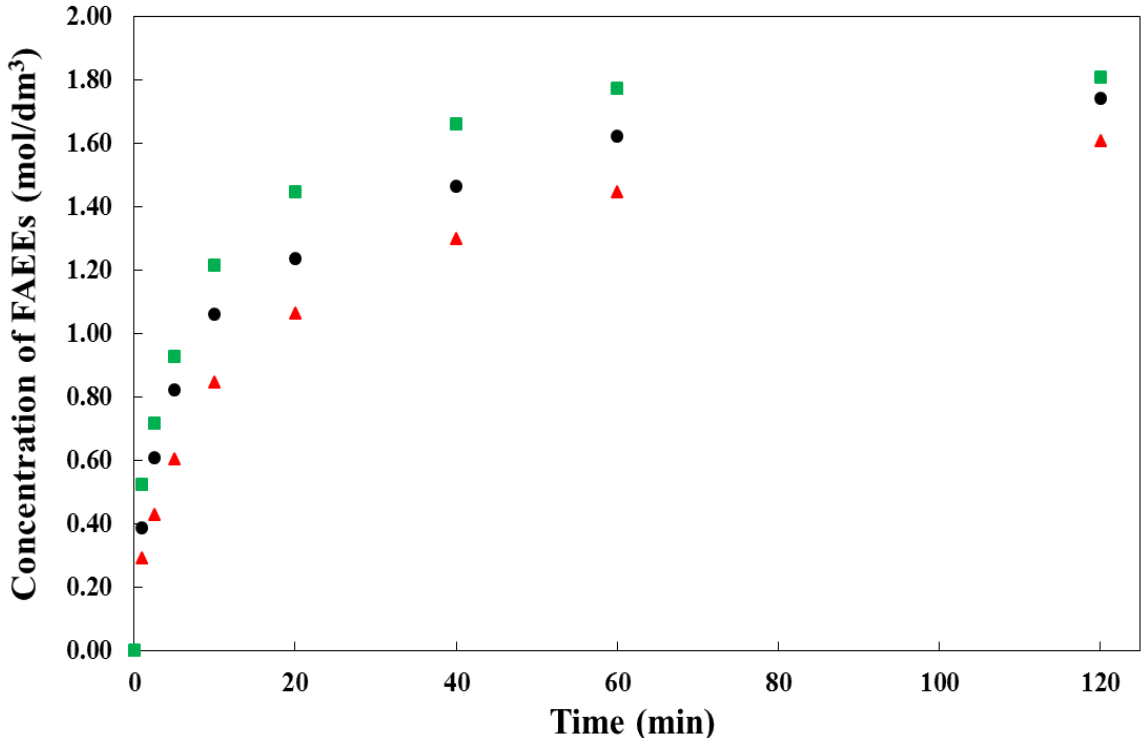

Figure 4.12: Effect of ethanol-to-oil molar ratio on the change in FAEEs concentration. (▲-6:1, ●-9:1, ■-12:1).

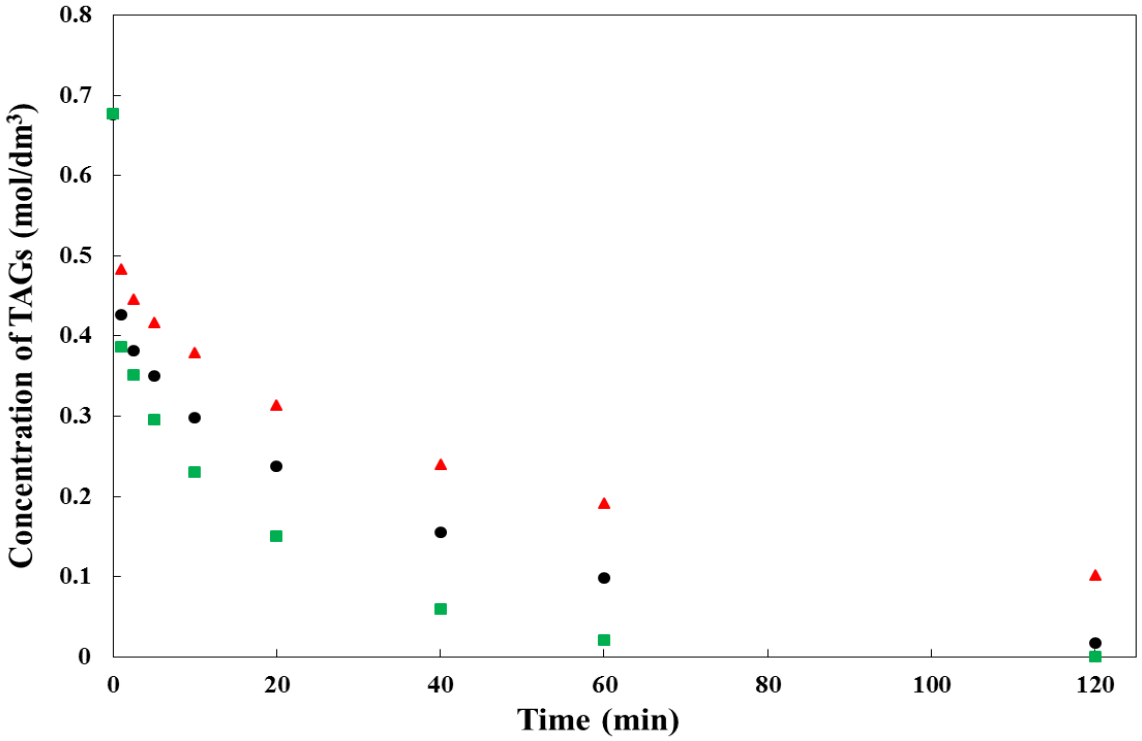

Figure 4.13: Effect of catalyst amount on the change in TAGs concentration. (▲-4 wt. %, ●-7 wt. %, ■-10 wt. %).

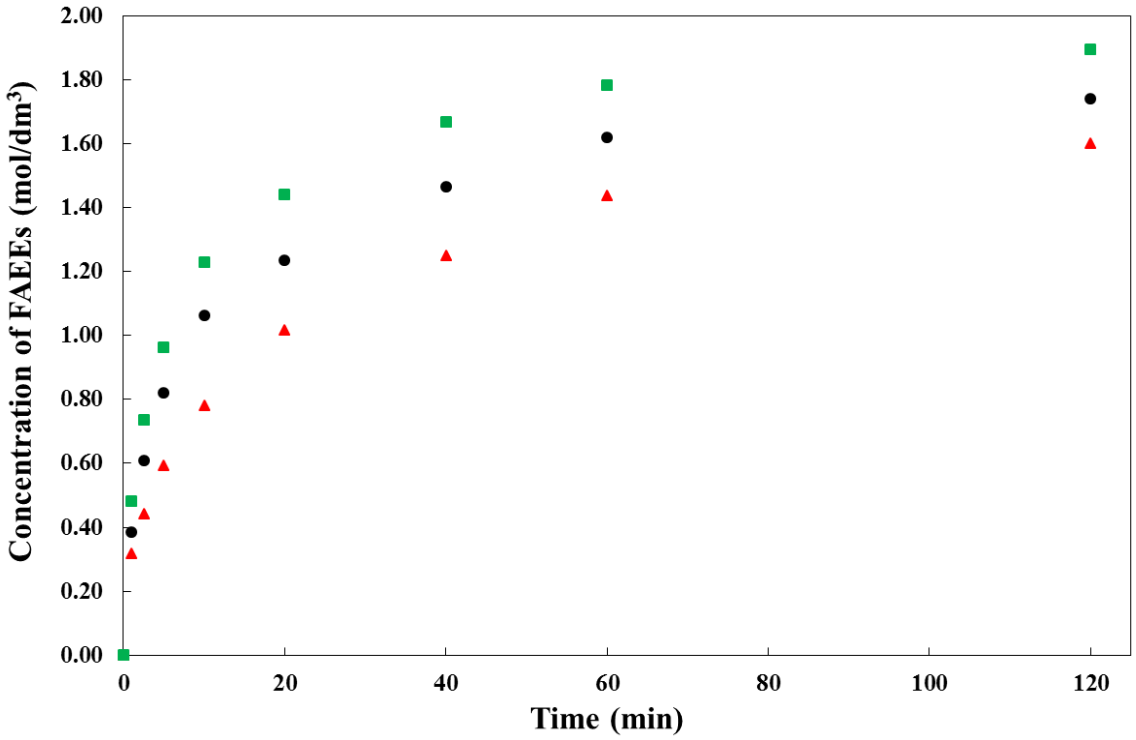

Figure 4.14: Effect of catalyst amount on the change in FAEEs concentration. (▲-4 wt. %, ●-7 wt. %, ■-10 wt. %).

4.3. Catalyst characterization

4.3.1. X-ray diffraction

The XRD patterns of the laboratory synthesized CaO and CaDg are given in Figure 4.15.

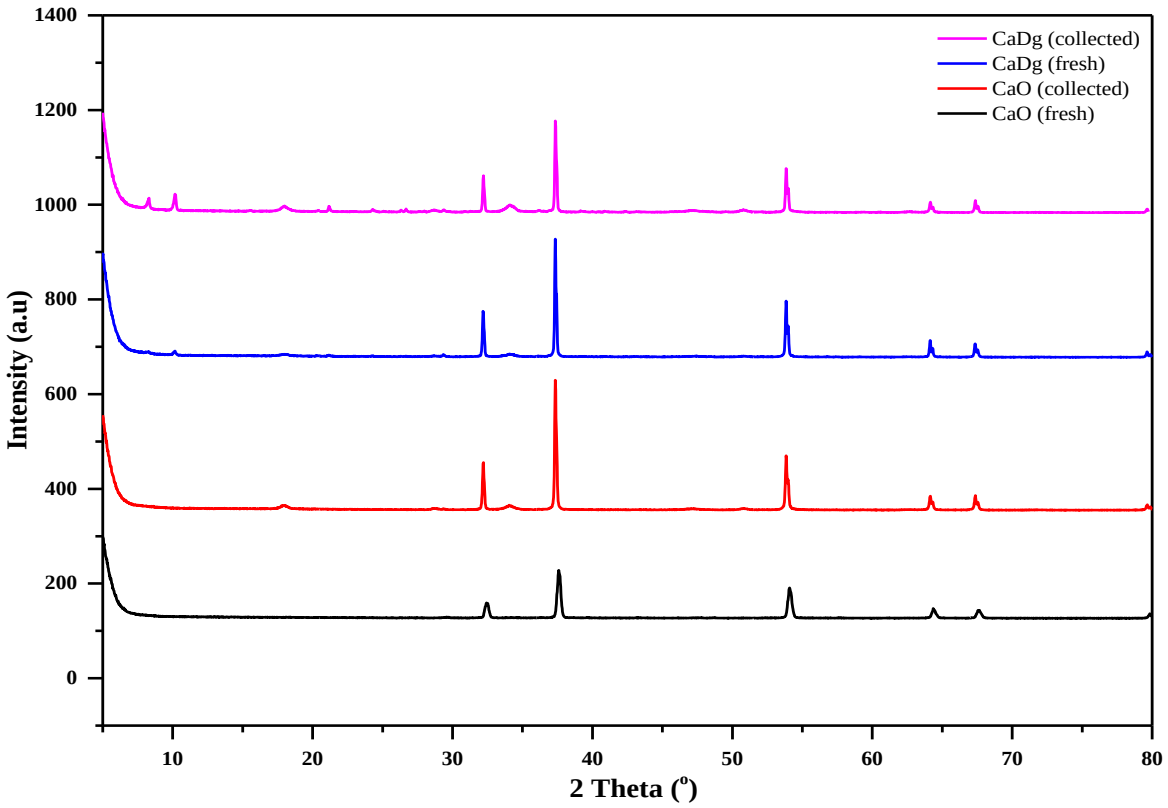

Figure 4.15: XRD patterns of fresh and collected CaO and CaDg.

The diffraction peaks at 2θ of 32, 37, 54, 64, and 67º were attributed to the CaO species. In the case of CaO, the absence of characteristic peaks for $CaCO_3$ at 2θ of 29.4º as well as for $Ca(OH)_2$ at 2θ of 18, 34, 47.2, and 50.8º confirmed that the calcination process of *M. Galloprovincialis* shells at 800 ºC resulted in the formation of only CaO species. After calcination at 800 ºC both $CaCO_3$ and calcium hydroxide ($Ca(OH)_2$) decompose. The diffraction pattern for CaDg was obtained after the reaction of CaO with glycerol, in the presence of plant oil at 65 ºC. Small but detectable characteristic peaks at 2θ of 8.2, 10.2, 24.4, 26.6, 34.4, and 36.2º in the diffractogram confirmed the formation of CaDg species. The characteristic peaks for CaDg are coincident with the values reported before [128, 154]. The XRD pattern for CaDg showed a small

contamination of $Ca(OH)_2$ (2θ of 18, 47.2, and 50.8º). This could be because of the presence of slight moisture in the plant oil.

The XRD patterns of the collected CaO and CaDg catalyst were also obtained and compared with those of fresh catalysts. In the case of collected CaO catalyst, the appearance of diffraction peaks at 2θ of 29.4º and of 18, 34, 47.2, and 50.8º indicated poisoning of CaO catalyst due to an adsorption of surrounding CO_2 and moisture, respectively. The hydration and carbonation reaction resulting in the formation of $CaCO_3$ and $Ca(OH)_2$ species might reduce the catalytic activity of CaO. In the case of collected CaDg catalyst, the increase in the intensity of diffraction peaks at 2θ of 8.2, 10.2, 24.4, 26.6, 34.4, and 36.2º indicated that untransformed CaO remained during the synthesis of CaDg reacted with glycerol produced during the alcoholysis reaction. The consistent generation of CaO-glycerol complex during the alcoholysis reaction was anticipated to promote the activity of CaDg catalyst.

4.3.2. Thermal analysis

The TGA profiles of the synthesized CaO and CaDg are shown in Figure 4.16 and 4.17, respectively. In the case of CaO, weight loss of 3.14 % was observed after heating the sample from 25 to 800 ºC. The two minor weight loss found at 100 ºC, and between 325 and 375 ºC could be due removal of the physisorbed moisture, and decomposition/oxidation of organic components, respectively. In the case of CaDg, a total weight loss of 17.88 % was obtained. The increase in weight loss indicated the formation of CaO-glycerol complex. A well-defined weight loss takes place between 150 and 450 ºC, which corresponds to the decomposition of glyceroxide ions to give calcite. The final weight loss registered between 600 and 700 ºC attributed to the decarbonation process to give CaO. The obtained pattern of weight loss of CaDg was in good agreement with that reported by Reyero et al. [128] and León Reina et al. [131]. Above 700 ºC, the CaDg sample seemed to be converted into CaO, because of the flat TGA line. Furthermore, TGA of the collected CaO and CaDg was carried out for the comparison purpose. The TGA profiles of the collected CaO and CaDg are shown in Figure 4.18 and 4.19, respectively. The thermal analysis can also be correlated with the XRD patterns. The weight loss in the case of the collected CaO catalyst increased to 9.43 %, from that of 3.14 % of the fresh catalyst. This behavior might be because of the adsorption of reaction products, and due to poisoning phenomenon of the catalyst. While, the weight loss in the case of CaDg

shifted from 17.88 % to 25.90 %. The increase in the weight loss is attributed to the occurring reaction between untransformed CaO and glycerol producing during the methanolysis reaction.

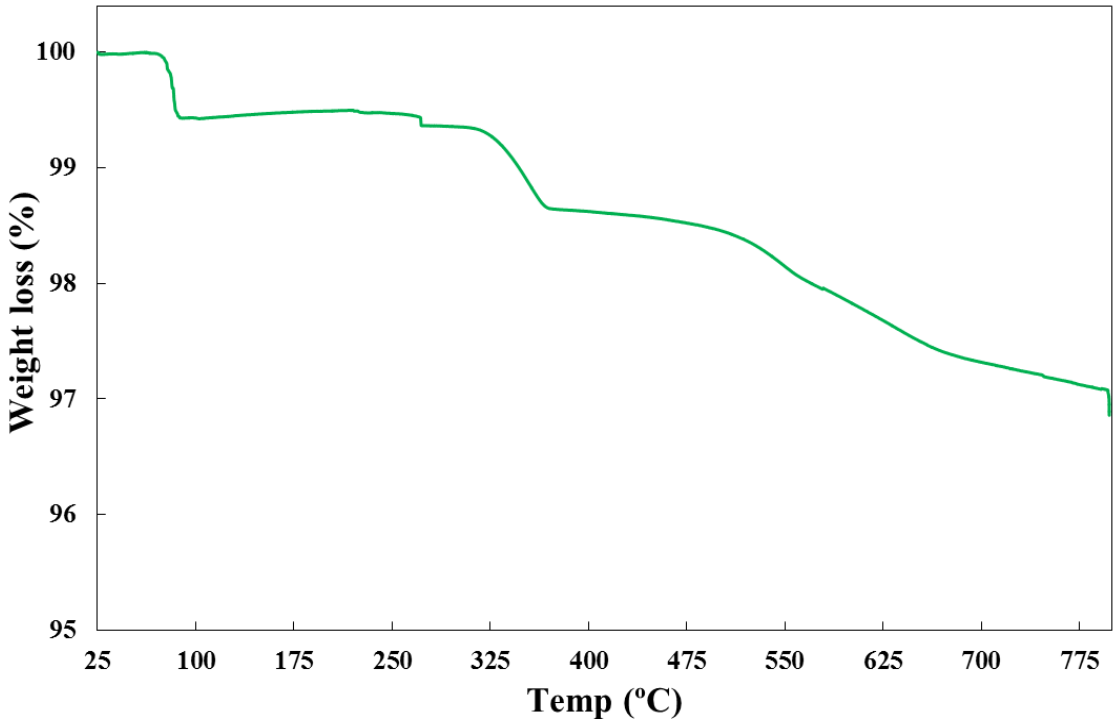

Figure 4.16: TGA profile of the synthesized CaO.

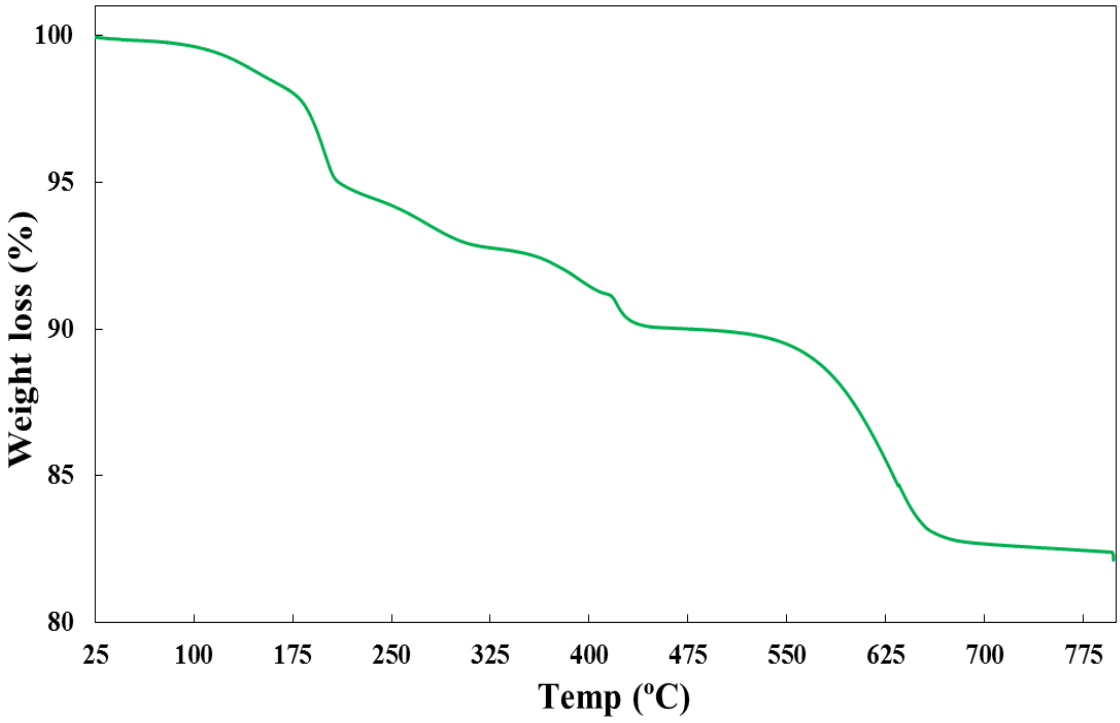

Figure 4.17: TGA profile of the synthesized CaDg.

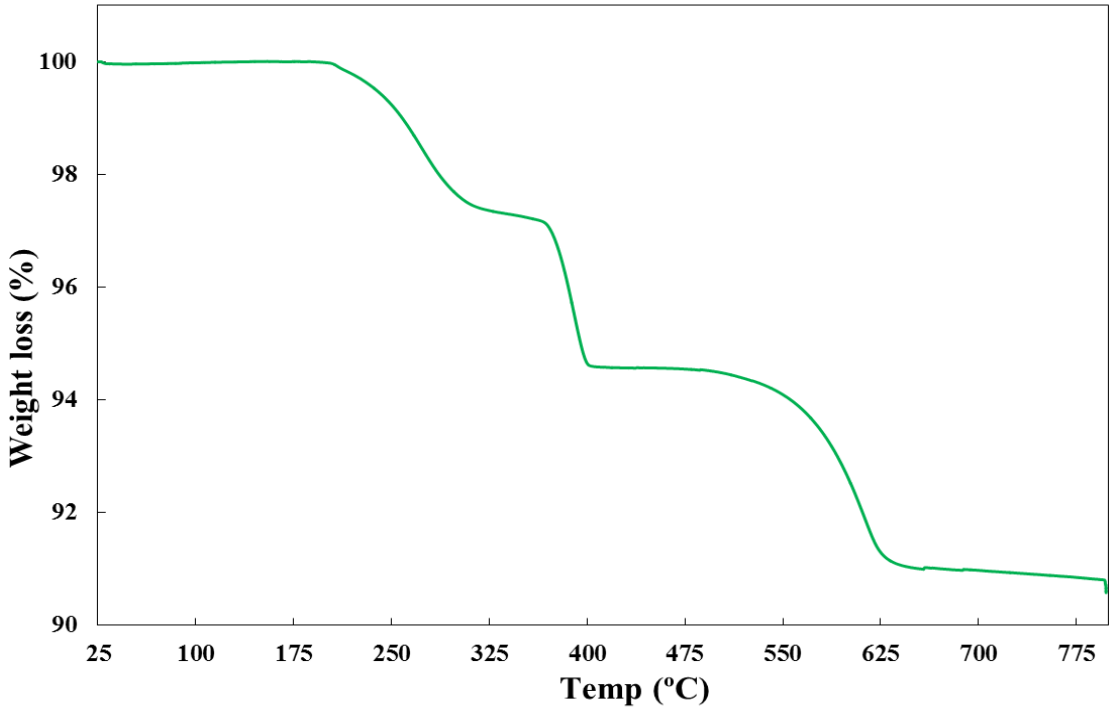

Figure 4.18: TGA profile of the collected CaO.

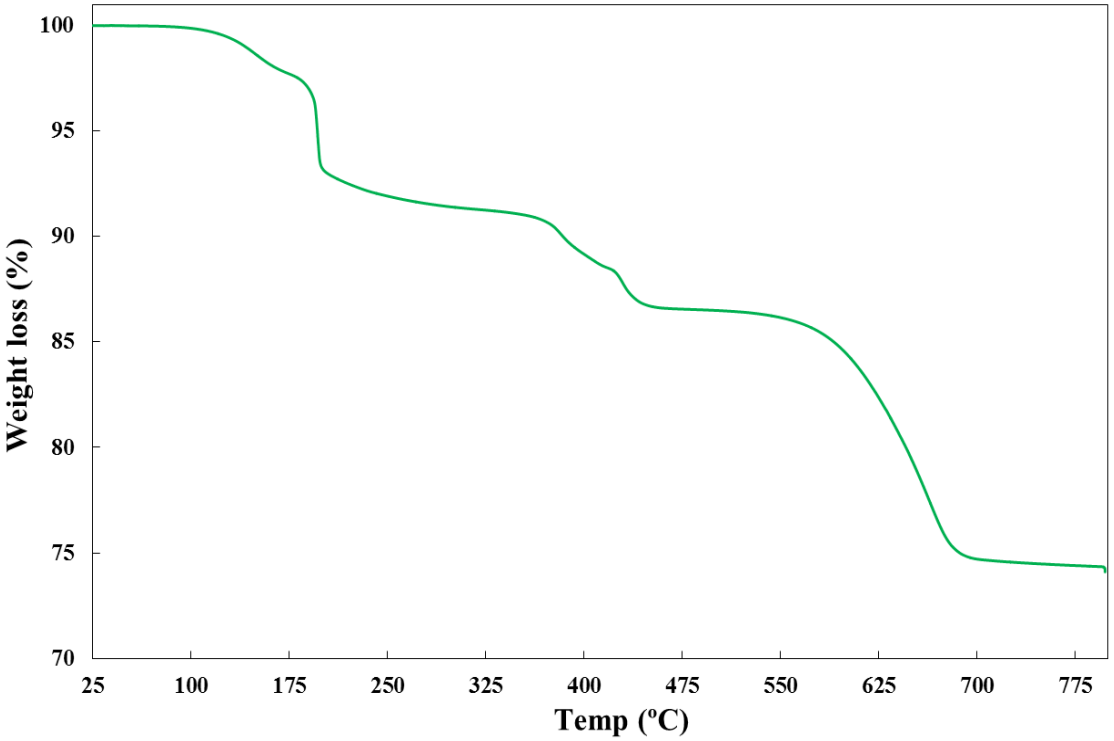

Figure 4.19: TGA profile of the collected CaDg.

4.4. Reactive extraction of Hass avocado seeds

Hass avocado fruit contains a single seed, which constituents on an average 13 % of the total weight of the fresh fruit. The seed is composed of a testa where most of the polyphenolic substances are localized. The embryo contains high content of TAGs. The cotyledons have the highest amount of carbohydrates [155]. Initially, we conducted the microscopical investigation of the embryo to witness the lipid bodies inside Hass avocado seeds. The microscopic images depicting lipid bodies in Hass avocado seeds are shown in Figure 4.20 (a and b). As can be seen in the Figure 4.20, the lipid bodies are confined inside the cellular wall. The use of Toluidine blue stain enabled the differentiation between the fat cells and starch grains. The lipid bodies stained blue (Figure 4.20a), while polysaccharides turned purple in color (Figure 4.20b).

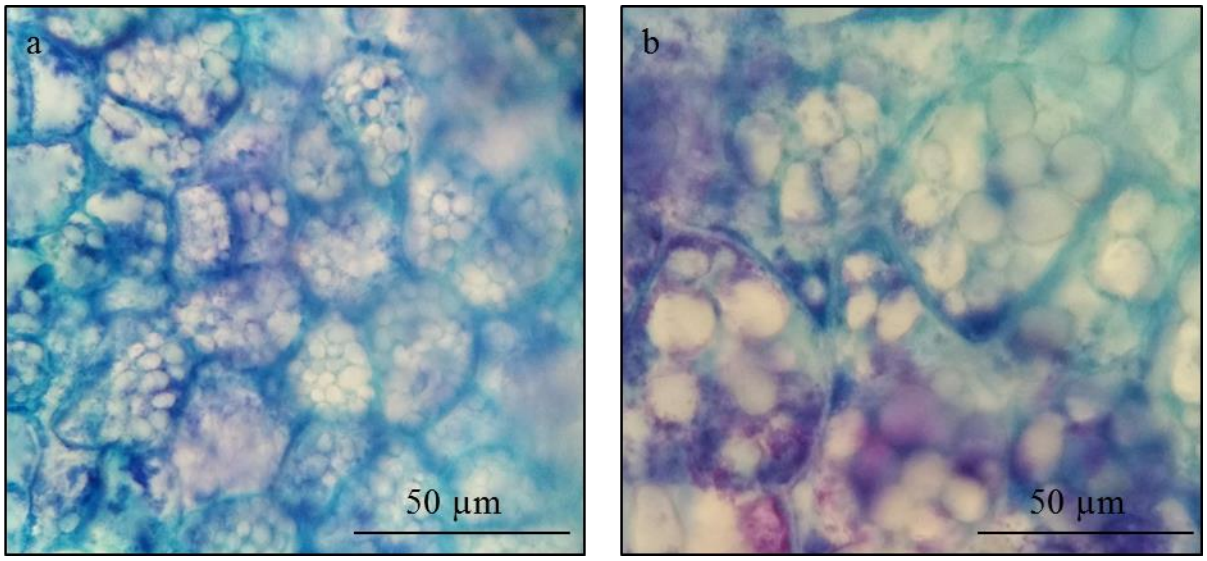

Figure 4.20: Microscopic image showing lipid bodies in Hass avocado seeds.

4.4.1. Drying stage

Water content in the fresh Hass avocado seeds, utilized in the present study, was 51.20 %. In order to effectively utilize Hass avocado seeds for the derivatization of combustible oil and chemicals, its moisture removal stage could be primary, but is a critical one because the presence of moisture could cause irreversible damage to the seeds and reduce the quality of the final product. The impact of five different air temperatures (40, 50, 60, 70, and 80 ºC) on the degree of moisture evaporation and quality of Hass avocado seeds was systematically reported in **Paper VI**. Hass avocado seeds were physically treated prior to the drying process and its

influence on the overall speed of moisture evaporation was carefully investigated. Firstly, the effect of drying air temperatures on the extent of moisture evaporation from the non-pretreated Hass avocado seeds was investigated. Increase in the drying air temperature accelerated the moisture evaporation process. After 720 min of drying, air temperature of 80 ºC resulted in 27.35 % reduction in the weight of the non-pretreated Hass avocado seeds, which was around 4.3 times higher than that observed using 40 ºC. The final weight loss of 45.59 % of the non-pretreated Hass avocado seed was reported after 5760 min of drying performed at 80 ºC. A graphical representation showing the impact of five different temperatures on the drying of non-pretreated Hass avocado seeds can be seen in Figure 2 in **Paper VI**. Afterwards, we investigated the impact of pretreatment (crushing and slicing) of Hass avocado seeds on the degree of moisture evaporation. The physical treatment prior to the drying process would not only allow the usage of less energy for drying but also would help faster removal of moisture. It was observed that after 1440 min of the drying process, a maximum weight loss of 54.50 and 56.76 % was achieved for the crushed and sliced Hass avocado seeds, respectively. Hence, it was understood that complete water was not evaporated from the non-pretreated Hass avocado seeds even after 5760 min of drying process at 80 ºC temperature. Even though the use of elevated drying temperatures accelerated the moisture evaporation, it had an unfavorable impact on the quality of the product. To effectively understand the influence of surrounding temperature on the nature of Hass avocado seeds, the physical appearance of Hass avocado seed was photographed consistently during the drying experiment. We observed that at 60 ºC or higher temperature resulted in hardening and charring of the outer surface of seed. This, consequently, might hinder the moisture evaporation. Furthermore, the employment of high drying temperature for the drying process could burn the cellular wall, which in return might cause complexity for the extraction of chemicals from Hass avocado seeds. The physical appearance of Hass avocado seeds at different time intervals is shown in Figure 4.21.

The phenomenon of having a negative influence of high temperatures on the drying of Hass avocado seeds was well-defined also in the case of pretreated seeds. In the case of crushed and sliced Hass avocado seeds, though elevated temperatures assisted acceleration in the moisture evaporation rate, the maximum weight loss of seeds was achieved when dried at 40 ºC. High temperature (80 ºC) resulted in lower weight loss, while, high weight loss was obtained when Hass avocado seeds were dried at 40 ºC air temperature. It was believed that the elevated

temperature critically affected the seed surface, which consequently, obstructed the evaporation of water residing inside the seeds. Therefore, the appliance of high temperature (80 ºC) resulted in incomplete drying of Hass avocado seeds, while, low temperature (40 ºC) though had an inferior moisture evaporation rate, assisted consistent removal of moisture with causing no damage to Hass avocado seeds.

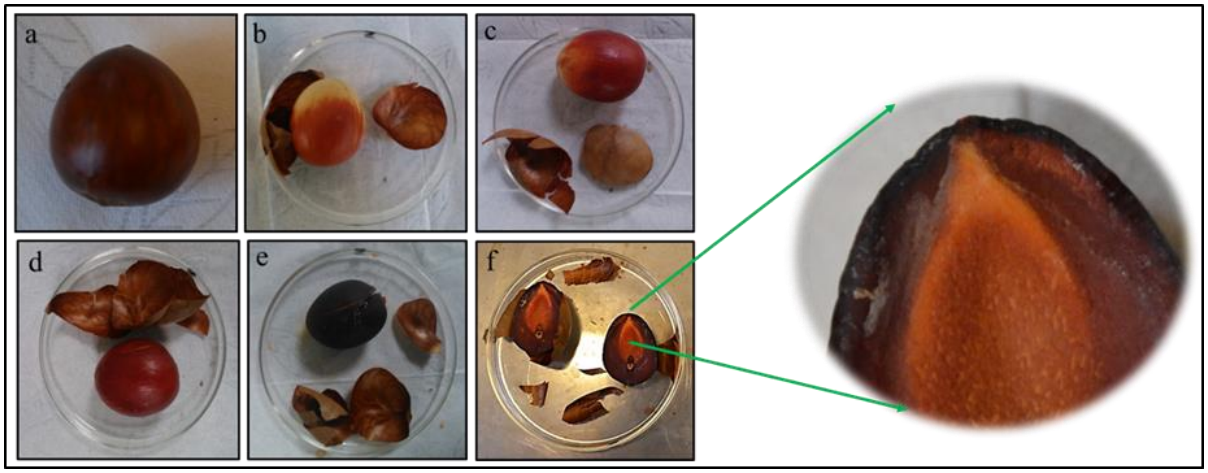

Figure 4.21: Physical appearance of Hass avocado seed at 60 ºC with time: a) 0 min; b) 60 min; c) 120 min; d) 180 min; e) 360 min; f) 720 min [53].

The crushing pretreatment process and the operative temperature of 40 ºC and 1440 min drying time was decided to be suitable for an satisfactory drying of Hass avocado seeds. This is because the objective of performing two different pretreatment process (slicing and crushing) was to have the accuracy in the experimental findings, and the outcome is briefly discussed in **Paper VI**. The experimental results explaining the drying curves of crushed Hass avocado seeds at different temperatures are presented in Figure 4.22. The residual moisture content in Hass avocado seeds after the drying process performed at 40 ºC for 1440 min was 4.57 %. This dried Hass avocado seeds can be safely stored because the final moisture content was below the sample safety storage level of 7 % [156].

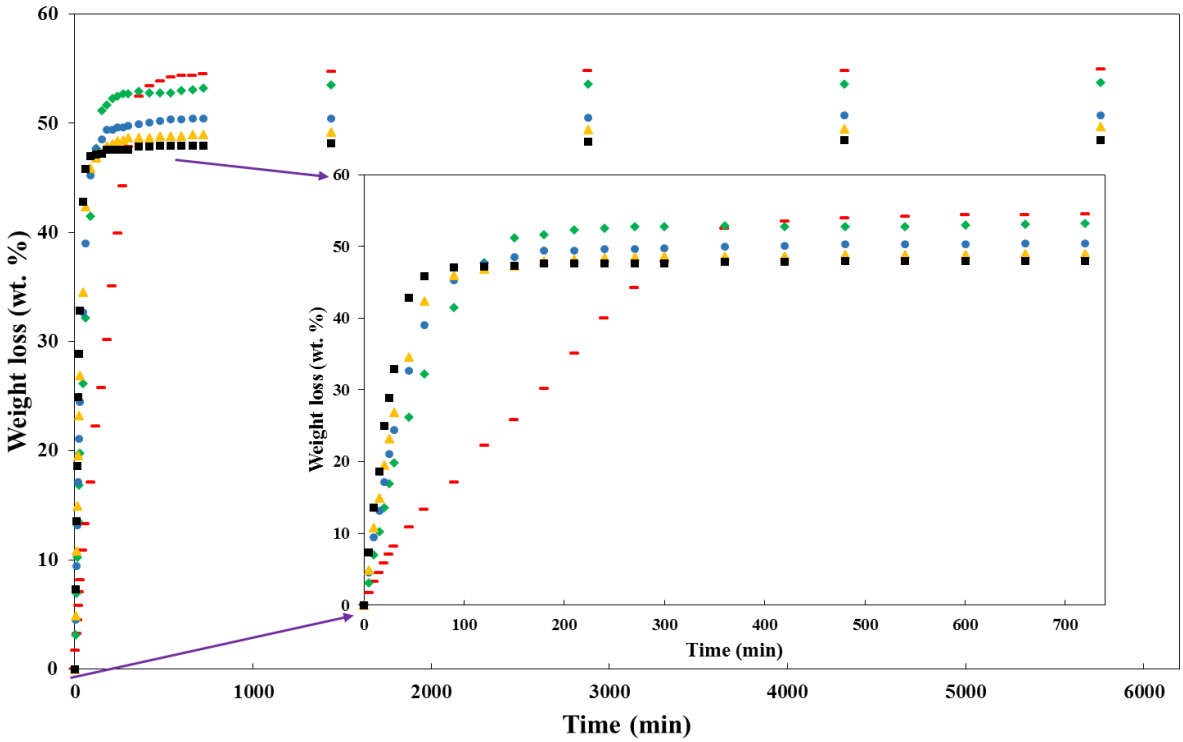

Figure 4.22: Weight loss profile for the crushed Hass avocado seeds at different temperatures. (-) 40 ºC, (♦) 50 ºC, (●) 60 ºC, (▲) 70 ºC, (■) 80 ºC [53].

The microscopic images of dried Hass avocado seeds after staining with Toluidine are shown in Figure 4.23. It can be seen that the lipid bodies are intact and preserved inside the seed. The dried powdered Hass avocado seeds were further utilized for the in-situ extraction and reaction process.

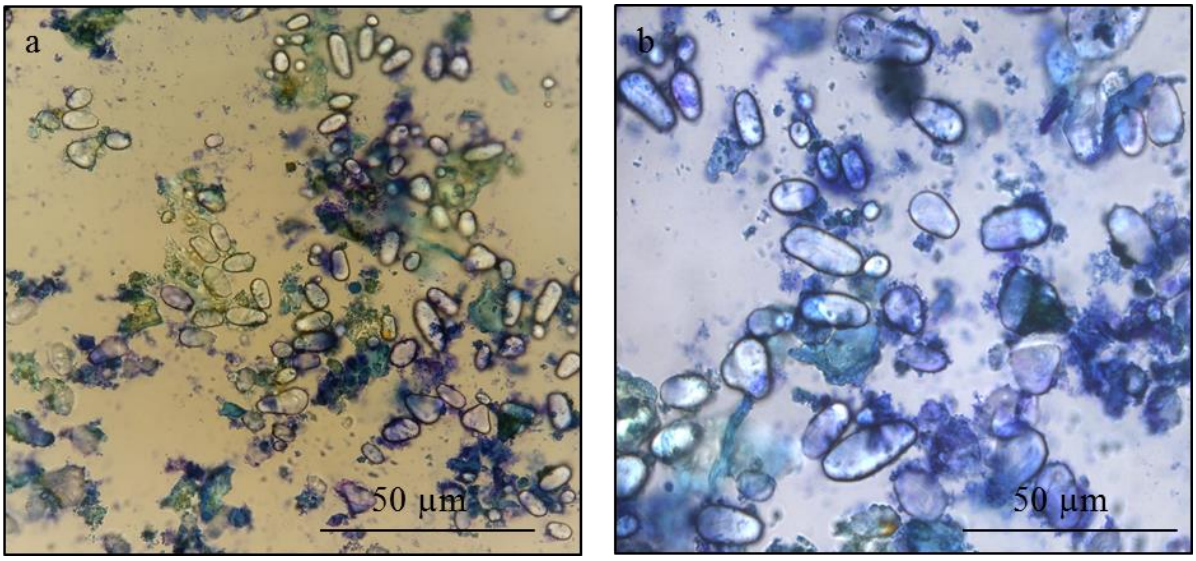

Figure 4.23: Microscopic images of dried Hass avocado seeds.

4.4.2. Reactive extraction

The effects of different temperatures and pressures on the in-situ extraction and reaction of Hass avocado seeds using ethanol were studied. The system pressure was observed to augment from 0.9 to 50.4 bar when the operating temperature was increased from 75 to 225 ºC. The color of the post-reaction mixture was found to be darkening with the increase in the temperature; indicating the positive impact of temperature on the reactive-extraction process. The change in the color of reactive extraction liquid at different temperatures is shown in Figure 4.24 (a, b, and c). On other hand, color of Hass avocado seeds turned from pale orange to black after the reactive extraction process performed at 225 ºC. The change in color of Hass avocado seeds after the reactive extraction processes is shown in Figure 4.24 (d, e, and f). The aliquots of the reaction mixture were periodically withdrawn (60, 120, 180, 240, 300 min) to understand the progression of extraction of biochemicals and reaction of lipid bodies. The product analysis of the experimental samples are currently under process.

Figure 4.24: Extractable liquid (a, b, and c) and avocado seeds after the reactive extraction (d, e, and f): 75 ºC (a and d), 150 ºC (b and e), 225 ºC (c and f).

4.4.3. Heat of combustion

The leftover Hass avocado seeds could be used for direct combustion in a biorefinery, and therefore measuring the heat of combustion of seeds is of importance. In the present study, we investigated the gross calorific value of Hass avocado seeds, before and after utilizing it for the reactive extraction process. The measured average calorific value of Hass avocado seeds before and after the reactive extraction process was 17.79 and 17.65 kJg^{-1}, respectively. The presented value for the heat of combustion of the leftover Hass avocado seeds was in the case of the reactive extraction performed at 150 ºC. The selection of the leftover Hass avocado seeds for the calorific value analysis was based on insignificant difference in the intensity of color of extractable liquid between 150 and 225 ºC. An insignificant reduction in the heating value of Hass avocado seeds after the extraction of chemicals observed. The heat of combustion even of the leftover being higher than coal indicated that this seed residue could be a potential combustion compound.

5. Mathematical modelling

5.1. Jojoba oil butanolysis process

In **Paper III**, the statistical analysis was initially performed to understand the interaction between the reaction variables and determine the optimal conditions affecting the CaO-catalyzed jojoba oil butanolysis process. The response for the statistical analysis is presented in Figure 1 in **Paper III**. The regression analysis indicated that the catalyst amount and butanol-to-oil molar ratio influenced the CaO-catalyzed jojoba oil butanolysis process, whereas, the butanol-to-oil molar ratio had a major impact on the process. The non-linear stage of the experimental design was also taken into consideration because the curvature value was higher than the confidence interval.

$$X_J = 54.04 + 4.51\,X_B + 5.97\,X_C - 4.69\,X_B^2 + 3.89\,X_{BC} - 3.89\,X_C^2 \quad (5.1)$$

$$X_J = -32.70 + 9.34\,X_B + 3.85\,X_C - 0.59\,X_B^2 + 0.34X_{BC} - 0.24\,X_C^2 \quad (5.2)$$

X_J is the conversion of jojoba oil occurring during the described butanolysis process.

The statistical quadratic regression equation was utilized to plot a three-dimensional graphical representation predicting the jojoba oil conversion with varying catalyst loading and butanol-to-oil molar ratio, which is shown in Figure 5.1. Within the studied experimental range, the jojoba oil conversion augmented with the increase in the n-butanol concentration and catalyst amount, indicating a possible interaction between n-butanol and CaO catalyst. However, the appliance of butanol-to-oil molar ratio and catalyst loading higher than the optimal value resulted in the slight drop of jojoba oil conversion. The regression model presented a good correlation between the experimental results and the predicted values, which validated that the regression model satisfactorily described the CaO-catalyzed jojoba oil butanolysis process within the studied range of reaction conditions.

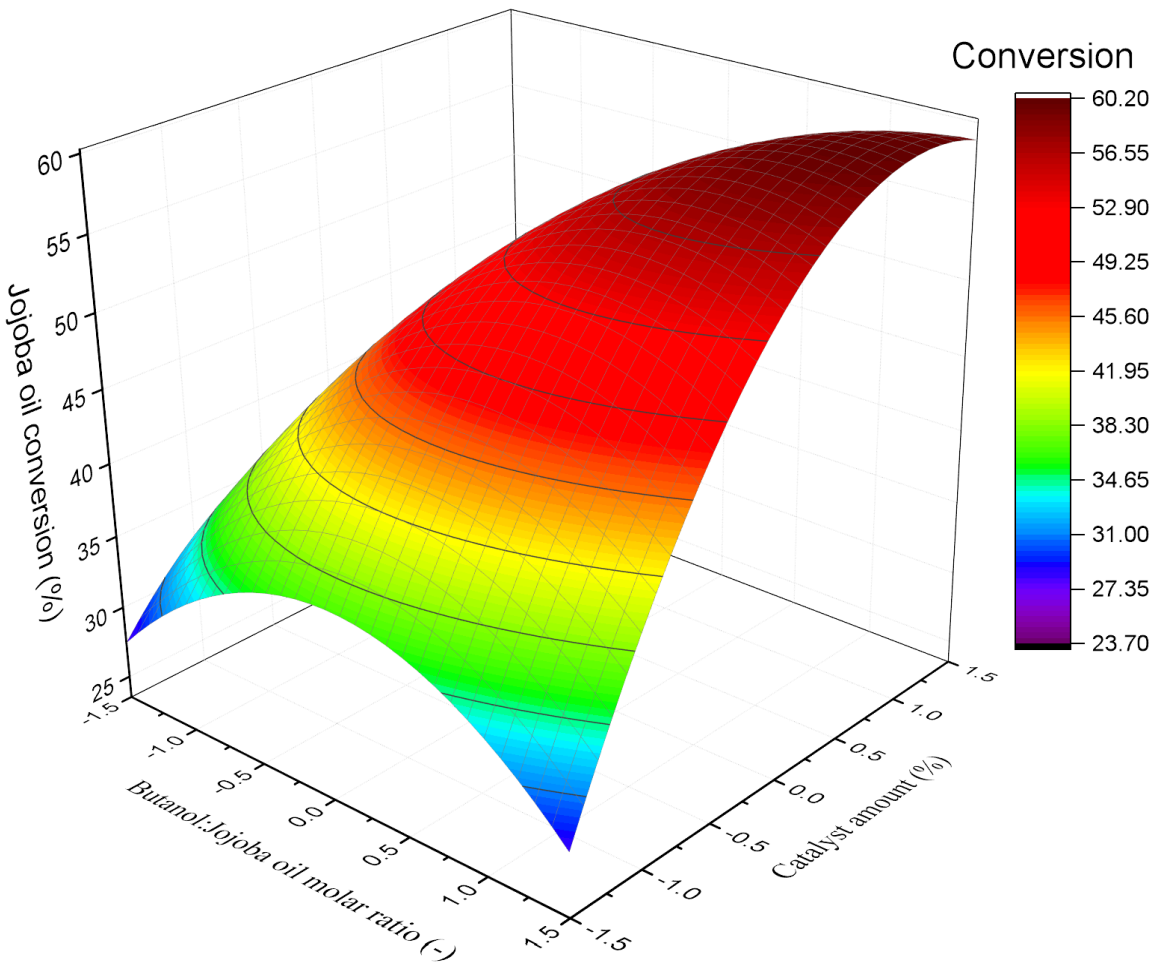

Figure 5.1: Response surface 3D plot indicating the influence of butanol-to-oil molar ratio and catalyst loading on the jojoba oil conversion. Temperature: 85 ºC, time: 600 min, stirring intensity: 350 rpm [157].

Furthermore, a mathematical model describing the chemical kinetics was developed to identify a step controlling the overall butanolysis process as well as to propose a plausible reaction mechanism. In regards to develop a best mathematical model for describing the kinetics of the CaO-catalyzed jojoba oil butanolysis process, several kinetic models were tested. For this purpose, different reaction pathways having adsorption of the reactant molecules on the catalytic sites, surface chemical reaction, and the reaction products desorption steps were taken into consideration. Different assumed reaction mechanisms for the heterogeneously catalyzed butanolysis reaction along with the model equations and the obtained SWE and MSC values are tabulated in Table 5.1.

Table 5.1: List of kinetic models applied for the CaO-catalyzed jojoba oil butanolysis reactions.

Model	Reaction pathway	Controlling Step	Model equation	Catalyst mass balance	MSC	SWE
1	$B + s \leftrightarrow Bs$ $Bs + J \leftrightarrow BE + JA + s$	1	$\frac{dX_J}{dt} = m\left[[C_B k_1] - \left[\frac{k_2 k_4 C_{BE} C_{JA}}{k_3 C_J}\right]\right]$	$m = \frac{m_0}{\left[1 + \left[\frac{k_4 C_{JA} C_{BE}}{C_J k_3}\right]\right]}$	3.93	1.24 x 10^{-2}
		2	$\frac{dX_J}{dt} = m\left[\left[\frac{k_3 k_1 C_B C_J}{k_2}\right] - k_4 C_{BE} C_{JA}\right]$	$m = \frac{m_0}{\left[1 + \left[\frac{k_1 C_B}{k_2}\right]\right]}$	4.13	4.39 x 10^{-3}
2	$B + s \leftrightarrow Bs$ $J + s \leftrightarrow Js$ $Bs + Js \leftrightarrow BEs + JA + s$ $BEs \leftrightarrow BE + s$	1	$\frac{dX_J}{dt} = m\left[k_1 C_B - \left[\frac{k_2 k_8 k_4 k_6 C_{BE} C_{JA}}{k_3 k_7 k_5 C_J}\right]\right]$	$m = \frac{m_0}{\left[1 + \left[\frac{k_4 k_6 k_8 C_{JA} C_{BE}}{C_J k_7 k_5 k_3}\right] + \left[\frac{k_3 C_J}{k_4}\right] + \left[\frac{k_8 C_{BE}}{k_7}\right]\right]}$	4.05	4.44 x 10^{-2}
		2	$\frac{dX_J}{dt} = m\left[k_3 C_J - \left[\frac{k_2 k_8 k_4 k_6 C_{BE} C_{JA}}{k_1 k_7 k_5 C_B}\right]\right]$	$m = \frac{m_0}{\left[1 + \left[\frac{k_2 k_6 k_8 C_{JA} C_{BE}}{C_B k_7 k_5 k_1}\right] + \left[\frac{k_1 C_B}{k_2}\right] + \left[\frac{k_8 C_{BE}}{k_7}\right]\right]}$	3.73	5.27 x 10^{-2}
		3	$\frac{dX_J}{dt} = m^2\left[\left[\frac{k_1 k_5 k_3 C_B C_J}{k_2 k_4}\right] - \left[\frac{k_6 k_8 C_{BE} C_{JA}}{k_7}\right]\right]$	$m = \frac{m_0}{\left[1 + \left[\frac{k_1 C_B}{k_2}\right] + \left[\frac{k_3 C_J}{k_4}\right] + \left[\frac{k_8 C_{BE}}{k_7}\right]\right]}$	3.66	6.04 x 10^{-3}
		4	$\frac{dX_J}{dt} = m\left[\left[\frac{k_7 k_1 k_5 k_3 C_B C_J}{k_2 k_4 k_6 C_{JA}}\right] - k_8 C_{BE} C_s\right]$	$m = \frac{m_0}{\left[1 + \left[\frac{k_1 C_B}{k_2}\right] + \left[\frac{k_3 C_J}{k_4}\right] + \left[\frac{k_3 k_5 k_1 C_B C_J}{k_4 k_2 k_6 C_{JA}}\right]\right]}$	3.12	7.55 x 10^{-2}

Table 5.1: List of kinetic models applied for the CaO-catalyzed jojoba oil butanolysis reactions.

Model	Reaction pathway	Controlling Step	Model equation	Catalyst mass balance	MSC	SWE
3	$B + s \leftrightarrow Bs$ $J + s \leftrightarrow Js$ $Bs + Js \leftrightarrow BE + JA + 2s$	1	$\frac{dX_J}{dt} = m\left[k_1 C_B - \left[\frac{k_2 k_4 k_6 C_{BE} C_{JA}}{k_3 k_5 C_J}\right]\right]$	$m = \frac{m_0}{\left[1 + \left[\frac{k_4 k_6 C_{JA} C_{BE}}{C_J k_5 k_3}\right] + \left[\frac{k_3 C_J}{k_4}\right]\right]}$	3.55	1.44 x 10^{-2}
		2	$\frac{dX_J}{dt} = m\left[k_3 C_J - \left[\frac{k_2 k_4 k_6 C_{BE} C_{JA}}{k_1 k_5 C_B}\right]\right]$	$m = \frac{m_0}{\left[1 + \left[\frac{k_2 k_6 C_{JA} C_{BE}}{C_B k_5 k_1}\right] + \left[\frac{k_1 C_B}{k_2}\right]\right]}$	3.60	1.27 x 10^{-2}
		3	$\frac{dX_J}{dt} = m^2\left[\left[\frac{k_3 k_5 k_1 C_B C_J}{k_2 k_4}\right] - k_6 C_{JA} C_{BE}\right]$	$m = \frac{m_0}{\left[1 + \left[\frac{k_4 k_6 C_{JA} C_{BE}}{C_J k_5 k_3}\right] + \left[\frac{k_3 C_J}{k_4}\right]\right]}$	3.90	4.33 x 10^{-3}
4	$B + s \leftrightarrow Bs$ $Bs + J \leftrightarrow BEs + JA$ $BEs \leftrightarrow BE + s$	1	$\frac{dX_J}{dt} = m\left[C_B k_1 - \left[\frac{k_4 k_6 k_2 C_{BE} C_{JA}}{C_J k_3 k_5}\right]\right]$	$m = \frac{m_0}{\left[1 + \left[\frac{k_4 k_6 C_{JA} C_{BE}}{k_5 k_3 C_J}\right] + \left[\frac{k_6 C_{BE}}{k_5}\right]\right]}$	3.58	9.65 x 10^{-3}
		2	$\frac{dX_J}{dt} = m\left[\left[\frac{k_1 k_3 C_B C_J}{k_2}\right] - \left[\frac{k_4 k_6 C_{BE} C_{JA}}{k_5}\right]\right]$	$m = \frac{m_0}{\left[1 + \left[\frac{k_1 C_B}{k_2}\right] + \left[\frac{k_6 C_{BE}}{k_5}\right]\right]}$	4.27	3.20 x 10^{-3}
		3	$\frac{dX_J}{dt} = m\left[\left[\frac{k_1 k_3 k_5 C_B C_J}{k_2 k_4 C_{JA}}\right] - k_6 C_{BE}\right]$	$m = \frac{m_0}{\left[1 + \left[\frac{k_1 k_3 C_J C_B}{C_{JA} k_4 k_2}\right] + \left[\frac{k_1 C_B}{k_2}\right]\right]}$	3.23	1.14 x 10^{-2}

By fitting the experimental data with the model, the best kinetic option for the described butanolysis process included the below mentioned features:

- It was understood that the alcoholysis reaction occurs between n-butanol molecules chemisorbed on the catalytic surface and jojoba oil molecules present in the butanol phase close to the active sites.
- The overall process rate is controlled by the surface reaction step occurring between chemisorbed butoxide ions and the jojoba oil molecules in the bulk phase.
- The butanol adsorption as well as desorption of the reaction product (FABE) is reached spontaneously, and does not limit the overall rate of the reaction.
- The overall alcoholysis reaction on the catalytic surface follows pseudo-first order kinetics with respect to jojoba oil.

The proposed reaction pathway for the heterogeneous CaO-catalyzed jojoba oil butanolysis process was found to be equivalent to the Eley-Rideal mechanism which includes three main steps: adsorption of alcohol, surface reaction and desorption of the reaction product. The butanolysis process occurred between the butoxide molecules chemisorbed on the catalytic active sites and jojoba oil molecules present in the liquid phase. In the biphasic reaction system, the rate of the butanolysis process was controlled by the surface reaction step, and the fractional conversion of jojoba oil was expressed as:

$$\frac{dX_J}{dt} = m\left[\left[\frac{1254.69\, e^{-(8844.77/RT)} * 182.61\, e^{-(10885.80/RT)} * C_B * C_J}{174.38\, e^{-(6644.63/RT)}}\right] - \left[\frac{11815.30\, e^{-(12437.30/RT)} * 135.75\, e^{-(9754.46/RT)} * C_{BE} * C_{JA}}{17.57\, e^{-(43.68/RT)}}\right]\right] \quad (5.3)$$

$$m = \frac{m_0}{\left[1 + \left[\frac{1254.69\, e^{-(8844.77/RT)} * C_B}{174.38\, e^{-(6644.63/RT)}}\right] + \left[\frac{135.75\, e^{-(9754.46/RT)} * C_{BE}}{17.57\, e^{-(43.68/RT)}}\right]\right]} \quad (5.4)$$

The graphical representation for the simulation of the experimental data using the proposed kinetic model at different reaction temperatures, butanol-to-oil molar ratios, and catalyst amounts are presented as solid lines in Figure 5.2, 5.3, and 5.4, respectively. The complete proposed reaction mechanism for the butanolysis reaction is shown in Figure 5.5.

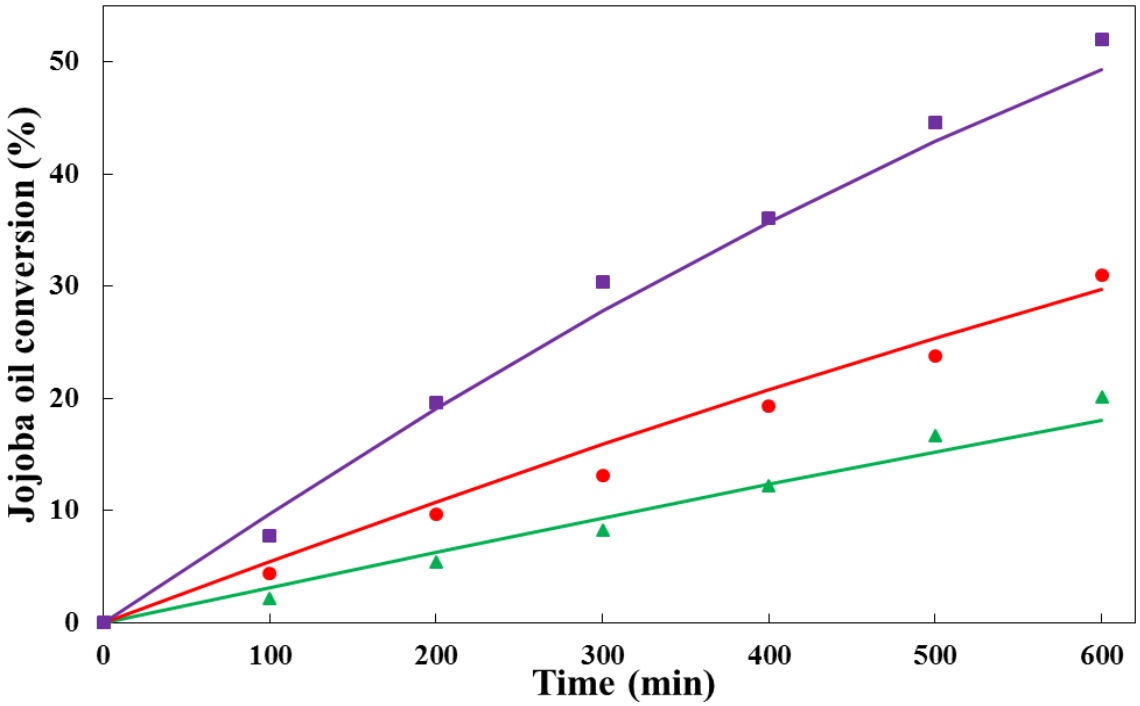

Figure 5.2: Comparison of the experimental data and simulated values for the temperature impact on the jojoba oil conversion. Temperature- (▲): 65 ºC, (●): 75 ºC, (■): 85 ºC. Experimental data: symbols, kinetic model: lines [158].

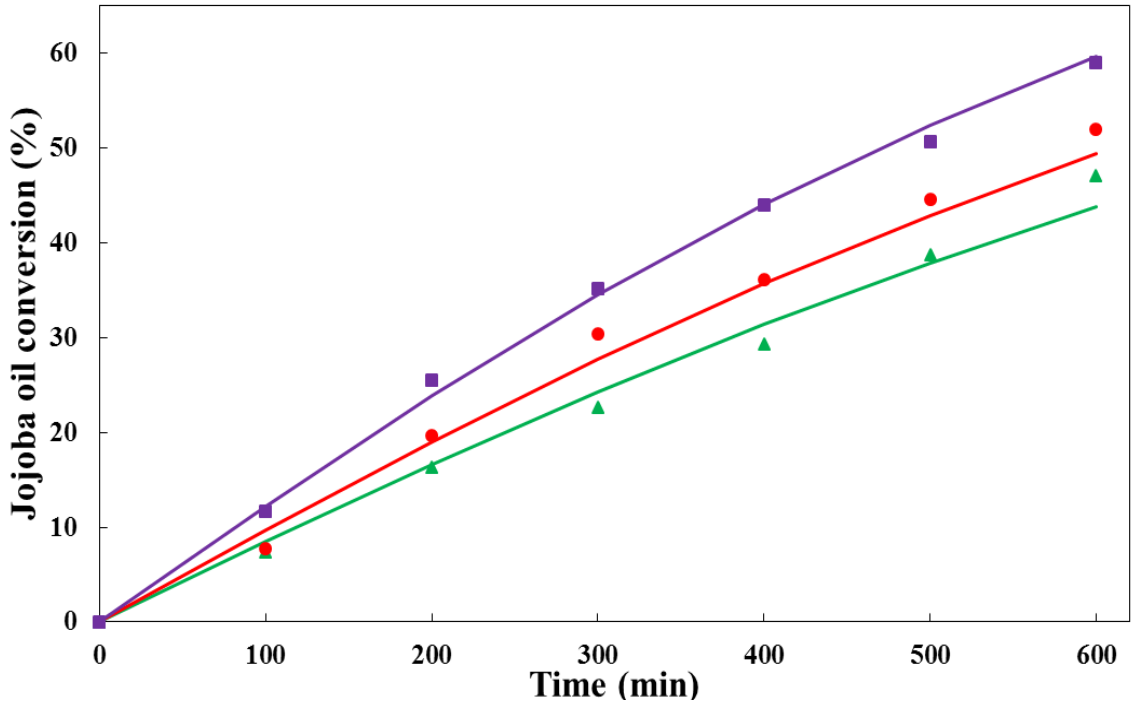

Figure 5.3: Comparison of the experimental data and simulated values for the butanol-to-oil impact on the jojoba oil conversion. Butanol-to-oil molar ratio- (▲): 7.2:1, (●): 10:1, (■): 12.8:1. Experimental data: symbols, kinetic model: lines [158].

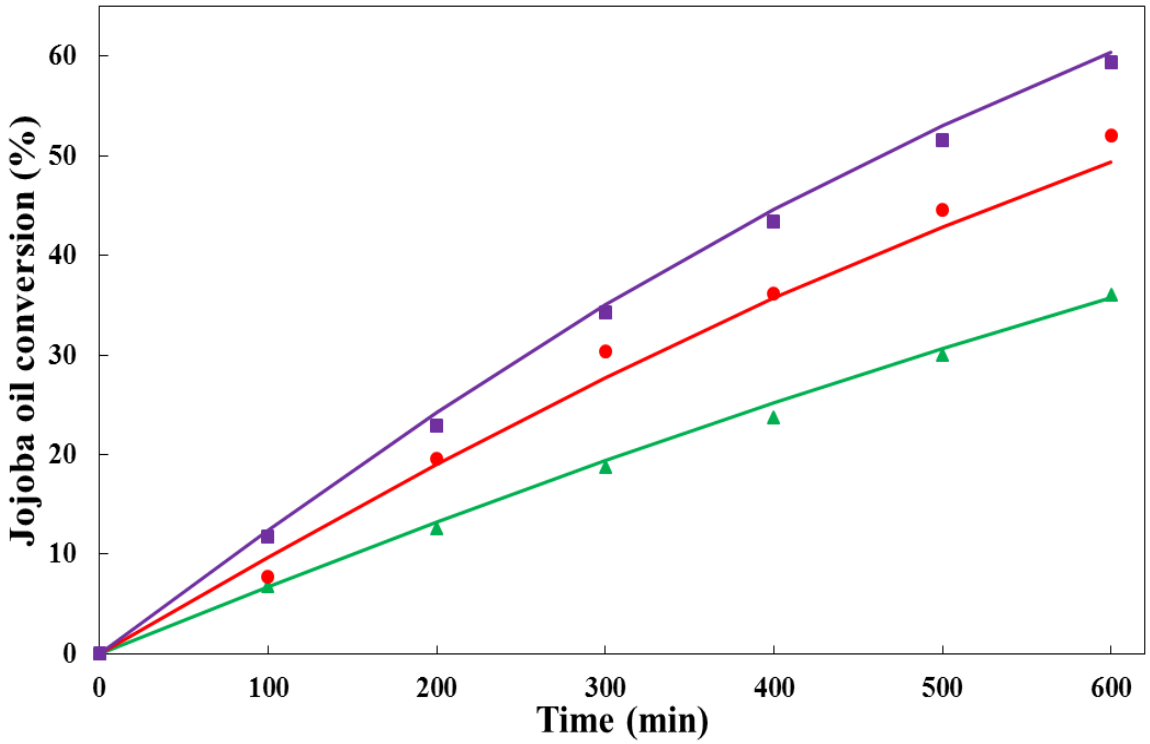

Figure 5.4: Comparison of the experimental data and simulated values for the impact of catalyst loading on the jojoba oil conversion. Catalyst loading- (▲): 8 wt. %, (●): 12 wt. %, (■): 16 wt. %. Experimental data: symbols, kinetic model: lines [158].

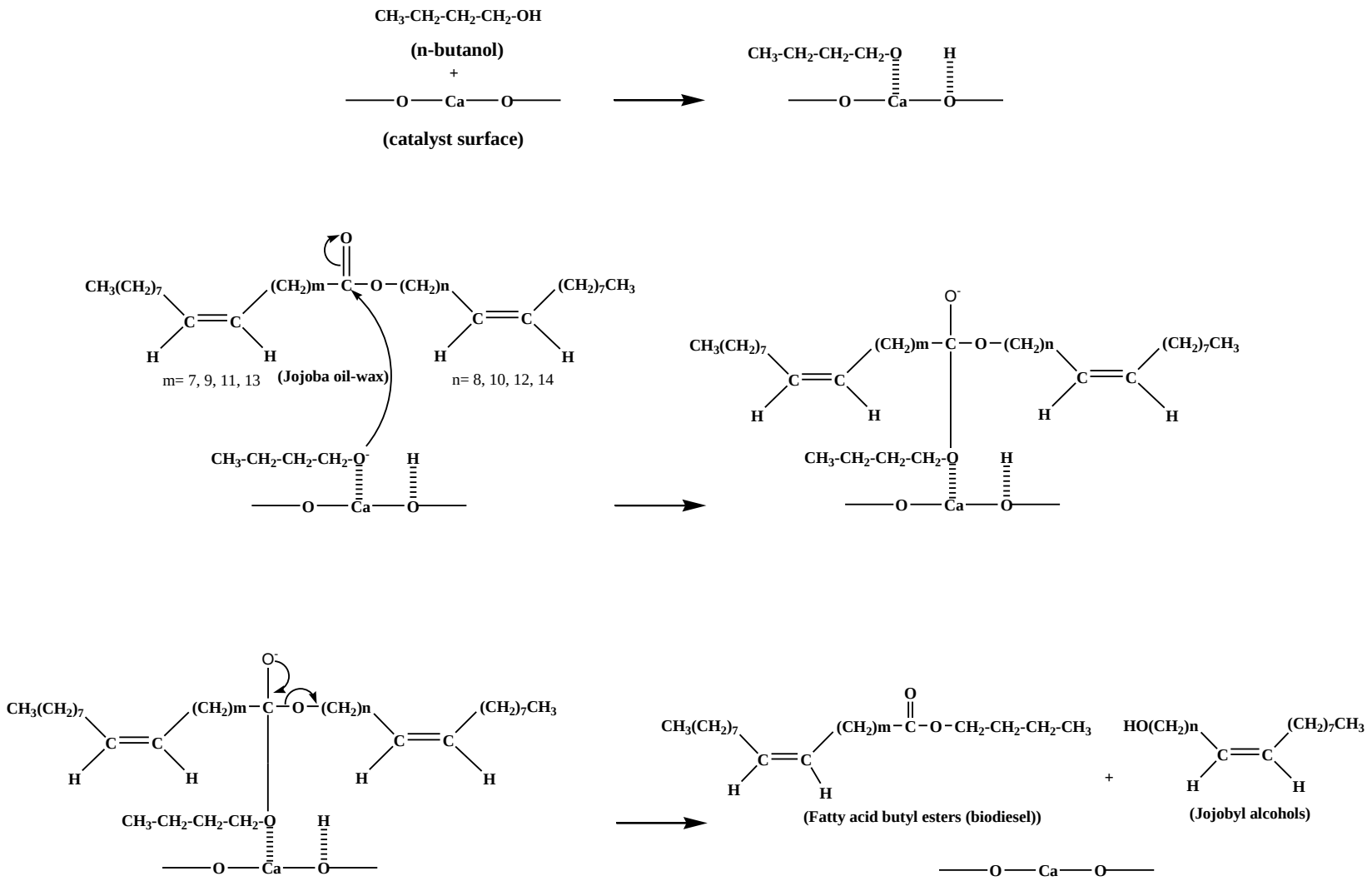

Figure 5.5: Proposed reaction mechanism for the CaO-catalyzed jojoba oil butanolysis reaction [158].

5.2. *Jatropha curcas* oil methanolysis process

In **Paper IV**, the statistical analysis was performed to determine the interaction between the reaction variables (methanol-to-oil molar ratio and catalyst amount), their influence on the methanolysis reaction, and optimum parameters affecting the CaDg-catalyzed CJCO methanolysis process. The response for the statistical analysis is presented in Table 2 in **Paper IV**. The obtained results suggested that both catalyst loading and methanol-to-oil molar ratio significantly affected the process, because the influence of both variables was considerably higher than the confidence interval. The regression analysis suggested that the curvature had a positive influence on the described methanolysis process under the investigated experimental range. The non-linear stage of the design of experiments was also taken into consideration to fit the experimental data with a quadratic model because the curvature was found to be higher than the confidence curvature interval. A superior-fitting response surface statistical and industrial quadratic mathematical model for the glycerol enriched CaO assisted CJCO methanolysis process are expressed in Equation 5.5 and 5.6, respectively.

$$X_{CJCO} = 93.12 + 4.19\,X_M + 3.23\,X_C - 1.80\,X_M^2 - 1.87\,X_{MC} - 1.03\,X_C^2 \quad (5.5)$$

$$X_{CJCO} = -5.39 + 8.13\,X_M + 6.32\,X_C - 0.20\,X_M^2 - 0.20\,X_{MC} - 0.11\,X_C^2 \quad (5.6)$$

The statistical quadratic regression equation was applied to plot a three-dimensional graphical representation predicting the CJCO conversion with varying catalyst loading and methanol-to-oil molar ratio, which is shown in Figure 5.6. Within the studied experimental range, the CJCO conversion augmented with the increase in methanol-to-CJCO molar ratio and catalyst loading, hinting towards the possible interaction between methanol and glycerol-enriched CaO catalyst. The presented regression model presented an appreciable correlation between the experimental results and the predicted values, which validated that the presented regression model satisfactorily described the glycerol enriched CaO assisted CJCO methanolysis process within the studied range of reaction conditions.

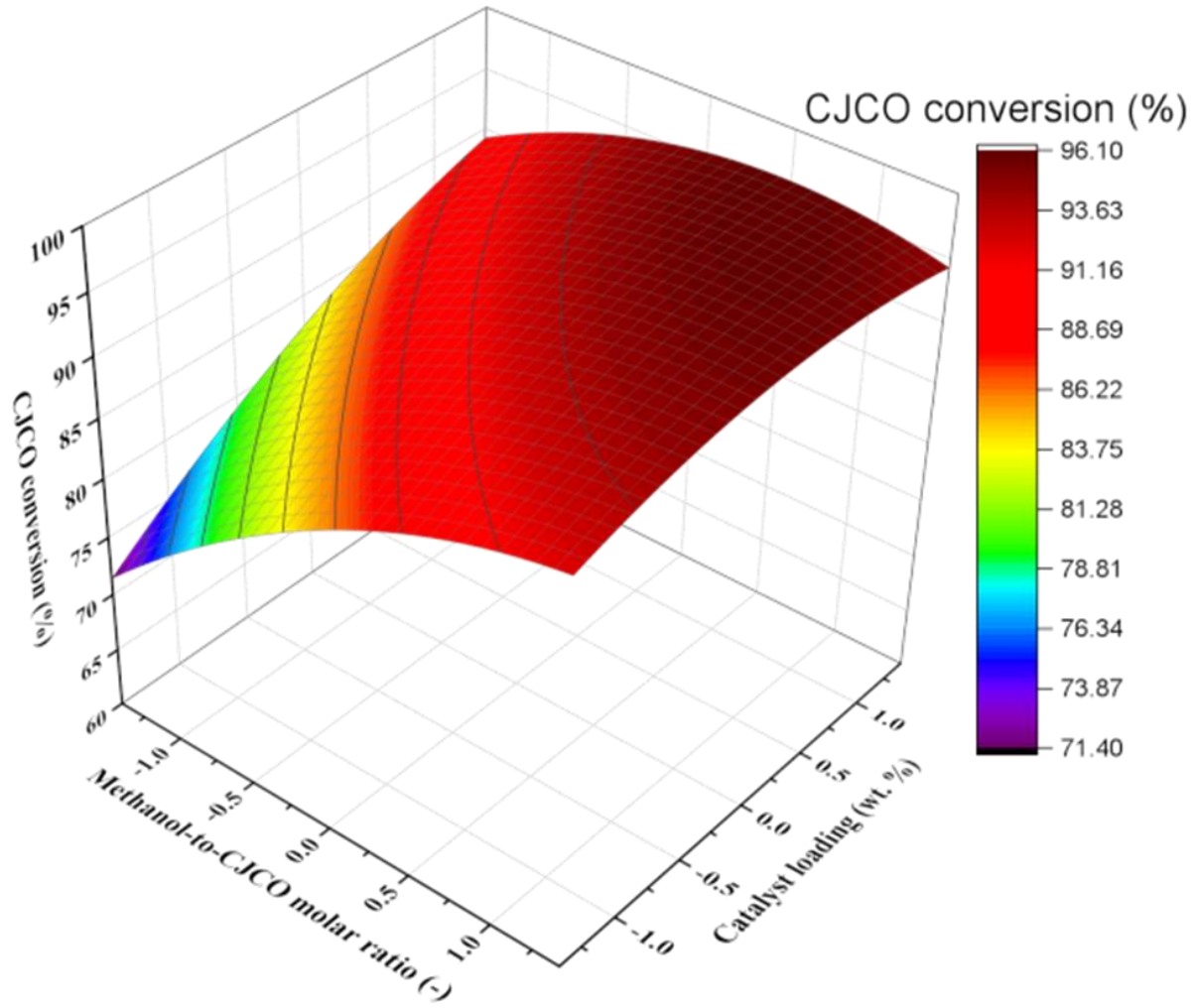

Figure 5.6: Response surface 3D plot indicating the influence of methanol-to-oil molar ratio and catalyst loading on the CJCO conversion. Glycerol dose: 10% (w.r.t. cat. wt.), temperature: 65ºC, time: 420 min, stirring intensity: 350 rpm.

5.3. Avocado oil ethanolysis process

In **Paper V**, initially a kinetic model proposed by Lukić et al. [158] for the CaDg-catalyzed sunflower oil methanolysis reaction was applied for the present ethanolysis process due to similar nature of the catalyst. However, no appreciable fitting between the experimental data and the predicted values was obtained; indicating that the kinetic model applied for the methanolysis process is not suitable for the current ethanolysis reaction. A previously developed mathematical model applied for the base-catalyzed ethanolysis process was subsequently tested for the current ethanolysis process [159].

The kinetic model included below mentioned features:

- The alcoholysis reaction occurred between ethanol molecules chemisorbed on the catalytic surface and oil molecules present in the ethanol phase close to the active sites.
- The overall process rate is controlled by the adsorption of an alcohol over the solid catalytic surface.
- The alcohol adsorption is rapid, and all reaction steps are elementary.
- FAEEs, due to their non-polar nature, does not adsorb on the catalytic surface.

The steps involved in the proposed reaction pathway could be presented as:

$$E + cs \underset{k_2}{\overset{k_1}{\longleftrightarrow}} Ecs \tag{5.7}$$

$$TAGs + Ecs \underset{k_4}{\overset{k_3}{\longleftrightarrow}} FAEEs + DAGs + cs \tag{5.8}$$

$$DAGs + Ecs \underset{k_6}{\overset{k_5}{\longleftrightarrow}} FAEEs + MAGs + cs \tag{5.9}$$

$$MAGs + Ecs \underset{k_8}{\overset{k_7}{\longleftrightarrow}} FAEEs + G + cs \tag{5.10}$$

where, cs is the catalytic active sites.

The differential equations to evaluate the variation in the concentration of the chemical components involved in the ethanolysis reaction are as below:

$$\frac{dC_{TAGs}}{dt} = [-k_3 C_{TAGs} C_E K + k_4 C_{DAGs} C_{FAEEs}] \cdot m \tag{5.11}$$

$$\frac{dC_{DAGs}}{dt} = [k_3 C_{TAGs} C_E K - k_4 C_{DAGs} C_{FAEEs} - k_5 C_{DAGs} C_E K + k_6 C_{MAGs} C_{FAEEs}] \cdot m \tag{5.12}$$

$$\frac{dC_{MAGs}}{dt} = [k_5 C_{DAGs} C_E K - k_6 C_{MAGs} C_{FAEEs} - k_7 C_{MAGs} C_E K + k_8 C_G C_{FAEEs}] \cdot m \tag{5.13}$$

$$\frac{dC_G}{dt} = [k_7 C_{MAGs} C_E K - k_8 C_G C_{FAEEs}] \cdot m \tag{5.14}$$

$$\frac{dC_{FAEEs}}{dt} = [k_3 C_{TAGs} C_E K - k_4 C_{DAGs} C_{FAEEs} + k_5 C_{DAGs} C_E K - k_6 C_{MAGs} C_{FAEEs} + k_7 C_{MAGs} C_E K - k_8 C_G C_{FAEEs}] \cdot m \tag{5.15}$$

$$\frac{dC_E}{dt} = -[k_3 C_{TAGs} C_E K - k_4 C_{DAGs} C_{FAEEs} + k_5 C_{DAGs} C_E K - k_6 C_{MAGs} C_{FAEEs} + k_7 C_{MAGs} C_E K - k_8 C_G C_{FAEEs}] \cdot m \quad (5.16)$$

$$k = A \cdot exp^{-E_a/RT} \quad (5.17)$$

$$m = \left[\frac{m_0}{(1+C_E K)}\right] \quad (5.18)$$

where, k_1, k_3, k_5, and k_7 are the specific rate constants for the reactions in the forward direction; k_2, k_4, k_6, and k_8 are the specific rate constants for the reactions in the reverse direction; C_{TAGs}, C_{DAGs}, C_{MAGs}, C_G, C_{FAEEs}, and C_E is the concentration of TAGs, DAGs, MAGs, G, FAEEs, and ethanol , respectively, at time t; m_0 is the initial mass of the catalyst (g); m is the mass of the catalytic sites involved in the reaction (g); A is the pre-exponential factor of the Arrhenius equation (min^{-1}); Ea is the activation energy (cal mol^{-1}); R is the universal gas constant (1.98 cal K^{-1} mol^{-1}); T is the absolute temperature (K).

The simulation curves for the variation in the concentration of TAGs at different temperature, ethanol-to-oil molar ratio, and the catalyst amount is presented as lines in Figure 5.7(a), 5.7(b), and 5.7(c), respectively. Whereas, the prediction for the change in the FAEEs concentration with time at different temperature, ethanol-to-oil molar ratio, and the catalyst amount can be seen as lines in Figure 5.8(a), 5.8(b), and 5.8(c), respectively.

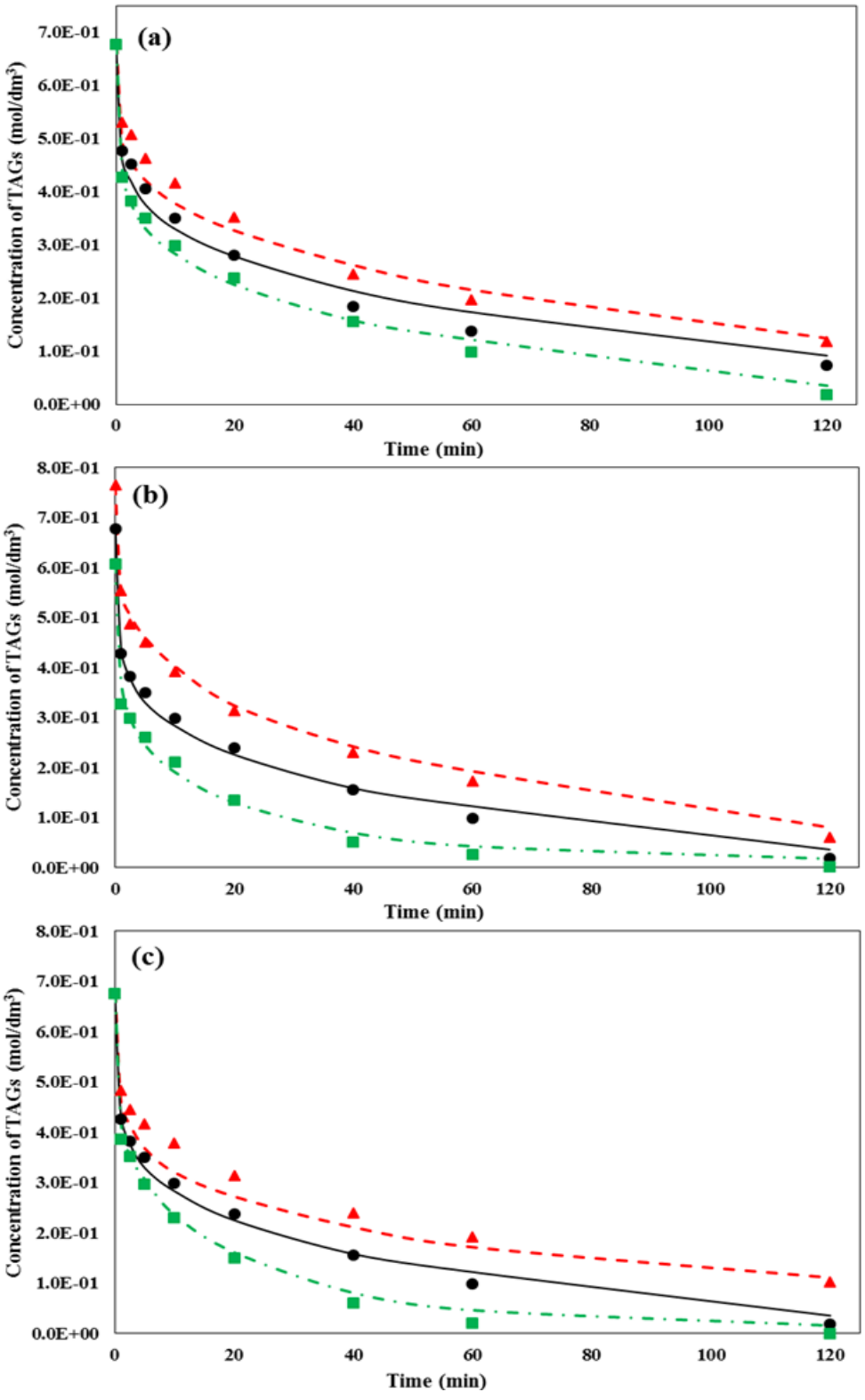

Figure 5.7: Comparison between the experimental data and the predicted values for the variation in the TAGs concentration due to the impact of (a) temperature (▲-55 ºC, ●-65 ºC, ■-75 ºC), (b) ethanol-to-oil molar ratio (▲-6:1, ●-9:1, ■-12:1), and (c) catalyst amount (▲-4 wt. %, ●-7 wt. %, ■-10 wt. %). Experimental data: symbols, kinetic model: lines [160].

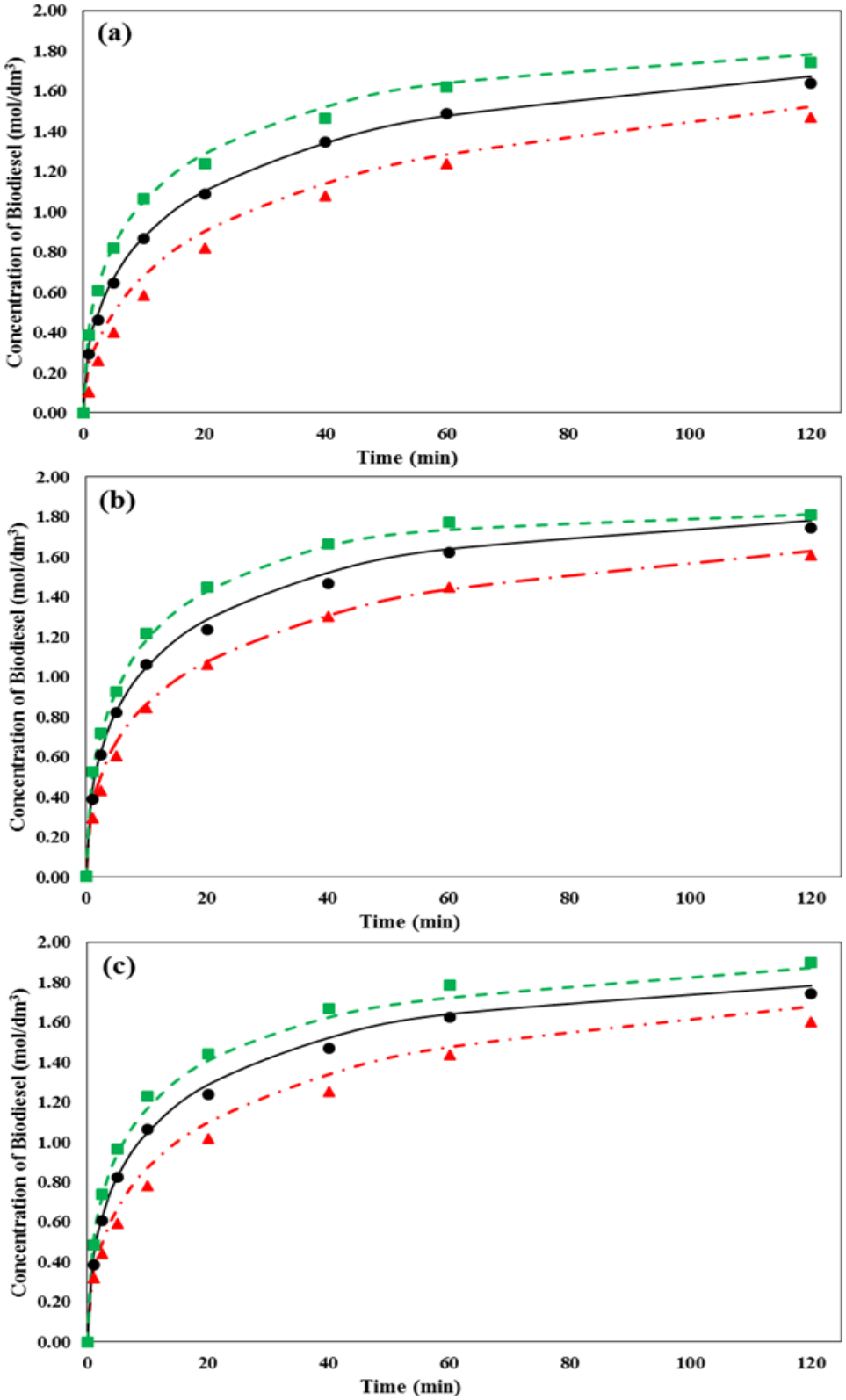

Figure 5.8: Comparison between the experimental data and the predicted values for the variation in the FAEEs concentration due to the impact of (a) temperature (▲-55 ºC, ●-65 ºC, ■-75 ºC), (b) ethanol-to-oil molar ratio (▲-6:1, ●-9:1, ■-12:1), and (c) catalyst amount (▲-4 wt. %, ●-7 wt. %, ■-10 wt. %). Experimental data: symbols, kinetic model: lines [160].

5.4. Mathematical modelling of the drying kinetics of Hass avocado seeds

In **Paper VII**, we performed the simulation of the experimental results for the drying process of Hass avocado seeds reported in **Paper VI**. In this study we presented a new semi-theoretical model, the proficiency of which to describe the drying kinetics of Hass avocado seeds was compared with the extensively applied Lewis, Henderson and Pabis, and Page mathematical model. Initially, four semi-theoretical mathematical models were compared versus the experimental drying curves obtained at 60 ºC for the non-pretreated, sliced, and crushed Hass avocado seeds, respectively. A comparison between four mathematical models to simulate the experimental data in the case of non-pretreated, sliced, and crushed is shown in Figure 3(a), 3(b), and 3(c), respectively in **Paper VII**. The graphical representation suggested that all four mathematical models are suitable to describe the drying kinetics of Hass avocado seeds; however, the best model was selected based on the statistical parameters, such as coefficient of determination, square error, root mean square error, mean bias error, and mean absolute error of the deviation. Among the four tested mathematical models, the Avhad and Marchetti model was found to have a better fitting with the experimental data, with the values of coefficient of determination in the case of non-pretreated, sliced, and crushed Hass avocado seeds being higher than 0.98, 0.99, and 0.99, respectively. Furthermore, the square error and root mean square error was lower using the Avhad and Marchetti model in all three cases (non-pretreated, sliced, and crushed). The Avhad and Marchetti model is represented as:

$$MR = a\,exp(-kt^N) \tag{5.19}$$

where, k, a, and N are the constants of model. k follows an Arrhenius expression.

The value of the activation energy for the non-pretreated, sliced, and crushed Hass avocado seeds in the case of Avhad and Marchetti model was 128.43, 34.18, and 31.10 kJ mol^{-1}, respectively. The computed activation energy in the case of sliced and crushed Hass avocado seeds were in agreement with those reported for other agricultural substances, such as grape seeds [161], kale [162], and hull-less seed pumpkin [163]. The graphical representation for the Avhad and Marchetti model prediction with the experimental data at 50-80 ºC air temperatures for the non-pretreated, sliced, and crushed Hass avocado seeds is shown in Figure 5.9, 5.10, and 5.11, respectively.

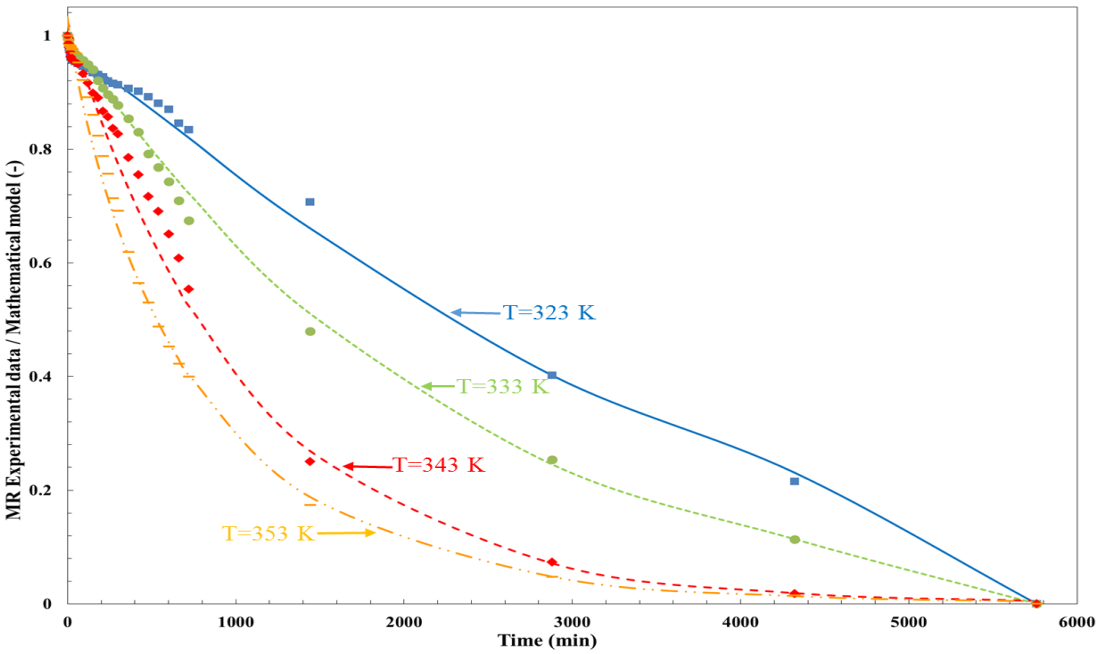

Figure 5.9: Comparison of the experimental and predicted moisture ratio using the Avhad and Marchetti drying mathematical models at 50-80 ºC air temperatures for the non-pretreated Hass avocado seeds: (■) Experimental data, (—) Model, (●) Experimental data, (—) Model, (♦) Experimental data, (—) Model, (—) Experimental data, (—) Model [164].

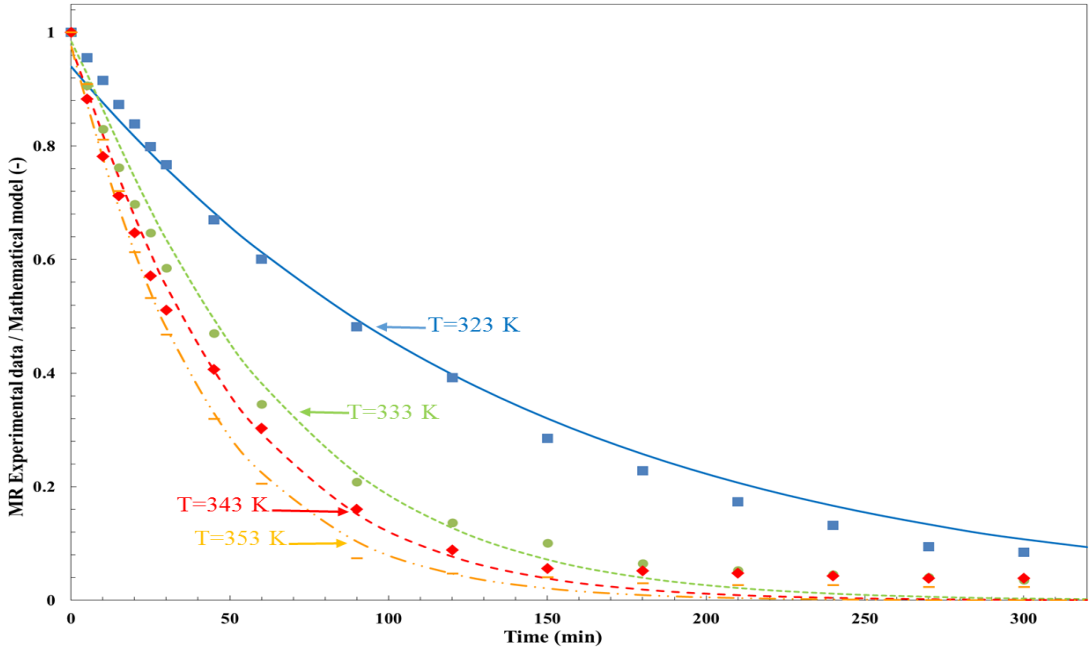

Figure 5.10: Comparison of the experimental and predicted moisture ratio using the Avhad and Marchetti drying mathematical models at 50-80 ºC air temperatures for the sliced Hass avocado seeds: (■) Experimental data, (—) Model, (●) Experimental data, (—) Model, (♦) Experimental data, (—) Model, (—) Experimental data, (—) Model [164].

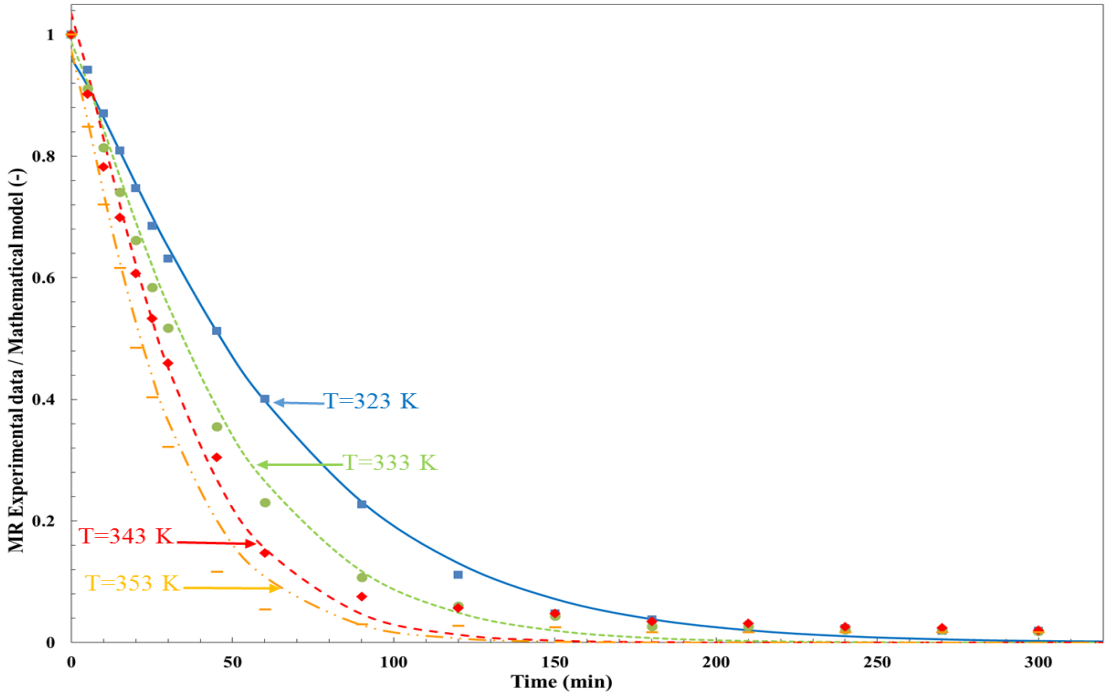

Figure 5.11: Comparison of the experimental and predicted moisture ratio using the Avhad and Marchetti drying mathematical models at 50-80 ºC air temperatures for the crushed Hass avocado seeds: (■) Experimental data, (—) Model, (●) Experimental data, (—) Model, (♦) Experimental data, (—) Model, (—) Experimental data, (—) Model [164].

6. Conclusion

The present thesis attempted to systematically address four segments related to the production of biochemicals, with an emphasis on biodiesel: (i) utilization of non-edible lipid biomass feedstock, (ii) application of highly active and cost-effective heterogeneous catalysts for the alcoholysis process, (iii) the reactive extraction methodology with a viewpoint of the process integration, and (iv) the mathematical modelling of the experimental findings.

Paper I prudently discussed different variety of lipid feedstocks, catalysts, and the methodologies recently applied for biodiesel production. Based on large number of publications, it was clear that the alcoholysis methodology has been widely applied for biodiesel production. Several non-edible feedstocks have emerged as a potential raw material for the synthesis of biodiesel in view of reducing the cost of this biofuel and eliminating the 'food versus fuel' debate. However, the presence of impurities and high free fatty acids content in the non-edible feedstocks have profoundly affected the performance of conventional homogeneous catalytic materials. This in return has hindered the upscaling of biodiesel production from non-edible oils. Consequently, great amount of scientific efforts are involved in developing an active and stable heterogeneous catalytic system that holds the potential to successfully convert non-edible and crude lipid feedstocks to biodiesel. Since recent few years, broad ranges of catalytic materials have been researched for the alcoholysis process to increase the biodiesel yield in low processing time. The proficiency of several heterogeneous catalysts to assist the alcoholysis process is distinctly reviewed in **Paper II**. Though heterogeneous catalysts are expedient due to their easy separation from the post-reaction mixture and reutilization for the next cycle, it is foremost relevance to consider the monetary investment made in regulating their textural morphology, surface area, and porosity. **Paper I** and **II** concluded that among different forms of heterogeneous catalysts, calcium oxide presently can gain scientific as well as industrial importance as a promising solid catalyst for biodiesel production from non-edible plant oils because of its high basicity, low solubility, easy synthesis from natural resources, and low cost.

In **Paper III**, the catalytic activity calcium oxide derived from waste *Mytilus Galloprovincialis* shells was tested for the butanolysis reaction of jojoba oil to produce value-added jojobyl alcohols and biodiesel. The presented study suggested that *M. Galloprovincialis* shells derived

calcium oxide was not only simple to synthesize and inexpensive but also displayed good capability to accelerate the butanolysis reaction of jojoba oil. The statistical analysis suggested that the n-butanol concentration had a major impact on the process. The maximum jojoba oil conversion of 96.11 % was registered after 1800 min of transesterification reaction performed at 85 ºC using butanol-to-oil molar ratio of 10:1, catalyst amount of 12 wt. %, and 350 rpm stirring intensity. The kinetics of the calcium oxide catalyzed jojoba oil butanolysis reaction was systematically studied to validate the reaction mechanism and simulate the process using a mathematical model. The developed kinetic model involved a three-step reaction pathway that was equivalent to the Eley-Rideal one. The present study concluded that the butanolysis reaction occurred between the surface chemisorbed butoxide ions and jojoba oil molecules in the liquid phase, whereas, the overall process was controlled by the surface reaction. The proposed kinetic model presented a good agreement between the predicted values and the experimental data. For this reason, the presented kinetic model can be considered as valid for the prediction of the calcium oxide-catalyzed jojoba oil butanolysis process. Since jojoba oil is a non-triglycerides based oil, the interaction of calcium oxide with glycerol is not existent. Calcium oxide, however, experiences material transformation during the progression of the alcoholysis of triglycerides based plant oils due to its reaction with the generating glycerol. The initial stage of the alcoholysis reaction is catalyzed by the calcium oxide phase of the catalyst, after which the material reacts with the co-generating glycerol and is transformed to calcium diglyceroxide. Since calcium diglyceroxide was characterized as chemically stable heterogeneous catalyst and not prone for deactivation due to the surrounding air and moisture, it was recommended to transform calcium oxide to calcium diglyceroxide compounds before applying for the alcoholysis process. In **Paper IV**, the waste *M. Galloprovincialis* shells derived calcium oxide was transformed to calcium diglyceroxide prior to the utilization of catalyst to assist a single-step methanolysis reaction of crude *jatropha curcas* oil consisting of high free fatty acids content. The results presented in the thesis concluded that calcium diglyceroxide displayed superior catalytic performance than the commercial as well as laboratory synthesized calcium oxide. The glycerol dose of 10 % with respect to catalyst weight was sufficient to enable the structural tuning of calcium oxide, while the newly prepared glycerol-activated calcium oxide catalyst was highly active for the methanolysis process merely at 65 ºC temperature. The experimental findings suggested that the application of methanol-to-oil molar

ratio of 9:1 and 15 wt. % catalyst amount was appropriate to achieve satisfactory oil conversion after 420 min of the methanolysis reaction. Whereas, the statistical analysis suggested that both methanol-to-oil molar ratio and the catalyst amount significantly affected the crude *jatropha curcas* oil methanolysis process. Because of high activity of calcium diglyceroxide for the methanolysis reactions, same heterogeneous catalyst was further applied for the ethanolysis of refined avocado oil with an objective to study the kinetics of the process in **Paper V**. This study carefully examined the impact of temperature, ethanol-to-oil molar ratio, and the catalyst amount of the oil conversion and biodiesel yield, wherein the increase in respective parameter accelerated the rate of the ethanolysis reaction. The experimental findings presented in the thesis concluded that the utilization of temperature of 75ºC, ethanol-to-oil molar ratio of 9:1, and 7 wt. % catalyst amount were suitable for the studied calcium diglyceroxide-catalyzed avocado oil ethanolysis process. The mathematical modelling of the present ethanolysis process concluded that the transesterification reaction occurred on between the surface chemisorbed ethoxide ions and oil molecules in the liquid phase, while, the overall process was controlled by the ethanol-adsorption step. A good agreement between the predicted values and experimental results validated the model for the glycerol-enriched calcium oxide assisted avocado oil ethanolysis process under the studied range of experimental conditions.

Although the utilization of refined avocado oil for non-food applications has been reported before, the multiple features of avocado pulp oil for human benefits do not make them a good resource for biofuel production. However, the seed of avocado fruit that is about 13 % of the total fresh weight of the fruit is considered as an agricultural waste and discarded with no further application. The lipid bodies, along with other chemicals, are also located inside the seed of avocado fruit. In a viewpoint to extract biochemicals, with an emphasis on combustible oil, from avocado seed, a research strategy was outlined to apply the seed for the reactive extraction methodology. Before applying avocado seed for the reactive extraction methodology, its drying process was essential because of the presence of high content of water. The initial moisture content in Hass avocado seed was 51.20 %. In **Paper VI**, the effects of five different temperatures on the degree of moisture evaporation and the physical appearance of seeds was systematically monitored. In addition, this study carefully examined the impact of the pretreatment of seeds on the drying mechanism. This study concluded that avocado seeds should be crushed or sliced before placing for drying to accelerate the moisture evaporation,

and that the seeds should be dried only at 40 ºC air temperature for 1440 min to satisfactorily eliminate the moisture and preserve the quality of Hass avocado seeds. This is because, the appliance of higher temperature resulted in a charring and hardening of the seed surface. After the drying process, Hass avocado seed sample was utilized for the reactive extraction methodology, in the presence of ethanol, to extract the lipid molecules and simultaneously convert it to biodiesel. The product analysis of the experiments are currently under process. After the reactive extraction process, the heat of combustion of the seed leftover was determined, and compared with that of the fresh seed. The measured average calorific value of Hass avocado seeds before and after the reactive extraction process was 17.79 and 17.65 kJg^{-1}, respectively. An insignificant reduction in the heating value of Hass avocado seeds after the extraction of chemicals indicated that the avocado leftover could be a potential combustion compound. **Paper VII** involved the mathematical modelling of the drying kinetics of the non-pretreated, sliced, and crushed Hass avocado seeds dried at 40, 50, 60, 70, and 80º C air temperature. The novelty of this study is that a new semi-theoretical mathematical model, named Avhad and Marchetti model, was developed, and its ability to describe the drying kinetics of non-pretreated as well as pretreated Hass avocado seeds was compared with three well-known and widely applied mathematical model. The present simulation concluded that the newly proposed Avhad and Marchetti model provided superior simulation of the drying kinetics of Hass avocado seeds than the Lewis, Henderson and Pabis, and Page model. The predictions made by the Avhad and Marchetti model were in an excellent agreement with the experimental data, and provided the coefficient of determination values higher than 0.97, 0.99, and 0.98 at all five studied temperatures for the non-pretreated, sliced, and crushed Hass avocado seeds, respectively.

7. Future perspective

The focus of this work has largely been the utilization of cost-effective raw materials and low-cost green heterogeneous catalysts for biodiesel production. The presented catalysts were easy to prepare and inexpensive. Therefore, there is a great opportunity to upscale the use of these heterogeneous catalysts for biodiesel production. The transformation of calcium oxide to calcium diglyceroxide have eliminated the concerns related to the catalyst deactivation occurring due to the surrounding carbon dioxide and moisture. However, in order to effective utilize calcium diglyceroxide catalyst for biodiesel production from different lipid feedstocks, the reutilization study of the catalyst must be fulfilled in future.

Given that jojoba oil is non-triglycerides based plant oil and the possibility for the formation of calcium diglyceride catalytic species due to an interaction between glycerol and calcium oxide during the transesterification is not existent, it is clear that the complete alcoholysis reaction is catalyzed only by the calcium oxide catalytic species. The catalytic performance of calcium diglyceroxide has been reported to be superior to calcium oxide. The investigation of the catalytic performance of calcium diglyceroxide to accelerate the alcoholysis of jojoba oil is suggested with an objective to achieve high yields of products in lesser reaction time and by using milder operating conditions. Moreover, because the alcoholysis of jojoba oil leads towards the formation of two value added chemicals (biodiesel and jojobyl alcohols) which are miscible and appear in a single phase, a novel distillation or separation technology could be established in future to expand and commercialize the use of jojoba oil for the synthesis of biochemicals.

In the present thesis, Hass avocado seeds were utilized for the reactive extraction methodology to produce biodiesel. Further advancements in the study is suggested, which are mentioned as follows:

- To investigate the capability of different alcohol solvents to extract chemicals from Hass avocado seeds.
- To investigate the chemical composition and yields of the extractable chemicals.
- To increase the selective of the desired product through monitoring the formation of products and regulating the experimental conditions.

8. References

[1] International Energy Outlook. U.S. Energy Information Administration. 2016. http://www.eia.gov/forecasts/ieo/ [accessed on 10.09.2016].

[2] Borugadda VB, Goud VV. Biodiesel production from renewable feedstocks: Status and opportunities. Renewable and Sustainable Energy Reviews. 2012;16(7):4763-84.

[3] Rosenberg E, Lind A, Espegren KA. The impact of future energy demand on renewable energy production–Case of Norway. Energy. 2013;61:419-31.

[4] Renewable Energy Directive 2009/28/2009. European Commission Directive of the European Parliament and of the Council on the production of the use of energy from renewable resources. https://ec.europa.eu/energy/en/topics/renewable-energy/renewable-energy-directive [accessed on 10.09.2016].

[5] Huber GW, Iborra S, Corma A. Synthesis of transportation fuels from biomass: Chemistry, catalysts, and engineering. Chemical Reviews. 2006;106(9):4044-98.

[6] Chheda JN, Huber GW, Dumesic JA. Liquid–phase catalytic processing of biomass-derived oxygenated hydrocarbons to fuels and chemicals. Angewandte Chemie International Edition. 2007;46(38):7164-83.

[7] The Roadmap for Biomass Technologies in the U.S. biomass R&D Technical Advisory Committee. U.S. Department of Energy. 2002; Accession No. ADA 436527.

[8] Enweremadu CC, Mbarawa MM. Technical aspects of production and analysis of biodiesel from used cooking oil–A review. Renewable and Sustainable Energy Reviews. 2009;13(9):2205-24.

[9] Yusuf NNAN, Kamarudin SK, Yaakub Z. Overview on the current trends in biodiesel production. Energy Conversion and Management. 2011;52(7):2741-51.

[10] Tsoutsos TD, Tournaki S, Paraíba O, Kaminaris SD. The used cooking oil–to–biodiesel chain in Europe assessment of best practices and environmental performance. Renewable and Sustainable Energy Reviews. 2016;54:74-83.

[11] Poddar T, Jagannath A, Almansoori A. Use of reactive distillation in biodiesel production: A simulation-based comparison of energy requirements and profitability indicators. Applied Energy. 2015; 75: 17-22.

[12] EurObserv'ER. Biofuels Barometer. 2015. http://www.eurobserv-er.org/biofuels-barometer-2015/ [accessed on 10.09.2016].

[13] Kotrba R. Swedish biodiesel producer acquires Norway plant. Biodiesel Magazine. 2015. http://www.biodieselmagazine.com/articles/516675/swedish-biodiesel-producer-acquires-norway-plant [accessed on 10.09.2016].

[14] Andersen O, Weinbach J-E. Residual animal fat and fish for biodiesel production. Potentials in Norway. Biomass and Bioenergy. 2010;34(8):1183-8.

[15] Bart JCJ, Palmeri N, Cavallaro S. 5–Feedstocks for biodiesel production. Biodiesel science and technology: From soil to oil. Woodhead Publishing. 2010: 130-225.

[16] Clean Cities Alternative Fuel Price Report. U.S. Department of Energy. 2016. http://www.afdc.energy.gov/fuels/prices.html [accessed on 10.09.2016].

[17] Stevens CV, Verhé RG. 1–Green chemistry and sustainability. Renewable bioresources: Scope and modifications for non-food applications. John Wiley & Sons Ltd. 2004: 1-2.

[18] Brundtland CG. Our common future–The World Commission on Environmental Development. Oxford University Press. 1987.

[19] Anastas PT, Warner JC. Green chemistry: Theory and practice. Oxford University Press. 1998;30.

[20] Tang SY, Bourne RA, Smith RL, Poliakoff M. The 24 principles of green engineering and green chemistry: "IMPROVEMENTS PRODUCTIVELY". Green Chemistry. 2008;10(3):268-9.

[21] Knothe G. Biodiesel and renewable diesel: A comparison. Progress in Energy and Combustion Science. 2010;36(3):364-73.

[22] Knothe G. 2–History of vegetable oil-based diesel fuels. The Biodiesel Handbook. Second Edition. AOCS Press. 2010:5-19.

[23] Lin L, Cunshan Z, Vittayapadung S, Xiangqian S, Mingdong D. Opportunities and challenges for biodiesel fuel. Applied Energy. 2011;88(4):1020-31.

[24] Marchetti JM. 1–General background about biodiesel. Biodiesel production technologies. First edition. New York: Nova science publisher, Inc.2010: 13-9.

[25] Marchetti JM. A summary of the available technologies for biodiesel production based on a comparison of different feedstock's properties. Process Safety and Environmental Protection. 2012;90(3):157-63.

[26] Marchetti JM, Miguel VU, Errazu AF. Heterogeneous esterification of oil with high amount of free fatty acids. Fuel. 2007;86(5–6):906-10.

[27] Marchetti JM, Errazu AF. Esterification of free fatty acids using sulfuric acid as catalyst in the presence of triglycerides. Biomass and Bioenergy. 2008;32(9):892-5.

[28] Atadashi IM, Aroua MK, Aziz AA. High quality biodiesel and its diesel engine application: A review. Renewable and Sustainable Energy Reviews. 2010;14(7):1999-2008.

[29] Demirbas A. Progress and recent trends in biodiesel fuels. Energy Conversion and Management. 2009;50(1):14-34.

[30] Agarwal AK. Biofuels (alcohols and biodiesel) applications as fuels for internal combustion engines. Progress in Energy and Combustion Science. 2007;33(3):233-71.

[31] Hazar H, Ozturk U. The effects of Al_2O_3–TiO_2 coating in a diesel engine on performance and emission of corn oil methyl ester. Renewable Energy. 2010;35(10):2211-6.

[32] Juan JC, Kartika DA, Wu TY, Hin T-YY. Biodiesel production from *jatropha* oil by catalytic and non-catalytic approaches: An overview. Bioresource Technology. 2011;102(2):452-60.

[33] Helwani Z, Aziz N, Bakar MZA, Mukhtar H, Kim J, Othman MR. Conversion of *jatropha curcas* oil into biodiesel using re-crystallized hydrotalcite. Energy Conversion and Management. 2013;73:128-34.

[34] Karmakar A, Karmakar S, Mukherjee S. Properties of various plants and animals feedstocks for biodiesel production. Bioresource Technology. 2010;101(19):7201-10.

[35] No S-Y. Inedible vegetable oils and their derivatives for alternative diesel fuels in CI engines: A review. Renewable and Sustainable Energy Reviews. 2011;15(1):131-49.

[36] Atabani AE, Silitonga AS, Badruddin IA, Mahlia TMI, Masjuki HH, Mekhilef S. A comprehensive review on biodiesel as an alternative energy resource and its characteristics. Renewable and Sustainable Energy Reviews. 2012;16(4):2070-93.

[37] Atabani AE, Silitonga AS, Ong HC, Mahlia TMI, Masjuki HH, Badruddin IA, et al. Non-edible vegetable oils: A critical evaluation of oil extraction, fatty acid compositions, biodiesel production, characteristics, engine performance and emissions production. Renewable and Sustainable Energy Reviews. 2013;18:211-45.

[38] Hoekman SK, Broch A, Robbins C, Ceniceros E, Natarajan M. Review of biodiesel composition, properties, and specifications. Renewable and Sustainable Energy Reviews. 2012;16(1):143-69.

[39] Ong HC, Silitonga AS, Masjuki HH, Mahlia TMI, Chong WT, Boosroh MH. Production and comparative fuel properties of biodiesel from non-edible oils: *Jatropha curcas*, *Sterculia foetida* and *Ceiba pentandra*. Energy Conversion and Management. 2013;73:245-55.

[40] Canoira L, Alcántara R, Jesús García-Martínez M, Carrasco J. Biodiesel from jojoba oil-wax: Transesterification with methanol and properties as a fuel. Biomass and Bioenergy. 2006;30(1):76-81.

[41] Sánchez M, Marchetti JM, Boulifi NE, Martínez M, Aracil J. Jojoba oil biorefinery using a green catalyst. Part I: Simulation of the process. Biofuels, Bioproducts and Biorefining. 2015;9(2):129-38.

[42] Al-Widyan MI, Al-Muhtaseb MtA. Experimental investigation of jojoba as a renewable energy source. Energy Conversion and Management. 2010;51(8):1702-7.

[43] El-Boulifi N, Sánchez M, Martínez M, Aracil J. Fatty acid alkyl esters and monounsaturated alcohols production from jojoba oil using short-chain alcohols for biorefinery concepts. Industrial Crops and Products. 2015;69:244-50.

[44] Food and Argiculture Organization of the United Nations Statistics Division. http://faostat3.fao.org/browse/Q/QC/E [accessed on 10.09.2016].

[45] Kozliak E, Mota R, Rodriguez D, Overby P, Kubátová A, Stahl D, et al. Non-catalytic cracking of jojoba oil to produce fuel and chemical by-products. Industrial Crops and Products. 2013;43:386-92.

[46] Wisniak J. Potential uses of jojoba oil and meal–a review. Industrial Crops and Products. 1994;3(1-2):43-68.

[47] Al-Hamamre Z, Rawajfeh KM. Investigating the energy value of jojoba as an alternative renewable energy source. International Journal of Green Energy. 2015;12(4):398-404.

[48] Sánchez M, Marchetti JM, El Boulifi N, Martínez M, Aracil J. Jojoba oil biorefinery using a green catalyst. Part II: Feasibility study and economical assessment. Biofuels, Bioproducts and Biorefining. 2015;9(2):139-46.

[49] Koh MY, Mohd. Ghazi TI. A review of biodiesel production from *jatropha curcas l.* oil. Renewable and Sustainable Energy Reviews. 2011;15(5):2240-51.

[50] Issariyakul T, Dalai AK. Biodiesel from vegetable oils. Renewable and Sustainable Energy Reviews. 2014;31:446-71.

[51] Dreher ML, Davenport AJ. Hass avocado composition and potential health effects. Critical Reviews in Food Science and Nutrition. 2013;53(7):738-50.

[52] Mexico: Avocado Annual. Unites States Department of Agriculture Foreign Agricultural Service. 2015. http://www.fas.usda.gov/data/mexico-avocado-annual-0 [accessed on 10.09.2016].

[53] Avhad MR, Marchetti JM. Temperature and pretreatment effects on the drying of Hass avocado seeds. Biomass and Bioenergy. 2015;83:467-73.

[54] Dabas D, Elias RJ, Lambert JD, Ziegler GR. A colored avocado seed extract as a potential natural colorant. Journal of Food Science. 2011;76(9):C1335-C41.

[55] Gómez F, Sánchez S, Iradi M, Azman N, Almajano M. Avocado seeds: Extraction optimization and possible use as antioxidant in food. Antioxidants. 2014;3(2):439.

[56] Weatherby LS, Sorber DG. Chemical composition of avocado seed. Industrial & Engineering Chemistry. 1931;23(12):1421-3.

[57] Lacerda L, Colman T, Bauab T, da Silva Carvalho Filho M, Demiate I, de Vasconcelos E, et al. Thermal, structural and rheological properties of starch from avocado seeds (*Persea americana, Miller*) modified with standard sodium hypochlorite solutions. Journal of Thermal Analysis and Calorimetry. 2014;115(2):1893-9.

[58] Bhaumik M, Choi HJ, Seopela MP, McCrindle RI, Maity A. Highly effective removal of toxic Cr(VI) from wastewater using sulfuric acid-modified avocado seed. Industrial & Engineering Chemistry Research. 2014;53(3):1214-24.

[59] Rodrigues LA, da Silva MLCP, Alvarez-Mendes MO, Coutinho AdR, Thim GP. Phenol removal from aqueous solution by activated carbon produced from avocado kernel seeds. Chemical Engineering Journal. 2011;174(1):49-57.

[60] Vinha AF, Moreira J, Barreira SVP. Physicochemical parameters, phytochemical composition and antioxidant activity of the algarvian avocado (*Persea americana Mill.*). Journal of Agricultural Science. 2013; 5(12): 100-9.

[61] Takenaga F, Matsuyama K, Abe S, Torii Y, Itoh S. Lipid and fatty acid composition of mesocarp and seed of avocado fruits harvested at northern range in Japan. Journal of Oleo Science. 2008;57(11):591-7.

[62] Ilkılıç C, Aydın S, Behcet R, Aydin H. Biodiesel from safflower oil and its application in a diesel engine. Fuel Processing Technology. 2011;92(3):356-62.

[63] Vedharaj S, Vallinayagam R, Yang WM, Chou SK, Chua KJE, Lee PS. Experimental investigation of kapok (*Ceiba pentandra*) oil biodiesel as an alternate fuel for diesel engine. Energy Conversion and Management. 2013;75:773-9.

[64] Demirbas A. Production of biodiesel fuels from linseed oil using methanol and ethanol in non-catalytic SCF conditions. Biomass and Bioenergy. 2009;33(1):113-8.

[65] Singh SP, Singh D. Biodiesel production through the use of different sources and characterization of oils and their esters as the substitute of diesel: A review. Renewable and Sustainable Energy Reviews. 2010;14(1):200-16.

[66] Marchetti JM, Miguel VU, Errazu AF. Possible methods for biodiesel production. Renewable and Sustainable Energy Reviews. 2007;11(6):1300-11.

[67] Meher LC, Vidya Sagar D, Naik SN. Technical aspects of biodiesel production by transesterification–a review. Renewable and Sustainable Energy Reviews. 2006;10(3):248-68.

[68] Collins S, Peace SK, Richards RW, MacDonald WA, Mills P, King SM. Transesterification in poly(ethylene terephthalate). Molecular weight and end group effects. Macromolecules. 2000;33(8):2981-8.

[69] Kim SC, Kim YH, Lee H, Yoon DY, Song BK. Lipase-catalyzed synthesis of glycerol carbonate from renewable glycerol and dimethyl carbonate through transesterification. Journal of Molecular Catalysis B: Enzymatic. 2007;49(1-4):75-8.

[70] Barrault J, Pouilloux Y, Clacens JM, Vanhove C, Bancquart S. Catalysis and fine chemistry. Catalysis Today. 2002;75(1-4):177-81.

[71] Brunschwig C, Moussavou W, Blin J. Use of bioethanol for biodiesel production. Progress in Energy and Combustion Science. 2012;38(2):283-301.

[72] Green S. Industrial Catalysis. Macmillan Company. New York. 1928.

[73] Berzelius JJ. Årsberättelsen om framstegi fysik och kemi. Royal Swedish Academy of Sciences. 1835.

[74] Lindström B, Pettersson LJ. A Brief History of Catalysis. CatTech. 2003;7(4):130-8.

[75] Davis BH. 1–Development of the science of catalysis. Handbook of heterogeneous catalysis: Wiley-VCH Verlag GmbH & Co. KGaA. 2008.

[76] Hagen J. 3–Homogeneously catalyzed industrial processes. Industrial catalysis: Wiley-VCH Verlag GmbH & Co. KGaA. 2006: 59-82.

[77] Hagen J. 8–Heterogeneously catalyzed processes in industry. Industrial catalysis: Wiley-VCH Verlag GmbH & Co. KGaA. 2006: 261-93.

[78] Uzun BB, Kılıç M, Özbay N, Pütün AE, Pütün E. Biodiesel production from waste frying oils: Optimization of reaction parameters and determination of fuel properties. Energy. 2012;44(1):347-51.

[79] Fadhil AB, Ali LH. Alkaline-catalyzed transesterification of *Silurus triostegus* heckel fish oil: Optimization of transesterification parameters. Renewable Energy. 2013;60:481-8.

[80] Fukuda H, Kondo A, Noda H. Biodiesel fuel production by transesterification of oils. Journal of Bioscience and Bioengineering. 2001;92(5):405-16.

[81] Marchetti JM, Miguel VU, Errazu AF. Techno-economic study of different alternatives for biodiesel production. Fuel Processing Technology. 2008;89(8):740-8.

[82] Soriano Jr NU, Venditti R, Argyropoulos DS. Biodiesel synthesis *via* homogeneous Lewis acid-catalyzed transesterification. Fuel. 2009;88(3):560-5.

[83] Aranda DAG, Santos RTP, Tapanes NCO, Ramos ALD, Antunes OAC. Acid-catalyzed homogeneous esterification reaction for biodiesel production from palm fatty acids. Catalysis Letters. 2008;122(1):20-5.

[84] Park J-Y, Wang Z-M, Kim D-K, Lee J-S. Effects of water on the esterification of free fatty acids by acid catalysts. Renewable Energy. 2010;35(3):614-8.

[85] Farag HA, El-Maghraby A, Taha NA. Optimization of factors affecting esterification of mixed oil with high percentage of free fatty acid. Fuel Processing Technology. 2011;92(3):507-10.

[86] Marchetti JM, Pedernera MN, Schbib NS. Production of biodiesel from acid oil using sulfuric acid as catalyst: Kinetics study. International Journal of Low-Carbon Technologies. 2011;6(1):38-43.

[87] Tasić MB, Stamenković OS, Veljković VB. Cost analysis of simulated base-catalyzed biodiesel production processes. Energy Conversion and Management. 2014;84:405-13.

[88] Kazemian H, Turowec B, Siddiquee MN, Rohani S. Biodiesel production using cesium modified mesoporous ordered silica as heterogeneous base catalyst. Fuel. 2013;103:719-24.

[89] Thitsartarn W, Kawi S. Transesterification of Oil by Sulfated Zr-Supported Mesoporous Silica. Industrial & Engineering Chemistry Research. 2011;50(13):7857-65.

[90] Kawashima A, Matsubara K, Honda K. Acceleration of catalytic activity of calcium oxide for biodiesel production. Bioresource Technology. 2009;100(2):696-700.

[91] Viola E, Blasi A, Valerio V, Guidi I, Zimbardi F, Braccio G, et al. Biodiesel from fried vegetable oils via transesterification by heterogeneous catalysis. Catalysis Today. 2012;179(1):185-90.

[92] Mootabadi H, Salamatinia B, Bhatia S, Abdullah AZ. Ultrasonic-assisted biodiesel production process from palm oil using alkaline earth metal oxides as the heterogeneous catalysts. Fuel. 2010;89(8):1818-25.

[93] Di Serio M, Cozzolino M, Giordano M, Tesser R, Patrono P, Santacesaria E. From homogeneous to heterogeneous catalysts in biodiesel production. Industrial & Engineering Chemistry Research. 2007;46(20):6379-84.

[94] Verziu M, Cojocaru B, Hu J, Richards R, Ciuculescu C, Filip P, et al. Sunflower and rapeseed oil transesterification to biodiesel over different nanocrystalline MgO catalysts. Green Chemistry. 2008;10(4):373-81.

[95] Jeon H, Kim DJ, Kim SJ, Kim JH. Synthesis of mesoporous MgO catalyst templated by a PDMS–PEO comb–like copolymer for biodiesel production. Fuel Processing Technology. 2013;116:325-31.

[96] Liu X, He H, Wang Y, Zhu S. Transesterification of soybean oil to biodiesel using SrO as a solid base catalyst. Catalysis Communications. 2007;8(7):1107-11.

[97] Patil P, Gude VG, Pinappu S, Deng S. Transesterification kinetics of *Camelina sativa* oil on metal oxide catalysts under conventional and microwave heating conditions. Chemical Engineering Journal. 2011;168(3):1296-300.

[98] D'Cruz A, Kulkarni MG, Meher LC, Dalai AK. Synthesis of biodiesel from canola oil using heterogeneous base catalyst. Journal of the American Oil Chemists' Society. 2007;84(10):937-43.

[99] Kaur M, Ali A. Ethanolysis of waste cottonseed oil over lithium impregnated calcium oxide: Kinetics and reusability studies. Renewable Energy. 2014;63:272-9.

[100] MacLeod CS, Harvey AP, Lee AF, Wilson K. Evaluation of the activity and stability of alkali-doped metal oxide catalysts for application to an intensified method of biodiesel production. Chemical Engineering Journal. 2008;135(1–2):63-70.

[101] Liu C-C, Lu W-C, Liu T-J. Transesterification of soybean oil using CsF/CaO catalysts. Energy & Fuels. 2012;26(9):5400-7.

[102] Woodford JJ, Parlett CMA, Dacquin J-P, Cibin G, Dent A, Montero J, et al. Identifying the active phase in Cs-promoted MgO nanocatalysts for triglyceride transesterification. Journal of Chemical Technology & Biotechnology. 2014;89(1):73-80.

[103] Xie W, Zhao L. Production of biodiesel by transesterification of soybean oil using calcium supported tin oxides as heterogeneous catalysts. Energy Conversion and Management. 2013;76:55-62.

[104] Samart C, Chaiya C, Reubroycharoen P. Biodiesel production by methanolysis of soybean oil using calcium supported on mesoporous silica catalyst. Energy Conversion and Management. 2010;51(7):1428-31.

[105] Alba-Rubio AC, Santamaría-González J, Mérida-Robles JM, Moreno-Tost R, Martín-Alonso D, Jiménez-López A, et al. Heterogeneous transesterification processes by using CaO supported on zinc oxide as basic catalysts. Catalysis Today. 2010;149(3–4):281-7.

[106] Wen Z, Yu X, Tu S-T, Yan J, Dahlquist E. Biodiesel production from waste cooking oil catalyzed by TiO_2–MgO mixed oxides. Bioresource Technology. 2010;101(24):9570-6.

[107] Taufiq-Yap YH, Lee HV, Hussein MZ, Yunus R. Calcium-based mixed oxide catalysts for methanolysis of *jatropha curcas* oil to biodiesel. Biomass and Bioenergy. 2011;35(2):827-34.

[108] Lee HV, Taufiq-Yap YH, Hussein MZ, Yunus R. Transesterification of *jatropha* oil with methanol over Mg–Zn mixed metal oxide catalysts. Energy. 2013;49:12-8.

[109] Woodford JJ, Dacquin J-P, Wilson K, Lee AF. Better by design: Nanoengineered macroporous hydrotalcites for enhanced catalytic biodiesel production. Energy & Environmental Science. 2012;5(3):6145-50.

[110] Di Serio M, Mallardo S, Carotenuto G, Tesser R, Santacesaria E. Mg/Al hydrotalcite catalyst for biodiesel production in continuous packed bed reactors. Catalysis Today. 2012;195(1):54-8.

[111] Kim M, Salley SO, Ng KYS. Transesterification of glycerides using a heterogeneous resin catalyst combined with a homogeneous catalyst. Energy & Fuels. 2008;22(6):3594-9.

[112] Ren Y, He B, Yan F, Wang H, Cheng Y, Lin L, et al. Continuous biodiesel production in a fixed bed reactor packed with anion-exchange resin as heterogeneous catalyst. Bioresource Technology. 2012;113:19-22.

[113] Correia LM, Saboya RMA, de Sousa Campelo N, Cecilia JA, Rodríguez-Castellón E, Cavalcante Jr CL, et al. Characterization of calcium oxide catalysts from natural sources and their application in the transesterification of sunflower oil. Bioresource Technology. 2014;151:207-13.

[114] Navajas A, Issariyakul T, Arzamendi G, Gandía LM, Dalai AK. Development of eggshell derived catalyst for transesterification of used cooking oil for biodiesel production. Asia-Pacific Journal of Chemical Engineering. 2013;8(5):742-8.

[115] Suryaputra W, Winata I, Indraswati N, Ismadji S. Waste capiz (*Amusium cristatum*) shell as a new heterogeneous catalyst for biodiesel production. Renewable Energy. 2013;50:795-9.

[116] Birla A, Singh B, Upadhyay SN, Sharma YC. Kinetics studies of synthesis of biodiesel from waste frying oil using a heterogeneous catalyst derived from snail shell. Bioresource Technology. 2012;106:95-100.

[117] Nakatani N, Takamori H, Takeda K, Sakugawa H. Transesterification of soybean oil using combusted oyster shell waste as a catalyst. Bioresource Technology. 2009;100(3):1510-3.

[118] Liu X, He H, Wang Y, Zhu S, Piao X. Transesterification of soybean oil to biodiesel using CaO as a solid base catalyst. Fuel. 2008;87(2):216-21.

[119] Thitsartarn W, Kawi S. An active and stable CaO-CeO_2 catalyst for transesterification of oil to biodiesel. Green Chemistry. 2011;13(12):3423-30.

[120] Molaei Dehkordi A, Ghasemi M. Transesterification of waste cooking oil to biodiesel using Ca and Zr mixed oxides as heterogeneous base catalysts. Fuel Processing Technology. 2012;97:45-51.

[121] Albuquerque MCG, Jiménez-Urbistondo I, Santamaría-González J, Mérida-Robles JM, Moreno-Tost R, Rodríguez-Castellón E, et al. CaO supported on mesoporous silicas as basic catalysts for transesterification reactions. Applied Catalysis A: General. 2008;334(1–2):35-43.

[122] Alonso DM, Mariscal R, Granados ML, Maireles-Torres P. Biodiesel preparation using Li/CaO catalysts: Activation process and homogeneous contribution. Catalysis Today. 2009;143(1–2):167-71.

[123] Kumar D, Ali A. Transesterification of low-quality triglycerides over a Zn/CaO heterogeneous catalyst: Kinetics and reusability studies. Energy & Fuels. 2013;27(7):3758-68.

[124] Lin L, Vittayapadung S, Li X, Jiang W, Shen, Xiangqian. Synthesis of magnetic calcium oxide hollow fiber catalyst for the production of biodiesel. Environmental Progress & Sustainable Energy. 2013;32(4):1255-61.

[125] Liu F, Zhang Y. Hydrothermal growth of flower-like CaO for biodiesel production. Ceramics International. 2012;38(4):3473-82.

[126] Ferrero GO, Almeida MF, Alvim-Ferraz MCM, Dias JM. Glycerol–enriched heterogeneous catalyst for biodiesel production from soybean oil and waste frying oil. Energy Conversion and Management. 2015;89:665-71.

[127] Esipovich A, Danov S, Belousov A, Rogozhin A. Improving methods of CaO transesterification activity. Journal of Molecular Catalysis A: Chemical. 2014;395:225-33.

[128] Reyero I, Arzamendi G, Gandía LM. Heterogenization of the biodiesel synthesis catalysis: CaO and novel calcium compounds as transesterification catalysts. Chemical Engineering Research and Design. 2014;92(8):1519-30.

[129] Sánchez-Cantú M, Reyes-Cruz FM, Rubio-Rosas E, Pérez-Díaz LM, Ramírez E, Valente JS. Direct synthesis of calcium diglyceroxide from hydrated lime and glycerol and its evaluation in the transesterification reaction. Fuel. 2014;138:126-33.

[130] Gupta AR, Yadav SV, Rathod VK. Enhancement in biodiesel production using waste cooking oil and calcium diglyceroxide as a heterogeneous catalyst in presence of ultrasound. Fuel. 2015;158:800-6.

[131] León-Reina L, Cabeza A, Rius J, Maireles-Torres P, Alba-Rubio AC, López Granados M. Structural and surface study of calcium glyceroxide, an active phase for biodiesel production under heterogeneous catalysis. Journal of Catalysis. 2013;300:30-6.

[132] Kouzu M, Tsunomori M, Yamanaka S, Hidaka J. Solid base catalysis of calcium oxide for a reaction to convert vegetable oil into biodiesel. Advanced Powder Technology. 2010;21(4):488-94.

[133] López Granados M, Alba-Rubio AC, Vila F, Martín Alonso D, Mariscal R. Surface chemical promotion of Ca oxide catalysts in biodiesel production reaction by the addition of monoglycerides, diglycerides and glycerol. Journal of Catalysis. 2010;276(2):229-36.

[134] Niemantsverdriet JW. Spectroscopic methods in heterogeneous catalysis. VCH, Weinheim. 1993.

[135] Cullity BD, Stock SR. 3–The directions of diffracted beams. Elements of X-ray diffraction. Third edition. Addison-Wesley Publishing Company Inc. 2001: 78-96.

[136] Henry NFM, Lipson J, Wooster WA. 1–The interpretation of X-ray diffraction photographs. D. Van Nostrand Company, Inc., London. 1951: 19-54.

[137] Brown ME. 2–Thermogravimetry. Introduction to thermal analysis: Techniques and applications. Dordrecht: Springer Netherlands. 2001: 13-17.

[138] Jiang Y, Li D, Li Y, Gao J, Zhou L, He Y. In situ self-catalyzed reactive extraction of germinated oilseed with short-chained dialkyl carbonates for biodiesel production. Bioresource Technology. 2013;150:50-4.

[139] Zakaria R, Harvey AP. Direct production of biodiesel from rapeseed by reactive extraction/in situ transesterification. Fuel Processing Technology. 2012;102:53-60.

[140] Georgogianni KG, Kontominas MG, Pomonis PJ, Avlonitis D, Gergis V. Conventional and in situ transesterification of sunflower seed oil for the production of biodiesel. Fuel Processing Technology. 2008;89(5):503-9.

[141] Shuit SH, Lee KT, Kamaruddin AH, Yusup S. Reactive extraction and in situ esterification of *jatropha curcas l*. seeds for the production of biodiesel. Fuel. 2010;89(2):527-30.

[142] Dufreche S, Hernandez R, French T, Sparks D, Zappi M, Alley E. Extraction of lipids from municipal wastewater plant microorganisms for production of biodiesel. Journal of the American Oil Chemists' Society. 2007;84(2):181-7.

[143] Haas MJ, Scott KM, Foglia TA, Marmer WN. The general applicability of in situ transesterification for the production of fatty acid esters from a variety of feedstocks. Journal of the American Oil Chemists' Society. 2007;84(10):963-70.

[144] Poirot R, Prat L, Gourdon C, Diard C, Autret JM. Fast batch to continuous solid–liquid extraction from plants in continuous industrial extractor. Chemical Engineering & Technology. 2007;30(1):46-51.

[145] Lian S, Li H, Tang J, Tong D, Hu C. Integration of extraction and transesterification of lipid from *jatropha* seeds for the production of biodiesel. Applied Energy. 2012;98:540-7.

[146] Mehta DU, Saxena P, Jawale S, Joshipura MH. A review on prediction of properties of biodiesel and blends of biodiesel. Procedia Engineering. 2013;51:395-402.

[147] Kouzu M, Yamanaka S-y, Hidaka J-s, Tsunomori M. Heterogeneous catalysis of calcium oxide used for transesterification of soybean oil with refluxing methanol. Applied Catalysis A: General. 2009;355(1–2):94-9.

[148] Sánchez M, Bergamin F, Peña E, Martínez M, Aracil J. A comparative study of the production of esters from *jatropha* oil using different short–chain alcohols: Optimization and characterization. Fuel. 2015;143:183-8.

[149] Sánchez M, Marchetti JM, El Boulifi N, Aracil J, Martínez M. Kinetics of jojoba oil methanolysis using a waste from fish industry as catalyst. Chemical Engineering Journal. 2015;262:640-7.

[150] Ilgen O. Investigation of reaction parameters, kinetics and mechanism of oleic acid esterification with methanol by using Amberlyst 46 as a catalyst. Fuel Processing Technology. 2014;124:134-9.

[151] Deshmane VG, Adewuyi YG. Synthesis and kinetics of biodiesel formation *via* calcium methoxide base catalyzed transesterification reaction in the absence and presence of ultrasound. Fuel. 2013;107:474-82.

[152] Kouzu M, Hidaka J-s, Wakabayashi K, Tsunomori M. Solid base catalysis of calcium glyceroxide for a reaction to convert vegetable oil into its methyl esters. Applied Catalysis A: General. 2010;390(1–2):11-8.

[153] Knothe G. Analyzing biodiesel: standards and other methods. Journal of the American Oil Chemists' Society. 2006;83(10):823-33.

[154] Fujii K, Kondo W. Calcium glyceroxides formed in the system of calcium oxide-glycerol. Zeitschrift für anorganische und allgemeine Chemie. 1968;359(5-6):296-304.

[155] Ramos-Jerz MdR. Phytochemical analysis of avocado seeds (*Persea Americana Mill., c.c. Hass*). Ph.D. dissertation. Technischen Universität Braunschweig. 2007.

[156] Gurtas Seyhan F, Evranuz Ö. Low temperature mushroom (*A. bisporus*) drying with desiccant dehumidifiers. Drying Technology. 2000;18(1-2):433-45.

[157] Avhad MR, Sánchez M, Peña E, Bouaid A, Martínez M, Aracil J, et al. Renewable production of value-added jojobyl alcohols and biodiesel using a naturally-derived heterogeneous green catalyst. Fuel. 2016;179:332-8.

[158] Lukić I, Kesić Ž, Zdujić M, Skala D. Calcium diglyceroxide synthesized by mechanochemical treatment, its characterization and application as catalyst for fatty acid methyl esters production. Fuel. 2016;165:159-65.

[159] Jasen P, Marchetti JM. Kinetic study of the esterification of free fatty acid and ethanol in the presence of triglycerides using solid resins as catalyst. International Journal of Low-Carbon Technologies. 2012;7(4):325-30.

[160] Avhad MR, Sánchez M, Bouaid A, Martínez M, Aracil J, Marchetti JM. Modeling chemical kinetics of avocado oil ethanolysis catalyzed by solid glycerol-enriched calcium oxide. Energy Conversion and Management. 2016. doi.org/10.1016/j.enconman.2016.07.060

[161] Roberts JS, Kidd DR, Padilla-Zakour O. Drying kinetics of grape seeds. Journal of Food Engineering. 2008;89(4):460-5.

[162] Mwithiga G, Olwal JO. The drying kinetics of kale (*Brassica oleracea*) in a convective hot air dryer. Journal of Food Engineering. 2005;71(4):373-8.

[163] Sacilik K. Effect of drying methods on thin-layer drying characteristics of hull-less seed pumpkin (*Cucurbita pepo L.*). Journal of Food Engineering. 2007;79(1):23-30.

[164] Avhad MR, Marchetti JM. Mathematical modelling of the drying kinetics of Hass avocado seeds. Industrial Crops and Products. 2016;91:76-87.

9. Papers

Paper I: Avhad MR, Marchetti JM. A review on recent advancement in catalytic materials for biodiesel production. *Renewable and Sustainable Energy Reviews*. 2015: 50; 696-718.

Paper II: Avhad MR, Marchetti JM. Innovation in solid heterogeneous catalysis for the generation of economically viable and ecofriendly biodiesel: A review. *Catalysis reviews: Science and Engineering*. 2016: 58(2); 157-208.

Paper III: Avhad MR, Sánchez M, Peña E, Bouaid A, Martínez M, Aracil J, Marchetti JM. Renewable production of value-added jojobyl alcohols and biodiesel using a naturally-derived heterogeneous green catalyst. *Fuel*. 2016: 179; 332-338.

Paper IV: Avhad MR, Sánchez M, Bouaid A, Martínez M, Aracil J, Marchetti JM. Glycerol-activated calcium oxide catalyst for the methanolysis of crude *jatropha curcas* oil. Submitted to *Fuel*.

Paper V: Avhad MR, Sánchez M, Bouaid A, Martínez M, Aracil J, Marchetti JM. Modeling chemical kinetics of avocado oil ethanolysis catalyzed by solid glycerol-enriched calcium oxide. Accepted by *Energy Conversion and Management*. 2016.

Paper VI: Avhad MR, Marchetti JM. Temperature and pretreatment effects on the drying of Hass avocado seeds. *Biomass and Bioenergy*. 2015: 83; 467-473.

Paper VII: Avhad MR, Marchetti JM. Mathematical modelling of the drying kinetics of Hass avocado seeds. *Industrial Crops and Products*. 2016: 91; 76-87.

Papers

Paper I

Renewable and Sustainable Energy Reviews 50 (2015) 696–718

Contents lists available at ScienceDirect

Renewable and Sustainable Energy Reviews

journal homepage: www.elsevier.com/locate/rser

A review on recent advancement in catalytic materials for biodiesel production

M.R. Avhad, J.M. Marchetti *

Department of Mathematical Sciences and Technology, Norwegian University of Life Sciences, Drøbakveien 31, Ås 1432, Norway

ARTICLE INFO

Article history:
Received 12 March 2015
Received in revised form
6 May 2015
Accepted 12 May 2015

Keywords:
Biodiesel
Alcoholysis reaction
Homogeneous catalyst
Heterogeneous catalyst

ABSTRACT

Biodiesel, which could be derived from plant oils and animal fats, is considered as a promising substitute for petroleum diesel fuel because of its advantages, such as renewability, biodegradability, less environmental toxicity, and superior combustion efficiency. The feedstock used for biodiesel production primarily include edible oils, non-edible oils, waste oils, and animal fats. Consistent scientific investigations are performed to locate innovative oil resources and minimize the utilization of expensive food-grade oils for biodiesel production. The extensive research information is available on the determination of physico-chemical properties of different plant oils. This review will present a general information related to the existing varieties of oil feedstocks, their lipid content, and fatty acid composition.

This article further discusses different methods employed to enable the usage of plant oils as biofuel, such as its direct use, blending, thermal cracking, microemulsion, and alcoholysis process. Among the possible methodologies for biodiesel production, alcoholysis process, in the presence or absence of a catalytic material, have been frequently employed. The benefits and limitations of using homogeneous, heterogeneous, enzyme catalysts, and supercritical method for the alcoholysis process are comprehensively discussed. In the current article, efforts have been made to review the recent inventions in homogeneous and heterogeneous catalytic materials utilized for biodiesel production. The present study shall provide a tool for the selection of an optimal catalyst for a large-scale biodiesel production.

Contents

* Corresponding author. Tel.: +47 67231647; fax: +47 64965401.
E-mail address: jorge.mario.marchetti@nmbu.no (J.M. Marchetti).

http://dx.doi.org/10.1016/j.rser.2015.05.038
1364-0321/

1. Introduction

Energy is a basic requirement for human existence. Due to a continuous growth in human population, the majority of the world total energy is utilized for the industrial applications, transportation, and for the power generation sector. According to the International Energy Outlook 2013 set by the U.S Energy Information Administration [1], the total energy consumed in 2010 was 5.5282×10^{20} J, which further is predicted to rise to 8.6510×10^{20} J by 2040. Accordingly, the total world energy consumption will grow by 56% between 2010 and 2040; this can be seen in Fig. 1.

Transportation is currently the second largest energy consuming sector and is increasing by an average of 1.1% per year [1]. In the current situation, the foremost amount of energy is supplied by the conventional fossil fuel resources, such as gasoline, liquefied petroleum gas, diesel fuel, and natural gas. However, the use of fossil fuels has several carcinogenic influences on the ecosystem, such as large greenhouse gas emissions, acid rain, and also global warming. In addition to serious environmental issues, dwindling reserves of crude oil, oscillating petroleum fuel prices, and the overconsumption of liquid fuels, especially for the transportation purposes, have made today's necessity to find an alternate "green" sources of energy which are sustainable, environmentally tolerable, economically competitive, and easily available. The numerous modes of renewable energy resources are anticipated to play a significant role in resolving the world's future power situation; therefore, over the past few years, researchers have driven their attention towards finding an appropriate replacement for fossil fuels. Renewable energy resources, such as solar energy, wind energy, hydro-energy, and biofuels (biodiesel, bioethanol, biogas, and biomass) have been considered as a potential alternative to reduce the entire dependency on the use of fossil fuels [2–4].

Amongst others, biodiesel is consistently gaining attention as a viable substitute for petroleum diesel in a near future due to its remarkable characteristics. Biodiesel production is persistently winning relevance and market due to its benefits, such as biodegradability, renewability, environmentally less toxicity, high combustion efficiency, high cetane number, high flash point, lower sulfur content, better lubrication, among others [5–6]. Furthermore, biodiesel, ensuring a flashpoint of 423 K, is a non-flammable and non-explosive fuel in contrast to petroleum diesel having flashpoint of 337 K. Consequently, handling, storage, and transportation of biodiesel becomes relatively easy and safe [7]. Additionally, biodiesel production could also provide an opportunity to improve the domestic oil market in developing countries, and enhance farm incomes and agricultural industries [6,8].

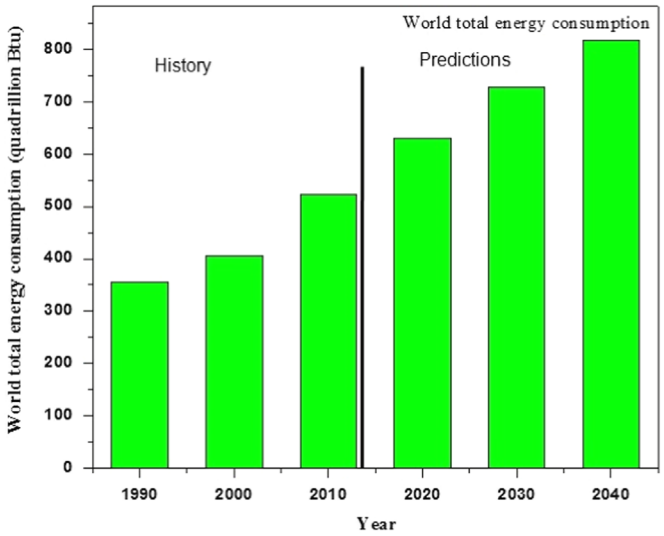

Fig. 1. World total energy consumption; history and projection.

In order to achieve the objective of understanding the valuable importance of biodiesel, the recent available literature were thoroughly reviewed to determine the current state-of-the-art and identify different oil sources, methodologies, and catalytic materials employed for biodiesel production. The current article will highlight the latest catalytic materials utilized for biodiesel production.

2. Biodiesel

According to the American Society for Testing and Materials (ASTM), biodiesel is defined as a mono-alkyl esters derived from lipid feedstocks, such as vegetable oils or animal fats [9]. The major components of plant oils and animal fats are triacylglycerol (TAGs); the esters of fatty acids and glycerol. The TAGs, also known as triglycerides, consists of different fatty acid composition which influences both physical and chemical properties of plant oils and animal fats; correspondingly also deciding the quality of biodiesel. There are two kinds of fatty acids: saturated fatty acids containing carbon-carbon single bond, and unsaturated fatty acids which include one or more carbon-carbon double bond. The most common fatty acids found in the lipid feedstocks are palmitic acid (16:0), stearic acid (18:0), oleic acid (18:1), linoleic acid (18:2), and linolenic acid (18:3). The other fatty acids which are also present in several plant oils include myristic acid (14:0), palmitoleic acid (16:1), arachidic acid (20:0), and erucic acid (22:1). Besides the presence of fatty acids, additional components, such as phospholipids, carotenes, tocopherols, sulphur compounds, and water might also be present in plant oils [5,10].

2.1. Different types of oils

The satisfactory replacement of petroleum diesel with biodiesel is feasible only if it encounters two basic requirements: first is its easy availability and environmentally acceptability, and second being economically reasonable. In current scenarios, cost of plant oils used accounts for about 60–80% of the total production cost of biodiesel [11–13]. Thus, wide ranges of feedstocks have been assessed for biodiesel production and could be divided into different categories, such as edible oils, non-edible oils, waste oils, animal fats, and algal lipids. The different forms of plant oils, animal fats, and other sources used for producing biodiesel are

listed in Table 1. The botanical name and oil content of edible and non-edible plant oils are illustrated in Table 2 [14–21].

2.1.1. Edible plant oils

The requirement of edible plant oils has been increased abruptly in the last few decades for two prime industrial reasons: first for the food industries, and second being its use as a biodiesel feedstock. Edible oils for biodiesel production mostly are used in countries like The United States of America, Argentina, Brazil, European nations, Malaysia, and Indonesia, where soybean oil [22], sunflower oil [23], rapeseed oil [24], and palm oil [25] are extensively used. In the current circumstances, around 95% of the world total biodiesel is produced from approximately 84%, 13%, and 3% amount of rapeseed oil, sunflower oil, and palm oil, respectively [17,26]. However, the continuous large-scale usage of edible plant oils for biodiesel production has been a great concern because their evolve problems, such as rise in the food prices, increasing starvation, deforestation, and usage of arable land for farming merely oil bearing plants. Furthermore, the cultivation of edible oil bearing plants depend heavily on the environmental conditions. Additionally, even its transportation to the biodiesel generation industry would possibly have an adverse effect on the capital cost of biodiesel. Thus, the current use of the food-grade plant oils as a feedstock for producing biodiesel are considered to be not worthy and stipulates search for relatively less expensive resources.

Table 1
Universal feedstocks utilized for biodiesel production.

Edible oils	Non-edible oils	Animal fats	Other resources
Coconut	Castor	Beef tallow	Algae
Corn	Cottonseed	Chicken fats	Cooking oil
Hemp seed	Desert date	Fish fats	Pomace oil
Mustard seed	Jatropha	Porklard	Soapstocks
Olive	Jojoba	Waste salmon	Tall oil
Palm	Karanja		
Peanut	Linseed		
Pumpkin seed	Mahua		
Rapeseed	Moringa		
Rice bran	Neem		
Safflower seed	Polonga		
Sesame seed	Rubeer seed		
Soybean	Tobacco seed		
Sunflower	Tung		

Table 2
Botanical name and oil content of edible and non-edible plant oils [9,14–21].

Type	Common name	Botanical name	Oil content (wt%)	Ref.
Edible	Cocunut	*Cocos Nucifera* L.	65–68	[9]
	Corn	*Zeamays*	3.1–5.7	[9]
	Hemp seed	*Cannabis Sativa* L.	22–38	[17]
	Mustard seed	*Brassica nigra*	33	[18]
	Olive	*Olea europaea*	45–70	[15]
	Palm	*Elaeis guineensis*	45–50	[9]
	Peanut	*Arachis hypogea* L.	45–50	[9]
	Pumpkin seed	*Cucurbita maxima*	31.5	[19]
	Rapeseed	*Brassica napus*	40–45	[9]
	Rice bran	*Oryza sativa*	15–23	[15]
	Safflower seed	*Carthamus tinctorius*	35	[20]
	Sesame seed	*Sesamum indicum*	50	[21]
	Soybean	*Glycine max*	18–20	[9]
	Sunflower	*Helianthus annuus*	25–30	[15]
Non-edible	Castor	*Ricinus communis* L.	45–50	[14]
	Cottonseed	*Gossypium hirsutum* L.	18–20	[9]
	Desert date	*Balanites aegyptiaca*	45–50	[16]
	Jatropha	*Jatropha curcas* L.	50–60	[14]
	Jojoba	*Simmondisa chincnsis*	45–50	[15]
	Karanja	*Pongamia pinnata*	30–40	[14]
	Linseed	*Linum usitatissimum*	35–45	[14]
	Mahua	*Madhuca indica*	35–40	[14]
	Neem	*Azadirachta indica*	20–30	[14]
	Polanga	*Calophyllum inophyllum*	65	[16]
	Rubber seed	*Hevea brasiliensis*	40–60	[16]
	Tobacco	*Nicotiana tabacum* L.	30–43	[15]
	Tung	*Vernicia montana*	16–18	[15]

2.1.2. Non-edible plant oils

Recently, non-edible plant oils have gained enormous attention as a new generation feedstock because of their high oil content, easy availability, and having the advantage that it could be grown in empty territories which are not suitable for agriculture. Also, the growth of non-edible oil bearing plants are not reliable on the regional weather conditions and could be grown with less intensive attention; thus, reducing the cost of cultivation. Some of the well-known and mostly investigated non-edible plant oils for biodiesel production include jatropha seed oil [27,28], jojoba oil [29], karanja oil [30], linseed oil [31], cottonseed oil [32], amongst other.

All the above mentioned edible and non-edible plant oils have dissimilar fatty acid composition, which consequently, influences physical as well as chemical properties of the produced biodiesel. The detail fatty acid composition of the edible plant oils can be seen in Table 3 [5,18,19,33–39] and those for the non-edible plant oils are depicted in Table 4 [15,27,28,40-50].

2.1.3. Waste oils and animal fats

The residual obtained after using oil for the cooking purposes is generally discarded with no further application. Over the last few years, waste cooking oil has been considered as a possible feedstock for biodiesel production due to its low cost [51]. However, waste oil is highly impure consisting mainly of high free fatty acid (FFA). Hence, waste cooking oil could be categorized in two groups based on its FFA content: the yellow grease (FFA $< 15\%$), and the brown grease (FFA $> 15\%$). These oils after the filtration and purification processes could be used for biodiesel production.

Animal fats, such as beef tallow [52], duck tallow [53], chicken fats [54], fish fats, amongst other are also tested as a feedstock for biodiesel production. Biodiesel obtained from animal fats have been reported to possess high cetane number; however, fuel derived from such resource have high cold filter plugging point due to the significant amount of saturated fatty acids in fats, and are less resistant towards the oxidation process due to the absence of natural antioxidants.

2.2. Use of straight plant oils

The direct use of peanut oil in a diesel engine is recognized to be the first step towards the invention of plant oils based renewable biofuel. It was said that the diesel engine ran successfully on peanut oil, but further studies have confirmed that the direct use of plant oils as a fuel is not appropriate due to their larger molecular mass, high kinematic viscosity, low volatility, and poor cold flow properties. These unfavorable properties of plant oils thus direct poor atomization of the fuel spray as well as coking of the injectors, combustion chamber, and valve [45,55–57]. Furthermore, the long term use of plant oils as a fuel in the diesel engine could also cause severe problems, such as thickening and gelling of lubricating oil, and ring sticking; thus, resulting in incomplete combustion of fuel and increasing the exhaust smoke level [56,57].

Table 3
Fatty acid composition profile of edible plant oils [5,18,19,33-39].

Species		Fatty acid composition (wt%)													
Common name	**Properties**	**Waste coconut oil**	**Corn**	**Hempseed(~)**	**Mustard seed**	**Olive**	**Palm**	**Peanut**	**Pumpkin seed**	**Rapeseed**	**Rice bran**	**Safflower seed**	**Sesame**	**Soybean**	**Sunflower**
Lauric acid 12:0[Abb]	$C_{12}H_{24}O_2$[MF] 200.32[M]	–	–	–	–	–	0.10	–	–	–	–	–	–	–	0.53
Myristic acid 14:0[Abb]	$C_{14}H_{28}O_2$[MF] 228.38[M]	0.50	–	–	0.05	–	0.70	0.10	–	–	–	–	–	–	–
Palmitic acid 16:0[Abb]	$C_{16}H_{32}O_2$[MF] 256.43[M]	21.40	–	6.0–8.5	5.54	11.60	36.70	8.0	13.80	–	22.00	11.07 (±0.10)	9.80 (±0.21)	16.29 (±0.54)	6.14
Palmitoleic acid 16:1[Abb]	$C_{16}H_{30}O_2$[MF] 254.42[M]	0.20	11.67	–	0.21	1.00	0.10	–	–	3.49	–	–	–	–	0.09
Stearic acid 18:0[Abb]	$C_{18}H_{36}O_2$[MF] 284.48[M]	3.00	1.85	2.5–3.0	1.51	3.10	6.60	1.80	11.20	0.85	3.00	4.37 (±0.10)	6.30 (±0.15)	6.66	4.11
Oleic acid 18:1[Abb]	$C_{18}H_{34}O_2$[MF] 282.47[M]	27.50	25.16	12.0–15.0	8.83	75.00	46.10	53.30	29.50	64.40	38.00	12.76 (±0.22)	41.82 (±0.91)	22.70 (±0.07)	34.30
Linoleic acid 18:2[Abb]	$C_{18}H_{32}O_2$[MF] 280.46[M]	47.40	60.60	52.0–56.0	10.79	7.80	8.60	28.40	45.5	22.30	35.00	69.65 (±0.24)	40.50 (±1.01)	44.13 (±0.60)	51.17
Linolenic acid 18:3[Abb]	$C_{18}H_{30}O_2$[MF] 278.44[M]	–	0.48	–	20.98	0.60	0.30	0.30	–	8.23	–	0.49 (±1.15)	0.32 (±0.01)	8.97 (±0.52)	2.23
Arachidic acid 20:0[Abb]	$C_{20}H_{40}O_2$[MF] 312.54[M]	–	0.24	0.5–0.8	1.21	0.30	0.40	0.90	–	–	–	0.78 (±0.05)	0.67 (±0.03)	0.62 (±0.11)	0.17
Gadoleic acid 20:1[Abb]	$C_{20}H_{38}O_2$ 310.51[M]	–	–	–	5.27	–	0.20	2.40	–	–	–	–	–	–	–
Behenic acid 22:0[Abb]	$C_{22}H_{44}O_2$[MF] 340.60[M]	–	–	–	1.09	0.10	0.10	3.00	–	–	–	0.59 (±0.09)	–	0.63 (±0.02)	0.41
Erucic acid 22:1[Abb]	$C_{22}H_{42}O_2$[MF] 338.58[M]	–	–	–	37.71	–	–	–	–	–	–	–	–	–	0.53
Lignoceric acid 24:0[Abb]	$C_{22}H_{42}O_2$[MF] 368.63[M]	–	–	–	1.68	0.50	0.10	1.80	–	–	–	0.29 (±0.13)	–	–	–
Nervonic acid 24:1[Abb]	$C_{24}H_{48}O_2$ [MF] 366.62[M]	–	–	–	2.22	–	–	–	–	–	–	–	–	–	–
Others/Unknown	–	–	–	α-Linolenic 15.5–18.0 γ-Linolenic 2.3–3.0	0.66	–	–	–	–	–	α-Linolenic 2.00	–	–	–	Margaric 0.09 Margaroleic 0.06 Eicosenic 0.17
References		[33]	[5]	[34]	[18]	[35]	[35]	[35]	[19]	[5]	[36]	[37]	[38]	[37]	[39]

MF – Molecular formula; Abb – Abbreviation; M – Molecular weight; (~) – The fatty acid composition was specified in an range.

Table 4
Fatty acid composition profile of non-edible plant oils [15,27,28,40-50].

Species		Fatty acid composition (wt%)													
Common name	**Properties**	**Castor seed**	**Cottonseed**	**Desert date Kernel**	**Jatropha**	**Jojoba**	**Karanja**	**Linseed**	**Mahua**	**Moringa**	**Neem**	**Polonga**	**Rubber seed**	**Tobacco seed**	**Tung**
Myristic acid 14:0[Abb]	$C_{14}H_{28}O_2$[MF] 228.38[M]	–	1.00	–	–	–	–	–	–	–	–	–	–	0.14	–
Palmitic acid 16:0[Abb]	$C_{16}H_{32}O_2$[MF] 256.43[M]	1.00	25.80	15.40(±0.26)	15.20	1.20	11.65	5.10	17.80	7.60	18.1	12.01	10.20	8.46	4.00
Palmitoleic acid 16:1[Abb]	$C_{16}H_{30}O_2$[MF] 254.42[M]	–	0.60	–	0.70	–	–	0.30	–	1.40	–	–	–	–	–
Stearic acid 18:0[Abb]	$C_{18}H_{36}O_2$[MF] 284.48[M]	–	2.50	19.01(±0.29)	6.80	–	7.50	2.50	14.00	5.50	18.1	12.95	8.70	3.38	1.00
Oleic acid 18:1[Abb]	$C_{18}H_{34}O_2$[MF] 282.47[M]	3.00	16.4+0.8=17.20	25.74(±0.35)	44.60	10.70	51.59	18.90	46.30	66.60	44.5	34.09	24.60	11.24	8.00
Linoleic acid 18:2[Abb]	$C_{18}H_{32}O_2$[MF] 280.46[M]	5.00	51.50	39.85(±0.48)	32.20	–	16.46	18.10	17.90	8.10	18.3	38.26	39.60	75.58	4.00
Linolenic acid 18:3[Abb]	$C_{18}H_{30}O_2$[MF] 278.44[M]	1.00	0.20	–	–	–	2.65	55.10	–	0.20	0.2	0.30	16.30	1.14	3.00
Arachidic acid 20:0[Abb]	$C_{20}H_{40}O_2$[MF] 312.54[M]	–	0.30	–	0.20	9.10	–	–	–	5.80	0.8	–	–	–	–
Gondoic acid 20:1[Abb]	$C_{20}H_{38}O_2$[MF] 310.53[M]	–	–	–	–	59.50	–	–	–	–	–	–	–	–	–
Gadoleic acid 20:1[Abb]	$C_{20}H_{38}O_2$ 310.51[M]	–	–	–	–	–	–	–	–	1.70	–	–	–	–	–
Behenic acid 22:0[Abb]	$C_{22}H_{44}O_2$[MF] 340.60[M]	–	0.20	–	–	–	–	–	–	–	–	––	–	–	–
Erucic acid 22:1[Abb]	$C_{22}H_{42}O_2$[MF] 338.58[M]	–	-	–	–	12.30	–	–	–	–	–	–	–	–	–
Lignoceric acid 24:0[Abb]	$C_{22}H_{42}O_2$[MF] 368.63[M]	–	–	–	–	–	–	–	–	–	–	–	–	–	–
Nervonic acid	$C_{24}H_{48}O_2$	–	–	–	–	1.70	–	–	–	–	–	–	–	–	–
24:1[Abb]	[MF] 366.62[M]														
Riconoleic acid	$C_{18}H_{34}O_3$	89.00	–	–	–	–	–	–	–	–	–	–	–	–	–
18:1(OH) [Abb]	[MF] 298.46[M]														
Others/ Unknown		Estearic acid 1.00	0.70	–	Heptadecanoic acid 0.10 α-Linolenic 0.20	Docot–trasenic acid 3.70	–	–	–	–	–	–	–	–	Eleostrearic80.00
References		[40]	[41]	[42]	[27,28]	[44]	[43]	[45]	[46]	47	[48]	[43]	[49]	[50]	[15]

MF – Molecular formula; Abb – Abbreviation; M – Molecular weight.

2.3. Blending of plant oils

Biodiesel is an oxygenated fuel and contains no petroleum products, but is compatible and could be blended with petroleum diesel in order to reduce the extensive utilization of the latter fuel. Blending plant oils with petroleum diesel could be one of the possible options to reduce its kinematic viscosity; thus, allowing its appliance as a fuel.

Rakopoulos et al. [58] utilized sunflower, cottonseed, corn, and olive oil blended with petroleum diesel for running a laboratory-installed heavy duty, direct injection, four-stroke, water cooled, six-cylinder diesel engine (Mercedes-Benz OM 366 LA). The reported study indicated that the use of blended fuel reduced the smoke emissions, but nitrogen oxides (NO_x), carbon monoxide (CO), and unburned hydrocarbons (UHCs) level intensified with increasing percentage of plant oils in diesel. On the other hand, Bajpai et al. [59] reported that blending diesel with maximum 10% of karanja oil reduced the exhaust smoke as well as the CO emissions. However, preheating of the blended fuel was recommended to reduce its kinematic viscosity. Misra and Murthy [60] explained that the reduction in CO emissions, when soapnut oil blended diesel was tested in a single-cylinder diesel engine, was due to the high availability of oxygen in the blended fuel. Furthermore, the NO_x emissions were dropped even after adding 40% soapnut oil in petroleum diesel. However, it was reported that the increase in the oil content amplified the viscosity of fuel; thus, preceded improper spraying pattern, and incomplete fuel combustion.

İşcan et al. [61] reported that insulating the engine combustion chamber decreased the heat transfer and improved its thermal efficiency. The zirconia coated engine, fueled with the waste corn oil blended diesel, running at an engine speed of 2750 rpm displayed improved air movements in the engine cylinder, thus resulting in a better homogeneous air-fuel charge and combustion. However, the determined engine performance and exhaust emissions indicated that due to a higher engine temperature, NO_x emissions were found to be rising. In a comparative study, Aydin [62] found that sunflower oil blended diesel fuel displayed better engine performance than the blended cottonseed oil fuel when both the blended fuels were tested to run a zirconia coated diesel engine.

The blending of plant oils with petroleum diesel could be considered as a possible option to reduce the entire dependency on the conventional fuel and to promote the use of renewable energy; however, the long term use of blended fuel in a diesel engine could result in the carbon deposition and coking of the injectors. The coating of the combustion chambers could improve the diesel engine efficiency and enable more effective use of blended fuel; however, its prolonged use might cause cracks on the coating surface. Furthermore, the utilization of high percentage of plant oils for blending could also increase exhaust smoke, CO, NO_x, and UHCs. The above mentioned complications take place because the blending process is associated with the physical alteration of oils, whereas, the chemical properties, such as the molecular structure of oil molecules remains the same. In order to make potential use of plant oils as a fuel, their chemical properties, such as molecular mass, kinematic viscosity, volatility, and cetane number are required to be modified.

3. Transformation of plant oils to biodiesel

The kinematic viscosity of plant oils fluctuates around 10–17 times higher than that of the petroleum diesel. The successful transformation of plant oils to biodiesel will not only reduce its kinematic viscosity but also modify the chemical properties. Biodiesel obtained through the conversion of plant oils has both physical and chemical properties adjacent to those of the petroleum diesel fuel; and thus, could be directly used in a diesel engine with less or no engine modifications. The methodologies employed for producing biodiesel, such as thermal cracking (pyrolysis), micro-emulsion, and alcoholysis will be further discussed.

3.1. Thermal cracking (pyrolysis)

Thermal cracking, also known as pyrolysis, is a process of a cleavage of oil molecules and fast forming a mixture of hydrocarbons with the properties similar to those of the petroleum fuel [63]. The thermal cracking process involving a decarboxylation reaction is performed at an elevated temperatures (above 350 °C), either in the presence, or in the absence of a catalyst. The thermal cracking of plant oils or animal fats takes place in two successive and distinct stages: the primary stage involves the formation of an acid species through the decomposition of TAGs molecules in which the breakage of C–O bonds occur within the glycerides part of a TAGs chain, while, the second stage is characterized by the degradation of acids produced in the first stage leading towa7rds the formation of hydrocarbons. Generally, the thermal cracking method is largely used for the production of biodiesel from animal fats and waste cooking oils, and widely employed in a region where the cultivation of raw oil bearing plants is in a scarcity.

Kozliak et al. [64] reported that in a bench-scale continuous thermal cracking process of non-triglycerides jojoba wax-oil performed in the presence of nitrogen pressure of 14.8×10^5 Pa, reaction temperature of 450 °C was required for the formation of the desired products. It was reported that jojoba wax-oil remained uncracked at 420 °C, while, the reaction temperature of 470 °C resulted in over-cracking which directed the generation of unwanted gas products. Furthermore, it was also reported that the thermal cracking of jojoba wax-oil was advantageous over that of soybean oil in producing low molecular weight hydrocarbons and fatty acids. The products obtained from thermal cracking of soybean oil contained high molecular weight viscous chemicals which were due to the presence of glycerol backbone in TAGs of soybean oil that promoted the formation of polymers/oligomers. Biswas et al. [65] reported a study focused on thermal cracking of jatropha oil in an isothermal and non-isothermal reaction conditions. The reaction was performed in an isothermal batch reactor in the presence of nitrogen gas flow of 120 ml h^{-1} revealed that the complete cracking of jatropha oil was achieved at a reaction temperature of 375 °C. The obtained product contained 73% liquid, 26% gaseous product, and less than 1% char. The liquid product contained 91% aliphatic carbon, and 6.9% aromatic carbon. It was concluded that TAGs molecules undergo dehydration, decarboxylation, decarbonylation, recombination, and rearrangement reactions to generate hydrocarbons. The generated gaseous products consisted of methane, pentane, iso-butane, and uncondensed compounds. The reaction kinetic studied in a non-isothermal reaction conditions indicated that during the thermal cracking process, bigger TAGs molecules breaks into smaller organic molecules, followed by their degradation. The average activation energy for the first and second step was 114.49 kJ mol^{-1} and 221.88 kJ mol^{-1}, respectively. The average activation energy for the complete degradation reaction was 168.18 kJ mol^{-1}. Luo et al. [66] reported that the presence of a hydrogen environment had no significant impact on thermal cracking of soybean oil, canola oil, and their respective methyl esters. The results obtained from a comparative study indicated that better yields of esters were obtained using canola oil. The difference in the results was assumed due to a higher oleic-to-linoleic acid chain ratio in the TAGs of canola oil. The oleic acid in canola oil has only one double bond at a ω-9 position which resulted in its cracking to compounds that are predominantly collected in the liquid crackate, while, linoleic acid chains in soybean oil have two double bonds (ω-9 and ω-6 positions) and a portion of ω-6 position associated in the cracking

resulted in the production of light alkanes that end up in the generation of non-condensable gas phase products. Prado and Filho [67] found that the catalytic thermal cracking have shorter reaction time compared to the non-catalytic one. The thermal cracking of soybean oil was performed in the presence of bauxite catalyst and with 10%, 20%, and 30% catalyst dose. The thermal cracking was studied at a temperature range between 380 °C and 400 °C in three different systems namely: simple cracking (SC), modified simple cracking (MSC), and fractionated cracking (FC). The products obtained from SC showed the presence of long chain fatty acids, such as oleic, palmitic, linoleic, linolenic, and stearic acids due to the incomplete secondary cracking; whereas, the MSC and FC systems were more efficient in decomposing the long chain fatty acids. It was reported that bauxite catalyst enhanced the secondary cracking. The secondary cracking process controlled the formation of hydrocarbons, such as alkanes, alkenes and aromatics, and few oxygenated compounds, such as carboxylic acids, ketones, and alcohols.

The thermal cracking process has an advantage of being adjusted to the usage of low quality feedstocks. However, this process follows different reaction mechanism; thus, keeping control on the selectivity of the desired product becomes extremely challenging. In addition, the reaction variables heavily decide the selectivity of the products. The presence of glycerol backbone in TAGs molecules directs the formation of intermediates, particularly ketene, ethyl radical, propylene, and ethylene oxides which initiates the polymerization reaction and are also responsible for the gaseous product formation [64,67].

3.2. Microemulsification

Microemulsions are clear and thermodynamically stable isotropic mixtures with three phases: aqueous, an oil, and a surfactant phase. The aqueous phase might contain salts or other ingredients, and the oil phase possibly will consist complex mixture of different hydrocarbons and alkenes [68]. This ternary phase system could improve spray characteristics by explosive vaporization of low boiling constituents in the micelles. The term “microemulsions” was described as an optically isotropic system and transparent oil and water dispersion consisting of approximately equal volumes of the two phases. The oil and water dispersion contained droplets of either water, or oil in the appropriate continuous phase, with the droplets having diameters that were somewhat greater than those of the swollen micelles. Microemulsions exist in four different forms: Winsor-Type-I (oil-in-water) microemulsions solubilize oil into spherical normal micelles within the continuous water phase, while, type-II (water-in-oil) microemulsions solubilize water in the reverse micelles occurring in the oil phase. The type-III (middle phase) microemulsions exhibits an excess oil and water phases in equilibrium with a bi-continuous phase when lamellar micelles are formed in the system. In the middle phase microemulsions, increasing surfactant concentration increases volume of the middle phase until all oil and water coexists in a Type-IV single-phase microemulsions [69,70]. Microemulsions using solvents such as ethanol, and ionic and non-ionic surfactants are demonstrated by several scientists and are discussed below.

Nguyen et al. [70] used reverse-miceller microemulsions of diesel to extract oil from peanut into the oil phase and produce a blend of peanut oil and diesel. The surfactants, such as rhamnolipid, sorphorolipid, lipcithin, and oleyl alcohol were utilized in this study. Using solid-to-solvent ratio of 1:5, temperature of 23 °C and 200 rpm stirring intensity, the highest oil extraction efficiency of around 95% was observed after 40 min of reaction in the presence of diesel based reverse-miceller microemulsions; while that produced by diesel and hexane was 89%. The remarkable results for reverse-miceller microemulsions were attributed to the presence of water which enhanced the extraction of the polar rich proteins, thus, releasing more oil trapped within them. Naksuk et al. [71] reported that the palm kernel oil extraction using surfactant-microemulsion method could be a good substitute for the hexane based oil extraction method. The non-ionic 3% Comperlan KD and an anionic extended 0.1 wt% Alfoterra 145-5PO or 145-8PO surfactants were employed for the oil extraction from palm kernel. Qi et al. [72] tested the performance, emissions, and combustion characteristics of a two-cylinder, four-stroke, water cooled, 17:1 compression ratio diesel engine which ran on microemulsions consisting of a rapeseed oil-diesel blend, an ethanol and a surfactant. The volume fraction of rapeseed oil in diesel was 20%, oleic oil was used as a surfactant, and ethanol composition varied from 0% to 30%. The viscosity and density of microemulsions was reduced with the ethanol addition, and reached similar to those of diesel with the addition of 30% ethanol amount. However, the surfactant quantity required for maintaining the steady state of microemulsion increased with the ethanol addition.

3.3. Alcoholysis

The alcoholysis process is the most frequently performed and is an established method for the transformation of plant oils to biodiesel. In general, the catalysts used for the alcoholysis reaction could be classified as homogeneous or heterogeneous ones; which further could be subdivided into three categories: acid, base, and acid-base bi-functional catalysts. Recently, several researchers have focused their attention towards finding a bio-catalytic pathway for biodiesel production. The non-catalytic or catalytic supercritical alcoholysis process has been also gaining the consideration as one of the developing methodologies for biodiesel production. A schematic representation for the different branches of feedstocks and catalytic systems used for biodiesel production can be seen in Fig. 2.

The alcoholysis reaction is also known as transesterification reaction of TAGs, and esterification reaction of FFA. In a stoichiometric transesterification reaction, one TAGs molecule reacts with three alcohol molecules to produce three moles of fatty acid alkyl esters (FAAE) and one molecule of glycerol. This process consists of three sequential reversible reactions where one triglyceride molecule delivers one diglyceride molecule and from them one monoglyceride molecule is formed; in each step, one molecule of biodiesel is being produced [9,73,74]. A general reaction and a sequence for the transesterification process can be seen in Fig. 3 and Fig. 4, respectively.

The transesterification reaction is a reversible process, and therefore, an excess of alcohol is usually required to shift the reaction equilibrium towards the formation of products. The types

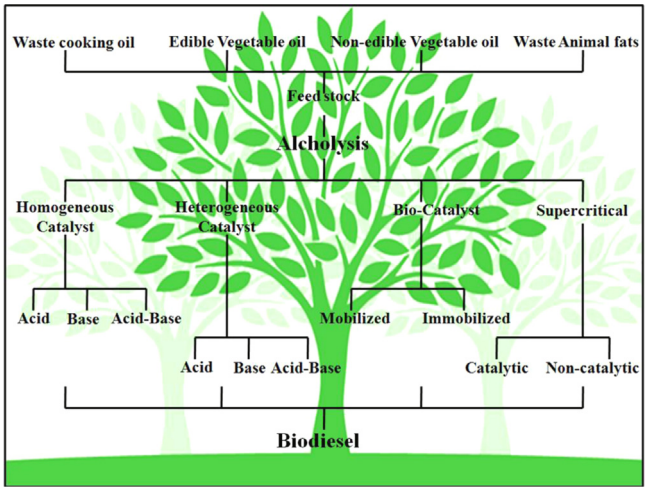

Fig. 2. Schematic diagram for alcoholysis reaction.

of alcohol that could be used for the alcoholysis reactions include short chain, long chain, and cyclic alcohols; however, methanol and ethanol are widely utilized because of their superior reactivity, polarity, availability, and low cost. Different techniques, such as microwave heating [75], ultrasonic-irradiation [76], and super-critical method [77] are tested to improve the miscibility between the oil and alcohol phase. Furthermore, the operative reaction variables, such as type of alcohol, alcohol-to-oil molar ratio, catalyst nature, catalyst amount, reaction temperature, reaction time, stirring intensity, presence of co-solvent, and reusability of catalytic materials also have significant role in deciding the alcoholysis reaction rate, final biodiesel yield, and consequently overall cost of biodiesel. Nevertheless, biodiesel production through the transesterification pathway is heavily reliant on the nature of feedstocks. The base-catalyzed transesterification reactions are faster than the one catalyzed by acidic materials; however, the applicability of base catalysts is restricted to high quality oils containing negligible amount of FFA and water. The presence of water in the feedstock results in the formation of FFA or promotes the hydrolysis reaction of esters. On the other hand, the presence of FFA in the base-catalyzed reaction mixture direct the reaction towards undesired route, such as the saponification [78]. The soap formation reduces the final biodiesel yield because the esters gets dissolved in the glycerol phase leading towards the formation of ester-glycerol emulsion, and thus, the separation and purification of products becomes complicated [79]. The soap formation due to the reaction between FFA and a base catalyst can be seen in Fig. 5.

One of the possible options to minimize the FFA amount in the low quality feedstocks is its removal via saponification process, and then introduce the remaining feedstock to the base-catalyzed transesterification reaction. However, decaying large proportion of feedstock for the soap formation could be considered economically irrelevant. Furthermore, this process will consume large amount of catalyst, and the additional separation and purification units will be required. The other alternative which is widely recommended

Fig. 5. Saponification reaction of free fatty acid.

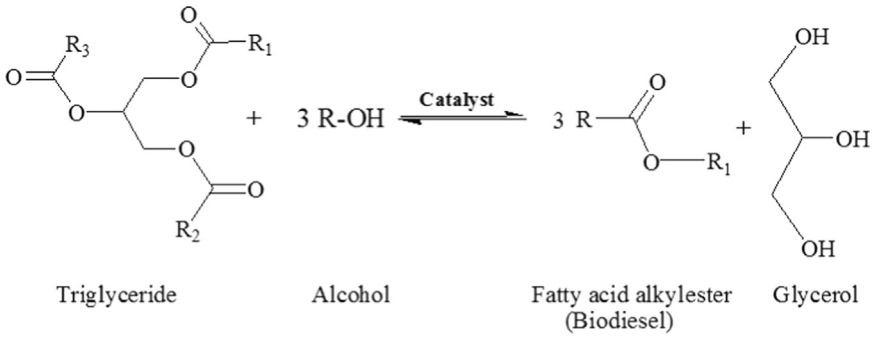

Fig. 3. General transesterification reaction of vegetable oils.

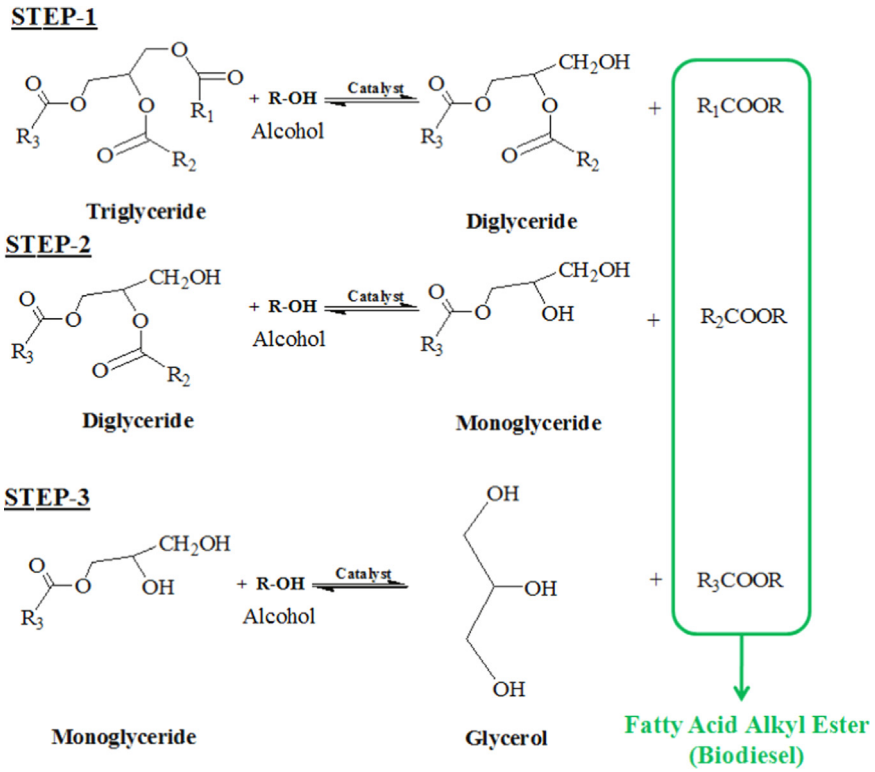

Fig. 4. Step-wise transesterification reaction.

is an acid-catalyzed esterification process of FFA. The FFA in the low quality is treated with an alcohol in the presence of acid catalyst to produce FAAE. The remaining feedstock is then subjected to a base-catalyzed transesterification process to produce additional esters. The general reaction for the FFA esterification process can be seen in Fig. 6.

Although acid catalyst could also be used to assist transesterification reaction, the rate of acid-catalyzed transesterification reaction is extremely slow and it could take around a day to achieve the complete transformation of oil to biodiesel [80]. However, the prime advantage of acid-catalyzed esterification process is that it enables usage of non-edible oils, waste cooking oils, poultry fats, industrial by-products, and other feedstocks containing elevated amount of FFA for biodiesel production.

4. Homogeneous catalysis for alcoholysis reaction

4.1. Homogeneous base-catalyzed alcoholysis reaction

The base-catalyzed alcoholysis process is well known to produce biodiesel in relatively short reaction time. The homogeneous alkali catalysts, such as sodium hydroxide (NaOH), and potassium hydroxide (KOH) have been widely used for producing biodiesel due to their high activity, low cost, and easy availability. The sodium based catalysts are usually reported to be better than the potassium based catalysts due to its lower molecular weight. However, using KOH could also be beneficial as the post reaction mixture then may possibly be neutralized with phosphoric acid to synthesize potassium phosphate and use it as a fertilizer. However, it is worth mentioning that the performance of these proficient catalysts depends heavily on the impurities content in the feedstock.

Keera et al. [81] suggested that when using 1 wt% amount of NaOH catalyst, around 97% biodiesel yield was achieved when transesterification reaction between cottonseed oil and methanol was carried out at 60 °C for 60 min. Furthermore, it was also investigated that esters produced from soybean oil possessed higher cetane number and lower kinematic viscosity than those produced from cottonseed oil, thus suggesting that soybean oil is a better feedstock for biodiesel production. Dias et al. [82] reported that sodium based catalysts, such as NaOH, and sodium methoxide ($NaOCH_3$) represented superior catalytic activity than the potassium based (KOH) counterpart for the alcoholysis reaction of soybean oil, sunflower oil, and waste frying oil. It was mentioned that the biodiesel yield using 0.4 wt% and 1 wt% catalyst amount were almost similar, but the kinematic viscosity of biodiesel produced using lower catalyst concentration was above the EN standards limiting value; thus indicating need of higher catalyst concentration to satisfy the viscosity factor. Uzun et al. [83] reported that sodium ethoxide-assisted transesterification between waste frying oil and methanol produced 96% biodiesel yield within 30 min of reaction performed at 50 °C using stirring rate of 600 rpm, and 0.5 wt% catalyst amount; however, it was highlighted that NaOH is an appropriate catalyst among the hydroxides, ethoxides, and methoxides of sodium and potassium due to its low cost and easy availability.

On the other hand, Chung et al. [84] reported that KOH is better catalyst than NaOH, and $NaOCH_3$. The KOH-catalyzed transesterification reaction between duck tallow and methanol resulted in 97% biodiesel yield after 180 min of reaction performed at 65 °C

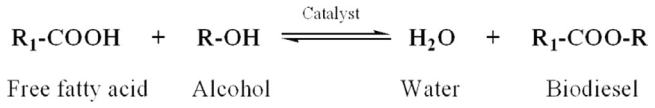

Fig. 6. Esterification reaction of free fatty acid.

using methanol-to-oil molar ratio of 6:1, and 1 wt% catalyst amount. Similar results were documented by Fadhil and Ali [85] where it was suggested that KOH is a superior catalyst than NaOH to transesterify silurus triostegus Heckel fish oil. In a multiple-step transesterification reaction, 96% biodiesel yield was reported after 60 min of reaction performed at 32 °C using methanol-to-oil molar ratio of 6:1, and 0.5 wt% catalyst dose. However, it was said that the multiple-step transesterification process had no significant role in improving biodiesel yield. Li et al. [86] suggested that adding dichloromethane (DCM) as a co-solvent into the reaction mixture, consisting soybean oil, methanol, and a KOH catalyst, increased miscibility between the oil and alcohol phase. The improved miscibility thus increased the transesterification reaction rate and the final biodiesel yield, producing 96% biodiesel yield after 120 min of reaction performed at 45 °C using methanol-to-oil molar ratio of 4.5:1, 4% of DCM, and 1 wt% of KOH amount. Fernandes et al. [87] reported that the addition of up to 300 mg Kg^{-1} of tert-butylhydroquinone improved the oxidation stability of biodiesel by 360 min produced from cottonseed oil using either methanol or ethanol, in the presence of KOH catalyst.

Chen et al. [88] studied the impact of heating methodology on the $NaOCH_3$-catalyzed transesterification reaction between waste cooking oil and methanol. It was found that the microwave heating outperforms the conventional heating system, producing almost 98% biodiesel yield within 3 min of transesterification reaction performed using methanol-to-oil molar ratio of 6:1, and 0.75 wt% catalyst amount. It was investigated that the absorption of microwave radiation directed the excitation of –OH group, thus exceeding the activation energy required for transesterification reaction. Furthermore, it was said that methanol is a good microwave absorber which improved the methanol-oil phase miscibility. Brito et al. [89] reported that the three-steps low frequency ultrasonic-assisted ethanolysis reaction of soybean oil produced more biodiesel in less time than that produced after two-steps of conventional transesterification reaction. The ultrasonic-assisted transesterification reaction performed in the presence of 1 wt% KOH amount and ethanol-to-oil molar ratio of 6:1 produced 98% biodiesel within 6 min of reaction.

Even though sodium and potassium based alkali catalysts have been widely utilized for biodiesel production, the usage of such catalysts have always amplified overall biodiesel cost interrelated with their separation and purification from the post-reaction mixture, and disposal issues of the generated waste water stream. Few organic bases have been also utilized as a catalyst for biodiesel production. Karavalakis et al. [90] reported a study focused on the use of amine-based liquid catalysts, such as tetramethyl ammonium hydroxide (TMAH) and benzyltrimethyl ammonium hydroxide (BTAH) for the methanolysis of cottonseed oil, and waste frying oil. The reported results suggested that both catalysts displayed superior activity for biodiesel production; however, the time required for the completion of transesterification of cottonseed oil was 120 and 90 min in the presence of TMAH and BTAH catalysts, respectively; indicating that BTAH is slightly better catalyst than TMAH for biodiesel production. In the case methanolysis of waste frying oil, greater amount of catalyst and reaction time was required to satisfactorily complete the transesterification reaction. The alkaline metal-free homogeneous 1,1,3,3-Tetramethylguanidine (TMG) catalyst was also tested for biodiesel production from cottonseed oil and waste frying oil [91]. It was reported that the soap formation was not observed because the FFA in oil reacted with amine catalyst and directed the formation of low acidity fatty acid amides and tetramethylguanidine organic salts. The use of TMG catalyst leaves no neutralization salts in the glycerol by-product, thus eliminating catalyst removal steps and minimizing the generation of waste water stream [91]. Yao et al. [92] tested tri-ethylamine (TEA), di-ethylamine (DEA), and tert-butylamine (t-BA) catalysts for transesterification of cottonseed oil. The reported study

stated that the addition of 367.1 mg kg^{-1} KOH as a co-catalyst augmented the biodiesel yield and NMR spectra revealed that no amines existed in the product. A summary of different basic homogeneous catalysts used for biodiesel production accompanied by the reaction variables, final performance of the alcoholysis reactions, and the corresponding references are tabulated in Table 5.

4.2. Homogeneous acid-catalyzed alcoholysis reaction

The formation of soap due to the reaction between FFA and a homogeneous base catalyst is considered to be detrimental for biodiesel production due to the fact that it reduces the final esters yield and triggers further complicated separation and purification steps. Accordingly, the acid-catalyzed esterification of FFA or acid-catalyzed simultaneous esterification and transesterification of feedstocks containing considerably higher amount of FFA is considered as a substitute option. The acid catalysts are tolerant to the presence of FFA in feedstocks; however, the existence of water in the reaction mixture above certain threshold value might have a negative impact on biodiesel production process.

Farag et al. [93] reported that among several homogeneous acid catalysts, such as sulfuric acid (H_2SO_4), hydrochloric acid (HCl), aluminum chloride, tin chloride, and iron sulfate, H_2SO_4 represented better catalytic activity for esterification of FFA. The H_2SO_4 catalyst was found to possess excellent catalytic activity for the esterification reaction, transforming 96% of FFA in the model oil which was prepared using oleic acid, and a mixture of sunflower oil and soybean oil. The highest FFA conversion was obtained after 60 min of esterification reaction performed at 60 °C using catalyst amount of 2.5 wt%, and 6:1 alcohol-to-oil molar ratio. The influence of the nature of alcohol on oil conversion was also investigated where methanol was found to be better reactant, followed by the mixture of alcohol (methanol+ethanol; 50/50 vol%), mixture of alcohol (methanol+propanol; 50/50 vol%), ethanol, and propanol. Aranda et al. [94] investigated the catalytic activity of H_2SO_4, methanesulfonic acid, phosphoric acid, and trichloroacetic acid for esterification of palm oil fatty acid. Among them, H_2SO_4 was observed to be the best catalyst, followed by methanesulfonic acid, and phosphoric acid. On the other side, trichloroacetic acid displayed no role in catalyzing the alcoholysis process and the obtained esters yield was lower than that obtained by the non-catalytic reaction. It was mentioned that H_2SO_4 represented superior catalytic activity because its higher acid strength donated more H^+ species to protonate the carboxylic moiety of fatty acid. Berrios et al. [95] reported that the model oil having the acid value of 5–7 mg KOH g^{-1} was satisfactorily esterified with the help of H_2SO_4 catalyst within 120 min of methanolysis reaction performed at 60 °C using 5 wt% catalyst amount; however, higher amount of alcohol (methanol-to-oil molar ratio of 60:1) was required for satisfactory completion of the reaction. The kinetic model was proposed for the H_2SO_4-catalyzed esterification of FFA in sunflower oil by considering following assumptions: the esterification was reversible reaction, the rate of the non-catalyzed reaction was negligible, alcohol-to-oleic acid molar ratio was high and constant throughout the process, and the reaction occurred in an oil phase. It was predicted that the reaction followed the pseudo-homogeneous first order in the forward direction and second order in the reverse direction. The influence of temperature on the kinetic constants was also determined by fitting the results into the Arrhenius equation where the activation energy for the forward reaction was found to be decreasing with increase in the catalyst concentration [95]. Marchetti and Errazu [96] explained that the esterification reaction rate is slow due to the dissolution versus kinetics effect; however, it was suggested that the esterification reaction rate increased with rise in reaction temperature, catalyst concentration, and initial FFA concentration. The studied

Table 5
Some homogeneous base catalysts for alcoholysis reaction [81–86,88–92].

Source	Catalyst	Catalyst (wt%)	Alcohol	Alcohol- to-oil molar ratio	Temperature (°C)/Time (min)	Performance	Ref.
Soybean oil	NaOH	1.0	Methanol	6:1	60/60	~90.00% Yield	[81]
Cotton seed oil	NaOH	1.0	Methanol	6:1	60/60	~97.00% Yield	[81]
Soybean oil	NaOH	0.8	Methanol	6:1	60/60	~97.00% Yield	[82]
Sunflower oil	NaOH	0.6	Methanol	6:1	60/60	~97.00% Yield	[82]
Waste frying oil	NaOH	0.8	Methanol	6:1	60/60	~95.00% Yield	[82]
Soybean oil	$NaOCH_3$	0.6	Methanol	6:1	60/60	~97.00% Yield	[82]
Sunflower oil	$NaOCH_3$	0.6	Methanol	6:1	60/60	~97.00% Yield	[82]
Waste frying oil	$NaOCH_3$	0.8	Methanol	6:1	60/60	~92.00% Yield	[82]
Soybean oil	KOH	1.0	Methanol	6:1	60/60	~96.00% Yield	[82]
Sunflower oil	KOH	1.0	Methanol	6:1	60/60	~95.00% Yield	[82]
Waste frying oil	KOH	1.2	Methanol	6:1	60/60	~96.00% Yield	[82]
Waste frying oil	NaOH	0.5	Methanol	7.5:1	50/30	96.00% Yield	[83]
Duck tallow	KOH	1.0	Methanol	6:1	65/180	97.10% Yield	[84]
Duck tallow	NaOH	1.0	Methanol	6:1	65/180	81.30% Yield	[84]
Duck tallow	$NaOCH_3$	1.0	Methanol	6:1	65/180	83.60% Yield	[84]
Heckel fish oil	KOH	0.5	Methanol	6:1	32/60	96.00% Yield	[85]
Soybean oil	KOH	1.0	Methanol +4% DCM	4.5:1	45/120	96.00% Yield	[86]
Waste cooking oil	$NaOCH_3$	0.75	Methanol	6:1	Microwave heating (750 W)/3	97.90% Yield	[88]
Waste cooking oil	$NaOCH_3$	0.75	Methanol	6:1	65/90	96.60% Yield	[88]
Soybean oil	KOH	0.5	Ethanol	12:1	60/60	95.00% Yield	[89]
Soybean oil	KOH	1.0	Ethanol	6:1	Ultrasonic (20 kHz, 750 W)/6	98.00% Yield	[89]
Cottonseed oil	TMAH	2	Methanol	6:1	65/120	~98.00% Yield	[90]
Waste frying oil	TMAH	3	Methanol	6:1	65/150	~95.00% Yield	[90]
Cottonseed oil	BTAH	2	Methanol	6:1	65/90	~98.00% Yield	[90]
Waste frying oil	BTAH	3	Methanol	6:1	65/150	~95.00% Yield	[90]
Cottonseed oil	TMG	3	Methanol	12:1	65/90	98.60% Yield	[91]
Waste frying oil	TMG	3	Methanol	12:1	65/90	93.80% Yield	[91]
Cottonseed oil	TEA	6	Methanol	9:1	190/180	55.30% Yield	[92]
Cottonseed oil	DEA	6	Methanol	9:1	190/180	67.50% Yield	[92]
Cottonseed oil	t-BA	6	Methanol	9:1	190/180	62.40% Yield	[92]
Cottonseed oil	TEA-KOH	6	Methanol	9:1	190/180	94.10% Yield	[92]
Cottonseed oil	DEA-KOH	6	Methanol	9:1	180/180	94.50% Yield	[92]
Cottonseed oil	t-BA-KOH	6	Methanol	9:1	200/300	94.20% Yield	[92]

esterification reaction was performed using ethanol as a reactant with an aim to synthesize biodiesel from a green source of energy, where 96% FFA conversion was reported after 240 min of ethanolysis reaction performed at 55 °C using alcohol-to-oil molar ratio of 6.126 and 2.261 wt% H_2SO_4 catalyst dose. Marchetti et al. [97] proposed a kinetic model for the H_2SO_4-catalyzed esterification reaction, and for the combination of esterification and transesterification process of a model acid oil. It was reported that in the case of FFA conversion, the simultaneous esterification-transesterification reaction represented more accuracy between the experimental data and the theoretical study. Park et al. [98] investigated the influence of water on the H_2SO_4-catalyzed esterification process of an acid oil and oleic acid. The acid oil, containing 96.9% FFA, was prepared via hydrolysis of soapstock using KOH catalyst and by the acidulation using H_2SO_4 at room temperature. It was reported that in the presence of H_2SO_4 and methanol-to-oil molar ratio of 6:1, the esterification reaction rate did not decrease even after the existence of 5% of water in the reaction mixture, indicating that under H_2SO_4, high methanol amount counterbalanced the reverse reaction caused by water. In a two-step H_2SO_4-catalyzed esterification process performed at 80 °C for 360 min using methanol-to-oil molar ratio of 3:1, 92.98% and 88.96% biodiesel yield was obtained from oleic acid and acid oil, respectively. Hanh et al. [99] investigated the influence of heating technique and type of alcohol employed for the H_2SO_4-catalyzed esterification of oleic acid, palmitic acid, and stearic acid. The ultrasonic assisted method, when compared to the conventional mechanical stirring method, was suggested to be beneficial in promoting the biodiesel yield. Furthermore, unlike the secondary chain alcohols, straight chain alcohols were reported to promote the esterification reaction rate, explaining that the steric hindrance limited access of the secondary alcohols to the reaction centre. The reactants favorable for biodiesel production could be arranged in the following order: ethanol > 1-propanol > 2-propanol > 1-butanol > 2-butanol.

Su [100,101] suggested that unlike H_2SO_4 and nitric acid (HNO_3), HCl catalyst can be recovered from the post reaction mixture and can be reutilized for the next esterification reaction cycle. The lipase-hydrolyzed feedstock (acid value of 201 mg KOH g m^{-1}) was subjected to the HCl-catalyzed esterification process, where it was found that HCl did not mix in the formed esters phase and remained in the reactant phase. It was said that all HCl catalyst might have left in the alcohol phase because the presence of 63% water in the catalyst increased the polarity of the methanol phase; thus, enabling its easy separation and further use. The reported study suggested that 99.75% HCl can be recovered after the esterification process compared to 57.75% and 69.25% for HNO_3 and H_2SO_4, respectively. Furthermore, higher than 97% FFA conversion obtained inside 120 min of methanolysis reaction indicated that HCl also is a suitable candidate to catalyze the esterification reactions. The kinetics for the above reactions were also studied by varying the catalyst loading, reaction temperature, and methanol-to-FFA molar ratio [101]. Miao et al. [102] reported that trifluoroacetic acid can also catalyze the alcoholysis reaction of soybean oil. It was reported that 98.40% biodiesel yield was achieved after 360 min of methanolysis reaction performed at 80 °C using methanol-to-oil molar ratio of 20:1 and 2.0M catalyst amount. Soriano et al. [103] investigated the catalytic activity of aluminum chloride ($AlCl_3$), and zinc chloride ($ZnCl_2$) for the simultaneous transesterification of TAGs and esterification of long chain fatty acids in the presence of methanol and a co-solvent, tetrahydrofuran (THF). The addition of co-solvent nowadays is practiced to improve the miscibility between the oil and alcohol phase, and thus, to reduce the dependency of mass transfer on the temperature, stirring intensity, and on the alcohol amount. The stronger Lewis acid $AlCl_3$ was reported to have better catalytic activity than $ZnCl_2$ for the alcoholysis reaction. However, the reported results suggest that it took 1080 min to achieve 98% canola oil conversion even in the presence of co-solvent (THF: methanol = 1), using reaction temperature of 110 °C, alcohol-to-oil molar ratio of 24:1, and 5 wt% $AlCl_3$ catalyst amount. Furthermore, close boiling point of THF and methanol might cause problems for their separation, purification, and reutilization. Guan et al. [104] reported that p-toluenesulfonic acid (PTSA) possess better catalytic activity than benzenesulfonic acid (BSA), and H_2SO_4 for transesterification reaction between corn oil and methanol. The transesterification reaction was performed in the presence of co-solvent, dimethyl ether (DME), which was injected in a 10 ml pressure-proof glass cylinder reactor containing methanol, oil, and the catalyst. The highest biodiesel yield of 97.10% was reported after 120 min of transesterification reaction performed at 80 °C in the presence of co-solvent (methanol:DME = 1:1.76), alcohol-to-oil molar ratio of 10:1, and 4 wt% catalyst amount. It was reported that FFA in the reaction mixture reacted with methanol and produced water which then was attached to the H^+ ions; thus, lowering the acid strength, and consequently, activity of PTSA catalyst. Table 6 summaries some of the effective homogeneous acid catalysts employed for biodiesel production along with the employed reaction conditions, obtained performance, and related references.

4.3. Homogeneous acid and base catalysts for the two-steps alcoholysis reaction

The base catalysts are well known to accelerate the transesterification reaction rate, while, acid catalysts are tolerant towards the FFA content in feedstocks. In a standpoint of producing high yield of biodiesel in less reaction time from waste and low-grade feedstocks, few studies have been addressed towards performing a two-step alcoholysis reaction in which an acid catalyst was initially used to promote the fatty acid esterification and then the remaining feedstock was subjected to the base-catalyzed transesterification process.

Hayyan et al. [105] studied the catalytic activity of H_2SO_4 and KOH for esterification and transesterification reaction of sludge palm oil, respectively. It was reported that 94% of FFA in the feedstock was esterified, and the intermediate was then subjected to the KOH-catalyzed transesterification process; thus producing 83.72% final biodiesel yield. Hayyan et al. [106] suggested that ethanesulfonic acid is an efficient catalyst to satisfactorily reduce FFA level in the feedstock and the catalyst can be recovered and reutilized for the next esterification reactions. The intermediate obtained after the ethanesulfonic acid-catalyzed esterification process of acidic crude palm oil was subjected to the KOH-catalyzed transesterification reaction to produce biodiesel. The two-step alcoholysis process was tried successfully also for biodiesel production from non-edible oils, such as karanja oil, and jatropha oil containing high amount of FFA and other toxic components [107,108]. Encinar et al. [109] tested three different animal fats varying in their FFA concentration for biodiesel production using the two-step alcoholysis process. The catalytic activity of acidic materials, such as H_2SO_4, PTSA, and phosphoric acid were tested for esterification of FFA, while the transesterification reaction was performed using a KOH catalyst. It was reported that phosphoric acid did not show any significant activity for the esterification reaction because of its lower acidity; however, H_2SO_4 and PTSA proved to be efficient catalyst with an adjustment that PTSA was required double the amount of H_2SO_4. The rise in the reaction temperature and methanol amount positively influenced the esterification process, but drop in the acid value was initially fast and was then stabilized. The reason for such behavior was explained due to the accumulation of water which resulted in sulfuric acid removal from the methanol phase and its migration into water, thus making it unavailable for the reaction. Suppalakpanya et al. [110] used a microwave heating technique for biodiesel production from crude palm oil. The two-step biodiesel production process included esterification of palm crude oil using

Table 6
Some homogeneous acid catalysts for alcoholysis reaction [93–96,98,99,102–104].

Source	Catalyst	Cat. (wt%)	Alcohol	Alcohol-to-oil molar ratio	Temperature (ºC)/Time (min)	Performance	Ref.
Oleic acid in Sunflower oil and Soybean oil	H_2SO_4	2.5	Methanol	6:1	60/60	96.6% Conv.	[93]
Oleic acid in Sunflower oil and Soybean oil	HCl	2.5	Methanol	6:1	60/120	87.90% Conv.	[93]
Oleic acid in Sunflower oil and Soybean oil	$AlCl_3$	2.5	Methanol	6:1	60/120	87.98% Conv.	[93]
Palm fatty acid	H_2SO_4	0.1	Methanol	3:1[a]	130/60	~ 92.00% Conv.	[94]
Palm fatty acid	CH_3SO_3H	0.1	Methanol	3:1[a]	130/60	~ 91.00% Conv.	[94]
Palm fatty acid	H_3PO_4	0.1	Methanol	3:1[a]	130/60	~50.00% Conv.	[94]
Palm fatty acid	H_2SO_4	0.1	Ethanol	3:1[a]	130/60	~82.00% Conv.	[94]
Palm fatty acid	CH_3SO_3H	0.1	Ethanol	3:1[a]	130/60	~80.00% Conv.	[94]
Oleic acid in Sunflower oil	H_2SO_4	2.261	Ethanol	6.126:1	55/240	96% Conv.	[96]
Acid oil (one-step)	H_2SO_4	–	Methanol	3:1	80/360	85.58% Yield	[98]
Acid oil (two-step)	H_2SO_4	–	Methanol	3:1	80/360	88.96% Yield	[98]
Oleic acid (one-step)	H_2SO_4	–	Methanol	3:1	80/360	91.47% Yield	[98]
Oleic acid (two-step)	H_2SO_4	–	Methanol	3:1	80/360	92.98% Yield	[98]
Olec acid	H_2SO_4	5 wt%	Ethanol	3:1[a]	60/120 Ultrasonic (40 kHz, 700 W)	~93.00% Conv.	[99]
Oleic acid	H_2SO_4	5 wt%	1-propanol	3:1[a]	60/300 Ultrasonic (40 kHz, 700 W)	~92.00% Conv.	[99]
Oleic acid	H_2SO_4	5 wt%	1-butanol	3:1[a]	60/300 Ultrasonic (40 kHz, 700 W)	~87.00% Conv.	[99]
Oleic acid	H_2SO_4	5 wt%	2-propanol	3:1[a]	60/300 Ultrasonic (40 kHz, 700 W)	~78.00% Conv.	[99]
Oleic acid	H_2SO_4	5 wt%	2-butanol	3:1[a]	60/300 Ultrasonic (40 kHz, 700 W)	~42.00% Conv.	[99]
Soybean oil	$C_2HF_3O_2$	2.0M	Methanol	20:1	80/360	98.40% Yield	[102]
Canola oil	$AlCl_3$	5%	Methanol+ THF (1:1)	24:1	110/1080	98.00% Conv.	[103]
Corn oil	PTSA	4 wt%	Methanol + DME(1:1.76)	10:1	80/120	97.10% Yield	[104]
Corn oil	BSA	4 wt%	Methanol + DME (1:1.76)	10:1	60/480	~ 82.00% Yield	[104]
Corn oil	H_2SO_4	4 wt%	Methanol + DME (1:1.76)	10:1	60/480	~ 65.00% Yield	[104]

[a] Alcohol-to- acid ratio.

H_2SO_4 catalyst followed by the KOH-catalyzed transesterification of the esterified oil. It was suggested that the microwave heating facilitated the cleavage of TAGs molecules; thus, the alcoholysis reaction rate was enhanced and the time required to achieve highest biodiesel was minimized.

The optimal reactor design to execute the two-stage biodiesel production in a batch or continuous reactor needs knowledge related to the kinetics of various possible reactions. Jansri et al. [111] studied the chemical kinetics for the H_2SO_4-catalyzed esterification reaction of mixed crude palm oil and for the NaOH-catalyzed transesterification reaction of the esterified oil. The two-step alcoholysis reaction was performed and the obtained experimental data were then used to calculate the rate coefficients with the help of curve-fitting tool of MatLab. The agreement between the experimental data and the model did not match, thus the predicted values were recalculated using Polymath and the Runge–Kutta method for determining the percentage mean data error and the standard deviation of error. The best-fit values of the rate coefficients were used for obtaining approximate activation energy. The lower activation energy for the forward reaction compared to the reverse reaction indicated that forward reaction is comparatively faster [111].

5. Heterogeneous catalysts for alcoholysis reaction

Even though homogeneous catalysts have been widely used for biodiesel production because of their high activity and relatively low cost, the post-reaction treatment required for the removal of residual catalyst from the reaction mixture and disposal of the generated large waste water stream have augmented the overall processing expenses, and consequently, of biodiesel. Moreover, the homogeneous catalysts are consumed during the process and cannot be reutilized.

In this regards, the heterogeneous catalysts are economically and ecologically benign, much easier to separate from the products, simplifies the purification stages, and could be reutilized. However, it is worth mentioning that the activity of heterogeneous catalysts is largely reliant on their nature, active sites, structural morphology, porosity, and thermal stability. Heterogeneous catalysts represents slower reaction rate but the limitation can be resolved by elevating the reaction temperature and the amount of reactants.

5.1. Heterogeneous base-catalyzed alcoholysis reaction

Numerous alkali and alkaline earth based metal oxide catalysts have been tested for transesterification reaction. The base catalysts, such as magnesium oxide (MgO), calcium oxide (CaO), strontium oxide (SrO), alkali and alkaline earth metal supported oxides, mixed metal oxides, hydrotalcites, anionic resins, amongst other have been employed for biodiesel production and are discussed below. Among these, calcium oxide is extensively researched heterogeneous catalyst because it ensures high basicity, little solubility, can be handled easily, and is economically less expensive.

The calcium oxide catalyst has gained scientific and industrial attention because of the abundance of calcium species from the natural resources. Kawashima et al. [112] suggested that CaO catalyst, when activated with an methanol, represented superior catalytic activity than the non-activated one for transesterification reaction between rapeseed oil and methanol. It was reported that higher the methanol amount was used for the catalyst activation, better was the transesterification reaction rate. Kawashima et al. [112] identified that CaO in the reaction mixture reacted with the formed glycerol during the transesterification reaction and resulted in the formation of CaO–glycerin complex. The CaO–glycerin complex was considered to function as a chief catalyst to accelerate the transesterification reaction. Kouzu et al. [113] investigated the reaction mechanism for the CaO-catalyzed transesterification between soybean oil and methanol. It was proposed that methanol, with the help of basic sites on the CaO surface, produces methoxide anions which serves as a nucleophile and effectively initiates the transesterification reaction. After a particular reaction interval which occurs due to mass transfer, the formed glycerol reacts with CaO to form calcium glyceroxide ($Ca[O(OH)_2C_3H_5]_2$). The presence of glyceroxyl carbon in the collected catalyst was verified using XRD and ^{13}C-NMR technique. It was reported that the collected catalyst and the reference ($Ca[O(OH)_2C_3H_5]_2$) sample possessed similar catalytic activity for the transesterification process but was lower than the fresh CaO catalyst, which was due to their lower basic strength; however, it is worth noting that the chemical alteration of CaO to ($Ca[O(OH)_2C_3H_5]_2$) makes the transformed catalyst stable and minimizes its deactivation phenomenon. Furthermore, the innovated ($Ca[O(OH)_2C_3H_5]_2$) catalyst was stated to be tolerant to the surrounding air which simplifies its utilization for biodiesel production.

Several natural and waste resources have been examined to derive low-cost and active calcium based catalysts. These calcium species, when thermally treated, gets converted to CaO catalyst which then could be used for biodiesel production. Suryaputra et al. [114] reported that waste capiz shells, after the calcination at 900 °C for 120 min, produced CaO catalyst which then was used to catalyze transesterification reaction between palm oil and methanol. It was reported that with the assistance of 3 wt% catalyst amount, 92.83% biodiesel yield was obtained after 360 min of methanolysis process performed at 60 °C using 8:1 alcohol-to-oil molar ratio. Correia et al. [115] documented the use of egg shells and crab shells as a source for CaO catalyst. The obtained catalyst was used to catalyze transesterification reaction between sunflower oil and methanol, where it was observed that CaO derived from egg shells possessed superior catalytic activity because of its higher basicity. The reported results suggested that 94.10% biodiesel yield was obtained after 180 min of transesterification reaction performed at 60 °C using methanol-to-oil molar ratio of 9:1 and 3 wt% catalyst amount. Rezaei et al. [116] reported that CaO catalyst derived from mussel shells is extracted in the reaction mixture by methanol during the alcoholysis process. Furthermore, the recyclability tests studied for 5 reaction cycles suggested that the re-calcination process had a negative impact on the chemical composition of the obtained catalyst; thus, directing the reduction in the active sites of catalyst, and consequently, lowering the biodiesel yield. The biodiesel yield, using calcined catalyst, in the first reaction cycle was 94.10%, which then was dropped to 37.13% after 5 reaction cycles. Kouzu and Hidaka [117] reported that among Amberlyst-15DRY resins was more efficient than Amberlite-200CTNA, Amberlite-IRC76, and Amberlyst-31WET resins in removing the leached calcium species from the reaction mixture. The reason for superior behavior of Amberlyst-15DRY resins was due to the difference in the counter-cation of sulfonic groups and the textile structure of the polymer matrix. Calero et al. [118] reported a study focused on the CaO-catalyzed partial transesterification reaction between soybean oil and methanol. In a 1, 3-selective TAGs partial transesterification process, one mole of TAGs resulted in the formation 2 mol of esters, while the remaining monoglycerides stayed in the product esters and acted as a lubricating agent; thus eliminating glycerol separation and purification steps. The commercial CaO catalyst was found to possess excellent activity for the partial transesterification reaction assisting complete conversion of oil, with 98% selectivity, even after 20 catalyst reutilization tests.

Some reports on the utilization of magnesium oxide catalyst for biodiesel production are available in the literature. The reported studies indicate that the structural morphology, particle size, crystallinity, and surface area of MgO catalyst had a significant impact on the final yield of biodiesel [119–120]. In a study reported by Jeon et al. [119], the catalytic activity of poly (dimethylsiloxane-ethyleneoxide) (PDMS-PEO) templated-MgO catalyst was compared with the non-templated MgO catalyst for biodiesel production from canola oil and methanol. It was found that the comb-like structure of PDMS-PEO template generated mesoporous and macroporous nature of MgO catalyst because the magnesium precursor entered into the hydrophilic PEO domains and the agglomerated PDMS generated nanopores; thus, the presence of macropores allowed the transportation of bulky TAGs and micropores increased the active catalytic sites. With the help of templated-MgO catalyst, maximum biodiesel yield of 98.20% was reported after 120 min of transesterification reaction performed at 190 °C using methanol-to-oil molar ratio of 20:3 and 3 wt% catalyst amount. Almerindo et al. [120] compared the catalytic activity of synthesized MgO-chitosan complex and commercial MgO catalyst for transesterification reaction between soybean oil and methanol. The amine groups of chitosan are the main effective bonding sites for the magnesium ions, thus resulting in complexes stabilized by coordination. The nitrogen electrons present in amine and N-acetylamine groups established coordinate covalent bonds with metal ions. The addition of biopolymer into the magnesium precursor, which was subsequently removed on calcination, directed the formation of porous structure of MgO catalyst and increased its surface area and pore volume. The surface area of the synthesized catalyst was determined to be 3.8 times higher than the commercial one. The biodiesel yield obtained from the MgO-chitosan complex-assisted ethanolysis reaction was 75%, while, under the same reaction conditions, 30% biodiesel yield was reported using commercial MgO catalyst. However, the MgO catalyst was found to be deactivating because of the formation of hydrogenocarbonates on the active basic sites. Among the alkaline earth metals, strontium oxide has also been considered as one of the catalysts for biodiesel production. Chen et al. [121] investigated the catalytic activity of different alkaline earth metal oxides (SrO, CaO, and MgO) for biodiesel production from olive oil and methanol. The SrO-catalyzed transesterification reaction performed at 65 °C for 15 min resulted in the formation of 82% biodiesel using catalyst concentration of 5 wt%, methanol-to-oil molar ratio of 6:1, and 600 rpm stirring speed. Viola et al. [122] reported that in a batch-scale reactor under the high speed mechanical stirring, 75% of granular SrO broke down into powder, while 90% CaO catalyst retained its granular structure. Thus, when a granulated catalyst was used for biodiesel production, SrO initiated reaction faster than the one catalyzed by CaO; however, the final biodiesel yield was higher with the CaO-catalyzed alcoholysis process. After 180 min of SrO-catalyzed transesterification reaction between fried oil and methanol performed at 65 °C using methanol-to-oil molar ratio of 6:1 and 5 wt% catalyst amount, 86% biodiesel yield was reported.

Several reports are focused on the synthesis and utilization of supported alkali and alkaline earth metal catalysts for biodiesel production in a viewpoint to minimize the lixiviation of the active catalyst into the reaction medium. Kaur and Ali [123] reported a

study focused on the utilization of lithium metal ion supported on CaO catalyst for biodiesel production from high FFA karanja and jatropha oil. It was reported that using reaction temperature of 65 °C, methanol-to-oil molar ratio of 6:1, and 5 wt% catalyst amount, the complete conversion of karanja oil and jatropha oil was achieved in 60 min and 120 min, respectively; the time difference was due to higher FFA content in jatropha oil. Tonetto and Marchetti [124] innovated a K/γ-Alumina loaded in a honeycomb structured cordierite monolithic catalyst for transesterification reaction between soybean oil and methanol. Primarily, different alkali (Na, K) and alkaline earth metal (Ca, Ba) catalyst supported on powder γ-Alumina were tested for transesterification reaction; K/γ-Alumina catalyst proving to be the best catalyst among other was then deposited on the cordierite monolith to study its reactivity and stability for biodiesel production. It was reported that after 360 min of transesterification reaction performed at 120 °C using methanol-to-oil molar ratio of 32:1 and 0.5 wt% catalyst amount, 59.10% biodiesel yield was achieved. Kazemian et al. [125] reported a work focused on the utilization of cesium metal impregnated high surface area mesoporous SBA-15 catalyst for transesterification reaction between canola oil and methanol. The influence of two different silica sources, used for the synthesis of SBA-15, on the overall catalytic activity for biodiesel production was investigated along with the different reaction conditions including reaction temperature, alcohol molar ratio, catalyst concentration, and reaction time. It was reported that SBA-15 prepared using metasilicate precursor had a positive impact on the cesium metal loading; thus increasing number of active sites of the synthesized catalyst, and consequently, the final oil conversion. The maximum biodiesel yield of 25.35% was obtained after 300 min of transesterification reaction performed at 135 °C using methanol-to-oil molar ratio of 40:1 and 100 mg catalyst dose. The changes in the structural morphology and the alteration in the chemical composition of the existing catalytic system is also considered as a possible option to increase the number of active basic sites, and stability as well as to reduce the diffusion of active catalytic species into the reaction medium. Furthermore, its persistence for longer period of time, robustness in harsh reaction conditions, and reutilization is also of peak importance. The mixed metal oxides could be one of the promising candidates for assisting biodiesel production. Rubio-Caballero et al. [126] used a calcium zincate dehydrate precursor, which after thermal treatment at 400 °C underwent dehydroxylation process to generate strong basic sites on the catalytic surface consisting of CaO and ZnO, for transesterification reaction between sunflower oil and ethanol. The biodiesel yield of approximately 95% was obtained after 180 min of transesterification reaction performed at 78 °C using ethanol-to-oil molar ratio of 20:1 and 3 wt% catalyst amount. Santiago-Tores et al. [127] utilized sodium zirconate catalyst for biodiesel production from soybean oil and methanol. It was reported that transesterification reaction performed at 65 °C for 180 min using methanol-to-oil molar ratio of 3:1 and 3 wt% catalyst amount resulted in 98.30% soybean oil conversion. Rashtizadeh et al. [128] proposed a highly basic Sr-Al mixed oxide nanocomposite catalyst for transesterification reaction between soybean oil and methanol. It was reported that the synthesized strontium based catalyst possessed basicity of 1615 μmol g^{-1} and the maximum esters yield of around 95.7% was obtained within 61 min of reaction performed using reaction temperature of 60 °C, methanol-to-oil molar ratio of 25:1, and 1.30 wt% catalyst amount. Meng et al. [129] reported Ca/Al composite oxide based catalyst for biodiesel production from rapeseed oil. It was stated that the synthesized catalyst had strong basicity due to the presence of $Ca_{12}Al_{14}O_{33}$ and CaO species. The methanolysis reactions were performed in a conventional and modified trickle bed reactor. The methanol pre-addition technique in a modified reactor increased the biodiesel yield with a margin of 20% when compared with that obtained using the conventional reactor. Furthermore, the precipitation experiment of the post-reaction mixture indicated that no calcium species leached even after 18,000 min of reaction time. It was concluded that the synthesized catalyst had better activity and stability for the transesterification reaction in the trickle bed reactor.

Together with several base catalyst systems discussed, layered double hydroxide or hydrotalcite catalysts have also been continuously studied and have gained enormous attention for biodiesel production. Dias et al. [130] reported higher than 90% biodiesel yield using cerium doped Mg–Al hydrotalcite catalyst for transesterification reaction between soybean oil and methanol. The cerium doped hydrotalcite catalyst was synthesized via co-precipitation method with Mg/Al ratio of 3, and cerium doping was reported to establish the rehydration and restructuration of the hydrotalcite catalyst displaying higher catalytic activity than Mg–Al mixed oxide for biodiesel production. Wang et al. [131] investigated the catalytic activity of transition metal doped hydrotalcite like materials consisting Mg^{2+}, Fe^{3+}, and Al^{3+} layered double hydroxide catalyst for biodiesel production from soybean oil. Four different catalysts with varying Mg/Fe molar ratio were synthesized with constant Al composition. It was reported that increasing magnesium content reduced the catalytic surface area, but improved the basicity of the final catalyst; and thus, the catalytic activity for transesterification reaction.

Recently, anion-exchange resins have also been tested for biodiesel production due to the fact that their separation from the post-reaction mixture is trouble-free compared to the fine powdered basic catalytic materials. The use of anion exchange resins not only reduces purification and separation steps but also produces highly pure glycerol by-product. Li et al. [132] reported a work focused on the use of weak and strong anion-exchange resins (Amberlite IRC-93 and Amberlite IRA-900) for transesterification reaction between yellow horn seed oil and methanol. The oil transformation was performed in a digital microwave-assisted reactor where it was concluded that the generated electromagnetic field accelerated the mobility and reactivity between the reaction molecules. Marchetti et al. [133] studied Dowex monosphere 550A and Dowex upcore Mono-625 alkaline anion-exchange resins for esterification of FFA in an acid oil. Marchetti and Errazu [134] used Dowex monosphere 550A anion-exchange resins for transesterification reaction of an acid oil prepared from a mixture of sunflower oil and oleic acid. The reported results indicated that increasing FFA in the feedstock raised the esterification reaction rate but the final conversion remained the same; however, in the case of simultaneous esterification and transesterification reaction, initial reaction rate as well as the final conversion increased with rise in the FFA content. The recent effective heterogeneous base catalysts used for obtaining biodiesel are listed in Table 7.

5.2. Heterogeneous acid-catalyzed alcoholysis reaction

The utilization of heterogeneous acid catalysts for biodiesel production could be advantageous over the heterogeneous base ones because acid catalysts are tolerant to FFA and water content in feedstocks. However, the ideal heterogeneous acid catalyst must possess high number of accessible active sites, moderate acid strength, hydrophobicity, and porosity to minimize the diffusional issues. Furthermore, the utilization of acid catalyst for biodiesel production requires severe reaction conditions to satisfactorily transform oil to biodiesel; thus, it is necessary to have thermally stable acid catalyst. Though acid catalysts have gained less attention compared to the basic counterparts due to their low reaction rate, recently, variety of solid acidic materials have been comprehensively tested for biodiesel

Table 7
Some heterogeneous base catalysts for alcoholysis reaction [112,114–116,119–128,130–132].

Source	Catalyst	Catalyst	Alcohol	Alcohol- to-oil molar ratio	Temperature (°C)/Time (minutes)	Performance	Ref.
Rapeseed oil	CaO	1.00 gm	Methanol	26 wt% of oil	60 °C/180	~90.00% Yield	[112]
Palm oil	CaO (Capiz shell)	3.00 wt%	Methanol	8:1	60 °C/360	92.83% Yield	[114]
Soybean oil	CaO (mussel shell)	12.00 wt%	Methanol	24:1	60 °C/480	94.10% Yield	[115]
Sunflower oil	CaO (Egg shell)	3.00 wt%	Methanol	9:1	60 °C/180	94.73% Conv.	[116]
Sunflower oil	CaO (Crab shell)	3.00 wt%	Methanol	6:1	60 °C/240	82.87% Conv.	[116]
Canola oil	MgO	3.00 wt%	Methanol	20:3	190 °C/120	82.80% Yield	[119]
Canola oil	Templated- MgO	3.00 wt%	Methanol	20:3	190 °C/120	98.20% Yield	[119]
Soybean oil	MgO	Ethanol:oil:cat. 600:100:5	Ethanol	600:100	150 °C/180	30.00% Yield	[120]
Soybean oil	MgO complex	Ethanol:oil:cat. 600:100:5	Ethanol	600:100	150 °C/180	75.00% Yield	[120]
Olive oil	SrO	5.00 wt%	Methanol	6:1	65 °C/15	82.00% Conv.	[121]
Fried oil	CaO	5.00 wt%	Methanol	6:1	65 °C/180	92.00% Yield	[122]
Fried oil	SrO	5.00 wt%	Methanol	6:1	65 °C/180	86.00% Yield	[122]
Fried oil	K_3PO4	5.00 wt%	Methanol	6:1	65 °C/180	78.00% Yield	[122]
Karanja oil	Li/CaO	5.00 wt%	Methanol	6:1	65 °C/60	~99.00% Conv.	[123]
Jatropha oil	Li/CaO	5.00 wt%	Methanol	6:1	65 °C/120	~99.00% Conv.	[123]
Soybean oil	Ca/Al_2O_3	1.00 wt%	Methanol	32:1	120 °C/360	94.70% Yield	[124]
Soybean oil	Na/Al_2O3	1.00 wt%	Methanol	32:1	120 °C/360	97.10% Yield	[124]
Soybean oil	K/Al_2O_3	1.00 wt%	Methanol	32:1	120 °C/360	98.90% Yield	[124]
Soybean oil	K/Al_2O_3-Monolith	0.50 wt%	Methanol	32:1	120 °C/360	59.10% Yield	[124]
Canola oil	Cs/SiO_2	100 mg	Methanol	40:1	135 °C/300	25.35% Yield	[125]
Sunflower oil	$CaZn(OH)_4$	3.00 wt%	Ethanol	20:1	78 °C/180	~95.00% Yield	[126]
Soybean oil	Na_2ZrO_3	3.00 wt%	Methanol	3:1	65 °C/180	98.30% Conv.	[127]
Soybean oil	Sr_3Al2O_6	1.30 wt%	Methanol	25:1	60 °C/61	~95.70% Yield	[128]
Soybean oil	Ce- Hydrotalcite	5.00 wt%	Methanol	9:1	67 °C/240	~90.00% Yield	[130]
Soybean oil	MgAlFe hydrotalcite	3.00 wt%	Methanol	21:1	65 °C/240	81.00% Conv.	[131]
Yellow horn seed oil	Amberlite IRA 900	3.00 wt%	Methanol	8:1	60 °C/90	~96.00% Conv.	[132]

production. Most of the recent heterogeneous catalysts used for biodiesel production are based on the modified inorganic mixed oxides, such as silica, sulfated and tungstated zirconia, or zeolites, heteropoly acids, superacid catalysts, sulfated carbon materials, and cation-exchange resins.

The high surface area mesoporous silica has been extensively studied as a support of the heterogeneous acid catalyst due to the fact that their mesostructure could be regulated and the hydrophobic or hydrophilic behavior of such materials could be reformed via functionalization with the different sulfonic acid groups. Melero et al. [135] used mesostructured SBA-15 silica catalysts functionalized with different sulfonic acid (–SO_3H) group, such as propyl-SO_3H, arene-SO_3H, and perfluoro-SO_3H for simultaneous esterification and transesterification of an high free acid crude palm oil. The performances of the above synthesized catalysts were compared with commercially available ion-exchange sulfonic resins, such as Amberlyst-36, Nafion SiO_2-composite (SAC-13), and with arene-sulfonic acid modified non-structured silica (SiO_2-Tosic acid). The reported results and the catalyst reutilization analysis suggested that arene-SO_3H modified SBA-15 displayed better catalytic performance than other synthesized and commercially available catalytic materials. Melero et al. [135] explained that the catalyst synthesis procedure was responsible for the superior performance of arene-SO_3H modified SBA-15 material. The co-condensation method employed for the incorporation of propyl-SO_3H, and arene-SO_3H moiety in SBA-15 resulted towards higher inclusion of –SO_3H groups compared to the reactive grafting method used for the synthesis of perfluoro-SO_3H modified SBA-15. In the case of arene-SO_3H modified mesostructured SBA-15, apart from the moiety dispersion, the co-condensation method also directed the incorporation of thermally stable covalent Si–C anchoring bonds; in contrast, the Si–O–C bonds of perfluoro-SO_3H acid sites were thermally less stable and got released into the reaction medium at high reaction temperatures and methanol amount. Melero et al. [135] further recommended that the hydrophobicity near sulfonic acid moieties can be improved by capping arene-SO_3H modified SBA-15 with trimethylmoethoxy silane; thus increasing the performance of the catalytic material, and consequently, improving the final biodiesel yield. García-Sancho et al. [136] investigated the catalytic performance of mesoporous niobosilicate molecular sieves for biodiesel production from sunflower oil. The Niobium incorporation into MCM-41 silica was done during the synthesis, or after via incipient wetness impregnation method, where it was reported that both catalysts possessed similar acid strength. The maximum biodiesel yield of 95% was achieved after 240 min of methanolysis reaction performed at 200 °C using methanol-to-oil molar ratio of 12:1 and 7.5 wt% catalyst amount. In addition, it was found that no catalytic species leached into the reaction medium, containing 0.2 wt% water and 1.1 wt% FFA, even after 5 recycle tests. Hence, it was recommended that niobosilicate molecular sieves are thermally stable, active, and suitable to assist biodiesel production.

Zirconia materials have been always considered as one of the potential heterogeneous catalysts for biodiesel production because of their strong acid properties and high catalytic activity for esterification reactions. Patel et al. [137] suggested that impregnating zirconia with sulfuric acid increases its acidity and activity for biodiesel the alcoholysis reaction. After sulfate dispersion, zirconia catalysts were used to assist the esterification reaction between oleic acid and methanol, where 90% biodiesel yield was achieved after 720 min of esterification reaction performed at 60 °C using methanol-to-oil molar ratio of 40:1 and 0.5 g catalyst amount. Zhang et al. [138] mentioned that the interaction between the sulfate species and zirconia is weak, and thus, the activity of the catalyst is reduced during the recyclability tests. Zhang et al. [138], in the reported study, used a stable chlorosulfonic functionalized zirconia ($HClSO_3$–ZrO_2) catalyst for esterification reaction between oleic acid and methanol. It was verified that $HClSO_3$–ZrO_2 catalyst consisted sulfate species 4 times higher than those in the H_2SO_4 modified zirconia. It was mentioned that the presence of higher number of acid sites in $HClSO_3$–ZrO_2 catalyst activated the protonation of carbonyl groups by proton transfer, and the enhanced acid strength resulted in more effective protonation of carbonyl groups of FFA. The reported results suggested that 100%

biodiesel yield was achieved even after 5 catalyst recycle tests of esterification reaction performed at 100 °C for 720 min using methanol-to-oil molar ratio of 8:1 and 3 wt% catalyst amount. The prime concern related to expanding the potential use of zirconia materials is its reduction in porosity and surface area after the thermal treatment. However, doping zirconia surface with a hetero species could maintain their structural morphology at high calcination temperatures. Jimenez-Lopez et al. [139] reported a study focused on the loading of tungsten oxide species on a zirconium doped MCM-41 silica. The obtained catalyst was then used to assist the methanolysis reaction of sunflower oil. The methanolysis reaction performed at 200 °C for 150 min resulted in the production of 82% biodiesel using methanol-to-oil molar ratio of 12:1 and 1.5 g catalyst amount. The 15% WO_3/ZrO_2-MCM-41 catalyst was found to be active and hydrophobic until 3 recycle tests and was resistant towards the water concentration of 5% and acidity degree of 9.1 in the feedstock. Xie and Yang [140] tested the activity of tungsten oxide supported on a high surface area and thermally stable aluminum phosphate catalyst for biodiesel production from soybean oil. It was reported that the calcination temperature had a significant role in deciding the performance of the catalyst for transesterification reaction. It was said that the calcination process at 800 °C was responsible for the generation of Brønsted acid sites; while, further rise in the calcination temperature reduced the tungsten oxide species from the catalyst surface. The IR analysis stated that the calcination process at 800 °C gave rise to an absorption peak at 928 cm^{-1} attributing to a fundamental $W=0$ stretching which delocalized the charge imbalance of the heteropolytungstate species; thus generating the Brønsted acid sites. The transesterification reaction performed at 180 °C for 300 min using methanol-to-oil molar ratio of 30:1 and 5 wt% catalyst amount resulted in 72.50% biodiesel yield.

The zeolite materials are known to be efficient solid acid catalyst on an industrial scale; however, their hydrophilic nature limits their usage for biodiesel production. Costa et al. [141] reported that the incorporation of tungsten oxide onto a USY zeolite surface gave rise to a notable hydrophobicity of the final catalyst. It was stated that though the incorporation of tungsten species blocked the acid sites of zeolite, the new acid sites were generated from the interaction of tungsten species with Brønsted and silanol groups inside the zeolite pores as well as from the supported WO_3 moieties on the external zeolite surface. The possibility of introduction of a hetero species in order to increase the overall catalytic stability of zeolite with an adjustment of reducing the number of acid sites was also proposed by Borges et al. [142]. The reported results suggested that the cerium doping on the HUSY zeolite surface increased the stability and activity of the catalyst. After cerium doping, HUSY zeolite catalyst assisted 99.80% soybean oil conversion after 1440 min of ethanolysis reaction performed at 200 °C using ethanol-to-oil molar ratio of 30:1 and 0.001 mol catalyst [142]. Vieira et al. [143] reported that sulfated lanthanum oxide impregnated HZSM-5 zeolite catalyst assisted complete conversion of oleic acid to biodiesel. It was reported that it took 420 min to achieve complete conversion of oleic acid when subjected to a methanolysis reaction using temperature of 100 °C, methanol-to-oleic acid molar ratio of 10:1, and 10 wt% catalyst amount.

Together with different mesoporous materials (e.g. silica) and microporous materials (e.g. zeolite), a macroporous vanadium phosphate, containing Brønsted (P–OH) and Lewis acid sites ($V=O$), was also reported as an efficient heterogeneous acid catalyst for biodiesel production. Domingues et al. [144] investigated the catalytic activity of vanadium phosphate catalyst for biodiesel production from a high acidity industrial by-product containing 26–39% FFA, 0.6% to 1.1% water, and 45–66% fatty acid methyl esters. It was suggested that the methyl esters, present in the reaction mixture, acted as a co-solvent which helped in reducing the mass transfer limitation during the methanolysis reaction. Alhassan et al. [145] tested the activity of ferric hydrogen sulfate [$Fe(HSO_4)_3$] catalyst for simultaneous transesterification and esterification of mixed waste oil. The alcoholysis reaction of waste oil performed at 205 °C for 240 min using methanol-to-oil molar ratio of 15:1 and 1 wt% catalyst amount resulted in 94.50% biodiesel yield. Narkhede and Patel. [146] investigated the catalytic activity of 12-tungstosilicic acid supported on zeolite-Hβ for an oleic acid esterification, and soybean oil transesterification process. The reported results indicated that the incorporation of 12-tungstosilicic acid on the zeolite surface generated the acid sites and increased the total acid strength of the final catalyst. For a transesterification process, 95% of soybean oil was transformed to biodiesel after 480 min of alcoholysis reaction performed at 65 °C using methanol-to-oil molar ratio of 4:1 and 200 mg catalyst amount. Srilatha et al. [147] tested cesium exchanged 12-tungstophosphoric acid catalyst for esterification reaction of rice bran fatty acid. It was mentioned that the partial exchange of cesium ions with the protons in 12-tungstophosphoric acid increased the acidity of the resulting catalyst; however, further increase in cesium content reduced the acidity of catalyst because the number of protons responsible for the acidity decreased. Hence, the complete substitution of proton with cesium ion was said to have a negative influence on the activity of the final catalyst; and consequently, on the biodiesel yield.

In recent days, the development of superacid catalysts is also gaining relevance for biodiesel production. Li et al. [148] tested the activity of a SO_4^{2-}/ZrO_2–TiO_2/La^{3+} heterogeneous superacid catalyst for biodiesel production from a cheap and low quality acid oil feedstock containing 60 wt% FFA. The proposed catalyst assisted more than 90% biodiesel yield for 5 recyclability tests of methanolysis reaction performed at 200 °C for 120 min using methanol-to-oil molar ratio of 15:1 and 5 wt% catalyst amount. Guan et al. [149] used a paramagnetic SO_4^{2-}/ZrO_2–B_2O_3–Fe_3O_4 solid acid catalyst for biodiesel production from acetic acid in the presence of n-butanol. It was suggested that the proposed catalyst enabled its separation, easy recovery from the reaction mixture, and thus, reduced the chances of getting deactivated during the post-reaction treatments. Furthermore, the incorporation of B_2O_3 species was said to improve the thermal stability of the resultant catalyst, while, the strong interaction between ZrO_2 and B_2O_3 reduced the agglomeration of zirconia materials during the calcination process.

Dawodu et al. [150] reported use of carbon catalysts, functionalized with the different sulfonic acid, such as H_2SO_4, and PTSA, for biodiesel production from polanga oil. It was reported that PTSA-sulfonated catalyst possessed less $-SO_3H$ species, and thus, displayed inferior catalytic activity than the H_2SO_4 doped carbon catalyst. However, after 240 min of reutilization tests, catalyst was found to be deactivating due to glycerol adhesion. Poonjarernsilp et al. [151] compared the catalytic activity and stability of sulfated single-walled carbon nanohorns (SWCN), sulfated oxidized SWCN, sulfated activated carbon, and sulfated carbon black for the esterification reaction between palmitic acid and methanol. It was reported that the oxidation process caused the structural destruction of carbon nanohorns, while, sulfonated SWCN comprised twice the number of acid sites than those of the sulfonated oxidized SWCN. It was concluded that the oxidation process improved the surface area of catalyst but inhibited the incorporation of sulfonic acid groups on the catalyst surface; thus, the oxidation of carbon nanohorns had no significant impact in promoting the activity of catalysts. It was reported that 93% biodiesel was obtained after 300 min of sulfonated SWCN catalyzed-methanolysis reaction using temperature of 64 °C, methanol-to-oil molar ratio of 33:1 and 3 wt% catalyst amount. The catalytic activity of cation-exchange resins have also been tested for biodiesel production. Jiang et al. [152] tested the catalytic activity of cation-exchange resins CH-A for a esterification reaction between oleic acid and ethanol. The alcoholysis reaction performed at 82 °C for 480 min using ethanol-to-acid molar ratio of 9:1 and 20 g catalyst amount

resulted in 93% oleic acid conversion. The recyclability tests in a batch reactor witnessed breakage of resins during the reaction and hydrolysis of sulfonic group in the presence of water; thus, resulting in the reduction of oleic acid conversion. Feng et al. [153] performed esterification of FFA in a fix bed reactor in the presence of NKC-9 cation-exchange resins catalyst. The reported results suggested that increase in the bed height augmented the biodiesel yield as more time was available for the interaction between catalytic active sites and reaction mixture. It was found that the proposed resins not only assisted alcoholysis reaction but also absorbed sulfur components present in the feedstock. The influence of different reaction parameters such as catalyst type, catalyst amount, type of alcohol, alcohol concentration, reaction temperature, and time on the performance of heterogeneous acid catalyzed-alcoholysis reactions are summarized in Table 8.

5.3. Heterogeneous bi-functional catalysts or two-steps alcoholysis process

Use of two different homogeneous catalysts for a two-steps biodiesel production might not be beneficial because large amount of catalyst is required and consumed during the neutralization steps. Furthermore, the utilization of homogeneous catalysts could also introduce concerns related to the separation, purification, and disposal of waste water stream. Replacing homogeneous catalysts with the heterogeneous ones for the two-steps biodiesel production could gain future relevance as catalyst could be reutilized. Srilatha et al. [154] reported a study focused on a two-steps biodiesel production from used cooking oil in which 25 wt% TPA/Nb_2O_5 catalyst was used for esterification of FFA, while, 20 wt% ZnO/NaY zeolite catalyst was used to transesterify the remaining feedstock. Shibasaki-Kitakawa et al. [155] studied biodiesel production from jatropha oil in a bench-scale series of reactors where the first bed-reactor packed with an cation-exchange Diaion PA306S resins was employed for esterification of FFA, and the second reactor packed with an anion-exchange Diaion PK208LH resins was used to assist transesterification of TAGs. It was reported that anion-exchange resins possessed ability to adsorb glycerol and water formed during the esterification step; consequently, cation-exchange resins did not deactivate, and hence, its regeneration treatment was not needed. However, anion-exchange resins were regenerated to remove the adsorbed glycerol.

Recently, development of a bi-functional catalyst for biodiesel production has also gained enormous scientific attention where a single catalyst, comprising both acidic and basic sites, was used to perform a synchronized esterification and transesterification reaction. The use of bi-functional catalyst would not only eliminate the elongated two-steps process but also reduce the need of high cost equipment; consequently, minimizing the capital cost of the processing technology for biodiesel production. The acidic and basic sites on a single catalyst surface could be generated during the synthesis procedure or by addition of hetero species. Farooq et al. [156] reported the synthesis and application of Mo–Mn/γ-Al_2O_3–15 wt% MgO bi-functional catalyst for transesterification reaction between waste cooking oil and methanol. The reported study suggested that weak Mg–O bonds due to poor electronegativity of Mg^{2+} ions in γ-Al_2O_3–MgO mixed oxides resulted in strong Mo-support interaction. The maximum biodiesel yield of 91.4% was achieved after 240 min of alcoholysis reaction of waste cooking oil performed at 95 °C using methanol-to-oil molar ratio of 27:1 and 5 wt% catalyst amount. Kondamudi et al. [157] reported economically cheap, naturally available and chemically similar to hydrotalcite, a bi-functional Quintine-3T catalyst for biodiesel production. The reported results suggested that even after 5 recycle tests and irrespective of FFA content in the feedstock, more than 96% biodiesel yield was obtained after 120 min of alcoholysis reaction performed at 75 °C using methanol-to-oil molar ratio of 12:1 and 10 wt% catalyst amount.

6. Biocatalysts for alcoholysis reaction

The utilization of enzymes as an effective biocatalyst has been an emerging contribution for biodiesel production. The prime advantages related to enzyme catalysts are their tolerance to FFA and water, and need to low energy for biodiesel production. The immobilized lipase Novozym-435 enzyme catalyst is a commercialized and extensively used catalyst for biodiesel production due to its faster reaction rate and world-wide availability. Cerveró et al. [158] used Novozym-435 (macroporous resins immobilized form of lipase *Candida antárctica*) for a step-wise biodiesel production from soybean oil. It was reported

Table 8
Some heterogeneous acid catalysts for alcoholysis reaction [135–138,140–143,145,146,148,150–152].

Source	Catalyst	Cat.	Alcohol	Alcohol-to-oil molar ratio	Temperature (°C)/Time (min)	Performance	Ref.
Crude palm oil	propyl-SO_3H-SBA-15	6.00 wt%	Methanol	20:1	140/120	~72.00% Yield	[135]
Crude palm oil	arene-SO_3H-SBA-15	6.00 wt%	Methanol	20:1	140/120	~78.00% Yield	[135]
Crude palm oil	arene-SO_3H-SBA-15 (capped)	6.00 wt%	Methanol	20:1	140/120	~90.00% Yield	[135]
Crude palm oil	Amberlyst-36	6.00 wt%	Methanol	20:1	140/120	~32.00% Yield	[135]
Crude palm oil	SiO_2-Tosic acid	6.00 wt%	Methanol	20:1	140/120	~65.00% Yield	[135]
Sunflower oil	Nb-MCM 41	7.50 wt%	Methanol	12:1	200/240	95.00% Yield	[136]
Oleic acid	Sulfated zirconia	0.50 gm	Methanol	40:1[a]	60/720	90.00% Yield	[137]
Oleic acid	Chlorosulfonic zirconia	3.00 wt%	Methanol	8:1[a]	100/720	100.00% Yield	[138]
Sunflower oil	15%WO_3/Zr-MCM 41	1.50 gm	Methanol	12:1	200/150	82.00% Yield	[139]
Soybean oil	30%WO_3/$AlPO_4$	5.00 wt%	Methanol	30:1	180/300	72.50% Yield	[140]
Oleic acid	11.4%WO_3-USY zeolite	10.00 wt%	Ethanol	6:1[a]	200/120	74.00% Yield	[141]
Soybean oil	Ce/HUSY zeolite	0.001 mol	Ethanol	30:1	200/1440	99.80% Conv.	[142]
Oleic acid	Sulfated LaO/HZSM-5	10.00 wt%	Methanol	5:1[a]	100/420	100.00% Conv.	[143]
Oleic acid	Sulfated LaO	10.00 wt%	Methanol	5:1[a]	100/420	96.00% Conv.	[143]
Oleic acid	HZSM-5	10.00 wt%	Methanol	20:1[a]	100/420	80.00% Conv.	[143]
Waste oil	Fe $(HSO_4)_3$	1.00 wt%	Methanol	15:1	205/240	94.50% Yield	[145]
Oleic acid	30% Tungstosicic acid/zeolite Hβ	100 mg	Methanol	20:1[a]	60/600	86.00% Conv.	[146]
Soybean oil	30%Tungstosicic acid/zeolite Hβ	200 mg	Methanol	4:1	65/480	95.00% Conv.	[146]
Acid oil	SO_4^{2-}/ZrO_2-TiO_2/La^{3+}	5.00 wt%	Methanol	15:1	200/120	96.24% Yield	[148]
Polanga oil	Sulfonated carbon	7.50 wt%	Methanol	30:1	180/300	99.00% Conv.	[150]
Palmitic acid	Sulfonated carbon nanohorn	3.00 wt%	Methanol	33:1[a]	64/300	93.00% Yield	[151]
Oleic acid	CH-A Cation exchange resins	20 gm	Ethanol	9:1[a]	82/480	93.00% Conv.	[152]

[a] Alcohol-to- acid ratio.

that the degree of deactivation of catalyst was inversely proportional to the number of carbon atoms in the linear lower alcohols. Furthermore, the step-wise ethanol addition did not had any significant impact on the final biodiesel yield, but it inhibited catalyst deactivation and facilitated biodiesel production in less reaction time. It was reported that the reaction temperature of 37 °C, ethanol-to-oil molar ratio of 3:1, and catalyst amount of 5 wt% was enough to achieve approximately 99% biodiesel yield. Ngo et al. [159] tested the catalytic activity of two catalysts, *Thermomyces lanuginosus* lipase and *Cándida antárctica* lipase B enzymes, each immobilized on a superparamagnetic iron oxide nanoparticles, for biodiesel production from high FFA grease. It was report that *T. lanuginosus* lipase represented activity for esterification and transesterification reaction, while, *C. antárctica* lipase B enzyme demonstrated the catalytic selectivity only for esterification reaction. Ngo et al. [159] further reported that the addition of silica beads into a reaction mixture could avoid step-wise addition of alcohol because silica beads hold methanol and release it slowly during the alcoholysis process. Furthermore, silica beads also enabled the absorption of water and glycerol formed during the esterification and transesterification reaction, respectively; thus, reducing the possibility of deactivation of the magnetic nano-biocatalyst.

Chattopadhyay and Sen. [160] tested the catalytic activity of IIT-SARKZYME lipase for biodiesel production in a continuous flow packed-bed reactor system. It was reported that oil was initially subjected to a partial transesterification process which improved methanol-oil mutual solubility; the formed product then was transferred to the packed-bed reactor, loaded with enzyme catalyst, to complete biotransformation of oil to biodiesel. Soares et al. [161] reported a study in which high FFA feedstock was initially hydroesterified in the presence of water in an sub-critical condition, after that, the obtained product was subjected to a esterification process in a bed reactor packed with a fermented solid made by cultivating *Burkholderia cepacia* LTEB11 on a mixture (1:1) of sugarcane bagasse and sunflower seed meal. The proposed procedure was said to be beneficial as the pure fatty acid product was obtained without usage of a catalyst and the glycerol removal, after the initial hydroesterification reaction, reduced the risk of enzyme deactivation. Jang et al. [162] reported that the presence of phospholipids in an oil feedstock also resulted in the biocatalyst deactivation. The degumming process was employed for phospholipids conversion to lypo-phospholipids and fatty acid with the help of Phospholipase A2 enzyme; the resulting product then was transesterified to achieve the final esters yield of 68.56%, 70.15%, and 84.25% using *Rhizopus oryzae*, *Candida rugosa*, and 1:1 (vol: vol) mixture of two enzymes, respectively. The mixed enzymes were then immobilized on silica gel to increase its thermal stability. It was investigated that using 24.4 wt% catalyst amount of supported enzyme catalyst, 88.9% of degummed crude canola oil was converted to biodiesel. However, Li et al. [163] reported that phospholipids, being one of the surfactants with an excellent amphipathic property, improved the catalytic activity of free lipase *Aspergillus niger* enzyme, and increasing its concentration in the reaction mixture augmented the final biodiesel yield. It was mentioned that the presence of phospholipids emulsified a reaction mixture containing soybean oil, methanol, and free lipase *A. niger* enzyme. After the completion of alcoholysis reaction, free lipase *A. niger* enzyme remained in an emulsion and water phase which enabled its easy separation and reutilization.

7. Supercritical method

The supercritical methodology for biodiesel production is under continuous scientific study because of several benefits. The main advantages of the supercritical technology exist in their prompt reaction for the conversion of oil feedstock to biodiesel even in the absence of a catalyst. Furthermore, the operating temperatures and pressures used for the supercritical technology enables mutual solubility between an oil and alcohol phase; thus, ruling out the concerns related to the limited mass transfer. On top of that, the elimination of catalyst system in the reaction process makes the product separation and purification comparatively straightforward and cost effective. However, biodiesel synthesis using current technology requires severe reaction conditions to achieve high esters yield and high quality biodiesel. The high energy consuming parameters would not only increase the capital cost of the process but also deteriorate biodiesel yield due to thermal decomposition phenomenon. Olivares-Carrillo and Quesada-Medina [164] studied biodiesel production from the non-catalyzed supercritical transesterification reaction between soybean oil and methanol. The supercritical alcoholysis reaction performed at 325 °C resulted in 84% biodiesel yield; however, rise in the reaction temperature to 350 °C resulted in thermal degradation of the methyl esters and reduced biodiesel yield to 70%.

In order to minimize the reaction temperature necessary for the supercritical alcoholysis reactions, several supplementary approaches, such as the addition of gaseous and liquid co-solvents, the addition of a catalyst are under the continuous scientific studies. It is anticipated that the addition of carbon dioxide gas, as a co-solvent, in a reaction mixture could improve alcohol–oil solubility. It is suggested that the addition of CO_2 to the reaction system will not only reduce the reaction mixture critical point but also enable its easy separation from the products. Trentin et al. [165] reported that increasing CO_2 concentration in the reaction system promoted the transesterification reaction between soybean oil and ethanol; thus, increasing the biodiesel yield. The transesterification reaction performed in a stainless steel microtube reactor indicated that the smaller internal space in the micro reactor and high surface area-to-volume ratio enhanced the mass and heat transfer. Tsai et al. [166] reported that the addition of CO_2 had no significant impact on the alcoholysis reaction between sunflower oil and methanol, studied in a continuous mode tubular reactor, under the supercritical reaction conditions. It was reported that the rise in the reaction temperature augmented the biodiesel yield, but increase in the system pressure and the addition of CO_2 had no influence on the same. Jiang and Tan [167] investigated the influence of 8 different organic co-solvents in the supercritical transesterification reaction between coconut oil and methanol. It was reported that among the tested co-solvents, ethers improved alcohol–oil miscibility and created single phase system at less extreme temperature. The alcoholysis reaction performed for 20 min at 285 °C and at a pressure of 14 MPa using methanol-to-coconut oil-to-ether molar ratio of 30:1:3, resulted in 72% biodiesel yield.

The catalytic supercritical technology for biodiesel production could also be beneficial in reducing elevated reaction conditions so as to avoid the thermal degradation of reactants and products. Santana et al. [168] studied the transesterification reaction of sunflower-based oil reacting with the supercritical ethanol in the presence of Nafion SAC-13 ion-exchange resins catalyst and carbon dioxide gas. Shin et al. [169] investigated the activity of a copper catalyst for the simultaneous transesterification and partial hydrogenation reaction of TAGs and polyunsaturated methyl esters, respectively. The conversion of polyunsaturated esters to monounsaturated esters increased the fuel characteristics of biodiesel such as the oxidation stability, iodine number, cetane number, and cold flow properties. It was suggested that the methanol decomposition under the supercritical reaction produced hydrogen gas, which then along with the copper catalyst promoted the hydrogenation reaction. Thus, it was concluded that two simultaneous reactions were performed using a single catalyst and no external addition of hydrogen gas was required.

8. Recent non-traditional development in catalysis and technology for biodiesel production

Biodiesel might not be the complete solution to fuel crisis; however, it's appropriate usage would definitely reduce the entire dependency on petroleum diesel. Despite significant advancement made in several stages of biodiesel production, challenge of competing with petroleum diesel still exists. At present, large fraction of total biodiesel is produced from expensive food-grade oils. This, consequently, has resulted in rise in the cost of biodiesel production. Hence, to minimize the prices of biodiesel, there evolves a requirement to search less expensive non-edible oil resources. The oils, such as jatropha seed oil, jojoba oil, karanja oil, amongst others, are not part of human food chain and could be utilized for biodiesel production. However, it is worth noting that such oils constituent high concentration of free fatty acids. Park et al. [98] and Soares et al. [161] selected a non-traditional method of biodiesel production in which feedstock containing elevated concentration of free fatty acid was first hydrolyzed followed with esterification reaction of the obtained product. The tested process could be advantageous as it would facilitate the usage of low-grade oils, minimize multiple reaction stages, and eliminate the need of additional catalyst for biodiesel production.

Other than raw material, it is also of foremost importance to consider the monetary investment made for catalysts. For successful commercialization of catalyst for biodiesel production, ideal catalyst should represent superior activity and selectivity for the alcoholysis reaction along with its easy availability, low cost, and reusability as these factors would have a direct impact on overall cost of the process. Among the base catalysts, calcium oxide material is widely utilized not only because of their stupendous physico-chemical properties but also due to economic benefits. In a conventional catalyst synthesis procedure, the naturally available calcium materials are thermally treated at high temperatures to derive CaO catalyst. However, consistent scientific efforts are still engaged to find a way to minimize its poisoning occurred when exposed to the surrounding atmosphere. Minimizing poisoning phenomenon of CaO catalyst is extremely crucial to allow its storage for longer duration without applying any special precautions. Granados et al. [170] suggested that after the calcination process, the pretreatment of CaO catalyst with biodiesel eliminated the diffusion of CO_2 and H_2O into the catalyst surface, thus protecting the catalyst from poisoning. Zhu et al. [171] reported that rinsing CaO with ammonium carbonate solution and then keeping for calcination resulted in the promotion of basic strength of catalyst. Huang et al. [172] reported that the addition of deep eutectic solvents into the reaction mixture would eliminate the necessity of traditional calcination procedure of calcium materials. It was concluded that deep eutectic solvent and methanol mixture directed the liberation of carbonate and hydroxide species from the surface of material, thus providing desired CaO active sites required to accelerate the alcoholysis reaction. Furthermore, the incorporation of CaO into hetero species during the catalyst synthesis or its loading on a porous support was also tested in order to promote the number of active centers, durability, and stability of catalyst [173–175]. This in return is anticipated to allow the reutilization of catalysts for several reaction cycles. Lin et al. [176] suggested that magnetic CaO/α-Fe fibers displayed excellent catalytic activity for transesterification of rapeseed oil, producing 85% biodiesel yield even after 20 recycle tests. Furthermore, the magnetic behavior of catalyst helped its easy separation from the post-reaction mixture with the appliance of magnetic field. The carbon materials are also considered as an excellent support for catalyst because of its hydrophobicity. The hydrophobic characteristic of catalyst is assumed to preclude the undesired side reactions caused due to the presence of moisture in the reaction medium. Furthermore, excellent thermal and mechanical stability of carbon would maintain its textural framework even under severe reaction conditions. However, challenge remains to find a suitable procedure to strongly anchor catalytic species onto the carbon support. The possibility of fabricating carbon material also from feedstock and reaction leftover, such as oil cake waste, canola de-oiled meal, microalgae residue, lignin, and glycerol is also newly tested and is expected to gain further consideration [177–181]. The successful synthesis of carbon materials from the industrial production plant waste would not only provide a catalytic material within the industry but also minimize waste disposal concerns. However, serious scientific efforts would still be required to regulate the textural framework of these carbon materials in order to achieve satisfactory dispersion of catalytic species on the support.

Along with catalysis, the upgradation in processing technology would also facilitate the up-scaling of biodiesel production from a laboratory scale to a commercial scale. The recently introduced technologies, such as microwave irradiation, ultrasonic technology, and supercritical technology though have gained adequate importance, the reactive extraction technology [182–185], a single-step oil extraction and its immediate transformation to biodiesel process, has been gaining serious scientific attention. However, more research evidences would be required to implement the reactive extraction process on the industrial scale.

9. Summary and conclusion

The availability and cost of oil feedstocks would play a vital role in deciding the capital cost of biodiesel production. In order to reduce the drawbacks associated with the usage of uneconomical food-grade oils, the utilization of potential non-edible oils, such as jatropha oil, karanja oil, polanga oil, jojoba oil, amongst other, for the production of biodiesel could gain industrial relevance. This is possible for the reason that, not the feedstocks, but the produced biodiesel has to meet the ASTM, EN standards specifications. However, it is important to note that the physical and chemical properties of feedstocks, such as fatty acid composition, free fatty level, moisture, impurities and unsaponifiables will decide the quality of biodiesel.

Amongst the different possible options known for the transformation of oil feedstock to biodiesel, alcoholysis process has been frequently utilized. The catalysts used for the alcoholysis process could be divided into two categories based on their active site: acid and base catalysts. The selection of appropriate catalyst profoundly depends on the free fatty acid and water content in the feedstock. The base catalysts are known to accelerate transesterification reaction rate and possible maximum biodiesel yield is achieved using mild reaction conditions, whereas, the acidic counterparts are tolerant towards the free fatty acid and water content in feedstocks and can catalyze both esterification and transesterification reaction, but is a time-consuming process. The homogeneous catalysts are conventionally used for biodiesel production; however, their use evolves problems, such as complicated separation and purification steps, and generate large amount of waste water stream. The heterogeneous catalysts, depending on the number and strength of the active sites, display superior catalytic activity and selectivity for biodiesel production, with an adjustment that the elevated reaction conditions are required to minimize the mass transfer limitation and improve the biodiesel yield. Moreover, heterogeneous catalysts enable their easy separation from the post-reaction mixture, regeneration, and reutilization. Thus, it is anticipated that heterogeneous catalysts would be possible substitute for the conventional homogeneous ones in a near future. The significant number of recently available publications on the development of heterogeneous catalysis for biodiesel production is an

indicative of an efforts made to replace the homogeneous catalysts with the modern heterogeneous materials. However, an extensive research is still a continuous process to regulate the textural morphology, specific surface area, and porosity of the heterogeneous catalyst systems in order to improve their activity, mechanical strength, thermal stability, and minimize the lixiviation of active species into the reaction mixture.

The catalytic activity of several heterogeneous base and acid catalysts has been investigated for biodiesel production. Among the different heterogeneous base catalysts, calcium oxide catalyst could gain future industrial relevance due to the natural abundance of calcium species, its trouble-free handling, easy synthesis methodology, and low cost. The CaO-catalyzed transesterification reactions have resulted in more than 90% biodiesel yield. However, its de-activation phenomenon, when exposed to the surrounding carbon dioxide and moisture, has indicated the need for its structural modifications. The incorporation of calcium species onto the heterospecies during the synthesis, or its anchoring on a metal oxide support might restrict the sintering and leaching of active calcium species. Moreover, the uniform dispersion of calcium catalyst into the pores of mesoporous metal oxide would also improve the activity of the final designed catalyst for the alcoholysis process. The reports on the excellent catalytic activity of mixed metal oxides catalysts, such as calcium zincate, sodium zirconate, Ca/Al nanocomposite, and Sr–Al nanocomposite for biodiesel production are available in the literature.

The employment of heterogeneous acid catalysts for biodiesel production could be crucial when it comes to the utilization of low quality feedstocks, such as industrial waste, and non-edible oils. Several heterogeneous acid catalysts have been tested for biodiesel production. The acid functionalization of a mesoporous support is considered as a foundation for the development of heterogeneous acid catalysts. It can be concluded that the carbon materials could be excellent supports for the acid catalyst because its porosity can be regulated during its synthesis, high thermal stability, hydrophobicity, and low cost. A bi-functional catalyst, which includes both acid and basic active sites, could be of future scientific interest because it can simultaneously catalyze transesterification and esterification reaction of triglycerides and free fatty acids, respectively. Thus, heterogeneous acid catalysts and bi-functional catalyst could be of an industrial relevance because these catalysts would enable biodiesel production from less expensive low-quality feedstocks.

The ideal heterogeneous catalyst for biodiesel production should possess high catalytic activity, high stability, minimal lixiviation, high reutilization, and low cost. Hence, to sum up, it could be said that in-depth knowledge about the selection of appropriate oil feedstock, catalyst, and processing reaction conditions is of foremost importance for a large-scale biodiesel production.

Acknowledgments

The authors would like to express their gratitude to the Norwegian University of Life Sciences (Project no. 1301051406) for their financial support.

References

[1] International Energy Outlook, U. S Energy Administration. ⟨http://www.eia.gov/forecasts/ieo/⟩; 2013 [accessed 19.02.15].
[2] BP statistical review of World Energy June 2013. ⟨http://www.bp.com/statisticalreview⟩ [accessed 19.02.15].
[3] Panwar NL, Kaushik SC, Kothari S. Role of renewable energy sources in environmental protection: a review. Renew Sustain Energy Rev 2011;15:1513–24.
[4] Twidell JW, Weir AD. Renewable energy resources. 2nd ed. Great Britain: Taylor & Francis; 2006.
[5] Marchetti JM. A summary of the available technologies for biodiesel production based on a comparison of different feedstock's properties. Process Saf Environ Prot 2012;90:157–63.
[6] Knothe G. Improving biodiesel fuel properties by modifying fatty ester composition. Energy Environ Sci 2009;2:759–66.
[7] Yusuf NNAN, Kamarudin SK, Yaakub Z. Overview on the current trends in biodiesel production. Energy Convers Manag 2011;52:2741–51.
[8] Demirbas A. Importance of biodiesel as transportation fuel. Energy Policy 2007;35:4661–70.
[9] Marchetti JM. Biodiesel production technologies. 1st ed. New York: Nova science publisher, Inc.; 2010.
[10] Ong HC, Silitonga AS, Masjuki HH, Mahlia TMI, Chong WT, Boosroh MH. Production and comparative fuel properties of biodiesel from non-edible oils: Jatropha curcas, Sterculia foetida and Ceiba pentandra. Energy Convers Manag 2013;73:245–55.
[11] Helwani Z, Aziz N, Bakar MZA, Mukhtar H, Kim J, Othman MR. Conversion of Jatropha curcas oil into biodiesel using re-crystallized hydrotalcite. Energy Convers Manag 2013;73:128–34.
[12] Zheng L, Hou Y, Li W, Yang S, Li Q, Yu Z. Exploring the potential of grease from yellow mealworm beetle (Tenebrio molitor) as a novel biodiesel feedstock. Appl Energy 2013;101:618–21.
[13] Azcan N, Yilmaz O. Microwave assisted transesterification of waste frying oil and concentrate methyl ester content of biodiesel by molecular distillation. Fuel 2013;104:614–9.
[14] Singh SP, Singh D. Biodiesel production through the use of different sources and characterization of oils and their esters as the substitute of diesel: a review. Renew Sustain Energy Rev 2010;14:200–16.
[15] Karmakar A, Karmakar S, Mukherjee S. Properties of various plants and animals feedstocks for biodiesel production. Bioresour Technol 2010;101:7201–10.
[16] No S-Y. Inedible vegetable oils and their derivatives for alternative diesel fuels in CI engines: a review. Renew Sustain Energy Rev 2011;15:131–49.
[17] Da Porto C, Decorti D, Tubaro F. Fatty acid composition and oxidation stability of hemp (Cannabis sativa L.) seed oil extracted by supercritical carbon dioxide. Ind Crop Prod 2012;36:401–4.
[18] Fadhil AB, Abdulahad WS. Transesterification of mustard (Brassica nigra) seed oil with ethanol: purification of the crude ethyl ester with activated carbon produced from de-oiled cake. Energy Convers Manag 2014;77:495–503.
[19] Mitra P, Ramaswamy HS, Chang KS. Pumpkin (Cucurbita maxima) seed oil extraction using supercritical carbon dioxide and physicochemical properties of the oil. J Food Eng 2009;95:208–13.
[20] Duz MZ, Saydut A, Ozturk G. Alkali catalyzed transesterification of safflower seed oil assisted by microwave irradiation. Fuel Process Technol 2011;92:308–13.
[21] Banapurmath NR, Tewari PG, Hosmath RS. Performance and emission characteristics of a DI compression ignition engine operated on Honge, Jatropha and sesame oil methyl esters. Renew Energy 2008;33:1982–8.
[22] Xie W, Zhao L. Heterogeneous CaO–MoO_3–SBA-15 catalysts for biodiesel production from soybean oil. Energy Convers Manag 2014;79:34–42.
[23] Martínez SL, Romero R, Natividad R, González J. Optimization of biodiesel production from sunflower oil by transesterification using Na_2O/NaX and methanol. Catal Today 2014;220–222:12–20.
[24] Kurayama F, Yoshikawa T, Furusawa T, Bahadur NM, Handa H, Sato M, et al. Microcapsule with a heterogeneous catalyst for the methanolysis of rape-seed oil. Bioresour Technol 2013;135:652–8.
[25] Choedkiatsakul I, Ngaosuwan K, Cravotto G, Assabumrungrat S. Biodiesel production from palm oil using combined mechanical stirred and ultrasonic reactor. Ultrason Sonochemistry.
[26] Zheng L, Li Q, Zhang J, Yu Z. Double the biodiesel yield: rearing black soldier fly larvae, Hermetia illucens, on solid residual fraction of restaurant waste after grease extraction for biodiesel production. Renew Energy 2012;41:75–9.
[27] Wang R, Hanna MA, Zhou W-W, Bhadury PS, Chen Q, Song B-A, et al. Production and selected fuel properties of biodiesel from promising non-edible oils: Euphorbia lathyris L., Sapium sebiferum L. and Jatropha curcas L. Bioresour Technol 2011;102:1194–9.
[28] Supamathanon N, Wittayakun J, Prayoonpokarach S. Properties of Jatropha seed oil from Northeastern Thailand and its transesterification catalyzed by potassium supported on NaY zeolite. J Ind Eng Chem 2011;17:182–5.
[29] Al Awad AS, Selim MYE, Zeibak AF, Moussa R. Jojoba ethyl ester production and properties of ethanol blends. Fuel.
[30] Thiruvengadaravi KV, Nandagopal J, Baskaralingam P, Sathya Selva Bala V, Sivanesan S. Acid-catalyzed esterification of karanja (Pongamia pinnata) oil with high free fatty acids for biodiesel production. Fuel 2012;98:1–4.
[31] Kumar R, Tiwari P, Garg S. Alkali transesterification of linseed oil for biodiesel production. Fuel 2013;104:553–60.
[32] Athalye S, Sharma-Shivappa R, Peretti S, Kolar P, Davis JP. Producing biodiesel from cottonseed oil using Rhizopus oryzae ATCC #34612 whole cell biocatalysts: culture media and cultivation period optimization. Energy Sustain Dev 2013;17:331–6.
[33] Oliveira JFG, Lucena IL, Saboya RMA, Rodrigues ML, Torres AEB, Fernandes FAN, et al. Biodiesel production from waste coconut oil by esterification with ethanol: the effect of water removal by adsorption. Renew Energy 2010;35:2581–4.
[34] Li S-Y, Stuart JD, Li Y, Parnas RS. The feasibility of converting Cannabis sativa L. oil into biodiesel. Bioresour Technol 2010;101:8457–60.
[35] Ramos MJ, Fernández CM, Casas A, Rodríguez L, Pérez Á. Influence of fatty acid composition of raw materials on biodiesel properties. Bioresour Technol 2009;100:261–8.

[36] Zhang Y, Wong W-T, Yung K-F. One-step production of biodiesel from rice bran oil catalyzed by chlorosulfonic acid modified zirconia via simultaneous esterification and transesterification. Bioresour Technol 2013;147:59–64.
[37] Mihaela P, Josef R, Monica N, Rudolf Z. Perspectives of safflower oil as biodiesel source for South Eastern Europe (comparative study: Safflower, soybean and rapeseed). Fuel 2013;111:114–9.
[38] Park YW, Chang P-S, Lee J. Application of triacylglycerol and fatty acid analyses to discriminate blended sesame oil with soybean oil. Food Chem 2010;123:377–83.
[39] Ghanei R, Moradi GR, TaherpourKalantari R, Arjmandzadeh E. Variation of physical properties during transesterification of sunflower oil to biodiesel as an approach to predict reaction progress. Fuel Process Technol 2011;92:1593–8.
[40] Hincapié G, Mondragón F, López D. Conventional and in situ transesterification of castor seed oil for biodiesel production. Fuel 2011;90:1618–23.
[41] Joshi H, Moser BR, Shah SN, Mandalika A, Walker T. Improvement of fuel properties of cottonseed oil methyl esters with commercial additives. Eur J Lipid Sci Technol 2010;112:802–9.
[42] Okia CA, Kwetegyeka J, Okiror P, Kimondo JM, Teklehaimanot Z, Obua J. Physico-chemical characteristics and fatty acid profile of desert date kernel oil. African Crop Sci J 2013;21:725–34.
[43] Sahoo PK, Das LM. Process optimization for biodiesel production from Jatropha, Karanja and Polanga oils. Fuel 2009;88:1588–94.
[44] Shah SN, Sharma BK, Moser BR, Erhan SZ. Preparation and evaluation of jojoba oil methyl esters as biodiesel and as a blend component in ultra-low sulfur diesel fuel. BioEnergy Res 2009;3:214–23.
[45] Demirbas A. Production of biodiesel fuels from linseed oil using methanol and ethanol in non-catalytic SCF conditions. Biomass Bioenergy 2009;33:113–8.
[46] Jena PC, Raheman H, Prasanna Kumar GV, Machavaram R. Biodiesel production from mixture of mahua and simarouba oils with high free fatty acids. Biomass Bioenergy 2010;34:1108–16.
[47] Kafuku G, Mbarawa M. Alkaline catalyzed biodiesel production from moringa oleifera oil with optimized production parameters. Appl Energy 2010;87:2561–5.
[48] Betiku E, Omilakin OR, Ajala SO, Okeleye AA, Taiwo AE, Solomon BO. Mathematical modeling and process parameters optimization studies by artificial neural network and response surface methodology: a case of non-edible neem (Azadirachta indica) seed oil biodiesel synthesis. Energy 2014;72:266–73.
[49] Satyanarayana M, Muraleedharan C. A comparative study of vegetable oil methyl esters (biodiesels). Energy 2011;36:2129–37.
[50] Parlak A, Ayhan V, Cesur İ, Kökkülünk G. Investigation of the effects of steam injection on performance and emissions of a diesel engine fuelled with tobacco seed oil methyl ester. Fuel Process Technol 2013;116:101–9.
[51] Al-Hamamre Z, Yamin J. Parametric study of the alkali catalyzed transesterification of waste frying oil for Biodiesel production. Energy Convers Manag 2014;79:246–54.
[52] Teixeira LSG, Assis JCR, Mendonça DR, Santos ITV, Guimarães PRB, Pontes LAM, et al. Comparison between conventional and ultrasonic preparation of beef tallow biodiesel. Fuel Process Technol 2009;90:1164–6.
[53] Kwon EE, Jeon E-C, Yi H, Kim S. Transforming duck tallow into biodiesel via noncatalytic transesterification. Appl Energy 2014;116:20–5.
[54] Marulanda VF, Anitescu G, Tavlarides LL. Investigations on supercritical transesterification of chicken fat for biodiesel production from low-cost lipid feedstocks. J Supercrit Fluids 2010;54:53–60.
[55] Ilkılıç C, Aydın S, Behcet R, Aydin H. Biodiesel from safflower oil and its application in a diesel engine. Fuel Process Technol 2011;92:356–62.
[56] Roy MM, Wang W, Bujold J. Biodiesel production and comparison of emissions of a DI diesel engine fueled by biodiesel–diesel and canola oil–diesel blends at high idling operations. Appl Energy 2013;106:198–208.
[57] Vedharaj S, Vallinayagam R, Yang WM, Chou SK, Chua KJE, Lee PS. Experimental investigation of kapok (Ceiba pentandra) oil biodiesel as an alternate fuel for diesel engine. Energy Convers Manag 2013;75:773–9.
[58] Rakopoulos DC, Rakopoulos CD, Giakoumis EG, Dimaratos AM, Founti MA. Comparative environmental behavior of bus engine operating on blends of diesel fuel with four straight vegetable oils of Greek origin: sunflower, cottonseed, corn and olive. Fuel 2011;90:3439–46.
[59] Bajpai S, Sahoo PK, Das LM. Feasibility of blending karanja vegetable oil in petro-diesel and utilization in a direct injection diesel engine. Fuel 2009;88:705–11.
[60] Misra RD, Murthy MS. Performance, emission and combustion evaluation of soapnut oil–diesel blends in a compression ignition engine. Fuel 2011;90:2514–8.
[61] İşcan B, Aydın H. Improving the usability of vegetable oils as a fuel in a low heat rejection diesel engine. Fuel Process Technol 2012;98:59–64.
[62] Aydin H. Combined effects of thermal barrier coating and blending with diesel fuel on usability of vegetable oils in diesel engines. Appl Therm Eng 2013;51:623–9.
[63] Santos ALF, Martins DU, Iha OK, Ribeiro RAM, Quirino RL, P.A.Z. Suarez. Agro-industrial residues as low-price feedstock for diesel-like fuel production by thermal cracking. Bioresour Technol 2010;101:6157–62.
[64] Kozliak E, Mota R, Rodriguez D, Overby P, Kubátová A, Stahl D, et al. Non-catalytic cracking of jojoba oil to produce fuel and chemical by-products. Ind Crop Prod 2013;43:386–92.
[65] Biswas S, Mohanty P, Sharma DK. Studies on co-cracking of jatropha oil with bagasse to obtain liquid, gaseous product and char. Renew Energy 2014;63:308–16.
[66] Luo Y, Ahmed I, Kubátová A, Šťávová J, Aulich T, Sadrameli SM, et al. The thermal cracking of soybean/canola oils and their methyl esters. Fuel Process Technol 2010;91:613–7.
[67] Prado CMR, Antoniosi Filho NR. Production and characterization of the biofuels obtained by thermal cracking and thermal catalytic cracking of vegetable oils. J Anal Appl Pyrol 2009;86:338–47.
[68] Koh MY, Mohd., Ghazi TI. A review of biodiesel production from Jatropha curcas L. oil. Renew Sustain Energy Rev 2011;15:2240–51.
[69] Acharya DP, Hartley PG. Progress in microemulsion characterization. Curr Opin Colloid Interface Sci 2012;17:274–80.
[70] Nguyen T, Do L, Sabatini DA. Biodiesel production via peanut oil extraction using diesel-based reverse-micellar microemulsions. Fuel 2010;89:2285–91.
[71] Naksuk A, Sabatini DA, Tongcumpou C. Microemulsion-based palm kernel oil extraction using mixed surfactant solutions. Ind Crop Prod 2009;30:194–8.
[72] Qi DH, Bae C, Feng YM, Jia CC, Bian YZ. Combustion and emission characteristics of a direct injection compression ignition engine using rapeseed oil based micro-emulsions. Fuel 2013;107:570–7.
[73] Marchetti JM, Miguel VU, Errazu AF. Possible methods for biodiesel production. Renew Sustain Energy Rev 2007;11:1300–11.
[74] Marchetti JM. Influence of economical variables on a supercritical biodiesel production process. Energy Convers Manag 2013;75:658–63.
[75] Kumar R, Ravi Kumar G, Chandrashekar N. Microwave assisted alkali-catalyzed transesterification of Pongamia pinnata seed oil for biodiesel production. Bioresour Technol 2011;102:6617–20.
[76] Badday AS, Abdullah AZ, Lee K-T. Optimization of biodiesel production process from Jatropha oil using supported heteropolyacid catalyst and assisted by ultrasonic energy. Renew Energy 2013;50:427–32.
[77] Rodríguez-Guerrero JK, Rubens MF, Rosa PTV. Production of biodiesel from castor oil using sub and supercritical ethanol: effect of sodium hydroxide on the ethyl ester production. J Supercrit Fluids 2013;83:124–32.
[78] Shahbazi MR, Khoshandam B, Nasiri M, Ghazvini M. Biodiesel production via alkali-catalyzed transesterification of Malaysian RBD palm oil – characterization, kinetics model. J Taiwan Inst Chem Eng 2012;43:504–10.
[79] Ramachandran K, Suganya T, Nagendra Gandhi N, Renganathan S. Recent developments for biodiesel production by ultrasonic assist transesterification using different heterogeneous catalyst: a review. Renew Sustain Energy Rev 2013;22:410–8.
[80] Sun H, Ding Y, Duan J, Zhang Q, Wang Z, Lou H, et al. Transesterification of sunflower oil to biodiesel on ZrO_2 supported La_2O_3 catalyst. Bioresour Technol 2010;101:953–8.
[81] Keera ST, El Sabagh SM, Taman AR. Transesterification of vegetable oil to biodiesel fuel using alkaline catalyst. Fuel 2011;90:42–7.
[82] Dias JM, Alvim-Ferraz MCM, Almeida MF. Comparison of the performance of different homogeneous alkali catalysts during transesterification of waste and virgin oils and evaluation of biodiesel quality. Fuel 2008;87:3572–8.
[83] Uzun BB, Kılıç M, Özbay N, Pütün AE, Pütün E. Biodiesel production from waste frying oils: optimization of reaction parameters and determination of fuel properties. Energy 2012;44:347–51.
[84] Chung K-H, Kim J, Lee K-Y. Biodiesel production by transesterification of duck tallow with methanol on alkali catalysts. Biomass Bioenergy 2009;33:155–8.
[85] Fadhil AB, Ali LH. Alkaline-catalyzed transesterification of Silurus triostegus Heckel fish oil: optimization of transesterification parameters. Renew Energy 2013;60:481–8.
[86] Li Y, Qiu F, Yang D, Sun P, Li X. Transesterification of soybean oil and analysis of bioproduct. Food Bioprod Process 2012;90:135–40.
[87] Fernandes DM, Serqueira DS, Portela FM, Assunção RMN, Munoz RAA, Terrones MGH. Preparation and characterization of methylic and ethylic biodiesel from cottonseed oil and effect of tert-butylhydroquinone on its oxidative stability. Fuel 2012;97:658–61.
[88] Chen K-S, Lin Y-C, Hsu K-H, Wang H-K. Improving biodiesel yields from waste cooking oil by using sodium methoxide and a microwave heating system. Energy 2012;38:151–6.
[89] Brito JQA, Silva CS, Almeida JS, Korn MGA, Korn M, Teixeira LSG. Ultrasound-assisted synthesis of ethyl esters from soybean oil via homogeneous catalysis. Fuel Process Technol 2012;95:33–6.
[90] Karavalakis G, Anastopoulos G, Karonis D, Stournas S. Biodiesel production using tetramethyl- and benzyltrimethyl ammonium hydroxides as strong base catalysts. Fuel Process Technol 2010;91:1585–90.
[91] Karavalakis G, Anastopoulos G, Stournas S. Tetramethylguanidine as an efficient catalyst for transesterification of waste frying oils. Appl Energy 2011;88:3645–50.
[92] Yao J, Ji L, Sun P, Zhang L, Xu N. Low boiling point organic amine-catalyzed transesterification of cottonseed oil to biodiesel with trace amount of KOH as co-catalyst. Fuel 2010;89:3871–5.
[93] Farag HA, El-Maghraby A, Taha NA. Optimization of factors affecting esterification of mixed oil with high percentage of free fatty acid. Fuel Process Technol 2011;92:507–10.
[94] Aranda DAG, Santos RTP, Tapanes NCO, Ramos ALD, Antunes OAC. Acid-catalyzed homogeneous esterification reaction for biodiesel production from palm fatty acids. Catal Lett 2007;122:20–5.
[95] Berrios M, Siles J, Martín MA, Martín A. A kinetic study of the esterification of free fatty acids (FFA) in sunflower oil. Fuel 2007;86:2383–8.

[96] Marchetti JM, Errazu AF. Esterification of free fatty acids using sulfuric acid as catalyst in the presence of triglycerides. Biomass Bioenergy 2008;32:892–5.
[97] Marchetti JM, Pedernera MN, Schbib NS. Production of biodiesel from acid oil using sulphuric acid as catalyst: kinetics study. Int J Low-Carbon Technol 2010;6:38–43.
[98] Park J-Y, Wang Z-M, Kim D-K, Lee J-S. Effects of water on the esterification of free fatty acids by acid catalysts. Renew Energy 2010;35:614–8.
[99] Hanh HD, Dong NT, Okitsu K, Nishimura R, Maeda Y. Biodiesel production by esterification of oleic acid with short-chain alcohols under ultrasonic irradiation condition. Renew Energy 2009;34:780–3.
[100] Su C-H. Recoverable and reusable hydrochloric acid used as a homogeneous catalyst for biodiesel production. Appl Energy 2013;104:503–9.
[101] Su C-H. Kinetic study of free fatty acid esterification reaction catalyzed by recoverable and reusable hydrochloric acid. Bioresour Technol 2013;130:522–8.
[102] Miao X, Li R, Yao H. Effective acid-catalyzed transesterification for biodiesel production. Energy Convers Manag 2009;50:2680–4.
[103] Soriano NU, Venditti R, Argyropoulos DS. Biodiesel synthesis via homogeneous Lewis acid-catalyzed transesterification. Fuel 2009;88:560–5.
[104] Guan G, Kusakabe K, Sakurai N, Moriyama K. Transesterification of vegetable oil to biodiesel fuel using acid catalysts in the presence of dimethyl ether. Fuel 2009;88:81–6.
[105] Hayyan A, Alam MZ, Mirghani MES, Kabbashi NA, N.I.N.M. Hakimi, Siran YM, et al. Reduction of high content of free fatty acid in sludge palm oil via acid catalyst for biodiesel production. Fuel Process Technol 2011;92:920–4.
[106] Hayyan A, Mjalli FS, Hashim MA, Hayyan M, AlNashef IM, Al-Zahrani SM, et al. Ethanesulfonic acid-based esterification of industrial acidic crude palm oil for biodiesel production. Bioresour Technol 2011;102:9564–70.
[107] Naik M, Meher L, Naik S, Das L. Production of biodiesel from high free fatty acid Karanja (Pongamia pinnata) oil. Biomass Bioenergy 2008;32:354–7.
[108] Berchmans HJ, Hirata S. Biodiesel production from crude Jatropha curcas L. seed oil with a high content of free fatty acids. Bioresour Technol 2008;99:1716–21.
[109] Encinar JM, Sanchez N, Martinez G, Garcia L. Study of biodiesel production from animal fats with high free fatty acid content. Bioresour Technol 2011;102:10907–14.
[110] Suppalakpanya K, Ratanawilai SB, Tongurai C. Production of ethyl ester from crude palm oil by two-step reaction with a microwave system. Fuel 2010;89:2140–4.
[111] Jansri S, Ratanawilai SB, Allen ML, Prateepchaikul G. Kinetics of methyl ester production from mixed crude palm oil by using acid-alkali catalyst. Fuel Process Technol 2011;92:1543–8.
[112] Kawashima A, Matsubara K, Honda K. Acceleration of catalytic activity of calcium oxide for biodiesel production. Bioresour Technol 2009;100:696–700.
[113] Kouzu M, Tsunomori M, Yamanaka S, Hidaka J. Solid base catalysis of calcium oxide for a reaction to convert vegetable oil into biodiesel. Adv Powder Technol 2010;21:488–94.
[114] Suryaputra W, Winata I, Indraswati N, Ismadji S. Waste capiz (Amusium cristatum) shell as a new heterogeneous catalyst for biodiesel production. Renew Energy 2013;50:795–9.
[115] Correia LM, Saboya RM, Campelo Nde S, Cecilia JA, Rodriguez-Castellon E, Cavalcante Jr CL, et al. Characterization of calcium oxide catalysts from natural sources and their application in the transesterification of sunflower oil. Bioresour Technol 2014;151:207–13.
[116] Rezaei R, Mohadesi M, Moradi GR. Optimization of biodiesel production using waste mussel shell catalyst. Fuel 2013;109:534–41.
[117] Kouzu M, Hidaka J-s. Purification to remove leached CaO catalyst from biodiesel with the help of cation-exchange resin. Fuel 2013;105:318–24.
[118] Calero J, Luna D, Sancho ED, Luna C, Bautista FM, Romero AA, et al. Development of a new biodiesel that integrates glycerol, by using CaO as heterogeneous catalyst, in the partial methanolysis of sunflower oil. Fuel 2014;122:94–102.
[119] Jeon H, Kim DJ, Kim SJ, Kim JH. Synthesis of mesoporous MgO catalyst templated by a PDMS–PEO comb-like copolymer for biodiesel production. Fuel Process Technol 2013;116:325–31.
[120] Almerindo GI, Probst LFD, Campos CEM, de Almeida RM, S.M.P. Meneghetti, Meneghetti MR, et al. Magnesium oxide prepared via metal–chitosan complexation method: application as catalyst for transesterification of soybean oil and catalyst deactivation studies. J Power Sources 2011;196:8057–63.
[121] Chen CL, Huang CC, Tran DT, Chang JS. Biodiesel synthesis via heterogeneous catalysis using modified strontium oxides as the catalysts. Bioresour Technol 2012;113:8–13.
[122] Viola E, Blasi A, Valerio V, Guidi I, Zimbardi F, Braccio G, et al. Biodiesel from fried vegetable oils via transesterification by heterogeneous catalysis. Catal Today 2012;179:185–90.
[123] Kaur M, Ali A. Lithium ion impregnated calcium oxide as nano catalyst for the biodiesel production from karanja and jatropha oils. Renew Energy 2011;36:2866–71.
[124] Tonetto GM, Marchetti JM. Transesterification of soybean oil over Me/Al_2O_3 (Me=Na, Ba, Ca, and K) catalysts and monolith K/Al_2O_3-cordierite. Top Catal 2010;53:755–62.
[125] Kazemian H, Turowec B, Siddiquee MN, Rohani S. Biodiesel production using cesium modified mesoporous ordered silica as heterogeneous base catalyst. Fuel 2013;103:719–24.
[126] Rubio-Caballero JM, Santamaría-González J, Mérida-Robles J, Moreno-Tost R, Alonso-Castillo ML, Vereda-Alonso E, et al. Calcium zincate derived heterogeneous catalyst for biodiesel production by ethanolysis. Fuel 2013;105:518–22.
[127] Santiago-Torres N, Romero-Ibarra IC, Pfeiffer H. Sodium zirconate (Na_2ZrO_3) as a catalyst in a soybean oil transesterification reaction for biodiesel production. Fuel Process Technol 2014;120:34–9.
[128] Rashtizadeh E, Farzaneh F, Talebpour Z. Synthesis and characterization of $Sr_3Al_2O_6$ nanocomposite as catalyst for biodiesel production. Bioresour Technol 2014;154:32–7.
[129] Meng YL, Tian SJ, Li SF, Wang BY, Zhang MH. Transesterification of rapeseed oil for biodiesel production in trickle-bed reactors packed with heterogeneous Ca/Al composite oxide-based alkaline catalyst. Bioresour Technol 2013;136:730–4.
[130] Soares Dias AP, Bernardo J, Felizardo P, Neiva Correia MJ. Biodiesel production over thermal activated cerium modified Mg–Al hydrotalcites. Energy 2012;41:344–53.
[131] Wang S-H, Wang Y-B, Dai Y-M, Jehng J-M. Preparation and characterization of hydrotalcite-like compounds containing transition metal as a solid base catalyst for the transesterification. Appl Catal A: Gen 2012;439–440:135–41.
[132] Li J, Fu Y-J, Qu X-J, Wang W, Luo M, Zhao C-J, et al. Biodiesel production from yellow horn (Xanthoceras sorbifolia Bunge.) seed oil using ion exchange resin as heterogeneous catalyst. Bioresour Technol 2012;108:112–8.
[133] Marchetti JM, Miguel VU, Errazu AF. Heterogeneous esterification of oil with high amount of free fatty acids. Fuel 2007;86:906–10.
[134] Marchetti JM, Errazu AF. Biodiesel production from acid oils and ethanol using a solid basic resin as catalyst. Biomass Bioenergy 2010;34:272–7.
[135] Melero JA, Bautista LF, Morales G, Iglesias J, Sánchez-Vázquez R. Biodiesel production from crude palm oil using sulfonic acid-modified mesostructured catalysts. Chem Eng J 2010;161:323–31.
[136] García-Sancho C, Moreno-Tost R, Mérida-Robles JM, Santamaría-González J, Jiménez-López A, Maireles-Torres P. Niobium-containing MCM-41 silica catalysts for biodiesel production. Appl Catal B: Environ 2011;108–109:161–7.
[137] Patel A, Brahmkhatri V, Singh N. Biodiesel production by esterification of free fatty acid over sulfated zirconia. Renew Energy 2013;51:227–33.
[138] Zhang Y, Wong W-T, Yung K-F. Biodiesel production via esterification of oleic acid catalyzed by chlorosulfonic acid modified zirconia. Appl Energy 2014;116:191–8.
[139] Jiménez-López A, Jiménez-Morales I, Santamaría-González J, Maireles-Torres P. Biodiesel production from sunflower oil by tungsten oxide supported on zirconium doped MCM-41 silica. J Mol Catal A: Chem 2011;335:205–9.
[140] Xie W, Yang D. Transesterification of soybean oil over WO_3 supported on $AlPO_4$ as a solid acid catalyst. Bioresour Technol 2012;119:60–5.
[141] Costa AA, Braga PRS, de Macedo JL, Dias JA, Dias SCL. Structural effects of WO_3 incorporation on USY zeolite and application to free fatty acids esterification. Microporous Mesoporous Mater. 2012;147:142–8.
[142] Borges LD, Moura NN, Costa AA, Braga PRS, Dias JA, Dias SCL, et al. Investigation of biodiesel production by HUSY and Ce/HUSY zeolites: influence of structural and acidity parameters. Appl Catal A: Gen 2013;450:114–9.
[143] Vieira SS, Magriotis ZM, Santos NA, Saczk AA, Hori CE, Arroyo PA. Biodiesel production by free fatty acid esterification using Lanthanum (La^{3+}) and HZSM-5 based catalysts. Bioresour Technol 2013;133:248–55.
[144] Domingues C, Correia MJ, Carvalho R, Henriques C, Bordado J, Dias AP. Vanadium phosphate catalysts for biodiesel production from acid industrial by-products. J Biotechnol 2013;164:433–40.
[145] Alhassan FH, Yunus R, Rashid U, Sirat K, Islam A, Lee HV, et al. Production of biodiesel from mixed waste vegetable oils using Ferric hydrogen sulphate as an effective reusable heterogeneous solid acid catalyst. Appl Catal A: Gen 2013;456:182–7.
[146] Narkhede N, Patel A. Biodiesel production by esterification of oleic acid and transesterification of Soybean oil using a new solid acid catalyst comprising 12-tungstosilicic acid and zeolite Hβ. Ind Eng Chem Res 2013;52:13637–44.
[147] Srilatha K, Sree R, Prabhavathi Devi BLA, Sai Prasad PS, Prasad RBN, Lingaiah N. Preparation of biodiesel from rice bran fatty acids catalyzed by heterogeneous cesium-exchanged 12-tungstophosphoric acids. Bioresour Technol 2012;116:53–7.
[148] Li Y, Zhang X-D, Sun L, Xu M, Zhou W-G, Liang X-H. Solid superacid catalyzed fatty acid methyl esters production from acid oil. Appl Energy 2010;87:2369–73.
[149] Guan D, Fan M, Wang J, Zhang Y, Liu Q, Jing X. Synthesis and properties of magnetic solid superacid: SO_4^{2-}/ZrO_2–B_2O_3–Fe_3O_4. Mater Chem Phys 2010;122:278–83.
[150] Dawodu FA, Ayodele O, Xin J, Zhang S, Yan D. Effective conversion of non-edible oil with high free fatty acid into biodiesel by sulphonated carbon catalyst. Appl Energy 2014;114:819–26.
[151] Poonjarernsilp C, Sano N, Tamon H. Hydrothermally sulfonated single-walled carbon nanohorns for use as solid catalysts in biodiesel production by esterification of palmitic acid. Appl Catal B: Environ 2014;147:726–32.
[152] Jiang Y, Lu J, Sun K, Ma L, Ding J. Esterification of oleic acid with ethanol catalyzed by sulfonated cation exchange resin: experimental and kinetic studies. Energy Convers Manag 2013;76:980–5.
[153] Feng Y, Zhang A, Li J, He B. A continuous process for biodiesel production in a fixed bed reactor packed with cation-exchange resin as heterogeneous catalyst. Bioresour Technol 2011;102:3607–9.

[154] Srilatha K, Prabhavathi Devi BL, Lingaiah N, Prasad RB, Sai Prasad PS. Biodiesel production from used cooking oil by two-step heterogeneous catalyzed process. Bioresour Technol 2012;119:306–11.
[155] Shibasaki-Kitakawa N, Kanagawa K, Nakashima K, Yonemoto T. Simultaneous production of high quality biodiesel and glycerin from Jatropha oil using ion-exchange resins as catalysts and adsorbent. Bioresour Technol 2013;142:732–6.
[156] Farooq M, Ramli A, Subbarao D. Biodiesel production from waste cooking oil using bifunctional heterogeneous solid catalysts. J Clean Prod 2013;59:131–40.
[157] Kondamudi N, Mohapatra SK, Misra M. Quintinite as a bifunctional heterogeneous catalyst for biodiesel synthesis. Appl Catal A: Gen 2011;393:36–43.
[158] Cerveró JM, Álvarez JR, Luque S. Novozym 435-catalyzed synthesis of fatty acid ethyl esters from soybean oil for biodiesel production. Biomass Bioenergy 2014;61:131–7.
[159] Ngo TP, Li A, Tiew KW, Li Z. Efficient transformation of grease to biodiesel using highly active and easily recyclable magnetic nanobiocatalyst aggregates. Bioresour Technol 2013;145:233–9.
[160] Chattopadhyay S, Sen R. Development of a novel integrated continuous reactor system for biocatalytic production of biodiesel. Bioresour Technol 2013;147:395–400.
[161] Soares D, Pinto AF, Gonçalves AG, Mitchell DA, Krieger N. Biodiesel production from soybean soapstock acid oil by hydrolysis in subcritical water followed by lipase-catalyzed esterification using a fermented solid in a packed-bed reactor. Biochem Eng J 2013;81:15–23.
[162] Jang MG, Kim DK, Park SC, Lee JS, Kim SW. Biodiesel production from crude canola oil by two-step enzymatic processes. Renew Energy 2012;42:99–104.
[163] Li Y, Du W, Liu D. Effect of phospholipids on free lipase-mediated methanolysis for biodiesel production. J Mol Catal B: Enzym 2013;91:67–71.
[164] Olivares-Carrillo P, Quesada-Medina J. Synthesis of biodiesel from soybean oil using supercritical methanol in a one-step catalyst-free process in batch reactor. J Supercrit Fluids 2011;58:378–84.
[165] Trentin CM, Lima AP, Alkimim IP, da Silva C, de Castilhos F, Mazutti MA, et al. Continuous production of soybean biodiesel with compressed ethanol in a microtube reactor using carbon dioxide as co-solvent. Fuel Process Technol 2011;92:952–8.
[166] Tsai Y-T, Lin H-m, Lee M-J. Biodiesel production with continuous supercritical process: non-catalytic transesterification and esterification with or without carbon dioxide. Bioresour Technol 2013;145:362–9.
[167] Jiang J-J, Tan C-S. Biodiesel production from coconut oil in supercritical methanol in the presence of cosolvent. J Taiwan Inst Chem Eng 2012;43:102–7.
[168] Santana A, Maçaira J, Larrayoz MA. Continuous production of biodiesel from vegetable oil using supercritical ethanol/carbon dioxide mixtures. Fuel Process Technol 2012;96:214–9.
[169] Shin H-Y, Ryu J-H, Bae S-Y, Kim YC. Biodiesel production from highly unsaturated feedstock via simultaneous transesterification and partial hydrogenation in supercritical methanol. J Supercrit Fluids 2013;82:251–5.
[170] Granados ML, Alba-Rubio AC, Vila F, Martín Alonso D, Mariscal R. Surface chemical promotion of Ca oxide catalysts in biodiesel production reaction by the addition of monoglycerides, diglycerides and glycerol. J Catal 2010;276:229–36.
[171] Zhu H, Wu Z, Chen Y, Zhang P, Duan S, Liu X, et al. Preparation of biodiesel catalyzed by solid super base of calcium oxide and its refining process. Chin J Catal 2006;27:391–6.
[172] Huang W, Tang S, Zhao H, Tian S. Activation of commercial CaO for biodiesel production from rapeseed oil using a novel deep eutectic solvent. Ind Eng Chem Res 2013;52:11943–7.
[173] Alba-Rubio AC, Santamaría-González J, Mérida-Robles JM, Moreno-Tost R, Martín-Alonso D, Jiménez-López A, et al. Heterogeneous transesterification processes by using CaO supported on zinc oxide as basic catalysts. Catal Today 2010;149:281–7.
[174] Xie W, Zhao L. Production of biodiesel by transesterification of soybean oil using calcium supported tin oxides as heterogeneous catalysts. Energy Convers Manag 2013;76:55–62.
[175] Zabeti M, W.M.A.W. Daud, Aroua MK. Biodiesel production using alumina-supported calcium oxide: an optimization study. Fuel Process Technol 2010;91:243–8.
[176] Lin L, Vittayapadung S, Li X, Jiang W, Shen X. Synthesis of magnetic calcium oxide hollow fiber catalyst for the production of biodiesel. Environ Prog Sustain Energy 201;32:1255–61.
[177] Shu Q, Nawaz Z, Gao J, Liao Y, Zhang Q, Wang D, et al. Synthesis of biodiesel from a model waste oil feedstock using a carbon-based solid acid catalyst: reaction and separation. Bioresour Technol 2010;101:5374–84.
[178] Shu Q, Gao J, Liao Y, Wang J. Reaction kinetics of biodiesel synthesis from waste oil using a carbon-based solid acid catalyst. Chin J Chem Eng 2011;19:163–8.
[179] Rao BVSK, Chandra Mouli K, Rambabu N, Dalai AK, Prasad RBN. Carbon-based solid acid catalyst from de-oiled canola meal for biodiesel production. Catal Commun 2011;14:20–6.
[180] Guo F, Xiu Z-L, Liang Z-X. Synthesis of biodiesel from acidified soybean soapstock using a lignin-derived carbonaceous catalyst. Appl Energy 2012;98:47–52.
[181] Fu X, Li D, Chen J, Zhang Y, Huang W, Zhu Y, et al. A microalgae residue based carbon solid acid catalyst for biodiesel production. Bioresour Technol 2013;146:767–70.
[182] Sulaiman S, Aziz ARA, Aroua MK. Reactive extraction of solid coconut aste to produce biodiesel. J Taiwan Inst Chem Eng 2013;44:233–8.
[183] Shuit SH, Lee KT, Kamaruddin AH, Yusup S. Reactive extraction and in situ esterification of Jatropha curcas L. seeds for the production of biodiesel. Fuel 2010;89:527–30.
[184] Jairurob P, Phalakornkule C, Na-udom A, Petiraksakul A. Reactive extraction of after-stripping sterilized palm fruit to biodiesel. Fuel 2013;107:282–9.
[185] Lim S, Lee KT. Process intensification for biodiesel production from Jatropha curcas L. seeds: supercritical reactive extraction process parameters study. Appl Energy 2013;103:712–20.

Paper II

CATALYSIS REVIEWS
2016, VOL. 58, NO. 2, 157–208
http://dx.doi.org/10.1080/01614940.2015.1103594

Taylor & Francis
Taylor & Francis Group

Innovation in solid heterogeneous catalysis for the generation of economically viable and ecofriendly biodiesel: A review

M. R. Avhad and J. M. Marchetti

Department of Mathematical Sciences and Technology, Norwegian University of Life Sciences, Drøbakveien, Norway

ABSTRACT

Among the possible options for the transformation of plant oils and animal fats to biodiesel, the alcoholysis process has been frequently selected. The rate of alcoholysis reaction is accelerated using a catalytic material. This article reviews different nature of catalysts utilized to assist the process of biodiesel production. The chemical properties of both homogeneous and heterogeneous catalysts enable their sub-division into acidic and basic materials. The proficiency of several heterogeneous catalytic systems and the possible route of alcoholysis reaction using different materials is systematically discussed. Furthermore, the factors influencing the performance of catalysts are also considered.

ARTICLE HISTORY
Received June 29 2015
Accepted October 1 2015

KEYWORDS
Acidic materials; alcoholysis; basic materials; biodiesel production; heterogenous catalysis; homogenous catalysis

1. Introduction

In recent decades, it has been consistently suspected that global warming, as a consequence of the greenhouse gas emissions, might lead to a serious climatic alterations, thus threatening human nature. The climate changes, induced to a significant extent due to the surplus utilization of fossil fuel, has hinted at a requirement for the development of environmental friendly and renewable energy resources (1, 2). Furthermore, fluctuating fossil fuel prices and growing hypotheses related to diminishing petroleum reserves have made today's necessity to establish the renewable energy prominence. Biofuels have aroused much attention in the green-tech revolution in parallel to energy demand and climate change around the world. However, it is important that biofuel must be technically feasible, economically benign, and readily available (3).

As a promising replacement of fossil diesel, biodiesel has gained broadening attention in recent years because of its renewable nature, negligible toxicity, and biodegradability (4, 5). Biodiesel does not contribute to the increase of net atmospheric carbon dioxide (CO_2) level as CO_2 produced

CONTACT J. M. Marchetti jorge.mario.marchetti@nmbu.no Department of Mathematical Sciences and Technology, Norwegian University of Life Sciences, Drøbakveien 31, Ås 1432, Norway

by the combustion of biodiesel could be recycled by the photosynthesis process, thus minimizing the impact of biodiesel combustion on the greenhouse effect (6). Furthermore, the presence of more than 10% oxygen in biodiesel would accelerate the rate of fuel combustion and minimize the production of pollutants, such as particulate matter, carbon monoxide (CO), and polycyclic aromatic hydrocarbons (7). It is also expected that the appropriate usage of biodiesel could be beneficial to that of petroleum diesel due to the fact that biodiesel is advantageous in representing higher flash point, ultra-low sulfur concentration, better lubricating efficacy, and superior cetane number (8, 9). The above-mentioned characteristics of biodiesel make it an excellent alternative to petroleum diesel and currently its usage in diesel engine is practiced in several nations. However, the prime drawback of usage of biodiesel is that the temperature within the engine cylinders is raised due to the enhanced fuel combustion. This amplified temperature stimulates the production of nitrogen oxide (NO_x) gas, which in comparison is higher than those produced from the conventional diesel fuel (10).

Biodiesel is the colloquial name for "fatty acid alkyl ester" (FAAE). According to the American Society for Testing and Materials (ASTM), biodiesel is defined as the monoalkyl esters derivative from lipid feedstocks, such as vegetable oils or animal fats (11, 12). Among the different possible routes for biodiesel synthesis, the most commonly studied methodology is the catalyst-assisted alcoholysis reaction of lipid feedstocks, which is also known as transesterification of triacylglycerols (TAGs) and esterification of free fatty acids (FFA). The transesterification reaction has been gaining ever-increasing scientific attention not only in the biodiesel industries but also in the polymer industries (13, 14), paint industries, detergent industries (15), and pharmaceutical industries for the generation of intermediates (16). The general schematic representation for the transesterification reaction and the esterification reaction are shown in Figs. 1 and 2, respectively.

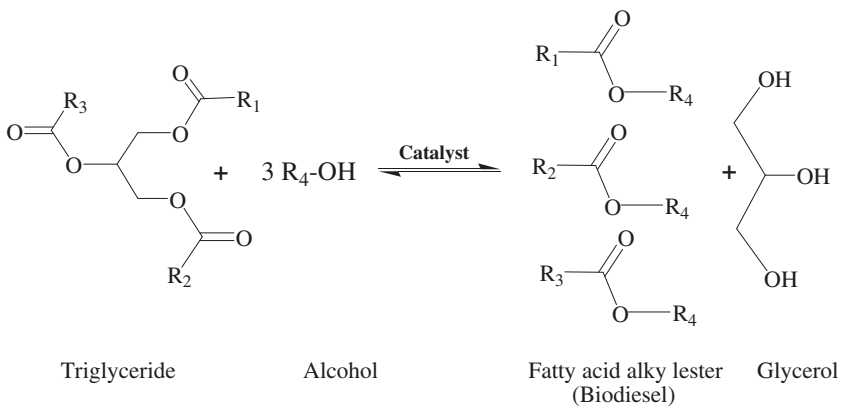

Figure 1. General transesterification reaction of vegetable oils.

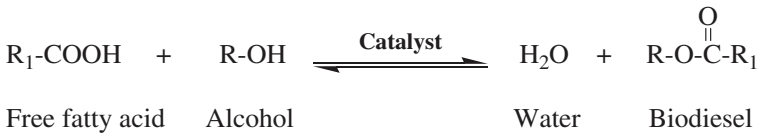

Figure 2. Esterification reaction of free fatty acid.

The typical transesterification reaction includes catalyzed chemical reaction between TAGs and a short-chain alcohol. The TAGs contain three long chain fatty acids attached to a glycerol structure. When the TAG reacts with an alcohol, the fatty acid chains are released from the glycerol skeleton to interact with the alcohol to produce biodiesel and the byproduct, glcyerol. This process, catalyzed by either bases or acids, consists of three sequential reversible reactions. In the reaction sequence, TAGs is converted stepwise to diacylglycerols (DAGs), monoacylglycerols (MAGs), and finally glycerol accompanied with the generation of esters during each step. The step-wise transesterification process can be seen in Fig. 3 (12, 17).

The main concern restricting the constructive commercialization and wide-spread usage of biodiesel is related to its higher capital cost than that of petroleum diesel. Even more, over 70% of the operational cost of the

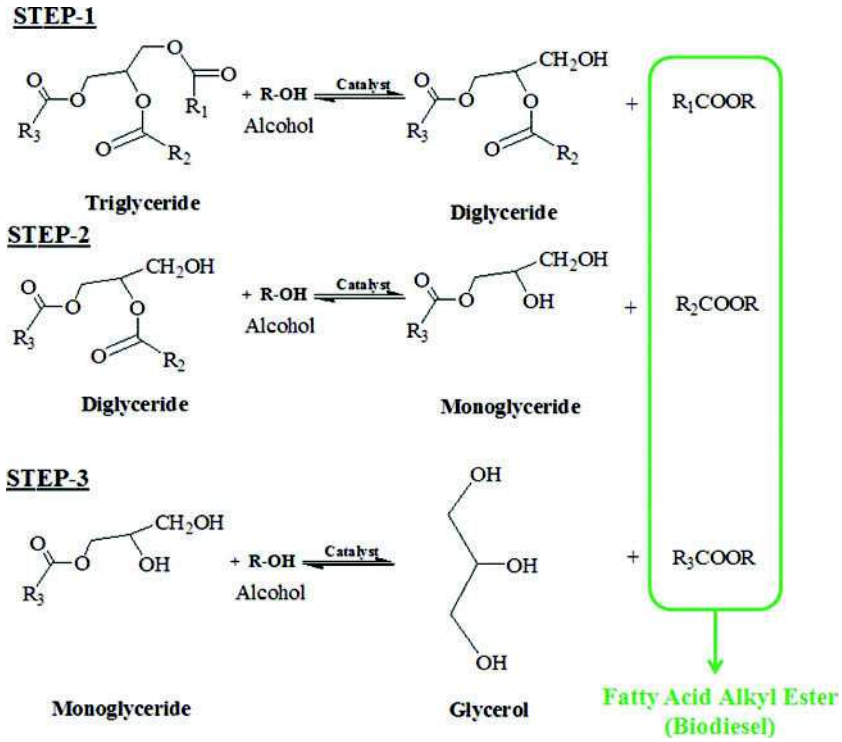

Figure 3. Stepwise transesterification reaction of vegetable oils.

biodiesel industry is related to the cost of the oil (raw material) and therefore new approaches and technologies that use waste or less refined vegetable oil are under consideration and study (4, 11). The limited use of biodiesel mostly could be due to three prime factors: (i) use of high-quality food-grade oils, (ii) multiple-step processing technology (18, 19), and (iii) use of expensive catalytic systems. In an standpoint to reduce the use of refined edible oils, the capability of non-edible oils, waste frying oil, animal fats, and industrial waste oil to produce biodiesel has been under continuous scientific investigation (20, 21). Furthermore, the multiple-step processing stages can possibly be simplified using the recently introduced reactive distillation technology (22), reactive extraction technology (23), and non-catalytic supercritical technology (24). Likewise, it is also of foremost importance to consider the monetary investment directed toward making available an appropriate catalyst system necessary to accelerate the biodiesel production process. From an economic point of view, an ideal catalyst for biodiesel production should not only represent superior activity and selectivity for the alcoholysis process but also be relatively abundant, less-expensive, durable, reusable, and easy-to-separate from the post reaction mixture. The prominent goal of producing less expensive biodiesel could be achieved by reducing the catalyst dose, lowering the reaction temperature on an energy input consideration, and using the lowest possible alcohol amount induced with the technical feasibility and safety considerations. Furthermore, the highest possible biodiesel yield must be achieved in a shortest reaction time for better productivity and lower overall energy requirement of the process.

There is a continuous growth in research efforts around the globe to find an uncomplicated method to derive active and stable catalytic materials for biodiesel production. The present article is focused on reviewing several forms of basic and acidic materials applied to accelerate the biodiesel production process. The different reaction pathway reported for different nature of homogeneous and heterogeneous catalysts were also systematically studied. Furthermore, the factors affecting the physico-chemical properties of catalyst, and consequently the biodiesel yield were also discussed.

2. Homogeneous catalysis for biodiesel production

The main advantage related to the usage of homogeneous catalysts is it reduces the mass transfer resistance concerns, which consequently leads to better reaction efficiency. The homogeneous catalysts utilized for the alcoholysis reactions are either basic or acidic in nature. On a commercial platform, homogeneous base catalysts are more commonly employed to assist the biodiesel production process. This is because the base-catalyzed transesterification reaction progresses faster than the acid-catalyzed one; consequently, the superior biodiesel yield could be obtained using relatively mild reaction

conditions. However, the selection of an appropriate catalyst is heavily reliant on the FFA and moisture concentration in the feedstock.

The most commonly known homogeneous base catalysts are hydroxides and alkoxides of alkali metals, such as sodium hydroxide (NaOH), potassium hydroxide (KOH), sodium methoxide (CH_3ONa), potassium methoxide (KCH_3O), and sodium ethoxide (C_2H_5ONa) (25, 26), as these catalysts are soluble in polar reactants. However, KOH and NaOH catalyst is frequently utilized for the industrial production of biodiesel due to several reasons, such as (i) low cost and easy availability, (ii) ability to catalyze transesterification reaction at relative low operative temperature, and (iii) high biodiesel yield could be obtained in short reaction time. Uzun et al. (26) reported that the reaction temperature of 50°C and time of 30 min was sufficient to achieve 96% biodiesel yield when NaOH was used to catalyze transesterification reaction between waste frying oil and methanol. Keera et al. (27) reported approximately 97% biodiesel yield after 60 min of reaction when NaOH was used to transesterify cottonseed oil with methanol, using reaction temperature of 60°C, methanol-to-oil molar ratio of 6:1, and 1 wt. % catalyst dose. Fadhil et al. (28) reported a study in which KOH-catalyzed transesterification of Heckel fish oil resulted in 96 % biodiesel yield after 60 min of reaction performed at 32°C, using methanol-to-oil molar ratio of 6:1, and 5.5 wt. % catalyst amount.

The precise reaction mechanism for homogeneous base-catalyzed transesterification reaction is yet not completely clarified. It is supposed that during the alcoholysis process, the reaction would proceed either in a biphasic reaction medium comprised of oil and an alcohol phase in which the catalyst is dissolved or in a monophasic medium depending heavily on the operative reaction variables, such as catalyst concentration, alcohol-to-oil molar ratio, and reaction temperature. Nevertheless, the general transesterification reaction pathway in the presence of homogeneous base catalyst could be explained as follows. In the initial step of the base-catalyzed alcoholysis reaction, the homogeneous base catalyst (KOH or NaOH) is dissolved in alcohol resulting in the formation of an alkoxide and a protonated catalyst. The strong nucleophile, i.e., the alkoxide species then attacks the carbonyl group of TAGs leading towards the formation of tetrahedral intermediate, from which after the rearrangement reaction the alkyl esters and the corresponding anion of DAGs are formed. The DAGs and MAGs are then transformed by the same mechanism into a mixture of alkyl esters and glycerol. After the satisfactory completion of reaction, the post-reaction mixture includes two liquid phases: FAAE and crude glycerol (29, 30). The plausible schematic representation for the reaction mechanism for the homogeneous base-catalyzed transesterification reaction is shown in Fig. 4.

It is important to note that these basic homogeneous catalysts face a variety of technical hurdles that limit their use for biodiesel production.

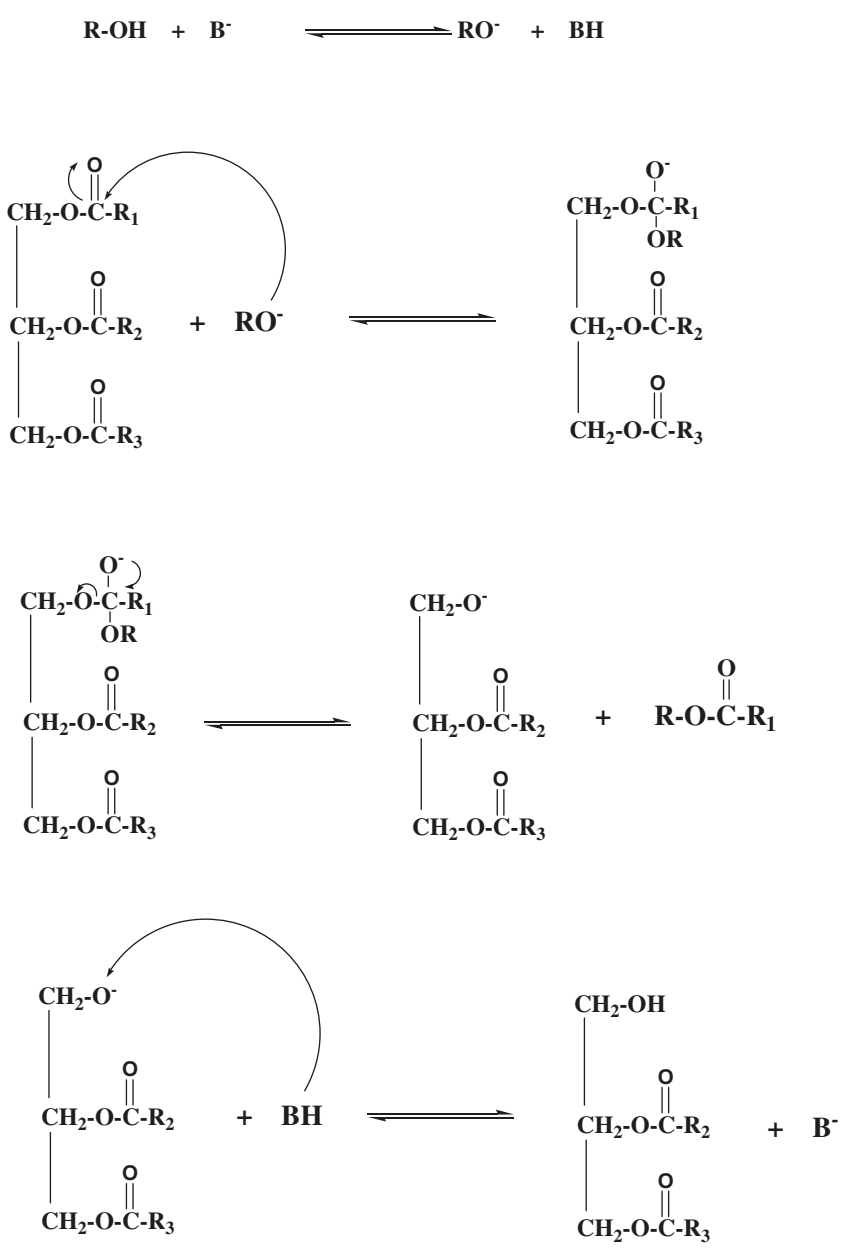

Figure 4. Plausible reaction mechanism for homogeneous base-catalyzed transesterification reaction.

For instance, the usage of such catalysts is restricted only for refined oils (containing less than 0.5 wt. % FFA or acid value less than 1 mg KOH g^{-1}) and under anhydrous conditions. The low-cost feedstocks containing a high concentration of FFA and moisture was found to cause a detrimental effect on the catalytic performance of homogeneous base catalysts. The base catalysts are not suitable for such raw materials because of the occurrence of

Figure 5. Saponification reaction of free fatty acid.

inevitable saponification reaction between the catalyst and FFA. The generation of soap could promote the formation of stable emulsions that prevent the separation of FAAE from glycerol; consequently, less biodiesel yield is obtained. Hence, the catalyst is consumed and additional expensive separation and purification equipment are required to achieve the final biodiesel product. The reaction of FFA with base catalyst leading toward the formation of soap is shown in Fig. 5. Furthermore, the presence of moisture in the reaction medium would hydrolyze the formed alkyl esters; thus minimizing the biodiesel yield.

The use of acid catalysts could be a possible option to solve the above-mentioned drawbacks associated with the usage of low-grade raw materials for biodiesel production. Although acid-catalyzed transesterification reaction is said to be about 4000 times slower than the homogeneous base-catalyzed ones, it is worth understanding that the performance of these catalysts is not strongly affected by the presence of FFA in feedstocks. Furthermore, acid catalysts can simultaneously assist both transesterification and esterification reaction of TAGs and FFA, respectively. Hence, acid catalysts are expected to be successfully practiced for the synthesis of biodiesel from a low-grade feedstocks, such as waste cooking oil, industrial waste oils, animal fats, wax, and grease. However, the requirement of severe reaction operative conditions (high reaction temperature, prolonged reaction time, and high alcohol amount) to promote the reaction rate and biodiesel yield in the case of acid-catalyzed alcoholysis reactions have been a major reason of concern for its upscaling on an industrial platform. Furthermore, the use of these non-green acid catalysts might also leads towards complicated and costly neutralization steps, and give rise to human safety and corrosion of equipment related concerns.

The leading homogeneous acid catalysts used for the alcoholysis process are sulfuric acid (H_2SO_4) and hydrochloric acid (HCl), while other homogeneous acid catalysts tested for the alcoholysis reaction include nitric acid (HNO_3), aluminium chloride ($AlCl_3$), phosphoric acid (H_3PO_4), and organic sulfonic acid. Marchetti et al. (31) reported 96% conversion of model oil, prepared using oleic acid and sunflower oil, when esterified at 55°C in the presence of H_2SO_4 catalyst, using ethanol-to-oil molar ratio of 6.126:1, and catalyst amount of 2.26 wt. %; but the time span of 240 min was needed to achieve the satisfactory completion of the reaction. Soriano et al. (32) reported that it took 1080 min to obtain 98% conversion of canola oil

when subjected to the methanolysis reaction at 110°C using Lewis acid $AlCl_3$ catalyst, even in the presence of co-solvent (THF : Methanol=1:1) and 5 wt. % catalyst amount.

The schematic representation for the plausible acid-catalyzed transesterification reaction mechanism is shown in Fig. 6. In the initial stage of reaction, the protonation of the acid carbonyl group is occurred to give an oxonium ion which increases electrophilicity of the adjoining carbon atom making it more susceptible to the nucleophilic attack. This then undergoes the exchange reaction with an alcohol to give an intermediate. The

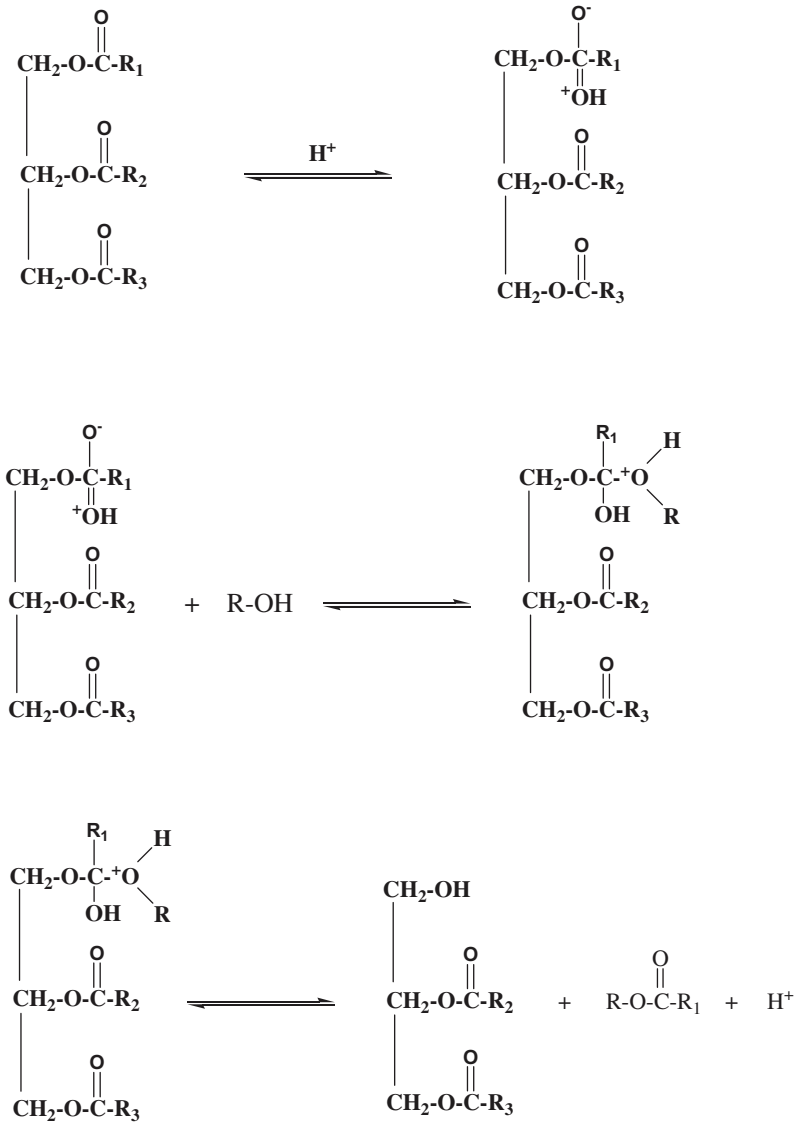

Figure 6. Plausible reaction mechanism for homogeneous acid-catalyzed transesterification reaction.

intermediate product then releases a proton to become esters. In the case of transesterification reaction, the same above sequential steps could be extended to di- and mono-acyl glycerol as well, resultantly, leading toward the formation of esters in each step. The prime reason responsible for the variation in the activity of different catalysts could be the formation of a more electrophilic species in acid catalysts and nucleophilic species in base catalysts (33, 34).

3. Heterogeneous catalysis for biodiesel production

The technical problems related to the utilization of homogeneous catalysts for biodiesel production is expected to be minimized by its replacement with the heterogeneous catalytic system. Over the last few years, heterogeneous catalysts have gained enormous scientific as well as industrial consideration due to their advantage on both economic and environmental standpoints. A successful application of heterogeneous catalyst is expected to quench multiple separation and purification steps, and decrease the amount of post-treatment waste water and other contaminants, thus enabling the process intensification via recyclability of catalyst, downsizing the processing equipment, and empowering a continuous biodiesel production (35, 36). The process intensification of biodiesel production by heterogenizing the reaction step is expected to improve the economics of the process only if the catalyst is neither consumed nor dissolved in the reaction medium, which in return would facilitate its separation from the post-reaction mixture. The catalyst can then be separated from the post-reaction mixture via physical methods, such as filtration and centrifugation. This in return will enable the re-utilization of the catalytic materials. Moreover, the concentration of metals or other elements arising from the catalyst in the obtained biodiesel, or glycerol, could be notably reduced when heterogeneous catalysts are utilized.

However, the prime drawback of the heterogeneous catalyst systems is their limited catalytic active centers in comparison to their homogeneous counterparts and, in general, they require more severe reaction conditions to reach oil conversion similar to that obtained by the homogenous-catalyzed processes (37). Also, the mass transfer resistance concern associated with the use heterogeneous catalyst due to the presence of three phases (oil/alcohol/catalyst) in the reaction mixture could be allied to the slower reaction rate for the transformation of lipid feedstock to biodiesel (38). It is also worth noting that the complicated and time-consuming synthesis procedure, and high price of materials required for the synthesis of heterogeneous catalysts, could also add to the total cost of the process, hence, making biodiesel more expensive. Furthermore, the poisoning of the active centers of catalysts when exposed to the surrounding atmospheric medium could also affect the stability and activity of catalysts; therefore, the detail information related to

the physical and chemical properties of solid materials become mandatory. A huge amount of scientific efforts are engaged in innovating a stable and active heterogeneous catalytic system for biodiesel production. The literature already contains a wide range of examples in this sense.

3.1. *Heterogeneous base catalysis for biodiesel production*

A great variety of basic materials have been utilized as a heterogeneous catalyst to assist the alcoholysis process, such as: (i) single alkaline earth metal oxides, (ii) supported alkali metal and alkaline earth metal oxides, (iii) mixed metal oxides, (iv) hydrotalcites, and (v) anionic ion-exchange resins, which are discussed below.

3.1.1. *Solid single alkaline earth metal oxides*

Solid base catalysts, such as alkaline earth metal oxides, are practiced to assist transesterification reaction due to their moderate basic strength. The basic strength of group II oxides and hydroxides is promoted with the increase in atomic number, i.e., from Magnesium (Mg) to Barium (Ba), which significantly affect their catalytic capability to transesterify lipid feedstocks (39). The origin of basic sites in the alkaline earth metal oxides could be attributed to the presence of the M^{2+}–O^{2-} ion pair and surface hydroxyl groups in different co-ordination environments (40). The amount of the surface oxygen could be affected by the surface compositions of the solid catalyst and the calcination temperature. Besides, the specific surface area, basicity, degree of leaching in the reaction medium, and selectivity toward the transesterification reaction products must also be considered as contributing factors for the selection of an appropriate catalysts for biodiesel production.

The plausible reaction mechanism for the alkaline earth metal oxide catalyst-assisted alcoholysis reaction could be discussed as follow. The catalytic alcoholysis reaction takes place on the surface of solid base catalyst and is explained in four steps: (i) alcohol and fatty acid are adsorbed onto the two neighboring available active centers, respectively; (ii) the two adsorbed groups react leading toward the formation of surface intermediates, which then further decompose in step (iii); and finally, the formed product then gets detached from the catalytic surface in step (iv). For catalysts having higher basicity, such as Strontium oxide (SrO) and Barium oxide (BaO), the surface reaction step becomes the rate determining step. While in the case of MgO catalyst, methanol adsorption was assumed to be the rate determining step of the mechanism (41). The schematic representation for the alkaline metal oxide-catalyzed alcoholysis reaction is shown in Fig. 7.

3.1.1.1. ***Calcium oxide (CaO) catalysis.*** Among the alkaline earth metal oxides, calcium oxide (CaO) is one of the well-researched heterogeneous

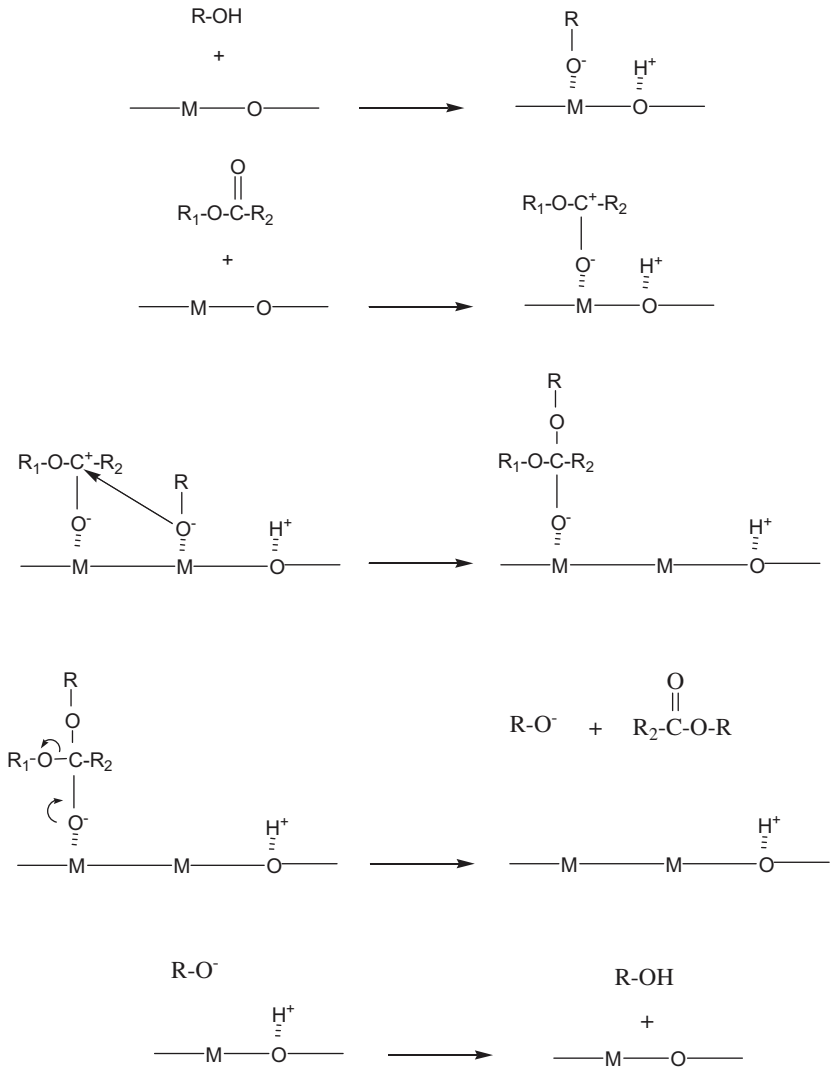

Figure 7. Plausible reaction mechanism for heterogeneous base-catalyzed transesterification reaction.

catalysts as it possesses high basicity, low solubility, low cost, and is easy to handle. Another reason for its popularity is the abundance of natural resources of calcium (Ca). Besides economic advantages, the performance of CaO as a catalyst for biodiesel production could also be comparable to homogeneous catalysts. Kawashima et al. (42) reported 90% biodiesel yield when transesterification reaction between rapeseed oil and methanol was performed at 60°C for 180 min, using 0.1 g CaO amount. It was reported that activating CaO with methanol prior to the reaction improved the transesterification reaction rate. The activation process performed at 25°C for 90 min enabled the formation of calcium methoxide ($Ca(OCH_3)_2$) which

then acted as an initiating agent and accelerated the reaction rate. It was mentioned that the small amount of CaO reacted with methanol leading towards the formation of $Ca(OCH_3)_2$, and the subsequent water generated reacted with CaO and resulted in the generation of calcium hydroxide ($Ca(OH)_2$) (42). Kouzu et al. (43) reported that during transesterification reaction between soybean oil and methanol, CaO catalyst present in the reaction medium reacted with the generating glycerol and, consequently, was converted to the calcium diglyceroxide. It was said that the collected catalyst containing calcium diglyceroxide although had lower basicity than the fresh one and displayed low biodiesel yield, no further change in its chemical properties were noticed. The similar catalytic activity for the collected catalyst and the fresh calcium diglyceroxide material confirmed that CaO was transformed to calcium diglyceroxide during transesterification reaction.

It is reported that in the initial stage of the CaO-catalyzed transesterification reaction, the role of CaO is to abstract the proton from alcohol and allow the generated nucleophile, i.e., calcium alkoxide, to attack the carbonyl carbon in a molecule of TAGs. The generating glycerol during the reaction then reacts with the remaining CaO, which consequently results in the formation of CaO-glycerin complex. Also, the two neighboring hydroxyl groups comprised in the calcium diglyceroxide adsorb alcohol due to the attractive intermolecular force causing hydrogen bond, thus promoting the catalytic activity for the transesterification reaction (43–45). The schematic representation for the proposed reaction mechanism for CaO-assisted alcoholysis reaction is shown in Fig. 8.

The CaO material, when exposed to the surrounding carbon dioxide (CO_2) and water (H_2O), lead toward the formation of a layer of calcium carbonate ($CaCO_3$) and $Ca(OH)_2$, respectively, on the catalytic surface. This poisoning effect alters and blocks the active catalytic sites; hence, resulting in lowering of biodiesel yield. Granados et al. (46) reported that CaO catalyst can be protected from poisoning when initially calcined at 800°C for 60 min and then pretreated with biodiesel (3 wt. % w.r.t. oil) at 60°C. This pretreatment process was reported to prevent the diffusion of CO_2 and H_2O into the catalyst surface, and maintain the activity of CaO catalyst. Also, the addition of small amount of biodiesel was said to promote the methanolysis reaction rate. However, it was not biodiesel, but MAGs and DAGs in the added biodiesel which were responsible for the enhancement in the FAME yield. The formed glycerol during the methanolysis reaction then reacted with the surface CaO leading towards the formation of active calcium glyceroxide species which are responsible for the increment of the alcoholysis reaction rate (47). Huang et al. (48) reported that the addition of deep eutectic solvents (DES), containing choline and glycerol (1:2 molar ratio), into the reaction mixture could play same role in activating CaO catalyst as thermal treatment at high temperature. It was proposed that due to the special

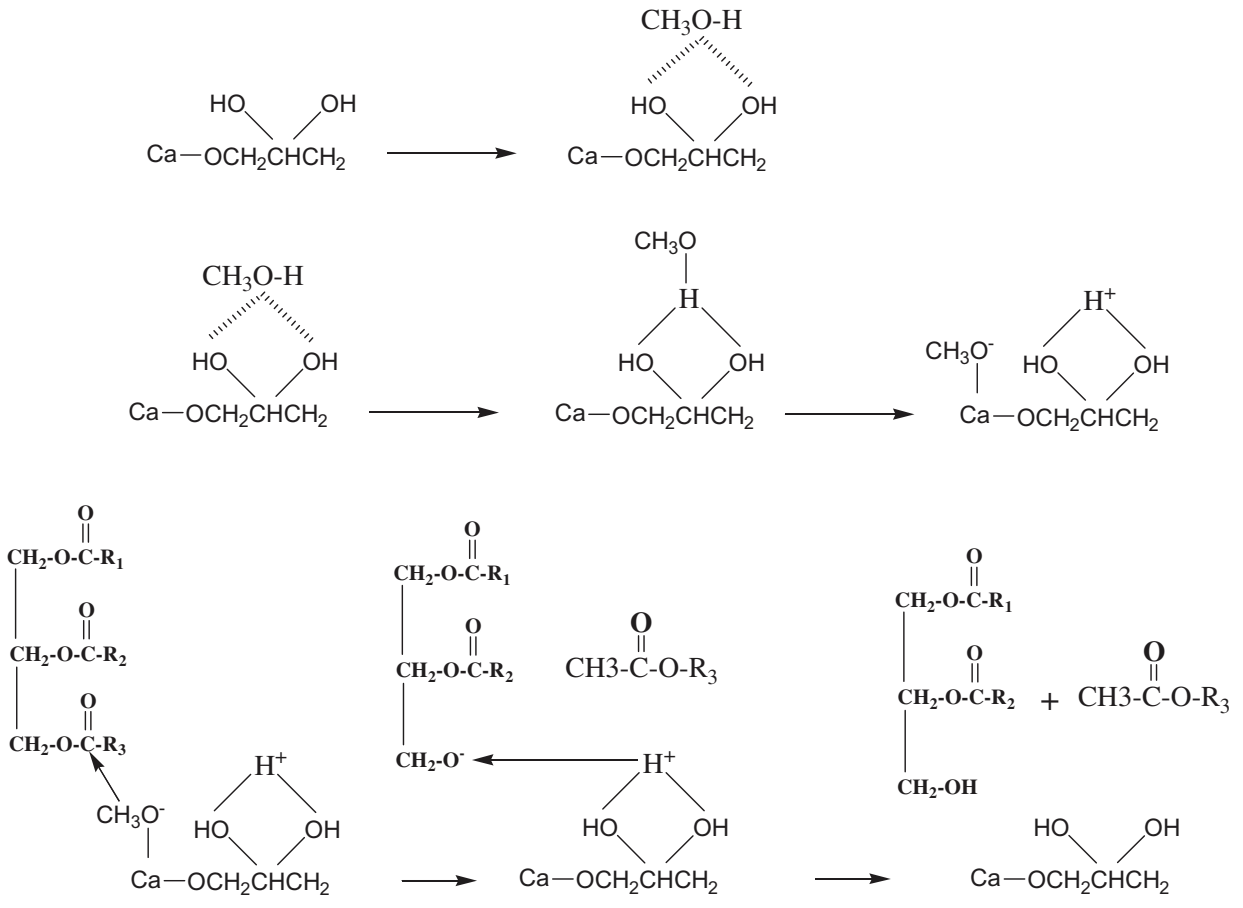

Figure 8. Plausible reaction mechanism for CaO-catalyzed transesterification reaction.

solvation properties for metal oxides, the addition of DES/methanol mixture resulted in the liberation of $CaCO_3$ and $Ca(OH)_2$ species; thus, directing towards the formation of only CaO surface species. The biodiesel yield of 91.9% was reported after 180 min of transesterification reaction between rapeseed oil and methanol. The methanolysis reaction was performed at 65°C in the presence of DES activated CaO catalyst using DES dosage of 10.74 wt. % (w.r.t. oil), methanol-to-oil molar ratio of 14.28:1, and 8.07 wt. % catalyst amount. Zhu et al. (49) reported that rinsing CaO in ammonium carbonate solution followed by the calcination process at 900°C promoted its basic strength higher than 26.5. It was documented that the reaction temperature of 70°C, catalyst amount of 1.5 wt. %, and methanol-to-oil molar ratio of 9:1 was sufficient to obtain 93% jatropha oil conversion after 150 min of methanolysis reaction. Lin et al. (50) reported a study focused on the synthesis and appliance of magnetic CaO hollow fibers modified with α-Fe catalyst for transesterification of rapeseed oil. The organic gel-precursor transformation process-assisted catalyst represented micro-structured hollow fibers structure associated with large pores which promoted the transportation of reaction molecules, thus enhancing the catalytic activity. While the magnetic behavior of this catalyst enabled its easy separation from the post-reaction mixture via imposed magnetic field. The Ca^{2+}:Fe^{3+} ratio of 1:2 was used for the successful synthesis of magnetic spun fibers which were then thermally treated in a reduced atmospheric condition to synthesize the fibers with the average fiber length of more than 10 cm and diameter of 1.5 μm. The reported results indicated that the biodiesel yield of 95.7% was obtained after 120 min of transesterification reaction between rapeseed oil and methanol performed at 60°C, using methanol-to-oil molar ratio of 12:1, and 5 wt. % catalyst amount. Dermirbas (51) reported that under the supercritical reaction conditions, merely 0.3 wt. % CaO catalyst dose and reaction time of 6 min was required for the complete transformation of sunflower oil to biodiesel. However, the need for elevated energy input (temperature of 252°C) and high methanol-to-oil molar ratio of 41:1 should not be neglected.

In a viewpoint to minimize the complication related to the catalyst synthesis and reduce the cost of required materials, the derivatization of CaO catalysts from abundantly available natural resources is considered as a viable possibility. Furthermore, non-toxicity, easy availability, and moderate basicity make them potential candidate for synthesizing CaO catalyst. The natural resources, such as crab shells (52), egg shells (52, 53), capiz shells (45), snail shells (54), oyster shells (55), mussel shells (56), among others, are inactive in the available form, but after annealing were found to be highly active for transesterification reaction. The appropriate utilization of these considerable waste shells for the synthesis of CaO catalyst is expected to decrease the entire dependency on limestone rocks which are non-renewable sources of $CaCO_3$. The $CaCO_3$ content in crab shells is 72.0%, and is 97.1%

in egg shells. This shells, when thermally treated at 900°C for 120 min, resulted in the formation of CaO catalyst. The subsequent catalysts were reported to show adequate activity to assist transesterification reaction between sunflower oil and methanol, displaying 83.1% and 97.75% biodiesel yield using thermally treated crab and egg shells, respectively. The higher activity of calcined egg shells for transesterification was due the difference in Ca content in the precursor (52). Navajas et al. (53) used CaO catalyst synthesized from the industrial waste egg shells to transesterify the esterified used cooking oil. The Ca content in the two types of tested egg shells was higher than 98%. After 300 min of transesterification reaction performed at 60°C using methanol-to-oil molar ratio of 24:1 and 4 wt. % catalyst amount, 100% esters yield was reported. Furthermore, it was also said that not only the chemical composition but also the surface morphology of the calcined catalyst has significantly affected its performance and the final biodiesel yield. The dissimilar morphology of the two catalysts was said to be because of the difference in the mechanical properties of the precursor, i.e., the eggshells (53). Nakatani et al. (55) reported that when oyster shells were calcined at 700°C for 180 min, the product catalyst represents similar XRD pattern as that of commercial CaO material. Rezaei et al. (56) used a CaO catalyst synthesized from the waste mussel shells and reported that the re-calcination process of the collected catalyst had a negative impact on the reusability study, and thus on the biodiesel yield and purity. The collected catalyst were differentiated in two categories where one was used without calcination for the reusability test, while other was calcined at 1050°C after every reaction cycle. In the first cycle, the biodiesel yield of 94.1% with 100% purity was reported. It was mentioned that in the case of re-calcination, after five reaction cycles, the biodiesel yield was dropped to 73.67% and purity to 37. 13%. While, in the case of uncalcination, the biodiesel yield and purity of 85.22% and 59.10%, respectively, was obtained after five reaction cycles. The lowering in the catalyst activity in the case of re-calcination was assumed to be due to the reduction in the specific surface area of the material. The XRF analysis revealed that the Ca content in the fresh mussel shells was 97.77% which then dropped to 38.94% after fifth re-calcination process. Futhermore, it was also suspected that calcium is extracted by methanol during the process. Thus, mussel shells catalyst were reported to be reusable only if not calcined after every reaction cycle.

3.1.1.2. ***Magnesium oxide (MgO) catalysis.*** The magnesium oxide (MgO) though does not possess strong basic sites as CaO, but is stable under ambient conditions and is easy to handle. Di Serio et al. (57) reported that 0.1 g of MgO catalyst was sufficient to achieve 75% biodiesel yield when transesterification reaction between soybean oil and methanol was performed at 180°C. This catalyst was found to also catalyze esterification reaction

between oleic acid and methanol; however, leaching of MgO into the reaction medium was observed. Dossin et al. (58) reported a study focused on the MgO-catalyzed transesterification of ethyl acetate with methanol. The transesterification reaction was accomplished between methanol adsorbed on an MgO free basic sites and ethyl acetate from the liquid phase. A kinetic model was developed based on a three elementary steps Eley-Rideal mechanism type which fits the obtained experimental values. The proposed reaction rate expression was presented based on the assumption that methanol adsorption is the rate determining step, while the surface reaction as well as the adsorption of produced alcohol is quasi-equilibrated.

In a viewpoint to improve the catalytic activity and the stability of MgO catalyst, several studies have been reported on tailoring its textural properties and altering the surface atomic arrangements. The modification in the surface morphology is expected to change the chemical and physical properties of the consequential catalyst, and promote their capability to assist the alcoholysis process. Almerindo et al. (59) synthesized and tested metal-chitosan complexation method-assisted MgO catalyst for transesterification of sunflower oil with ethanol. It was reported that the addition of the biopolymer to the magnesium precursor resulted in the generation of pores and contributed in the expansion of surface porosity. The newly proposed MgO catalyst was reported to possess higher surface area (3.8 times higher) and pore volume than that of commercially available MgO material. The amine groups of chitosan were mentioned to be the main effective bonding sites for the metallic ions, thus resulting in the complexes stabilized by coordination. The nitrogen electrons present in amine and N-acetylamine groups established the coordinate covalent bonds with metal ions and some hydroxyl groups present in chitosan acted as a donor. During the calcination process, the volatile materials were evaporated and the cavities were produced. Also, the rearrangement of solid material takes place, thus forming a crystalline matrix. The biodiesel yield of 75% was reported after 180 min of transesterification reaction performed at 150°C, using ethanol-oil-catalyst molar ratio of 600:100:5. However, the synthesized catalyst was found to be deactivating due to the formation of hydrogenocarbonates on the active catalytic sites when exposed to the surrounding CO_2 and H_2O; thus, resulting in lowering of the catalytic activity. However, the poisoning of the proposed MgO material was reported to be slower than that of commercial MgO, which was related to the presence of moderate Brønsted sites in the proposed catalyst. Verziu et al. (60) reported a study focused on the synthesis of three nano-scale MgO catalysts with different morphologies: (i) sol-gel method assisted MgO nano-sheets (111), (ii) chemical vapor deposition leading to cubic MgO nanoparticles (110), and (iii) aerogel prepared MgO catalysts consisting of interconnected network of cubic particles (100), and its appliance for transesterification of sunflower oil and rapeseed oil in an autoclave,

microwave, and ultrasounds conditions. The MgO (iii) catalyst displayed high specific surface area among other, followed by MgO (i) and MgO (ii). However, MgO (i) consisted of a higher number of basic active sites than other counterparts. Furthermore, the facet was said to have important influence on the catalyst activity. The MgO (i) catalyst with (111) facet was found to be highly active. The (111) lattice plane of the catalyst indicated the presence of alternating monolayers of anions and cations, hence, a strong electrostatic field perpendicular to the (111) surface is created. The superior activity of MgO nano-sheets were attributed to the novel crystalline structure. Furthermore, the maximum conversion of lipid feedstock and the selectivity toward esters was observed using the microwave assisted methodology. Also, it was investigated that not the microwave system, but the ultrasound conditions directed the leaching of all three catalysts in to the reaction mixture. Montero et al. (61) reported the appliance of MgO nanoparticle for transesterification reaction between tributyrin and methanol. The in-situ spectroscopic and microscopic methodologies used to investigate the thermal evolution of strong base sites in MgO particles indicated that the prepared material consisted mixture of MgO and a residual metastable magnesium hydroxymethoxide. The thermal annealing enabled the formation of low coordination defect sites and resulted in the transformation of amorphous species to large cuboidal nanoparticles, while the atomic arrangement of the surface changed from (100) to (111) or (110). The thermal treatment of the catalyst, containing physisorbed water and surface carbonate, above 300°C resulted in the decomposition of the residual precursor and surface carbonate; however, the carbonate multi-layer formed on the magnesium carbonate was said to persist up to 700°C. The persistence of surface carbon even at 700°C is indicative of stable carbonaceous/carbonate residues. However, the calcination even at 300°C gave rise to weak basic sites and the high temperature treatment (500°C and above) was reported to increase the density of basic sites (10–20% at 700°C) and the fraction of O-/O^{2-} species. The increase in the strong basic site density was considered to be responsible for the enhanced catalytic performance of the calcined catalyst. The surface composition and electronic properties determined from XPS analysis reveal that the thermal treatment does not affect the overall Mg content, but changes only the form of the material.

Jeon et al. (62) reported the synthesis of sol-gel process assisted mesoporous MgO catalyst using a magnesium nitrate hexahydrate precursor, and a amphiphilic comb-like copolymer poly(dimethylsiloxane-ethylene oxide) which acted as an structure-directing agent. It was stated that the morphology of PDMS-PEO was reliant on the interaction and solubility between the polymer and the casting solvent, where terahydrofuran (THF) was considered to be better solvent than chloroform, toluene, and water. It was mentioned that in the aqueous solution the interfacial energy between PDMS

chains and water is augmented, thus resulting in reduced swelling of PDMS chains and increased the stretching of PEO chains. Hence, PDMS chains aggregated to form micelle cores, whereas PEO chains formed coronas outside the cores. As the hydrophilic magnesium nitrate preferentially incorporates into the hydrophilic PEO domains, due to the favorable interactions, the PDMS domains generated nanopores. It was further mentioned that the PDMS-PEO comb-like copolymer played important role in directing the structure and reducing the particle aggregation during the hydrothermal and the calcination steps. Also, the comb-like graft copolymer is more attractive than a block copolymer due to its low cost and the ease with which it can be synthesized. The co-polymer, attached with the magnesium precursor, started degrading between 250–350°C and was able to liberate completely at 500°C, leading toward the formation of high specific surface area mesoporous MgO catalyst. The SEM analysis revealed the formation of bimodal pore in the material, i.e., mesopores 10–200 nm and macropores 1–4 μm. It was explained that the generation of macropores in the templated MgO enabled easy transportation of the bulky TAGs to a deeply penetrated active catalytic sites on the inner MgO surface by mass transport, while the mesopores increases catalytic sites on the MgO surface. The surface area analysis revealed that the copolymer had huge contribution in increasing the porosity of the catalyst. The BET surface area of the templated catalyst was 79.6 m^2 g^{-1}, while that of the non-templated material was 32.9 m^2 g^{-1}. Furthermore, the basic site density of the templated catalyst was 2.5 times higher than the non-templated MgO, which could help in increasing the catalytic performance. It was reported that the templated-MgO showed stable catalytic activity for up to five runs, with an average FAME yield of approximately 95%. The non-templated MgO always exhibited lower catalytic activities than the templated MgO with an average FAME yield of approximately 83%.

3.1.1.3. ***Strontium oxide (SrO) and barium oxide (BaO) catalysis.*** The strontium oxide (SrO) is a strong base and is used in the chemical reactions, such as the oxidative coupling of methane, the selective oxidation of propane, nitroaldol reactions, and the mixed Tishchenko reactions. Liu et al. (63) reported a study in which the catalytic activity of SrO was compared with the homogeneous catalysts, such as NaOH, KOH, CH_3ONa, and KCH_3O. It was reported that though homogeneous catalysts displayed better reaction rate, the equilibrium biodiesel yield using SrO was 10% higher than those obtained using homogeneous catalysts. In the transesterification reaction between soybean oil and methanol, 95% biodiesel yield was obtained after 30 min of reaction performed at 65°C, using methanol-to-oil molar ratio of 12:1 and 3 wt. % catalyst amount. Chen et al. (64) reported that SrO catalyst displayed better catalytic performance than CaO and MgO for

transesterification reaction between olive oil and methanol. The SrO catalyst was reported to be highly active exhibiting 82% biodiesel yield within 15 min of the methanolysis reaction. However, the Sr^{2+} species were found to be leaching into the reaction mixture, thus leading toward the saponification reaction with the available FFA. Yoo et al. (65) reported that the active SrO species dissolved into the reaction mixture under sub- and super-critical conditions. Nevertheless, due to higher basicity than CaO, ZnO, TiO_2, and ZrO, the SrO-assisted transesterification reaction between rapeseed oil and methanol produced biodiesel yield higher than 90% at the temperature range between 200°C and 270°C, whereas using ZrO and TiO_2 catalyst, the biodiesel yield did not reach 80% even at the highest operative temperature of 270°C. It was concluded that at temperature of 250°C and pressure of 10500 kPa, the SrO material was transformed to strontium methoxide which in the homogeneous phase catalyzed the transesterification reaction. Hence, the dissolution phenomenon of the active catalytic species hinted that SrO does not behave as a heterogeneous catalyst.

The barium hydroxide (BaO) is a strong base but its high toxicity and high methanol solubility make them not appropriate heterogeneous catalyst for biodiesel production. Babak et al. (66) reported that BaO catalyst displayed better catalytic performance than SrO, CaO, and MgO for transesterification reaction between palm oil and methanol. The biodiesel yield of 95% was reported after 240 min of the methanolysis reaction performed at 60°C, using methanol-to-oil molar ratio of 9:1. However, it was stated that the reaction conditions caused changes in the physical morphology of BaO catalyst and also resulted toward the lixiviation of the catalytic species. Patil et al. (67) reported that under the microwave heating, BaO and SrO display better catalytic performance than CaO and MgO. Despite low specific surface area, BaO and SrO were found to be very active for transesterification reaction between C. sativa oil and methanol, resulting in 94 and 80% biodiesel yield, respectively. With an anticipation that the ultrasonic irradiation could significantly affect the extent of interaction between the two immiscible reactants, Mootabadi et al. (68) tested the influence of ultrasonic energy on the catalytic performance of BaO, SrO, and CaO catalyst for transesterification of palm oil in the presence of methanol. It was observed that BaO had higher catalytic activity than SrO and CaO, producing 83.2% biodiesel yield after 20 min (up to 95% in 60 min of reaction) of transesterification reaction. However, the dissolution effect resulted in severe drop in the catalytic activity of BaO. Furthermore, the solubility in the ultrasonic irradiation conditions was more than that in the mechanical stirring method. It was proposed that the micro-cavitation and liquid jets caused by the ultrasonic irradiation would impart shear force to the catalyst particles to affect the fragile portions of the particles, and resultantly 14% of BaO catalyst was dissolved into the reaction mixture. Thus, it could be said that although

SrO and BaO are active for the alcoholysis reaction, their lixiviation into the reaction medium does not make them potential heterogeneous catalyst. The presence of barium could cause severe environmental concerns and its removal from the post-reaction mixture could also be cumbersome, thus could not be considered as an appropriate catalyst for biodiesel production.

3.1.2. *Supported alkali metal catalysis*

The dissolution phenomenon of the active metal catalytic species into the reaction medium can possibly be counterattacked by anchoring the active catalytic sites on a support. Also, the diffusion of big oil molecules at the active center is not completely possible in the case of unsupported single metal oxide catalysts. It is believed that the uniform dispersion of base metal catalyst onto the porous support would enable availability of large number of active surface base sites and increase the accessible surface for the reaction. The replacement of M^{2+} by M^{+} in the crystal framework generates an O- basic site. The enhancement in the basicity of the active sites is expected to increase the catalytic performance of the material.

The BaO material, although, has superior basicity among the alkaline earth metal oxides utilized for biodiesel production, the dissolubility of this toxic species in the reaction medium do not make them appropriate support for the loading of alkali metal catalysts. D'Cruz et al. (69) reported a study in which alkali metals, such as Na, K, and Li were loaded on MgO, CaO, and BaO support via wetness impregnation method and the subsequent catalysts were used to assist transesterification of canola oil in the presence of methanol. It was reported that the supported CaO catalysts contained few weak basic sites in the addition to the strong basic sites while the alkali metal-loaded MgO catalysts were weakly basic. The Li (1.25 wt. %) supported on CaO displayed 70.7 wt. % esters yield after 240 min of reaction performed at 50°C, using methanol-to-oil ratio of 6:1 and 2 wt. % catalyst amount. Watkins et al. (70) recommended that Li content of 1.23 wt. % supported on CaO was sufficient to achieve 100% glyceryl tributyrate conversion when transesterified in the presence of methanol. The incorporation of alkali metal ions into the oxide lattice is thought to induce a significant morphological change, thus favoring more polarizable low coordination step and corner sites. It was suggested that Li^{+} dopants preferentially coordinate to these highly active corner and step sites upon the thermal processing which regulate the basicity. Furthermore, the Li ion incorporation into the oxide lattice generated (Li^{+} O-) ion pairs and oxygen vacancies, which promoted the activity of the catalyst. Kaur and Ali (71) reported a work in which wet chemical method-assisted basic Li/CaO catalyst was used to transesterify variety of oil feedstocks having different FFA concentration. The incorporation of Li ions onto the CaO surface resulted in minimizing the specific surface area but enhanced the basic strength of the catalyst. The recyclability test revealed that even after four tests of recyclability,

Li (3 wt. %)/CaO assisted 84% conversion of waste oil; however, a partial deactivation of catalyst was observed due to the leaching of Li^+ species from the support. Furthermore, the specific surface area and the basicity of the reused catalyst were also depleted signifying that the catalyst underwent structural modification during the alcoholysis process, thus lowering the activity during the recyclability tests. In a standpoint to increase the basicity of CaO catalyst, Puna et al. (72) reported a work in which CaO is decorated with lithium nitrate solution (Li/Ca=0.3 atomic ratio) followed by its calcination at 575°C or 800°C for 300 min. It was reported that 93–98% biodiesel yield was produced after 240 min of transesterification reaction of rapeseed oil in the presence of methanol. However, it was observed that the Li loading increased the adsorption of glyceroxide species on the catalyst surface, which in return increased the dissolution of Ca species into the reaction mixture, thus leading towards the catalytic deactivation and reducing the biodiesel yield during the recyclability tests. Maclead et al. (73) reported that all alkali metals loaded CaO catalysts represented superior basic strength than those supported on MgO and alumina materials. The reason for such behavior was associated to the size of alkali metal ions and alkaline earth metal ions. The Na^+ ions are too large to substitute in the Mg^{2+} ions, whereas the bulky Ca^{2+} species enabled the easy substitution of all alkali metal ions. It was stated that the calcination process promoted the basic strength of Li/MgO catalyst, but had no significant effect on the basicity of Na/MgO and K/MgO material. Furthermore, none of the alumina supported catalysts represented a satisfactory level of base strength; however, the same was elevated after the thermal treatment. The origin of the basicity in the case of alumina support was thought to arise from the decomposition of salt anion (carbonate or nitrate) to form O- anion. Among all the tested catalysts, alkali doped CaO and calcined Li/MgO were found to be active for transesterification reaction, converting more than 90% oil after 180 min of reaction. However, the dissolution phenomenon of Ca and Mg species into the reaction medium was observed. The leached metal species displayed 54% biodiesel production via transesterification; thus, the generation of biodiesel was not entirely heterogeneously catalyzed. (73). Kumar and Ali (74) reported the appliance of heterogeneous K^+ impregnated CaO catalyst for the methanolysis of mutton fat, soybean oil, virgin cottonseed oil, waste cottonseed oil, castor oil, karanja oil, and jatropha oil. The potassium ion impregnation up to 3.5% on CaO support resulted in the formation of defects on the catalytic surface, and increased the specific surface area and the basicity of the catalyst. It was further mentioned that with the increase in the size of impregnated alkali metal ion (Li to K), the catalytic performance was lowered. Although the Li /CaO displayed better catalytic performance in shorter reaction time, the leaching of Li species into the reaction medium was higher than that observed in the case of K/CaO catalyst.

Supamathanon et al. (75) reported that when potassium acetate was used as an potassium precursor for the impregnation of potassium species on NAY zeolite support, the structural morphology of NaY zeolite was not altered. However, elevating the potassium loading on the support directed the decomposition of the precursor on the support surface and resulted in the decrease in the crystallinity of zeolite, thus reducing the specific surface area of the catalyst. After the thermal treatment at 400°C for 240 min, the obtained catalyst was used for transesterification of jatropha oil where it was observed that loading 12 wt. % K on NAY zeolite and using 4 wt. % catalyst amount resulted in 73.4% esters yield after 180 min of reaction. Xie et al. (76) used a zeolite material from the Faujasite structure family as a support for the decoration of KOH material. The KOH (10%) loaded on NaX zeolites was synthesized via impreganation method and used for transesterification of soybean oil where the reported results indicated that 85.6% soybean oil conversion was achieved after 480 min of reaction.

Arzamendi et al. (77) used NaOH supported on a commercially available alumina catalyst to assist transesterification of sunflower oil in the presence of methanol. It was mentioned that the introduction of NaOH caused structural damage to alumina and reduced the specific surface area and pore volume of the support. The high loading of NaOH (19%) on the alumina support resulted in the catalyst instability and leaching of the active catalytic species. The higher conversion of oil was obtained when the non-calcined material (99%) was used, in comparison to the calcined catalyst (86%), which was explained due to the vitrification phenomenon of the catalyst during the thermal treatment. It was said that the catalyst surface became inert and poorly active due to the calcination process, thus resulting in lowering of the catalytic performance. Similar behavior was reported in the case of NaOH loaded silica (Aerolyst 350) catalyst, where (i) the incorporation of NaOH caused destruction to the textural appearance of silica, (ii) the calcination process exhibited adverse impact on the performance of catalyst, and (iii) the excessive loading on NaOH caused the partial dissolution of silica. It was concluded that NaOH reacted with silica Si-OH surface and results in the formation of Si-ONa active groups, which were considered to catalyze the alcoholysis process. It was reported that almost 50% of the total oil conversion was due to the leached sodium species. The final oil conversion using the calcined catalyst was 36%, whereas that obtained using non-calcined catalyst was 88%. The superior performance of NaOH/alumina catalyst compared to NaOH/silica was attributed to higher surface area of the former catalyst. Furthermore, alumina is more resistant for the vitrification phenomenon than silica (78).

Liu et al. (79) reported CsF/CaO catalyst to be highly active for transesterification reaction between soybean oil and methanol as approximately 90% esters yield was observed within 10 min when the reaction was performed at

65°C, using methanol-to-oil molar ratio of 12:1 and 8 wt. % catalyst amount. It was reported that the CsF loading augmented the basicity of the final catalyst. Furthermore, the enhanced activity of the CsF/CaO catalyst was attributed to the formation of stable $CsCaF_3$ material. Also, it is easier for methanol to be transformed into CH_3O- species in the presence of $CsCaF_3$. Woodford et al. (80) reported the synthesis of Cs (20 wt. %)/MgO nanoparticle catalyst via supercritical sol-gel method and tested its capability to transesterify model triglyceride and olive oil in the presence of methanol. It was stated that after the impregnation of Cs on MgO support, only one-third of the total BET surface area was available, however, the density of the surface basic sites augmented by 46%. The generation of new CsMg phase was considered to be responsible for the improved basicity of the catalyst. The transesterification reaction performed at 90°C for 1440 min resulted in 93% olive oil conversion. However, the activity of catalyst was reported to be dropping with the increase in the fatty acid chain length in the raw material. This was explained due to falling oil solubility and slower diffusion through the bulk medium for bulkier TAGs, together with the steric effects hampering the base site accessibility. Furthermore, the unsaturation in TAGs could cause irreversible C=C binding to MgO, resulting into the blocking of the active sites. For instance, using Cs/MgO catalyst, 100% conversion for C_4 and C_8 triglyceride was observed after 1440 min of reaction, while conversion for C_{12} and C_{18} carbon were 89% and 11%, respectively.

Barputian et al. (81) employed KOH loaded activated carbon catalyst for transesterification process between palm oil and methanol. It was expected that the large surface of carbon will allow effective and uniform dispersion of KOH species. It was observed that the graphitic structure of carbon was intact even after the dispersion of KOH. The catalyst amount of 30.3 wt. %, methanol-to-oil molar ratio of 24:1, and reaction temperature of 64.1°C was required for obtaining 97.72% esters yield. It was concluded that 90% biodiesel yield was obtained even after three recycle tests. However, a little amount of K^+ species were found to be leaching which was because of the weak interaction between the alkali metal and carbon, thus hinting that the capability of the catalyst to assist the alcoholysis process could be improved with few modifications in the existing material synthesis procedure. Xie et al. (82) reported that using Li (5 wt. %)/ZnO catalyst, soybean oil conversion of 96.3% was obtained after 180 min of transesterification reaction. It was mentioned that the dispersion of lithium nitrate on a thermally treated ZnO support improved the catalyst surface oxygen species (O 1s). Furthermore, the activity of the synthesized catalyst for transesterification reaction was directly proportional to its basic strength. The number of basic sites of the catalyst was not related to the loading amount of lithium nitrate but on the degree of decomposition of the precursor loaded on the support. The impregnation of the excessive lithium precursor (above 3 mmol g^{-1}) was

not recommended as it resulted in its incomplete decomposition during the calcination process. This was because of the agglomeration of the active species on the support, thus lowering the specific surface area, and consequently, the activity of the catalyst.

3.1.3. *Supported alkaline earth metal catalysis*

Like alkali metal, anchoring of alkaline earth metal oxide catalysts onto a hetero species is also practiced so as to minimize the dissolution of the active catalytic species into the reaction medium. The negligible leaching of catalytic species into the reaction medium would prompt the alcoholysis reaction catalyzed by the heterogeneous phase of catalyst, and not the homogeneous one. This in return is expected to allow its reutilization for several alcoholysis reaction cycles. It is anticipated that the uniform dispersion of alkaline earth metal oxide on an appropriate support would not only increase the number of active basic sites but also fabricate a new structure of the resultant catalyst and provide more accessible surface area for the alcoholysis reaction.

Xie et al. (83) tested the efficacy of tin oxide (SnO_2) loaded CaO catalyst (Ca/Sn=4) for transesterification of soybean oil in the presence of methanol. The wet impregnation of CaO on SnO_2 followed by the calcination at 700°C resulted in the formation of calcium stannate. It was concluded that there occurred a solid state reaction which resulted in electron transfer between the catalyst components, thus minimizing the leaching of the catalytic species from the catalyst surface. Furthermore, a strong interaction between the basic and acidic moiety improved the durability and the stability of the consequent catalyst. The transesterification reaction performed at 65°C for 360 min resulted in the methyl esters yield of around 90%, using methanol-to-oil ratio of 12:1 and 8 wt. % catalyst amount (83). Zu et al. (84) reported that the introduction of oxygen species into the graphite sheets resulted in the increase in the interlayer spacing of graphite oxide. The abundant surface oxygen groups on the graphite oxide acts as an anchoring center for the dispersion of CaO material. It was found that using CaO (8 wt. %)/graphite oxide catalyst, more than 95% biodiesel yield was obtained when transesterification reaction between soybean oil and methanol was performed for 120 min. Zabeti et al. (85) reported that when CaO/Al_2O_3 catalyst, calcined at 718°C for 300 min, was applied for transesterification reaction between palm oil and methanol, negligible amount of catalytic species leached from the material. It was reported that after 300 min of transesterification reaction performed at 65°C, biodiesel yield of about 98% was obtained using methanol-to-oil molar ratio of 12:1 and 6 wt. % catalyst amount. Samart et al. (86) reported that using CaO (15wt. %) dispersed on mesoporous silica, around 95% oil conversion was achieved when soybean oil was transesterified with methanol at 60°C for 480 min, using methanol-to-oil molar ratio of 16:1 and 5 wt. % catalyst dose. Alba-Rubio et al. (87) reported a study in which it was

mentioned that CaO can be uniformly dispersed on the surface and inside mesopores of hexagonal structured crystalline ZnO support. The ZnO material enables the stabilization of CaO on its surface and preclude leaching of the catalytic species into the reaction mixture. The derived catalyst was mentioned to have weak basic sites on the support surface and strong basic sites on the CaO surface. The CaO/ZnO catalyst was tested for producing biodiesel from ethyl butyrate and sunflower oil. Using CaO (16 wt. %)/ZnO catalyst, when activated at 800°C for 600 min, the lixiviation of catalytic species into the reaction medium was found be insignificant, producing biodiesel yield higher than 90% after 120 min of transesterification reaction performed at 60°C, using methanol-to-oil molar ratio of 12:1 and 1.3 wt. % catalyst amount. Yang et al. (88) reported the use of Strontium nitrate/ZnO catalyst, when calcined at 600°C for 300 min, for the alcoholysis of soybean oil. It was reported that 94.7% oil conversion was obtained when the reaction was performed at 65°C, using methanol-to-oil molar ratio of 12:1 and 5 wt. % catalyst amount which further increased to 96.8% in the presence of co-solvent, THF. However, the same catalyst when used for the second recycle test, oil conversion was depleted to 15% indicating that catalytic species were poisoned during the first reaction cycle. Furthermore, when ZnO was replaced by other supportive materials, such as γ-alumina and zirconia, the resulting supported strontium nitrate catalysts displayed very low catalytic performance even in the first test of transesterification reaction; thus hinting that ZnO is a better support for anchoring alkaline earth metal oxides (88).

Other than the basic and acidic supports, the nature of neutral materials, such as carbon in anchoring alkaline earth metal oxide catalysts was also investigated (89, 90). Wan and Hameed (91) reported a study focused on the appliance of CaO/activated carbon catalyst for transesterification reaction between palm oil and methanol. The transesterification reaction performed at 190°C for 81 min resulted in approximately 81% esters yield, using methanol-to-oil molar ratio of 15:1 and 5.5 wt.% catalyst amount.

3.1.4. *Anion exchange resins*

In the recent days, the anion-exchange resins are also considered as a possible base catalyst for biodiesel production. Also, their large particle diameter makes them advantageous in being used in a fix-bed reactor for the continuous production of biodiesel. The strong anion-exchange resins could be classified in two types: (i) a quaternized amine product made by the reaction of trimethylamine with copolymer of styrene and divinylbenzene and (ii) while, in the other type of resin, the functionality is obtained by the reaction of styrene-divinylbenzene copolymer with dimethylethanolamine. The latter type of resins is said to have lower basicity than the former counterpart, however, the efficiency for the regeneration for this resins to the hydroxide form is higher. The resins obtained from the reaction between

trimethylamine and copolymers have better chemical stability and are favored for relatively high-temperature applications. The superior catalytic activity of anion exchange resins is associated also with its adsorption efficacy for alcohol. This in return is expected to activate the adsorbed molecules during the course of reaction, and consequently, facilitate the alcoholysis process (92).

Li et al. (92) reported the microwave-assisted transesterification of yellow horn seed oil in the presence of methanol using solid basic Amberlite IRA-900 and Amberlite IRC-93 ion exchange resins. It was concluded that Amberlite IRA-900 was more active than the other counterpart, producing approximately 96% methyl esters yield after 180 min of reaction performed at 60°C, using methanol-to-oil ratio of 8:1 and 3 wt. % catalyst dose. Vicente et al. (93) reported that basic Amberlyst A26 and Amberlyst A27 anion exchange resins hardly had any activity for transesterification of sunflower oil at 60°C, using twice the stoichiometric amount of methanol. Shibasaki-Kitakawa et al. (94) tested the ability of several ion exchange resins (PK208, PA308, PA306, PA306s, and HPA25) to catalyze transesterification reaction between triolein and ethanol. It was reported that PA306s resins, possessing lower crosslinking density and smaller particle size, effectively accelerated the reaction rate and displayed high conversion ratio. Using PA306s resin, triolien conversion of 80% was documented. The gel-type (Marathon A and Monosphere 550A) and macroporous-type (Marathon MSA and Amberlite 900) resins differentiating in the degree of crosslinking, textural properties, and basicity were also tested to catalyze transesterification reaction between soybean oil and methanol (95). The amount of basic sites in Marathon A and Monosphere 550A resins were three times higher than that in Marathon MSA and Amberlite 900 resins. The gel-type resins though had higher basicity, they showed inferior initial catalytic activity when compared with the macroporous-type resins; however, the final oil conversion was dependent on the basic site density. Hence, because of the higher basicity, the gel-type resins displayed superior equilibrium biodiesel yield. Furthermore, it was reported that the addition of 0.018% CH_3ONa to resins resulted in obtaining 100% biodiesel yield after 300 min of the alcoholysis reaction performed at 55°C. It was postulated that CH_3ONa reacted with the adsorbed water molecules responsible for the catalytic deactivation, thus allowing the regeneration of hydroxide group which then helped methanol to react with the bonded organic anions and TAGs to liberate methyl esters (95). Long et al. (96) reported that the introduction of N-methylimidazolium improved the polarity of chloromethylated styrene-divinylbenzene copolymer and, hence, the miscibility between oil and methanol. The N-methylimidazole hydroxyl anion exchange resins ((R^+OH-(Na))-assisted transesterification reaction between soybean oil and methanol performed at 50°C for 600 min, using methanol-to-oil molar ratio of 12:1, catalyst dose of

2.5 wt. %, and stirring intensity of 570 rpm resulted in 97.25% oil conversion. The elevated activity of $R^{+}OH$-(Na) resins catalyst was due to high content of OH- moiety, which was mentioned to be three times higher than the quaternary ammonium functionalized Marathon MSA and PA 306s anion exchange resins. Furthermore, it was documented that NaOH adsorption on $R^{+}OH$- resulted in the activation of OH- moiety, thus promoting the catalytic efficacy. Ren et al. (97) studied transesterification of soybean oil with methanol in a continuous bed reactor using a strongly basic D261 anion exchange resins. It was reported that the presence of THF, TBA, and n-hexane as a co-solvent helped in obtaining more than 95% biodiesel yield. However, the activity of the catalyst was said to begin to deplete after 240 min of reaction, where 23.7% biodiesel yield was reported after 480 min of reaction. This behavior was explained due to the adsorption of organic compounds, such as glycerol and TAGs on the active centers and due to the desorption of hydroxyl ions. Other than that, the catalyst position in the bed reactor was also mentioned to have a significant impact in dropping the biodiesel yield. He et al. (98) reported that lowering of the activity of resins was lesser when the catalyst was positioned at the bottom of the reactor. This was explained due to up-flow of TAGs. Furthermore, the three-steps regeneration process of resins using methanol and 5 wt. % KOH was said to preserve the activity of the catalyst, thus producing more than 90% biodiesel.

3.2. *Heterogeneous acid catalysis for biodiesel production*

Over the last few years, the advancement in heterogeneous acid catalysts for biodiesel production has been a very active research area because their utilization includes several advantages which are not present while using their homogeneous counterparts. The successful utilization of heterogeneous acid catalysts is expected to produce superior grade biodiesel as well as glycerol. Furthermore, replacing conventional homogeneous catalysts with the heterogeneous ones could be more beneficial as the catalyst would not cause concerns related to corrosion of the equipment. The usage of acid catalysts to assist the alcoholysis process could be valuable because they can accelerate both transesterification of TAGs and FFA esterification reaction. The Brønsted acid species catalyze esterification reaction while the Lewis acid species accelerate the transesterification process. It is assumed that the alcoholysis reaction mechanism is similar for both homogenous and heterogeneous acid catalyst except the fact that the heterogeneous acid-catalyzed alcoholysis reaction is governed by the catalyst surface depending heavily on the interconnected system of large pores, surface acid sites, and hydrophobicity.

The alcoholysis reaction assisted by heterogeneous acid catalyst following the Langmuir-Hinshelwood mechanism could be explained as follows. First, the hydroxyl group of methanol is protonated by Brønsted acid on the

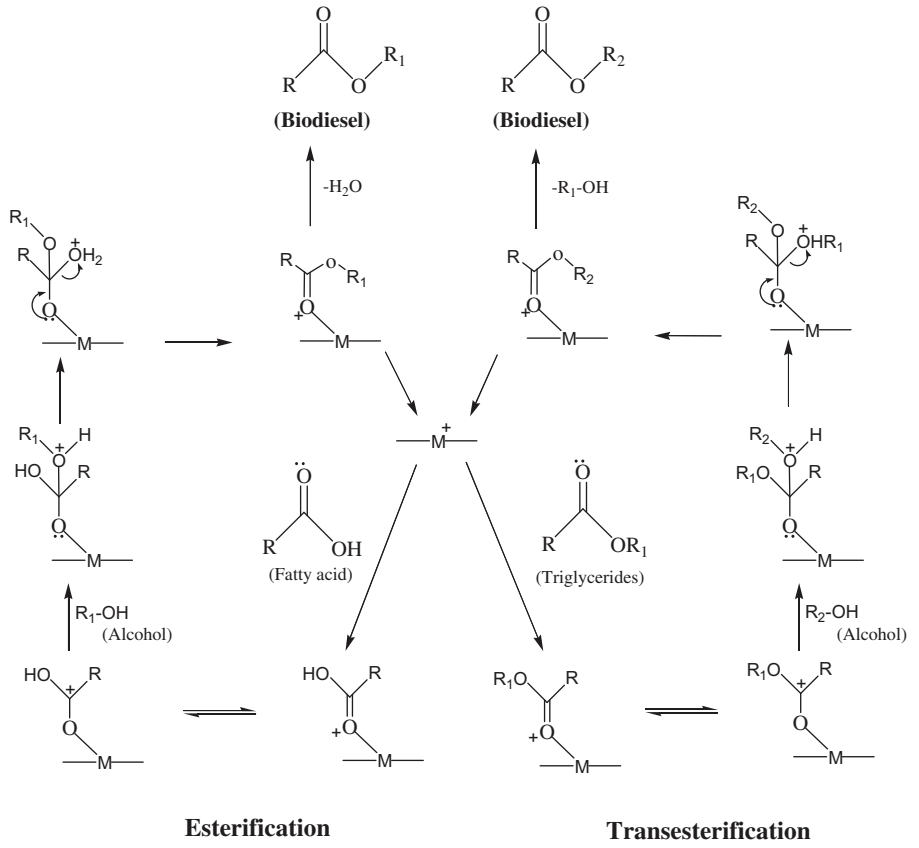

M^+- Acid site on the catalyst surface

R- Alkyl group of fatty acid

R_1- Alkyl esters of triglycerides

Figure 9. Plausible reaction mechanism for heterogeneous acid-catalyzed alcoholysis reaction.

catalyst surface, while the protonation of FFA/TAGs occurring on the adjacent catalytic site leads to the formation of carbocation. The deprotonation of methanol oxygen produces the nucleophile which attacks the carbocation to generate a tetrahedral intermediate. The tetrahedral intermediate then eliminates water to form esters. In transesterification process, this intermediate eliminates glycerol to generate new esters. This mechanism can be extended to di- and tri-glycerides (99). The plausible reaction mechanism for the simultaneous esterification and transesterification catalyzed by Brønsted acid catalyst surface sites is shown in Fig. 9. Sani et al. (100) and Lotero et al. (101) also reviewed some of the research related to the development of heterogeneous acid catalysts for biodiesel production.

3.2.1. *Zirconia-based catalysis*

Due to their strong acidic properties, high stability, and durability, the sulphated zirconia catalysts have been widely used to catalyze several reactions, such as transesterification, esterification, hydrocarbon isomerization, methanol conversion to hydrocarbons, alkylation, acylation, etherification, condensation, nitration, cyclization, etc. (102).

Patel et al. (103) reported a study in which zirconia impregnated with different concentration of H_2SO_4 was used to accelerate esterification reaction between oleic acid and methanol. It was investigated using XRD and FTIR analysis that the incorporation of sulphate species and the calcination process resulted in the zirconia phase modification from the thermodynamically stable monoclinic to the metastable tetragonal phase. The methyl oleate yield of 90% was reported after 1440 min of esterification reaction performed at 60°C, using methanol-to-oleic acid molar ratio of 40:1 and 0.5 g catalyst amount. Thiruvengadaravi et al. (104) documented that when sulphated zirconia was used as a catalyst, the acid value of karanja oil was dropped from 12.27 mg KOH g^{-1} to 1.3 mg KOH g^{-1} within 120 min of esterification reaction, using operative reaction temperature of 60°C, methanol-to-oil molar ratio of 9:1, and 1 wt. % catalyst dose. The reduction in the acid value was initially faster and slowed down after 60 min, which was explained due to the formation of water during the esterification process. Rattanaphra et al. (99) reported that sulphated zirconia catalyst synthesized using a solvent-free method represented superior catalytic activity for the alcoholysis reaction than the one synthesized using wet-impregnation method. The methyl esters produced from the simultaneous transesterification and esterification reaction using solvent-free assisted catalyst was 85% after 60 min of reaction performed at 170°C while 45% yield was obtained at similar reaction condition using wet-impregnation method-assisted catalyst. The elevated catalytic activity in the case of solvent-free method-assisted catalyst was attributed to its higher surface area, and due to the presence of Lewis acid sites and additional number of Brønsted acid sites. Garcia et al. (105) reported that the solvent-free assisted catalyst represented better catalytic efficacy for the methanolysis and ethanolysis reaction than the precipitation method assisted catalyst. The reason for such behavior was not only because of the elevated surface area but also more Brønsted acid sites formed due to the tetragonal phase of solvent-free sulfated zirconia material. However, both Garcia et al. (105) and Rattanaphra et al. (99) reported the lixiviation of sulphur species from the catalyst surface, hence, rendering its applicability for the recyclability tests. Rattanaphra et al. (106) reported a study in which sulphated zirconia catalyst was used to promote the alcoholysis reactions. It was mentioned that the reaction parameters were reliant on the molecular structure of feedstock. For instance, operative temperature of 170°C was required for the transformation of rapeseed oil, while reaction temperature

of 120°C was found to be adequate to esterify myristic acid. However, the appliance of elevated temperature and catalyst dose resulted in the formation of FFA due to the side-reactions of TAGs, such as thermal cracking, hence higher concentration of methanol was necessary to complete the alcoholysis reaction. However, water was generated via dehydration of methanol which occurred due to rise in reaction temperature. Hence, the additional quantity of water was generated which then directed the hydrolysis of TAGs. The proposed reaction mechanism for the simultaneous transesterification and esterification process was explained in three steps as: (i) esterification of myristic acid (0–20 min); (ii) transesterification of TAGs, thermo/catalytic cracking of TAGs followed by esterification of fatty acids, and hydrolysis of TAGs followed by esterification of fatty acids (20–90 min); thus, increasing the yield of methyl esters and FFA, and generating water; and (iii) the final metyl esters and FFA yield reach equilibrium but higher operative variables causes methanol dehydration, thus directing the generation of additional water (Fig. 9). The highest methyl esters yield of 86% was reported after 60 min of the alcoholysis reaction, using temperature of 170°C, methanol-to-oil molar ratio of 20:1, and 3 wt. % catalyst amount. Suwannakarn et al. (107) concluded that the sulfate species leached from the sulfated zirconia when the catalyst was used to assist the high temperature (120°C) transesterification reaction between tricaprylin and a series of alcohol differentiating in the number of carbon atoms in the alkyl chain. It was documented that the degree of catalyst deactivation was similar irrespective of the type of alcohol used. The reported investigation suggested that not the carbonaceous deposition, but leaching of sulfate species from the catalyst surface on its contact with alcohol directed the deactivation of catalyst. The leached sulfate species was said to react with alcohol and result in the formation of monoalkyl hydrogen sulfate and dialkyl sulfate. The spent catalyst, when used for the next recycle test, resulted in the lowering of tricaprylin conversion and the extent of drop in conversion was severe with the increase in the carbon chain length of alcohol.

The supported tungsten oxide (WO_3) catalysts recently received enormous attention because of their acidic properties and ability to catalyze both esterification and transesterification reactions. Another advantage of tungsted zirconia (WZ) material is that it is robust, withstands higher temperatures, and the catalytic deactivation appears to be not rapid (108). Park et al. (109, 110) reported that WO_3/ZrO_2 material was highly stable and hardly any tungsten moiety leaching from the support when the catalyst was used to accelerate the alcoholysis process. It was explained that the calcinations process at 800°C and the addition of tungsten species generated the tetragonal phases in zirconia framework. The WO_3 addition higher than 10% resulted in the formation of triclinic phase which, in together with the tetragonal phase of zirconia, promoted the catalytic activity for the

esterification reaction. Furthermore, the loading of WO_3 (20 wt. %) on the zirconia surface resulted in the generation of moderate as well as strong acid sites. The alcoholysis reaction performed at 150°C for 120 min using methanol-to-oil molar ratio of 9:1, catalyst amount of 0.4 gm ml^{-1}, and 800 rpm stirring intensity resulted in 96% conversion of dark acid oil. It was assumed that the addition of WO_3 species avoided the sintering of ZrO_2 and allowed the transesterification reaction to occur at higher temperature as the oil conversion increased with the rise in temperature. However, it is worth noting there evolves a risk that the use of high reaction temperature could lead towards the undesired side reactions (111). The pellet WO_3/ZrO_2 catalyst, which is required for the packed-bed continuous flow reactor, was found to be less active than the powdered catalyst. The proposed catalyst was said to rapidly accelerate the FFA transformation during initial 1440 min of reaction and then resulted in the steady FFA conversion of 65% in an 8400 min continuous esterification process, indicative that the catalyst is stable and active for the esterification process. After 8400 min of reaction, it was found that only 0.3% catalyst active species were leached from the material. The XPS analysis revealed that W^{6+} and W^{5+} species underwent reduction during the first 2340 min of reaction due to the presence of oleic acid; however, after 2340, the extent of reduction was minimized due the coverage of catalyst surface by oil. Therefore, it was believed that the reduction of the tungsten species resulted in the decrease of the catalytic activity for the esterification reaction. Thus, the spent catalyst was re-oxidized to enhance further activity for the esterification reaction (111).

3.2.2. *Silica-based catalysis*

The ordered mesostructure combined with the high specific surface area, flexible pore size, and tunable surface property make silica materials one of the ideal catalysts for biodiesel production. The silica mesopores are connected with the micropores enabling the pore surface to be accessed in three dimensions for the catalytic reaction. The large number of silanol groups at the surface of its channels serves as a robust support. Moreover, the silica materials, such as SBA-15 and MCM-41 display remarkable hydrothermal stabilities (112).

Corro et al. (113) reported the appliance of hydrofluoric acid (HF) pretreated silica (SiO_2) material for esterification of FFA in waste frying oil in the presence of methanol. It was mentioned that HF loading generated the Lewis acid sites on the silica surface. The pretreated silica catalyst, after the thermal annealing at 500°C for 300 min, was tested for esterification reaction at 70°C, using catalyst dose of 4 wt. % and methanol-to-oil molar ratio of 30:1, where 86% FFA conversion was reported after 240 min of reaction time. Furthermore, it was reported that the proposed catalyst did not deactivate due to hydration/carbonation phenomenon when exposed to the

surrounding air and moisture. Đokić et al. (114) tested the activity of ferric sulfate functionalized silica gel catalyst for esterification of model oil prepared using sunflower oil and oleic acid. The oleic acid conversion of 96.9% was obtained after 240 min of alcoholysis reaction performed at 95°C, using the system pressure of 301.1 kPa, methanol-to-oil molar ratio of 10:1, and 8.1 wt. % catalyst amount.

The mesoporous silica materials, such as mesoporous molecular sieves MCM-41 materials developed by the Mobil Oil Corporation, are also considered as an appropriate material to potentially anchor the heterospecies. The physical properties of MCM-41, such as the high specific surface area, pore volume, and pore diameter enable them to be used as an adsorbents, heterogeneous catalyst, and catalyst support in several branches of chemical industries. Moreover, having a highly ordered distribution of mesopores, MCM-41 solids offers the possibility for the strong anchoring of metals into their structures, which improves their hydrothermal stability, thus broadening their fields of application (115, 116). García-Sancho et al. (117) investigated the catalytic performance of Niobium (Nb) incorporated MCM-41 and Niobium loaded MCM-41 catalyst for transesterification of sunflower oil in the presence of methanol. The structurally incorporated Nb-MCM-41 catalyst was said to possess superior textural properties than the one prepared using wetness impregnation method. However, irrespective of the catalyst synthesis procedure, both catalysts represented similar acidity. The alcoholysis reaction performed at 200°C for 240 min resulted in 95% biodiesel yield, using methanol-to-oil molar ratio of 12:1 and 7.5 wt. % Nb (8 wt. %)-MCM-41 catalyst amount. The crucial point to note was that the insignificant leaching Nb species was observed which could make it a promising heterogeneous catalyst for biodiesel production. Carmo Jr. (118) reported that the incorporation of Aluminium (Al) into the structural lattice of MCM-41 increased the acidity of the subsequent catalyst. The improved catalytic activity of the catalyst was due to the generation of Brønsted acid sites. It was suggested that the Al incorporation resulted in the structural transformation of the support but the hexagonal orientation of aluminosilicate MCM-41 was intact. The resultant catalyst was then used to assist esterification of palmitic acid in the presence of variety of alcohol differing in their carbon chain length. Xu (119) reported transesterification reaction between soybean oil and methanol in a ceramic membrane reactor loaded with a MCM-41 supported p-toluenesulfonic acid catalyst. The biodiesel yield of 84.1% was reported using reaction temperature of 80°C, circulation velocity of 4.15 ml min^{-1}, and 0.27 gm ml^{-1} catalyst amount.

The mesoporous SBA-15 materials, along with the high surface area and ordered porosity, are stable at high temperatures and possess easy functionalization properties. The SBA-15 materials are considered to have high concentration of silanol groups on its framework surface and these silanol

groups are expected to act as a anchoring sites for the organic moieties because the surface hydroxyl reacts readily with the alkoxy groups in silane compounds by the silylation reaction (120). Shah et al. (121) tested the catalytic activity of co-condensation method assisted sulfonic acid functionalized SBA-15 catalyst for the alcoholysis reaction of high FFA acid oil. It was verified that the hexagonal orientation of SBA-15 was not damaged after the introduction of acid moiety; however, the functionalization and high temperature hydrothermal treatment resulted in the broadening of the mesopores of the same. The increase in the porosity facilitated the transportation of the bulky TAGs and promoted the interaction between the active acid centers and reactants. Using the proposed catalyst, 99% FFA conversion was reported after 360 min of methanolysis reaction performed at 80°C, using methanol-to-oil molar ratio of 15:1 and 4 wt. % catalyst dose. Xie et al. (122) studied esterification of FFA in model oil using a phenylsulfonic acid functionalized SBA-15 catalyst. In a synthesis methodology, the synthesized mesoporous SBA-15 silica was treated with phenyltrimethoxysilane leading towards the formation of phenyl SBA-15, followed by the sulfonation reaction with chlorosulfonic acid. It was presented that the FFA conversion upgraded with the increase in the chlorosulfonic loading and with the sulfonation duration. It was further mentioned that the functionalization process resulted in the reduction in the specific surface area, however, the textural hexagonal mesostructure of parent SBA-15 was not damaged. The esterification reaction performed at 67°C resulted in 96.7% biodiesel yield after 300 min, using methanol-to-oil molar ratio of 15:1 and 7 wt. % catalyst amount. Iglesias et al. (123) investigated the catalytic stability and the deactivation pattern of Zr-SBA-15 catalyst against the impurities and the natural componenets present in a low-grade feedstock when subjected to the methanolysis process in a batch reactor and a continuous packed-bed reactor. With the confirmation studies from XPS analysis, it was concluded that lecithin, a natural substance present in both animal and vegetal lipids, is adsorbed on the surface of zirconium Lewis acid sites during the methanolysis reaction. This, in consequence, blocked the interaction between the glyceride molecules and the catalytic active centers. Although the interaction between phosphate/phosphonate groups of the unsaponifiable organic compounds (phospholipids and retinoids) and zirconia atoms is energetically favorable and chemically stable, the re-calcination process of the spent catalyst was suggested to successfully remove the adsorbed lecithin species making the catalyst active for the next recycle test. Chen et al. (124) reported use of the co-condensation method assisted titanium (Ti) incorporated mesoporous SBA-15 catalyst for biodiesel production from crude jatropha oil. In comparison to TiO_2 and SBA-15, the Ti-SBA-15 material displayed superior catalytic performance for the methanolysis reaction. The higher catalytic activity of Ti-SBA-15 catalyst was attributed to the tetrahedral cordinated Ti (IV)

species having a weak Lewis acid nature. The methyl esters yield of 98.4% was reported after 180 min of the methanolysis reaction performed at 200°C, using methanol-to-oil molar ratio of 108:1. Furthermore, the proposed catalyst was mentioned to be tolerant to the presence of 5 wt. % water and 30 wt. % FFA in the reaction mixture, while no leaching of acid species from the support was reported. Cruz et al. (125) reported a study focused on the usage of Pt and Ni supported SBA-15 and SBA-16 catalysts for biodiesel production. It was suggested that all the supported catalysts represented adequate capability to assist the alcoholysis reactions, however, the SBA-15 silica was found to be better support than the SBA-16 silica. The maximum biodiesel yield of 89% was reported after 240 min of reaction performed at 60°C, using methanol-to-oil molar ratio of 6:1 and 2.5 wt. % catalyst amount.

3.2.3. *Heteropoly acid-based catalysis*

The heteropolyacids (HPAs) are oxygenated compounds based on polyoxometalates. The HPAs and their salts are useful acid catalysts for diverse reactions that require strong acidity. Although HPAs hold strong Brønsted acidity and are environmentally friendly, they are highly soluble in, and difficult to separate from, the polar media. It was said that the unsupported keggin type HPAs, such as $H_4PNbW_{11}O_{40}$, $H_3PW_{12}O_{40}$, $H_4SiW_{12}O_{40}$, and $H_4SiMo_{12}O_{40}$, although displayed better catalytic performance, were found to be dissolving in the reaction medium (126). Therefore, in order to make an appropriate use of HPAs as heterogeneous catalysts, they must be grafted on the high surface area porous materials. This is, in consequence, anticipated to promote the anchoring of the active catalysts on the support and avoid its dissolution into the reaction medium. Tropecelo et al. (127) tested three SBA-15 supported HPAs catalysts: (i) tungstophosphoric acid (PW), (ii) molydophosphoric acid (PMo), and (iii) tungstosilicic acid (SiW) for esterification reaction between palmitic acid and methanol. Among all the synthesized catalysts, PW/SBA-15 was reported to possess higher acidity. The catalytic activity of the supported catalysts was said to be increasing with the augmentation in the HPAs loading. Based on their performance to assist esterification reaction, the supported HPAs catalyst could be ordered as: PW/SBA-15>SiW/SBA-15>PMo/SBA-15. The SBA-16 material possesses Lewis acid sites due to their cationic nature. Khayoon and Hameed (128) reported that loading HPAs on SBA-16 will result in the generation of both Lewis and Brønsted acid sites on the resultant catalyst. It was mentioned that the interaction between surface silanol groups and HPAs moieties directed the formation of Si-O-Mo species. A series of SBA-16 supported 12-molybdophosphoric acid ($H_3PMo_{12}O_{40}$), varying in the HPAs concentration, were tested for biodiesel production from karanja oil. The HPAs loading of 15 wt. % was found to be optimum for its uniform dispersion on SBA-16 surface. The further increment in the HPAs amount resulted in the blockage of the

silica mesopores, thus minimizing the accessible catalytic active sites for esterification reaction. The highest biodiesel yield of 81.8% was recorded after 300 min of reaction performed at 140°C, using catalyst dose of 2.5 wt. %, methanol-to-oil molar ratio of 8:1, and 250 rpm stirring intensity. Zou et al. (129) used the inclusion complex of $Cs_{2.5}H_{0.5}PW_{12}O_{14}$ with the bridged bis-clyclodextrin catalyst to assist the transformation of waste cooking oil to biodiesel. The maximum conversion of waste cooking oil of 94.2% was reported after 180 min of reaction performed at 65°C, using methanol-to-oil molar ratio of 9:1 and 3 wt. % catalyst amount. Katada et al. (130) reported a study in which the ability of $H_4PNbW_{11}O_{40}/WO_3$-Nb_2O_5 catalyst, after the calcination at 500°C for 180 min, was investigated for transesterification of triolein in the presence of ethanol. The HPAs dispersion on WO_3-Nb_2O_5 support and succeeding calcination of the synthesized catalyst was said to generate the Brønsted acid sites on the acid catalyst surface and create an insoluble material keeping the catalyst active without any significant dissolution of the acid species into the reaction medium.

3.2.4. *Other acid catalysis*

The anchoring of different nature of acidic species on various support materials are studied with an objective to develop a catalyst system withstanding severe reaction conditions. Lam and Lee (131) reported a study in which So_4^{2-}/ SnO_2 was used to assist the alcoholysis of waste cooking oil. The maximum biodiesel yield of 91.5% was obtained after 180 min of the methanolysis reaction performed at 150°C, using methanol-to-oil molar ratio of 30:1, stirring intensity of 350 rpm, and 6 wt. % catalyst amount. Maksimov et al. (132) reported that WO_3/ SnO_2 catalyst exhibited a superior activity than WO_3/ZrO_2 material when used for the liquid phase-catalyzed reactions. Xie and Wang (133) reported that the WO_3/SnO_2 catalyst represented promoted catalytic activity because the impregnation of ammonium metatungstate on SnO_2 surface followed by the calcination process directed the formation of WO_x clusters which have delocalized negative charge across the extended W-O network and accommodate the protons responsible for the Brønsted acid sites generation. The resulting WO_3/SnO_2 catalyst was employed for transesterification of soybean oil and esterification of FFA in model oil prepared using soybean oil, oleic acid, and water. The WO_3/SnO_2 catalyst was said to be active under severe reaction conditions than that required using SO_4^{2-}/SnO_2 catalyst; but then the former catalyst display better stability and represented negligible leaching of the active WO_3 species from the catalyst surface. The reported results suggested that the maximum oil and FFA conversion of 79.2% and 93.8%, respectively, were obtained after 300 min of the alcoholysis reaction performed at 180°C, using methanol-to-oil molar ratio of 30:1 and 5 wt. % catalyst amount. Under the similar reaction conditions, WO_3 (30%)/$AlPO_4$ catalyst, calcined at 800°C for 300

min, assisted 72.5% oil conversion when soybean oil was transesterified with methanol. The activity of the above-mentioned catalyst was said to be superior to that of $TiO_2/AlPO_4$, $MoO_3/AlPO_4$, $SnO_2/AlPO_4$, $ZrO_2/AlPO_4$, and $CeO_2/AlPO_4$ catalysts. The structure of $AlPO_4$ is similar to silica consisting of tetrahedral units of AlO_4 and PO_4; thus, representing large surface properties and high thermal stability, and allows easy incorporation of heterospecies. However, WO_3(30%)/SnO_2 was found to be better catalyst than WO_3 (30%)/$AlPO_4$ because the former catalyst displayed better resistance towards 10% FFA and water (133).

Ramchandran et al. (134) reported the appliance of the sulfonation method assisted aluminium hydrogen phosphate (Al $(HSO_4)_3$) catalyst to assist the alcoholysis of waste vegetable oil. It was mentioned that H_2SO_4 reacted with the large pores of $AlCl_3$ and resulted in the generation of covalently bonded Aluminium with $–SO_3H$ moieties which promoted the overall hydrophilicity of the catalyst. The highest oil conversion of 81% was reported after 50 min of reaction performed at 220°C, using methanol-to-oil molar ratio of 16:1, stirring intensity of 300 rpm, and 0.5 wt. % catalyst amount. However, it is worth noting that the generation of hydrophilic $–SO_3H$ species could also direct the hydration of –OH groups and generate the additional amount of water which eventually will reduce the conversion of TAGs. Hence, the catalyst was found to be deactivating after two recycle tests. Alhassan et al. (135) used ferric hydrogen sulfate ($(Fe(SO_4)_3$) for the simultaneous esterification and transesterification of waste oil containing 14.7 wt. % FFA. The $(Fe(SO_4)_3$ catalyst, after the crystallization due to the thermal treatment at 400°C for 180 min, assisted the formation of 94.5% methyl esters yield when the methanolysis reaction was performed at 205°C, using methanol-to-oil molar ratio of 15:1 and 1 wt. % catalyst amount. The macroporous vanadium phosphate catalyst with V/P=1 having both Brønsted (P-OH) and Lewis acid sites (V=O) have been also tried for biodiesel production from high acidity industrial by-products containing FFA, FAME, and water (136). Chen et al. (137) used the hydrothermal method assisted copper vanadium phosphate catalyst having a three-dimensional network structure for transesterification reaction between soybean oil and methanol. The maximum oil conversion of 65.5% was reported after 300 min of the methanolysis reaction performed at 65°C, using methanol-to-oil molar ratio of 6.75:1, and 1.5% catalyst amount.

3.2.5. *Carbon-based catalysis*

Together with the density of multiple Brønsted acid sites, the hydrophobic feature of catalyst could be of paramount importance in determining the overall activity of solid acid materials for the alcoholysis process. The hydrophobicity of catalyst would hinder unfavorable side reactions caused by the presence of water molecules. The ordered mesoporous carbon materials,

which could be replicated from the ordered mesoporous silica, has hydrophobic surface and could be an ideal support for anchoring the acidic materials. Furthermore, the outstanding hydrothermal and mechanical stability of carbon material is expected to maintain their textural framework even under harsh reaction conditions.

Ong et al. (138) reported a study in which the sol-gel method assisted copper nanoparticles impregnated on activated carbon (AC) catalyst, calcined at 400°C for 360 min, was used to assist esterification of FFA in rubber seed oil. The maximum FFA conversion of 95% was obtained after 360 min of esterification reaction performed at 65°C, using methanol-to-FFA ratio of 10:1, and 8 wt. % Cu (7 wt. %)/AC catalyst amount. Shuit and Tan (139) presented a work focused on different methods used for the functionalization of the multi-walled carbon nanotubes (MWCNTs). The sulfonation of the MWCNTs was performed using different methodologies, such as in-situ polymerization of acetic anhydride and sulfuric acid, thermal decomposition of ammonium sulphate, thermal treatment with sulfuric acid, and in-situ polymerization of poly(sodium 4-stryenesulponate). The obtained catalysts were then used to assist the methanolysis of palm fatty acid distillate. The alcoholysis reactions performed at 170°C for 180 min, using methanol-to-acid molar ratio of 20:1 and 2 wt. % catalyst amount suggested that the maximum biodiesel yield of 93.4% was obtained employing the MWCNTs sulfonated via in-situ polymerization of poly(sodium 4-stryenesulponate). This was due to the higher sulfonic acid group density decorated on the surface of MWCNTs. It was explained that the generated benzenesulfonic acid groups resulted in the resonance. Furthermore, the presence of three electronegative oxygen atoms not only makes SO_3H a strong acidic groups but also the electron-withdrawing groups when the SO_3H species are attached to the benzene molecules. It was stated that when the SO_3H group is attached to the benzene ring, it will remove the electron density from the conjugated π-system of benzene ring via resonance or inductive electron withdrawal; which deactivates the π-system by making it more electrophilic. However, the presence of positive charges in the ortho position via deactivation of the benzene ring by SO_3H favors an esterification reaction because the charges at these positions can play a role similar to that of the sulfur atom in the SO_3H groups to serve as active sites for esterification reaction. Hence, the additional active sites of the catalyst leads toward enhanced biodiesel yields.

Due to the fact that the carbon nanofibers are advantageous in having smaller hydrodynamic resistance, fibrous shape, and high mass transfer rate, these materials are also considered as a viable support for the loading of the active acid catalytic species. Alcaniz-Monge et al. (140) used activated carbon fibers as a support for impregnating HPAs, such as phosphomolybdic acid (HPAMo) and phosphotungstic acid (HPAW). The subsequent catalysts were then utilized for esterification reaction between palmitic acid and methanol.

The reported results suggested that the micro-porosity of carbon fibers restricted the transportation of reagents to the catalyst active centers, thus resulting in low biodiesel yield.

Liu et al. (141) presented a work in which sulfonic acid functionalized ordered mesoporous carbon was used to assist the ethanolysis of oleic acid. The SBA-15 templated mesoporous carbon was treated with 4-benzenediazoniumsulfonate in the presence of hypophosphoric acid. Hence, the sulfonic acid containing aryl radicals reacted with the carbon surface resulting in the formation of sulfonic acid functionalized ordered mesoporous carbon. Zhang et al. (142) documented a work in which the monolithic carbon based nanostructured catalyst with medium acid density were tested for transesterification reaction between soybean oil and methanol. In the synthesis procedure, the carbon nanotubes reacted with sodium polysulfide leading towards the formation of CNT-SH material, followed with its oxidation using hydrogen peroxide to convert –C-SH to –C-SO_3H on the surface of the CNTs. Due to the oxidation step, beside the formation of SO_3H species, the tubular CNTs were abundant with –COOH and –OH moieties. The methanolysis reaction was performed in a catalytic distillation column and the soybean oil conversion higher than 98 % was reported even after 5700 min of continuous biodiesel production process. Poonjarernsilp et al. (143) reported that the chemically resistant, thermally stable, hydrophobic, and high specific surface area sulfonated single-walled carbon nanohorns (SWCNH) represented superior catalytic performance than the homogeneous H_2SO_4 catalyst. The four different carbon based catalysts namely: SO_3H-SWCNH, SO_3H-oxi-SWCNH, SO_3H-activated carbon, and SO_3H-carbon black were synthesized via hydrothermal sulfonation method, and their catalytic performance for esterification reaction between palmitic acid and methanol was investigated. The high catalytic performance of SO_3H-SWCNH was observed and was explained due to higher acid site density. It was a small wonder that the surface area of the SWCNH increased, while that of the oxi-SWCNH depleted on the introduction of sulfonic acid species. It was suggested that the rise in the surface area of SWCNH was due to the opening of small mesopores, whereas the weak sites in the oxi-SWCNH, which were already opened due to the oxidation at 500°C, underwent the structural destruction during the further hydrothermal sulfonation treatment. The sulfonation process directed the re-aggregation of the horn nanostructure, which was explained due to the bridging of acid functional groups formed on the surface of the SWCNH and oxi-SWCNH. However, the micropores in the horn structure remains intact and are responsible for the high surface area of the material. Furthermore, no significant change in the surface area before and after the sulfonation of activated carbon indicated that the sulfonic acid species did not incorporate into the pores and were adsorbed on the external surface of carbon. Hence, it was concluded that the

oxidation process though increased the surface area of the carbon nanohorns, but hindered the incorporation of sulfonic acid species. The SO_3H-SWCNH-assisted alcoholysis reaction performed at 64°C for 300 min, using methanol-to-acid molar ratio of 33:1, stirring intensity of 600 rpm, and 3 wt. % catalyst amount resulted in more than 90% biodiesel yield.

The generation of water during the esterification process usually result toward the deactivation of catalyst due to the adsorption of water molecules on the active centers or due to the lixiviation of catalytic species from the support. Hence, the hydrophobic behavior of carbonaceous materials could encourage the utilization of carbon-based catalysts for the transformation of low-grade feedstocks to biodiesel. Looking at the phenomenal advantages of the carbonaceous materials, the derivatization of carbon materials from the leftover materials, such as glycerol, lignin, microalgae residue, oil cake waste, and canola de-oiled meal are also proposed. The produced hydrophobic carbons were used as a support for anchoring the acid species, and the subsequent catalysts were used to accelerate the alcoholysis reactions (144–148).

3.2.6. *Cation exchange resins*

Park et al. (149) investigated the catalytic performance of Amberlyst 15 and Amberlyst BD 20 ion-exchange resins for esterification of FFA in model oil prepared using soybean oil and oleic acid, and waste trap grease and oleic acid. It was reported that the increment in FFA concentration in the reaction medium resulted in the lowering of the Amberlyst 15 activity. Explaining the reason for such behavior, Park et al. (149) mentioned that the large pore size of Amberlyst 15 resins was responsible for its deactivation because it adsorbs water formed during the esterification process on its inner and outer surface; hence, blocking the active acid sites. Li et al. (92) reported the microwave-assisted transesterification of yellow horn seed oil using the solid acid Amberlyst 15 and Amberlite IRC-72 ion-exchange resins. In this instance, the Amberlyst 15 resins was found to be more active than the other counterpart producing approximately 83% methyl esters yield after 90 min of the alcoholysis reaction performed 60°C, using 5 wt. % catalyst amount. The superior activity of Amberlyst 15 resins was related to its high acidity compared to the Amberlite IRC-72 resins. Hence, it could be said that Amberlyst 15 resins display the good catalytic performance at low concentration of FFA in the reaction medium.

Kouzu et al. (150) reported that the lower cross-linkage of gelular type Amberlyst-31 WET resins were effective in swelling with methanol; thus, eased the methanolysis process. In the published research article, it was mentioned that the gelular-type sulfonated Amberlyst-31WET displayed higher catalytic performance than the mesoporous macro-reticular type sulfonated Amberlyst-15DRY resins for esterification of oleic acid with methanol. It was suggested that the swelling phenomenon increased the surface area of resins,

thereby exposing additional internal acid sites for the reaction. Lopez et al. (151) reported that other than swelling, the surface area and the resultant reactivity of the solid acid resins can be promoted also by supporting the polymers on an inert high surface area oxide materials. The presented paper dealt with the investigation of the catalytic performance of Nafion® SAC-13 and Nafion® NR50 resin catalysts for transesterification between triacetin and methanol. The silica supported Nafion® displayed surface areamore than 200 times higher than that of the non-supported Nafion® resin. Hence, it was said that the reactivity of the supported polymer actually was less reliant on the swelling extent but more on the catalytic active centers.

Feng et al. (152) reported that a macro reticular copolymer styrene-divinyl benzene NKC- 9 cation exchange resins-assisted 98% FFA conversion during 30,000 min of a continuous esterification reaction of FFA from the acidified oil. However, the involvement of water into the reaction medium hindered the performance of the cation exchange resins which was explained due to the blocking of the active centers due to the adsorption of water molecules on $-SO_3H$ groups on the surface of the polymer resins. However, it was said that the continuous removal of the reaction product from the reactor bed also enabled elimination of water and methanol, thus preserving the catalytic activity of resins. Jiang et al. (153) used sulfonated CH-A cation exchange resins to promote esterification reaction between oleic acid and ethanol. The ethanolysis reaction performed in a batch reactor resulted in 92.75% oleic acid conversion after 480 min of reaction performed at 82°C, using 9:1 ethanol-to-acid molar ratio.

4. Influence of different parameters on catalyst and biodiesel production

4.1. *Influence of thermal treatment on physico-chemical properties of catalysis*

It is well known that the calcination process of the solid catalysts, which generally are in carbonate and hydroxide forms, will maximize the active base sites responsible to catalyze the transesterification reaction. Therefore, it could be concluded that the annealing process is one of the indispensable factors influencing the catalytic activity of the heterogeneous catalysts. However, understanding the optimum temperature for the calcination process would also of foremost relevance.

Lin et al. (50) reported that calcining magnetic CaO/α-Fe fibers at low temperature indicated the presence of $CaFe_2O_4$ compounds; however, the calcination at 900°C and above signified the generation of CaO. Thus, it was recommended that the Ca-based materials should be calcined at the temperature minimum of 900°C to achieve CaO compounds, as the carbonate species

decompose at the temperature between 650–850°C (154). Furthermore, the specific surface area and the porosity of the resultant catalyst was also improved with the maximized calcination temperature, which ensured more accessible active centers for the alcoholysis reaction. Similar findings were reported by Sharma et al. (155) where it was stated that the calcination of eggshells at 900°C resulted in the liberation of carbonate and hydroxide species, and in the generation of the active oxide phase. Granados et al. (156), however, stated that the complete removal of OH groups is not possible after the calcination because, after cooling the calcined catalyst to room temperature, the surface moisture is enough to cover the surface of catalyst by layers of $Ca(OH)_2$. Xie et al. (82) demonstrated that the basicity of the catalyst is altered with the calcination temperature. The catalytic activity of Li/ZnO was found to be stimulating with rising calcination temperature from 300–600°C; however, further increment in the calcination temperature to 800°C resulted in the significant decrease in the basicity, and consequently, in the activity of the proposed catalyst. Furthermore, using too high calcination temperature would also lead toward the undesired material transformation. Yang and Xie (88) reported that $Sr(NO_3)_2$/ZnO and $Ba(NO_3)_2$/ZnO, calcined at 500°C and 550°C, respectively, displayed low basic strength; however, the promotion in the calcination temperature to 600°C and 650°C, respectively, resulted in the generation of the additional basic sites and the resultant catalyst exhibited excellent activity for the transesterification reaction. According to Patel et al. (103), on calcination at 600°C for 240 min, the specific surface area and pore volume of SO_4^{2-}/ZrO_2 was reduced but the acidity was increased by 65%. This behavior was due to the formation of the tetragonal phase and augmentation in the Lewis acidity. The increased acidity thus was responsible for the increment in the biodiesel yield. Park et al. (110) reported that the calcination temperature above 800°C resulted in minimizing the tetragonal phase of WO_3/ZrO_2 catalysts. At the calcination temperature above 800°C, the WO_x species were said to agglomerate into a monoclinic WO_3 crystallites and become less effective sintering inhibitors. Lam et al. (157) reported that, along with the temperature, the duration of calcination also decides the quality of the derived catalyst. This is because the reduction in time required for the thermal treatment could direct the incomplete crystallization of the catalytic material. Thus, optimizing the appropriate calcination temperature and time could be of foremost importance in order to develop an active and stable heterogeneous catalyst.

4.2. *Influence of thermal treatment of catalyst on biodiesel production*

It is worth noting that the calcination temperature significantly would affect the physico-chemical properties of the heterogeneous catalysts which, in return, would also affect the yield and the quality of biodiesel. Zhu et al. (49) reported that jatropha curcas oil conversion was decreased from ˜93% to ˜89% when the

CaO catalyst calcination temperature was increased from 900°C to 1100°C. Nakatani et al. (55) observed that when the Oyster shells were annealed at the temperature range between 100–500°C, the biodiesel purity was less than 1 wt. %; however, when the same shells were calcined at 700°C, the biodiesel purity jumped over 95 wt. %. In the case of CaO derived from mussel shells, the yield and the purity of biodiesel were directly proportional to the calcination temperature. When the calcination temperature was increased from 950°C to 1050°C, the biodiesel yield and purity were intensified from ˜38% to ˜72% and from ˜52% to 90%, respectively. The maximum purity and yield of 94.33% and 85.58%, respectively, were obtained when catalyst was calcined at temperature of 1050°C (56). Xie and Zhao (83) found that CaO/SnO_2 catalyst, calcined at 500°C, assisted only 43.1% soybean oil conversion. The rise in the calcination temperature to 700°C promoted the activity of the catalyst resulting in 89.3% oil conversion, however further increment in the calcination temperature reduced the catalytic activity as severe temperature resulted in the sintering of fine crystals and cluster agglomeration. Xie and Wang (158) reported that WO_3/SnO_2 catalyst, when calcined at 200°C, assisted merely 34.2% methyl esters production from soybean oil, however the same catalyst when calcined at 900°C helped in achieving 79.2% biodiesel yield.

4.3. *Reusability of heterogeneous catalysts for biodiesel production*

One of the key aspect related to the development of heterogeneous catalysis for biodiesel production is the possibility of their reutilization. The reusability of catalysts for biodiesel production could be of great industrial relevance. The reutilization of catalytic materials will not only simplify the processing technology but also minimize the economic and environmental concerns. Out of the number of catalyst reviewed, few catalysts have shown promising recyclability and could gain future relevance in biodiesel industries.

Lin et al. (50) reported that the magnetic CaO/α-Fe fibers possessed high catalytic activity for biodiesel production and did not significantly deactivate even after 20 recycle tests. It was presented that even after 20 recycle tests, more than 85% biodiesel yield was achieved. Moreover, due to the magnetic properties, its fast separation from the post-reaction mixture could also be easily done by the appliance of the magnetic field. Huang et al. (48) found that the DES activated CaO catalyst was active for transesterification reaction between rapeseed oil and methanol producing about 85% biodiesel even after 5 recycle tests. Garcia-Sancho et al. (117) reported that Nb_2O_5(8wt. %)/MCM-41 catalyst maintained its activity for 5 recycle runs even in the presence of 1.1 wt. % acidity and 0.2 wt. % water present in the feedstock. With no significant leaching of Nb species into the reaction medium, the biodiesel yield close to 80% was obtained even after five catalytic tests. Corro et al. (113) reported that HF (10%)/SiO_2 catalyst esterified FFA in waste

frying oil for 10 consecutive catalytic tests without any significant loss in its activity. Furthermore, it is noteworthy that the esterification produces water and its presence did not affect the catalytic activity of the proposed catalyst which makes it even more potential candidate for biodiesel production. Liu et al. (141) reported that the sulfonated ordered mesoporous carbon catalyst was active for four catalytic cycles producing around 70% esters yield when oleic acid was esterified in the presence of ethanol.

5. Conclusion

The current article reviewed different forms of heterogeneous catalysts used in biodiesel production where it can be seen that an enormous scientific efforts are invested to improve the performance of the existing catalytic systems. A successful replacement of homogeneous catalysts with heterogeneous materials at industrial scale is anticipated to minimize the elongated separation and purification stages, and consequently, eliminate the generation of wastewater. Furthermore, the reutilization of heterogeneous materials would facilitate their application and help in reducing the cost of biodiesel production. However, governing the catalytic sites concentration along with surface area and porosity of these materials is of foremost relevance. Hence, the type of precursor, catalysis synthesis procedure, and calcination temperature employed was found to have a significant impact on the quality of catalysts. Among the base catalysts, calcium oxide material was found to be gaining consistent scientific as well industrial attention because of its high basicity, low solubility in methanol, and its easy derivatization from natural resources. The uniform dispersion of CaO on an appropriate support, such as ZnO would further enhance the stability and durability of the catalyst under severe reaction conditions. The proficiency of several heterogeneous acid catalysts have also been investigated as acidic materials are known to catalyze both transesterification and esterification reactions. The ordered mesoporous silica supported acid catalysts were discovered to possess excellent ability to assist the alcoholysis reactions with negligible deactivation. The catalysts were stable under harsh reaction conditions and the textural morphology of silica, such as SBA-15 and MCM-41 remained intact. The carbon materials were also considered as an outstanding support for acid catalysts because of their hydrophobic nature.

Funding

The authors would like to express their gratitude to the Norwegian University of Life Sciences (Project No. 1301051406) for their financial support.

References

1. Roy, M.M.; Wang, W.; Bujold, J.; Biodiesel production and comparison of emissions of a DI diesel engine fueled by biodiesel–diesel and canola oil–diesel blends at high idling operations. *Appl. Ener*. 2013, *106*, 198–208.
2. Rashid, U.; Anwar, F.; Knothe, G.; Biodiesel from Milo (Thespesia populnea L.) seed oil. *Biomass Bioener*. 2011, *35*, 4034–4039.
3. U. S Energy Administration. International Energy Outlook 2013; http://www.eia.gov/forecasts/ieo/ (Accessed on April 26, 2015).
4. Marchetti, J.M.; Influence of economical variables on a supercritical biodiesel production process. *Ener. Convers. Manage*. 2013, *75*, 658–663.
5. Li, Q.; Zheng, J.; Yan Y.; Biodiesel preparation catalyzed by compound-lipase in co-solvent. *Fuel Process. Technol*. 2010, *91*, 1229–1234.
6. Peterson, C.L.; Hustrulid, T.; Carbon cycle for rapeseed oil biodiesel fuels. *Biomass Bioener*. 1998, *14*, 91–101.
7. Agarwal, A.K.; Biofuels (alcohols and biodiesel) applications as fuels for internal combustion engines. *Progr. Ener. Combust. Sci*. 2007, *33(3)*, 233–271.
8. Knothe, G.; Improving biodiesel fuel properties by modifying fatty ester composition. *Ener. Environ. Sci*. 2009, *2*, 759–766.
9. Marchetti, J.M.; A summary of the available technologies for biodiesel production based on a comparison of different feedstock's properties. *Process Safety Environ. Protect*. 2012, *90*, 157–163.
10. Hazar, H.; Ozturk, U.; The effects of Al_2O_3–TiO_2 coating in a diesel engine on performance and emission of corn oil methyl ester. *Renew. Ener*. 2010, *35*, 2211–2216.
11. Marchetti, J.M.; Miguel, V.U.; Errazu, A.F.; Techno-economic study of different alternatives for biodiesel production. *Fuel Process. Technol*. 2008, *89*, 740–748.
12. Marchetti, J.M. *Biodiesel Production Technologies*, 1st ed., Nova Science Publisher: New York, 2010.
13. Kenwright, A.M.; Peace, S.K.; Richards, R.W.; Bunn, A.; MacDonald, W.A.; Transesterification in poly(ethylene terephthalate) and poly(ethylene naphthalene 2, 6-dicarboxylate) blends; the influence of hydroxyl end groups. *Polymer* 1999, *40*, 5851–5856.
14. Farahat, M.S.; Abdel-Azim, A-A.A.; Abdel-Raowf, M.E.; Modified unsaturated polyester resins synthesized from poly(ethylene terephthalate) waste, 1. Synthesis and curing characteristics. *Macromolec. Mater. Eng*. 2000, *283*, 1–6.
15. Kim, S.C.; Kim, Y.H.; Lee, H.; Yoon, D.Y.; Song, B.K.; Lipase-catalyzed synthesis of glycerol carbonate from renewable glycerol and dimethyl carbonate through transesterification, *J. Molec. Catal. B Enzym*. 2007, *49*, 75–78.
16. Barrault, J.; Pouilloux, Y.; Clacens, J.M.; Vanhove, C.; Bancquart, S.; Catalysis and fine chemistry. *Catal. Today* 2002, *75*, 177–181.
17. Marchetti, J.M.; Miguel, V.U.; Errazu, A.F.; Possible methods for biodiesel production, *Renew. Sustain. Ener. Rev*. 2007, *11*, 1300–1311.
18. Canakci, M.; Sanli, H.; Biodiesel production from various feedstocks and their effects on the fuel properties. *J. Ind. Microbiol. Biotechnol*. 2008, *35*, 431–441.
19. Zhang, Y.; Dubé, M.A.; McLean, D.D.; Kates, M.; Biodiesel production from waste cooking oil: 1. Process design and technological assessment. *Bioresour. Technol*. 2003, *89*, 1–16.
20. Mohammadshirazi, A.; Akram, A.; Rafiee, S.; Bagheri Kalhor, E.; Energy and cost analyses of biodiesel production from waste cooking oil. *Renew. Sustain. Ener. Rev*. 2014, *33*, 44–49.

21. Andersen, O.; Weinbach, J-E.; Residual animal fat and fish for biodiesel production. Potentials in Norway. *Biomass Bioener*. 2010, *34*, 1183–1188.
22. Noshadi, I.; Amin, N.A.S.; Parnas, R.S.; Continuous production of biodiesel from waste cooking oil in a reactive distillation column catalyzed by solid heteropolyacid: Optimization using response surface methodology (RSM). *Fuel*. 2012, *94*, 156–164.
23. Georgogianni, K.G.; Kontominas, M.G.; Pomonis, P.J.; Avlonitis, D.; Gergis, V.; Conventional and in situ transesterification of sunflower seed oil for the production of biodiesel. *Fuel Process. Technol*. 2008, *89*, 503–509.
24. Velez, A.; Soto, G.; Hegel, P.; Mabe, G.; Pereda, S.; Continuous production of fatty acid ethyl esters from sunflower oil using supercritical ethanol. *Fuel*. 2012, *97*, 703–709.
25. Dias, J.M.; Alvim-Ferraz, M.C.M.; Almeida, M.F.; Comparison of the performance of different homogeneous alkali catalysts during transesterification of waste and virgin oils and evaluation of biodiesel quality. *Fuel* 2008, *87*, 3572–3578.
26. Uzun, B.B.; Kılıç, M.; Özbay, N.; Pütün, A.E.; Pütün, E.; Biodiesel production from waste frying oils: Optimization of reaction parameters and determination of fuel properties. *Energy* 2012, *44*, 347–351.
27. Keera, S.T.; El Sabagh, S.M.; Taman, A.R.; Transesterification of vegetable oil to biodiesel fuel using alkaline catalyst. *Fuel* 2011, *90*, 42–47.
28. Fadhil, A.B.; Ali, L.H.; Alkaline-catalyzed transesterification of Silurus triostegus Heckel fish oil: Optimization of transesterification parameters. *Renew. Ener*. 2013, *60*, 481–488.
29. Brunschwig, C.; Moussavou, W.; Blin, J.; Use of bioethanol for biodiesel production. *Progr. Ener. Combust. Sci*. 2012, *38*, 283–301.
30. Issariyakul, T.; Dalai, A.K.; Biodiesel from vegetable oils. *Renew. Sustain. Ener. Rev*. 2014, *31*, 446–471.
31. Marchetti, J.M.; Errazu, A.F.; Esterification of free fatty acids using sulfuric acid as catalyst in the presence of triglycerides. *Biomass Bioener*. 2008, *32*, 892–895.
32. Soriano, N.U.; Venditti, R.; Argyropoulos, D.S.; Biodiesel synthesis via homogeneous Lewis acid-catalyzed transesterification. *Fuel* 2009, *88*, 560–565.
33. Demirbas, A.; Progress and recent trends in biodiesel fuels. *Ener. Convers. Manage*. 2009, *50*, 14–34.
34. Lam, M.K.; Lee, K.T.; Mohamed, A.R.; Homogeneous, heterogeneous and enzymatic catalysis for transesterification of high free fatty acid oil (waste cooking oil) to biodiesel: A review. *Biotechnol. Adv*. 2010, *28*, 500–518.
35. Tonetto, G.M.; Marchetti, J.M.; Transesterification of soybean oil over Me/Al_2O_3 (Me = Na, Ba, Ca, and K) catalysts and monolith K/Al_2O_3-cordierite. *Topics Catal*. 2010, *53*, 755–762.
36. Sánchez-Cantú, M.; Pérez-Díaz, L.M.; Pala-Rosas, I.; Cadena-Torres, E.; Juárez-Amador, L.; Rubio-Rosas, E.; Rodríguez-Acosta, M.; Valente, J.S.; Hydrated lime as an effective heterogeneous catalyst for the transesterification of castor oil and methanol. *Fuel* 2013, *110*, 54–62.
37. Kazemian, H.; Turowec, B.; Siddiquee, M.N.; Rohani, S.; Biodiesel production using cesium modified mesoporous ordered silica as heterogeneous base catalyst. *Fuel* 2013, *103*, 719–724.
38. Thitsartarn, W.; Kawi, S.; Transesterification of Oil by Sulfated Zr-Supported Mesoporous Silica. *Industr. Eng. Chem. Res*. 2011, *50*, 7857–7865.
39. Weckhuysen, B.M.; Mestl, G.; Rosynek, M.P.; Krawietz, T.R.; Haw, J.F.; Lunsford, J.H.; Destructive adsorption of carbon tetrachloride on alkaline earth metal oxides. *J. Phys. Chem. B* 1998, *102*, 3773–3778.
40. Meher, L.C.; Kulkarni, M.G.; Dalai, A.K.; Naik, S.N.; Transesterification of karanja (Pongamia pinnata) oil by solid basic catalysts. *Eur. J. Lipid Sci. Technol*. 2006, *108*, 389–397.

41. Hattori, H.; Shima, M.; Kabashima, H.; Alcoholysis of ester and epoxide catalyzed by solid bases. *Stud. Surf. Sci. Catal.* 2000, *130*, 3507–3512.
42. Kawashima, A.; Matsubara, K.; Honda, K.; Acceleration of catalytic activity of calcium oxide for biodiesel production. *Bioresour Technol.* 2009, *100*, 696–700.
43. Kouzu, M.; Kasuno, T.; Tajika, M.; Yamanaka, S.; Hidaka, J.; Active phase of calcium oxide used as solid base catalyst for transesterification of soybean oil with refluxing methanol. *Appl. Catal. A Gen.* 2008, *334*, 357–365.
44. Kouzu, M.; Tsunomori, M.; Yamanaka, S.; Hidaka, J.; Solid base catalysis of calcium oxide for a reaction to convert vegetable oil into biodiesel. *Adv. Powder Technol.* 2010, *21*, 488–494.
45. Suryaputra, W.; Winata, I.; Indraswati, N.; Ismadji, S.; Waste capiz (Amusium cristatum) shell as a new heterogeneous catalyst for biodiesel production. *Renew. Ener.* 2013, *50*, 795–799.
46. Granados, M.L.; Martín Alonso, D.; Alba-Rubio, A.C.; Mariscal, R.; Ojeda, M.; Brettes, P.; Transesterification of triglycerides by CaO: increase of the reaction rate by biodiesel addition. *Ener. Fuels.* 2009, *23*, 2259–2263.
47. Granados, M.L.; Alba-Rubio, A.C.; Vila, F.; Martín Alonso, D.; Mariscal, R.; Surface chemical promotion of Ca oxide catalysts in biodiesel production reaction by the addition of monoglycerides, diglycerides and glycerol. *J. Catal.* 2010, *276*, 229–236.
48. Huang, W.; Tang, S.; Zhao, H.; Tian, S.; Activation of commercial CaO for biodiesel production from rapeseed oil using a novel deep eutectic solvent. *Indust. Eng. Chem. Res.* **2013**, *52*, 11943–11947.
49. Zhu, H.; Wu, Z.; Chen, Y.; Zhang, P.; Duan, S.; Liu, X.; MaO, Z.; Preparation of biodiesel catalyzed by solid super base of calcium oxide and its refining process. *Chin. J. Catal.* 2006, *27*, 391–396.
50. Lin, L.; Vittayapadung, S.; Li, X.; Jiang, W.; Shen, X.; Synthesis of magnetic calcium oxide hollow fiber catalyst for the production of biodiesel. *Environ. Progr. Sustain. Ener.* 2013, *32*, 1255–1261.
51. Demirbas, A.; Biodiesel from sunflower oil in supercritical methanol with calcium oxide. *Ener. Convers. Manage.* 2007, *48*, 937–941.
52. Correia, L.M.; Saboya, R.M.A.; de Sousa Campelo, N.; Cecilia, J.A.; Rodríguez-Castellón, E.; Cavalcante Jr, C.L.; Vieira, R.S.; Characterization of calcium oxide catalysts from natural sources and their application in the transesterification of sunflower oil. *Bioresour. Technol.* 2014, *151*, 207–213.
53. Navajas, A.; Issariyakul, T.; Arzamendi, G.; Gandía, L.M.; Dalai, A.K.; Development of eggshell derived catalyst for transesterification of used cooking oil for biodiesel production. *Asia-Pacific J. Chem. Eng.* 2013, *8*, 742–748.
54. Birla, A.; Singh, B.; Upadhyay, S.N.; Sharma, Y.C.; Kinetics studies of synthesis of biodiesel from waste frying oil using a heterogeneous catalyst derived from snail shell. *Bioresour. Technol.* 2012, *106*, 95–100.
55. Nakatani, N.; Takamori, H.; Takeda, K.; Sakugawa, H.; Transesterification of soybean oil using combusted oyster shell waste as a catalyst *Bioresour. Technol.* 2009, *100*, 1510–1513.
56. Rezaei, R.; Mohadesi, M.; Moradi, G.R.; Optimization of biodiesel production using waste mussel shell catalyst. *Fuel.* 2013, *109*, 534–541.
57. Di Serio, M.; Cozzolino, M.; Giordano, M.; Tesser, R.; Patrono, P.; Santacesaria, E.; From homogeneous to heterogeneous catalysts in biodiesel production. *Industr. Eng. Chem. Res.* 2007, *46*, 6379–6384.
58. Dossin, T.; Reyniers, M.; Marin, G.; Kinetics of heterogeneously MgO-catalyzed transesterification. *Appl. Catal. B Environ.* 2006, *62*, 35–45.

59. Almerindo, G.I.; Probst, L.F.D.; Campos, C.E.M.; de Almeida, R.M.; Meneghetti, S.M. P.; Meneghetti, M.R.; Clacens J-M.; Fajardo, H.V.; Magnesium oxide prepared via metal–chitosan complexation method: Application as catalyst for transesterification of soybean oil and catalyst deactivation studies. *J. Power Sour*. 2011, *196*, 8057–8063.
60. Verziu, M.; Cojocaru, B.; Hu, J.; Richards, R.; Ciuculescu, C.; Filip, P.; Parvulescu, V.I.; Sunflower and rapeseed oil transesterification to biodiesel over different nanocrystalline MgO catalysts. *Green Chem*. 2008, *10*, 373–381.
61. Montero, J.M.; Brown, D.R.; Gai, P.L.; Lee, A.F.; Wilson, K.; In situ studies of structure–reactivity relations in biodiesel synthesis over nanocrystalline MgO. *Chem. Eng. J*. 2010, *161*, 332–339.
62. Jeon, H.; Kim, D.J.; Kim, S.J.; Kim, J.H.; Synthesis of mesoporous MgO catalyst templated by a PDMS–PEO comb-like copolymer for biodiesel production. *Fuel Process. Technol*. 2013, *116*, 325–331.
63. Liu, X.; He, H.; Wang, Y.; Zhu, S.; Transesterification of soybean oil to biodiesel using SrO as a solid base catalyst. *Catal. Commun*. 2007, *8*, 1107–1111.
64. Chen, C.L.; Huang, C.C.; Tran, D.T.; Chang, J.S.; Biodiesel synthesis via heterogeneous catalysis using modified strontium oxides as the catalysts. *Bioresour. Technol*. 2012, *113*, 8–13.
65. Yoo, S.J.; Lee, H.S.; Veriansyah, B.; Kim, J.; Kim, J.D.; Lee, Y.W.; Synthesis of biodiesel from rapeseed oil using supercritical methanol with metal oxide catalysts. *Bioresour. Technol*. 2010, *101*, 8686–8689.
66. Babak, S.; Iman, H.; Abdullah, A.Z.; Alkaline earth metal oxide catalysts for biodiesel production from palm oil: elucidation of process behaviors and modeling using response surface methodology. *Iran. J. Chem. Chem. Eng*. 2013, *32 (1)*, 113–126.
67. Patil, P.; Gude, V.G.; Pinappu, S.; Deng, S.; Transesterification kinetics of Camelina sativa oil on metal oxide catalysts under conventional and microwave heating conditions. *Chem. Eng. J*. 2011, *168*, 1296–1300.
68. Mootabadi, H.; Salamatinia, B.; Bhatia, S.; Abdullah, A,Z.; Ultrasonic-assisted biodiesel production process from palm oil using alkaline earth metal oxides as the heterogeneous catalysts. *Fuel* 2010, *89*, 1818–1825.
69. D'Cruz, A.; Kulkarni, M.; Meher, L.; Dalai, A.; Synthesis of biodiesel from canola oil using heterogeneous base catalyst. *J. Am. Oil Chem. Soc*. 2007, *84*, 937–943.
70. Watkins, R.S.; Lee, A.F.; Wilson, K.; Li-CaO catalysed tri-glyceride transesterification for biodiesel applications. *Green Chem*. 2004, *6*, 335–340.
71. Kaur, M.; Ali, A.; Ethanolysis of waste cottonseed oil over lithium impregnated calcium oxide: Kinetics and reusability studies. *Renew. Ener*. 2014, *63*, 272–279.
72. Puna, J.F.; Gomes, J.F.; Bordado, J.C.; Correia, M.J.N.; Dias, A.P.S.; Biodiesel production over lithium modified lime catalysts: Activity and deactivation. *Appl. Catal. A Gen*. 2014, *470*, 451–457.
73. MacLeod, C.S.; Harvey, A.P.; Lee, A.F.; Wilson, K.; Evaluation of the activity and stability of alkali-doped metal oxide catalysts for application to an intensified method of biodiesel production. *Chem. Eng. J*. 2008, *135*, 63–70.
74. Kumar, D.; Ali, A.; Nanocrystalline K–CaO for the transesterification of a variety of feedstocks: Structure, kinetics and catalytic properties. *Biomass Bioener*. 2012, *46*, 459–468.
75. Supamathanon, N.; Wittayakun, J.; Prayoonpokarach, S.; Properties of Jatropha seed oil from Northeastern Thailand and its transesterification catalyzed by potassium supported on NaY zeolite. *J. Industr. Eng. Chem*. 2011, *17*, 182–185.
76. Xie, W.; Huang, X.; Li, H.; Soybean oil methyl esters preparation using NaX zeolites loaded with KOH as a heterogeneous catalyst. *Bioresour. Technol*. 2007, *98*, 936–939.

77. Arzamendi, G.; Campo, I.; Arguiñarena, E.; Sánchez, M.; Montes, M.; Gandía, L.M.; Synthesis of biodiesel with heterogeneous NaOH/alumina catalysts: Comparison with homogeneous NaOH. *Chem. Eng. J*. 2007, *134*, 123–130.
78. Arzamendi, G.; Campo, I.; Arguiñarena, E.; Sánchez, M.; Montes, M.; Gandía, L.M.; Synthesis of biodiesel from sunflower oil with silica-supported NaOH catalysts. *J. Chem. Technol. Biotechnol*. 2008, *83*, 862–870.
79. Liu, C-C.; Lu, W-C.; Liu T-J.; Transesterification of soybean oil using CsF/CaO catalysts. *Ener. Fuels* 2012, *26*, 5400–5407.
80. Woodford, J.J.; Parlett, C.M.A.; Dacquin, J-P.; Cibin, G.; Dent, A.; Montero, J.; Wilson, K.; Lee, A.F.; Identifying the active phase in Cs-promoted MgO nanocatalysts for triglyceride transesterification. *J. Chem. Technol. Biotechnol*. 2014, *89*, 73–80.
81. Baroutian, S.; Aroua, M.K.; Raman, A.A.A.; Sulaiman, N.M.N.; Potassium hydroxide catalyst supported on palm shell activated carbon for transesterification of palm oil. *Fuel Process. Technol*. 2010, *91*, 1378–1385.
82. Xie, W.; Yang, Z.; Chun, H.; Catalytic properties of lithium-doped ZnO catalysts used for biodiesel preparations. *Industr. Eng. Chem. Res*. 2007, *46*, 7942–7949.
83. Xie, W.; Zhao, L.; Production of biodiesel by transesterification of soybean oil using calcium supported tin oxides as heterogeneous catalysts. *Ener. Convers. Manage*. 2013, *76*, 55–62.
84. Zu, Y.; Tang, J.; Zhu, W.; Zhang, M.; Liu, G.; Liu, Y.; Zhang, W.; Jia, M.; Graphite oxide-supported CaO catalysts for transesterification of soybean oil with methanol. *Bioresour. Technol*. 2011, *102*, 8939–8944.
85. Zabeti, M.; Daud, W.M.A.W.; Aroua, M.K.; Biodiesel production using alumina-supported calcium oxide: An optimization study. *Fuel Process. Technol*. 2010, *91*, 243–248.
86. Samart, C.; Chaiya, C.; Reubroycharoen, P.; Biodiesel production by methanolysis of soybean oil using calcium supported on mesoporous silica catalyst. *Ener. Convers. Manage*. 2010, *51*, 1428–1431.
87. Alba-Rubio, A.C.; Santamaría-González, J.; Mérida-Robles, J.M.; Moreno-Tost, R.; Martín-Alonso, D.; Jiménez-López, A.; Maireles-Torres, P.; Heterogeneous transesterification processes by using CaO supported on zinc oxide as basic catalysts. *Catal. Today* 2010, *149*, 281–287.
88. Yang, Z.; Xie, W.; Soybean oil transesterification over zinc oxide modified with alkali earth metals. *Fuel Process. Technol*. 2007, *88*, 631–638.
89. Buasri, A.; Ksapabutr, B.; Panapoy, M.; Chaiyut, N.; Biodiesel production from waste cooking palm oil using calcium oxide supported on activated carbon as catalyst in a fixed bed reactor. *Kor. J. Chem. Eng*. **2012**, *29*, 1708–1712.
90. Zu, Y.; Liu, G.; Wang, Z.; Shi, J.; Zhang, M.; Zhang, W.; Jia, M.; CaO supported on porous carbon as highly efficient heterogeneous catalysts for transesterification of triacetin with methanol. *Ener. Fuels* 2010, *24*, 3810–3816.
91. Wan, Z.; Hameed, B.H.; Transesterification of palm oil to methyl ester on activated carbon supported calcium oxide catalyst. *Bioresour. Technol*. 2011, *102*, 2659–2664.
92. Li, J.; Fu, Y.J.; Qu, X.J.; Wang, W.; Luo, M.; Zhao, C.J.; Zu, Y.G.; Biodiesel production from yellow horn (Xanthoceras sorbifolia Bunge.) seed oil using ion exchange resin as heterogeneous catalyst. *Bioresour. Technol*. 2012, *108*, 112–118.
93. Vicente, G.; Coteron, A.; Martinez, M.; Aracil, A.; Applications of the factorial design of experiments and response surface methodology to optimize biodiesel production. *Industr. Crops Products*. 1998, *8(1)*, 29–35.
94. Shibasaki-Kitakawa, N.; Honda, H.; Kuribayashi, H.; Toda, T.; Fukumura, T.; Yonemoto, T.; Biodiesel production using anionic ion-exchange resin as heterogeneous catalyst. *Bioresour. Technol*. 2007, *98*, 416–421.

95. Kim, M.; Salley, S.O.; Ng, K.Y.S.; Transesterification of glycerides using a heterogeneous resin catalyst combined with a homogeneous catalyst. *Ener. Fuels*. 2008, *22*, 3594–3599.
96. Long, T.; Deng, Y.; Li, G.; Gan, S.; Chen, J.; Application of N-?methylimidizolium functionalized anion exchange resin containing NaOH for production of biodiesel. *Fuel Process. Technol*. 2011, *92*, 1328–1332.
97. Ren, Y.; He, B.; Yan, F.; Wang, H.; Cheng, Y.; Lin, L.; Feng, Y.; Li, J.; Continuous biodiesel production in a fixed bed reactor packed with anion-exchange resin as heterogeneous catalyst. *Bioresour. Technol*. 2012, *113*, 19–22.
98. He, B.; Ren, Y.; Cheng, Y.; Li, J.; Deactivation and in situ regeneration of anion exchange resin in the continuous transesterification for biodiesel production. *Ener. Fuels* 2012, *26*, 3897–38902.
99. Rattanaphra, D.; Harvey, A.; Srinophakun, P.; Simultaneous conversion of triglyceride/free fatty acid mixtures into biodiesel using sulfated zirconia. *Top Catal*. 2010, *53*, 773–782.
100. Sani, Y.M.; Daud, W.M.A.W.; Abdul Aziz, A.R.; Activity of solid acid catalysts for biodiesel production: a critical review. *Appl. Catal. A Gen*. 2014, *470*, 140–161.
101. Lotero, E.; Liu, Y.; Lopez, D.E.; Suwannakarn, K.; Bruce, D.A.; Goodwin, J.G.; Synthesis of biodiesel via acid catalysis. *Industr. Eng. Chem. Res*. 2005, *44*, 5353–5363.
102. Yadav, G.D.; Nair, J.J.; Sulfated zirconia and its modified versions as promising catalysts for industrial processes. *Micropor. Mesopor. Mater*. 1999, *33*, 1–48.
103. Patel, A.; Brahmkhatri, V.; Singh, N.; Biodiesel production by esterification of free fatty acid over sulfated zirconia. *Renew. Ener*. 2013, *51*, 227–233.
104. Thiruvengadaravi, K.V.; Nandagopal, J.; Baskaralingam, P.; Sathya Selva Bala, V.; Sivanesan, S.; Acid-catalyzed esterification of karanja (Pongamia pinnata) oil with high free fatty acids for biodiesel production. *Fuel* 2012, *98*, 1–4.
105. Garcia, C.M.; Teixeira, S.; Marciniuk, L.L.; Schuchardt, U.; Transesterification of soybean oil catalyzed by sulfated zirconia. *Bioresour. Technol*. 2008, *99*, 6608–6613.
106. Rattanaphra, D.; Harvey, A.P.; Thanapimmetha, A.; Srinophakun, P.; Simultaneous transesterification and esterification for biodiesel production with and without a sulphated zirconia catalyst. *Fuel* 2012, *97*, 467–475.
107. Suwannakarn, K.; Lotero, E.; Goodwin Jr, J.G.; Lu, C.; Stability of sulfated zirconia and the nature of the catalytically active species in the transesterification of triglycerides. *J. Catal*. 2008, *255*, 279–286.
108. López, D.E.; Goodwin, J.G.; Bruce, D.A.; Lotero, E.; Transesterification of triacetin with methanol on solid acid and base catalysts. *Appl. Catal. A Gen*. 2005, *295*, 97–105.
109. Park, Y-M.; Lee, J.Y.; Chung, S-H.; Park, I.S.; Lee, S-Y.; Kim, D-K.; Lee, J-S.; Lee K-Y.; Esterification of used vegetable oils using the heterogeneous WO_3/ZrO_2 catalyst for production of biodiesel. *Bioresour. Technol*. 2010, *101*, S59–S61.
110. Park, Y-M.; Chung, S-H.; Eom, H.J.; Lee, J-S.; Lee, K-Y.; Tungsten oxide zirconia as solid superacid catalyst for esterification of waste acid oil (dark oil). *Bioresour. Technol*. 2010, *101*, 6589–6593.
111. Park, Y-M.; Lee, D-W.; Kim, D-K.; Lee, J-S.; Lee, K-Y.; The heterogeneous catalyst system for the continuous conversion of free fatty acids in used vegetable oils for the production of biodiesel. *Catal. Today* 2008, *131*, 238–243.
112. Galarneau, A.; Cambon, H.; Di Renzo, F.; Fajula, F.; True microporosity and surface area of mesoporous SBA-15 silicas as a function of synthesis temperature. *Langmuir* 2001, *17*, 8328–8335.
113. Corro, G.; Tellez, N.; Jimenez, T.; Tapia, A.; Banuelos, F.; Vazquez-Cuchillo, O.; Biodiesel from waste frying oil. Two step process using acidified SiO_2 for esterification step. *Catal. Today*. 2011, *166*, 116–122.

114. Đokić, M.; Kesić, Ž.; Krstić, J.; Jovanović, D.; Skala, D.; Decrease of free fatty acid content in vegetable oil using silica supported ferric sulfate catalyst. *Fuel* 2012, *97*, 595–602.
115. Grün, M.; Unger, K.K.; Matsumoto, A.; Tsutsumi, K.; Novel pathways for the preparation of mesoporous MCM-41 materials: control of porosity and morphology. *Micropor. Mesopor. Mater*. 1999, *27*, 207–216.
116. Zhao, X.S.; Lu, G.Q.; Millar, G.J.; Advances in mesoporous molecular sieve MCM-41. *Industr. Eng. Chem. Res*. 1996, *35*, 2075–2090.
117. García-Sancho, C.; Moreno-Tost, R.; Mérida-Robles, J.M.; Santamaría-González, J.; Jiménez-López, A.; Maireles-Torres, P.; Niobium-containing MCM-41 silica catalysts for biodiesel production. *Appl. Catal. B Environ*. 2011, 108–109, 161–167.
118. Carmo Jr, A.C.; de Souza, L.K.C.; da Costa, C.E.F.; Longo, E.; Zamian, J.R.; da Rocha Filho, G.N.; Production of biodiesel by esterification of palmitic acid over mesoporous aluminosilicate Al-MCM-41. *Fuel* 2009, *88*, 461–468.
119. Xu, W.; Gao, L.; Wang, S.; Xiao, G.; Biodiesel production in a membrane reactor using MCM-41 supported solid acid catalyst. *Bioresour. Technol*. 2014, *159*, 286–291.
120. Margolese, D.; Melero, J.A.; Christiansen, S.C.; Chmelka, B.F.; Stucky, G.D.; Direct syntheses of ordered SBA-15 mesoporous silica containing sulfonic acid groups. *Chem. Mater*. 2000, *12*, 2448–2459.
121. Shah, K.A.; Parikh, J.K.; Maheria, K.C.; Biodiesel synthesis from acid oil over large pore sulfonic acid-modified mesostructured SBA-15: Process optimization and reaction kinetics. *Catal. Today*. 2014, *237*, 29–37.
122. Xie, W.; Qi, C.; Wang, H.; Liu, Y.; Phenylsulfonic acid functionalized mesoporous SBA-15 silica: A heterogeneous catalyst for removal of free fatty acids in vegetable oil. *Fuel Process. Technol*. 2014, *119*, 98–104.
123. Iglesias, J.; Melero, J.A.; Bautista, L.F.; Morales, G.; Sánchez-Vázquez, R.; Continuous production of biodiesel from low grade feedstock in presence of Zr-SBA-15: catalyst performance and resistance against deactivation. *Catal. Today*. 2014, *234*, 174–181.
124. Chen, S-Y.; Mochizuki, T.; Abe, Y.; Toba, M.; Yoshimura, Y.; Production of high-quality biodiesel fuels from various vegetable oils over Ti-incorporated SBA-15 mesoporous silica. *Catal. Commun*. 2013, *41*, 136–139.
125. Barrón Cruz, A.E.; Melo Banda, J.A.; Mendoza, H.; Ramos-Galvan, C.E.; Meraz Melo, M.A.; Esquivel, D.; Pt and Ni supported catalysts on SBA-15 and SBA-16 for the synthesis of biodiesel. *Catal. Today*. 2011, *166*, 111–115.
126. Sharma, Y.C.; Singh, B.; Korstad, J.; Advancements in solid acid catalysts for eco-friendly and economically viable synthesis of biodiesel. *Biofuels Bioprod. Biorefin*. 2011, *5*, 69–92.
127. Tropecêlo, A.I.; Casimiro, M.H.; Fonseca, I.M.; Ramos, A.M.; Vital, J.; Castanheiro, J.E.; Esterification of free fatty acids to biodiesel over heteropolyacids immobilized on mesoporous silica. *Appl. Catal. A Gen*. 2010, *390*, 183–189.
128. Khayoon, M.S.; Hameed, B.H.; Single-step esterification of crude karanj (Pongamia pinnata) oil to fatty acid methyl esters over mesostructured SBA-16 supported 12-molybdophosphoric acid catalyst. *Fuel Process. Technol*. 2013, *114*, 12–20.
129. Zou, C.; Zhao, P.; Shi, L.; Huang, S.; Luo, P.; Biodiesel fuel production from waste cooking oil by the inclusion complex of heteropoly acid with bridged bis-cyclodextrin. *Bioresour. Technol*. 2013, *146*, 785–788.
130. Katada, N.; Hatanaka, T.; Ota, M.; Yamada, K.; Okumura, K.; Niwa, M.; Biodiesel production using heteropoly acid-derived solid acid catalyst $H_4PNbW_{11}O_{40}/WO_3$–Nb_2O_5. *Appl. Catal. A Gen*. 2009, *363*, 164–168.
131. Lam, M.K.; Lee, K.T.; Accelerating transesterification reaction with biodiesel as co-solvent: A case study for solid acid sulfated tin oxide catalyst. *Fuel* 2010, *89*, 3866–3870.

132. Maksimov, G.M.; Fedotov, M.A.; Bogdanov, S.V.; Litvak, G.S.; Golovin, A.V.; Likholobov, V.A.; Synthesis and study of acid catalyst 30% WO_3/SnO_2. *J. Molec. Catal. A Chem*. 2000, *158*, 435–438.
133. Xie, W.; Yang, D.; Transesterification of soybean oil over WO_3 supported on $AlPO_4$ as a solid acid catalyst. *Bioresour. Technol*. 2012, *119*, 60–65.
134. Ramachandran, K.; Sivakumar, P.; Suganya, T.; Renganathan, S.; Production of biodiesel from mixed waste vegetable oil using an aluminium hydrogen sulphate as a heterogeneous acid catalyst. *Bioresour. Technol*. 2011, *102*, 7289–7293.
135. Alhassan, F.H.; Yunus, R.; Rashid, U.; Sirat, K.; Islam, A.; Lee, H.V.; Taufiq-Yap, Y.H.; Production of biodiesel from mixed waste vegetable oils using Ferric hydrogen sulphate as an effective reusable heterogeneous solid acid catalyst. *Appl. Catal. A Gen*. 2013, *456*, 182–187.
136. Domingues, C.; Correia, M.J.; Carvalho, R.; Henriques, C.; Bordado, J.; Dias, A.P.; Vanadium phosphate catalysts for biodiesel production from acid industrial by-products. *J. Biotechnol*. 2013, *164*, 433–440.
137. Chen, L.; Yin, P.; Liu, X.; Yang, L.; Yu, Z.; Guo, X.; Xin, X.; Biodiesel production over copper vanadium phosphate. *Energy* 2011, *36*, 175–180.
138. Ong, H.R.; Khan, M.R.; Chowdhury, M.N.K.; Yousuf, A.; Cheng, C.K.; Synthesis and characterization of CuO/C catalyst for the esterification of free fatty acid in rubber seed oil. *Fuel* 2014, *120*, 195–201.
139. Shuit, S.H.; Tan, S.H.; Feasibility study of various sulphonation methods for transforming carbon nanotubes into catalysts for the esterification of palm fatty acid distillate. *Ener. Convers. Manage*. 2014, *88*, 1283–1289.
140. Alcañiz-Monge, J.; Trautwein, G.; Marco-Lozar, J.P.; Biodiesel production by acid catalysis with heteropolyacids supported on activated carbon fibers. *Appl. Catal. A Gen*. 2013, *468*, 432–441.
141. Liu, R.; Wang, X.; Zhao, X.; Feng, P.; Sulfonated ordered mesoporous carbon for catalytic preparation of biodiesel. *Carbon* **2008**, *46*, 1664–1669.
142. Zhang, D.; Wei, D.; Ding, W.; Zhang, X.; Carbon-based nanostructured catalyst for biodiesel production by catalytic distillation. *Catal. Commun*. 2014, *43*, 121–125.
143. Poonjarernsilp, C.; Sano, N.; Tamon, H.; Hydrothermally sulfonated single-walled carbon nanohorns for use as solid catalysts in biodiesel production by esterification of palmitic acid. *Appl. Catal. B Environ*. 2014, *147*, 726–732.
144. Shu, Q.; Nawaz, Z.; Gao, J.; Liao, Y.; Zhang, Q.; Wang, D.; Wang, J.; Synthesis of biodiesel from a model waste oil feedstock using a carbon-based solid acid catalyst: reaction and separation. *Bioresour. Technol*. 2010, *101*, 5374–5384.
145. Shu, Q.; Gao, J.; Liao, Y.; Wang, J.; Reaction kinetics of biodiesel synthesis from waste oil using a carbon-based solid acid catalyst. *Chin. J. Chem. Eng*. 2011, *19*, 163–168.
146. Rao, B.V.S.K.; Chandra Mouli, K.; Rambabu, N.; Dalai, A.K.; Prasad, R.B.N.; Carbon-based solid acid catalyst from de-oiled canola meal for biodiesel production. *Catal. Commun*. 2011, *14*, 20–26.
147. Guo, F.; Xiu, Z-L.; Liang, Z-X.; Synthesis of biodiesel from acidified soybean soapstock using a lignin-derived carbonaceous catalyst. *Appl. Ener*. 2012, *98*, 47–52.
148. Fu, X.; Li, D.; Chen, J.; Zhang, Y.; Huang, W.; Zhu, Y.; Yang, J.; Zhang, C.; A microalgae residue based carbon solid acid catalyst for biodiesel production. *Bioresour. Technol*. 2013, *146*, 767–770.
149. Park, J.Y.; Kim, D.K.; Lee, J.S.; Esterification of free fatty acids using water-tolerable amberlyst as a heterogeneous catalyst. *Bioresour. Technol*. 2010, *101(Suppl 1)*, S62–S65.
150. Kouzu, M.; Nakagaito, A.; Hidaka, J-S.; Pre-esterification of FFA in plant oil transesterified into biodiesel with the help of solid acid catalysis of sulfonated cation-exchange resin. *Appl. Catal. A Gen*. 2011, *405*, 36–44.

151. Lopez, D.; Goodwinjr, J.; Bruce, D.; Transesterification of triacetin with methanol on Nafion® acid resins. *J. Catal.* 2007, *245*, 381–391.
152. Feng, Y.; Zhang, A.; Li, J.; He, B.; A continuous process for biodiesel production in a fixed bed reactor packed with cation-exchange resin as heterogeneous catalyst. *Bioresour. Technol.* 2011, *102*, 3607–3609.
153. Jiang, Y.; Lu, J.; Sun, K.; Ma, L.; Ding, J.; Esterification of oleic acid with ethanol catalyzed by sulfonated cation exchange resin: experimental and kinetic studies. *Ener. Convers. Manage.* 2013, *76*, 980–985.
154. Smith, S.M.; Oopathum, C.; Weeramongkhonlert, V.; Smith, C.B.; Chaveanghong, S.; Ketwong, P.; Boonyuen, S.; Transesterification of soybean oil using bovine bone waste as new catalyst. *Bioresour. Technol.* 2013, *143*, 686–690.
155. Sharma, Y.C.; Singh, B.; Korstad, J.; Application of an efficient nonconventional heterogeneous catalyst for biodiesel synthesis from pongamia pinnata oil. *Ener. Fuels* 2010, *24*, 3223–3231.
156. Granados, M.L.; Poves, M.D.Z.; Alonso, D.M.; Mariscal, R.; Galisteo, F.C.; Moreno-Tost, R.; Santamaria, J.; Fiero, J.L.G.; Biodiesel from sunflower oil by using activated calcium oxide. *Appl. Catal. B Environ.* 2007, *73*, 317–326.
157. Lam, M.K.; Lee, K.T.; Mohamed, A.R.; Sulfated tin oxide as solid superacid catalyst for transesterification of waste cooking oil: an optimization study. *Appl. Catal. B Environ.* 2009, *93*, 134–139.
158. Xie, W.; Wang, T.; Biodiesel production from soybean oil transesterification using tin oxide-supported WO_3 catalysts. *Fuel Process. Technol.* 2013, *109*, 150–155.

Paper III

Fuel 179 (2016) 332–338

Contents lists available at ScienceDirect

Fuel

journal homepage: www.elsevier.com/locate/fuel

Renewable production of value-added jojobyl alcohols and biodiesel using a naturally-derived heterogeneous green catalyst

M.R. Avhad [a], M. Sánchez [b], E. Peña [b], A. Bouaid [b], M. Martínez [b], J. Aracil [b], J.M. Marchetti [a,*]

[a] Department of Mathematical Science and Technology, Norwegian University of Life Sciences, Drøbakveien 31, 1432 Ås, Norway
[b] Chemical Engineering Department, Faculty of Chemistry, Complutense University, 28040 Madrid, Spain

HIGHLIGHTS

- Green catalyst for the production of value-added alcohols and biodiesel.
- All raw materials could be obtained from the underutilized natural resources.
- Butanol-to-jojoba oil molar ratio had a major impact on the alcoholysis process.
- The surface reaction controlled the overall butanolysis process.

GRAPHICAL ABSTRACT

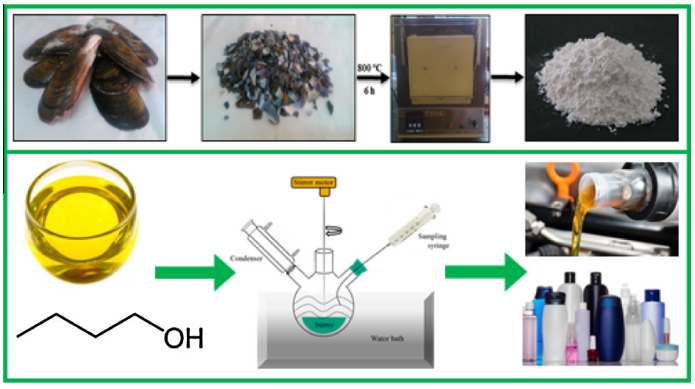

ARTICLE INFO

Article history:
Received 19 February 2016
Received in revised form 29 March 2016
Accepted 31 March 2016
Available online 7 April 2016

Keywords:
Jojoba oil
Butanol
Mytilus Galloprovincialis shells
Calcium oxide
Biodiesel
Kinetic model

ABSTRACT

The present article addresses the generation of value-added jojobyl alcohols and biodiesel using the underutilized renewable natural resources. The butanolysis reaction of jojoba oil required for its transformation to jojobyl alcohols and fatty acid butyl esters was performed over mussel shells derived calcium oxide as a heterogeneous base catalyst. This study systematically investigated the influence of temperature, time, n-butanol concentration and catalyst loading on the butanolysis process. The results of the present study indicated that n-butanol concentration had a major impact on the reaction. The maximum jojoba oil conversion of 96.11% was registered after 1800 min of transesterification reaction performed at 85 °C using butanol-to-oil molar ratio of 10:1, 12 wt.% catalyst amount and 350 rpm stirring intensity. A mathematical model for its kinetics was developed based on a three-step mechanism equivalent to the Eley–Rideal one. It was concluded that the butanolysis reaction occurred between the surface chemisorbed butoxide ions and jojoba oil molecules in the liquid phase, whereas, the overall process was controlled by the surface reaction.

1. Introduction

Plant biomass, the only current sustainable source of organic carbon, has been considered as the promising equivalent to petroleum for the production of fuel and value-added chemicals. The establishment of plant biomass-based energy is anticipated to minimize the entire dependency on the utilization of fossil fuels [1]. Additionally, biomass feedstocks feature a closed carbon cycle in which the carbon dioxide released during the energy conversion is recaptured by the existing plants via photosynthesis during biomass regrowth. The "Roadmap for Biomass Technologies", set by

* Corresponding author.
E-mail address: jorge.mario.marchetti@nmbu.no (J.M. Marchetti).

http://dx.doi.org/10.1016/j.fuel.2016.03.107
0016-2361/

the U.S. Department of Energy, has predicted that by 2030, 20% of transportation fuel and 25% of chemicals would be produced from biomass [2]. The occurring dynamic transition of the global dependence on fossil fuels to renewable energy is understood not only for the effective management of environmental situations but also to augment the agriculture-based economy. However, the nature of biomass feedstock applied for the large-scale production of fuel and chemicals is an important aspect affecting the economics of the process [3]. Consistent scientific efforts are underway in finding a cost-effective and abundantly available non-edible oil-rich biomass. Jojoba oil is a light golden color fluid that differs profoundly from other seed oils because of the absence of glycerol molecules. Its chemical structure could be explained as a mixture of esters of straight long-chain fatty acids and fatty alcohols [4,5]. The available reports indicate that jojoba oil is not poisonous to human, but is poorly digestible and is not considered a part of human food chain; hence, is categorized as the non-edible oil [4]. The presence of 20–44 carbon atoms make it good combustion substance and is utilized as lubricant in high-speed machinery in the automotive industry [6,7]. The studies reported by Al-Widyan and Al-Muhtaseb [8] and Al-Hamamre and Rawajfeh [9] suggested that jojoba oil, having energy content higher than 40 MJ kg^{-1}, can possibly be used as direct fuel for the compression-ignition engines. However, the high kinematic viscosity of oil could cause several operational problems, such as poor atomization of the fuel spray, carbon deposits due to incomplete combustion, and gelling of lubricating oil. Since the last few years, several methodologies have emerged as a possible way to lower the kinematic viscosity of oil, out of which the alcoholysis procedure is well known and extensively applied. The alcoholysis process would enable the transformation of jojoba oil to fatty acid alkyl esters (FAAE) and jojobyl alcohol (11-eicosenol, 13-docosenol and 15-tetracosenol). The derivatives of jojoba oil, such as jojobyl alcohols finds their high relevance in the pharmaceuticals, cosmetics and coating industries, while, the fatty acid alkyl esters (biodiesel) could be utilized as biofuel in the automotive industries [6,7]. After the synthesis of jojobyl alcohols and biodiesel, the seed residue, having heating value higher than 13 MJ kg^{-1}, could be used for direct combustion or as a substrate for the biogasification process [8,9]. Therefore, the environmental and economic benefits gained through the appropriate utilization of jojobyl alcohols, FAAE and jojoba leftover could lead to a successful jojoba-based biorefinery and encourage the expansion of agriculture of jojoba plant.

In the present study, the alcoholysis reactions were performed between jojoba oil and n-butanol, the rate of which was accelerated using calcium oxide (CaO) catalyst. The utilization of n-butanol for the alcoholysis reaction could be advantageous because it can be synthesized through the Acetone–Butanol–Ethanol fermentation process using the reasonable cost and easily available lignocellulosic materials, such as wood forestry residues, corn stover, wheat and barley straw [10,11]. In comparison to fatty acid methyl esters (FAME), the synthesis of fatty acid butyl esters (FABE) is beneficial as the extra carbon atoms introduced by the butanol molecule will improve the cetane number, oxidation stability, cold filter plugging point, cloud point, pour point and heating value of biodiesel [12]. However, the kinematic viscosity of FABE is higher than that of FAME. The production of FABE could be of considerable relevance because, unlike methanol, butanol is renewable and is safe to handle. Additionally, the CaO catalyst was derived from mussel shells (*Mytilus Galloprovincialis*), which is a waste generated from the fish industry. Therefore, all the raw materials utilized for the production of fuel and chemicals are available from natural resources; following the principles of green chemistry. To the best of our knowledge, no studies on the CaO-catalyzed jojoba oil butanolysis process and its kinetic modeling have been so far reported. The influence of temperature, catalyst amount, n-butanol concentration and time on the CaO-catalyzed butanolysis process of jojoba oil was systematically investigated. The interaction between the reaction variables and the optimal conditions affecting the process were determined by means of the response surface methodology (RSM). Furthermore, the Eley–Rideal approach was used to select a mathematical model capable of describing the kinetics of the CaO-catalyzed butanolysis process of jojoba oil over the applied range of experimental conditions.

2. Experimental section

2.1. Materials

Jojoba oil was supplied by Jojoba Israel (Kibbutz Hatzerim, Israel). Its physico-chemical properties were determined in accordance to the AOCS official methods, and published elsewhere [13]. The n-butanol (Cor Quimica, Spain), n-octyl octanoate (Sigma–Aldrich) and carbon disulphide (Panreac) were utilized as received. The waste mussel shells required for the synthesis of CaO catalyst were obtained from the local fish market in Madrid, Spain.

2.2. Catalyst preparation

The mussel shells were carefully washed under the flow of tap water to remove the adsorbed superfluous materials. The cleaned shells were dried in an oven, set at 100 °C, for 60 min. The shells were subsequently pulverized, placed in a silica crucible and calcined in a ceramic muffle heating furnace, set at 800 °C, for 360 min. The selection of the calcination temperature was based on the former investigation performed in the same laboratory [14]. This is because the appliance of too low temperatures could result in the incomplete formation of the oxide species, whereas, too high temperatures could direct the undesired material transformation and reduction in the basic strength of the catalyst. The heating furnace was shut down after 360 min. of the calcination process and allowed to cool. The obtained white colored solid was removed from the furnace, preserved in an airtight container to avoid poisoning due to ambient air while handling or weighing, and utilized instantaneously to assist the butanolysis reaction. The results obtained for the characterization of the catalytic material by means of X-ray diffraction, specific surface area analysis, induced coupled plasma atomic emission spectroscopy and transmission electron microscopy have been reported elsewhere [14].

2.3. Reaction and analysis

The CaO-catalyzed butanolysis reaction between jojoba oil and n-butanol was conducted in a three-neck curved bottom glass reactor of 250 cm^3 volume capacity. Both the diameter and the length of the glass reactor is equivalent to 12.0 cm. The middle neck of the reactor was used to insert the mechanical stirrer equipped with an impeller of 6.0 cm diameter placed centrically close to the bottom. One of the side necks was fitted with the water cooling condenser; while the other neck, was fitted with a rubber cork through which the aliquots of the reaction mixture were periodically withdrawn using a glass syringe. The glass reactor was immersed into a thermostatically controlled water bath (Heto-Holten A/S, Denmark), the temperature of which was controlled by a PID controller with 1 °C precision. The speed of the mechanical stirrer was monitored by a motor (Eurostar Basic IKA).

Initially, the measured quantities of jojoba oil and CaO catalyst were added to the glass reactor and heated to the desired temperature. Once the temperature reached the set point, an appropriate

volume of n-butanol was introduced into the agitated reactor using a conical funnel; this was considered as the starting time of the butanolysis reaction. The stirring intensity was maintained at 350 rpm for all experiments to overcome the mass-transfer limitations [14]. The aliquots (approximately 1 mL) of the reaction mixture were withdrawn at a specified time intervals (100, 200, 300, 400, 500, 600 min) to study the progress of the reaction. The extracted samples were immediately applied to a rota-evaporator attached to a vacuum pump (10 mg Hg), set at 80 °C, for 30 min. to eliminate the residual n-butanol. The catalyst was separated through centrifugation (1500 rpm for 15 min). The reaction samples were analyzed using the gas chromatography (GC) analyzer (Hewlett–Packard HP-5890 Series II) equipped with a flame ionization detector and a fused silica capillary column (12 m length, 0.31 mm internal diameter and 0.71 μm thickness). A Hewlett–Packard 3396SA integrator was connected to the chromatograph. The injection system was split–splitless, and helium was the carrier gas at a 1 mL min^{-1} flowrate. The injector and the detector temperature were set at 275 °C and 325 °C, respectively. The GC column temperature was initially held at 130 °C for 1 min, then raised at 2 °C min^{-1} to 160 °C, and finally heating at a ramp rate of 30 °C min^{-1} to 320 °C. The n-octyl octonoate was used as an internal standard and the extracted reaction samples were dissolved in carbon disulfide. The GC analysis was conducted by injecting 1 μL volume of the prepared samples into the instrument.

2.4. Design of experiments

A set of experiments was designed and the data obtained from the experimental findings were fit to a two-level factorial design for the application of the RSM using the Statgraphics centurion XV software (Statpoint technologies, Inc., USA), utilized for the regression and graphical analyses. The response selected was the conversion of jojoba oil, while, the factors investigated were butanol-to-oil molar ratio (X_B) and catalyst amount (X_C). The influences associated with interactions were estimated considering the oil conversion at the high and low values of each factor. The variability in the dependent parameters was determined by the multiple coefficients of regression, while, the model equation was utilized to predict the optimal conditions affecting the CaO-catalyzed butanolysis process of jojoba oil.

2.5. Theoretical background

The overall alcoholysis reaction between jojoba oil and n-butanol, in the presence of solid CaO catalyst with stoichiometry could be represented as:

$$J + B \xleftrightarrow{catalyst} JA + BE \quad (1)$$

where J is jojoba oil, B is n-butanol, JA is jojobyl alcohols and BE is fatty acid butyl esters.

For the purpose of modeling the described butanolysis process of jojoba oil, the following commonly applied assumptions were taken into considerations [15–18]:

(1) The reaction mixture was perfectly mixed, and its composition, catalyst distribution and temperature were uniform throughout the process because the reaction was performed in a batch reactor under continuous, vigorous stirring [15–17].
(2) The internal diffusion rate inside the catalyst particles does not influence the rate of the butanolysis reaction because of low porosity and small surface area of CaO catalyst [15,16].
(3) The contribution of homogeneous and thermal catalysis is insignificant because CaO is poorly soluble in the reaction mixture and acts as a heterogeneous catalyst [15,17,18].

3. Results and discussion

3.1. Statistical analysis

The statistical analysis of the CaO-catalyzed jojoba oil butanolysis process was performed using the components involved in the reactor, such as n-butanol and catalyst, in all cases keeping a fixed reaction temperature of 85 °C and 350 rpm stirring intensity. The linear and non-linear stage of the two-level factorial design consisted of four experiments each, along with four replicates of the center points. The natural factors, the coded factors and the experimental results for the jojoba oil conversion obtained after 600 min of the described butanolysis reaction are summarized in Table 1.

3.1.1. Linear stage

The evaluation of the interaction between the reaction variables as well as their influence on the overall CaO-catalyzed jojoba oil butanolysis process was done using the linear stage and center points of the experiments. The responses of the statistical analysis are listed in Table 2. Based on the calculated parameters, it was understood that both catalyst amount and butanol-to-oil molar ratio had a significant impact on the described butanolysis process because the influence of both variables was considerably higher than the confidence interval. The linear statistical and industrial mathematical regression models were developed using the coded and natural values, respectively. The linear statistical and industrial model for the CaO-catalyzed jojoba oil butanolysis process

Table 1
Two-level factorial design of experiments. Stages of experiments along with the natural and coded values of the reaction variables, and the obtained jojoba oil conversion.

Type of experiment	Run	Butanol-to-oil molar ratio	Catalyst amount (%)	X_B	X_C	Conversion (%)
Linear stage	1	12.8:1	16	1	1	63.21
	2	12.8:1	8	1	−1	45.10
	3	7.2:1	16	−1	1	42.31
	4	7.2:1	8	−1	−1	39.77
Center stage	5	10:1	12	0	0	55.15
	6	10:1	12	0	0	53.28
	7	10:1	12	0	0	52.01
	8	10:1	12	0	0	55.73
Non-linear stage	9	14.1	12	1.41	0	46.02
	10	6:1	12	−1.41	0	39.00
	11	10:1	17.7	0	1.41	53.71
	12	10:1	6.3	0	−1.41	34.53

X_B for butanol-to-oil molar ratio and X_C for catalyst amount.

Table 2
Results for the statistical analysis of the experimental design.

Parameters	Response
Main influence and interactions	$\bar{y} = 47.59$ $I_B = 13.11$ $I_C = 10.32$ $I_{BC} = 7.78$
Significance test: *c confidence level: 95%*	
Mean response	54.04
Standard deviation	$t = 3.18$; $s = 1.71$
Confidence interval	±2.72
Significant variables	B, C, BC
Significance of curvature	
Curvature	6.44
Confidence curvature interval	3.85
Significance	Yes

B: butanol-to-oil molar ratio, *C*: catalyst loading, *s*: standard deviation, *t*: student's t.

are represented in Eqs. (2) and (3), respectively. It is important to understand that the mathematical expressions are valid only within the studied experimental range.

$$X_J = 47.59 + 6.55X_B + 5.16X_C + 3.89X_{BC} \quad (2)$$

$$X_J = 51.68 - 1.82X_B - 2.18X_C + 0.34X_{BC} \quad (3)$$

X_J is the conversion of jojoba oil occurring during the described butanolysis process.

3.1.2. Non-linear stage

The regression analysis suggested that the curvature had a positive impact on the CaO-catalyzed jojoba oil butanolysis process. Since the value for the curvature was found to be greater than the confidence curvature interval, the non-linear stage of the design of experiments was also taken into consideration to fit the experimental data with a quadratic model. An additional four experiments, known as star-points and coded as ±α, were performed and included into the two-level factorial design to form a central composite design as summarized in Table 1. The distance between the origin and star-points is expressed as $\alpha = 2^{n/4}$ (In the present study: $n = 2$ and $\alpha = 1.41$). To complete the central composite design, adapted from Box and Wilson [19], the linear, center and non-linear stages were combined in the design of experiments to investigate the significance of n-butanol concentration and catalyst loading on the CaO-catalyzed jojoba oil butanolysis process. The present analysis involves all the independent variables and their within interactions, regardless of their significance level. The superior-fitting response surface statistical and industrial quadratic mathematical model for the CaO-catalyzed jojoba oil butanolysis process are expressed in Eqs. (4) and (5), respectively.

$$X_J = 54.04 + 4.51X_B + 5.97X_C - 4.69X_B^2 + 3.89X_{BC} - 3.89X_C^2 \quad (4)$$

$$X_J = -32.70 + 9.34X_B + 3.85X_C - 0.59X_B^2 + 0.34X_{BC} - 0.24X_C^2 \quad (5)$$

The three-dimensional surface plot of the predicted jojoba oil conversion with varying catalyst loading and n-butanol concentration is presented in Fig. 1. The response surface graphical representation was achieved using the statistical quadratic regression equation. The results shown in Fig. 1 indicated the change in jojoba oil conversion with varying n-butanol concentration and catalyst amount. Within the studied experimental range, the jojoba oil conversion augmented with the increase in the n-butanol concentration and catalyst amount, indicating the possible interaction between n-butanol and CaO catalyst. However, the appliance of butanol-to-oil molar ratio and catalyst loading higher than the optimal value resulted in the slight drop of jojoba oil conversion. The regression model presented a good correlation between the experimental results and the predicted values, which validated that the presented model is appropriate to represent the described

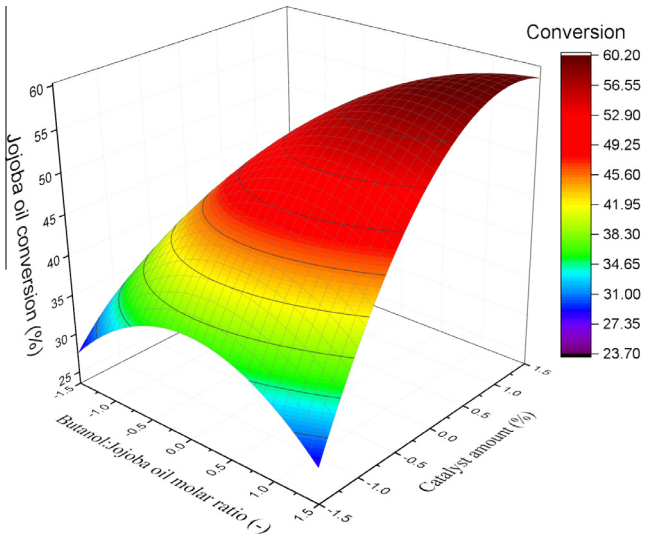

Fig. 1. Response surface 3D plot indicating the influence of butanol-to-oil molar ratio and catalyst loading on the jojoba oil conversion. Temperature: 85 °C, Time: 600 min, Stirring intensity: 350 rpm.

butanolysis process within the studied range of reaction conditions (Supplementary Fig. S1). The contour plot for the jojoba oil conversion with varying n-butanol concentration and catalyst loading can be seen in Supplementary Fig. S2.

3.2. Impact of reaction parameters

3.2.1. Impact of temperature

Like many chemical reactions, the kinetics of alcoholysis reaction is a function of the reaction conditions. Since the transesterification reaction is assumed to be endothermic in nature [20], the effect of temperature on the rate of CaO-catalyzed jojoba oil butanolysis reaction was initially examined. Also, from the kinetics perspective, the rise in the reaction temperature is expected to accelerate the rate of the alcoholysis process. This is because the appliance of elevated temperature would promote the miscibility and reactivity between the reactants. The impact of three different temperatures (65, 75 and 85 °C) on the CaO-catalyzed butanolysis process of jojoba oil was studied keeping constant butanol-to-oil molar ratio of 10:1 and 12 wt.% catalyst amount. The experimental results for the effect of temperature (65, 75 and 85 °C) on the jojoba oil conversion are presented as symbols in Fig. 2. The results depicted in Fig. 2 indicated that the reaction temperature had a positive impact on the described butanolysis process. The rise in the reaction temperature resulted in the reduction of time of the described butanolysis process. To achieve approximately 20% conversion of jojoba oil, the reaction time decreased from 600 min to 200 min when temperature was raised from 65 °C to 85 °C. Using 85 °C reaction temperature, jojoba oil conversion higher than 52% was observed after 600 min of the CaO-catalyzed jojoba oil butanolysis process. Further extending the reaction time to 1800 min, maximum jojoba oil conversion of 96.11% was achieved (Supplementary Fig. S3).

3.2.2. Impact of butanol-to-oil molar ratio

The other important variable affecting the alcoholysis process is the alcohol-to-oil molar ratio. The stoichiometry of the jojoba oil alcoholysis reaction requires a ratio of 1 mol of butanol to 1 mol of oil to produce 1 mol of jojobyl alcohols and 1 mol of FABE. However, the transesterification reaction is an equilibrium reaction; therefore, an excess of n-butanol was required to shift the reaction equilibrium towards the formation of jojobyl alcohols

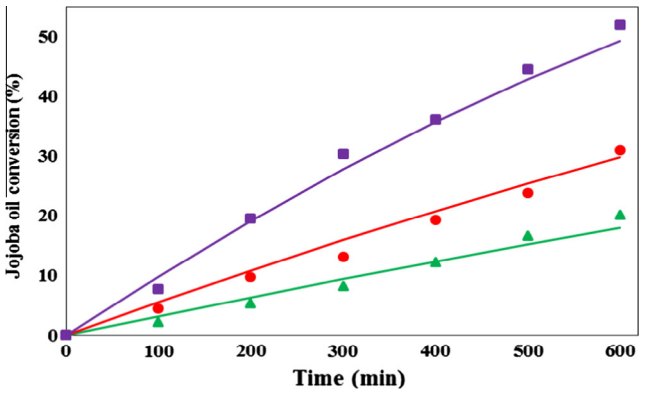

Fig. 2. Comparison of the experimental data and simulated values for the impact of reaction temperature on the jojoba oil conversion. Temperature- (▲): 65 °C, (●): 75 °C, (■): 85 °C. Experimental data: symbols, kinetic model: lines. Catalyst loading 12 wt.%, butanol-to-oil molar ratio: 10:1, Time: 600 min, Stirring intensity: 350 rpm.

and FABE [20,21]. To investigate the effect of n-butanol concentration on the CaO-catalyzed jojoba oil butanolysis process, the butanol-to-molar ratio was varied keeping fixed reaction temperature of 85 °C and 12 wt.% catalyst amount. The obtained results suggested that increasing the butanol-to-oil molar ratio from 6:1 to 12.8:1 resulted in the augmentation of jojoba oil conversion from 39.00% to 58.93% after 600 min of reaction time. However, amplifying the butanol-to-oil molar ratio to 14:1 directed the drop in the jojoba oil conversion to 46.02%. A possible explanation for such behavior is that n-butanol amount higher than the optimal value resulted in the dilution of the reaction mixture which prevented the interaction between jojoba oil and butoxide ions chemisorbed on the CaO catalytic sites. The presented explanation was in agreement with the literature [22]. The catalytic ionization of butanol molecule resulting in the formation of the butoxide ion has been mentioned earlier [12]. The experimental results for the effect of butanol-to-oil molar ratio (7.2-10-12.8:1) on the jojoba oil conversion are presented as symbols in Fig. 3, while, the influence of butanol-to-molar ratio ranging between 6:1 and 14:1 on the described butanolysis process is summarized in Supplementary Fig. S4.

3.2.3. Impact of catalyst loading

The dependence of the conversion of jojoba oil on the catalyst amount at the constant n-butanol concentration and temperature was also systematically investigated. The effect of five different catalyst loading ranging between 6.3 wt.% and 17.7 wt.% on the rate of the described butanolysis process was examined setting the reaction temperature and butanol-to-oil molar ratio to 85 °C and 10:1, respectively. Increase in the catalyst loading from 6.3 wt.% to 16 wt.% resulted in the acceleration of the rate of butanolysis reaction. The maximum jojoba oil conversion of 59.30% was recorded after 600 min of the CaO-catalyzed butanolysis reaction. This is attributed to the increase in the availability of the catalytic active centers; thus, producing additional number of butoxide ions. However, further rise in the catalyst loading to 17.7 wt.% resulted in lowering of jojoba oil conversion to 53.71%. The reason for the reduced conversion of jojoba oil at higher catalyst amount could be related to increase in the viscosity of the reaction mixture [23,24]. It is supposed that the rise in viscosity of the reaction mixture obstructed the interaction between the reactant molecules as a result of the external mass transfer resistance. However, the appliance of additional energy to the reaction system through amplifying the reaction temperature and stirring intensity might alter the jojoba oil conversion. The experimental results of the study evaluating the effects of 8, 12 and 16 wt.% catalyst loading on the jojoba oil conversion of the described butanolysis process are shown as symbols in Fig. 4, while, that of the catalyst loading ranging between 6.3 wt.% and 17.7 wt.% is presented in Supplementary Fig. S5. Furthermore, the dissolution phenomenon of the mussel shells derived CaO species as well as the possibility of contribution of homogeneous catalysis in the jojoba oil butanolysis process was examined. For the discussed investigation, CaO catalyst of 12 wt.% amount with respect to the total volume of the reaction mixture was stirred in n-butanol solution equivalent to 10:1 molar ratio. The CaO-butanol mixture was agitated with the stirring intensity of 350 rpm at room temperature for 720 min. and subsequently filtered using a Whatman filter paper. The obtained catalyst-free n-butanol filtrate was added into the reactor having a calculated volume of jojoba oil, and the butanolysis reaction was performed at 85 °C temperature. The jojoba oil conversion of 4.74% was achieved after 600 min. of reaction time. The contribution of the homogeneous catalysis in the described butanolysis process could be considered negligible when compared with the jojoba oil conversion obtained through thermal catalysis, which was 2.20% after 600 min of reaction performed at 85 °C using 10:1 butanol-to-oil molar ratio. Therefore, the CaO catalyst can possibly be recovered and further utilized for another experimental run provided that the reaction products are completely desorbed from

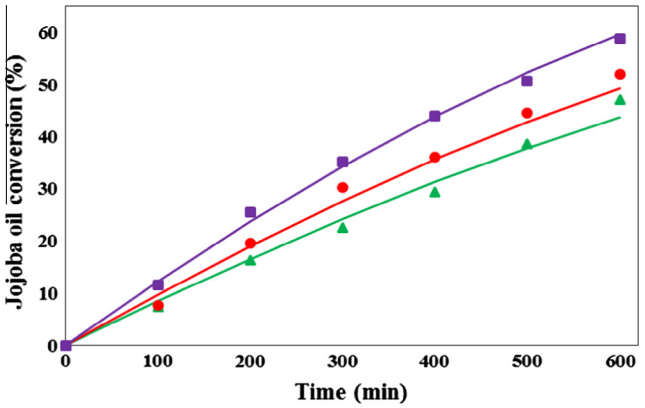

Fig. 3. Comparison of the experimental data and simulated values for the impact of n-butanol concentration on the jojoba oil conversion. Butanol-to-oil molar ratio-(▲): 7.2:1, (●): 10:1, (■): 12.8:1. Experimental data: symbols, kinetic model: lines. Temperature: 85 °C, Catalyst loading 12 wt.%, Time: 600 min, Stirring intensity: 350 rpm.

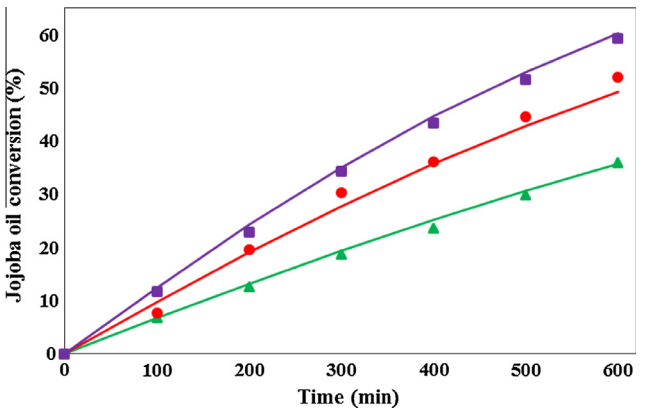

Fig. 4. Comparison of the experimental data and simulated values for the impact of catalyst loading on the jojoba oil conversion. Catalyst loading- (▲): 8 wt.%, (●): 12 wt.%, (■): 16 wt.%. Experimental data: symbols, kinetic model: lines. Temperature: 85 °C, butanol-to-oil molar ratio: 10:1, Time: 600 min, Stirring intensity: 350 rpm.

the catalytic active surface and poisoning of the catalyst due to the surrounding carbon dioxide and moisture is prevented.

3.3. Kinetic modeling of the butanolysis process

The appliance of heterogeneous catalysts to the alcoholysis process, in general, results in the formation of three-phasic (liquid–liquid–solid) reaction system. Consequently, the initial rate of the reaction is slow because of the external mass transfer resistance resulting in the sigmoidal pattern of the reaction curve [13–16]. However, in the present study, only two phases (liquid–solid) were observed due to excellent miscibility between n-butanol and jojoba oil. Nevertheless, the adsorption of the reactant molecules on the catalytic sites, surface chemical reaction and the reaction products desorption steps were taken into consideration to develop a model for the correct prediction of the kinetics of the CaO-catalyzed jojoba oil butanolysis process. In order to identify the rate-controlling step of the described butanolysis process, the reaction kinetics for all the reversible reactions has been considered and the rate constants for the overall reaction were evaluated. A total of 18 different kinetic models were tested, and the selection of the best mathematical model was based on the parameters, such as sum of weighted errors and model selection criteria. By fitting the model with the experimental data, the appropriate kinetic model for the described butanolysis process included below mentioned features:

(1) It was understood that the alcoholysis reaction occurs between n-butanol molecules chemisorbed on the catalytic surface and jojoba oil molecules present in the butanol phase close to the active sites.
(2) The overall process rate is controlled by the surface reaction step occurring between chemisorbed butoxide ions and the jojoba oil molecules in the bulk phase.
(3) The butanol adsorption as well as desorption of the reaction product (FABE) is reached spontaneously, and does not limit the overall rate of the reaction.
(4) The overall alcoholysis reaction on the catalytic surface follows pseudo-first order kinetics with respect to jojoba oil.

The reaction steps involved in the proposed reaction mechanism could be presented as:

$$B + s \leftrightarrow Bs \tag{6}$$

$$Bs + J \leftrightarrow BEs + JA \tag{7}$$

$$BEs \leftrightarrow B + s \tag{8}$$

where s is the catalytic active sites.

When the surface reaction was proposed to be the rate-limiting step, the fractional conversion of jojoba oil can be expressed as:

$$\frac{dX_J}{dt} = m\left[\left[\frac{k_a k_s C_B C_J}{k_{-a}}\right] - \left[\frac{k_{-s} k_{-d} C_{BE} C_{JA}}{k_d}\right]\right] \tag{9}$$

$$k = Ae^{-E_a/RT} \tag{10}$$

The equation for the mass balance of the catalyst is presented as:

$$m = \frac{m_0}{\left[1 + \left[\frac{k_a C_B}{k_{-a}}\right] + \left[\frac{k_{-d} C_{BE}}{k_d}\right]\right]} \tag{11}$$

while,

$$C_J = C_{J0}[1 - X_J] \tag{12}$$

$$C_B = C_{B0} - C_{J0} * X_J \tag{13}$$

$$C_{BE} = C_{JA} = C_{J0} * X_J \tag{14}$$

where k_a, k_s and k_d are the specific rate constants of the adsorption, surface and desorption reaction, respectively, in the forward direction; k_{-a}, k_{-s} and k_{-d} are the specific rate constants of the adsorption, surface and desorption reaction, respectively, in the reverse direction; C_{B0} is the n-butanol initial concentration (mol L^{-1}); C_B is the n-butanol concentration at time t (mol L^{-1}); C_{J0} is the jojoba oil initial concentration (mol L^{-1}); C_J is the jojoba oil concentration at time t (mol L^{-1}); C_{JA} is the concentration of jojobyl alcohols (mol L^{-1}); C_{BE} is the concentration of FABE (mol L^{-1}); m_0 is the initial mass of the catalyst (g); m is the mass of the catalytic sites involved in the reaction (g); A is the pre-exponential factor of the Arrhenius equation (min^{-1}); E_a is the activation energy (cal mol^{-1}); R is the universal gas constant (1.98 cal K^{-1} mol^{-1}); T is the absolute temperature (K).

The curve fitting procedure was performed using Aspen custom modeler software (Version 8.4, Aspen Technology, Inc., USA). After the substitution of the obtained reaction parameters, the Eqs. (9) and (11) can be rearranged as:

$$\frac{dX_J}{dt} = m\left[\left[\frac{1254.69e^{-(8844.77/RT)} * 182.61e^{-(10885.80/RT)} * C_B * C_J}{174.38e^{-(6644.63/RT)}}\right] - \left[\frac{11815.30e^{-(12437.30/RT)} * 135.75e^{-(9754.46/RT)} * C_{BE} * C_{JA}}{17.57e^{-(43.68/RT)}}\right]\right] \tag{15}$$

$$m = \frac{m_0}{\left[1 + \left[\frac{1254.69e^{-(8844.77/RT)} * C_B}{174.38e^{-(6644.63/RT)}}\right] + \left[\frac{135.75e^{-(9754.46/RT)} * C_{BE}}{17.57e^{-(43.68/RT)}}\right]\right]} \tag{16}$$

The proposed kinetic model displayed excellent fitting with the experimental data where the value for the sum of weighed errors and model selection criteria was equivalent to 3.20 E-3 and 4.27, respectively. The graphical representation for the simulation of the experimental data using the proposed kinetic model at different reaction temperature, butanol-to-oil molar ratio and catalyst amount is presented as solid lines in Figs. 2–4, respectively. In addition, the complete reaction mechanism for the described butanolysis process was also explained from chemistry perspective (Supplementary Fig. S6). The proposed reaction pathway for the heterogeneous CaO-catalyzed jojoba oil butanolysis process was found to be equivalent to the Eley–Rideal mechanism which includes three main steps: adsorption of alcohol, surface reaction and desorption of the reaction product. The validation of precision of the proposed kinetic model for the described butanolysis process was additionally carried out using a simplified expression of Eley–Rideal mechanism consisting of an adsorption and desorption coefficient [25]. The pseudo-first order kinetic model based on the simplified Eley–Rideal model was found to provide a good correlation with the experimental data having the sum of weighed errors and model selection criteria of 4.45 E-3 and 4.08, respectively. The achieved low value of the sum of weighed errors and high value of the model selection criteria even with using the simplified equation of the Eley–Rideal mechanism provided the confirmation that the proposed kinetic model correctly simulated the CaO-catalyzed jojoba oil butanolysis process.

4. Conclusion

The transformation of jojoba oil to jojobyl alcohols and biodiesel was performed in the presence of n-butanol using a heterogeneous CaO catalyst synthesized from the waste of the fish industry. The mussel shells derived CaO catalyst was not only simple to synthesize, inexpensive and environmentally benign but also displayed good capability to accelerate the butanolysis reaction of jojoba oil. The interactions between the reaction variables (n-butanol concentration and catalyst loading) and their

influence on the described butanolysis process was studied using a two-factorial design by means of the RSM. A response equation was generated which could be utilized to determine the optimal reaction parameters required to attain maximum conversion of jojoba oil. The statistical analysis suggested that butanol-to-oil molar ratio of 12.8:1 and 16 wt.% catalyst loading are optimal conditions for achieving maximum jojoba oil conversion. However, from process economic and ecological perspective, the utilization of butanol-to-oil molar ratio of 10:1, 12 wt.% catalyst loading could be beneficial as the described butanolysis reaction performed at 85 °C using 350 rpm stirring intensity resulted in 96.11% jojoba oil conversion after 1800 min of reaction time.

The kinetics of the CaO-catalyzed jojoba oil butanolysis reaction was systematically studied to validate the reaction mechanism and simulate the process using a mathematical model. The proposed kinetic model involved a three-step reaction pathway which was equivalent to the Eley–Rideal mechanism. The butanolysis process occurred between the butoxide molecules chemisorbed on the catalytic active sites and jojoba oil molecules present in the liquid phase. In the biphasic reaction system, the rate of the butanolysis process was controlled by the surface reaction step, and the overall process followed the pseudo-first order reaction kinetics. The proposed kinetic model presented a good agreement between the predicted values and the experimental data. For this reason, the presented kinetic model could be considered as valid for the prediction of the CaO-catalyzed jojoba oil butanolysis process and to determine the optimal reaction variables for large-scale jojoba alcohols and biodiesel production.

Competing financial interests

The authors declare no competing financial interests.

Acknowledgements

The authors would like to express their gratitude to the Norwegian University of Life Sciences, Norway (Project No. 1301051406), Complutense University of Madrid and NILS mobility Grants (009-ABEL-CM-2013) for their financial support.

Appendix A. Supplementary material

Supplementary data associated with this article can be found, in the online version, at http://dx.doi.org/10.1016/j.fuel.2016.03.107.

References

[1] Huber GW, Iborra S, Corma A. Synthesis of transportation fuels from biomass: chemistry, catalysts, and engineering. Chem Rev 2006;106:4044–98.
[2] The Roadmap for Biomass Technologies in the U.S. Biomass R&D Technical Advisory Committee. US Department of Energy 2002; Accession No. ADA 436527.
[3] Avhad MR, Marchetti JM. A review on recent advancement in catalytic materials for biodiesel production. Renew Sustain Energy Rev 2015;50:696–718.
[4] Kozliak E, Mota R, Rodriguez D, Overby P, Kubatova A, Stahl D, et al. Non-catalytic cracking of jojoba oil to produce fuel and chemical by-products. Ind Crops Prod 2013;43:386–92.
[5] Canaoira L, Alcántara R, Garcia-Martinez MJ, Carrasco J. Biodiesel from jojoba oil: transesterification with methanol and properties as a fuel. Biomass Bioenergy 2006;30:76–81.
[6] Wisniak J. Potential uses of jojoba oil and meal-a review. Ind Crops Prod 1994;3:43–68.
[7] Palla C, Hegel P, Pereda S, Bottini S. Extraction of jojoba oil with liquid CO_2 + propane solvent mixtures. J Supercrit Fluids 2014;91:37–45.
[8] Al-Widyan MI, Al-Muhtaseb MA. Experimental investigation of jojoba as a renewable energy source. Energy Convers Manage 2010;51:1702–7.
[9] Al-Hamamre Z, Rawajfeh KM. Investigating the energy value of jojoba as an alternative renewable energy source. Int J Green Energy 2015;12(4):398–404.
[10] Qureshi N, Ezeji TC. Butanol,'a superior biofuel' production from agricultural residues (renewable biomass): recent progress in technology. Biofuels, Bioprod Biorefin 2008;2:319–30.
[11] García V, Päkkilä J, Ojamo H, Muurinen E, Keiski R. Challenges in biobutanol production: how to improve the efficiency? Renew Sustain Energy Rev 2011;15:964–80.
[12] El-Boulifi N, Sánchez M, Martínez M, Aracil J. Fatty acid alkyl esters and monounsaturated alcohols production from jojoba oil using short-chain alcohols for biorefinery concepts. Ind Crops Prod 2015;69:244–50.
[13] Sánchez M, Marchetti JM, El-Boulifi N, Martínez M, Aracil J. Jojoba oil biorefinery using a green catalyst. Part I: simulation of the process. Biofuels, Bioprod Biorefin 2015;9(2):129–38.
[14] Sánchez M, Marchetti JM, El-Boulifi N, Aracil J, Martínez M. Kinetics of jojoba oil methanolysis using a waste from fish industry as catalyst. Chem Eng J 2015;262:640–7.
[15] Lukíc I, Kesić Z, Maksimović S, Zdujić M, Liu H, Krstić J, et al. Kinetic of sunflower and used vegetable oil methanolysis catalyzed by CaO·ZnO. Fuel 2013;113:367–78.
[16] Tasić MB, Miladinović MR, Stamenković OS, Veljković VB, Skala DU. Kinetic modeling of sunflower oil methanolysis catalyzed by calcium-based catalysts. Chem Eng Technol 2015;38(9):1550–6.
[17] Veljković VB, Stamenković OS, Todorović ZB, Lazić ML, Skala DU. Kinetics of sunflower oil methanolysis catalyzed by calcium oxide. Fuel 2009;88:1554–62.
[18] Zhao L, Qiu Z, Stagg-Williams SM. Transesterification of canola oil catalyzed by nanopowder calcium oxide. Fuel Process Technol 2013;114:154–62.
[19] Bouaid A, El-boulifi N, Hahati K, Martínez M, Aracil J. Biodiesel production from biobutanol. Improvement of cold flow properties. Chem Eng J 2014;238:234–41.
[20] Farooq M, Ramli A, Subbarao D. Biodiesel production from waste cooking oil using bifunctional heterogeneous solid catalysts. J Clean Prod 2013;59:131–40.
[21] Fu B, Gao L, Niu L, Wei R, Xiao G. Biodiesel from waste cooking oil via heterogeneous superacid catalyst SO_4^{2-}/ZrO_2. Energy Fuels 2009;23:569–72.
[22] Ilgen O. Investigation of reaction parameters, kinetics and mechanism of oleic acid esterification with methanol by using Amberlyst 46 as a catalyst. Fuel Process Technol 2014;124:134–9.
[23] Deshmane VG, Adewuyi YG. Synthesis and kinetics of biodiesel formation via calcium methoxide base catalyzed transesterification reaction in the absence and presence of ultrasound. Fuel 2013;107:474–82.
[24] Birla A, Singh B, Upadhyay SN, Sharma YC. Kinetics studies of synthesis of biodiesel from waste frying oil using a heterogeneous catalyst derived from snail shell. Bioresour Technol 2012;106:95–100.
[25] Endalew A, Kiros Y, Zanzi R. Inorganic heterogeneous catalysts for biodiesel production from vegetable oils. Biomass Bioenergy 2011;35:3787–809.

Paper IV

Glycerol-activated calcium oxide catalyst for the methanolysis of crude *Jatropha curcas* oil.

M.R. Avhad[a*], M. Sánchez[b], A. Bouaid[b], M. Martínez[b], J. Aracil[b], J. M. Marchetti[a*]

[a] Department of Mathematical Science and Technology, Norwegian University of Life Sciences, Drøbakveien 31, 1432 Ås, Norway.

[b] Chemical Engineering Department, Faculty of Chemistry, Complutense University, 28040 Madrid, Spain.

* Correspondence and requests for materials should be addressed to J.M. Marchetti (Tel: +4767231647; Fax: +4764965401; E-mail: jorge.mario.marchetti@nmbu.no) and M.R. Avhad (E-mail: avhad.mangesh@ymail.com).

Abstract

Calcium oxide catalyst, when utilized for biodiesel production, experiences material transformation due to its reaction with glycerol present in the transesterification reaction mixture. In the present study, calcium oxide catalyst was interacted with glycerol prior to its application for biodiesel production. The catalytic activity of glycerol-activated calcium oxide was tested for the methanolysis of high free fatty acid crude *Jatropha curcas* oil. The glycerol-enriched calcium oxide presented superior catalytic activity for the methanolysis reaction than the commercial as well as laboratory synthesized calcium oxide, and calcium methoxide. This study systematically investigated the influence of different variables, such as reaction temperature, reaction time, catalyst amount, glycerol dose, and methanol-to-oil molar ratio on the conversion of *Jatropha curcas* oil. The interaction between the reaction variables (methanol-to-oil molar ratio and catalyst amount), their influence on the methanolysis reaction, and the optimum parameters affecting the process were determined by means of the response surface methodology. The obtained results suggested that both catalyst loading and methanol-to-oil molar ratio significantly affected the *Jatropha curcas* oil methanolysis process.

Keywords

Biodiesel; *Jatropha curcas* oil; Calcium oxide; Glycerol activation; Methanolysis.

1. Introduction

The diminishing of the petroleum reserves, the increase of environmental pollution as a consequence of the burning of fossil fuels, and the fluctuating fuel prices have hinted the necessity of utilizing renewable source of energy which are sustainable, ecologically benign, and economically reasonable [1]. In this respect, biodiesel has been recognized as a potential replacement of petroleum diesel not only due to the fact that this oxygenated fuel can be synthesized from oil-rich biomass but also because its combustion offers minor environmental toxicity in comparison to the petroleum-based diesel fuel [2, 3]. The overall physical and fuel properties of biodiesel are dependent on the fatty acid profile of the lipid feedstock [4, 5]. Among several methodologies applied for biodiesel production, the catalyst-assisted alcoholysis process of plant oil has been frequently selected. The alcoholysis processes are also known as the transesterification of triacylglycerol (TAGs) and the esterification of free fatty acid (FFA). The base-catalyzed alcoholysis reactions were reported to be faster than those catalyzed by the acid catalysts [6-9]. The ability of homogeneous catalysts to promote the production of biodiesel in a short reaction time using mild reaction conditions have resulted in its widespread utilization. However, the post-alcoholysis treatments required for the removal of residual homogeneous catalyst from the reaction mixture have resulted in the generation of large amount of contaminated water as well as stable emulsions, which reduces the biodiesel as well as glycerol yield [10, 11]. The appliance of homogeneous acid catalysts could also result in the corrosion of the reaction equipment [12]. Furthermore, homogeneous catalysts are consumed during the course of the alcoholysis reaction and cannot be reutilized. The introduction of heterogeneous catalytic materials for biodiesel production have offered an imperative solution to the previous mentioned drawbacks related to the use of homogeneous counterpart. The utility of heterogeneous base and acid catalysts

has been widely investigated, wherein they offer the possibility of elimination of the neutralization process, enabling simple purification and separation steps, allowing a continuous operation of the process, enabling the recovery and reutilization of the catalyst, and enhancing the purity of the reaction products [13, 14]. In this regards, research efforts are consistently engaged in developing not only a high-performance and stable but also a low cost heterogeneous catalyst for biodiesel production [15].

Among the variety of basic heterogeneous catalysts, calcium oxide (CaO) has been extensively applied for the alcoholysis reaction because of its high basicity, low solubility in short-chain alcohols, low cost, and is easy to handle [16]. The utilization of CaO catalyst for biodiesel production was reported to be advantageous also from the process economics perspective because the catalyst could be generated from inexpensive and abundantly available natural resources, such as egg shells [17], crab shells [17], mussel shells [18], scallop shells [19], amongst others. Kouzu et al. [20] concluded that 0.78 g of CaO catalyst applied for the transesterification of soybean oil with reflux methanol resulted in the fatty acid methyl esters (FAME) yield of 99 % after 120 min of reaction performed using 12:1 methanol-to-oil molar ratio. The recent studies have reported that CaO catalyst experiences material transformation during the progression of the alcoholysis reaction [21-24]. The initial stage of the alcoholysis reaction is catalyzed by the CaO phase of the catalyst, after which the material reacts with the by-producing glycerol and is transformed to calcium diglyceroxide (CaDg) [21]. This was because CaO was more reactive with glycerol than methanol. León-Reina et al. [22] described CaDg as a set of molecular calcium tetramers interlinked by H-bonds; and reported its superior catalytic activity when compared with CaO catalyst. The superior activity of CaDg catalyst was due to the availability of basic oxygen anion as a consequence of interruption of the crystal structure at the surface which can abstract proton

from OH group of methanol leading towards the formation of surface methoxide ion [22]. The CaDg catalyst was characterized as a chemically stable heterogeneous catalyst, weakly basic in nature, and not prone for deactivation due to hydration/carbonation reaction when exposed to the surrounding air [23, 24]. Taking the mentioned advantages of CaDg catalyst into consideration, Kouzu et al. [23] and López Granados et al. [25] recommended to transform CaO to CaDg compound prior to its application for biodiesel production.

Different procedures have been employed for the synthesis of CaDg catalyst. Lukić et al. [26] applied mechanochemical method synthesized CaDg catalyst for the alcoholysis reaction between sunflower oil and methanol, where it was concluded that CaDg catalyst acted as an emulsifier and significantly influenced the initial rate of the methanolysis reaction. Li et al. [27] utilized precipitation-based method using potassium hydroxide, glycerol, and calcium chloride for the synthesis of CaDg catalyst. The synthesized catalyst was used to assist the alcoholysis reaction between refined *Jatropha* oil and methanol. In addition, CaDg catalyst have been successfully employed for biodiesel production from several lipid feedstocks, such as soybean oil [28, 29], sunflower oil [30], castor oil [31], and waste cooking oil [32]. In the present study, mussel shells (*Mytilus Galloprovincialis*) derived CaO was utilized for the synthesis of CaO-glycerol complex, which subsequently was applied for the methanolysis reaction of high FFA crude *Jatropha curcas* oil (CJCO). The influence of catalyst loading, glycerol dose, reaction temperature, reaction time, and methanol-to-oil molar ratio on the conversion of CJCO was systematically investigated. Furthermore, the interactions between the reaction variables, their influence on the described methanolysis reaction, and optimum process parameters were determined by means of the response surface methodology (RSM).

2. Experimental section

2.1. Materials

CJCO was supplied by IBERINCO (Spain). Its fatty acid composition and the physico-chemical properties were determined earlier, in accordance to the AOCS official methods and the UCM methods, and the results were published elsewhere [33]. CJCO was filtered using the Whatman filter paper prior to its utilization for the methanolysis reactions. Methanol (Cor Quimica, Spain), glycerol (Sigma-Aldrich), n-octyl octanoate (Sigma-Aldrich), and carbon disulphide (Panreac) with purity higher than 99 % were utilized. The commercial reagent grade CaO was purchased from Sigma-Aldrich and used as received, while, for the synthesis of laboratory-grade CaO, mussel shells were collected from the local fish market in Madrid, Spain.

2.2. Catalyst preparation

For the synthesis of CaO, the mussel shells initially were neatly cleaned under the flow of tap water to remove the adsorbed superfluous substances, followed with its drying in an oven set at 100 ºC for 60 min. Subsequently, the mussel shells were pulverized using a mortar-pestle, evenly placed in a silica crucible, and applied for the calcination process in a ceramic muffle heating furnace set at 800 ºC for 360 min. The selection of the calcination temperature was based on the previous research work performed in the same laboratory [18]. The appliance of an appropriate calcination temperature is considered to be of foremost relevance because lower temperatures could result in the incomplete formation of the oxide species, whereas, higher temperatures might cause undesired transformation of the material. After 360 min of the calcination process, the oven was switched off and allowed to cool. The formed white colored powder was removed from the furnace and preserved in a desiccator to avoid its poisoning due to moisture in the ambient air

while handling or weighing. The calcination process resulted in approximately 45 % loss of the total fresh weight of the precursor, mussel shells. The characterization of the CaO material was performed earlier by means of X-ray diffraction, specific surface area analysis, induced coupled plasma atomic emission spectroscopy, and transmission electron microscopy, the results of which were published elsewhere [18].

The obtained CaO powder was further treated with different amount of glycerol to conduct the material transformation. The glycerol activation process of CaO was performed by pouring the desired amount of CaO and glycerol in an air tight glass reactor. Instead of allowing the material transformation to occur in the absence [24, 28], or presence [22, 29] of methanol, the mixture of CaO and glycerol was agitated in the presence of CJCO. This was done to eliminate even a minor possibility of the formation of the calcium methoxide catalytic species, and produce only glycerol-enriched CaO catalyst. The possibility for the formation of the calcium methoxide catalytic species was suspected because a study reported by Kawashima et al. [34] suggested that a small amount of CaO reacts with methanol resulting towards the generation of calcium methoxide. Additionally, the CaO activation by glycerol was performed in the presence of oil so as to prevent the poisoning of CaO due to the surrounding air inside the reactor. This mixture was vigorously agitated at 60 ºC for 60 min using 350 rpm stirring intensity and under atmospheric pressure. For the synthesis of calcium methoxide, the immersion of CaO in methanol was stirred at 60 ºC for 60 min, followed with the filtration for the separation of the solid catalyst. To understand the homogeneous contribution of mussel shells derived CaO (HMC) for the described methanolysis process, initially a measured amount of CaO and methanol were agitated using 350 rpm stirring intensity at room temperature for 720 min. Subsequently, the solution was filtered and only the filtrate methanol was used for the CJCO methanolysis reaction performed in the absence of a solid catalytic material.

147 The term thermal catalysis (TC) refers to the performance of the alcoholysis reaction between
148 CJCO and methanol performed at 65 ºC reaction temperature, in the absence of a catalytic material.
149
150 **2.3. Reaction**
151 The methanolysis reaction of CJCO was conducted in a three-neck curved bottom glass
152 reactor of 250 cm^3 volume capacity. The mechanical stirrer equipped with an impeller of 6.0 cm
153 diameter was inserted through the middle neck and placed centrically close to the bottom of the
154 reactor. The water condenser was attached to one of the side necks, while, a rubber cork was fitted
155 to the other neck of the reactor. The water condenser allowed the refluxing of methanol back into
156 the reactor. The glass reactor was placed in a thermostatically controlled water bath (Heto-Holten
157 A/S, Denmark), the temperature of which was controlled by a PID controller with 1 ºC precision.
158 The velocity of the mechanical stirrer was monitored by a motor (Eurostar Basic IKA). After the
159 glycerol activation process of CaO catalyst, the temperature of the system was shifted to the desired
160 reaction temperature. Once the system temperature had reached the set point, a measured volume
161 of methanol was charged into the reactor using a conical flask; this was considered as the initiating
162 time of the methanolysis reaction. The stirring intensity of 350 rpm was maintained for all
163 experiments to avoid the mass transfer limitations [22, 26]. The post-reaction mixture was
164 centrifuged, allowing the separation of different phases of the components. The biodiesel phase
165 was then washed with water to remove the calcium soap, if any, lixiviated into the reaction
166 products during the methanolysis process. The trace amount of methanol as well as water present
167 in the biodiesel phase were subsequently removed using a rotary evaporator attached to a vacuum
168 pump (10 mg Hg) set at 60 ºC for 30 min. Every experiments were replicated twice to obtain the

reproducibility in the experimental finding, and the average of the experimental values were considered.

2.4. Analysis

The reaction samples were analyzed using the gas chromatography (GC) analyzer (Hewlett-Packard HP-5890 Series II) equipped with a flame ionization detector and a fused silica capillary column (12 m length, 0.31 mm internal diameter and 0.71 μm thickness). A Hewlett-Packard 3396SA integrator was connected to the chromatograph. The injection system was split-splitless, and helium was the carrier gas at a 1 ml min^{-1} flowrate. The injector and the detector temperature were set at 275 ºC and 325 ºC, respectively. The GC column temperature was initially held at 130 ºC for 1 min, then raised at 4 ºC min^{-1} to 160 ºC, and finally heating at a ramp rate of 30 ºC min^{-1} to 320 ºC. The n-octyl octanoate was used as an internal standard and the reaction samples were dissolved in carbon disulfide. The GC analysis was conducted by injecting 1 μl volume of the prepared samples into the instrument. The acid value of CJCO and biodiesel was determined in accordance to the ASTM D664 method, using a Metrohm Swiss, model 702SM Titrino. The titration endpoint was determined and verified automatically with the help of phenolphthalein indicator.

The CJCO conversion (X_{CJCO}) is expressed as

$$X_{CJCO} = \frac{\text{Initial moles of TAGs} - \text{Final moles of TAGS}}{\text{Initial moles of TAGs}} \text{ x } 100\ \% \quad (1)$$

2.5. Design of experiments

The regression analyses was conducted by designing a set of experiments, the results of which were fitted to a two-level factorial design for the application of the RSM using the

Statgraphics centurion XV software (Statpoint technologies, Inc., USA). The linear and the non-linear stage of the two-level factorial design consisted of four experiments each, along with four replicates of the center points, as shown in Table 1. The non-linear stage of the two-factorial design is also known as the star-points and coded as ± α. The distance between the origin and the star-points is expressed as $\alpha = 2^{n/4}$ (in the present study: n = 2 and α = 1.41). The linear, the center-points, and the non-linear stage of the experimental design were combined to form a central composite design, and utilized to investigate the influence of methanol-to-CJCO molar ratio and the catalyst loading on the described methanolysis process. The successful implementation of such method requires an appropriate selection of the independent variables, levels, and the response. The catalyst loading (X_C) and methanol-to-oil molar ratio (X_M) were selected as the investigating factors, while, the response chosen was the CJCO conversion. The statistical analysis enabled the determination of influences associated with interactions considering the CJCO conversion at high and low values of each factor. The model equation was used to elucidate the interaction between the variables, and predict the optimum conditions affecting the described methanolysis process.

3. Results and discussion

3.1. Selection of catalyst type

Initially, the capability of different catalytic materials to assist the alcoholysis reaction between CJCO and methanol was investigated. The activity of commercial CaO, laboratory-synthesized mussel shells derived CaO, calcium methoxide, glycerol-enriched CaO, lixiviated CaO, and thermal catalyst for the CJCO methanolysis reaction was examined. The methanolysis reactions were performed at 65 ºC for 420 min, using methanol-to-oil molar ratio of 9:1, catalyst amount of 15 wt. %, glycerol dose (in the case of glycerol activated catalyst) of 10 % with respect to (w.r.t.) catalyst weight, and 350 rpm stirring intensity. The experimental results of the study evaluating the efficiency of different catalyst to assist the CJCO methanolysis reaction are presented in Figure 1. An insignificant difference obtained in the CJCO conversion while comparing the activity of the lixiviated CaO species (HMC) with thermal catalysis (TC) attributed towards CaO being a good heterogeneous catalyst for biodiesel production. The application of commercial CaO catalyst for the described methanolysis reaction resulted in 53.80 % CJCO conversion, which was 2.25 times higher than that obtained using the mussel shells derived CaO catalyst. However, the CJCO conversion was found to be enhanced by 3.88 times when the mussel shells derived CaO was applied for the glycerol activation process prior to its utilization for the described methanolysis reaction. The utilization of glycerol-enriched CaO (GMC) catalyst for the methanolysis reaction resulted in 93.56 % CJCO conversion using the previous mentioned reaction variables. The elevation in the CJCO conversion was due to the reaction between glycerol and the basic sites of CaO, leading towards the formation of Ca-glycerol complex. The presence of hydrophobic as well as hydrophilic sites on the surface of GMC, in comparison to the polar surface of CaO, favor the approach of triglycerides and alcohol to the catalytic sites [22, 29].

The CJCO conversion raised from 23.88 % to 47.27 % when the catalytic active species were transformed from CaO to calcium methoxide. The elevation in the CJCO conversion when calcium methoxide was applied for the methanolysis reaction indicated the existence of interaction between mussel shells derived CaO and methanol. Therefore, the scheme presented in the current study of using oil, and not methanol, as a medium for enhancing the interaction between CaO and glycerol would prove to be beneficial in eliminating even a slight possibility of the generation of catalytic methoxide species, and synthesize only the glycerol-enriched CaO catalytic material. A research study reported by Esipovich et al. [29] presented a mechanism in which it was shown that CM would react with glycerol, resulting in the release of methanol molecule and directing the formation of GMC. The final catalytic material (GMC), therefore, is similar when either MC or CM was treated with glycerol. Therefore, based on the mechanism presented before [29], the glycerol activated CM and the glycerol treated MC might possess similar efficiency to assist the CJCO methanolysis process.

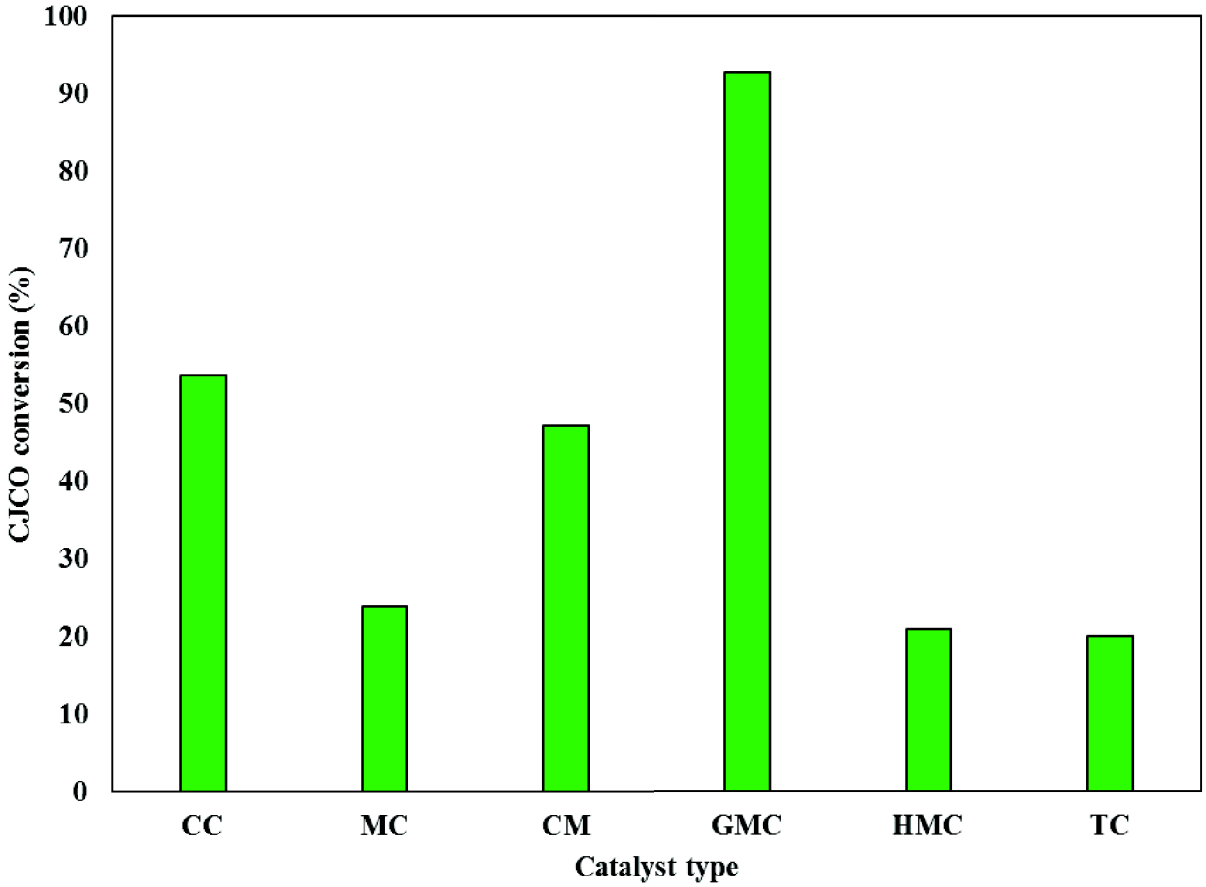

Figure 1: CJCO conversion using different types of catalyst. CC: commercial CaO, MC: mussel shells derived CaO, CM: calcium methoxide, GMC: glycerol-activated mussel shells derived CaO, HMC: Homogeneous contribution of mussel shells derived CaO, TC: thermal catalysis. Reaction temperature: 65 ºC, time: 420 min, CaO catalyst loading: 15 wt. %, glycerol dosage: 10 % (only in the case of GMC), methanol-to-CJCO molar ratio: 9:1, stirring intensity: 350 rpm.

3.2. Effect of reaction variables

3.2.1. Effect of glycerol dose

The evaluation of an appropriate amount of glycerol, required for the transformation of CaO, could be of foremost relevance because the reported study suggested that the availability of surplus glycerol in the reaction mixture due to its by-production during the methanolysis reaction

255 directs the deactivation of CaO catalytic material [35]. Additionally, Ferrero et al. [28] reported
256 that the glycerol dosage higher than the optimum amount resulted in decrease of the biodiesel
257 yield. In the present study, the impact of glycerol dose of 5, 10, and 15 % (w.r.t. catalyst weight)
258 on the CJCO conversion was examined. The CJCO methanolysis reaction with different glycerol
259 dosage was performed keeping fixed reaction temperature of 65 ºC, methanol-to-CJCO molar ratio
260 of 9:1, catalyst amount of 15 wt. %, time of 420 min, and 350 rpm stirring intensity. The effect of
261 CaO catalyst, activated by different amount of glycerol, on the conversion of CJCO is shown in
262 Figure 2. The CJCO conversion increased from 85.60 % to 93.56 % with increase in the glycerol
263 dosage from 5 % to10 % (w.r.t. catalyst weight); however, further increment in the glycerol dosage
264 had an insignificant impact on the CJCO conversion. Similar pattern of experimental findings were
265 reported by López Granados [25]; where it was presented that the addition of glycerol to the
266 reaction mixture significantly affected the rate of methanolysis reaction; however, increasing the
267 glycerol dosage above optimal value had a negligible impact on the biodiesel yield. Therefore, the
268 present study concluded that the glycerol dosage of 10 % (w.r.t. catalyst weight) was appropriate
269 to occur the structural transformation of CaO as well as to enhance the catalytic activity of
270 heterogeneous glycerol-enriched CaO for the described methanolysis reaction.
271

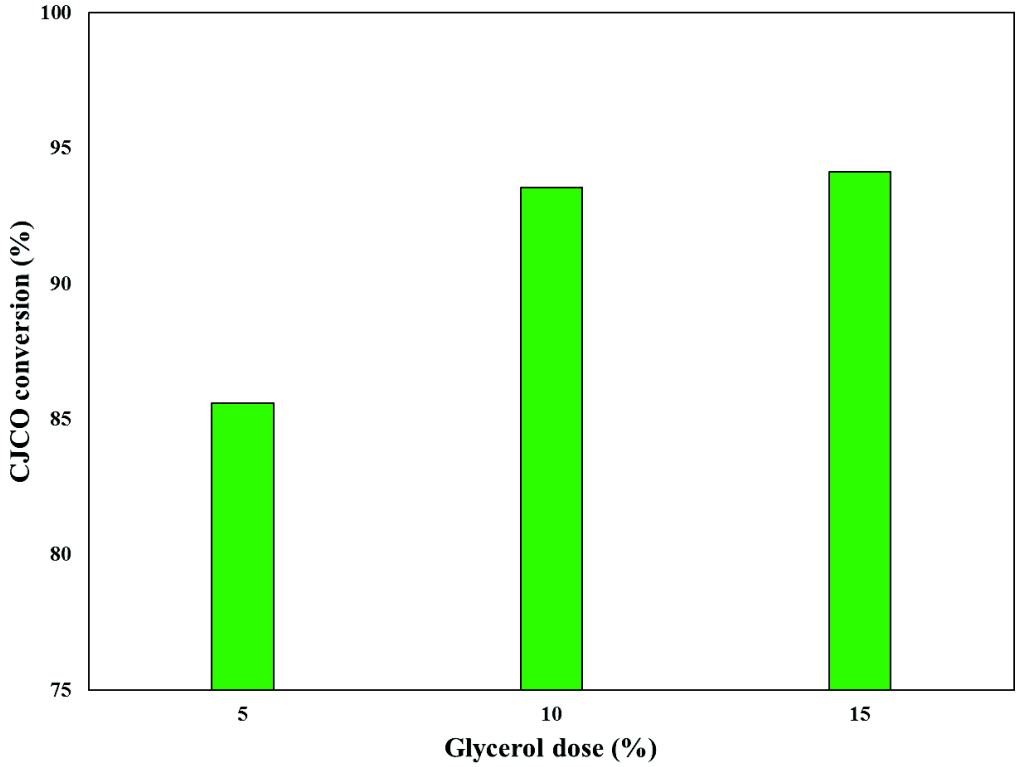

Figure 2: Effect of glycerol dosage for CaO catalyst activation on CJCO conversion. Reaction temperature: 65 ºC, time: 420 min, CaO catalyst loading: 15 wt. %, methanol-to-CJCO molar ratio: 9:1, stirring intensity: 350 rpm.

3.2.2. Effect of reaction temperature

The study of effect of temperature on the described methanolysis process could be of high relevance because the available report suggested that an adequate temperature is required not only to promote the miscibility and reactivity between the reactants but also for the activation of the heterogeneous glycerol-enriched CaO catalyst [25, 35]. The experimental results for the effect of temperature (45, 55, and 65 ºC) on the conversion of CJCO are presented in Figure 3. Under similar operating parameters, the methanolysis reaction performed at 65 ºC resulted in the highest conversion of CJCO; maximum oil conversion being 93.56 % after 420 min of reaction. Approximately identical oil conversion obtained at reaction temperature of 45 and 55 ºC hinted that the catalytic phase of glycerol-enriched CaO was not activated at the mentioned temperatures.

The obtained experimental findings could be correlated with those reported by Kouzu et al. [35], where it was concluded that CaDg was interacted with methanol at 60 ºC temperature. Therefore, the reaction temperature of 65 ºC was concluded as optimum for the described methanolysis process.

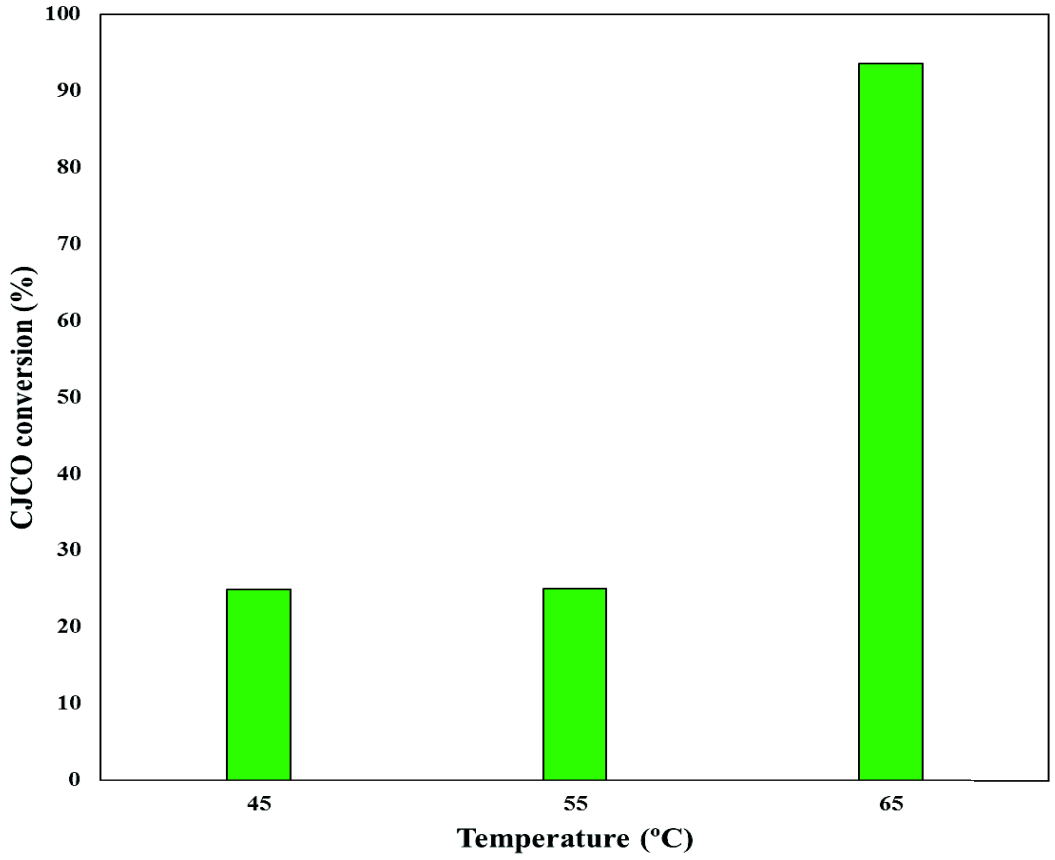

Figure 3: Effect of temperature on CJCO conversion. Reaction time: 420 min, CaO catalyst loading: 15 wt. %, glycerol dosage: 10 %, methanol-to-CJCO molar ratio: 9:1, stirring intensity: 350 rpm.

3.2.3. Effect of reaction time

From a process economics perspective, it would be important to determine the optimal time required for achieving the maximum biodiesel production. The effect of reaction time (60, 180, 300, 420, and 540 min) on the CJCO conversion was studied using reaction temperature of 65 ºC, catalyst loading of 15 wt. %, glycerol dosage of 10 % (w.r.t. catalyst weight), methanol-to-CJCO

molar ratio of 9:1, and 350 rpm stirring intensity; the results of which are shown in Figure 4. As observed, the methanolysis reaction progressed till 420 min. The described methanolysis reaction performed for 420 min allowed 93.56 % conversion of CJCO; its further continuation, however, had an insignificant impact on the oil conversion. Hence, all experiments in the present study were performed for 420 min.

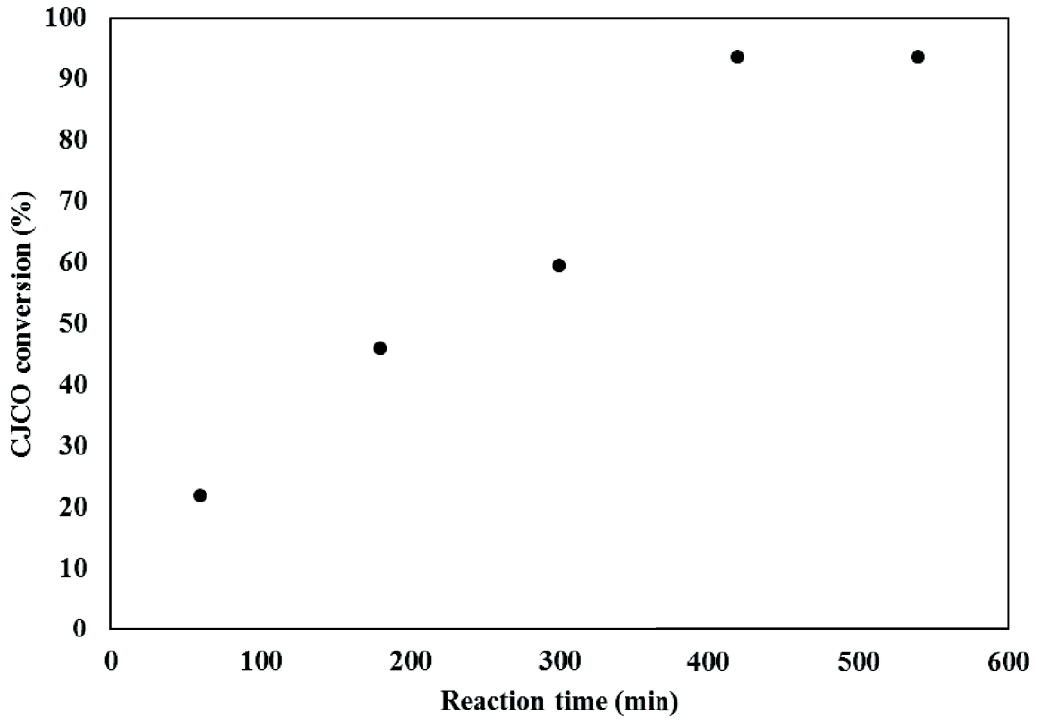

Figure 4: Effect of time on CJCO conversion. Reaction temperature: 65 ºC, CaO catalyst loading: 15 wt. %, glycerol dosage: 10 %, methanol-to-CJCO molar ratio: 9:1, stirring intensity: 350 rpm.

3.2.4. Effect of methanol-to-CJCO molar ratio

Theoretically, 3 molecules of alcohol are required to react with 1 molecule of TAGs for the synthesis of 3 molecules of fatty acid alkyl esters (biodiesel) and 1 molecule of glycerol. However, it is generally recognized that an excess of alcohol is essential to promote the forward reaction leading towards the complete transformation of TAGs to biodiesel [1]. The effect of the

mole ratio of methanol-to-CJCO, varied from 4.8:1 to 13.2:1, on the CJCO conversion is shown in Figure 5. The experimental results showed that the CJCO conversion augmented gradually with increasing amount of methanol. The increase in methanol-to-CJCO molar ratio from 4.8:1 to 9:1 resulted in the elevation of CJCO conversion from 80.93 % to 93.56 %, however, further increase in the mole ratio of methanol-to-CJCO to 12:1 resulted only in slight improvement in oil conversion. The highest oil conversion of 95.03 % was achieved using methanol-to-CJCO molar ratio of 13.2:1; however, from the process economics perspective, methanol-to-CJCO molar ratio of 9:1 could be ideal.

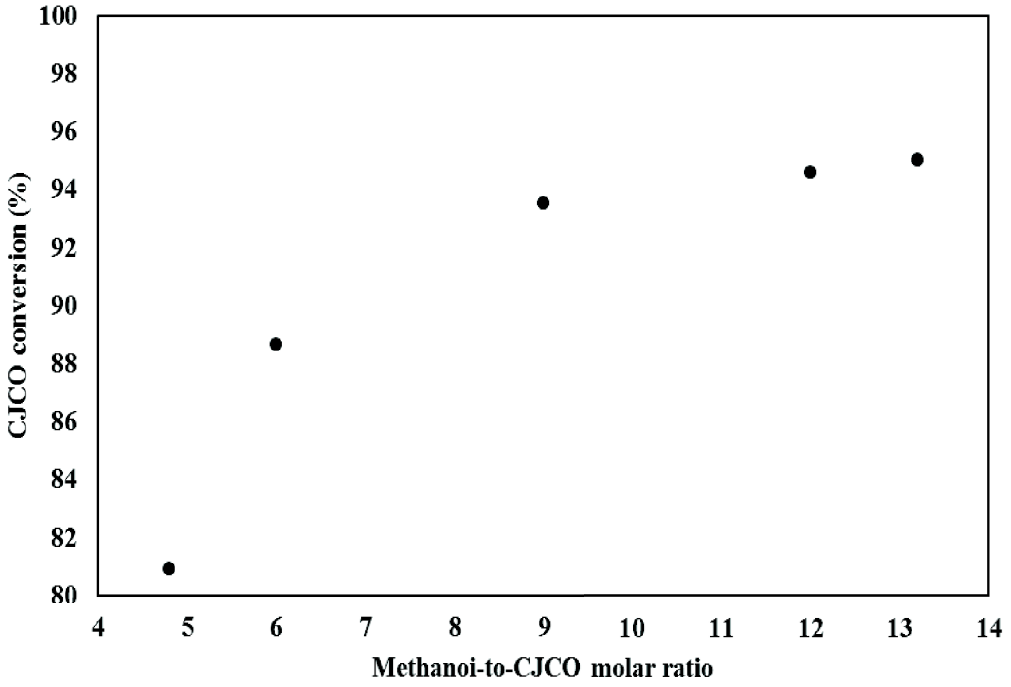

Figure 5: Effect of methanol-to-CJCO molar ratio on CJCO conversion. Reaction temperature: 65 ºC, time: 420 min, CaO catalyst loading: 15 wt. %, glycerol dosage: 10 %, stirring intensity: 350 rpm.

3.2.5. Effect of catalyst amount

The effect of five different catalyst amount on the described methanolysis reaction was also examined using constant glycerol dosage of 10 % (w.r.t. catalyst weight), temperature of 65

ºC, time of 420 min, methanol-to-CJCO molar ratio of 9:1, and 350 rpm stirring intensity. The effect of catalyst amount, ranging between 10.8 wt. % and 19.2 wt. %, on the CJCO conversion is presented in Figure 6. The experimental results indicated that increase in the catalyst loading from 10.8 wt. % to 15 wt. % resulted in the augmentation of CJCO conversion from 84.30 % to 93.56 %. However, insignificant improvement in oil conversion observed when the catalyst amount was further increased was indicative of the catalyst amount of 15 wt. % being optimum for the described methanolysis reaction. The increase in the viscosity of the reaction mixture caused due to higher catalyst loading could be the reason for stagnation in the advancement of the CJCO methanolysis process. Furthermore, it was reported earlier that the by-production of glycerol limited the biodiesel yield to around 95 % as a consequence of reverse transformation of CaDg catalyst [35]. This could be correlated with the experimental results presented in the current investigation.

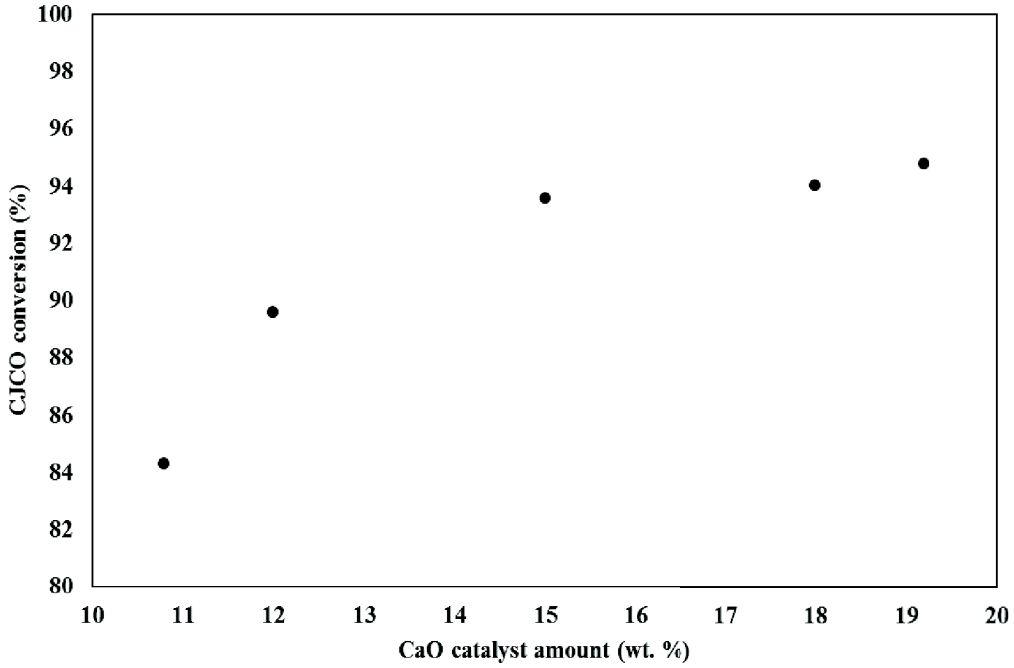

Figure 6: Effect of catalyst amount on CJCO conversion. Reaction temperature: 65 ºC, time: 420 min, glycerol dosage: 10 %, methanol-to-CJCO molar ratio: 9:1, stirring intensity: 350 rpm.

3.3. Acid value analysis

Since, crude *Jatropha curcas* oil having high FFA was utilized for biodiesel production, the determination of acid value of the produced biodiesel is of foremost relevant. The acid value of biodiesel produced from CJCO using reaction temperature of 65 ºC, time of 420 min, CaO catalyst loading of 15 wt. %, glycerol dosage of 10 % (w.r.t. catalyst weight), methanol-to-CJCO molar ratio of 9:1, and 350 rpm stirring intensity was determined. The acid value of CJCO was determined to be 24.75 mg KOH g^{-1}, which subsequently dropped to 0.18 mg KOH g^{-1} after its transformation to biodiesel. However, it is important to note that the water-washing step of biodiesel phase was required. The acid value of biodiesel was found to follow the specifications of EN 14214 and ASTM D6751-08 official methods [36].

3.4. Statistical analysis

The statistical analysis of glycerol-activated CaO assisted CJCO methanolysis reaction was conducted utilizing methanol-to-CJCO molar ratio and catalyst loading as the investigating factors, in all experiments keeping fixed reaction temperature of 65 ºC, glycerol dosage of 10 % (wr.t. to catalyst weight), time of 420 min, and 350 rpm stirring intensity. The reaction temperature was not included in the experimental design because the glycerol-activated CaO catalyst was activated only at 65 ºC, and displayed insignificant activity at 45 and 55 ºC to assist the methanolysis process (Figure 3). The water condenser, attached to the reactor, enabled the refluxing of methanol back to the reactor when the methanolysis reaction was performed at 65 ºC. However, increasing reaction temperature to 75 ºC resulted in rapid evaporation of methanol despite having the water cooling condenser, and in incompletion of the methanolysis process. Whereas, the reaction time was not involved because low reaction time resulted in too low CJCO conversion, while, high

reaction time directed an insignificant improvement in the CJCO conversion (Figure 4). The real factors, the coded factors, and the experimental CJCO conversion of the described methanolysis reaction are summarized in Table 1.

Table 1: Two-level factorial design of experiments. Stages of experiments along with the natural and the coded values (X_M for methanol-to-CJCO molar ratio and X_C for catalyst amount) of the reaction variables, and the obtained CJCO conversion.

Type of experiment	Run	Methanol-to-oil molar ratio	Catalyst amount (%)	X_M	X_C	Conversion (%)
Linear stage	1	12	18	1	1	96.09
	2	12	12	1	-1	94.31
	3	6	18	-1	1	93.04
	4	6	12	-1	-1	83.78
Center stage	5	9	15	0	0	92.70
	6	9	15	0	0	93.56
	7	9	15	0	0	93.59
	8	9	15	0	0	92.63
Non-linear stage	9	13.2	15	1.41	0	95.03
	10	4.8	15	-1.41	0	80.93
	11	9	19.2	0	1.41	94.77
	12	9	10.8	0	-1.41	84.30

3.4.1. Linear Stage

The linear stage and the center points of the experimental design were utilized to evaluate the interaction within the reaction variables, and also their influence on the described methanolysis process. The results of the statistical analysis are presented in Table 2. The evaluated parameters indicated that the influence of methanol-to-CJCO molar ratio and catalyst loading was higher than the confidence interval; consequently, both parameters significantly affected the described methanolysis process. The natural and the coded values of the considered experimental parameters were utilized for the establishment of the linear statistical and industrial mathematical regression models, respectively, for the described methanolysis process. The linear statistical and industrial model for the glycerol-enriched CaO assisted methanolysis process, under the investigated range of experimental conditions, are presented in equation (2) and (3), respectively.

$$X_{CJCO} = 91.80 + 3.39\ X_M + 2.76\ X_C - 1.87\ X_{MC} \quad (2)$$

$$X_{CJCO} = 40.42 + 4.24\ X_M + 2.79\ X_C - 0.20\ X_{MC} \quad (3)$$

Table 2: Results for the statistical analysis of the experimental design. M: Methanol-to-CJCO molar ratio, C: catalyst loading, $\bar{Y}$: mean response, s: standard deviation, t: student's t.

Parameters	Response
Main influence and interactions	$\bar{Y} = 91.80$
	$I_M = 6.79$
	$I_C = 5.52$
	$I_{MC} = -3.74$
Significance test: *c confidence level: 95 %*	
Mean response (only center points)	93.12
Standard deviation	t = 3.18; s = 0.52
Confidence interval	± 0.83
Significant variables	M, C, MC
Significance of curvature	
Curvature	1.31
Confidence curvature interval	1.18
Significance	Yes

3.4.2. Non-linear Stage

The results of the regression analysis, presented in Table 2, indicated that the curvature had a positive influence on the described methanolysis process under the investigated experimental range. The non-linear stage of the design of experiments was also taken into consideration because the curvature was found to be higher than the confidence curvature interval. The present analysis involves all the independent variables and their within interactions. The response surface statistical and industrial quadratic mathematical model for the glycerol-activated CaO assisted methanolysis process, under the studied range of experimental conditions, are expressed in equation (4) and (5), respectively.

$$X_{CJCO} = 93.12 + 4.19\ X_M + 3.23\ X_C - 1.80\ X_M^2 - 1.87\ X_{MC} - 1.03\ X_C^2 \quad (4)$$

$$X_{CJCO} = -5.39 + 8.13\ X_M + 6.32\ X_C - 0.20\ X_M^2 - 0.20\ X_{MC} - 0.11\ X_C^2 \quad (5)$$

The statistical quadratic regression expression (equation 4) was applied to achieve the response surface graphical representation. The three-dimensional surface plot of the predicted

CJCO conversion with varying methanol-to-CJCO molar ratio and catalyst loading is presented in Figure 7. Within the studied experimental range, the CJCO conversion augmented with the increase in methanol-to-CJCO molar ratio and catalyst loading, hinting towards the possible interaction between methanol and glycerol-enriched CaO catalyst. The present regression analysis provided an appreciable correlation between the predicted values and experimental findings, which validated the statistical quadratic mathematical model being appropriate to describe the glycerol-activated CaO assisted methanolysis process of CJCO within the studied range of reaction conditions. The graphical representation for the comparison between the predicted values and the experimental results for the CJCO conversion is shown in Figure 8.

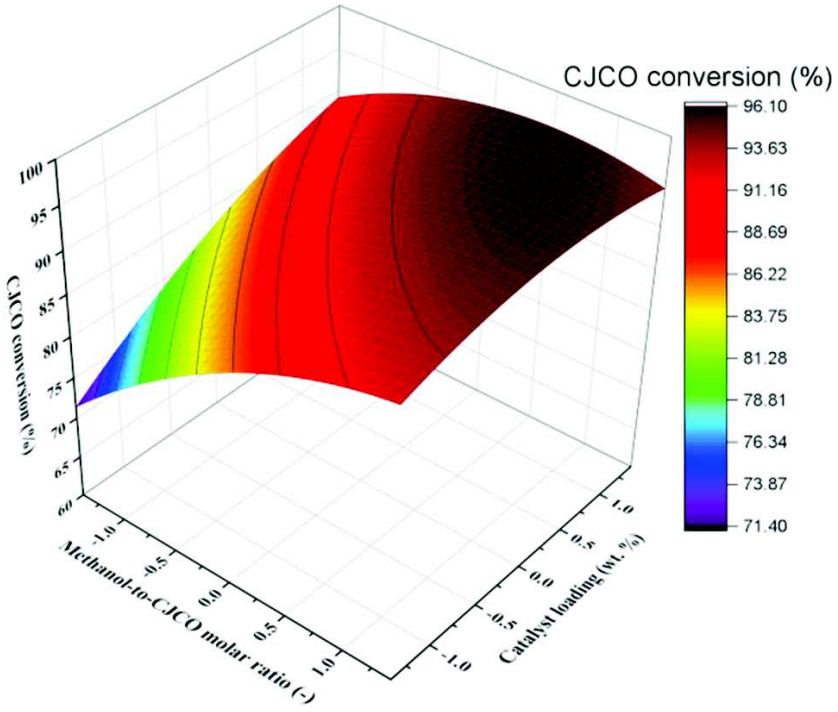

Figure 7: Response surface 3D plot indicating the influence of methanol-to-oil molar ratio and catalyst loading on the CJCO conversion. Temperature: 65 ºC, time: 420 min, glycerol dose: 10 % (w.r.t. catalyst weight), stirring intensity: 350 rpm.

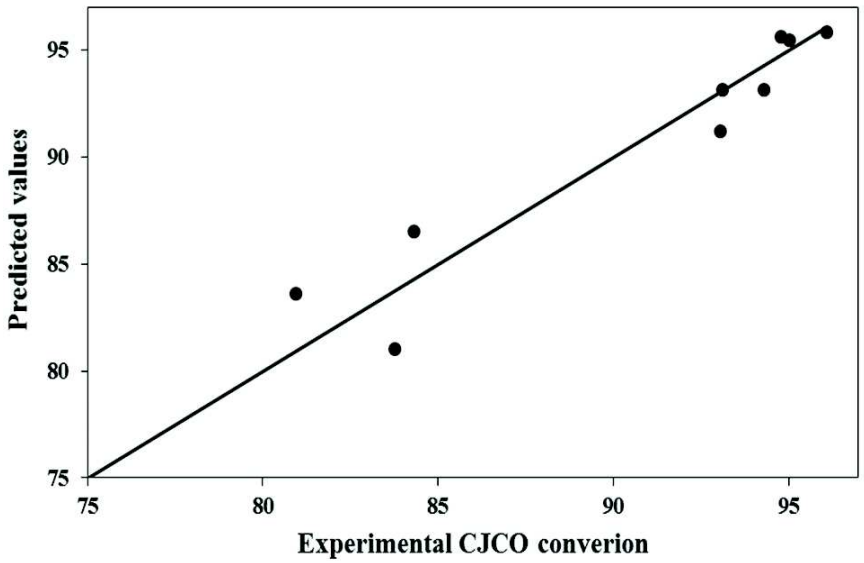

417

418 **Figure 8**: Parity plot between predicted and experimental CJCO conversion. Line corresponds to zero error between

419 the experimental data and predicted values.

4. Conclusion

The present research article addresses the applicability of heterogeneous glycerol-activated CaO catalyst for biodiesel production from CJCO having high free fatty acid content. For the current research investigation, CaO catalyst was derived from mussel shells. The obtained results suggested that the temperature had a significant impact on the activation of glycerol-enriched CaO catalyst, which was found to be active for the methanolysis at 65 ºC temperature. The glycerol dose of 10 % (w.r.t. catalyst weight) was found to be suitable to allow the structural transformation of CaO as well as to improve the activity of the heterogeneous glycerol-enriched CaO catalyst for the described methanolysis reaction. Based on the experimental findings, presented in Figure 4, the reaction time of 420 min was optimum for the described methanolysis process. The statistical analysis suggested that the appliance of methanol-to-CJCO molar ratio of 12:1 and 18 wt. % catalyst loading resulted in the maximum CJCO conversion. The experimental results presented in Figure 5 and Figure 6 indicated that the utilization of methanol-to-CJCO molar ratio of 9:1 and 15 wt. % catalyst loading, respectively, could be appropriate for the glycerol-activated CaO assisted CJCO methanolysis process, under the investigated range of experimental conditions.

436 **Acknowledgements**

437 The authors would like to express their gratitude to the Norwegian University of Life
438 Sciences (Project No. 1301051406), Complutense University of Madrid, and NILS mobility grants
439 (009-ABEL-CM-2013) for their financial support.

440

References

[1] Avhad MR, Marchetti JM. A review on recent advancement in catalytic materials for biodiesel production. Renewable and Sustainable Energy Reviews. 2015; 50: 696-718.

[2] Marchetti JM. A summary of the available technologies for biodiesel production based on a comparison of different feedstock's properties. Process Safety and Environmental Protection. 2012; 90(3): 157-63.

[3] Marchetti JM. The effect of economic variables over a biodiesel production plant. Energy Conversion and Management. 2011; 52(10): 3227-33.

[4] Knothe G. Dependence of biodiesel fuel properties on the structure of fatty acid alkyl esters. Fuel Processing Technology. 2005; 86(10): 1059-70.

[5] Knothe G. Improving biodiesel fuel properties by modifying fatty ester composition. Energy & Environmental Science. 2009; 2(7): 759-66.

[6] Marchetti JM, Pedernera MN, Schbib NS. Production of biodiesel from acid oil using sulfuric acid as catalyst: kinetics study. International Journal of Low-Carbon Technologies. 2011; 6(1): 38-43.

[7] Uzun BB, Kılıç M, Özbay N, Pütün AE, Pütün E. Biodiesel production from waste frying oils: Optimization of reaction parameters and determination of fuel properties. Energy. 2012; 44(1): 347-51.

[8] Dias JM, Alvim-Ferraz MCM, Almeida MF. Comparison of the performance of different homogeneous alkali catalysts during transesterification of waste and virgin oils and evaluation of biodiesel quality. Fuel. 2008; 87(17–18): 3572-8.

[9] Soriano Jr NU, Venditti R, Argyropoulos DS. Biodiesel synthesis via homogeneous Lewis acid-catalyzed transesterification. Fuel. 2009; 88(3): 560-5.

[10] Xie W, Zhao L. Production of biodiesel by transesterification of soybean oil using calcium supported tin oxides as heterogeneous catalysts. Energy Conversion and Management. 2013; 76: 55-62.

[11] Kim M, Salley SO, Ng KYS. Transesterification of Glycerides Using a Heterogeneous Resin Catalyst Combined with a Homogeneous Catalyst. Energy & Fuels. 2008; 22(6): 3594-9.

[12] Kazemian H, Turowec B, Siddiquee MN, Rohani S. Biodiesel production using cesium modified mesoporous ordered silica as heterogeneous base catalyst. Fuel. 2013; 103: 719-24.

[13] Zabeti M, Wan Daud WMA, Aroua MK. Activity of solid catalysts for biodiesel production: A review. Fuel Processing Technology. 2009; 90(6): 770-7.

[14] Semwal S, Arora AK, Badoni RP, Tuli DK. Biodiesel production using heterogeneous catalysts. Bioresource Technology. 2011; 102(3): 2151-61.

[15] Endalew AK, Kiros Y, Zanzi R. Inorganic heterogeneous catalysts for biodiesel production from vegetable oils. Biomass and Bioenergy. 2011; 35(9): 3787-809.

[16] Avhad MR, Marchetti JM. Innovation in solid heterogeneous catalysis for the generations of economically viable and ecofriendly biodiesel: a review. Catalysis reviews. 2015. (DOI: 10.1080/01614940.2015.1103594).

[17] Correia LM, Saboya RMA, de Sousa Campelo N, Cecilia JA, Rodríguez-Castellón E, Cavalcante Jr CL, et al. Characterization of calcium oxide catalysts from natural sources and their application in the transesterification of sunflower oil. Bioresource Technology. 2014;151:207-13.

[18] Sánchez M, Marchetti JM, El Boulifi N, Aracil J, Martínez M. Kinetics of Jojoba oil methanolysis using a waste from fish industry as catalyst. Chemical Engineering Journal. 2015; 262: 640-7.

[19] Sirisomboonchai S, Abuduwayiti M, Guan G, Samart C, Abliz S, Hao X, et al. Biodiesel production from waste cooking oil using calcined scallop shell as catalyst. Energy Conversion and Management. 2015; 95: 242-7.

[20] Kouzu M, Kasuno T, Tajika M, Sugimoto Y, Yamanaka S, Hidaka J. Calcium oxide as a solid base catalyst for transesterification of soybean oil and its application to biodiesel production. Fuel. 2008; 87(12): 2798-806.

[21] Kouzu M, Kasuno T, Tajika M, Yamanaka S, Hidaka J. Active phase of calcium oxide used as solid base catalyst for transesterification of soybean oil with refluxing methanol. Applied Catalysis A: General. 2008; 334(1–2): 357-65.

[22] León-Reina L, Cabeza A, Rius J, Maireles-Torres P, Alba-Rubio AC, López Granados M. Structural and surface study of calcium glyceroxide, an active phase for biodiesel production under heterogeneous catalysis. Journal of Catalysis. 2013; 300: 30-6.

[23] Kouzu M, Tsunomori M, Yamanaka S, Hidaka J. Solid base catalysis of calcium oxide for a reaction to convert vegetable oil into biodiesel. Advanced Powder Technology. 2010; 21(4): 488-94.

[24] Kouzu M, Yamanaka S-y, Hidaka J-s, Tsunomori M. Heterogeneous catalysis of calcium oxide used for transesterification of soybean oil with refluxing methanol. Applied Catalysis A: General. 2009; 355(1–2): 94-9.

[25] López Granados M, Alba-Rubio AC, Vila F, Martín Alonso D, Mariscal R. Surface chemical promotion of Ca oxide catalysts in biodiesel production reaction by the addition of monoglycerides, diglycerides and glycerol. Journal of Catalysis. 2010; 276(2): 229-36.

[26] Lukić I, Kesić Ž, Zdujić M, Skala D. Calcium diglyceroxide synthesized by mechanochemical treatment, its characterization and application as catalyst for fatty acid methyl esters production. Fuel. 2016; 165: 159-65.

[27] Li C, Huang Z, He Y, Zhou D, Du C, Zhang S, Chen J. Transesterification of *Jatropha* oil to biodiesel by using catalyst containing $Ca(C_3H_7O_3)_2$ as a solid base catalyst. Advanced Materials Research. 2013; 666: 93-102.

[28] Ferrero GO, Almeida MF, Alvim-Ferraz MCM, Dias JM. Glycerol-enriched heterogeneous catalyst for biodiesel production from soybean oil and waste frying oil. Energy Conversion and Management. 2015; 89: 665-71.

[29] Esipovich A, Danov S, Belousov A, Rogozhin A. Improving methods of CaO transesterification activity. Journal of Molecular Catalysis A: Chemical. 2014; 395: 225-33.

[30] Reyero I, Arzamendi G, Gandía LM. Heterogenization of the biodiesel synthesis catalysis: CaO and novel calcium compounds as transesterification catalysts. Chemical Engineering Research and Design. 2014; 92(8): 1519-30.

[31] Sánchez-Cantú M, Reyes-Cruz FM, Rubio-Rosas E, Pérez-Díaz LM, Ramírez E, Valente JS. Direct synthesis of calcium diglyceroxide from hydrated lime and glycerol and its evaluation in the transesterification reaction. Fuel. 2014; 138: 126-33.

[32] Gupta AR, Yadav SV, Rathod VK. Enhancement in biodiesel production using waste cooking oil and calcium diglyceroxide as a heterogeneous catalyst in presence of ultrasound. Fuel. 2015; 158: 800-6.

[33] Sánchez M, Bergamin F, Peña E, Martínez M, Aracil J. A comparative study of the production of esters from *Jatropha* oil using different short-chain alcohols: Optimization and characterization. Fuel. 2015; 143: 183-8.

[34] Kawashima A, Matsubara K, Honda K. Acceleration of catalytic activity of calcium oxide for biodiesel production. Bioresource Technology. 2009; 100(2): 696-700.

[35] Kouzu M, Hidaka J-s, Wakabayashi K, Tsunomori M. Solid base catalysis of calcium glyceroxide for a reaction to convert vegetable oil into its methyl esters. Applied Catalysis A: General. 2010; 390(1–2): 11-8.

[36] Knothe G. Analyzing biodiesel: standards and other methods. J Am Oil Chem Soc. 2006; 83(10): 823-3.

Paper V

Energy Conversion and Management xxx (2016) xxx–xxx

Contents lists available at ScienceDirect

Energy Conversion and Management

journal homepage: www.elsevier.com/locate/enconman

Modeling chemical kinetics of avocado oil ethanolysis catalyzed by solid glycerol-enriched calcium oxide

M.R. Avhad [a,*], M. Sánchez [b], A. Bouaid [b], M. Martínez [b], J. Aracil [b], J.M. Marchetti [a,*]

[a] Department of Mathematical Science and Technology, Norwegian University of Life Sciences, Drøbakveien 31, 1432 Ås, Norway
[b] Chemical Engineering Department, Faculty of Chemistry, Complutense University, 28040 Madrid, Spain

ARTICLE INFO

Article history:
Received 7 June 2016
Received in revised form 8 July 2016
Accepted 23 July 2016
Available online xxxx

Keywords:
Biodiesel production
Calcium oxide
Glycerol activation
Avocado oil
Ethanolysis
Kinetics

ABSTRACT

The catalytic activity of glycerol-enriched calcium oxide for the alcoholysis reaction between avocado oil and ethanol was investigated. The calcium oxide was derived from *Mytilus Galloprovincialis* shells. This study systematically examined the influence of temperature, ethanol-to-oil molar ratio, and the catalyst amount on the variation in the concentration of triacylglycerols and biodiesel with reaction time. The interaction between the reaction variables (ethanol-to-oil molar ratio and catalyst amount), their influence on the ethanolysis process, and the optimum variables affecting the process were determined through the response surface methodology. A previously developed mathematical model was applied for the current ethanolysis process, and the model parameters were determined. The ethanolysis reaction occurred between the surface chemisorbed ethoxide ions and oil molecules in the liquid phase, while, the overall process was controlled by the ethanol-adsorption step. The physico-chemical properties of biodiesel, produced using potassium methoxide catalyst, were additionally measured.

1. Introduction

Biodiesel, comprising fatty acid alkyl esters (FAAEs), is considered as a viable alternative or additive to current petroleum-derived diesel due to its environmental benefits, such as negligible toxicity, biodegradability, and renewability [1]. According to the American Society for Testing and Materials (ASTM), biodiesel is referred as the mono-alkyl esters derived from lipid feedstocks, such as vegetable oils and animal fats [2]. A well-known and extensively applied methodology for biodiesel production is the catalyst-assisted alcoholysis process, which is also known as the transesterification reaction of triacylglycerol (TAGs) and the esterification of free fatty acid (FFA). Since the last few years, heterogeneously catalyzed alcoholysis reactions are preferred over the homogeneous process. This is because, the utilization of heterogeneous catalysts allows an easy recovery of the materials which might be re-utilized, eliminates the neutralization process, simplifies the purifications stages, and could enable the continuous operation of the process; which in return would improve the yield and the purity of biodiesel as well as glycerol [3,4]. However, the use of heterogeneous catalysts for biodiesel production have not been yet implemented on an industrial scale. The major challenges associated with the utilization of heterogeneous catalysts includes: (i) restricted catalytic active sites in comparison to the homogeneous counterparts, (ii) generally need of severe reactions conditions, (iii) sometimes tri-phasic reaction system (liquid-liquid-solid) resulting in the mass transfer limitations, (iv) expensive and time-consuming material synthesis procedure, and (v) catalyst poisoning due to the surrounding atmosphere. In this regards, consistent scientific efforts are involved in developing not only an active and stable but also a low-cost heterogeneous catalyst for biodiesel production.

The recent literature demonstrated that calcium oxide (CaO) catalyst has been widely applied for the alcoholysis reactions, because of its high basicity, low solubility in short-chain alcohols, low cost, and is easy to handle [5–7]. In addition, the utilization of CaO catalyst for biodiesel production could be advantageous because the material can be generated from abundantly available natural and waste sources [8–10]. The CaO-based catalyst have been utilized in several forms, including neat [11–13], mixed oxides [14–17], supported [18–22], doped [23,24], amongst others [25,26]. Besides the above mentioned CaO-based catalysts, the catalytic activity of glycerol-CaO complex, described as glycerol-enriched CaO or calcium diglyceroxide (CaDg), for the alcoholysis reaction have been also investigated [27–31]. León-Reina et al. [32] described glycerol-enriched CaO as a set of molecular calcium tetramers interlinked by H-bonds; and reported its superior catalytic activity when compared with CaO catalyst. The superior activity

* Corresponding authors.
E-mail addresses: avhad.mangesh@ymail.com (M.R. Avhad), jorge.mario.marchetti@nmbu.no (J.M. Marchetti).

http://dx.doi.org/10.1016/j.enconman.2016.07.060
0196-8904/

of CaDg catalyst was due to the availability of basic oxygen anion as a consequence of interruption of the crystal structure at the surface which can abstract proton from OH group of methanol leading towards the formation of surface methoxide ion [22]. The CaDg catalyst was characterized as a chemically stable heterogeneous catalyst, weakly basic in nature, and not prone for deactivation due to the hydration/carbonation reaction when exposed to the surrounding air [33,34]. Because CaO catalyst experiences material transformation due to its interaction with glycerol, co-producing during the transesterification reaction, Kouzu et al. [33] and López Granados et al. [35] recommended to transform CaO to CaDg compound prior to its application for biodiesel production.

In the present study, glycerol-enriched CaO catalyst was applied for the alcoholysis reaction between avocado oil and ethanol. The CaO was derived from mussel shells (*Mytilus Galloprovincialis*), which is a waste generated from the fish industry. It is generally believed that the production of fatty acid ethyl esters (FAEEs) could be valuable from an ecological standpoint because ethanol can be synthesized through the fermentation process of a reasonable cost and abundantly available lignocellulosic biomass [36,37]. This study, therefore, addressed the utilization of only renewable resources for biodiesel production; thereby attaining total independence from petroleum-based materials and following the principles of green chemistry. Moreover, the application of ethanol for biodiesel production offers several advantages, including superior miscibility with plant oils, low toxicity, higher cetane number, lower cloud point, improved pour point, and lower nitrogen oxides as well as carbon monoxide emissions [38,39]. The synthesis of FAEEs is of high relevance because it can also be used as alcohol markers for the retrospective drug analysis in forensic cases [40,41]. Furthermore, FAEEs can be useful internal standard for the determination of fatty acid methyl esters in food and other samples [42]. Due to the previous mentioned advantages, the number of recent studies focused on the ethanolysis process of the lipid feedstocks have augmented [38,39,43–50]. The present research uses avocado oil as the lipid feedstock for the ethanolysis process. The emergy analysis presented by Takahashi and Ortega [51] concluded that avocado can be used as a raw material for biodiesel production because oil can be generated from the pulp, while, ethanol can be extracted from the pit. The renewability index of avocado was reported to be higher than the other oleaginous crops used for biodiesel production, such as rapeseed, sunflower, soybean, and cotton [51]. The use of avocado as a raw material for biodiesel production could be possible because, in its oil content, avocado fruit is exceeded only by the fruits of the palm and olive trees [52]. Though literature on the alcoholysis of avocado oil are available [53,54], no studies on glycerol-enriched CaO catalyst assisted avocado oil ethanolysis and its kinetic modeling have been so far reported.

This study systematically investigated the influence of temperature, the catalyst amount, and ethanol-to-oil ratio on the described ethanolysis process. The interactions within the reaction variables, their influence on the described ethanolysis reaction, and the optimum parameters affecting the process were determined by means of the response surface methodology (RSM). A mathematical model predicting the change in the TAGs and FAEEs concentration over the applied range of the experimental conditions is also presented. Furthermore, the physico-chemical properties of FAEEs, produced using a homogeneous catalyst, were measured and compared with the ASTM D6751 and EN 14214 official standards for biodiesel.

2. Experimental section

2.1. Materials

Avocado oil was supplied by Jedwards International, Inc. (Braintree, USA). Its fatty acid composition and properties, provided by the suppliers, are listed in the Supplementary Table S1. Ethanol (Cor Quimica, Spain), glycerol (Sigma-Aldrich), K-methylate (methanol/potassium methoxide: 68/32 wt.%, BASF, Germany), n-octyl octanoate (Sigma-Aldrich), and carbon disulfide (Panreac) with purity higher than 99% were utilized as received. The waste mussel shells needed for the synthesis of CaO were collected from the local fish market in Madrid, Spain.

2.2. Catalyst preparation

The detailed procedure for the synthesis of CaO material from mussel shells has been documented in the previous work [55]. The results for the characterization of CaO material, carried out earlier by means of X-ray diffraction, specific surface area analysis, induced coupled plasma atomic emission spectroscopy, and transmission electron microscopy, were published elsewhere [56]. For the synthesis of glycerol-enriched CaO catalyst, measured amount of CaO and glycerol (10% with respect to (w.r.t.) catalyst weight) were initially added into an airtight three-neck curved bottom glass reactor of 250 cm^3 volume capacity. Subsequently, an appropriate volume of avocado oil was poured into the reactor and the mixture was vigorously stirred at 60 °C for 60 min under atmospheric pressure. The selection of glycerol dose and the mixing temperature was based on the previous reports [55,57]. The CaO material transformation was conducted in the presence of avocado oil, and not ethanol, so as to not only produce merely glycerol-enriched CaO catalyst but also to eliminate even a minor possibility of the formation of the calcium ethoxide catalytic species [55,58]. In addition, performing the material transformation in the presence of avocado oil would prevent poisoning of CaO occurring due to the surrounding air inside the reactor.

2.3. Reaction and analysis

The transesterification reaction was performed in a three-neck curved bottom glass reactor of 250 cm^3 volume capacity. The middle neck of the glass reactor was used to insert a mechanical stirrer equipped with an impeller of 6.0 cm diameter which was placed centrically close to the bottom of the reactor. Both the diameter and the length of the glass reactor are 12.0 cm. The water condenser was attached to one of the side necks, while, a rubber cork was fitted to the other neck of the reactor through which the aliquots of the reaction mixture were periodically withdrawn using a glass syringe. The glass reactor was immersed in a thermostatically controlled water bath (Heto-Holten A/S, Denmark), the temperature of which was controlled by the PID controller with 1 °C precision. The speed of the mechanical stirrer was monitored by a motor (Eurostar Basic IKA). After the glycerol activation process of CaO, the reaction system was heated to the desired temperature. Once the system temperature reached the set point, an appropriate volume of ethanol was charged into the reactor using a conical flask; this was considered as the starting time of the ethanolysis reaction. The stirring intensity of 350 rpm was maintained for all experiments to overcome the mass transfer limitations [56]. The aliquots (approximately 1 ml) of the reaction mixture were withdrawn at a specific time intervals (1, 2.5, 5, 10, 20, 40, 60, and 120 min) to understand the progression of the reaction. The extracted samples were immediately applied to a rotaevaporator, attached to a vacuum pump (10 mg Hg), set at 70 °C for 30 min to eliminate the residual ethanol. The catalyst and glycerol was separated through the centrifugation (1500 rpm for 15 min).

The potassium methoxide-catalyzed ethanolysis of avocado oil was carried out in a semi-batch 3 dm^3 capacity glass reactor, equipped with the mechanical stirrer, the water condenser, a distillation unit and a decantation valve. The avocado oil ethanolysis

Please cite this article in press as: Avhad MR et al. Modeling chemical kinetics of avocado oil ethanolysis catalyzed by solid glycerol-enriched calcium oxide. Energy Convers Manage (2016), http://dx.doi.org/10.1016/j.enconman.2016.07.060

reaction was performed at 75 °C for 60 min, using 2 dm^3 of oil, 1 wt.% catalyst amount, ethanol-to-oil molar ratio of 6:1, and 600 rpm stirring intensity. Initially, avocado oil was added to the reactor and then the system temperature was raised to the desired set point. Once the system temperature was stable at the set point, potassium methoxide catalyst dissolved in ethanol was poured to the reactor. After the ethanolysis reaction, excess ethanol was removed using the distillation unit attached to a vacuum pump (70 mg Hg). The glycerol phase was separated from the biodiesel one through the decantation process. The FAEEs phase containing trace amount of ethanol, residual catalyst, and glycerol were removed using the waster washing step. The water washing step was repeated until the pH value of the waste water reached approximately neutral. Finally, the distillation process was repeated so as to eliminate the trace amount of water present in FAEEs. The produced biodiesel was subsequently utilized for the characterization purpose. The physico-chemical properties of avocado oil and FAEEs were analyzed using different analytical instruments, the details of which and the official methods followed are listed in the Supplementary Table S2.

The reaction samples were analyzed using a gas chromatography (GC) analyzer (Hewlett-Packard HP-5890 Series II) equipped with a flame ionization detector and a fused silica capillary column (12 m length, 0.31 mm internal diameter, and 0.71 μm thickness). The GC was connected to a Hewlett-Packard 3396SA integrator. The injection system was split-splitless, and helium was the carrier gas at a 1 ml min^{-1} flowrate. The injector and the detector temperature were set at 275 °C and 325 °C, respectively. The GC column temperature was initially held at 130 °C for 1 min, then raised at 4 °C min^{-1} to 160 °C, and finally heating at a ramp rate of 30 °C min^{-1} to 320 °C. The n-octyl octanoate was used as an internal standard, and the extracted reaction samples were dissolved in carbon disulfide. The GC analyses was conducted by injecting 1 μl volume of the prepared samples into the instrument. The TAGs, diacylglycerols, monoacylglycerols, and FAEEs concentration were determined and all four components were taken into consideration for the data analysis; however, only TAGs and FAEEs values were presented because of their high concentration and interest.

The avocado oil conversion ($X_{Avocado}$) is expressed as

$$X_{Avocado} = \frac{Initial\ moles\ of\ TAGs - Final\ moles\ of\ TAGS}{Initial\ moles\ of\ TAGs} \times 100\% \quad (1)$$

The FAEEs yield is expressed as

$$FAEEs\ yield = \frac{Total\ moles\ of\ FAEEs}{3 \times Moles\ of\ oil} \times 100\% \quad (2)$$

2.4. Design of experiments

For the purpose of regression analyses, a set of experiments was designed and the experimental findings were fitted to a two-level factorial design for the application of the RSM using the Statgraphics centurion XV software (Statpoint technologies, Inc., USA). The successful implementation of such method requires an appropriate selection of the independent variables, levels, and the response. The catalyst amount (X_C) and ethanol-to-oil molar ratio (X_E) were selected as the investigating factors, while, the response chosen was the FAEEs yield. The influences associated with the interactions were estimated considering the biodiesel yield at the high and low values of each factor. The model equation was used to elucidate the interaction between the variables, and predict the optimum conditions affecting the glycerol-enriched CaO assisted avocado oil ethanolysis process.

2.5. Theoretical background

The stoichiometry of transesterification reaction between plant oil and ethanol requires a mole TAGs and 3 mol of ethanol to produce 3 mol of FAEEs and a mole of glycerol [59]. The overall avocado oil ethanolysis is shown as

$$TAGs + 3E \overset{Catalyst}{\longleftrightarrow} 3FAEEs + G \quad (3)$$

where E is ethanol, and G is glycerol.

The ethanolysis process consists of three consecutive reversible reaction, where in a mole of FAEEs is released in each steps, and monoacylglycerol (MAGs) and diacylglycerol (DAGs) are intermediate products. The step wise ethanolysis process is represented as:

$$TAGs + E \overset{Catalyst}{\longleftrightarrow} FAEEs + DAGs \quad (4)$$

$$DAGs + E \overset{Catalyst}{\longleftrightarrow} FAEEs + MAGs \quad (5)$$

$$MAGs + E \overset{Catalyst}{\longleftrightarrow} FAEEs + G \quad (6)$$

For the purpose of modeling the described ethanolysis process, the following initial assumptions were taken into consideration [60–62]:

(1) The reaction mixture was perfectly mixed; and its composition, the catalyst distribution, and temperature were uniform throughout the process because the reaction was performed in a batch reactor under continuous and vigorous agitation [60,61].
(2) The contribution of homogeneous and thermal catalysis is insignificant [60,61].
(3) The proportion of FFA in avocado oil was negligible, hence the FFA neutralization is insignificant [60,62].
(4) The saponification reaction is negligible and the catalyst concentration remains constant during the ethanolysis process [60,62].
(5) Because of the nature of the catalyst, the initial mass transfer step resistance is not existent [32,63].

The curve fitting procedure was performed using the Aspen custom modeler software (version 8.4, Aspen Technology, Inc., USA). The selection of an appropriate mathematical model for the described ethanolysis process was based on the statistical parameters, such as the sum of weighted errors and the model selection criteria (MSC). The mathematical expression for the MSC is presented as:

$$MSC = \ln\left[\frac{\sum\left(\beta_{exp,i-}\beta_{exp,a}\right)^2}{\sum\left(\beta_{exp,i-}\beta_{pre,i}\right)^2}\right] - \frac{2p}{n} \quad (7)$$

where $\beta_{exp,i}$ is the experimental data at ith reaction time; $\beta_{exp,a}$ is an average of the experimental data; $\beta_{pre,i}$ is the predicted values at ith reaction time; p is the number of the parameter involved in the model; n is the number of the experimental data.

3. Results and discussion

3.1. Statistical analysis

The statistical analysis of glycerol-enriched CaO assisted avocado oil ethanolysis was conducted using ethanol-to-oil molar ratio and the catalyst amount as the investigating factors; in all experiments keeping fixed reaction temperature of 75 °C, glycerol dosage of 10% (w.r.t. catalyst weight), time of 120 min, and 350 rpm mixing intensity. The linear and the non-linear stage of

Please cite this article in press as: Avhad MR et al. Modeling chemical kinetics of avocado oil ethanolysis catalyzed by solid glycerol-enriched calcium oxide. Energy Convers Manage (2016), http://dx.doi.org/10.1016/j.enconman.2016.07.060

the two-level factorial design consisted of four experiments each, along with four replicates of the center points. The real factors, the coded factors, the experimental avocado oil conversion, and the experimental FAEEs yield of the described methanolysis reaction are summarized in Table 1.

3.1.1. Linear stage

The evaluation of the interaction between the reaction variables and their influences on the overall mentioned ethanolysis process was initially performed using the linear stage and the center points of the experimental design. The results of the statistical analysis are presented in Table 2. The obtained values suggested that both ethanol-to-oil molar ratio and the catalyst amount significantly affected the described ethanolysis process, because the influence of both variables was higher than the confidence interval. The natural and the coded values were utilized for the development of the linear statistical and the industrial mathematical regression models, respectively. The linear statistical and the industrial model for the glycerol-enriched CaO avocado oil ethanolysis process, under the investigated experimental conditions, are presented in Eqs. (8) and (9), respectively.

$$X_Y = 74.35 + 9.98X_C + 3.30X_E - 1.42X_{EC} \quad (8)$$

$$X_Y = 33.77 + 4.75X_C + 2.20X_E - 0.15X_{EC} \quad (9)$$

X_Y is the FAEEs yield occurring during the described ethanolysis process.

3.1.2. Non-linear stage

The results of the regression analysis, presented in Table 2, suggested that the curvature had a positive impact on the mentioned ethanolysis process. Since the value of the curvature was found to be higher than the confidence curvature interval, the non-linear stage of the experimental design was also taken into consideration to fit the experimental data with the quadratic model. The non-linear stage, also known as the star-points and coded as $\pm\alpha$, of the two-factorial design consisted of four experiments as shown in Table 1. The distance between the origin and star-points is expressed as $\alpha = 2^{n/4}$ (in the present study: $n = 2$ and $\alpha = 1.41$). The linear, the center-points, and the non-linear stage of the experimental design were combined to form a central composite design, and utilized to investigate the influence of ethanol-to-oil molar ratio and the catalyst amount on the described ethanolysis process. The present analysis involves all the independent variables and their within interactions. The response surface statistical and the industrial quadratic mathematical model for the glycerol-enriched CaO assisted avocado oil ethanolysis process, under the studied range of experimental conditions, are expressed in Eqs. (10) and (11), respectively.

Table 2
Results for the statistical analysis of the experimental design.

Parameters	Response
Main influence and interactions	$\overline{Y} = 74.35$ $I_E = 6.60$ $I_C = 19.97$ $I_{EC} = -2.84$
Significance test: *c confidence level: 95%*	
Mean response	79.53
Standard deviation	t = 3.18; s = 0.56
Confidence interval	±0.90
Significant variables	E, C, EC
Significance of curvature	
Curvature	5.18
Confidence curvature interval	1.27
Significance	Yes

E: ethanol-to-oil molar ratio, C: catalyst amount, $\overline{Y}$: mean response, s: standard deviation, t: student's t.

$$X_Y = 79.53 + 10.73X_C + 6.82X_E - 3.09X_{C^2} - 1.42X_{CE} - 1.69X_{E^2} \quad (10)$$

$$X_Y = -6.85 + 9.52X_C + 6.83X_E - 0.32X_{C^2} - 0.15X_{CE} - 0.19X_{E^2} \quad (11)$$

The three-dimensional surface plot for the predicted FAEEs yield with varying ethanol-to-oil molar ratio and the catalyst amount is presented in Fig. 1. The statistical quadratic regression expression (Eq. (10)) was applied to achieve the response surface graphical representation. The increase in the biodiesel yield with the rise in ethanol-to-oil molar ratio and the catalyst amount indicated a possible interaction between an alcohol and the catalyst. The present regression analysis provided an appreciable correlation between the predicted values and the experimental findings within the studied range of reaction conditions, which validated the statistical quadratic mathematical model being an appropriate one to describe the glycerol-enriched CaO assisted avocado oil ethanolysis process. The Supplementary Fig. S3 shows the comparison between the predicted values and the experimental results for the FAEEs yield.

3.2. Effect of reaction parameters

3.2.1. Effect of temperature

The effect of temperature on glycerol-enriched CaO assisted avocado oil ethanolysis process was initially studied because with

Table 1
Two-level factorial design of experiments. Stages of experiments along with the natural and the coded values of the reaction variables, and the obtained biodiesel yield.

Type of experiment	Run	Ethanol-to-oil molar ratio	Catalyst amount (%)	X_E	X_C	Conversion (%)	Biodiesel yield (%)
Linear stage	1	12	10	1	1	99.99	86.22
	2	12	4	1	−1	89.11	69.09
	3	6	10	−1	1	98.78	82.46
	4	6	4	−1	−1	81.84	59.64
Center stage	5	9	7	0	0	97.30	79.31
	6	9	7	0	0	96.74	78.86
	7	9	7	0	0	97.95	79.84
	8	9	7	0	0	98.31	80.14
Non-linear stage	9	13.24	7	1.41	0	99.99	91.18
	10	4.58	7	−1.41	0	86.28	61.93
	11	9	11.24	0	1.41	99.99	90.01
	12	9	2.58	0	−1.41	82.02	57.51

X_E for ethanol-to-oil molar ratio and X_C for catalyst amount.

Please cite this article in press as: Avhad MR et al. Modeling chemical kinetics of avocado oil ethanolysis catalyzed by solid glycerol-enriched calcium oxide. Energy Convers Manage (2016), http://dx.doi.org/10.1016/j.enconman.2016.07.060

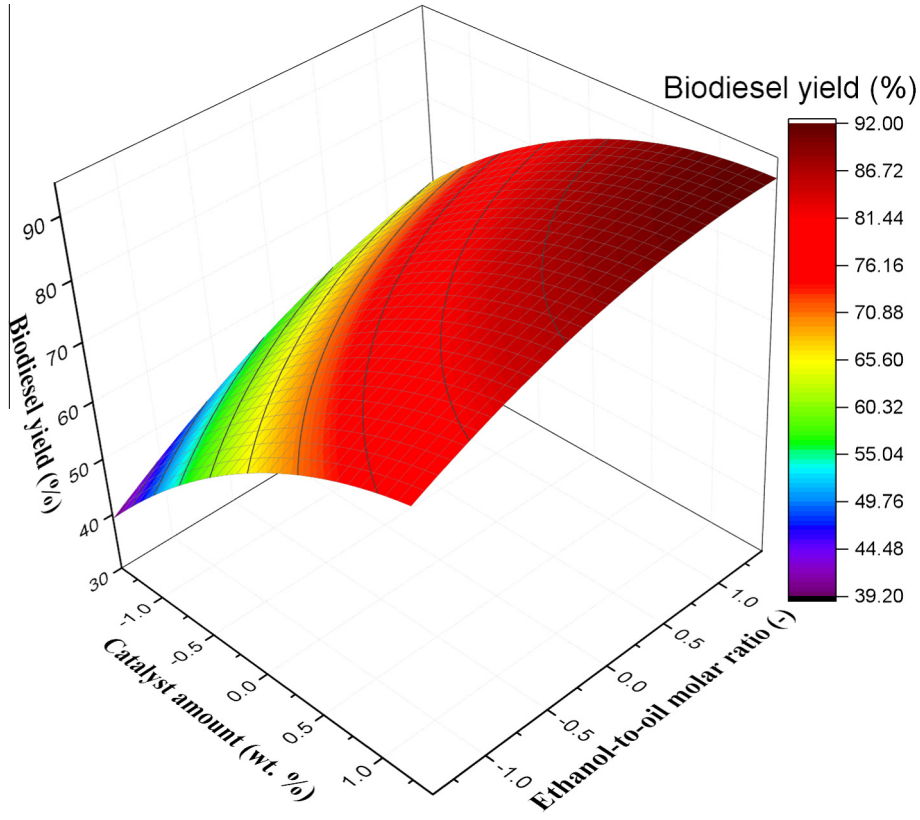

Fig. 1. Response surface 3D plot indicating the influence of ethanol-to-oil molar ratio and catalyst amount on the biodiesel yield. Temperature: 75 °C, Time: 120 min, Stirring intensity: 350 rpm.

the rise in temperature, the improvement in the miscibility and the reactivity between the reactants was expected. Also, from a chemical kinetics perspective, the rise in reaction temperature could accelerate the rate of the alcoholysis process. The effect of three different temperatures (55, 65, and 75 °C) on the described ethanolysis process was studied keeping constant ethanol-to-oil molar ratio of 9:1, catalyst amount of 7 wt.%, time of 120 min, and 350 rpm stirring intensity. The experimental results for the effect of temperature on the change in the concentration of TAGs and FAEEs are presented as symbols in Figs. 2a and 3a, respectively. The experimental findings suggested that an increase in reaction temperature had a positive impact on the described ethanolysis process. As shown in Fig. 2a, to achieve an about similar drop in the TAGs concentration, the reaction time reduced from 20 min to 5 min when temperature was elevated from 55 °C to 75 °C. Furthermore, it can be seen in Fig. 3a that the rise in temperature from 55 °C to 75 °C resulted in the reduction of reaction time from 120 min to 40 min to produce nearly equal concentration of biodiesel. Therefore, reaction temperature of 75 °C was found to be optimal for the described ethanolysis process.

3.2.2. Effect of ethanol-to-oil molar ratio

Since the transesterification is an equilibrium reaction, an excess of alcohol would be essential to shift the reaction equilibrium towards the formation of FAEEs [64]. The effect of ethanol-to-oil molar ratio on the described ethanolysis process was investigated using fixed reaction temperature of 75 °C, time of 120 min, catalyst amount of 7 wt.%, and 350 rpm stirring intensity. The variation in the TAGs and FAEEs concentration with the change in ethanol-to-oil molar ratio is presented as symbols in Figs. 2b and 3b, respectively. The obtained results suggested that the rise in ethanol-to-oil molar ratio significantly affected the rate of the avocado oil ethanolysis process. To achieve around similar FAEEs concentration, the reaction time decreased from 40 min to 10 min when ethanol-to-oil molar ratio was raised from 6:1 to 12:1. Though, the rise in ethanol-to-oil molar ratio from 9:1 to 12:1 improved the rate of the ethanolysis reaction, not a significant difference in the final TAGs and biodiesel concentration was observed. Therefore, ethanol-to-oil molar ratio of 9:1 was considered to be appropriate for the described ethanolysis process under the investigated range of experimental conditions.

3.2.3. Effect of catalyst amount

The effect of three different catalyst amount (4, 7, and 10 wt.%) on the mentioned ethanolysis process was also examined setting the constant reaction temperature of 75 °C, ethanol-to-oil molar ratio of 9:1, time of 120 min, and 350 rpm stirring intensity. The experimental results of the study evaluating the effect of the catalyst amount on the variation in the TAGs and FAEEs concentration are shown as symbols in Figs. 2c and 3c, respectively. A faster drop in the TAGs concentration and the rise in the FAEEs concentration was observed with an increase in the catalyst amount. This is attributed to an increase in the availability of the catalytic active centers; thus, providing an additional number of ethoxide ions for the reaction. The increase in the catalyst amount from 4 wt.% to 10 wt.% reduced the ethanolysis reaction time from 60 min to 20 min to achieve around similar biodiesel concentration. However, when the catalyst amount was raised from 7 wt.% to 10 wt.%, a minor difference in the final TAGs as well as the biodiesel concentration was obtained; therefore, the catalyst amount of 7 wt.% was considered optimal for the described ethanolysis process. The homogeneous contribution of the catalyst was additionally investigated. In this case, glycerol-enriched CaO catalyst was prepared in the presence of ethanol at 60 °C for 60 min under

Please cite this article in press as: Avhad MR et al. Modeling chemical kinetics of avocado oil ethanolysis catalyzed by solid glycerol-enriched calcium oxide. Energy Convers Manage (2016), http://dx.doi.org/10.1016/j.enconman.2016.07.060

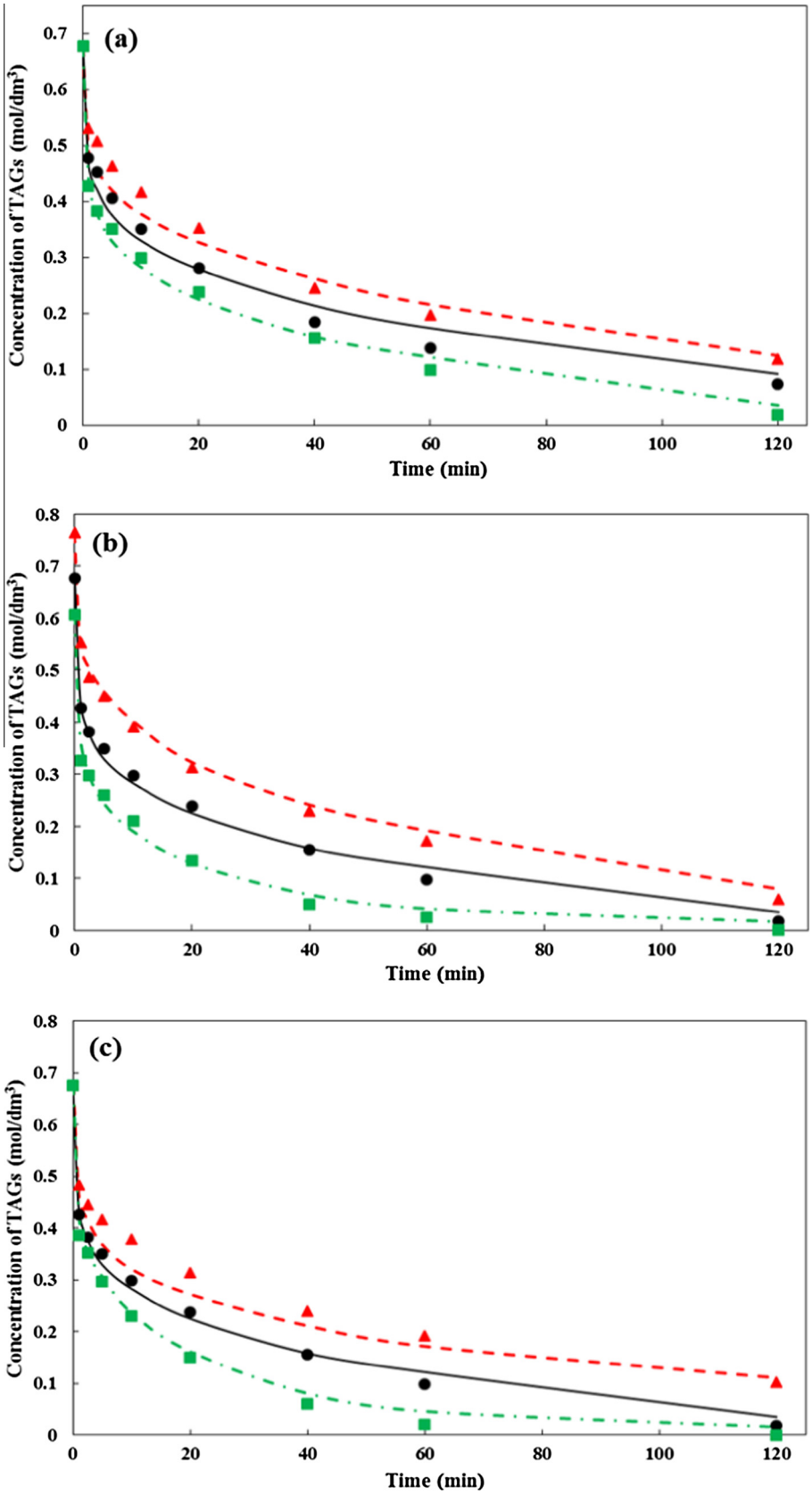

Fig. 2. Comparison between the experimental data and the predicted values for the variation in the TAGs concentration due to the impact of (a) temperature (▲-55 °C, ●-65 °C, ■-75 °C), (b) ethanol-to-oil molar ratio (▲-6:1, ●-9:1, ■-12:1), and (c) catalyst amount (▲-4 wt.%, ●-7 wt.%, ■-10 wt.%). Experimental data: symbols, kinetic model: lines.

Please cite this article in press as: Avhad MR et al. Modeling chemical kinetics of avocado oil ethanolysis catalyzed by solid glycerol-enriched calcium oxide. Energy Convers Manage (2016), http://dx.doi.org/10.1016/j.enconman.2016.07.060

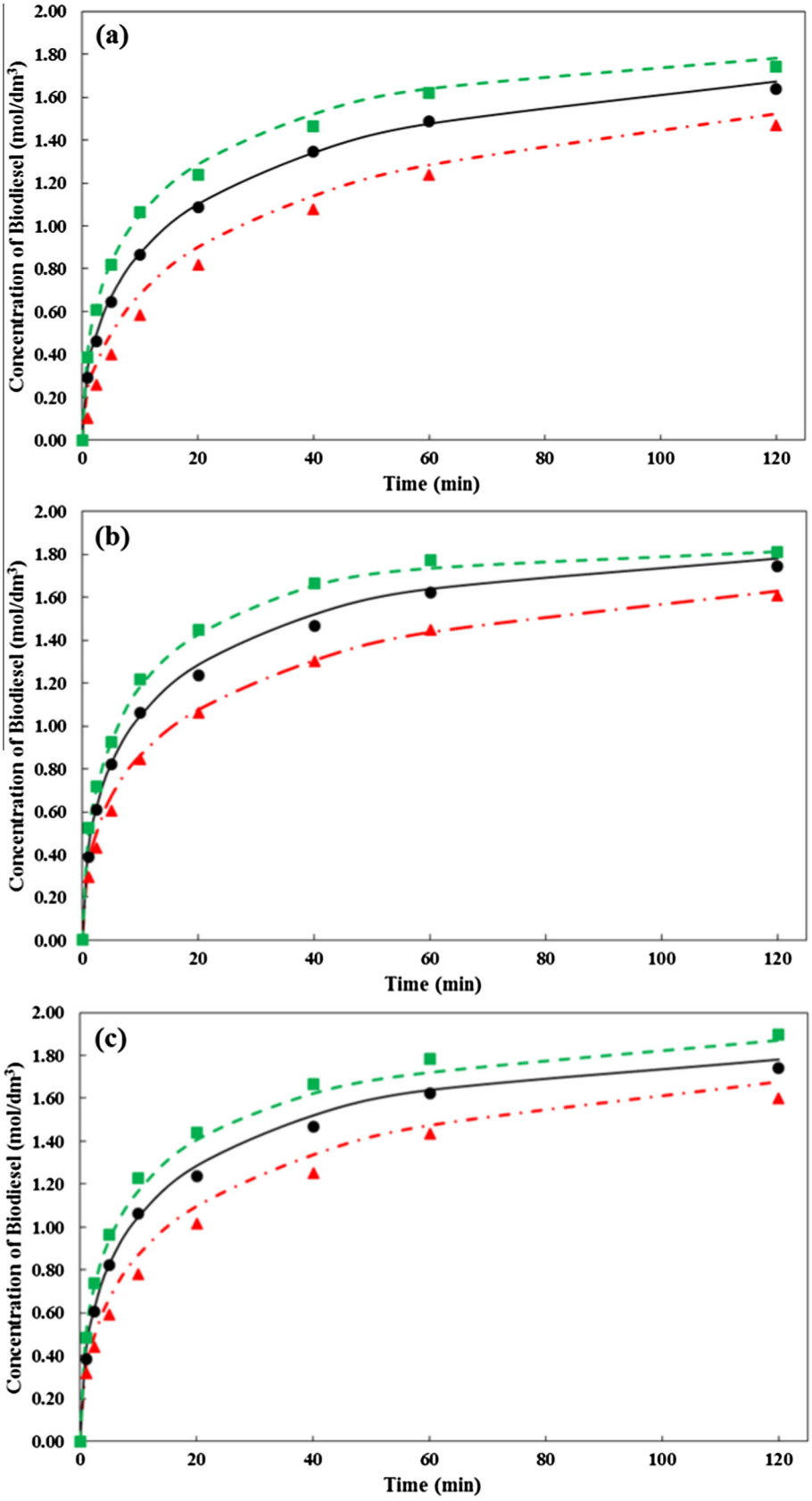

Fig. 3. Comparison between the experimental data and the predicted values for the variation in the FAEEs concentration due to the impact of (a) temperature (▲-55 °C, ●-65 °C, ■-75 °C), (b) ethanol-to-oil molar ratio (▲-6:1, ●-9:1, ■-12:1), and (c) catalyst amount (▲-4 wt.%, ●-7 wt.%, ■-10 wt.%). Experimental data: symbols, kinetic model: lines.

Please cite this article in press as: Avhad MR et al. Modeling chemical kinetics of avocado oil ethanolysis catalyzed by solid glycerol-enriched calcium oxide. Energy Convers Manage (2016), http://dx.doi.org/10.1016/j.enconman.2016.07.060

atmospheric pressure. Subsequently, the mixture was filtered using the Whatman filter paper and only the filtrate was used for the ethanolysis reaction. The avocado oil conversion of 5.08% was obtained when no catalyst was used for the ethanolysis reaction, while using the filtrate ethanol 6.34% oil conversion was achieved. An insignificant acceleration in the ethanolysis reaction indicated that the catalyst did not leach into ethanol. The slight increase in oil conversion obtained during the testing of homogeneous contribution could be because a little amount of glycerol might have mixed with ethanol which acted as a co-solvent. Furthermore, the available reports have also concluded CaDg to be chemically stable heterogeneous catalyst [33,34].

3.3. Kinetic modeling of the ethanolysis process

Initially, a kinetic model proposed by Lukić et al. [63] for the CaDg-catalyzed sunflower oil methanolysis reaction was applied for the present ethanolysis process due to probably a similar nature of the catalyst. However, no appreciable fitting between the experimental data and the predicted values was obtained; indicating that the kinetic model applied for the methanolysis process is not suitable for the current ethanolysis reaction. A study reported by Jasen and Marchetti [65] presented the kinetic simulations of the ethanolysis process, in the presence of heterogeneous basic resin catalyst. The validity of this previously developed kinetic model was tested for the present heterogeneous base-catalyzed ethanolysis process. The determination of the rate-controlling step for the glycerol-enriched CaO assisted avocado oil ethanolysis was carried out considering the reaction kinetics for all the reversible reactions, and the rate constants for the overall reaction were evaluated. The kinetic model included below mentioned features:

(1) The alcoholysis reaction occurred between ethanol molecules chemisorbed on the catalytic surface and oil molecules present in the ethanol phase close to the active sites.
(2) The overall process rate is controlled by the adsorption of an alcohol over the solid catalytic surface.
(3) The alcohol adsorption is rapid, and all reaction steps are elementary.
(4) FAEEs, due to their non-polar nature, does not adsorb on the catalytic surface.

The steps involved in the proposed reaction pathway could be presented as:

$$E + cs \underset{k_2}{\overset{k_1}{\leftrightarrow}} Ecs \tag{12}$$

$$TAGs + Ecs \underset{k_4}{\overset{k_3}{\leftrightarrow}} FAEEs + DAGs + cs \tag{13}$$

$$DAGs + Ecs \underset{k_6}{\overset{k_5}{\leftrightarrow}} FAEEs + MAGs + cs \tag{14}$$

$$MAGs + Ecs \underset{k_8}{\overset{k_7}{\leftrightarrow}} FAEEs + G + cs \tag{15}$$

where cs is the catalytic active sites.

$$K = \frac{k_1}{k_2} \tag{16}$$

The equation for the mass balance of the catalyst is given as:

$$m = \left[\frac{m_0}{(1 + C_E K)}\right] \tag{17}$$

The differential equations to evaluate the variation in the concentration of the chemical components involved in the ethanolysis reaction are as below:

$$\frac{dC_{TAGs}}{dt} = [-k_3 C_{TAGs} C_E K + k_4 C_{DAGs} C_{FAEEs}] \cdot m \tag{18}$$

$$\frac{dC_{DAGs}}{dt} = [k_3 C_{TAGs} C_E K - k_4 C_{DAGs} C_{FAEEs} - k_5 C_{DAGs} C_E K + k_6 C_{MAGs} C_{FAEEs}] \cdot m \tag{19}$$

$$\frac{dC_{MAGs}}{dt} = [k_5 C_{DAGs} C_E K - k_6 C_{MAGs} C_{FAEEs} - k_7 C_{MAGs} C_E K + k_8 C_G C_{FAEEs}] \cdot m \tag{20}$$

$$\frac{dC_G}{dt} = [k_7 C_{MAGs} C_E K - k_8 C_G C_{FAEEs}] \cdot m \tag{21}$$

$$\frac{dC_{FAEEs}}{dt} = [k_3 C_{TAGs} C_E K - k_4 C_{DAGs} C_{FAEEs} + k_5 C_{DAGs} C_E K - k_6 C_{MAGs} C_{FAEEs} + k_7 C_{MAGs} C_E K - k_8 C_G C_{FAEEs}] \cdot m \tag{22}$$

$$\frac{dC_E}{dt} = -[k_3 C_{TAGs} C_E K - k_4 C_{DAGs} C_{FAEEs} + k_5 C_{DAGs} C_E K - k_6 C_{MAGs} C_{FAEEs} + k_7 C_{MAGs} C_E K - k_8 C_G C_{FAEEs}] \cdot m \tag{23}$$

$$k = A \cdot \exp^{-E_a/RT} \tag{24}$$

where k_1, k_3, k_5, and k_7 are the specific rate constants for the reactions in the forward direction; k_2, k_4, k_6, and k_8 are the specific rate constants for the reactions in the reverse direction; C_{TAGs}, C_{DAGs}, C_{MAGs}, C_G, C_{FAEEs}, and C_E is the concentration of TAGs, DAGs, MAGs, G, FAEEs, and ethanol, respectively, at time t; m_0 is the initial mass of the catalyst (g); m is the mass of the catalytic sites involved in the reaction (g); A is the pre-exponential factor of the Arrhenius equation (min^{-1}); Ea is the activation energy (cal mol^{-1}); R is the universal gas constant (1.98 cal K^{-1} mol^{-1}); T is the absolute temperature (K).

The above mentioned kinetic model provided a good correlation between the experimental finding and the predicted values, with the sum of weighed errors equivalent to 0.182. In the present scenario, a sigmoidal pattern of the curves was not witnessed as obtained for the CaO-catalyzed alcoholysis processes [56,61]; as a consequence of the nature of the catalyst [32,63]. The simulation curves for the variation in the concentration of TAGs at different temperature, ethanol-to-oil molar ratio, and the catalyst amount is presented as solid lines in Fig. 2a, b, and c, respectively. Whereas, the prediction for the change in the FAEEs concentration with time at different temperature, ethanol-to-oil molar ratio, and the catalyst amount can be seen as solid lines in Fig. 3a, b, and c, respectively. The kinetic parameters obtained through the simulation of the experimental data are presented in the Supplementary Table S4. The activation energy values could be correlated with those reported before for the ethanolysis processes catalyzed by the calcium-based catalysts [21,22]. The MSC value, calculated using Eq. (5), for the TAGs and FAEEs concentration was 3.79 and 4.96, respectively. The achieved low value of sum of weighed errors and high value of the MSC validated the kinetic model being an appropriate to predict the glycerol-enriched CaO assisted avocado oil ethanolysis process under the studied range of the experimental conditions.

Please cite this article in press as: Avhad MR et al. Modeling chemical kinetics of avocado oil ethanolysis catalyzed by solid glycerol-enriched calcium oxide. Energy Convers Manage (2016), http://dx.doi.org/10.1016/j.enconman.2016.07.060

Table 3
Physico-chemical properties avocado oil and fatty acid ethyl esters.

Properties	Units	ASTM D6751	EN 14214	Avocado oil	Ethyl esters
Kinetic viscosity	$mm^2\ s^{-1}$ @ 40 °C	1.9–6.0	3.5–5.0	41.66	4.87
Iodine number	g I_2 100 g^{-1}	–	120 max.	83.75	80.42
Moisture	%	0.05	0.05	0.03	0.03
Acid value	mg KOH g^{-1}	0.5	0.5	0.064	0.099
Oxidation stability	h @ 110 °C	3 min.	8 min.	18.38	9.30

3.4. Characterization

The glycerol-enriched CaO assisted ethanolysis process of avocado oil resulted in maximum FAEEs yield of 91.18%. This biodiesel containing 8.82% of other components might not be suitable for the industrial implementation. Therefore, to have biodiesel (FAEEs) from avocado oil with highest possible purity only for the characterization purpose, the FAEEs synthesis was done through the conventional route by using potassium methoxide catalyst. The analyzed physico-chemical properties of avocado oil as well as FAEEs, produced using potassium methoxide catalyst, are listed in Table 3. The obtained characterization results were compared with the ASTM D6751 and EN 14214 official standards, and it can be seen that all the measured properties of biodiesel follow most of the specifications set by the pervious mentioned standards.

4. Conclusion

The current research article presents an experimental as well as the simulation investigations for the glycerol-enriched CaO catalyst assisted ethanolysis of avocado oil. The CaO was synthesized through the thermal treatment of *Mytilus Galloprovincialis* shells, which is a waste generated from the fish industry, and subsequently treated with glycerol before its application for the ethanolysis reactions. The glycerol dosage of 10% (w.r.t. catalyst weight) was utilized for the preparation of glycerol-CaO complex. The results for the regression analyses indicated that both catalyst amount and ethanol-to-oil molar ratio significantly affected the described ethanolysis process. The presented response equations could be applied to determine the optimal reaction parameters to attain the desired biodiesel (FAEEs) yield, under the investigate range of experimental conditions. The utilization of temperature of 75 °C, ethanol-to-oil molar ratio of 9:1, and 7 wt.% catalyst amount was concluded to be suitable for the studied glycerol-enriched CaO assisted avocado oil ethanolysis process. However, the maximum FAEEs yield of 91.18% was registered using the presented catalyst which cannot be considered suitable for the industrial implementation. Therefore, further research to increase the FAEEs yield would be crucial. Kouzu et al. reported that the biodiesel yield was limited around 95% because the co-generating glycerol affected the performance of the CaDg catalyst. A continuous removal of glycerol from the reaction mixture might increase the biodiesel yield. Furthermore, the kinetics of the described ethanolysis reactions was studied to simulate the process using a mathematical model. The validity of a previously developed kinetic model was tested for the current ethanolysis process, which presented a good agreement between the predicted values and the experimental data. Therefore, the applied kinetic model could be considered as valid for the prediction of the glycerol-enriched CaO assisted avocado oil ethanolysis process.

Competing financial interests

The authors declare no competing financial interests.

Acknowledgements

The authors would like to express their gratitude to the Norwegian University of Life Sciences – Norway [Project No. 1301051406], Complutense University of Madrid – Spain, and NILS mobility grants [009-ABEL-CM-2013] for their financial support.

Appendix A. Supplementary material

Supplementary data associated with this article can be found, in the online version, at http://dx.doi.org/10.1016/j.enconman.2016.07.060.

References

[1] Marchetti JM, Miguel VU, Errazu AF. Possible methods for biodiesel production. Renew Sustain Energy Rev 2007;11(6):1300–11.
[2] Marchetti JM. Biodiesel production technologies. 1st ed. New York: Nova science publisher, Inc.; 2010.
[3] Avhad MR, Marchetti JM. A review on recent advancement in catalytic materials for biodiesel production. Renew Sustain Energy Rev 2015;50:696–718.
[4] Lee AF, Bennett JA, Manayil JC, Wilson K. Heterogeneous catalysis for sustainable biodiesel production via esterification and transesterification. Chem Soc Rev 2014;43(22):7887–916.
[5] Marinković DM, Stanković MV, Veličković AV, Avramović JM, Miladinović MR, Stamenković OO, et al. Calcium oxide as a promising heterogeneous catalyst for biodiesel production: Current state and perspectives. Renew Sustain Energy Rev 2016;56:1387–408.
[6] Kouzu M, Hidaka J-s. Transesterification of vegetable oil into biodiesel catalyzed by CaO: a review. Fuel 2012;93:1–12.
[7] Ngamcharussrivichai C, Nunthasanti P, Tanachai S, Bunyakiat K. Biodiesel production through transesterification over natural calciums. Fuel Process Technol 2010;91(11):1409–15.
[8] Boey P-L, Ganesan S, Maniam GP, Khairuddean M. Catalysts derived from waste sources in the production of biodiesel using waste cooking oil. Catal Today 2012;190(1):117–21.
[9] Viriya-empikul N, Krasae P, Puttasawat B, Yoosuk B, Chollacoop N, Faungnawakij K. Waste shells of mollusk and egg as biodiesel production catalysts. Bioresour Technol 2010;101(10):3765–7.
[10] Chakraborty R, Bepari S, Banerjee A. Transesterification of soybean oil catalyzed by fly ash and egg shell derived solid catalysts. Chem Eng J 2010;165(3):798–805.
[11] Verziu M, Coman SM, Richards R, Parvulescu VI. Transesterification of vegetable oils over CaO catalysts. Catal Today 2011;167(1):64–70.
[12] Liu X, He H, Wang Y, Zhu S, Piao X. Transesterification of soybean oil to biodiesel using CaO as a solid base catalyst. Fuel 2008;87(2):216–21.
[13] Cho YB, Seo G, Chang DR. Transesterification of tributyrin with methanol over calcium oxide catalysts prepared from various precursors. Fuel Process Technol 2009;90(10):1252–8.
[14] Taufiq-Yap YH, Lee HV, Hussein MZ, Yunus R. Calcium-based mixed oxide catalysts for methanolysis of Jatropha curcas oil to biodiesel. Biomass Bioenergy 2011;35(2):827–34.
[15] Thitsartarn W, Kawi S. An active and stable CaO-CeO_2 catalyst for transesterification of oil to biodiesel. Green Chem 2011;13(12):3423–30.
[16] Molaei Dehkordi A, Ghasemi M. Transesterification of waste cooking oil to biodiesel using Ca and Zr mixed oxides as heterogeneous base catalysts. Fuel Process Technol 2012;97:45–51.
[17] Taufiq-Yap YH, Teo SH, Rashid U, Islam A, Hussien MZ, Lee KT. Transesterification of Jatropha curcas crude oil to biodiesel on calcium lanthanum mixed oxide catalyst: effect of stoichiometric composition. Energy Convers Manage 2014;88:1290–6.
[18] Samart C, Chaiya C, Reubroycharoen P. Biodiesel production by methanolysis of soybean oil using calcium supported on mesoporous silica catalyst. Energy Convers Manage 2010;51(7):1428–31.
[19] Albuquerque MCG, Jiménez-Urbistondo I, Santamaría-González J, Mérida-Robles JM, Moreno-Tost R, Rodríguez-Castellón E, et al. CaO supported on mesoporous silicas as basic catalysts for transesterification reactions. Appl Catal A 2008;334(1–2):35–43.
[20] Pasupulety N, Gunda K, Liu Y, Rempel GL, Ng FTT. Production of biodiesel from soybean oil on CaO/Al_2O_3 solid base catalysts. Appl Catal A 2013;452:189–202.
[21] Kaur N, Ali A. Biodiesel production via ethanolysis of jatropha oil using molybdenum impregnated calcium oxide as solid catalyst. RSC Adv 2015;5(18):13285–95.
[22] Kaur M, Ali A. Ethanolysis of waste cottonseed oil over lithium impregnated calcium oxide: kinetics and reusability studies. Renew Energy 2014;63:272–9.
[23] Kumar D, Ali A. Transesterification of low-quality triglycerides over a Zn/CaO heterogeneous catalyst: kinetics and reusability studies. Energy Fuels 2013;27(7):3758–68.

Please cite this article in press as: Avhad MR et al. Modeling chemical kinetics of avocado oil ethanolysis catalyzed by solid glycerol-enriched calcium oxide. Energy Convers Manage (2016), http://dx.doi.org/10.1016/j.enconman.2016.07.060

[24] Alonso DM, Mariscal R, Granados ML, Maireles-Torres P. Biodiesel preparation using Li/CaO catalysts: activation process and homogeneous contribution. Catal Today 2009;143(1–2):167–71.
[25] Lin L, Vittayapadung S, Li X, Jiang W, Shen Xiangqian. Synthesis of magnetic calcium oxide hollow fiber catalyst for the production of biodiesel. Environ Progress Sustain Energy 2013;32(4):1255–61.
[26] Liu F, Zhang Y. Hydrothermal growth of flower-like CaO for biodiesel production. Ceram Int 2012;38(4):3473–82.
[27] Ferrero GO, Almeida MF, Alvim-Ferraz MCM, Dias JM. Glycerol-enriched heterogeneous catalyst for biodiesel production from soybean oil and waste frying oil. Energy Convers Manage 2015;89:665–71.
[28] Esipovich A, Danov S, Belousov A, Rogozhin A. Improving methods of CaO transesterification activity. J Mol Catal A: Chem 2014;395:225–33.
[29] Reyero I, Arzamendi G, Gandía LM. Heterogenization of the biodiesel synthesis catalysis: CaO and novel calcium compounds as transesterification catalysts. Chem Eng Res Des 2014;92(8):1519–30.
[30] Sánchez-Cantú M, Reyes-Cruz FM, Rubio-Rosas E, Pérez-Díaz LM, Ramírez E, Valente JS. Direct synthesis of calcium diglyceroxide from hydrated lime and glycerol and its evaluation in the transesterification reaction. Fuel 2014;138:126–33.
[31] Gupta AR, Yadav SV, Rathod VK. Enhancement in biodiesel production using waste cooking oil and calcium diglyceroxide as a heterogeneous catalyst in presence of ultrasound. Fuel 2015;158:800–6.
[32] León-Reina L, Cabeza A, Rius J, Maireles-Torres P, Alba-Rubio AC, López Granados M. Structural and surface study of calcium glyceroxide, an active phase for biodiesel production under heterogeneous catalysis. J Catal 2013;300:30–6.
[33] Kouzu M, Tsunomori M, Yamanaka S, Hidaka J. Solid base catalysis of calcium oxide for a reaction to convert vegetable oil into biodiesel. Adv Powder Technol 2010;21(4):488–94.
[34] Kouzu M, Yamanaka S-y, Hidaka J-s, Tsunomori M. Heterogeneous catalysis of calcium oxide used for transesterification of soybean oil with refluxing methanol. Appl Catal A 2009;355(1-2):94–9.
[35] López Granados M, Alba-Rubio AC, Vila F, Martín Alonso D, Mariscal R. Surface chemical promotion of Ca oxide catalysts in biodiesel production reaction by the addition of monoglycerides, diglycerides and glycerol. J Catal 2010;276(2):229–36.
[36] Limayem A, Ricke SC. Lignocellulosic biomass for bioethanol production: current perspectives, potential issues and future prospects. Prog Energy Combust Sci 2012;38(4):449–67.
[37] Sarkar N, Ghosh SK, Bannerjee S, Aikat K. Bioethanol production from agricultural wastes: an overview. Renew Energy 2012;37(1):19–27.
[38] Marjanović AV, Stamenković OS, Todorović ZB, Lazić ML, Veljković VB. Kinetics of the base-catalyzed sunflower oil ethanolysis. Fuel 2010;89(3):665–71.
[39] Encinar JM, González JF, Rodríguez-Reinares A. Ethanolysis of used frying oil. Biodiesel preparation and characterization. Fuel Process Technol 2007;88(5):513–22.
[40] Hartwig S, Auwärter V, Pragst F. Effect of hair care and hair cosmetics on the concentrations of fatty acid ethyl esters in hair as markers of chronically elevated alcohol consumption. Forensic Sci Int 2003;131(2–3):90–7.
[41] Suesse S, Pragst F, Mieczkowski T, Selavka CM, Elian A, Sachs H, et al. Practical experiences in application of hair fatty acid ethyl esters and ethyl glucuronide for detection of chronic alcohol abuse in forensic cases. Forensic Sci Int 2012;218(1–3):82–91.
[42] Thurnhofer S, Vetter W. Application of ethyl esters and d3-methyl esters as internal standards for the gas chromatographic quantification of transesterified fatty acid methyl esters in food. J Agric Food Chem 2006;54(9):3209–14.
[43] Surya Abadi Ginting M, Tazli Azizan M, Yusup S. Alkaline in situ ethanolysis of Jatropha curcas. Fuel 2012;93:82–5.
[44] Rubio-Caballero JM, Santamaría-González J, Mérida-Robles J, Moreno-Tost R, Alonso-Castillo ML, Vereda-Alonso E, et al. Calcium zincate derived heterogeneous catalyst for biodiesel production by ethanolysis. Fuel 2013;105:518–22.
[45] Kumar D, Kumar G, Poonam, Singh CP. Fast, easy ethanolysis of coconut oil for biodiesel production assisted by ultrasonication. Ultrason Sonochem 2010;17(3):555–9.
[46] Kaur N, Ali A. Kinetics and reusability of Zr/CaO as heterogeneous catalyst for the ethanolysis and methanolysis of Jatropha crucas oil. Fuel Process Technol 2014;119:173–84.
[47] Shahla S, Ngoh GC, Yusoff R. The evaluation of various kinetic models for base-catalyzed ethanolysis of palm oil. Bioresour Technol 2012;104:1–5.
[48] Marchetti JM, Errazu AF. Esterification of free fatty acids using sulfuric acid as catalyst in the presence of triglycerides. Biomass Bioenergy 2008;32(9):892–5.
[49] Kaur N, Ali A. One-pot transesterification and esterification of waste cooking oil via ethanolysis using Sr: Zr mixed oxide as solid catalyst. RSC Adv 2014;4(82):43671–81.
[50] Kaur M, Ali A. An efficient and reusable Li/NiO heterogeneous catalyst for ethanolysis of waste cottonseed oil. Eur J Lipid Sci Technol 2015;117(4):550–60.
[51] Takahashi F, Ortega E. Emergy evaluation of avocado crop as raw material for biodiesel production. State University of Campinas. <https://www.academia.edu/16379323/EMERGY_EVALUATION_OF_AVOCADO_CROP_AS_RAW_MATERIAL_FOR_BIODIESEL_PRODUCTION> [accessed on July 6, 2016].
[52] Werman MJ, Neeman I. Avocado oil production and chemical characteristics. J Am Oil Chem Soc 1987;64(2):229–32.
[53] Knothe G. Avocado and olive oil methyl esters. Biomass Bioenergy 2013;58:143–8.
[54] Giraldo L, Moreno-Piraján JC. Lipase supported on mesoporous materials as a catalyst in the synthesis of biodiesel from Persea americana mill oil. J Mol Catal B Enzym 2012;77:32–8.
[55] Avhad MR, Sánchez M, Bouaid A, Martínez M, Aracil J, Marchetti JM. Glycerol-activated calcium oxide catalyst for the methanolysis of crude Jatropha Curcas oil [submitted for publication].
[56] Sánchez M, Marchetti JM, El Boulifi N, Aracil J, Martínez M. Kinetics of Jojoba oil methanolysis using a waste from fish industry as catalyst. Chem Eng J 2015;262:640–7.
[57] Kouzu M, Hidaka J-s, Wakabayashi K, Tsunomori M. Solid base catalysis of calcium glyceroxide for a reaction to convert vegetable oil into its methyl esters. Appl Catal A 2010;390(1-2):11–8.
[58] Liu X, Piao X, Wang Y, Zhu S. Calcium ethoxide as a solid base catalyst for the transesterification of soybean oil to biodiesel. Energy Fuels 2008;22(2):1313–7.
[59] Avhad MR, Marchetti JM. Innovation in solid heterogeneous catalysis for the generation of economically viable and ecofriendly biodiesel: a review. Catal Rev 2016:1–52.
[60] Veljković VB, Stamenković OS, Todorović ZB, Lazić ML, Skala DU. Kinetics of sunflower oil methanolysis catalyzed by calcium oxide. Fuel 2009;88(9):1554–62.
[61] Lukić I, Kesić Ž, Maksimović S, Zdujić M, Liu H, Krstić J, et al. Kinetics of sunflower and used vegetable oil methanolysis catalyzed by CaO·ZnO. Fuel 2013;113:367–78.
[62] Tasić MB, Miladinović MR, Stamenković OS, Veljković VB, Skala DU. Kinetic modeling of sunflower oil methanolysis catalyzed by calcium-based catalysts. Chem Eng Technol 2015;38(9):1550–6.
[63] Lukić I, Kesić Ž, Zdujić M, Skala D. Calcium diglyceroxide synthesized by mechanochemical treatment, its characterization and application as catalyst for fatty acid methyl esters production. Fuel 2016;165:159–65.
[64] Farooq M, Ramli A, Subbarao D. Biodiesel production from waste cooking oil using bifunctional heterogeneous solid catalysts. J Clean Prod 2013;59:131–40.
[65] Jasen P, Marchetti JM. Kinetic study of the esterification of free fatty acid and ethanol in the presence of triglycerides using solid resins as catalyst. Int J Low-Carbon Technol 2012;7(4):325–30.

Please cite this article in press as: Avhad MR et al. Modeling chemical kinetics of avocado oil ethanolysis catalyzed by solid glycerol-enriched calcium oxide. Energy Convers Manage (2016), http://dx.doi.org/10.1016/j.enconman.2016.07.060

Paper VI

Biomass and Bioenergy 83 (2015) 467–473

Contents lists available at ScienceDirect

Biomass and Bioenergy

journal homepage: http://www.elsevier.com/locate/biombioe

Research paper

Temperature and pretreatment effects on the drying of Hass avocado seeds

M.R. Avhad, J.M. Marchetti*

Department of Mathematical Sciences and Technology, Norwegian University of Life Sciences, Drøbakveien 31, Ås, 1432, Norway

ARTICLE INFO

Article history:
Received 18 February 2015
Received in revised form
28 October 2015
Accepted 31 October 2015
Available online 9 November 2015

Keywords:
Hass avocado (*Persea Americana Mill.*) seed
Pretreatment process
Drying
Physical appearance

ABSTRACT

The objective of the present experimental work was to determine the influence of five different drying air temperatures (313, 323, 333, 343, and 353 K) on the drying kinetics and the degree of moisture evaporation from Hass avocado seeds. The drying experiments of the non-pretreated and pretreated (sliced and crushed) Hass avocado seeds were performed in a heating furnace, where the pretreatment process was found to accelerate the drying process. The obtained results suggested that increase in the operating air temperature stimulated the rate of moisture evaporation, but resulted in the charring of the seed surface. The drying air temperature of 313 K was concluded to be suitable for the reasonable drying of Hass avocado seeds. The slicing pretreatment process was found to be better indicative of the total moisture amount present in Hass avocado seeds. The drying process removed a maximum of 58% of the initial water mass of Hass avocado seeds. An additional investigation was performed where the physical appearance of Hass avocado seeds immersed in water at different temperatures (303, 318, 325.5, 333, and 348 K) was examined. The observed study suggested that the surrounding temperature higher than 313 K could damage the physical appearance and reduce the quality of Hass avocado seeds.

1. Introduction

The data presented by the statistics division of the Food and Agriculture organization of the United Nations suggested that the production of avocado fruit in the year 2013 was 2.81 times higher than that in 1983; Mexico being the top producer of the fruit [1]. The presence of micro- and macro-nutrients, such as minerals, dietary fibers, proteins, lipids, vitamins, and phytochemicals in the fruit pulp is the prime reason for the consistent rise in the requirement, and in consequence, for the agriculture of avocado fruit [2]. Among the different varieties of avocado fruit, Hass variety is commonly grown because of its longer shelf life and demand in foreign markets [3]. However, it is important to understand that only the pulp of the fruit is consumed; the seed of avocado, which is about 13% of the total fresh weight of the fruit, is considered as an agricultural waste and is discarded with no further applications. The average share of the pulp, skin, and seed in Hass avocado fruit is presented in Fig. 1.

The world total production of avocado in the year 2013 was 4.71 million tonnes [1]; thus, it could be estimated that in the year 2013 alone, approximately 613 thousand tonnes of avocado seeds were treated as a waste material. In addition, there are reports suggesting that avocado plant leaves and, fruit seed and skin are all potentially poisonous to animals and cannot be served as food because of the presence of substance named Persin. The consumption of avocado waste by animals could trigger several carcinogenic effects, such as fluid accumulation around the heart, difficulty in breathing, and even death due to oxygen deprivation. Moreover, high fat content of avocado can lead to pancreatitis [4,5]. However, reports on the possible utilization of avocado seeds for human benefit purpose are available. Furthermore, a market established from the usage of avocado seeds could also help in reducing the overall cost of avocado fruit. Dabas et al. [6] reported that Hass avocado seeds, when crushed in the presence of water and incubated at 297 K for 35 min, resulted in the generation of orange pigments. It was proposed that the development of color was assisted by enzyme, while, the excess heat treatment (373 K) has a negative impact on the extraction of color from seeds. Lacerda et al. [7], and Weatherby and Sober [8], in their study, revealed that avocado seeds consist also of a natural biopolymer, i.e. starch. Reports on the utilization of carbonized avocado seeds as an adsorbent are also available. Bhaumik et al. [9] reported a study focused on the usage of carbonized form of sulfuric acid modified avocado seed for the removal of toxic

* Corresponding author.
E-mail address: jorge.mario.marchetti@nmbu.no (J.M. Marchetti).

http://dx.doi.org/10.1016/j.biombioe.2015.10.028
0961-9534/

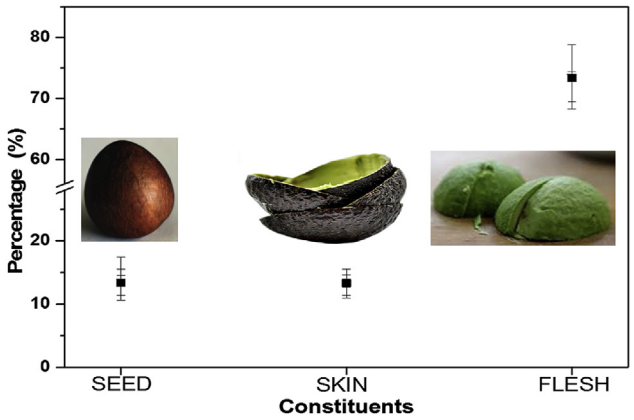

Fig. 1. Constituents of Hass avocado fruit.

hexavalent chromium (Cr (VI)) from the aquatic system. Moreover, a study reported by Rodrigues et al. [10] demonstrated that avocado seeds, after the carbonization process, could be utilized for the removal of phenol from the wastewater. In addition, several reports are available which confirm the presence of lipid components as well in avocado seeds [11–14]. Therefore, we assume that the derivatization of combustible oil from a waste resource, such as Hass avocado seed could be of industrial relevance. This is because its combustion would have negligible contribution on the net increase in the atmospheric carbon dioxide, while, the feedstock might necessitate less monetary investments. However, reports on the utilization of avocado seeds for biofuel generation are scarce. The study reported by Rachimoellah et al. [15] and Risnoyatiningsih [16], have demonstrated a possibility for the synthesis of biodiesel from avocado seed oil, in the presence of methanol and a sodium hydroxide catalyst.

The derivatization of value-added chemicals and biofuel from a waste biomass material, such as Hass avocado seeds may require several steps. The drying of Hass avocado seeds is a primary step for the oil and chemical extraction process, but is a critical one due to the fact that the presence of moisture could cause irreversible damage to the seeds and reduce the quality of the final product. Additionally, the quantity of substrate utilized for the value-added chemicals and biofuel production processes is based on dry matter content. Furthermore, deciding the drying conditions could also be of foremost importance. This is because the drying temperature might have a significant impact on the nature of oil cell walls, which in return, would decide simplicity or complexity for the oil extraction process. It is also worth noting that the mechanical cold pressing methodology that promises to yield best quality oil demands seeds with moisture content below 100 g kg^{-1} [17]; thus, hinting the need for the absolute moisture removal from Hass avocado seeds. The comprehensive removal of moisture from Hass avocado seeds is supposed to prevent the growth and reproduction of microorganisms, and subsequently, minimize several possible moisture-mediated deteriorative reactions. The drying process will also reduce the bulk weight of Hass avocado seeds, minimize the required storage space, facilitate its transportation, and enable its storage for a long period. Therefore, deciding the appropriate drying conditions and understanding its proficiency in minimizing moisture from Hass avocado seeds might be basic, but could be of a foremost importance. To our knowledge, till date, no effort on studying the influence of different temperatures on the degree of moisture removal from, and on the physical appearance of Hass avocado seeds is reported. In the present study, we investigated the impact of five different drying air temperatures (313, 323, 333, 343, and 353 K) on the moisture removal rate and on the final yield of dry matter. The influence of different pretreatment process on the overall speed of moisture evaporation during the drying process was also studied. In addition, the physical appearance of Hass avocado seeds when immersed in water at different temperatures (303, 318, 325.5, 333, and 348 K) was carefully monitored.

2. Materials and methods

2.1. Materials

Riped Hass avocado fruits were purchased from a local market of Norway. For the crushing pretreatment process, a bowl-shaped mortar-pestle, made from stone, was employed to pulverize Hass avocado seeds. For another pretreatment process, Hass avocado seeds were sliced using a stainless steel slicer to maintain a uniform thickness of every sample. All the seed samples were weighed on a digital balance machine having 1 mg accuracy (Mettler-Toledo, PG 5002 Delta Range, Switzerland). The drying experiments of the seed samples were performed using a heating furnace (Narbetherm P300, Germany). The initial and residual water content in Hass avocado seeds were determined using the automated Karl Fischer (KF) volumetric system (Metrohm, Tampa, FL, USA) consisting of an oven sample unit (Model 774) for water extraction, a dosing device (Model 901) connected to two mechanical burettes (Model 80; one for titrant and other for methanol) for control of titrant, and a titration cell with electrode and stirrer (Model 801). The complete system was operated by a computer using the software Tiamo 2.3, for the data analysis. For the moisture analysis, methanol (Sigma–Aldrich), and CombiTitrant 5 (Merck, Darmstadt, Germany) was used.

2.2. Experimental procedure

This work was performed on Hass avocado fruits of unknown provenance, for which the chain of custody is not known; while, the authors believe that this work exemplifies the drying process of Hass avocado seeds, there is a reasonable concern that there may be substrate factors that influence the results obtained. Hass avocado seeds were carefully separated from the mesocarp and cleaned under continuous flow of tap water. Subsequently, water attached to the seed surface while cleaning was removed with the help of tissue paper. The seeds were then separated in three sections. The first section of Hass avocado seeds were dried without any pretreatment. In the second section, Hass avocado seeds were crushed before applying for the drying process. The average particle size of the pulverized Hass avocado seeds was on average 4.2 mm; the smallest and largest unit size being 3.5 mm and 5.5 mm, respectively. In the third section, Hass avocado seeds were sliced, and utilized for the drying experiments. The average length, width, and thickness of the sliced seed samples were 43.7 cm, 30.6 cm, and 2.7 mm, respectively. All the seed samples were kept in separate pyrex glass petri plates and then placed in the heating furnace for the drying process. The efficacy of five drying temperatures (313, 323, 333, 343, and 353 K) on the moisture evaporation from Hass avocado seeds was systematically investigated for 5760 min. To understand the rate of moisture evaporation, the seeds samples were weighed at a predetermined time interval taking less than 0.25 min to weigh the samples. The seed samples were weighed until the weight of two consecutive samples fluctuated less than 1% to ensure acceptable moisture evaporation. Every experiments were replicated twice to obtain reproducibility in the experimental findings.

2.3. Physical appearance of Hass avocado seeds

The present study was performed to examine the influence of temperature on the physical appearance of Hass avocado seeds immersed in water. Furthermore, studying the physical appearance of Hass avocado seeds in water was considered beneficial because the chemical components, if any, extracting from the seeds at different operating temperatures was anticipated to remain in water. To investigate the physical appearance of Hass avocado seeds at different temperatures and encircling water environment, seeds were pretreated by the procedure mentioned by Egger [18]. First, the seed coat was carefully removed to promote the water imbibition and oxygen diffusion. Then, seeds were submerged in a glass vessel containing water in such a way that 60% of the seed was dipped in water, and remaining was exposed to the surrounding air. The physical appearance of avocado seeds in the presence of water was studied at five temperatures: 303, 318, 325.5, 333, and 348 K. The water in the vessel was replaced every alternate day. The above mentioned experiment was performed for the duration of 21 days to investigate also the degree of germination of avocado seeds at different temperatures. This could be of relevance as the lipase generated from the germination process could be utilized as a catalyst to perform enzyme-assisted reactions.

2.4. Moisture content analysis

First, 0.3 mg–0.4 mg of seed samples were weighed in a glass vials capped with airtight septa and the vials were placed in a sampler carousel. For analysis, the samples were automatically placed in the oven for heating. A double-hollow needle was pierced through the vial septum and a stream of dry air was passed through the inlet of the needle, leaving the vial through the outlet part of the needle containing released moisture from the sample. The air stream was directed to the titration beaker via a heated tube. The extraction temperature and time was set at 433 K and 75 min, respectively.

3. Results and discussion

3.1. Drying of Hass avocado seeds

The effect of drying air temperatures on the extent of moisture evaporation from the non-pretreated Hass avocado seeds is graphically represented in Fig. 2. From Fig. 2 it is clearly evident that the rise in operative temperature accelerated the drying process. After 720 min of drying, air temperature of 353 K resulted in 27.35% reduction in the weight of the non-pretreated Hass avocado seeds, which was around 4.3 times higher than that observed using 313 K.

This behavior was in agreement with the findings reported by Siqueira et al. [19], where it was found that the evaporation of water from jatropha seed was 80 times faster when temperature was increased from 309 K to 378 K. Thus, it could be said that the rise in operating temperature minimizes time required for the drying process. The final weight loss of 45.59% of the non-pretreated Hass avocado seed was reported after 5760 min of drying performed at 353 K. However, it was also of foremost importance to investigate the impact of drying temperature on the physical properties of seeds, which is rarely investigated. This is because, as on the pulp [20], the drying conditions might also have a significant influence on the physical and chemical properties of Hass avocado seeds. To effectively understand the influence of surrounding temperature on the nature of Hass avocado seeds, the physical appearance of Hass avocado seeds were photographed consistently during the drying experiment performed at 333 K air temperature. The physical appearance of Hass avocado seeds at different time intervals can be seen in Fig. 3. It was observed that during the initial stage of the drying process, water was evaporated from the seed integument. The seed coat when detached (see Fig. 3b), enabled the moisture evaporation from the inner layer of the seed. It was found that 333 K and higher temperature resulted in rupturing of avocado seed into two pieces (See Fig. 3f). Therefore, more surfaces were available for the evaporation for water allowing to continue the drying process. However, the employment of such high temperature resulted in hardening and charring of the outer surface of seeds.

The utilization of high operative temperature was predicted to damage the seeds due to charring, which consequently, might also lead for the incomplete evaporation of water. Furthermore, the employment of high drying temperature for the drying process could also burn the cell walls, which in return might cause complexity for the extraction of the value-added chemicals. The physical treatment prior to the drying process would not only allow the usage of less energy for drying but also would help faster removal of moisture. The effect of pretreatment, such as crushing and slicing of Hass avocado seed on the extent of moisture evaporation can be seen in Figs. 4 and 5, respectively. From Figs. 4 and 5, it was observed that after 720 min of drying, a maximum weight loss of 54.50% and 56.76% was achieved for the crushed and sliced Hass avocado seeds, respectively.

In comparison, the pretreated seeds lose approximately twice the amount of moisture that was evaporated with the non-pretreated seeds after 720 min of the drying process. The obtained results in this study can be contrasted with a study reported by Mwithiga and Olwal [21], where it was mentioned that decreasing the thickness of kale reduced the time for the moisture removal process. After 5760 min of drying, a final weight loss of 54.93% and 57.45% was achieved for the crushed and sliced avocado seeds, respectively. However, a negligible fluctuation in seed weight after 1440 min was indicative of accomplishment of possible maximum evaporation of water. From Figs. 2, 4 and 5 it was also understood that in the case of non-pretreated seeds, water was not completely removed even after 5760 min of the drying process. It is also worth noting that the time required to attain the constant weight of pretreated seed samples was same for all drying air temperatures. On the other hand, though elevated temperature assisted acceleration in the moisture evaporation rate, the maximum weight loss of Hass avocado seeds was achieved when dried at 313 K. From Figs. 4 and 5, it could been seen that high temperature (353 K) resulted in lower weight loss, while, high weight loss was obtained when Hass avocado seeds were dried at 313 K air temperature. It was believed that the elevated temperature critically affected the seed surface, which consequently, obstructed the evaporation of water residing inside the seeds. The utilization of high temperatures resulted in charring also of the surface of crushed and sliced seeds. Therefore, the appliance of high temperature (353 K) resulted in incomplete drying of Hass avocado seeds, while, low temperature (313 K) though had inferior moisture evaporation rate, but assisted consistent removal of moisture with causing no damage to Hass avocado seeds. Therefore, the pretreatment process, operative temperature of 313 K, and 1440 min drying time was considered optimal for drying and preserving high quality Hass avocado seeds.

From an industrial viewpoint, the selection of type of pretreatment process might have less significance because it had no impact on the final quality of the seed samples, and air temperature and time required to complete the drying process was also similar; however, we studied the slicing method to improve the accuracy in the experimental findings. We observed that during the crushing pretreatment of Hass avocado seeds, few liquid fragments adhered on the inner wall of the mortar-pestle. Thus, having in-depth

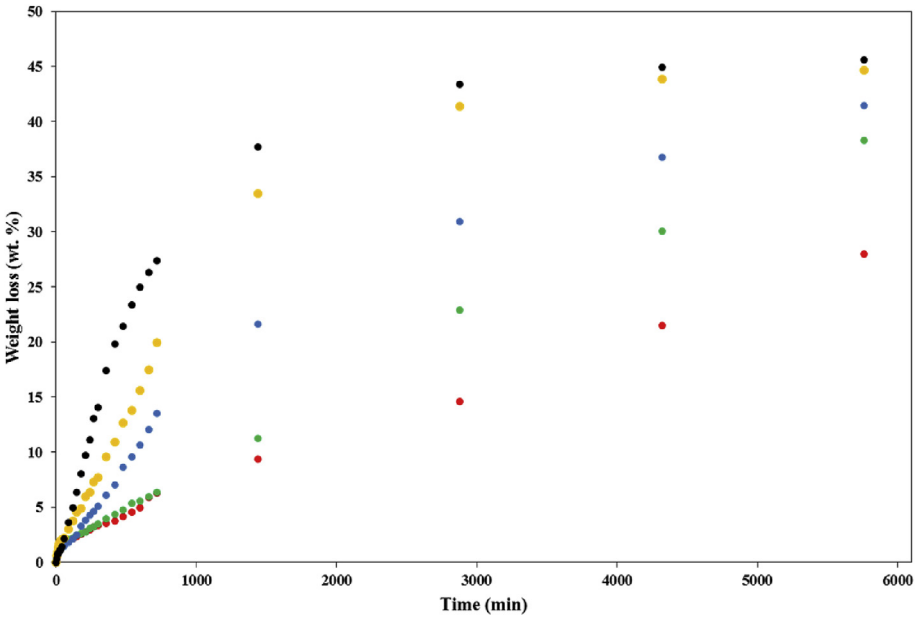

Fig. 2. Weight loss profile for the non-pretreated Hass avocado seed at different temperatures. ((•)) 313 K, ((•)) 323 K, ((•)) 333 K, ((•)) 343 K, (●) 353 K.

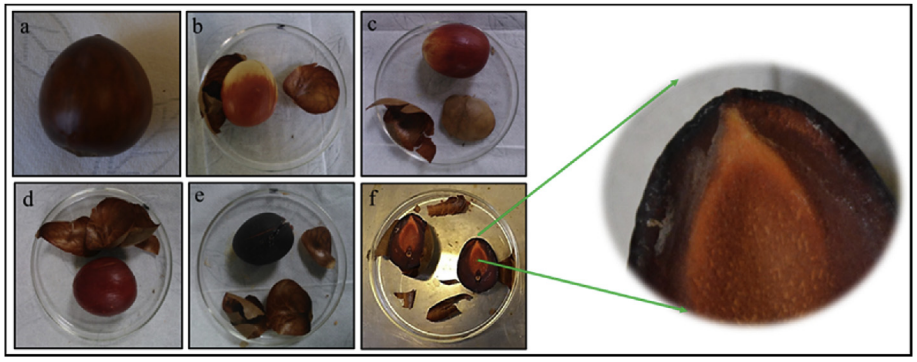

Fig. 3. Physical appearance of Hass avocado seed at 333 K with time: a) 0 min; b) 60 min; c) 120 min; d) 180 min; e) 360 min; f) 720 min.

knowledge about the moisture content in the case of crushed Hass avocado seeds was difficult. During slicing Hass avocado seeds, negligible loss of liquid fragments was observed. In addition, uniform thin layers of the sliced seeds were anticipated to enable straightforward transportation of water molecules as compared to the uneven size of clusters in the case of crushing methodology. The impact of crushing and slicing pretreatment on the water evaporation process from Hass avocado seeds can be seen in Fig. 6.

The moisture removal rate using both pretreatment processes was almost similar; however, the final weight loss in the case of sliced Hass avocado seeds was higher than that obtained using the crushed Hass avocado seeds. The obtained difference justified that some amount of moisture was lost during the crushing process. Therefore, prior to drying, slicing method was considered more beneficial than crushing of seeds in a viewpoint to comprehensively determine moisture content in Hass avocado seeds. The moisture content in Hass avocado seeds, before and after the drying process, was also measured using a KF titrator. The initial moisture content in Hass avocado seeds was 51.20%. The determined moisture content in the fresh seed samples was in close agreement with that reported by Vinha et al. [11]. The residual moisture content in Hass avocado seeds after the drying process performed at 313 K for 1440 min was 4.57%.

3.2. Physical appearance of Hass avocado seeds

The physical appearance of Hass avocado seeds immersed in water at five different temperatures can be seen in Fig. 7. The obtained results suggested that the water temperature of 318 K directed the leaching of orange pigments from Hass avocado seeds in to water, the intensity of which increased with the rise in temperature from 318 K to 348 K.

It was assumed that the rise in temperature promoted the solubility between the natural color inside seeds and water. However, the leaching phenomenon was not observed when Hass avocado seeds were immersed in water at 313 K, indicating that orange pigments were preserved inside the seeds. Thus, surrounding temperature of 313 K did not hold capability to remove orange pigments from physically non-pretreated Hass avocado seeds. Similar results were observed when Hass avocado seeds were placed in water at 303 K, but the seed started germinating after 14 days of experiment. Hass avocado seeds, when placed in water at temperature 318 K or higher, resulted in change in the color of seed surface from off-white to dark brown, indicating that the surrounding temperature higher than 318 K could change the physical properties of the seeds. Moreover, water temperature higher than 333 K resulted in breakage of the seeds into two pieces and caused

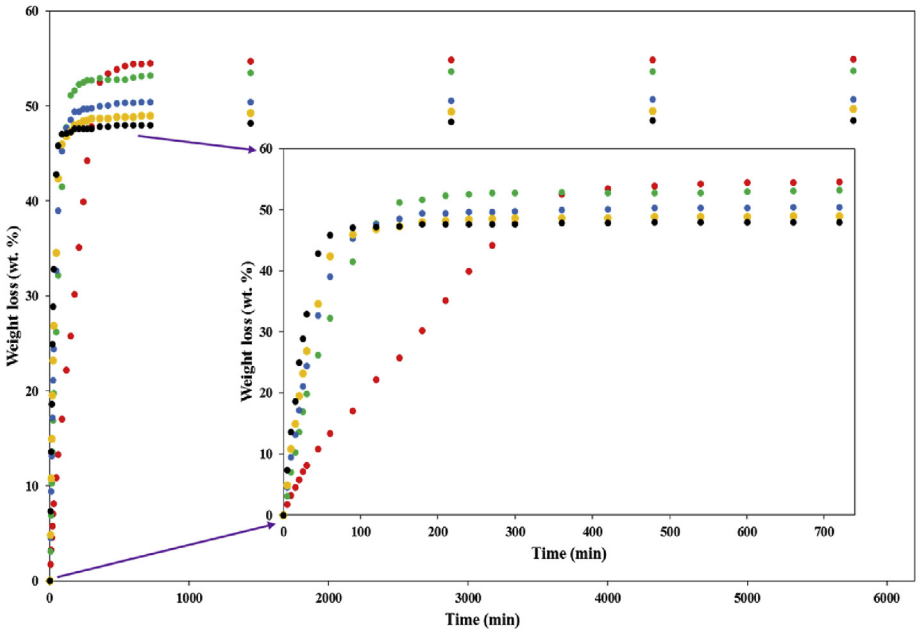

Fig. 4. Weight loss profile for the crushed Hass avocado seeds at different temperatures. ((•)) 313 K, ((•)) 323 K, ((•)) 333 K, ((•)) 343 K, (●) 353 K.

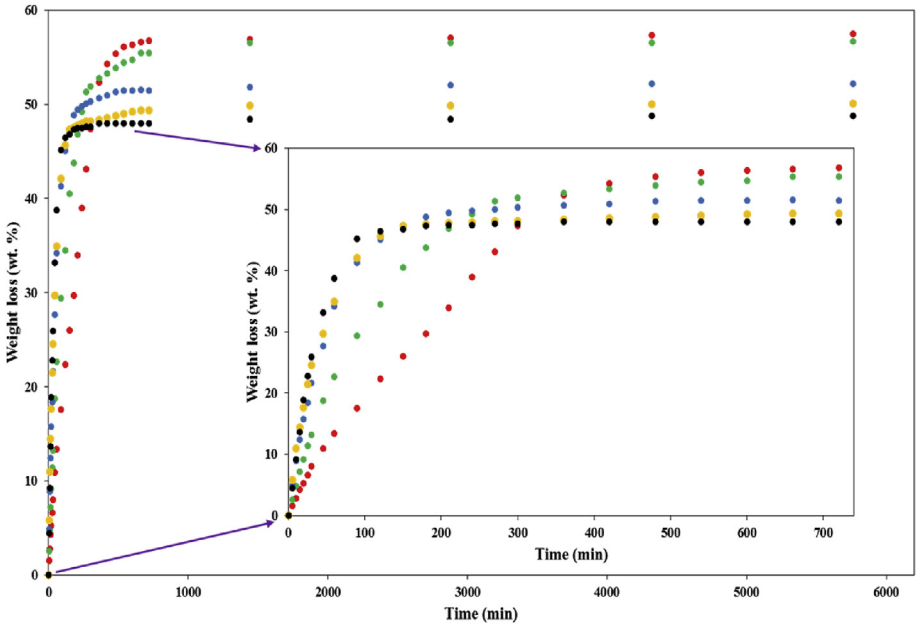

Fig. 5. Weight loss profile for the sliced Hass avocado seeds at different temperatures. ((•)) 313 K, ((•)) 323 K, ((•)) 333 K, ((•)) 343 K, (●) 353 K.

immediate leaching of the orange color. Hence, it was concluded that the surrounding temperature higher than 313 K could cause damage and change the physical as well as chemical properties of Hass avocado seeds.

4. Conclusion

Hass avocado seeds generally are discarded with no further applications. However, Hass avocado seeds constituents for several value-added chemicals which could gain relevance in food, cosmetic, pharmaceutical, and biofuel industries. In order to avoid irreversible damage happening to Hass avocado seeds and elongate its storage duration, its drying is of foremost importance. The present experimental study was performed to study the influence of five different air temperature on the drying kinetics of Hass avocado seeds. Furthermore, the impact of physical pretreatment process of Hass avocado seeds on the drying process was systematically investigated. The obtained results suggested that the rise in operating temperature accelerated the drying process of Hass avocado seeds; however, the appliance of high temperature resulted in charring of the seed surface. The drying process of the non-pretreated Hass avocado seeds was very slow and resulted in incomplete evaporation of water even after 5760 min of the drying process. However, the pretreatment process resulted in the reduction of the drying time. The drying process performed at 313 K for 1440 min resulted in weight loss of 54.50% and 56.75% in

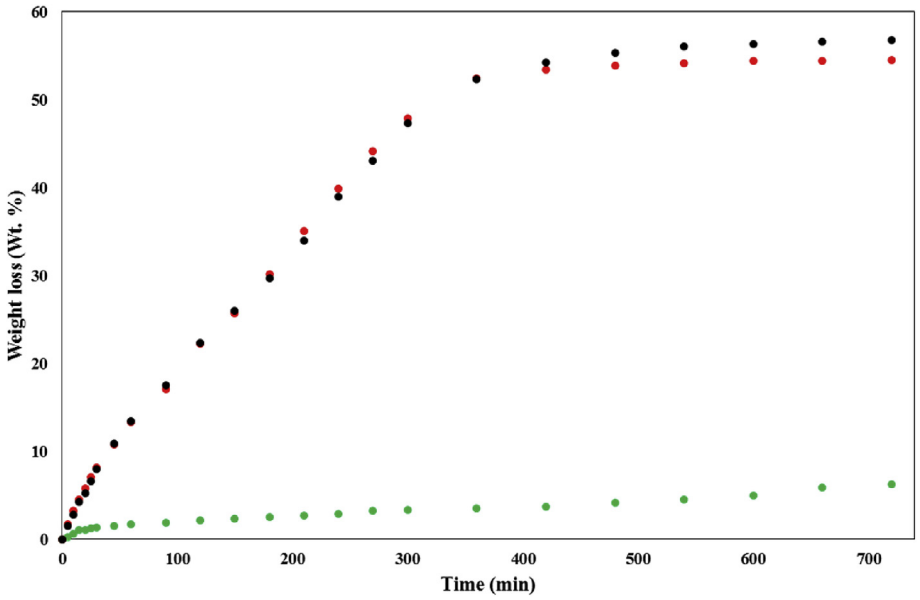

Fig. 6. Effect of the pretreatment process on drying of Hass avocado seeds at 313 K. (•) Non-pretreatment, (•) Crushed, (●) Sliced.

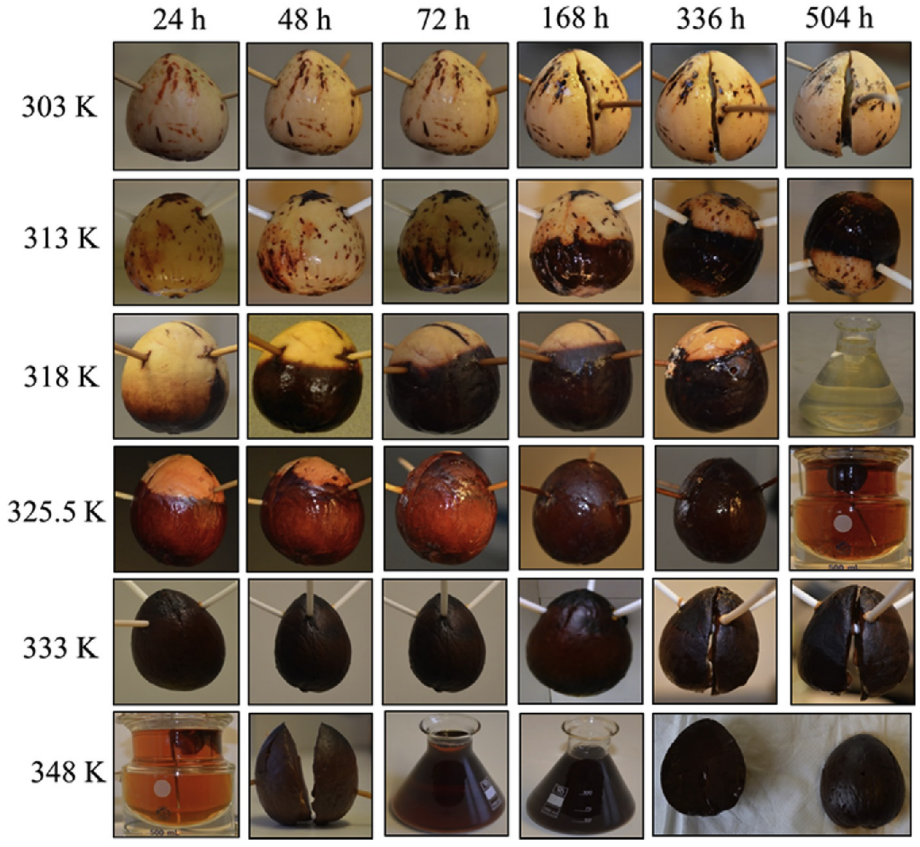

Fig. 7. Effect of temperature on the physical appearance of Hass avocado seeds.

the case of crushed and sliced Hass avocado seeds, respectively. The slicing pretreatment process was found to provide accuracy in the experimental findings. An additional experimental studies were performed in which the physical appearance of Hass avocado seeds immersed in water at different temperatures was monitored. The obtained results suggested that water temperature 318 K and higher resulted in leaching of orange pigments present inside the seeds. Therefore, it was concluded that drying air temperature of 313 K was optimal for satisfactory drying and preserving the quality of Hass avocado seed.

Acknowledgment

The authors would like to express their gratitude to the Norwegian University of Life Sciences (Project No. 1301051406) for their financial support.

References

[1] Food and Argiculture Organization of the United Nations Statistics Division. [cited 2015 October 22]. Availabe from: http://faostat3.fao.org/browse/Q/QC/E.
[2] M.L. Dreher, A.J. Davenport, Hass avocado composition and potential health effects, Crit. Rev. Food Sci. Nutr. 53 (7) (2013) 738–750.
[3] Mexico: Avocado Annual. United States Department of Agriculture Foreign Agricultural Service. [cited 2015 October 22]. Available from: http://www.fas.usda.gov/data/mexico-avocado-annual.
[4] N. Kovalkovičová, I. Šutiaková, J. Pistl, V. Šutiak, Some food toxic for pets, Interdiscip. Toxicol. 2 (3) (2009) 169–176.
[5] Foods that are hazardous to dogs, The American Society for the Prevention of Cruelty to Animals [US]. [cited 2015 October 22]. Available from: https://www.aspca.org/pet-care/virtual-pet-behaviorist/dog-behavior/foods-are-hazardous-dogs.
[6] D. Dabas, R.J. Elias, J.D. Lambert, G.R. Ziegler, A colored avocado seed extract as a potential natural colorant, J. Food Sci. 76 (9) (2011) C1335–C1441.
[7] L. Lacerda, T. Colman, T. Bauab, M. da Silva Carvalho Filho, I. Demiate, E. de Vasconcelos, E. Schnitzler, Thermal, structural and rheological properties of starch from avocado seeds (Persea americana, Miller) modified with standard sodium hypochlorite solutions, J. Therm. Analysis Calorim. 115 (2) (2014) 1893–1899.
[8] L.S. Weatherby, D.G. Sorber, Chemical composition of avocado seed, Ind. Eng. Chem. 23 (12) (1931) 1421–1423.
[9] M. Bhaumik, H.J. Choi, M.P. Seopela, R.I. McCrindle, A. Maity, Highly effective removal of toxic Cr(VI) from wastewater using sulfuric acid-modified avocado seed, Ind. Eng. Chem. Res. 53 (3) (2014) 1214–1224.
[10] L.A. Rodrigues, M.L.C.P. da Silva, M.O. Alvarez-Mendes, A. dR. Coutinho, G.P. Thim, Phenol removal from aqueous solution by activated carbon produced from avocado kernel seeds, Chem. Eng. J. 174 (1) (2011) 49–57.
[11] A.F. Vinha, J. Moreira, S.V.P. Barreira, Physicochemical parameters, phytochemical composition and antioxidant activity of the algarvian avocado (Persea americana Mill.), J. Agric. Sci. 5 (12) (2013) 100–109.
[12] F. Takenaga, K. Matsuyama, S. Abe, Y. Torii, S. Itoh, Lipid and fatty acid composition of mesocarp and seed of avocado fruits harvested at northern range in Japan, J. oleo Sci. 57 (11) (2008) 591–597.
[13] P.S. Bora, N. Narain, R.V.M. Rocha, M.Q. Paulo, Characterization of the oils from the pulp and seeds of avocado (cultivar: Fuerte) fruits, Grasas Y. Aceites 52 (3–4) (2001) 171–174.
[14] T. Gutfinger, A. Letan, Studies of unsaponifiables in several vegetable oils, Lipids 9 (9) (1974) 658–663.
[15] H.M. Rachimoellah, D.A. Resti, A. Zibbeni, dI.W. Susila, Production of biodiesel through tranesterification of avocado (persea gratissima) seed oil using base catalyst, J. Tek. Mesin 11 (2) (2009) 85–90.
[16] S. Risnoyatiningsih, Biodiesel from avocado seeds by tranesterification process, J. Tek. Kim. 5 (1) (2010) 345–351.
[17] J.S. Roberts, D.R. Kidd, O. Padilla-Zakour, Drying kinetics of grape seeds, J. Food Eng. 89 (4) (2008) 460–465.
[18] E.R. Egger, Effect of the removal of the seed coats on avocado seed germination, Calif. Avocado Soc. 24 (1942) 41–43.
[19] V.C. Siqueira, O. Resende, T.H. Chaves, Determination of the volumetric shrinkage in jatropha seeds during drying, Acta Sci. Agron. 34 (2012) 231–238.
[20] M.Z. dos Santos, T.R. Alicieo, C.P. Pereira, G. Ramis-Ramos, C.B. Mendonça, Profile of bioactive compounds in avocado pulp oil: influence of the drying processes and extraction methods, J. Am. Oil Chem. Soc. 91 (1) (2014) 19–27.
[21] G. Mwithiga, J.O. Olwal, The drying kinetics of kale (Brassica oleracea) in a connective hot air dryer, J. Food Eng. 71 (2005) 373–378.

Paper VII

Industrial Crops and Products 91 (2016) 76–87

Contents lists available at ScienceDirect

Industrial Crops and Products

journal homepage: www.elsevier.com/locate/indcrop

Mathematical modelling of the drying kinetics of Hass avocado seeds

M.R. Avhad, J.M. Marchetti*

Department of Mathematical Sciences and Technology, Norwegian University of Life Sciences, Drøbakveien 31, Ås 1432, Norway

ARTICLE INFO

Article history:
Received 7 December 2015
Received in revised form 24 May 2016
Accepted 28 June 2016
Available online 15 July 2016

Keywords:
Hass avocado seeds (*Persea americana mill.*)
Drying kinetics
Mathematical modelling
Avhad and Marchetti model

ABSTRACT

The seed of Hass avocado (*Persea Americana Mill.*), which is about 13% of the total weight of the fresh fruit, is considered as an agricultural waste and discarded with no proper applications. The current research article presents a study focused on the mathematical modelling of the drying kinetics of Hass avocado seeds. The drying experiments of the non-pretreated and pretreated (sliced and crushed) Hass avocado seeds were performed in a heating furnace where the influence of five different air temperatures (313, 323, 333, 343, and 353 K) on the rate of moisture evaporation was systematically studied. It was observed that the pretreatment process stimulated the drying progression of Hass avocado seeds. Four different semi-theoretical drying mathematical models were compared based on their coefficient of determination, reduced mean square error, root mean square error, mean bias error, and mean absolute error of the deviation to characterize the drying curves at previous mentioned conditions. The rise in the air temperature resulted in steeper decline in the curve shape of moisture ratio. The obtained scientific findings suggested that a newly proposed Avhad and Marchetti model provided superior simulation of the drying kinetics of Hass avocado seeds than the Lewis model, the Henderson and Pabis model, and the Page model over the experimental temperature range.

1. Introduction

According to the statistics division of the Food and Agriculture organization of the United Nations, the world total production of avocado fruit from the year 1993 until 2013 was augmented by 58.30%; the aggregate production of fruit being 4.71 million tonnes in the year 2013 (Food and Agriculture Organization of the United Nations, 2016). The consistent rise in the agriculture of avocado fruit is attributed to its increasing requirement as a consequence of numerous benefits of the same on human health (Dreher and Davenport, 2012; Pieterse et al., 2003). The augmenting demand for such a nutrient dense fruit has resulted in the growth of export business. Mexico is the top producer of Hass avocado fruits. According to the report published by USDA Foreign Agricultural Service in November 2014, Mexico has been exporting avocados to 21 countries; the nations which are the top importers of avocado fruit include, the United States, Japan, Canada, and Costa Rica (Mexico: Avocado Annual, 2014). It is important to note that only the pulp of the fruit is consumed; the seeds of Hass avocado, which constituents on an average 13% of the total weight of the fresh fruit, is considered as an agricultural waste and is discarded with no further application. Therefore, it could be estimated that in the year 2013 alone, approximately 613 thousand tonnes of avocado seeds were treated as a waste material. The natural orange pigments reside in Hass avocado seeds, which can be extracted in the presence of water and utilize in the food and the cosmetics industries (Dabas et al., 2011). Furthermore, the polyphenolic components are also present in Hass avocado seeds and can possibly be extracted (Gómez et al., 2014). The research articles focused on the availability of the starch compounds in avocado seeds are also available (Weatherby and Sorber, 1931; Lacerda et al., 2014). The carbon material synthesized from avocado seeds holds the capability to be served as an adsorbent for the treatment of the aquatic systems (Bhaumik et al., 2014; Rodrigues et al., 2011). In addition, few reports also indicated the existence of lipid components in avocado seeds, which depending on the physico-chemical properties could be utilized as combustible oil, or be transformed to biofuel (Vinha et al., 2013; Takenaga et al., 2008). The derivatization of combustible oil or biofuels from a waste resources, such as avocado seeds could be of industrial relevance because the combustion of fuel would have negligible contribution on the net increase in the atmospheric carbon dioxide. Furthermore, the trade of the raw materials would require less monetary investments.

In order to effectively utilize avocado seeds, its storage for elongated duration of time would be essential. The process of removal of moisture is anticipated to improve the shelf-life of avocado

* Corresponding author.
E-mail address: jorge.mario.marchetti@nmbu.no (J.M. Marchetti).

http://dx.doi.org/10.1016/j.indcrop.2016.06.035
0926-6690/

seeds. This is because the presence of moisture in avocado seeds is suspected to encourage the growth and reproduction of microorganisms causing irreversible damage to seeds; hence, downgrading the quality of the product. Furthermore, the moisture removal procedure would also provide a significant reduction in the total weight of the product and shorten the space required for packaging; thus, minimizing the packaging and transportation expenditure (Arabhosseini et al., 2009). The drying process in the presence of surrounding hot air could be considered as one of the viable option to accomplish the satisfactory evaporation of moisture from avocado seeds. The drying process could be defined as a progression of removal of moisture via simultaneous heat and mass transfer between the sample and the surrounding atmosphere by means of vaporization, generally caused by temperature and air convection forces (Perea-Flores et al., 2012). With the purpose of maintaining the quality of the bioproduct, studying the kinetics of the drying process could be of foremost relevance so as to select the appropriate temperature and time required for the satisfactory drying process. Furthermore, the development of the mathematical model for the drying process could be crucial as it would allow the design engineers to not only choose the most suitable operating conditions required for the effective drying but also size the drying equipment accordingly to meet the desired operating parameters (Perea-Flores et al., 2012; Gunhan et al., 2005). The simulation of the drying kinetics is based on setting a mathematical equation that can effectively describe the system. The solution of these mathematical equations is anticipated to allow the prediction of the process parameters as a function of time at any point in the drying equipment based on the initial conditions. The authors believe that the drying equipment should be designed considering the following criterion: (i) the dryer must provide sufficient heat for the evaporation of moisture from the samples, (ii) appropriate air must be provided to eliminate moisture in the dryer, (iii) the surrounding conditions should not drop the quality of the product, and (iv) to decide adequate time required for satisfactory drying of the material.

In recent years, the scientific efforts on investigating the influence of different temperatures on the drying kinetics of several seeds, such as castor oil seeds (Perea-Flores et al., 2012), soybean seeds (Barrozo et al., 2006), jatropha seeds (Siqueira et al., 2012), rapeseed (Duc et al., 2011), grape seeds (Roberts et al., 2008), amongst others have been reported. However, to our knowledge, no research investigation on the simulation of the drying kinetics of Hass avocado seeds yet has been reported. The previous work related to the experimental findings focused on examining the influence of air temperatures and pretreatment on the drying characteristics as well as physical appearance of Hass avocado seeds performed in the same laboratory has been published earlier (Avhad and Marchetti, 2015). The prime objective of the current study was to develop a mathematical model for predicting the drying kinetics of Hass avocado seed at five drying air temperatures. The simulated results were compared with the experimental data; while, the selection of the best model was based on the calculated statistical parameters.

2. Experimental section

2.1. Drying process

The detail experimental procedure employed for the drying process of Hass avocado seeds has been presented elsewhere (Avhad and Marchetti, 2015). The pretreatment process for Hass avocado seeds were tested so as to accelerate the rate of the drying process. For the crushing pretreatment process, a bowl-shaped mortar-pestle was used to pulverize Hass avocado seeds. In the slicing pretreatment process, Hass avocado seeds were sliced using a stainless steel slicer in order to maintain the uniform thickness of every samples. The average particle size of the crushed avocado seeds was 4.2 mm; the smallest and largest unit size being 3.5 mm and 5.5 mm. The average length, width, and thickness of the sliced Hass avocado seeds was 4.3 cm, 3.0 cm, and 2.7 mm respectively (Avhad and Marchetti, 2015). The pretreated and non-pretreated seed samples kept in separate Pyrex-glass petri plates were applied for the drying process performed at five different air temperatures (313, 323, 333, 343, and 353 K). The impact of five different air temperatures on the drying process was investigated because several reports have claimed that temperature is the dominant factor directing the drying process (Lahsasni et al., 2004; Mwithiga and Olwal, 2005). The drying experiments of the seed samples were performed in a heating furnace (Narbetherm P300, Germany). The seed samples were weighted on a digital balance machine having 0.01 g accuracy (Mettler-Toledo, PG 5002 Delta Range, Switzerland). For the drying experiments, the temperature of the heating furnace was first raised to the set point and was maintained for 60 min prior inserting the samples to ensure that there is no fluctuation in the surrounding air temperature. The weight of the seed samples during the experiments were measured at a predetermined time interval taking less than 15 s to weigh the samples. The drying experiments were performed for 5760 min in order to make sure that there is negligible fluctuation in the weight of seed samples, which was assumed to be the stage of dynamic equilibrium. Every experiments were replicated twice to obtain the reproducibility in the experimental findings.

The initial and equilibrium moisture content in Hass avocado seeds were determined using the automated Karl Fischer (KF) volumetric system (Metrohm, Tampa, FL, USA) consisting of an oven sample unit (Model 774) for water extraction, a dosing device (Model 901) connected to two mechanical burettes (Model 80; one for titrant and other for methanol) for control of titrant, and a titration cell with electrode and stirrer (Model 801) (Avhad and Marchetti, 2015).

The moisture content in the seed samples was determined according to the following equation:

$$\text{Moisture content}\,(\%) = \frac{V\,(mL)\cdot 5\left(gL^{-1}\right)\cdot 0.1}{m\,(g)} \quad (1)$$

where, $5\,g\,L^{-1}$ is the concentration of water equivalents in the titrant, V is the total volume of titrant consumed during the titration, and m is the initial weight of the sample.

For the determination of the initial moisture content, Hass avocado seeds were pretreated. It was not possible to measure the initial moisture content of non-pretreated Hass avocado seeds because of its big size and hardness. The final moisture content in the case of the non-pretreated Hass avocado seeds was not measured because the drying process was not completed even after using high temperature of 353 K and 5760 min processing time (Avhad and Marchetti, 2015). The initial and the equilibrium moisture content, in the case of the pretreated seed samples, was measured thrice and the average of the analyzed value was considered. The initial moisture content in Hass avocado seeds was 51.20%. The equilibrium moisture content of Hass avocado seeds, measured after 1440 min of drying process performed at 313 K, was 4.57% (Avhad and Marchetti, 2015). The initial and equilibrium moisture content of the seed samples were analyzed thrice and the values displayed insignificant fluctuation. The equilibrium moisture content measured in the case of sliced and crushed Hass avocado seeds were almost similar.

2.2. Mathematical model for the drying kinetics

In order to predict the drying kinetics of Hass avocado seeds, it is foremost importance to accurately model its drying behavior. Therefore, in the present study the experimental drying data for each of the five applied temperatures were fitted with four semi-theoretical drying mathematical models. The moisture contents at each time interval were calculated from both weight loss data and dry solid weight of the samples. The moisture content data at different temperatures were converted to moisture ratio (MR), which is a dimensionless expression and fitted as a function of drying time. The dimensionless MR of Hass avocado seeds during the drying experiments was written in the following form.

$$MR = \frac{M_t - M_e}{M_0 - M_e} \quad (2)$$

where, M_0 is the initial moisture content, M_t is the moisture content at time t, and M_e is the equilibrium moisture content.

The activation energy (E_a) for the non-pretreated and pretreated Hass avocado seeds was calculated using the Arrhenius equation, which is expressed as

$$k = Aexp\left(-E_a/RT\right) \quad (3)$$

where, k is the specific rate constant, A is the pre-exponential factor of the Arrhenius equation, E_a is the activation energy (KJ mol^{-1}), R is the universal gas constant (8.314 J mol^{-1} K), and T is the absolute air temperature (K).

Then the curve-fitting procedure was performed where three well-known and widely used, and one newly introduced semi-theoretical mathematical models were applied to describe the drying kinetics of Hass avocado seeds which are discussed below.

2.2.1. Lewis model

The Lewis model was initially tested to fit the experimental data of the drying kinetics because of its simplicity. The assumption made for this model is that there occurs negligible internal resistance, indicative of no resistance to moisture movement from within the interior of the material out to the surface of the material (Lewis, 1921). The drying rate is proportional to the difference in the moisture content between the drying material and equilibrium moisture content at the drying air condition. This model was successfully applied to model the drying kinetics of grape seeds (Roberts et al., 2008), black tea (Panchariya et al., 2002), amongst other. The Lewis model is represented as

$$MR = \exp(-kt) \quad (4)$$

where, k is the constant of the model following an Arrhenius expression and t is the time.

2.2.2. Henderson and Pabis model

The Henderson and Pabis model is also known as a bi-parametric exponential model (Iguaz et al., 2003). This model is the first term of a general series solution of Fick's second law. The slope of this model, coefficient k, is linked to effective moisture diffusivity when the drying process takes place only in the falling rate period and liquid diffusion control process. This model was successfully utilized to simulate the drying of corn (Henderson and Pabis, 1961). The simplest approximation form when only one term of the infinite series is utilized can be written as

$$MR = aexp(-kt) \quad (5)$$

where, a and k are the constants of the model following an Arrhenius expression.

2.2.3. Page model

Page proposed a modification of the Lewis model by introducing a new coefficient affecting time. The modifications were suggested so as to correct some shortcomings. This model suggests the use of two empirical constants. This model has produced good fits to characterize the drying of several agricultural products, such as bay leaves (Gunhan et al., 2005), rapeseed (Duc et al., 2011), pistachio nuts (Kashaninejad et al., 2007), amongst others. The modified Page model was utilized to describe the drying process of kale (Mwithiga and Olwal, 2005). The Page model is written in the following form:

$$MR = exp(-kt^N) \quad (6)$$

where, k and N are the constants of the model. k follows an Arrhenius expression.

2.2.4. Avhad and Marchetti model

Avhad and Marchetti proposed a new mathematical model to predict the drying kinetics of Hass avocado seeds. The development of this model originated from the combination of the Page and, the Henderson and Pabis model. In the case of the Page model, the estimated value for the coefficient, N, affecting time was constant and did not exhibited temperature dependence (Gunhan et al., 2005; Simal et al., 2005; Senadeera et al., 2003; Demir et al., 2004). The Henderson and Pabis model successfully predicted the drying kinetics of the materials with the approximation that diffusion controls the drying process and the material shrinkage is negligible (Jaiyeoba and Raji, 2012; Phanphanich and Mani, 2009). However, depending upon the characteristics of Hass avocado seeds obtained earlier from the experimental findings (Avhad and Marchetti, 2015), following assumptions were taken into consideration:

(a) The initial moisture content in Hass avocado seeds is high and uniformly distributed throughout the mass of the seed.
(b) The initial stage of the drying process was air temperature dependent.
(c) The change in the water content in Hass avocado seed during the initial period of drying was non-linear and the constant drying rate period is not existent.
(d) Resistance to mass transfer at the surface is negligible compared to the internal resistance of the sample.
(e) The drying process resulted in slight shrinkage of Hass avocado seeds.

The proposed mathematical model is represented as

$$MR = a\exp\left(-kt^N\right) \quad (7)$$

where, k, a, and N are the constants of model. k follows an Arrhenius expression.

This model was developed so as to improve the fitting between the model and the experimental data obtained for the drying of Hass avocado seeds.

2.3. Statistical parameters

The selection of the best mathematical model for predicting the drying kinetics of Hass avocado seeds was decided based on various statistical parameters, such as coefficient of determination, reduced mean square error, root mean square error, mean bias error, and mean absolute error.

The coefficient of determination (R^2) is considered as one of the prime criteria for the selection of the best model (Taylor, 1997). Furthermore, the evaluation of the goodness of fit of the model was also determined by various widely used statistical parameters, such as square error (χ^2), root mean square error (E_{RMS}), mean bias

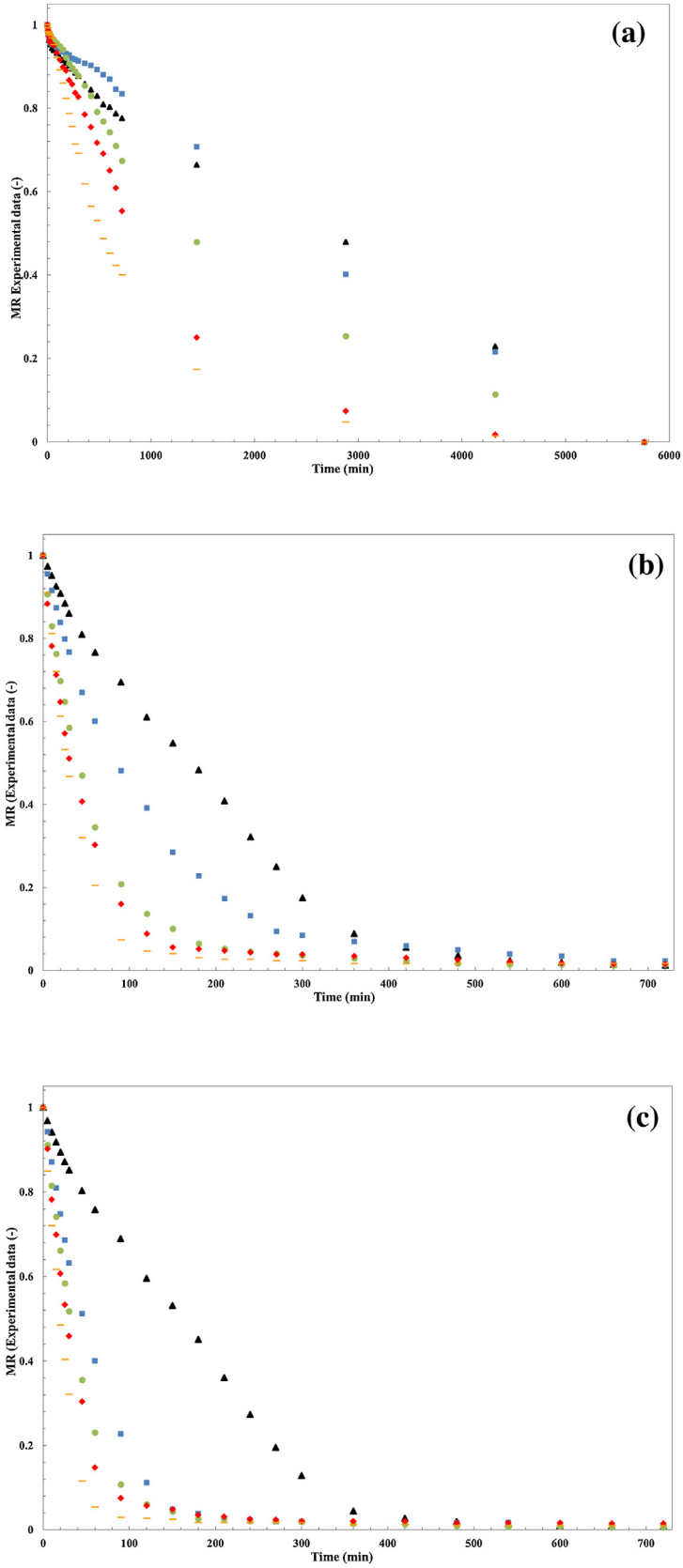

Fig. 1. (a): Moisture ratio vs. drying time at different air temperatures for the non-pretreated Hass avocado seeds: (▲) 313 K, (■) 323 K, (●) 333 K, (♦) 343 K, (_) 353. (b): Moisture ratio vs. drying time at different air temperatures for the sliced Hass avocado seeds: (▲) 313 K, (■) 323 K, (●) 333 K, (♦) 343 K, (_) 353. (c): Moisture ratio vs. drying time at different air temperatures for the crushed Hass avocado seeds: (▲) 313 K, (■) 323 K, (●) 333 K, (♦) 343 K, (_) 353.

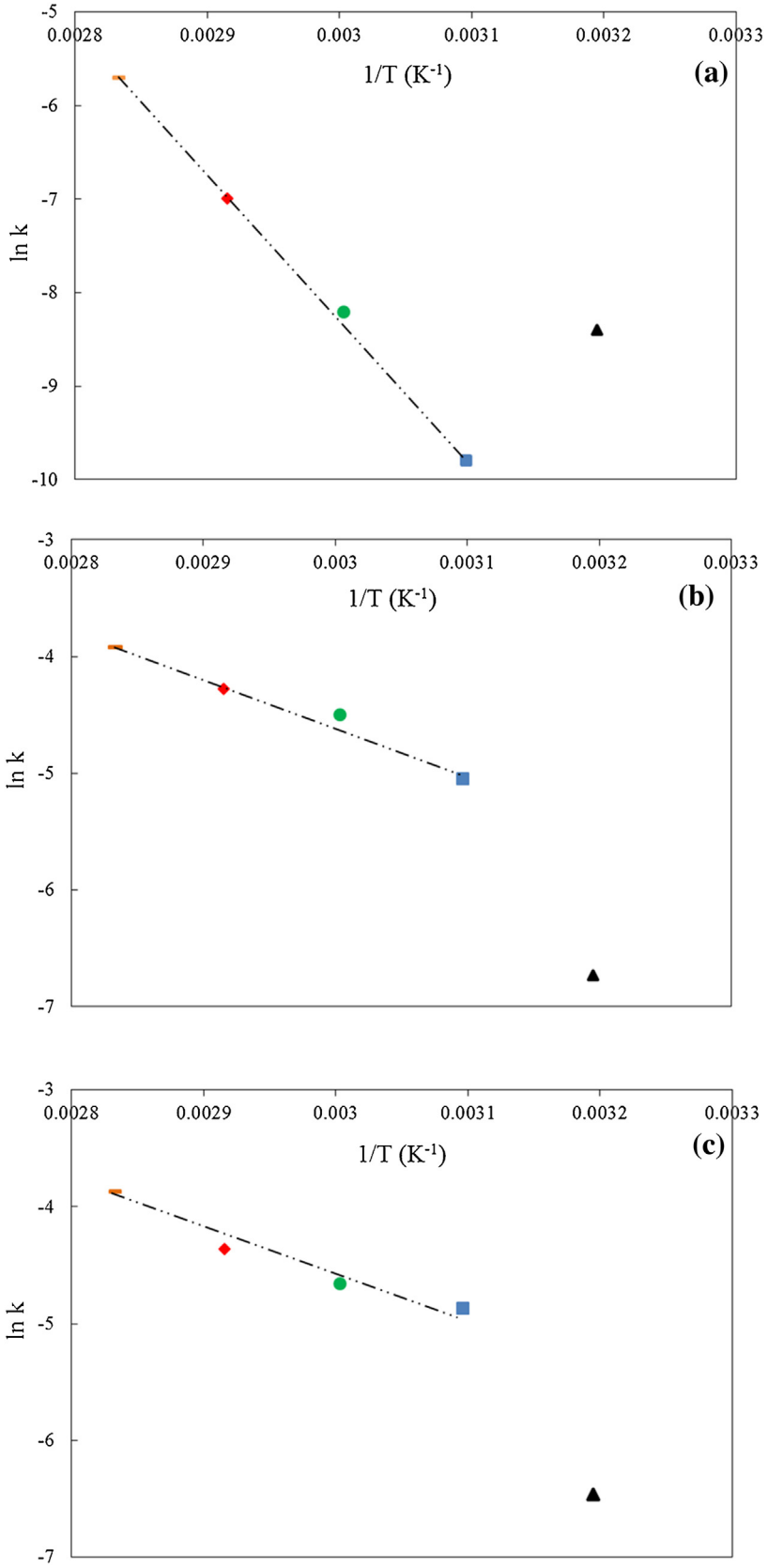

Fig. 2. (a): Arrhenius plot between ln (k) versus 1/T for the non-pretreated Hass avocado seeds: (▲) 313 K, (■) 323 K, (●) 333 K, (♦) 343 K, (_) 353 K. (b): Arrhenius plot between ln (k) versus 1/T for the sliced Hass avocado seeds: (▲) 313 K, (■) 323 K, (●) 333 K, (♦) 343 K, _) 353 K. (c): Arrhenius plot between ln (k) versus 1/T for the crushed Hass avocado seeds: (▲) 313 K, (■) 323 K, (●) 333 K, (♦) 343 K, (_) 353 K.

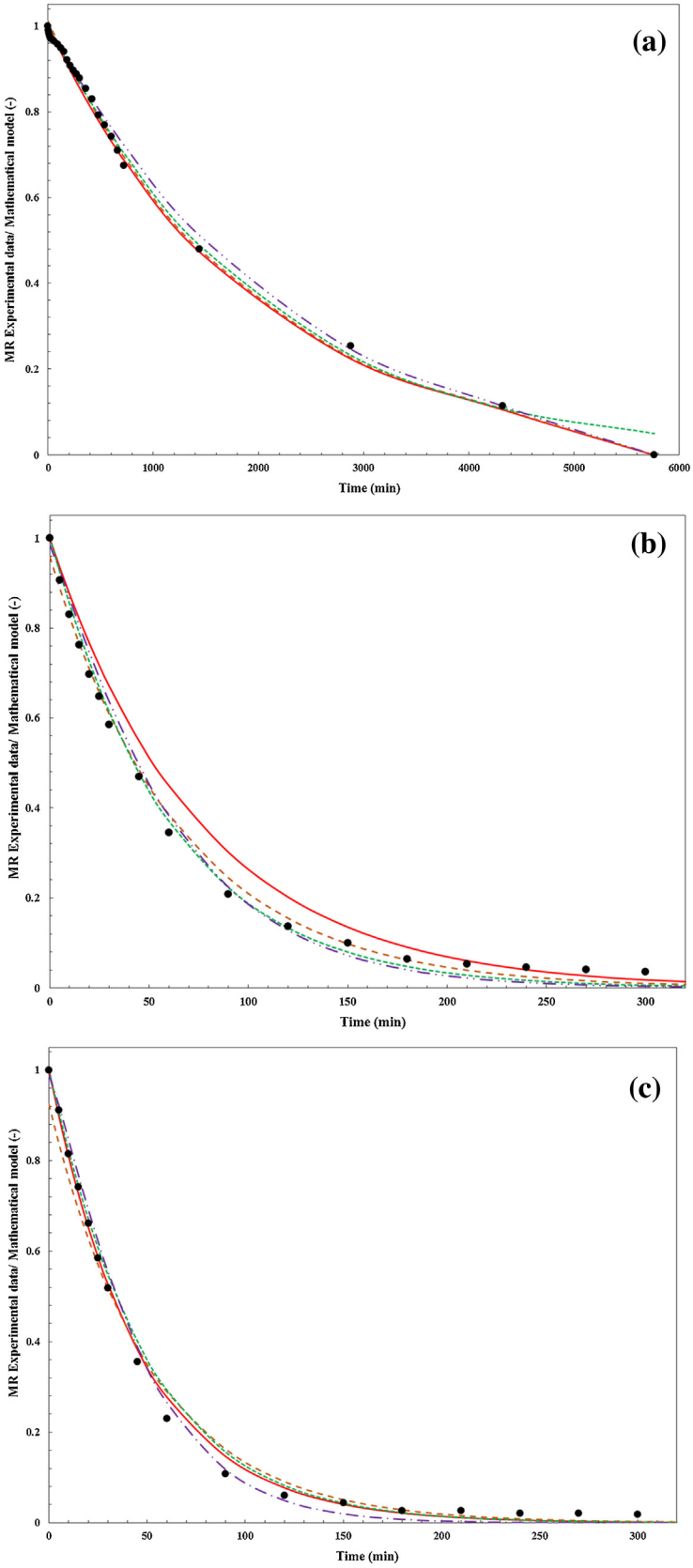

Fig. 3. (a): Comparison of the experimental and predicted moisture ratios using the four different drying mathematical models at 333 K for the non-pretreated Hass avocado seeds: (●) Experimental data, (—) Lewis model, (—) Henderson and Pabis model, (—) Page model, (—) Avhad and Marchetti model. (b): Comparison of the experimental and predicted moisture ratios using the four different drying mathematical models at 333 K for the sliced Hass avocado seeds: (●) Experimental data, (—) Lewis model, (—) Henderson and Pabis model, (—) Page model, (—) Avhad and Marchetti model. (c): Comparison of the experimental and predicted moisture ratios using the four different drying mathematical models at 333 K for the crushed Hass avocado seeds: (●) Experimental data, (—) Lewis model, (—) Henderson and Pabis model, (—) Page model, (—) Avhad and Marchetti model.

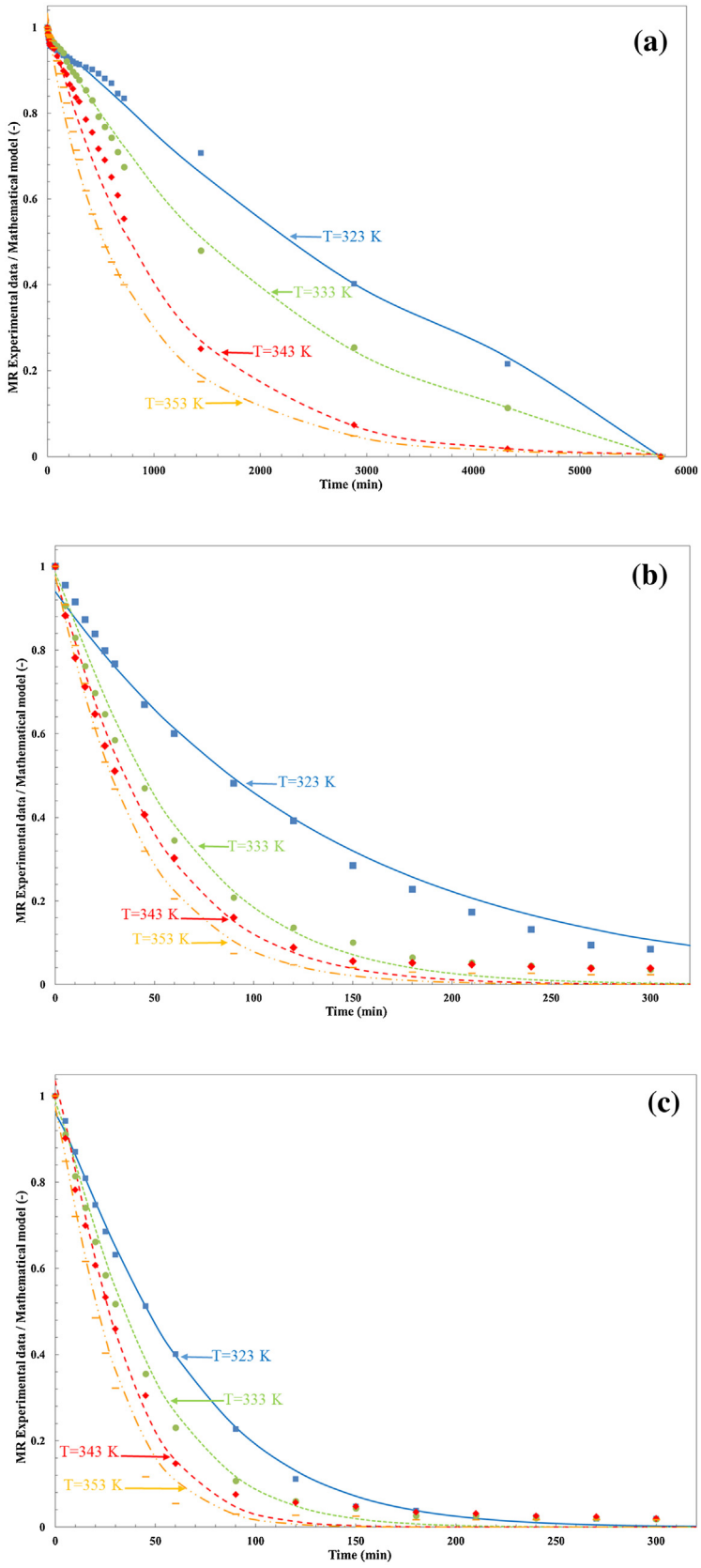

Fig. 4. (a): Comparison of the experimental and predicted moisture ratio using the Avhad and Marchetti drying mathematical models at 323–353 K air temperatures for the non-pretreated Hass avocado seeds: (■) Experimental data, (—) Model, (●) Experimental data, (—) Model, (♦) Experimental data, (—) Model, (—) Experimental data, (—) Model. (b): Comparison of the experimental and predicted moisture ratio using the Avhad and Marchetti drying mathematical models at 323–353 K air temperatures for the sliced Hass avocado seeds: (■) Experimental data, (—) Model, (●) Experimental data, (—) Model, (♦) Experimental data, (—) Model, (—) Experimental data, (—) Model. (c): Comparison of the experimental and predicted moisture ratio using the Avhad and Marchetti drying mathematical models at 323–353 K air temperatures for the crushed Hass avocado seeds: (■) Experimental data, (—) Model, (●) Experimental data, (—) Model, (♦) Experimental data, (—) Model, (—) Experimental data, (—) Model.

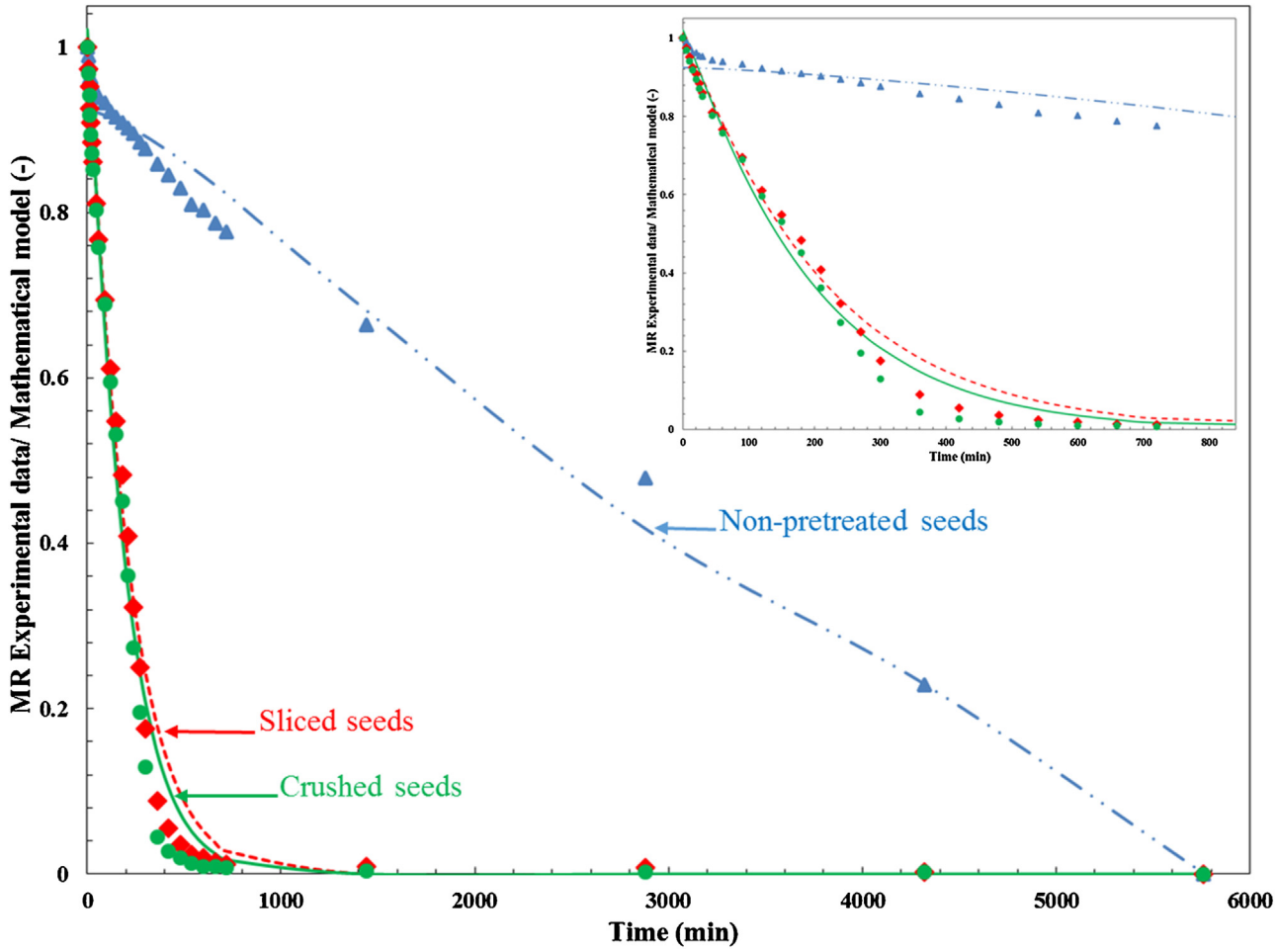

Fig. 5. Comparison of the experimental and predicted moisture ratios using the Avhad and Marchetti drying mathematical models at 313 K air temperature. (▲) Experimental data, (—) Model, (♦) Experimental data, (—) Model, (●) Experimental data, (—) Model.

error (MBE), and mean absolute error (MAE). For the quality fit, R^2 value should be higher; while, χ^2, E_{RMS}, and MBE value should be lower. As χ^2 and E_{RMS} reach 'zero', the closer the prediction is to the experimental data. The value for E_{RMS} is positive and it provides information on the short term performance. While, MBE provides information on the long term performance of the correlations by allowing a comparison of actual deviation between the predicted and measured values term by term (Gunhan et al., 2005).

The expression for the above mentioned parameters were written as:

$$R^2 = \frac{\sum_{i=1}^{N}\left(MR_{exp,i} - \overline{MR}_{pre,i}\right) * \left(MR_{exp,i} - \overline{MR}_{pre,i}\right)}{\sqrt{\sum_{i=1}^{N}\left(MR_{exp,i} - \overline{MR}_{pre,i}\right)^2 * \sum_{i=1}^{N}\left(MR_{exp,i} - \overline{MR}_{pre,i}\right)^2}} \quad (8)$$

$$\chi^2 = \frac{\sum_{i=1}^{N}\left(MR_{exp,i} - MR_{pre,i}\right)^2}{N - z} \quad (9)$$

$$E_{RMS} = \left[\frac{1}{N}\sum_{i=1}^{N}\left(MR_{exp,i} - MR_{pre,i}\right)^2\right]^{1/2} \quad (10)$$

$$MBE = \frac{1}{N}\sum_{i=1}^{N}\left(MR_{exp,i} - MR_{pre,i}\right) \quad (11)$$

where, $MR_{exp,i}$ is the ith experimental dimensionless moisture ratio; $MR_{pre,i}$ is the ith predicted dimensionless moisture ratio; N is the number of observation; z is the number of constants in the model.

3. Results and discussion

The graphical representation for the drying pattern of Hass avocado seeds were prepared by transforming the weight loss data to a dimensionless parameter moisture ratio and then plotting it

Table 1
Estimated activation energy and pre-exponential factor for the non-pretreated, sliced and crushed Hass avocado seeds.

Model	Non-pretreated		Sliced		Crushed	
	E_a (KJ mol^{-1})	A	E_a (KJ mol^{-1})	A	E_a (KJ mol^{-1})	A
Lewis	43.93	4.02×10^3	34.81	3829.15	24.41	143.16
Henderson and Pabis	43.93	4.02×10^3	34.81	3829.15	24.41	143.16
Page	127.92	2.72×10^{16}	35.20	5044.22	31.32	1487.72
Avhad and Marchetti	128.43	3.37×10^{16}	34.18	2301.69	31.10	756.01

Table 2
Results obtained of the statistical analysis from four selected drying mathematical models at 323–353 K temperatures for Hass avocado seeds.

Model	Temp (K)	Non-pretreated avocado seeds					Sliced avocado seeds					Crushed avocado seeds				
		R^2	χ^2	E_{RMS}	MBE	MAE	R^2	χ^2	E_{RMS}	MBE	MAE	R^2	χ^2	E_{RMS}	MBE	MAE
	323	0.984	1.974×10^{-5}	4.44×10^{-3}	−0.001	0.0237	0.996	7.152×10^{-6}	0.0026	0.0166	0.016	0.997	2.723×10^{-6}	0.0016	$7.667 \times 10{-3}$	0.0144
Lewis	333	0.997	1.198×10^{-6}	1.09×10^{-3}	0.0048	0.0123	0.98	1.15×10^{-4}	0.0107	−0.0217	0.032	0.992	1.826×10^{-6}	1.351×10^{-3}	1.693×10^{-3}	0.0118
	343	0.99	1.966×10^{-5}	4.43×10^{-3}	0.0098	0.0235	0.992	1.345×10^{-5}	0.0036	0.0011	0.021	0.994	7.441×10^{-6}	2.727×10^{-3}	0.01634	0.0199
	353	0.996	2.731×10^{-6}	1.65×10^{-3}	0.0084	0.0141	0.994	8.547×10^{-6}	0.0029	0.0188	0.197	0.992	1.076×10^{-5}	3.281×10^{-3}	1.223×10^{-3}	0.0166
Henderson	323	0.984	2.102×10^{-5}	4.50×10^{-3}	5.7×10^{-3}	0.0224	0.998	1.171×10^{-6}	1.06×10^{-3}	6.45×10^{-3}	0.01	0.994	1.096×10^{-5}	3.250×10^{-3}	4.650×10^{-3}	0.0018
and	333	0.996	1.611×10^{-6}	1.24×10^{-3}	−0.0042	0.0122	0.996	3.821×10^{-6}	0.00191	0.005	0.015	0.99	2.790×10^{-5}	0.00518	0.0084	0.0217
Pabis	343	0.99	1.8138×10^{-5}	0.0041	0.0072	0.0232	0.995	5.164×10^{-6}	0.0022	0.0124	0.016	0.98	9.935×10^{-5}	0.0097	0.0269	0.0321
	353	0.997	1.686×10^{-6}	0.0012	0.0029	0.0131	0.996	3.184×10^{-6}	0.0017	0.0116	0.014	0.964	2.4×10^{-4}	0.0154	0.021	0.0331
Page	323	0.986	1.514×10^{-5}	3.82×10^{-3}	−0.0109	0.0174	0.998	8.233×10^{-7}	8.9×10^{-4}	0.0048	0.009	0.998	8.002×10^{-7}	8.7×10^{-4}	5.771×10^{-3}	0.0102
Page	333	0.996	1.523×10^{-6}	1.21×10^{-3}	−0.005	0.0111	0.996	3.893×10^{-6}	1.937×10^{-3}	0.0039	0.016	0.995	5.792×10^{-6}	2.36×10^{-3}	−0.00412	0.0143
	343	0.996	3.137×10^{-6}	1.73×10^{-3}	−0.0054	0.0143	0.993	1.132×10^{-5}	3.304×10^{-3}	−0.003	0.021	0.999	5.169×10^{-6}	2.232×10^{-3}	0.0134	0.0177
	353	0.989	3.437×10^{-5}	5.75×10^{-3}	0.0204	0.2407	0.994	7.278×10^{-6}	2.649×10^{-3}	0.0099	0.017	0.994	5.942×10^{-6}	2.393×10^{-3}	0.0104	0.0166
	323	0.995	1.568×10^{-6}	1.20×10^{-3}	0.0047	0.0111	0.994	1.246×10^{-5}	3.40×10^{-3}	3.28×10^{-3}	0.02	0.998	1.413×10^{-6}	1.145×10^{-3}	5.243×10^{-3}	0.0115
Avhad and Marchetti	333	0.996	1.401×10^{-6}	1.14×10^{-3}	−0.0042	0.0088	0.993	1.566×10^{-5}	3.81×10^{-3}	1.25×10^{-3}	0.023	0.995	5.313×10^{-6}	2.22×10^{-3}	−0.0012	0.017
	343	0.982	6.810×10^{-5}	7.94×10^{-3}	0.0084	0.3314	0.992	1.380×10^{-5}	3.58×10^{-3}	8.43×10^{-3}	0.022	0.993	1.223×10^{-5}	3.370×10^{-3}	0.0092	0.0214
	353	0.993	1.476×10^{-5}	3.70×10^{-3}	0.0089	0.02	0.996	4.12×10^{-6}	1.95×10^{-3}	0.0109	0.016	0.991	1.574×10^{-5}	3.823×10^{-3}	−0.0026	0.0195

Table 3
Results for the Avhad and Marchetti model constants for the non-pretreated, sliced and crushed Hass avocado seeds.

Temp (K)	Non-pretreated		Sliced		Crushed	
	a	N	a	N	a	N
323	0.967	1.206	0.940	1.009	0.960	1.177
333	0.984	1.084	0.984	1.110	0.988	1.190
343	1.025	0.996	0.974	1.080	1.035	1.200
353	1.032	0.854	0.975	1.046	0.975	1.160

versus time. Fig. 1(a–c) presents the characteristic drying curves of Hass avocado seeds at five different air temperatures (313, 323, 333, 343, and 353 K). The numerical values for the weight loss and the moisture ratio at different drying temperatures for the non-pretreated, sliced and crushed Hass avocado seeds are tabulated in Tables S1, S2, and S3, respectively of the supplementary information. Every experiments were performed twice. Though no significant difference in the experimental readings were noticed, the average of the weight loss was considered. The detail information of the obtained experimental findings is published elsewhere (Avhad and Marchetti, 2015). It was clearly evident that the rise in the surrounding air temperature resulted in the acceleration of the rate of the drying process. It was observed that moisture ratio reduced with drying time and the curve shape was steeper decreasing with the rise in the operating temperature; the similar behavior was reported for several agricultural materials (Gunhan et al., 2005; Duc et al., 2011; Mwithiga and Olwal, 2005; Demir et al., 2007). In the case of non-pretreated avocado seeds (Fig. 1(a)), the drying time required to reduce the moisture ratio below 0.5 when using 313 K was approximately 5 times more than that required at 353 K drying temperature. Furthermore, when the thickness of seed samples was reduced via the pretreatment process so as to promote the moisture evaporation progression, the drying time required to reduce the moisture ratio below 0.5 for the sliced avocado seeds (Fig. 1(b)) and crushed avocado seeds (Fig. 1(c)) even at an operating temperature of 313 K was 16 times less than that required for the non-pretreated avocado seeds. The present results were in agreement with the studies reported by Mwithiga and Olwal (Mwithiga and Olwal, 2005), where it was suggested that increase in the sample thickness of sliced kale from 10 mm to 50 mm resulted in elongation of drying time from 390 min to 1200 min, respectively. In the case of sliced (Fig. 1(b)) and crushed (Fig. 1(c)) pretreatment process, the rate of moisture evaporation was rapid in initial 360 min of the drying process and then slowed down; thus, indicating that the drying rate decreased consistently with the moisture content and drying time. Hence, the constant drying rate period in these curves was not existent, and the drying of Hass avocado seeds occurs in the falling rate period.

The activation energy for the non-pretreated and pretreated (sliced and crushed) Hass avocado seeds was determined from the slope of the plot, ln (k) versus T^{-1}. It is important to understand that the determination of E_a was performed considering air temperature range 323 K to 353 K. The moisture evaporation mechanism for Hass avocado seeds switched from a temperature-controlled to a diffusion-controlled at low air temperature of 313 K. This is because the drying temperature of 313 K was too low to accelerate the moisture evaporation from Hass avocado seeds. The plot, ln (k) versus T^{-1} for all five air temperatures and in all three cases is shown in Fig. 2(a–c). The estimated value for the activation energies and pre-exponential factors for the four studied models are presented in Table 1. The value of the E_a for the non-pretreated, sliced, and crushed Hass avocado seeds varied between 43 and 129, 34–36, and 24–32 KJ mol^{-1}, respectively. The computed activation energies in the case of sliced and crushed Hass avocado seeds were in agreement with those reported for other agricultural substances, such as grape seeds (Roberts et al., 2008) kale (Mwithiga and Olwal, 2005), and hull-less seed pumpkin (Sacilik, 2007). The calculated value of the activation energies were subsequently utilized for simulating the drying kinetics of Hass avocado seeds.

The curve fitting simulation with the obtained experimental data were performed using four different mathematical models. Fig. 3a–c shows the comparison of different drying mathematical models versus experimental data obtained for the non-pretreated, sliced, and crushed Hass avocado seeds, respectively, at 333 K air temperature. The graphical representation suggested that all four mathematical models appropriately described the drying kinetics of Hass avocado seeds; however, the selection of the best model was based on the statistical parameters, such as R^2, χ^2, E_{RMS}, MBE, and MAE. These statistical parameters were calculated for the non-pretreated and pretreated (sliced and crushed) Hass avocado seeds at a 323 K–353 K drying air temperature range. The results of the statistical analysis for all four models are presented in Table 2. It was investigated that in the case of non-pretreatment process, the R^2, χ^2, and E_{RMS} values changed from 0.982 to 0.997, 1.198×10^{-6} to 6.810×10^{-5}, and 1.090×10^{-3} to 7.940×10^{-3}, respectively. For the sliced pretreatment process, the R^2, χ^2, and E_{RMS} values fluctuated between 0.980 to 0.998, 8.223×10^{-7} to 1.150×10^{-4}, and 8.900×10^{-4} to 3.814×10^{-3}, respectively; while, R^2, χ^2, and E_{RMS} values varied from 0.980 to 0.999, 8.002 10^{-7} to 2.470×10^{-4}, and 8.700×10^{-4} to 0.015, respectively, in the case of crushed Hass avocado seeds. Among the four tested mathematical models, the Avhad and Marchetti model was found to have a better fitting with the experimental data, with the values of coefficient of determination in the case of non-pretreated, sliced, and crushed Hass avocado seeds being higher than 0.98, 0.99, and 0.99, respectively. Furthermore, the χ^2 values for the non-pretreated, sliced, and crushed Hass avocado seeds were lower than 6.82×10^{-5}, 1.57×10^{-5}, and 1.58×10^{-5}, respectively. Additionally, the E_{RMS} values were found to be below 8.0×10^{-3}, 3.9×10^{-3}, and 3.9×10^{-3} in the case of non-pretreated, sliced, and crushed Hass avocado seeds, respectively. The graphical representation for the Avhad and Marchetti model prediction with the experimental data at 323–353 K air temperatures for the non-pretreated and pretreated (sliced and crushed) Hass avocado seeds is shown in Fig. 4(a–c). The values obtained for the constants, a and N, of the Avhad and Marchetti model are presented in Table 3. The values obtained for the constant a (in the case of the Henderson and Pabis model) and N (in the case of the Page model) are presented in Table S4 and S5 of the supplementary information. The estimated values for the parameter N of the Avhad and Marchetti model were not constant and exhibited temperature dependence. Conversely, Simal et al. (Simal et al., 2005) and Senadeera et al. (Senadeera et al., 2003) reported studies in which the calculated value for N was constant and, a function of air velocity and the initial moisture content. Therefore, the authors concluded that the Page model had an excellent fitting with the experimental data (Simal et al., 2005; Senadeera et al., 2003).

Moreover, the activation energies and the pre-exponential factors calculated at an air temperature range of 323–353 K were also utilized to estimate the moisture evaporation rate constant, and subsequently the statistical parameters for the drying process performed at the low air temperature of 313 K. The additional investigation was performed to examine the precision of all four

models in predicting the drying process at an air temperature other than those in which the models were developed. The results of the statistical analysis for the non-pretreated, sliced, and crushed Hass avocado seeds at 313 K drying air temperature is presented in Table 4. The obtained results suggested that the R^2, χ^2, and E_{RMS} values changed between 0. 790 to 0.990, 4.584×10^{-5} to 0.026, and 1.60×10^{-3} to 0.163, respectively. Even in this scenario, it was evident that the Avhad and Marchetti model presented a superior fitting with the experimental data. The statistical analysis suggested that the R^2 value for the non-pretreated, sliced, and crushed Hass avocado seeds was equal to 0.97, 0.99, and 0.98 respectively. Furthermore, the χ^2 values for the non-pretreated, sliced, and crushed Hass avocado seeds were minimal in the case of the Avhad and Marchetti model. The graphical representation for the Avhad and Marchetti model prediction with the experimental data at 313 K air temperature for the non-pretreated and pretreated (sliced and crushed) Hass avocado seeds is shown in Fig. 5.

Table 4
Results obtained of the statistical analysis from four selected drying mathematical models at 313 K temperature for Hass avocado seeds.

Model	Temp (K)	Non-pretreated avocado seeds					Sliced avocado seeds					Crushed avocado seeds				
		R^2	χ^2	E_{RMS}	MBE	MAE	R^2	χ^2	E_{RMS}	MBE	MAE	R^2	χ^2	E_{RMS}	MBE	MAE
Lewis	313	0.888	8.90×10^{-4}	0.0298	−0.0633	0.0633	0.974	3.74×10^{-4}	0.0193	0.0321	0.0396	0.790	0.0268	0.1638	0.1205	0.1205
Henderson and Pabis		0.957	1.34×10^{-4}	0.0113	−0.0075	0.0302	0.976	3.317×10^{-3}	0.0178	0.0282	0.0372	0.869	0.0107	0.1017	0.05204	0.9625
Page		0.956	1.39×10^{-4}	0.0016	−0.0257	0.0380	0.951	1.449×10^{-3}	0.0373	0.0533	0.0537	0.932	0.0029	0.0529	0.0621	0.0644
Avhad and Marchetti		0.975	4.584×10^{-5}	0.0065	5.04×10^{-3}	0.0281	0.990	6.089×10^{-5}	0.0151	−0.0200	0.1336	0.987	9.179×10^{-5}	0.0092	−0.0216	0.0340

4. Conclusion

The information provided in this article could be utilized to simulate the drying kinetics of Hass avocado seeds between 313 K–353 K temperature ranges. The experimental results suggested that the rise in the operating temperature resulted in the acceleration of the rate of moisture evaporation and the drying was carried out in falling-rate period. In order to accurately describe the drying behavior of Hass avocado seeds, four different semi-theoretical mathematical models were compared based on their coefficient of determination, reduced mean square error, root mean square error, mean bias error, and mean absolute error of the deviation. From the obtained results it was concluded that the predictions made by the Avhad and Marchetti model were in good agreement with the experimental data. The resulting mathematical model provided R^2 value higher than 0.97, 0.99, and 0.98 at all five temperatures for the non-pretreated, sliced, and crushed Hass avocado seeds, respectively.

Author contributions

M.A.- main author of the article; J.M.- main lead of the article.

Competing financial interests

The authors declare no competing financial interests.

Acknowledgement

The authors would like to express their gratitude to the Norwegian University of Life Sciences (Project No. 1301051406) for their financial support.

Appendix A. Supplementary data

Supplementary data associated with this article can be found, in the online version, at http://dx.doi.org/10.1016/j.indcrop.2016.06.035.

References

Food and Agriculture Organization of the United Nations Statistics Division. http://faostat3.fao.org/browse/Q/QC/E (accessed 20.05.16).

Arabhosseini, A., Huisman, W., van Boxtel, A., Müller, J., 2009. Modeling of thin layer drying of tarragon (Artemisia dracunculus L.). Ind. Crops Prod. 29 (1), 53–59.

Avhad, M.R., Marchetti, J.M., 2015. Temperature and pretreatment effects on the drying of Hass avocado seeds. Biomass Bioenergy 83, 467–473.

Barrozo, M.A.S., Henrique, H.M., Sartori, D.J.M., Freire, J.T., 2006. The use of the orthogonal collocation method on the study of the drying kinetics of soybean seeds. J. Stored Prod. Res. 42 (3), 348–356.
Bhaumik, M., Choi, H.J., Seopela, M.P., McCrindle, R.I., Maity, A., 2014. Highly effective removal of toxic Cr(VI) from wastewater using sulfuric acid-modified avocado seed. Ind. Eng. Chem. Res. 53 (3), 1214–1224.
Dabas, D., Elias, R.J., Lambert, J.D., Ziegler, G.R., 2011. A colored avocado seed extract as a potential natural colorant. J. Food Sci. 76 (9), C1335–C1341.
Demir, V., Gunhan, T., Yagcioglu, A.K., Degirmencioglu, A., 2004. Mathematical modelling and the determination of some quality parameters of air-dried bay leaves. Biosyst. Eng. 88 (3), 325–335.
Demir, V., Gunhan, T., Yagcioglu, A.K., 2007. Mathematical modelling of convection drying of green table olives. Biosyst. Eng. 98 (1), 47–53.
Dreher, M.L., Davenport, A.J., 2012. Hass avocado composition and potential health effects. Crit. Rev. Food Sci. Nutr. 53 (7), 738–750.
Duc, L.A., Han, J.W., Keum, D.H., 2011. Thin layer drying characteristics of rapeseed (Brassica napus L.). J. Stored Prod. Res. 47 (1), 32–38.
Gómez, F., Sánchez, S., Iradi, M., Azman, N., Almajano, M., 2014. Avocado seeds: extraction optimization and possible use as antioxidant in food. Antioxidants 3 (2), 439–454.
Gunhan, T., Demir, V., Hancioglu, E., Hepbasli, A., 2005. Mathematical modelling of drying of bay leaves. Energy Convers. Manage. 46 (11–12), 1667–1679.
Henderson, S.M., Pabis, S., 1961. Grain drying theory I: temperature effect on drying coefficient. J. Agric. Eng. Res. 6, 169–174.
Iguaz, A., San Martín, M.B., Maté, J.I., Fernández, T., Vírseda, P., 2003. Modelling effective moisture diffusivity of rough rice (Lido cultivar) at low drying temperatures. J. Food Eng. 59 (2–3), 253–258.
Jaiyeoba, K.F., Raji, A.O., 2012. Effects of drying temperature on the effective coefficient of moisture diffusivity and activation energy in Ibadan-local tomato variety (Lycopersicum esculentum). J. Inf. Eng. Appl. 2 (4), 24–38.
Kashaninejad, M., Mortazavi, A., Safekordi, A., Tabil, L.G., 2007. Thin-layer drying characteristics and modeling of pistachio nuts. J. Food Eng. 78 (1), 98–108.
Lacerda, L., Colman, T., Bauab, T., da Silva Carvalho Filho, M., Demiate, I., de Vasconcelos, E., Schnitzler, E., 2014. Thermal, structural and rheological properties of starch from avocado seeds (Persea americana, Miller) modified with standard sodium hypochlorite solutions. J. Therm. Anal. Calorim. 115 (2), 1893–1899.
Lahsasni, S., Kouhila, M., Mahrouz, M., Jaouhari, J.T., 2004. Drying kinetics of prickly pear fruit (Opuntia ficus indica). J. Food Eng. 61 (2), 173–179.
Lewis, W.K., 1921. The rate of drying of solid materials. J. Ind. Eng. Chem. 13 (5), 427–432.
Mexico: Avocado Annual United States Department of Agriculture Foreign Agricultural Service 2014. http://www.fas.usda.gov/data/mexico-avocado-annual (Accessed on 5.12.15.).
Mwithiga, G., Olwal, J.O., 2005. The drying kinetics of kale (Brassica oleracea) in a convective hot air dryer. J. Food Eng. 71 (4), 373–378.
Panchariya, P.C., Popovic, D., Sharma, A.L., 2002. Thin-layer modelling of black tea drying process. J. Food Eng. 52, 349–357.
Perea-Flores, M.J., Garibay-Febles, V., Chanona-Pérez, J.J., Calderón-Domínguez, G., Méndez-Méndez, J.V., Palacios-González, E., Gutiérrez-López, G.F., 2012. Mathematical modelling of castor oil seeds (Ricinus communis) drying kinetics in fluidized bed at high temperatures. Ind. Crops Prod. 38, 64–71.
Phanphanich, M., Mani, S., 2009. Drying characteristics of pine forest residues. BioResources 5 (1), 108–121.
Pieterse, Z., Jerling, J., Oosthuizen, W., 2003. Avocados (monosaturated fatty acids), weight loss and serum lipids. South Afr. Avocado Growers Assoc. Yearbook 26, 65–71.
Roberts, J.S., Kidd, D.R., Padilla-Zakour, O., 2008. Drying kinetics of grape seeds. J. Food Eng. 89 (4), 460–465.
Rodrigues, L.A., da Silva, M.L.C.P., Alvarez-Mendes, M.O., Coutinho, A.dR., Thim, G.P., 2011. Phenol removal from aqueous solution by activated carbon produced from avocado kernel seeds. Chem. Eng. J. 174 (1), 49–57.
Sacilik, K., 2007. Effect of drying methods on thin-layer drying characteristics of hull-less seed pumpkin (Cucurbita pepo L.). J. Food Eng. 79 (1), 23–30.
Senadeera, W., Bhandari, B.R., Young, G., Wijesinghe, B., 2003. Influence of shapes of selected vegetable materials on drying kinetics during fluidized bed drying. J. Food Eng. 58 (3), 277–283.
Simal, S., Femenia, A., Garau, M.C., Rosselló, C., 2005. Use of exponential, Page's and diffusional models to simulate the drying kinetics of kiwi fruit. J. Food Eng. 66 (3), 323–328.
Siqueira, V.C., Resende, O., Chaves, T.H., 2012. Determination of the volumetric shrinkage in jatropha seeds during drying. Acta Sci. Agron. 34, 231–238.
Takenaga, F., Matsuyama, K., Abe, S., Torii, Y., Itoh, S., 2008. Lipid and fatty acid composition of mesocarp and seed of avocado fruits harvested at northern range in Japan. J. Oleo. Sci. 57 (11), 591–597.
Taylor, J.R., 1997. An Introduction to Error Analysis, second edition. University Science Books.
Vinha, A.F., Moreira, J., Barreira, S.V.P., 2013. Physicochemical parameters, phytochemical composition and antioxidant activity of the Algarvian Avocado (Persea americana mill.). J. Agric. Sci. 5 (12), 100–109.
Weatherby, L.S., Sorber, D.G., 1931. Chemical composition of avocado seed. Ind. Eng. Chem. 23 (12), 1421–1423.